Modulation of the secondary metabolism of a Cophinforma mamane endophytic fungal strain by epigenetics and cultivation-based approaches

Romina Géraldine Pacheco Tapia

THÈSE

En vue de l'obtention du

DOCTORAT DE L'UNIVERSITÉ DE TOULOUSE

Délivré par l'Université Toulouse 3 - Paul Sabatier

Présentée et soutenue par

Romina Geraldine PACHECO TAPIA

Le 25 octobre 2021

Modulation du métabolisme secondaire dune souche endophyte de Cophinforma mamane par des approches épigénetiques et basées sur les conditions de culture

Ecole doctorale : **SDM - SCIENCES DE LA MATIERE - Toulouse**

Spécialité : **Chimie-Biologie-Santé**

Unité de recherche :
PHARMA-DEV -Laboratoire Pharmacochimie et Pharmacologie pour le Développement

Thèse dirigée par
Mohamed HADDAD et Marieke VANSTEELANDT

Jury

Mme Gwenael RUPRICH-ROBERT, Rapporteure
Mme Nadia PONTS, Rapporteure
Mme Alexandra MAGRO, Examinatrice
M. Xavier CACHET, Examinateur
Mme Jacqueline GRIMA, Examinatrice
M. Mohamed HADDAD, Directeur de thèse

ACKNOWLEDGEMENTS

Throughout these three years of doctoral work between France and Peru, I have received a great deal of support and assistance. Here, I would like to thank all my colleagues, friends, family and everyone who contributed in any way to the realization of this thesis work in the best conditions.

I am specially thankful to the Institut de recherche pour le développement (IRD) for the funding sources that allowed the execution of this doctoral work in collaboration with Cayetano Heredia University in Lima, Peru and also for their constant concern during this particular and not easy pandemic period.

First, I would like to thank Mohamed Haddad, my thesis director, by giving me the opportunity to enroll a doctoral thesis while I was finishing my Master in Lima. Thank you for your confidence and for opening the doors of your house and family when I first arrived in Toulouse and for all your support during the course of my PhD degree.

I would also like to thank Marieke Vansteelandt, my thesis co-director, whose expertise and insightful feedback pushed me to sharpen my thinking and brought my work to a higher level. I truly appreciate your support and patience on the analysis, writing and the rereading of the manuscript and article.

I would like to extend my sincere gratitude to Valerie Julian and Nicolas Fabre, for accepting me and allowing me to be part of the incredible scientific group of PHARMA-DEV and the UMR-152 unit. Thank you for your advice, support and concerning to make my whole period a satisfying experience.

Thanks to the members of the dissertation defense committee for willing and making the time to read the manuscript, Pr Gwenaël Ruprich-Robert, Pr Nadia Ponts, Pr Alexandra Magro, Pr Xavier Cachet and Pr Jacqueline Grima. It is a privilege to have the opportunity of sharing my work with you. I particularly thank Dr Michel Sauvain for his brilliant remarks and advice during my period in LMI-LAVi in Lima and in Toulouse.

Of course, I would also like to express my deeply gratitude to all the members of the research unit that I will always remember as a big joyful family. Many thanks to Anne-Cécile, Karine, Guillaume, Geneviève, Hélène, Valerie, Alice, Jan, Pierre, Sandra, François and Franck for their constant concern, advices, kind help and support but also for all the fun moments inside and outside the lab. Many thanks to Pedro, Sergio and Simon, it has been a pleasure sharing ideas as colleagues but also sharing good moments as lab mates and friends with Inés, Manon, Fátima, Elise, Julia, Monivan, Chio, Messi, Alexandre, Chinedu, Jade, Mathias and the new future doctors, Maëlle and Emi (good luck!) during these years. You all made me feel at home despite of the distance.

Thanks to all the lab members and my lab mates of the LMI-LAVi unit in Lima for also helping and supporting me before and during these years, Dr Rosario Rojas, Denis, Billy, Yesenia, Daniela, Milagros, Karina and Candy.

I appreciate all the support I received from my best friends, Paola, Yamileth, Claudia, Katherin, who are like sisters for me and always believed in me. I would also like to give a special thanks to the good friends I met during this journey, Ximena, Ana, Yngrid, Mariella, Fiorella, Allison, Dušan, Kenneth and Reda for all the nice and fun moments, including of course, Peruvian food. Thanks also to Vincent and Yunuo for the fun moments and nice experiences!

Finally, I would like to thank and express my love to my family, my dad, my mom and my sister for being there across the distance, supporting me and giving me words of encouragement. I could not have made it this far without them. I have no words to express my love and gratitude to my better half, Edwin, for being a very understanding person that supported me in every way during the good and difficult times and for being the person on whom I can count on unconditionally. Thank you for being there and let's go for more adventures together!

Many thanks again to everyone who made this thesis possible and that contributed to the succesful realization of my PhD.

Table of Contents

LIST OF FIGURES

LIST OF TABLES

LIST OF ABBREVIATIONS

TDKP	Thiodiketopiperazine
DKP	Diketopiperazine
CM	*Cophinforma mamane*
UHPLC	Ultra High-Performance Liquid Chromatography
HRMS	High Resolution Mass Spectrometry
LC-MS	Liquid Chromatography – Mass Spectrometry
PI	Positive Ionization
OSMAC	One Strain – Many Compounds
HDAC	Histone Deacetylase
DNMT	DNA methyltransferase
AZA	5-azacytidine
SB	Sodium butyrate
NIC	Nicotinamide
HSL	Homoserin lactone
QS	*Quorum* sensing
RT	Retention time
PCA	Principal Component Analysis
PLS-DA	Partial Least-squares Discriminant Analysis
PDB	Potato Dextrose Broth
MEA	Malt Extract Agar
ISP2	International Streptomyces Project-2 Medium
CZA	Czapek solution Agar
TSA	Trypticase soy agar
GNPS	Global Natural Products Social Molecular Networking
IC_{50}	Half-maximal Inhibitory Concentration
EC_{50}	Half-maximal Effective Concentration

LIST OF SCIENTIFIC PRODUCTION

Publications

1. Book chapter (Elsevier), expected publication date April 2022

Book title: Medicinal plants as anti-infectives: current knowledge and new perspectives

Chapter title: Fungal endophytes: A source of anti-infectives

Authors: R. Pacheco, S. Ortiz, M. Haddad, M. Vansteelandt

2. Submitted manuscript

Journal: Fungal Biology

Title: Chemical modulation of the metabolism of an endophytic fungal strain of *Cophinforma mamane* using epigenetic modifiers and amino-acids

Authors: R. Pacheco, P. Vásquez-Ocmín, S. Duthen, S. Ortiz, P. Jargeat, C. Amasifuen, M. Haddad, M. Vansteelandt

3. Manuscript in preparation

Journal: Chemistry and Biodiversity

Title: Metabolome time-variations and induction of secondary metabolites through OSMAC approaches of an endophytic fungal strain of *Cophinforma mamane*

Authors: R. Pacheco, S. Ortiz, P. Jargeat, C. Amasifuen, M. Vansteelandt, M. Haddad

Poster presentation

1. **Analysis of metabolome time-variations of an endophytic fungal strain of Botryosphaeria mamane through untargeted LC-MS profiling.** R. Pacheco; M. Haddad; P. Jargeat; B. Cabanillas; C. Amasifuen; N. Fabre; M. Vansteelandt. European RFMF Metabomeeting 2020, 22 – 24 Janvier 2020, Toulouse – France

Oral presentations

1. **Epigenetic modifiers alter the secondary metabolite production of an endophytic fungal strain of *Botryosphaeria mamane* isolated from *Bixa orellana*.** R. Pacheco, M. Vansteelandt, P. Jargeat, B. Cabanillas, C. Amasifuen, N. Fabre, M. Haddad. IV Encuentro cientifico de Peruanos en Europa SINAPSIS 23 – 25 Octobre 2019, Ghent – Belgium

2. **Modulation non ciblée d'une souche fongique endophyte de *Cophinforma mamane* par le traitement de modificateurs épigénétiques et l'addition des acides aminés.** R. Pacheco. Treizièmes Journées de l'Ecole Doctorale EDSDM. 21 – 22 Mai 2021, Tolouse – France

RÉSUMÉ

Modulation du métabolisme secondaire d'une souche endophyte de *Cophinforma mamane* par des approches épigénetiques et basées sur les conditions de culture

Dans le contexte actuel d'émergence croissante de souches microbiennes résistantes et de déclin du taux de découverte de nouveaux médicaments à partir de produits naturels, les champignons endophytes représentent une source potentielle de molécules actives aux structures chimiques nouvelles relativement peu étudiée. En effet, les champignons endophytes ont fait l'objet d'une attention accrue en raison de leur capacité importante à produire des métabolites chimiquement diversifiés ayant des propriétés antimicrobiennes, antiparasitaires, antivirales et de nombreuses autres bioactivités avec des applications potentielles dans les domaines de la santé et de l'agriculture. Dans cette étude, nous nous sommes concentrés sur une souche fongique endophyte de *Cophinforma mamane* (Botryosphaeriaceae) isolée de *Bixa orellana* (Bixaceae), à partir de laquelle 4 thiodikétopipérazines (TDKPs), les botryosulfuranols A-D, présentant une activité anti-leishmanienne ont précédemment été isolées. Afin de moduler le métabolisme secondaire de *C. mamane* pour mieux comprendre la production des TDKPs et espérer induire la production de métabolites anti-infectieux, nous avons utilisé différentes approches basées sur la modification des conditions de culture ainsi qu'une approche épigénétique. Des analyses UHPLC - spectrométrie de masse couplées à une approche par métabolomique non ciblée ont été utilisées pour traiter l'ensemble de nos résultats. L'étude cinétique réalisée sur 28 jours de culture a mis en évidence une production dans le temps très courte (jours 6 à 9) du botryosulfuranol C, un TDKP qui possède un pont disulfure dans sa structure. Il est également intéressant de noter que le traitement avec l'homosérine lactone (HSL), une molécule impliquée dans le *quorum*-sensing des bactéries gram-négatives, a induit la production du botryosulfuranol C ainsi que celle d'autres dicétopipérazines mises en évidence par réseau moléculaire. La production de métabolites, annotés comme étant des cyclopentapeptides et détectés à un stade précoce (jours 4 à 8), a été significativement induite en présence des co-cultures de *C. mamane* avec *Pseudomonas aeruginosa* et *Staphylococcus aureus*. En outre, le traitement de la culture de *C. mamane* avec différents modificateurs épigénétiques nous a permis d'identifier la 5-azacytidine (AZA) comme étant un puissant modulateur chimique du métabolome de *C. mamane* via l'induction de gènes silencieux ou faiblement exprimés. Ces résultats par approche métabolomique nous ont ainsi aidé à mieux comprendre l'effet des conditions de culture sur le métabolome de *C. mamane*, le but étant de trouver les conditions optimales de culture afin d'une part d'obtenir des rendements plus importants en TDKPs, nécessaires pour approfondir l'évaluation de leur activité antileishmanienne *in vivo* et d'autre part d'identifier puis isoler de nouveaux composés bioactifs produits par *C. mamane*.

Mots clés : champignons endophytes, *Cophinforma mamane*, modificateurs épigénétiques, co-culture, métabolomique, dicétopipérazines.

ABSTRACT

Modulation of the secondary metabolism of a *Cophinforma mamane* endophytic fungal strain by epigenetics and cultivation-based approaches

In the context of an increasing emergence of microbial resistant strains added to decline in drug discovery rate from natural products, endophytic fungi represent a potential source of new metabolites with novel and diverse chemical structures. Endophytic fungi have gained an increased attention due to their great capacity to produce chemically diverse metabolites with antimicrobial, antiparasitic, antiviral and many other bioactivities with potential applicacions in health and agriculture. In this study, we focused on an endophytic fungal strain of *Cophinforma mamane* (Botryosphaeriaceae) isolated from *Bixa orellana* (Bixaceae) and from which 4 antileishmanial thiodiketopiperazines (TDKPs), botryosulfuranols A-D, were previously isolated. We performed different culture-based approaches as well as an epigenetic approach in order to alter the secondary metabolism of *C. mamane* for a better understanding of TDKPs production and to induce the production of anti-infective metabolites. UHPLC – Mass Spectrometry analysis and untargeted metabolomics tools have been used to evaluate our results. The 28-days kinetic study highlighted a short time-frame production (day 6 – 9) of botryosulfuranol C, a TDKP that possesses a di-sulfur bridge on its structure. Interestingly, the treatment with homoserin lactone (HSL), a quorum-sensing molecule of gram-negative bacteria, induced the production of botryosulfuranol C and other diketopiperazines revealed by molecular networking. Also, the production of metabolites putatively annotated as cyclopentapeptides and their detection at an early production stage (day 4 – 8), was significantly induced during the co-culture with *Pseudomonas aeruginosa* and *Staphylococcus aureus*. Moreover, treating *C. mamane* culture with different 4 epigenetic modifiers allowed us to identify 5-azacytidine (AZA) as a potent chemical modulator of the metabolome of *C. mamane* via the induction of silent or lowly expressed genes. These results will help us to improve the culture conditions of *C. mamane* to obtain better yields from TDKPs for further investigation of their *in vivo* antileishmanial activity and to isolate and identify other potential novel bioactive compounds revealed thanks to the metabolomics tools.

Keywords: endophytic fungi, *Cophinforma mamane*, epigenetic modifiers, co-culture, metabolomics, diketopiperazines

RESUME EN FRANÇAIS

Modulation du métabolisme secondaire d'une souche endophyte de *Cophinforma mamane* par des approches épigénétiques et basées sur les conditions de culture

I. Introduction générale

Les produits naturels ont été historiquement utilisés pour le développement de médicaments et de candidats médicaments. Actuellement, près de 50% du total des petites molécules approuvées comme médicaments, entre 1981 et 2019, sont dérivées ou inspirées de produits naturels (Newman & Cragg 2020). Un grand nombre de principes actifs proviennent de microorganismes, notamment de bactéries, d'actinomycètes et de champignons (Hutchings *et al.* 2019), avec 45% de la production de métabolites microbiens issue des micromycètes (Bérdy 2012), montrant ainsi l'importance des produits naturels microbiens.

Cependant, l'arsenal de médicaments à activité antimicrobienne devient très limité, parallèlement à l'émergence croissante de souches microbiennes résistantes qui nous conduit à des prévisions alarmantes de 10 millions de décès d'ici 2050, ainsi qu'à un énorme fardeau économique pour les systèmes de soins de santé du monde entier (Browne *et al.* 2020). En outre, l'Organisation mondiale de la santé (OMS) n'a signalé que six médicaments en cours de développement clinique dans la liste des antiinfectieux ciblant des agents pathogènes prioritaires, considérés comme innovants. Pour faire face à cette problématique, de nouvelles molécules avec de nouvelles structures et/ou de nouveaux mécanismes d'action sont nécessaires, et elles peuvent potentiellement être trouvés dans des sources inhabituelles comme dans des environnements peu explorés ou inexplorés tels que les endophytes (Challinor & Bode 2015).

Les endophytes sont des micro-organismes qui colonisent les tissus internes des plantes sans provoquer de symptomes apparents. Ceci est possible grâce à de multiples interactions entre la plante et son microbiome, avant, pendant et après l'invasion de la plante hôte, *via* des molécules de signalisation (Khare *et al.* 2018). Il est considéré que presque toutes les plantes sur Terre sont en interaction constante et proche avec des endophytes (Arnold 2007). Malgré cela, seulement 1 à 2% de toutes les plantes connues ont été étudiées pour leur composition endophytique (Strobel 2018).

La plupart des endophytes isolés et étudiés correspondent à des champignons endophytes qui sont capables de produire des composés chimiquement diversifiés (Gao *et al.* 2018; Zheng *et al.* 2021) avec des propriétés antibactériennes, antifongiques, antiparasitaires, antivirales, anticancéreuses, antioxydants, immunosuppressives et antidiabétiques (Manganyi & Ateba 2020; Adeleke & Babalola 2021). Un grand nombre de ces composés présentent des applications potentielles dans divers domaines

tels que la santé publique, l'agriculture et les industries pharmaceutiques (Gupta *et al.* 2020) avec un total de 245 demandes de brevets rapportées, entre 2001 et 2019, impliquant la production de métabolites secondaires et dans les processus de biotransformation (Torres-Mendoza *et al.* 2020). À cet égard, les champignons endophytes représentent une source renouvelable et prometteuse de produits naturels.

Dans cette étude, nous nous sommes intéressés à une souche fongique endophyte de *Cophinforma mamane* (D.E. Gardner) A. J. L. Phillips & A. Alves (Botryosphaeriaceae) isolée des feuilles de la plante médicinale *Bixa orellana* (Bixaceae). La collecte des échantillons de feuilles a été effectuée dans la forêt amazonienne du Pérou permettant ainsi l'isolement de 17 souches fongiques endophytes appartenant aux genres suivants: *Diaporthe*, *Nigrospora*, *Phyllosticta*, *Endomelanconiopsis*, *Sporothrix*, *Xylaria*, et *Cophinforma* (données non publiées). Un extrait brut de la souche E224 (*Cophinforma mamane*) a montré une activité antileishmanienne *in vitro* contre *Leishmania infantum* (valeur IC_{50} de 1.96 µg/mL) et a conduit à l'isolement de quatre nouveaux alcaloïdes thiodikétopipérazines (TDKP), les botryosulfuranols A, B, C et D (Barakat 2018). Ces composés présentent des atomes de soufre sur les positions α- et β- des résidus de phénylalanine et deux centres spirocycliques en C-4 et C-2 jamais décrits dans la littérature (**Figure 1**).

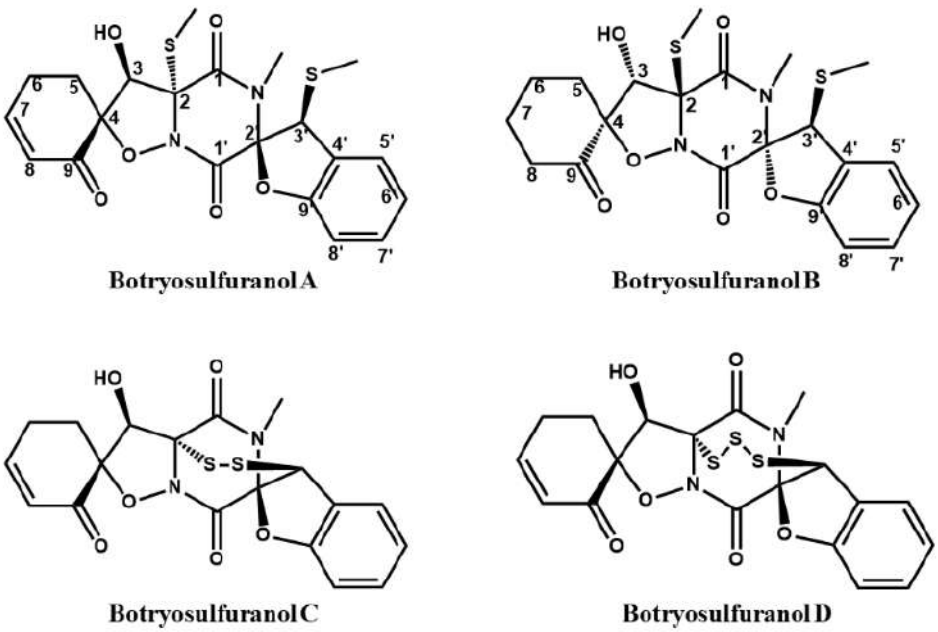

Figure 1. Structures chimiques des thiodicétopiperazines, botryosulfuranols A - D

L'activité antileishmanienne des quatre TDKPs a été évaluée *in vitro* contre les amastigotes axéniques de *Leishmania infantum*. Le botryosulfuranol D a présenté la plus forte activité avec une valeur de CI_{50} de 0.03 µM et un indice de sélectivité (IS) de 190, suivi du botryosulfuranol C (CI_{50} = 0.44 µM) ; du

botryosulfuranol A (CI_{50} = 0.69 μM) et du botryosulfuranol B (CI_{50} = 3.87 μM) (données non publiées). Les botryosulfuranols A, B et C ont également présenté une activité cytotoxique faible à modérée (GI_{50} = 8.0 – 115.7 μM) contre 4 lignées cellulaires cancéreuses (Barakat *et al.* 2019a). Bien que ces nouveaux composés aient présenté une activité antileishmanienne intéressante, les faibles quantités isolées n'ont pas permis d'approfondir leur activité biologique.

Un projet de pré-maturation, soutenu financièrement par la région Occitanie (porteur : N. Fabre), a été lancé avec l'objectif de poursuivre les recherches sur l'activité biologique par des tests *in vivo*. L'obtention de plus grandes quantités de molécules d'intérêt nécessaires aux tests *in vivo* a été possible grâce à une collaboration avec le Critt Bioindustries qui a pris en charge la fermentation du champignon à grande échelle. Parallèlement à ce projet auquel j'ai participé, notamment pour l'extraction et l'isolement des botryosulfuranols à partir des cultures en fermenteurs, la majeure partie de mon travail de recherche doctorale a porté sur l'étude des modifications du métabolisme de *C. mamane* soumis à différentes conditions de culture.

Il est connu que chez les champignons, le nombre de cluster de gènes est largement supérieur au nombre de groupes de gènes connus, impliqués dans la biosynthèse des métabolites secondaires isolés (Pettit 2011) en raison de la présence de gènes silencieux ou faiblement exprimés (Brakhage & Schroeckh 2011) en conditions standards de laboratoire. Ainsi, différentes approches ont été appliquées afin d'induire la production de métabolites secondaires chez les champignons, telles que les méthodologies basées sur la culture, comme l'approche OSMAC, la co-culture avec d'autres micro-organismes et l'ajout d'éliciteurs chimiques aux milieux de culture, tels que les modificateurs épigénétiques. Lors d'un travail doctoral précédent, une étude portant sur *C. mamane* a évalué l'influence de deux modificateurs épigénétiques (acide suberoylanilide hydroxamique et valproate de sodium) (Triastuti *et al*. 2019) et d'une co-culture avec *Fusarium solani* (Triastuti *et al.* 2021), sur le métabolisme de la souche *C. mamane* E224. Ce travail avait mis en évidence la production de métabolites induits *de novo* dans ces conditions.

Afin d'éviter le ré-isolement de composés déjà connus, l'approche métabolomique est devenu un outil puissant pour l'analyse, l'identification et la quantification des petits métabolites (Zhao *et al.* 2018). La spectrométrie de masse (SM) est la technique la plus utilisée en raison de sa grande sensibilité, du faible volume d'échantillon nécessaire, de l'acquisition de données de fragmentation SM/SM pour l'élucidation structurale suivie d'une comparaison avec des bases de données spécifiques. En outre, l'association avec des outils informatiques et statistiques peut offrir une bonne vue d'ensemble qui simplifie les vastes analyses de données (Demarque *et al.* 2020). Plus précisément, la métabolomique non ciblée se concentre sur la détection d'autant de métabolites que possible pour élaborer un ensemble de données complet afin de mieux comprendre le métabolome de l'objet étudié.

Après une revue de la littérature, nous avons appliqué différentes approches culturales et épigénétiques pour modifier le métabolisme secondaire d'une souche fongique endophyte de *Cophinforma mamane* (Botryosphaeriaceae) isolée de la plante médicinale *Bixa orellana* (Bixaceae). Une importance particulière a été accordée aux 4 thiodicétopipérazines bioactives précédemment isolées dans notre équipe par F. Barakat (Barakat *et al.* 2019a). Les deux objectifs principaux de cette étude sont :

1. **Une meilleure compréhension de la production des botryosulfuranols précédemment isolés ainsi qu'une induction de leur production, et plus généralement l'induction des dicétopipérazines et autres alcaloïdes par une approche cinétique et OSMAC incluant l'utilisation de modificateurs épigénétiques et de précurseurs biosynthétiques.**
2. **La production de nouveaux composés, notamment des métabolites anti-infectieux, par la co-culture de *C. mamane* avec des souches bactériennes pathogènes ainsi que des cultures en présence de parasites inactivés.**

Des analyses de CLUHP-SM couplées à des outils de métabolomique ont été utilisées afin d'atteindre nos objectifs.

Afin de répondre à notre premier objectif, une étude des variations temporelles de la production de métabolites secondaires a été réalisée. Cette analyse a été suivie par l'application de l'approche OSMAC consistant à utiliser différents milieux de culture et différentes conditions de lumière comme facteurs pouvant induire le métabolisme secondaire de ce champignon endophyte.

Le métabolisme de cette souche fongique soumise à la présence de modificateurs épigénétiques dans le milieu de culture a également été analysé, afin de mettre en évidence, via la production de nouveaux composés, une éventuelle stimulation de transcription de gènes silencieux ou faiblement exprimés en conditions standards de laboratoire. Nous avons également évalué l'impact de l'ajout d'acides aminés dans le milieu de culture sur le métabolisme, et notamment sur la production de dicétopipérazines et autres alcaloïdes via une stimulation des voies de biosynthèse spécifiques.

Enfin, pour répondre à notre deuxième objectif, des parasites de *Leishmania infantum* thermiquement inactivés ont été ajoutés à la culture du champignon endophyte afin de simuler la présence d'autres micro-organismes qui pourraient induire la production de métabolites secondaires antileishmaniens, tels que les botryosulfuranols. Des co-cultures de *C. mamane* avec des souches bactériennes pathogènes vivantes ont également été réalisées afin d'induire la production de métabolites antibactériens.

II. Matériels et méthodes

a) Matériels biologiques

Matériel fongique

La souche E224 de *Cophinforma mamane* (D.E. Gardner) A. J. L. Phillips & A. Alves a été isolée à partir des feuilles fraîches de *Bixa orellana* L. collectées en novembre 2013 par Carlos Amasifuen et Mohamed Haddad dans la réserve nationale d'Allpahuayo Mishana dans la forêt amazonienne d'Iquitos, Pérou (coordonnées GPS : 3°58'2.3" S, 73°25'3.9" W). Les processus d'isolement, d'identification et de stockage réalisés pour cette souche ont été précédemment décrits dans la littérature (Triastuti *et al.* 2019; Barakat *et al.* 2019).

Brièvement, les tissus collectés ont été stérilisés avec de l'hypochlorite de sodium à 5%, de l'éthanol à 70% (2 fois) et rincés à l'eau distillée. Les feuilles stérilisées en surface ont été coupées en petits fragments (5x5 mm) et placées sur une boîte de Pétri contenant du milieu MEA et du chloramphénicol (100 mg/L). Les isolats purs ont ensuite été identifiés par biologie moléculaire, via le séquençage des ITS1 et ITS2. La séquence correspondant à celle de la souche *C. mamane* E224 est disponible dans la base de données GenBank sous le numéro d'accession MG457709.1. Les cryotubes sont conservés à -80 °C dans 30% de glycérol dans la mycothèque de l'UMR 152.

Matériel bactérien

Pour les expériences de co-culture, trois souches bactériennes provenant de l'American Type Culture Collection (ATCC) ont été utilisées: *Escherichia coli* ATCC® 25922™; *Pseudomonas aeruginosa* ATCC® 27853™ et *Staphylococcus aureus* ATCC® 25923™.

Parasites de Leishmania

Pour la culture de *C. mamane* et pour les tests biologiques, des parasites *Leishmania infantum* exprimant une activité luciférase ont été utilisés (MHOM/MA/67/ITMAP-263, CNR Leishmania, Montpellier, France).

b) Conditions de culture et procédures d'extraction

Les étapes générales de la méthodologie, de l'isolement des champignons à l'analyse métabolomique, réalisées au cours de ce travail de doctorat sont résumées dans le schéma suivant (**Figure 2**)

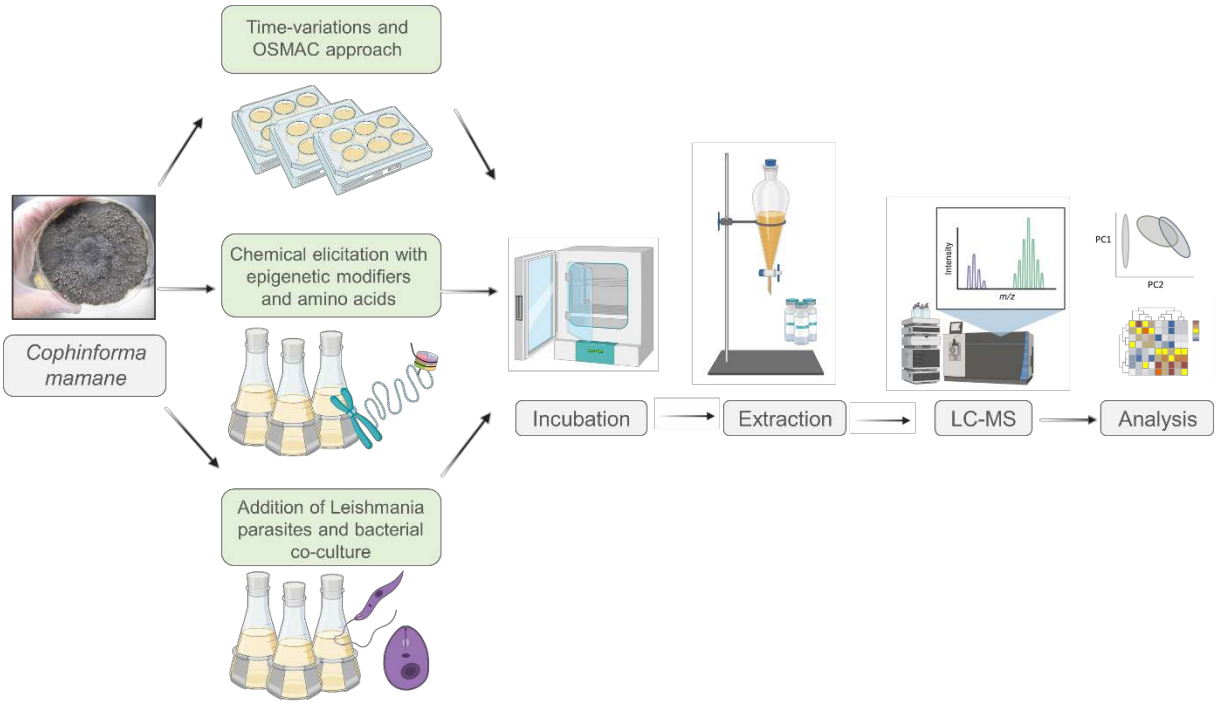

Figure 2. Étapes de la méthodologie générale: les différentes approches pour l'induction de métabolites secondaires de *C. mamane* (création propre avec biorender.com)

Étude cinétique et approche OSMAC

Pour l'étude cinétique, *C. mamane* a été incubé dans des plaques 6 puits contenant 4 mL/puits de MEA pendant 28 jours à 27°C sous lumière naturelle. A la fin de chaque jour de culture, une plaque de culture et une plaque témoin ont été placées à -80°C. Chaque culture (biomasse et milieu) a ensuite été lyophilisée. Le matériel sec a été transféré dans un tube de verre avec 10 mL de solvant. L'extraction a été réalisée à l'aide d'un mélange dichlorométhane-méthanol-eau 64:36:8 (v/v/v) préparé extemporanément (Bertrand *et al.* 2014).

En ce qui concerne l'approche OSMAC, *C. mamane* a été incubé dans des plaques 6 puits contenant du milieu CZA et du milieu ISP2 pendant 6 et 10 jours à 27 °C en présence ou en l'absence de lumière naturelle. A la fin de chaque temps d'incubation, les plaques de culture et les plaques témoins ont été placées à -80 °C. Chaque culture a ensuite été extraite avec 10 mL d'acétate d'éthyle. Le milieu et les mycéliums ont été broyés dans le solvant et soumis à un traitement par ultrasons pendant 60 minutes.

Dans les deux expériences (cinétique et OSMAC), les surnageants ont été filtrés à travers un coton de verre. Les filtrats ont ensuite été déshydratés sur du sulfate de magnésium puis filtrés à l'aide d'un papier filtre. Enfin, le solvant de toutes les phases organiques a ét évaporé sous pression réduite (évaporateur rotatif KNF RC 600) à 40 °C afin d'obtenir les extraits bruts secs.

Élicitation chimique avec des modificateurs épigénétiques et ajout d'acides aminés

La souche *C. mamane* E224 a été cultivée sur milieu PDA pendant 7 jours. Puis le prélèvement d'un morceau de mycélium a permis l'inoculation de 50 mL de PDB. Après 3 jours de cette culture à 27°C, 2 ml ont été utilisés pour inoculer des flacons Erlenmeyer de 250 ml contenant 50 ml de PDB. Cette culture a été traitée avec 4 modulateurs épigénétiques différents, NIC, SB, AZA et HSL, dissous dans du DMSO et ajoutés aux 50 ml de PDB. NIC et SB ont été ajoutés à 1 µM, AZA a été ajouté à 25 µM et HSL a été ajouté à 100 µM comme concentrations finales. La fermentation a été réalisée pendant 2 semaines à 27 °C dans des conditions statiques. Toutes les conditions, y compris les contrôles négatifs, ont été réalisées en triplicata.

Pour l'ajout d'acides aminés, *C. mamane* a été cultivé dans du MEB et dans du MEB supplémenté avec 2 mg/L de L-Trp et L-Phe. La fermentation a été effectuée dans des flacons Erlenmeyer de 250 mL contenant 50 mL de MEB ou 50 mL de MEB supplémenté pendant 2 semaines à 27°C sous agitation constante. Toutes les conditions et les contrôles négatifs ont été réalisés en triplicata.

Pour les deux études et après deux semaines d'incubation, un partage liquide/liquide a été réalisé avec 50mL d'acétate d'éthyle sous 60 minutes de traitement aux ultrasons. Les mycéliums ont été retirés par filtration avec du coton de verre. Les phases organiques ont ensuite été déshydratées sur du sulfate de magnésium et filtrées avec du papier filtre. Enfin, elles ont été évaporées à sec sous pression réduite (évaporateur rotatif KNF RC 600) à 40 °C.

Ajout de parasites inactivés et co-culture avec des bactéries

Des cultures fraîches de promastigotes et d'amastigotes de *Leishmania infantum* ont d'abord été centrifugées à 2100 RPM pendant 10 minutes. Après élimination du surnageant, chaque culot a été remis en suspension dans de l'eau distillée et autoclavé à 121°C pendant 15 minutes afin d'inactiver les parasites.

La souche de *C mamane* a été cultivée dans du MEB en présence de trois concentrations différentes d'amastigotes tués par la chaleur : C1=5.2 x 10^5, C2=1.06 x 10^6 et C3=2.12 x 10^6 parasites/mL. La fermentation a été effectuée dans des flacons Erlenmeyer de 250 ml contenant 50 ml de MEB pendant 2 semaines à 27 °C et sous agitation constante. Toutes les conditions, y compris les contrôles négatifs, ont été réalisées en triplicata.

Après 2 semaines d'incubation, un partage liquide/liquide a été réalisé avec 50mL d'acétate d'éthyle sous 60 minutes de traitement aux ultrasons. Les mycéliums ont été retirés par filtration avec du coton de verre. Le surnageant a été filtré à l'aide de membranes en acétate de cellulose régénérée (0.45 µm) pour éliminer les débris cellulaires. Les phases organiques ont ensuite été déshydratées sur du sulfate de

magnésium et filtrées avec du papier filtre. Enfin, elles ont été évaporées à sec sous pression réduite (évaporateur rotatif KNF RC 600) à 40°C.

Pour les expériences de co-culture, les souches *Escherichia coli* ATCC® 25922™; *Pseudomonas aeruginosa* ATCC® 27853™ et *Staphylococcus aureus* ATCC® 29923™ ont d'abord été cultivées dans du TSA et incubés à 30°C pendant 24 h. Une colonie de chaque souche a ensuite été cultivée dans du bouillon LB à 30°C pendant 48 h à 150 RPM. En parallèle, *C. mamane* a été cultivé sur PDA pendant 7 jours avant d'inoculer 50 mL de PDB. Après 3 jours de culture à 27°C, 1 ml a été utilisé pour inoculer des flacons Erlenmeyer de 250 ml contenant 50 ml de PDB auquel sont ajoutés 200 µL de bouillon LB 48 h de chaque souche bactérienne. Ces co-cultures ont été mises à incuber à 27°C pendant 10 jours.

Un partage liquide/liquide a été réalisé avec 50mL d'acétate d'éthyle sous 60 minutes de traitement aux ultrasons. Les mycéliums ont été retirés par filtration avec du coton de verre. Les phases organiques ont ensuite été déshydratées sur sulfate de magnésium et filtrées avec du papier filtre. Enfin, elles ont été évaporées à sec sous pression réduite.

Les différentes conditions de culture utilisées dans ce travail sont résumées dans le **Tableau 1**.

Tableau 1. Résumé des conditions de culture pour la modification du métabolisme de *C. mamane*

Etude	Milieu de culture	Temps d'incubation	Autres conditions
Cinétique	MEA	28 jours	27ºC
OSMAC	ISP2, CZA	6 and 10 jours	27ºC, 24h de lumière et 24 h d'obscurité
Modificateurs épigénétiques	PDB	14 jours	27ºC, sans agitation
Acides aminés	MEB	14 jours	27ºC, 120 RPM
Leishmania inactivés	MEB	14 jours	27ºC, 120 RPM
Co-culture	PDB	10 jours	27ºC, sans agitation

c) Evaluation de l'activité biologique

Un test d'activité antiparasitaire a été réalisé pour les extraits bruts obtenus à partir de la culture de *C. mamane* en présence des amastigotes thermiquement inactivés de *L. infantum*. Pour cela, les promastigotes de *L. infantum* ont été cultivés dans un milieu RPMI 1640 complété par 10% de sérum de veau fœtal (FCS), 2 mM L-glutamine, 100 U/mL de pénicilline et 100 µg/mL de streptomycine, puis récoltés en phase logarithmique de croissance par centrifugation à 900 g pendant 10 min. Le surnageant a été soigneusement éliminé et a été remplacé par le même volume de milieu complet RPMI 1640 à pH 5,4 et incubé pendant 24 h à 24°C. Les promastigotes acidifiés ont ensuite été incubés pendant 24 h à

37°C dans un flacon ventilé pour transformer les promastigotes acidifiés en amastigotes axéniques (Sereno & Lemesre 1997). Les effets des extraits sur la croissance des amastigotes axéniques de *L. infantum* ont été évalués comme suit: des amastigotes de *L. infantum* ont été incubés (2×10^6 parasites/mL) dans des plaques stériles96 puits avec chaque échantillon dissous dans du MeOH (concentration finale de 0.5 % v/v), en duplicata. Des témoins solvants (DMSO ou MeOH) et un contrôle positif (amphotéricine B), ont été ajoutés à chaque série d'expériences.

Après une période d'incubation de 48 heures à 37 °C, chaque puits de plaque a été examiné au microscope pour détecter toute formation de précipité. Pour estimer l'activité luciférase des amastigotes axéniques, 80 µL de chaque puits ont été transférés dans des plaques blanches à 96 puits, le réactif Steady Glow® (Promega) a été ajouté conformément aux instructions du fabricant, et les plaques ont été incubées pendant 2 min. La luminescence a été mesurée dans le compteur de luminescence Microbeta (PerkinElmer). La concentration efficace à 50 % (CE_{50}) a été définie comme la concentration du composé nécessaire pour inhiber de 50 % l'activité métabolique des amastigotes de *L. infantum* par rapport au contrôle. Les valeurs de la CE_{50} ont été calculées par analyse de régression non linéaire traitée sur des courbes dose-réponse, à l'aide du logiciel TableCurve 2D (version 5.0).

d) Analyse UHPLC-spectrométrie de masse

Des solutions méthanoliques à 2 mg/mL de tous les extraits ont été préparées pour l'analyse par chromatographie liquide à ultra-haute performance - MS. Des échantillons de contrôle de qualité (QC) ont été préparés en regroupant un aliquot de tous les extraits pour chaque expérience. Les analyses ont été réalisées sur un système UHPLC Ultimate 3000 (Dionex) couplé à un spectromètre de masse LTQ Orbitrap XL (Thermo Fisher Scientific, Hemel Hempstead, UK). Les échantillons ont été séparés sur une colonne C18 Acquity (100 × 2.1 mm i.d, 1.7 µm, Waters, MA, USA) équipée d'une colonne de garde. La phase mobile A était de l'eau ultrapure acidifiée avec 0.1% de FA et la phase mobile B était de l'acétonitrile acidifiée avec 0.1% de FA. Le gradient de solvant était le suivant : 0 min, 95 % A ; 10 min, 95 % B ; 12.5 min, 95 % B. Le débit était de 0.45 mL/min, la température de la colonne était réglée à 40 °C, la température de l'échantillonneur automatique était réglée à 15 °C et le volume d'injection fixé à 5 µL pour les extraits. La détection de masse a été réalisée à l'aide d'une source électrospray (ESI) en mode d'ionisation positive (PI) à un pouvoir de résolution de 15 000 [largeur totale à mi-hauteur (FWHM) à 400 *m/z*]. La plage de balayage de masse était de *m/z* 100-2000 pour tous les échantillons. La tension du spray d'ionisation était réglée à 3,5 kV et la température du capillaire était réglée à 300°C. Pour chaque scan MS complet, une fragmentation MS/MS des trois ions les plus intenses a été réalisée (mode « data dependant-scan) en utilisant la dissociation induite par collision (CID) à 35 unités d'énergie arbitraires.

e) Analyse des données

Traitement des données

Les données LC-MS de chaque expérience ont été traitées séparément avec MS-DIAL version 4.7 (Tsugawa *et al.* 2015) pour l'extraction du signal de masse entre 100 et 1500 Da de 0.5 à 12.5 min. Les tolérances MS1 et MS2 ont été fixées à 0.01 et 0.025 Da, respectivement, en mode centroïde pour chaque ensemble de données. Les pics ont été alignés sur un fichier de référence QC avec une tolérance de temps de rétention (RT) de 0.05 min et une tolérance de masse de 0.025 Da. La hauteur minimale des pics a été fixée à 70 % en dessous de la ligne de base du chromatogramme d'ions totaux (TIC) observé pour les échantillons témoins. Les données MS-DIAL ont été nettoyées avec le flux de travail MS-CleanR en utilisant les paramètres par défaut (Fraisier-Vannier *et al.* 2020) : tous les filtres avec un rapport minimum de blanc fixé à 0.8, un écart-type relatif (RSD) maximum fixé à 30 et un défaut de masse relatif (RMD) allant de 50 à 3000. La différence de masse maximale pour la détection des relations entre les caractéristiques a été fixée à 0.005 Da et la différence de RT maximale a été fixée à 0.025 min. Les liens de corrélation de Pearson ont été considérés avec une corrélation $\geq$0,8 et statistiquement significative $\alpha = 0.05$. Deux pics ont été conservés dans chaque cluster: le plus intense et le plus connecté aux autres ions.

Les caractéristiques conservées ont été annotées avec MS-FINDER version 3.5 (Tsugawa *et al.* 2016). Les tolérances MS1 et MS2 ont été fixées à 0.005 et 0.05 Da, respectivement. La recherche de formules chimiques a considéré les atomes C, H, O, N, P et S. L'annotation a été faite en utilisant les bases de données génériques internes de MS-FINDER: LipidMaps, YMDB, ChEBI, NPA, NANPDB, COCONUT, KNApsacK et UNPD. Seules les annotations ayant un score supérieur à 5 ont été retenues tout au long de l'analyse, tandis que les caractéristiques non annotées sont désignées comme "inconnues". Les données ont finalement été exportées sous forme de fichiers *.msp* pour les informations spectrales MSMS et de fichiers *.csv* pour les informations relatives aux métadonnées (surface des pics, temps de rétention, résultats des annotations, etc.).

Réseau moléculaire

Les fichiers MSP et de métadonnées générées après le flux de travail MS-CleanR ont été importés dans MetGem (version 1.3.4) (Olivon *et al.* 2018). Les données ont été filtrées en supprimant tous les pics MS/MS situés à ±17 Da du *m/z* du précurseur. Les spectres MS/MS ont été filtrés par fenêtre en utilisant les 6 pics supérieurs dans la fenêtre de ±50 Da dans tout le spectre. La tolérance des ions fragments MS/MS a été fixée à 0.2 Da. Un réseau de similarité de spectres de masse a été créé où les liens ont été filtrés pour avoir un score de cosinus supérieur à 0.7 et au moins six pics appariés. D'autres arêtes entre deux nœuds ont été conservées dans le réseau de similarité uniquement si chacun des nœuds apparaissait

dans le top 10 des nœuds les plus similaires de l'autre. Le réseau résultant a ensuite été importé dans Cytoscape (version 3.8.2, Institute for Systems Biology, Seattle, WA, USA) pour en améliorer la visualisation (Shannon 2003). Les nœuds ont été colorés en fonction de leurs conditions de culture et la taille des nœuds, quant à elle, indique leur surface de pic totale normalisée.

Analyses statistiques

Les analyses statistiques ont été réalisées en téléchargeant le fichier CSV sur la plateforme Metaboanalyst version 5.0 (https://www.metaboanalyst.ca/) (Chong *et al.* 2019). Les données ont été prétraitées, d'abord par normalisation (par la médiane) des échantillons, puis les variables ont été pondérées par auto échelle (centrée sur la moyenne et divisée par la racine carrée de l'écart-type de chaque variable). Une analyse en composantes principales (PCA) puis une analyse discriminante par moindres carrés partiels (PLS-DA) ont été réalisées. Enfin, le *m/z* et le temps de rétention des principales caractéristiques associées à leur aire de pic normalisée ont été reportés sur une carte thermique (regroupement hiérarchique) en utilisant l'ANOVA.

III. Résultats et discussions

Ce travail a porté sur l'étude des variations du métabolome sous différentes approches de culture d'une souche fongique endophyte de *Cophinforma mamane* (Botryosphaeriaceaee), isolée de *Bixa orellana* (Bixaceae), une plante médicinale du Pérou. Cette thèse de doctorat est un travail qui poursuit les recherches menées par les docteurs Fatima Barakat et Asih Triastuti dans le cadre de leurs travaux de doctorat, et qui ont permis d'une part l'étude du métabolome de ce champignon (Triastuti *et al.* 2019, 2021) et d'autre part l'isolement de 4 composés antiparasitaires, les botryosulfuranols A, B, C (Barakat *et al.* 2019) et D (Barakat 2018) (données non publiées).

Nos principaux objectifs étaient les suivants :

1) Mieux comprendre la production du TDKP botryosulfuranols A-D et d'autres DKPs par des approches cinétiques, et d'induction de leur production notamment par l'ajout de modificateurs épigénétiques et d'acides aminés (bioprécurseurs) dans les milieux de culture

2) Induire la production de métabolites, notamment anti-infectieux.

Afin de mener à bien ce travail, différentes approches ont été suivies.

Une étude cinétique a été réalisée pour analyser les changements du métabolome au fil du temps, tandis que l'approche OSMAC a été appliquée afin d'observer l'influence des milieux de culture et de la

présence de lumière sur le profil chimique global de *C. mamane*. Pour tenter d'induire l'expression des gènes faiblement exprimés ou silencieux en conditions standards de laboratoire, différents éliciteurs chimiques ont été ajoutés à la culture fongique, dont trois modificateurs épigénétiques qui agissent au niveau des chromosomes (protéines histones) et une molécule impliquée dans le quorum-sensing bactérien (homosérine lactone). Afin de stimuler spécifiquement les voies de biosynthèse des alcaloïdes, y compris les TDKPs, botryosulfuranols A-D, les acides aminés L-tryptophane et L-phénylalanine ont été ajoutés comme précurseurs de biosynthèse dans la culture fongique.

Enfin, dans le cadre de la recherche de nouveaux anti-infectieux, *C. mamane* a été mis en co-culture avec 3 souches bactériennes pathogènes différentes. De plus, une méthodologie utilisant des parasites de *Leishmania* inactivés par la chaleur a été développée afin d'induire la production par *C. mamane* de métabolites antileishmaniens, y compris les TDKPs, botryosulfuranols A-D.

a) Modulation générale de la diversité chimique de *C. mamane*

Les méthodologies utilisées nous ont permis d'identifier différents groupes chimiques produits par *C. mamane* dans la plupart des conditions, comme les dicétopipérazines, les peptides cycliques, les acides gras à chaîne longue et moyenne, les eicosanoïdes, suivis des sphingolipides, des terpénoïdes, des quinones, des coumarines, des hydropyridines et des benzénoïdes, qui sont les moins fréquents parmi les métabolites annotés. Parmi les méthodologies appliquées, l'ajout de modificateurs épigénétiques a été celle qui a le plus modifié le métabolisme général de *C. mamane*, et en particulier l'ajout de 5-azacytidine (un inhibiteur de l'ADN méthyltransférase) à la fois dans la régulation positive et négative des métabolites. De même, la culture de *C. mamane* dans le milieu de culture ISP2 pendant 10 jours dans des conditions lumineuses a semblé modifier le métabolisme général, à la fois dans la régulation positive et négative de nombreux métabolites, par rapport aux autres méthodologies utilisées.

L'un des principaux résultats, portant sur les métabolites annotés, nous a permis de constater que ce champignon endophyte produit un groupe de métabolites identifiés comme des cyclopentapeptides. Les pics chromatographiques correspondants ont été, dans la plupart des conditions, observés comme les pics principaux. L'étude cinétique nous a permis de mettre en évidence que ces métabolites apparaissent à un stade précoce (D4-D8) et diminuent rapidement après cette période. Cependant, dans une étude précédente portant sur la dynamique de la co-culture entre *C. mamane* et *Fusarium solani*, la production de ces cyclopentapeptides par les deux champignons avait été maintenue dans le temps après 10 jours de co-culture dans la MEA (Triastuti *et al.* 2021). Cette condition permettrait ainsi peut-être de favoriser la production de ces composés dans le temps, et ceci soulève l'hypothèse du rôle de ces composés dans les interactions fongiques.

De plus, la production de cyclopentapeptides a été régulée négativement en présence d'amastigotes de *Leishmania* inactivés par la chaleur, mais elle a été induite de manière significative en présence de bactéries vivantes, notamment *P. aeruginosa* (Gram-) et *S. aureus* (Gram +). Dans des études antérieures, les cyclopentapeptides fongiques ont présenté diverses activités biologiques contre d'autres champignons, bactéries, virus et parasites avec des applications potentielles (Wang *et al.* 2017). Cependant, leur rôle écologique a été moins discuté et à cet égard, certains auteurs ont suggéré leur rôle dans la communication inter-espèces, comme dans le cas des cyclopentapeptides produits par le champignon endophyte *Fusarium decemcellulare* (Li *et al.* 2016) ou les hexocyclopeptides produits par le champignon endophyte *Fusarium solani* (Wang *et al.* 2015). La régulation négative de la production de cyclopentapeptides par *C. mamane* en présence de parasites inactivés par la chaleur et la régulation positive en présence de bactéries vivantes, renforce leur rôle potentiel en tant que molécules de communication entre différentes espèces microbiennes, mais des recherches supplémentaires sont nécessaires afin de comprendre les mécanismes de déclenchement, comme cela est connu pour le processus de *quorum-sensing* bactérien.

b) Modulation de la production des TDKPs, botryosulfuranols A-D

Les méthodologies appliquées dans cette thèse de doctorat avaient également pour objectif d'induire la production de 4 TDKPs, précédemment isolées de *C. mamane*, les botryosulfuranols A-C (Barakat *et al.* 2019b) et D (données non publiées). Un résultat intéressant issue de l'étude cinétique est la production à court terme, par rapport aux autres TDKPs, du botryosulfuranol C (**Figure 3**), une TDKP qui possède un pont disulfure dans sa structure qui pourrait jouer un rôle important sur son activité biologique (Jiang & Guo 2011; Barakat *et al.* 2019b). Il est suggéré que l'organisme producteur de TDKPs avec pont disulfure pourrait activer des mécanismes de défense qui impliquent l'ouverture du pont disulfure pour éviter sa toxicité comme cela a été observé pour la biosynthèse de la gliotoxine produite par *Aspergillus fumigatus* (Scharf *et al.* 2014), ce qui pourrait expliquer la production à court terme de botryosulfuranol C observée chez *C. mamane*.

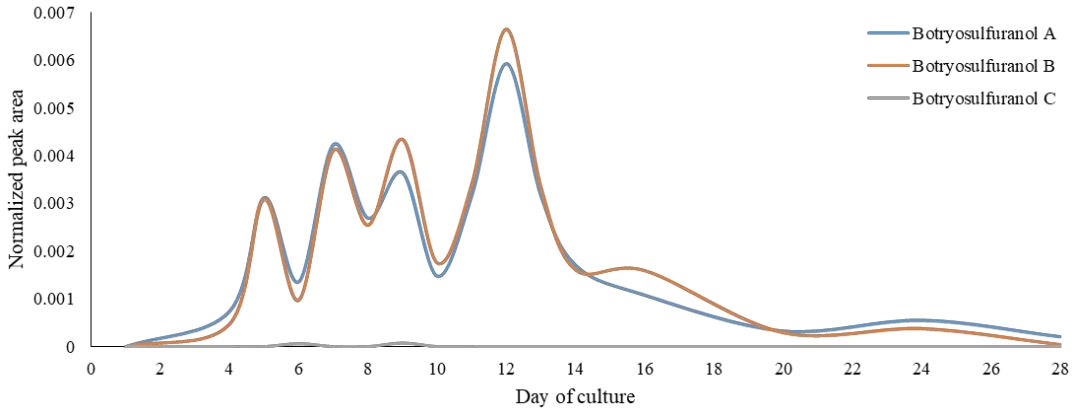

Figure 3. Tendance de production des TDKP en fonction de leur aire de pic normalisée

De plus, la culture de *C. mamane* dans ISP2 pendant 6 jours et dans des conditions d'obscurité a semblé exercer un effet retardateur sur la production de TDKPs pendant l'étude de l'approche OSMAC (**Figure 4**). Il est connu que les gènes codant pour ce type de composés répondent à différents signaux environnementaux, y compris la lumière (Brakhage 2013), tandis qu'une grande partie du génome fongique répond à différentes intensités et longueurs d'onde de la lumière (Yu & Fischer 2019). Ce résultat met en évidence que la lumière peut influencer la production de ces métabolites par *C. mamane* et que c'est un facteur important à prendre en compte lors de la culture dans des conditions de laboratoire et lors de fermentations à grande échelle dans des bioréacteurs au niveau industriel.

D'autres expériences impliquant différentes longueurs d'onde lumineuses lors de la culture de *C. mamane* seront envisagées.

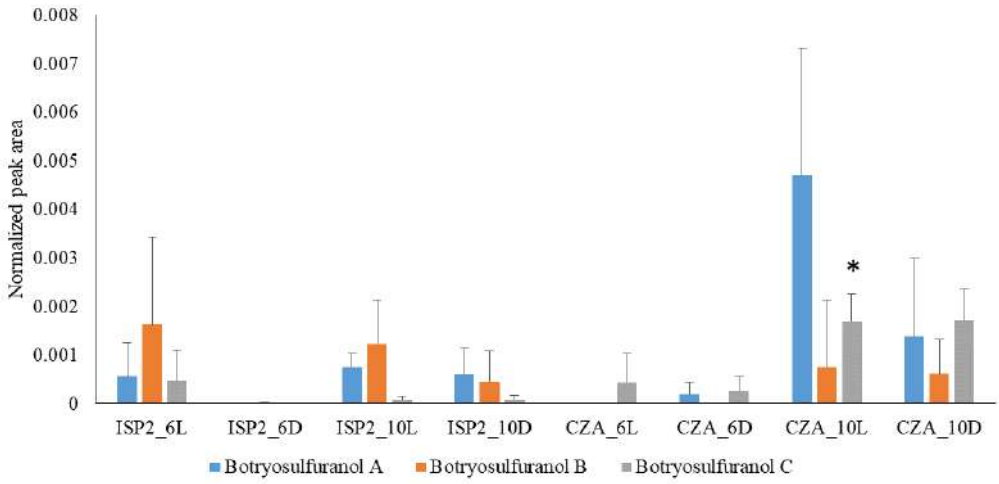

Figure 4. Aires de pic normalisées des TDKP botryosulfuranols A, B et C lors de la culture de *C. mamane* dans les milieux ISP2 et CZA pendant 6 et 10 jours dans des conditions de lumière (L) et d'obscurité (D). Les changements significatifs (test T avec p<0,05) sont indiqués (*).

En ce qui concerne l'ajout de modulateurs chimiques, le DNMTi AZA a régulé négativement la production des botryosulfuranols A, B et C (**Figure 5**), indiquant que l'inhibition de la méthylation de l'ADN a un effet négatif sur leur production, soit directement, soit indirectement sur leur voie de biosynthèse. Cependant, l'ajout de HSL, qui est une molécule de quorum-sensing impliquée dans la communication des bactéries gram-négatives avec d'autres espèces, a induit de manière significative la production de botryosulfuranol C.

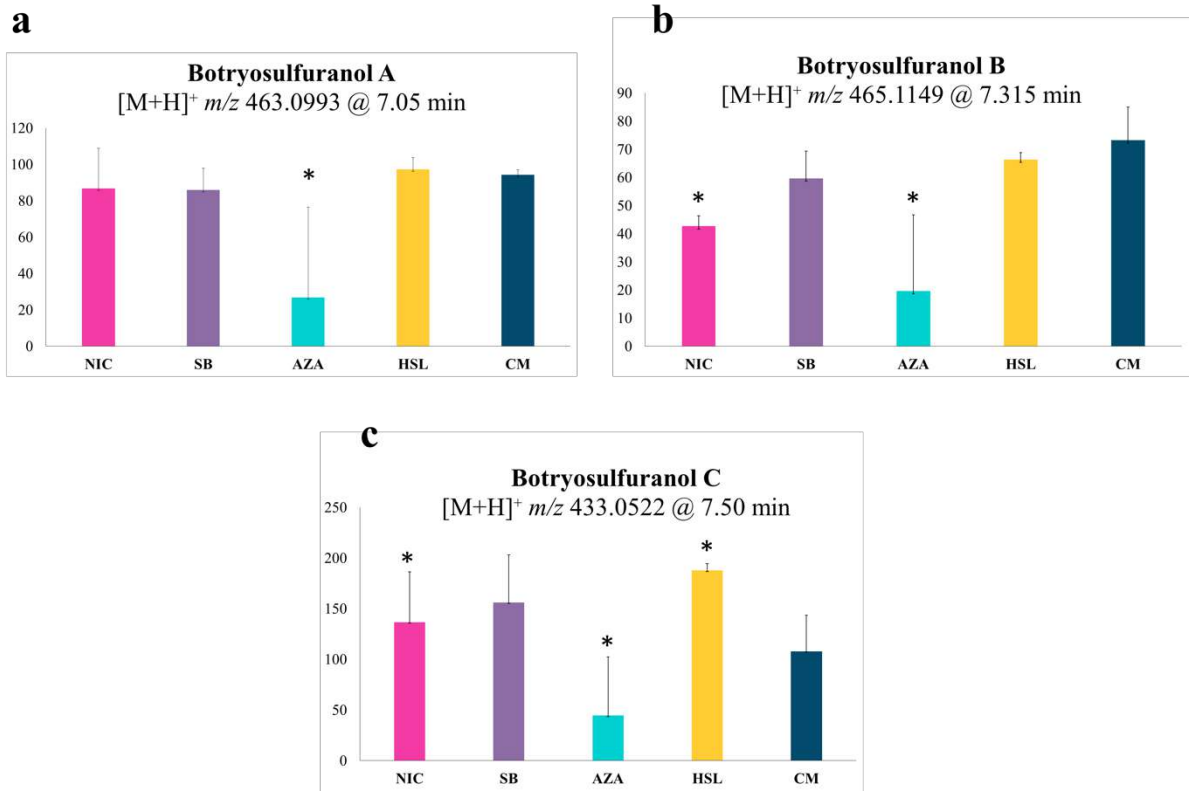

Figure 5. Aire de pic normalisée des TDKP (a) botryosulfuranol A, (b) botryosulfuranol B et (c) botryosulfuranol C détectés sous le traitement avec les modificateurs épigénétiques nicotinamide (NIC), butyrate de sodium (SB), 5-azacytidine (AZA) et homosérine lactone (HSL) en comparaison avec la culture non traitée de *C. mamane* (CM). Les changements significatifs (test T avec $p<0,05$) sont indiqués (*).

Il est important de mentionner que HSL a non seulement induit de manière significative la production de ce TDKP mais également la production d'autres DKPs qui ont pu être annotées, dont la diphénylalazine B et la bisdethiobis(méthylthio)gliotoxine, soulignant que ces types de métabolites pourraient être impliqués dans la communication inter-espèces. Leur rôle en tant que molécules du QS avait été suggéré pour des DKPs produites lors d'interactions bactériennes entre *Cronobacter sakazakii* et *Bacillus cereus* (Bofinger *et al.* 2017) mais aussi pour les DKPs, emestrines A et B, produites par *Aspergillus fumigatus* en présence de HSL et lors de la co-culture avec *Streptomyces bulli* (Rateb *et al.* 2013).

Afin de mieux comprendre le rôle de ces composés dans les interactions entre microorganismes, la souche *C. mamane* E224 a été cultivé en présence de bactéries vivantes, et en présence de parasites inactivés. L'ajout de leishmanies inactivées par la chaleur à la culture de *C. mamane* a considérablement réduit la production de botryosulfuranol C (**Figure 6**), tandis que l'ajout de bactéries vivantes n'a pas affecté de manière significative sa production dans les conditions testées.

Au vu des résultats encourageants obtenus avec l'ajout de la molécule de QS, HSL dans le milieu de culture, des périodes de fermentation plus longues et des co-cultures avec d'autres espèces bactériennes et fongiques seront réalisées afin de vérifier l'influence des microorganismes vivants sur la production de TDKPs, et le rôle potentiel des TDKPs dans la communication microbienne.

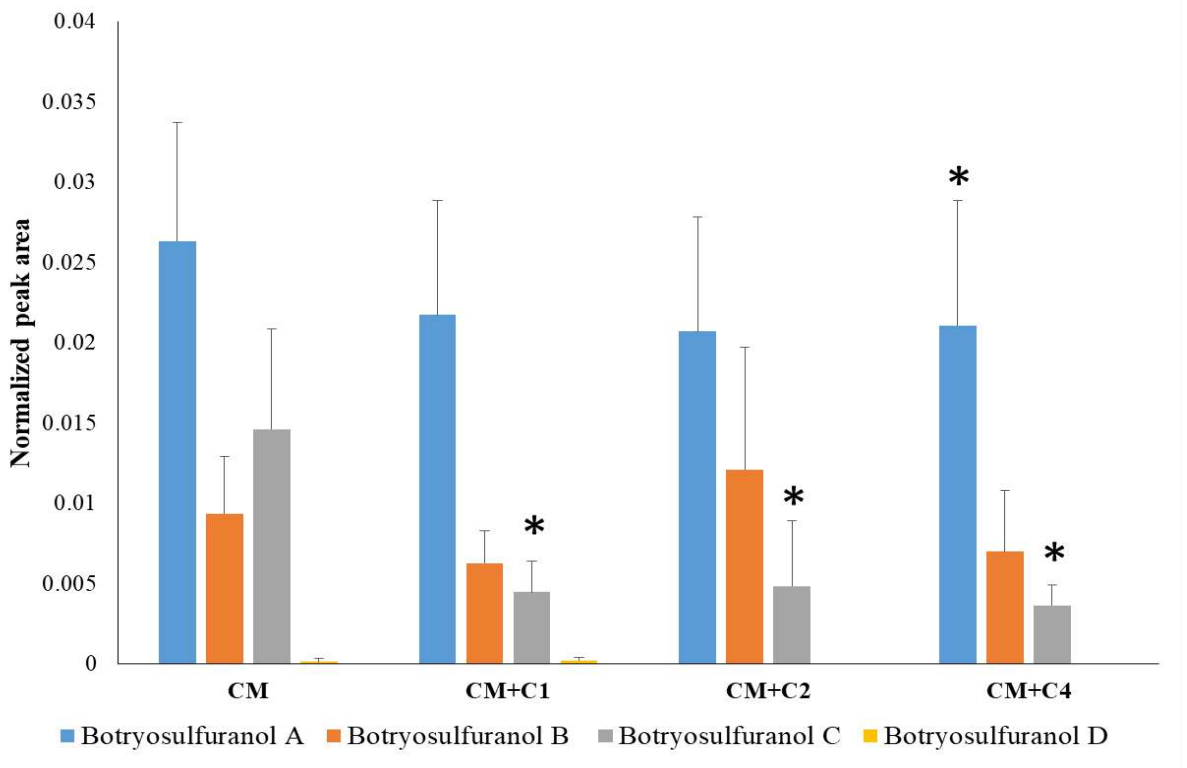

Figure 6. Aire de pic normalisée des TDKP botryosulfuranols A, B, C et D détectée sous l'addition d'amastigotes de Leishmania inactivés par la chaleur à 3 concentrations différentes (C1, C2 et C4) en comparaison avec la culture non traitée de *C. mamane* (CM). Les changements significatifs (test T avec p<0,05) sont indiqués (*).

Par ailleurs, contrairement à ce qui était attendu avec l'ajout de deux bioprécurseurs de DKP, L-phe et L-trp, la production de botryosulfuranols A-D a été régulée négativement par rapport à la culture non traitée (**Figure 7**), alors que ces métabolites sont biogénétiquement dérivés de deux résidus de phénylalanine (Barakat *et al.* 2019b). Plus généralement, l'ajout de ces deux acides aminés n'a pas semblé induire d'autres DKPs dérivées d'au moins une phénylalanine, tyrosine ou tryptophane (Welch & Williams 2014).

Des investigations supplémentaires sont nécessaires afin de comprendre les effets négatifs que ces acides aminés exercent sur la production de TDKP tandis que l'ajout de différents acides aminés à différentes concentrations sera également testé.

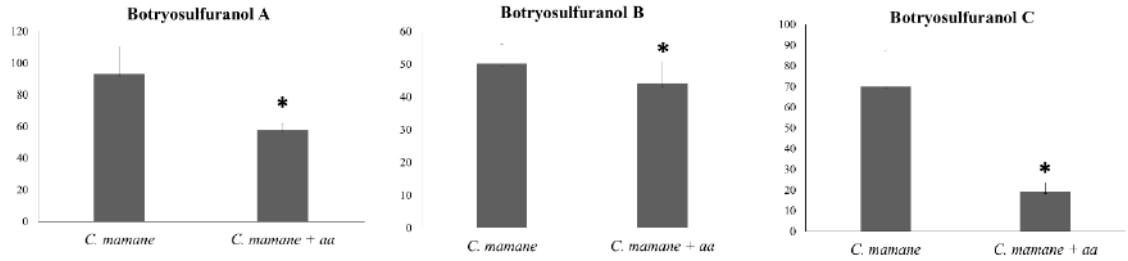

Figure 7. Aire de pic normalisée des botryosulfuranols A, B et C détectés sous l'addition d'acides aminés (*C.mamane* + aa) en comparaison avec la culture non traitée de *C. mamane*. Les changements significatifs (test T avec $p<0,05$) sont indiqués (*).

En ce qui concerne le botryosulfuranol D, qui est l'un des TDKP les plus actifs contre *Leishmania infantum* par rapport aux botryosulfuranols A-C (données non publiées), il a présenté une faible production dans les différentes cultures réalisées au cours de ce travail et n'a pas été détecté dans la majorité des cas. Sa production semble donc suivre un modèle différent avec une étape cruciale sur sa voie de biosynthèse influencée par les conditions de culture et autres facteurs. Sa très faible détection n'a pas permis de l'inclure dans les analyses par réseau moléculaire (absence de données de fragmentation).

c) Induction de la production de métabolites anti-infectieux

L'ajout de parasites inactivés dans le milieu de culture ainsi que la co-culture avec des bactéries pathogènes ont modifié le métabolome global de *C. mamane* en régulant significativement un certain nombre de métabolites. Néanmoins, aucune famille chimique de métabolites n'a pu être identifiée comme étant spécifiquement influencée par chacune des conditions. Cette modification du métabolome lors de co-cultures a déjà été démontré que ce soit dans le cadre de co-culture champignon-champignon ou de co-cultures champignon-bactérie où des métabolites non produits dans des conditions axéniques ou faiblement détectés, ont été induits (Kamdem *et al.* 2018). Ceci peut s'expliquer par diverses interactions complexes concernant la compétition pour les nutriments ou les interactions antagonistes dans des environnements partagés (Deshmukh *et al.* 2018).

Différentes souches bactériennes pathogènes avec différents profils de résistance ainsi que la co-culture avec des endophytes précédemment isolés de *Bixa orellana*, conservés dans la mycothèque de l'UMR 152, seront considérées pour de futures expériences de co-culture.

De plus, toujours dans cette optique de recherche de nouveaux antiinfectieux, nous envisageons l'ajout de leishmanies vivantes dans la culture de *C. mamane* afin d'évaluer la différence avec les parasites tués par la chaleur. Les principales limites de cette méthodologie sont le pH et les nutriments du milieu de culture, ainsi que la température et le temps d'incubation, ce qui pourrait nécessiter une chambre de culture plus appropriée ou un dispositif différent pour la réaliser.

La métabolomique, utilisée tout au long de ce travail, représente une stratégie qui facilite et accélère les processus laborieux d'isolement des produits naturels et permet d'éviter la ré-isolement de composés connus en fournissant des informations MS/MS utiles pour l'élucidation structurale et la comparaison avec les bases de données disponibles (Demarque *et al.* 2020). Cependant, elle présente certaines limites et défis en raison de sa complexité inhérente, de la préparation des échantillons et de l'acquisition des données aux problèmes de reproductibilité et d'interprétation (Marshall & Powers 2017). En outre, l'absence de consensus dans les données structurales provenant de différentes plateformes et la faible disponibilité des bases de données gratuites peuvent générer de faibles taux d'annotation putative (Van Santen *et al.* 2019). Par conséquent, les études de déréplication manuelle continuent d'être une partie très importante pour compléter ce type de travail. En dépit de ses limites, la métabolomique nous a permis d'accéder à des informations qui n'auraient pu être dévoilées, notamment concernant les métabolites minoritaires. Cette approche relativement nouvelle utilisée dans la découverte de produits naturels s'est ainsi souvent avérée efficace pour réduire de grands ensembles de données en des ensembles beaucoup plus petits qui contiennent potentiellement des métabolites nouveaux ou actifs (Caesar *et al.* 2019). Une optimisation de cet outil, un focus sur certains métabolites spécifiques, ainsi qu'une augmentation du nombre de réplicats seront envisagées pour les futures expériences avec *C. mamane* et les métabolites produits par cette souche endophyte.

IV. Conclusions et perspectives

Les résultats obtenus dans le cadre d'une analyse métabolomique non ciblée nous fournissent des informations directes et utiles sur ce qui est produit par les cellules au cours de leur métabolisme, dans ce cas, ce que la souche endophyte *C. mamane* E224 produit à un moment précis dans des conditions de culture spécifiques, ce qui nous donne un aperçu de son état physiologique et de son activité cellulaire.

L'intégration de ces informations avec d'autres techniques -omiques telles que la génomique, la protéomique et la transcriptomique, qui relèvent du domaine de recherche de la biologie des systèmes, permettra d'obtenir une compréhension plus holistique des micro-organismes et même des communautés, en particulier pour les micro-organismes endophytes, ce qui représente en même temps un défi permanent (Pinu *et al.* 2019). En ce sens, la compréhension des réponses physiologiques de *C. mamane* aux changements environnementaux et aux différentes conditions de culture peut conduire à l'activation ou à la manipulation de voies spécifiques. Ceci est utile pour la recherche de métabolites

spécifiques, principalement pour déterminer les conditions optimales de cultures, y compris le temps d'incubation optimal pour leur production et leur extraction, comme c'est le cas dans ce travail avec les TDKP.

En plus de cela et des expériences supplémentaires nécessaires citées précédemment, l'isolement des métabolites induits les plus significatifs ainsi que des métabolites chimiquement liés aux TDKPs annotés et révélés par les réseaux moléculaires réalisés, sera également au centre des travaux futurs. La compréhension de leurs mécanismes biologiques et de leurs rôles écologiques potentiels dans la nature fera également l'objet de notre attention.

Par ailleurs, il est important de noter que grâce au projet de pré-maturation soutenu financièrement par la région Occitanie, et à la collaboration avec le Critt Bioindustries, une fraction enrichie en TDKPs a été obtenue à partir d'extraits de cultures de *C. mamane* en fermenteurs à l'échelle semie-industrielle. Ceci a permis de commencer les tests *in vivo* sur souris et permettra d'approfondir l'étude de l'activité biologique *in vivo* des botryosulfuranols A-D.

Références

Adeleke B, Babalola O, 2021. Pharmacological Potential of Fungal Endophytes Associated with Medicinal Plants: A Review. *Journal of Fungi* **7**: 147. https://doi.org/10.3390/jof7020147

Arnold AE, 2007. Understanding the diversity of foliar endophytic fungi: progress, challenges, and frontiers. *Fungal Biology Reviews* **21**: 51–66. https://doi.org/10.1016/j.fbr.2007.05.003

Barakat F, 2018. Etude mycochimique et activités leishmanicides de composés issus de Botryosphaeria mamane, un champignon endophyte isolé de Bixa orellana L. Université Paul Sabatier Toulouse III.

Barakat F, Vansteelandt M, Triastuti A, Jargeat P, Jacquemin D, Graton J, Mejia K, Cabanillas B, Vendier L, Stigliani J-L, Haddad M, Fabre N, 2019a. Thiodiketopiperazines with two spirocyclic centers extracted from Botryosphaeria mamane, an endophytic fungus isolated from Bixa orellana L. *Phytochemistry* **158**: 142–148. https://doi.org/10.1016/j.phytochem.2018.11.007

Bérdy J, 2012. Thoughts and facts about antibiotics: Where we are now and where we are heading. *Journal of Antibiotics* **65**: 385–395. https://doi.org/10.1038/ja.2012.27

Bertrand S, Azzollini A, Schumpp O, Bohni N, Schrenzel J, Monod M, Gindro K, Wolfender JL, 2014. Multi-well fungal co-culture for de novo metabolite-induction in time-series studies based on untargeted metabolomics. *Molecular BioSystems* **10**: 2289–2298. https://doi.org/10.1039/c4mb00223g

Bofinger MR, de Sousa LS, Fontes JEN, Marsaioli AJ, 2017. Diketopiperazines as Cross-Communication Quorum - Sensing Signals between Cronobacter sakazakii and Bacillus cereus. *ACS Omega* **2**: 1003–1008. https://doi.org/10.1021/acsomega.6b00513

Brakhage AA, 2013. Regulation of fungal secondary metabolism. *Nature Reviews Microbiology* **11**: 21–32. https://doi.org/10.1038/nrmicro2916

Brakhage AA, Schroeckh V, 2011. Fungal secondary metabolites – Strategies to activate silent gene

clusters. *Fungal Genetics and Biology* **48**: 15–22. https://doi.org/10.1016/j.fgb.2010.04.004

Browne K, Chakraborty S, Chen R, Willcox MDP, Black DS, Walsh WR, Kumar N, 2020. A new era of antibiotics: The clinical potential of antimicrobial peptides. *International Journal of Molecular Sciences* **21**: 1–23. https://doi.org/10.3390/ijms21197047

Caesar LK, Kellogg JJ, Kvalheim OM, Cech NB, 2019. Opportunities and Limitations for Untargeted Mass Spectrometry Metabolomics to Identify Biologically Active Constituents in Complex Natural Product Mixtures. *Journal of Natural Products* **82**: 469–484. https://doi.org/10.1021/acs.jnatprod.9b00176

Challinor VL, Bode HB, 2015. Bioactive natural products from novel microbial sources. *Annals of the New York Academy of Sciences* **1354**: 82–97. https://doi.org/10.1111/nyas.12954

Chong J, Wishart DS, Xia J, 2019. Using MetaboAnalyst 4.0 for Comprehensive and Integrative Metabolomics Data Analysis. *Current Protocols in Bioinformatics* **68**. https://doi.org/10.1002/cpbi.86

Demarque DP, Dusi RG, de Sousa FDM, Grossi SM, Silvério MRS, Lopes NP, Espindola LS, 2020. Mass spectrometry-based metabolomics approach in the isolation of bioactive natural products. *Scientific Reports* **10**: 1–9. https://doi.org/10.1038/s41598-020-58046-y

Deshmukh S, Gupta M, Prakash V, Saxena S, 2018. Endophytic Fungi: A Source of Potential Antifungal Compounds. *Journal of Fungi* **4**: 77. https://doi.org/10.3390/jof4030077

Fraisier-Vannier O, Chervin J, Cabanac G, Puech V, Fournier S, Durand V, Amiel A, André O, Benamar OA, Dumas B, Tsugawa H, Marti G, 2020. MS-CleanR: A Feature-Filtering Workflow for Untargeted LC–MS Based Metabolomics. *Analytical Chemistry* **92**: 9971–9981. https://doi.org/10.1021/acs.analchem.0c01594

Gao H, Li G, Lou H-X, 2018. Structural Diversity and Biological Activities of Novel Secondary Metabolites from Endophytes. *Molecules* **23**: 646. https://doi.org/10.3390/molecules23030646

Gupta S, Chaturvedi P, Kulkarni MG, Van Staden J, 2020. A critical review on exploiting the pharmaceutical potential of plant endophytic fungi. *Biotechnology Advances* **39**: 107462. https://doi.org/10.1016/j.biotechadv.2019.107462

Hutchings MI, Truman AW, Wilkinson B, 2019. Antibiotics: past, present and future. *Current Opinion in Microbiology* **51**: 72–80. https://doi.org/10.1016/j.mib.2019.10.008

Jiang C-S, Guo Y-W, 2011. Epipolythiodioxopiperazines from Fungi: Chemistry and Bioactivities. *Mini-Reviews in Medicinal Chemistry* **11**: 728–745. https://doi.org/10.2174/138955711796355276

Kamdem RST, Wang H, Wafo P, Ebrahim W, Özkaya FC, Makhloufi G, Janiak C, Sureechatchaiyan P, Kassack MU, Lin W, Liu Z, Proksch P, 2018. Induction of new metabolites from the endophytic fungus Bionectria sp. through bacterial co-culture. *Fitoterapia* **124**: 132–136. https://doi.org/10.1016/j.fitote.2017.10.021

Khare E, Mishra J, Arora NK, 2018. Multifaceted Interactions Between Endophytes and Plant: Developments and Prospects. *Frontiers in Microbiology* **9**. https://doi.org/10.3389/fmicb.2018.02732

Li G, Kusari S, Golz C, Strohmann C, Spiteller M, 2016. Three cyclic pentapeptides and a cyclic lipopeptide produced by endophytic Fusarium decemcellulare LG53. *RSC Advances* **6**: 54092–54098. https://doi.org/10.1039/C6RA10905E

Manganyi MC, Ateba CN, 2020. Untapped potentials of endophytic fungi: A review of novel bioactive compounds with biological applications. *Microorganisms* **8**: 1–25. https://doi.org/10.3390/microorganisms8121934

Marshall DD, Powers R, 2017. Beyond the paradigm: Combining mass spectrometry and nuclear magnetic resonance for metabolomics. *Progress in Nuclear Magnetic Resonance Spectroscopy* **100**: 1–16. https://doi.org/10.1016/j.pnmrs.2017.01.001

Newman DJ, Cragg GM, 2020. Natural Products as Sources of New Drugs over the Nearly Four Decades from 01/1981 to 09/2019. *Journal of Natural Products* **83**: 770–803. https://doi.org/10.1021/acs.jnatprod.9b01285

Olivon F, Elie N, Grelier G, Roussi F, Litaudon M, Touboul D, 2018. MetGem Software for the Generation of Molecular Networks Based on the t-SNE Algorithm. *Analytical Chemistry* **90**: 13900–13908. https://doi.org/10.1021/acs.analchem.8b03099

Pettit RK, 2011. Small-molecule elicitation of microbial secondary metabolites. *Microbial Biotechnology* **4**: 471–478. https://doi.org/10.1111/j.1751-7915.2010.00196.x

Pinu FR, Beale DJ, Paten AM, Kouremenos K, Swarup S, Schirra HJ, Wishart D, 2019. Systems Biology and Multi-Omics Integration: Viewpoints from the Metabolomics Research Community. *Metabolites* **9**: 76. https://doi.org/10.3390/metabo9040076

Rateb ME, Hallyburton I, Houssen WE, Bull AT, Goodfellow M, Santhanam R, Jaspars M, Ebel R, 2013. Induction of diverse secondary metabolites in Aspergillus fumigatus by microbial co-culture. *RSC Advances* **3**: 14444. https://doi.org/10.1039/c3ra42378f

Van Santen JA, Jacob G, Singh AL, Aniebok V, Balunas MJ, Bunsko D, Neto FC, Castaño-Espriu L, Chang C, Clark TN, Cleary Little JL, Delgadillo DA, Dorrestein PC, Duncan KR, Egan JM, Galey MM, Haeckl FPJ, Hua A, Hughes AH, Iskakova D, Khadilkar A, Lee JH, Lee S, Legrow N, Liu DY, Macho JM, McCaughey CS, Medema MH, Neupane RP, O'Donnell TJ, Paula JS, Sanchez LM, Shaikh AF, Soldatou S, Terlouw BR, Tran TA, Valentine M, Van Der Hooft JJJ, Vo DA, Wang M, Wilson D, Zink KE, Linington RG, 2019. The Natural Products Atlas: An Open Access Knowledge Base for Microbial Natural Products Discovery. *ACS Central Science* **5**: 1824–1833. https://doi.org/10.1021/acscentsci.9b00806

Scharf DH, Habel A, Heinekamp T, Brakhage AA, Hertweck C, 2014. Opposed effects of enzymatic gliotoxin N - And S -methylations. *Journal of the American Chemical Society* **136**: 11674–11679. https://doi.org/10.1021/ja5033106

Sereno D, Lemesre JL, 1997. Axenically cultured amastigote forms as an in vitro model for investigation of antileishmanial agents. *Antimicrobial Agents and Chemotherapy* **41**: 972–976. https://doi.org/10.1128/AAC.41.5.972

Shannon P, 2003. Cytoscape: A Software Environment for Integrated Models of Biomolecular Interaction Networks. *Genome Research* **13**: 2498–2504. https://doi.org/10.1101/gr.1239303

Strobel G, 2018. The emergence of endophytic microbes and their biological promise. *Journal of Fungi* **4**. https://doi.org/10.3390/jof4020057

Torres-Mendoza D, Ortega HE, Cubilla-Rios L, 2020. Patents on endophytic fungi related to secondary metabolites and biotransformation applications. *Journal of Fungi* **6**. https://doi.org/10.3390/jof6020058

Triastuti A, Haddad M, Barakat F, Mejia K, Rabouille G, Fabre N, Amasifuen C, Jargeat P, Vansteelandt M, 2021. Dynamics of Chemical Diversity during Co-Cultures: An Integrative Time-Scale Metabolomics Study of Fungal Endophytes Cophinforma mamane and Fusarium solani. *Chemistry & Biodiversity* **18**. https://doi.org/10.1002/cbdv.202000672

Triastuti A, Vansteelandt M, Barakat F, Trinel M, Jargeat P, Fabre N, Amasifuen Guerra CA, Mejia K, Valentin A, Haddad M, 2019. How Histone Deacetylase Inhibitors Alter the Secondary Metabolites of Botryosphaeria mamane, an Endophytic Fungus Isolated from Bixa orellana. *Chemistry and Biodiversity* **16**. https://doi.org/10.1002/cbdv.201800485

Tsugawa H, Cajka T, Kind T, Ma Y, Higgins B, Ikeda K, Kanazawa M, VanderGheynst J, Fiehn O, Arita M, 2015. MS-DIAL: data-independent MS/MS deconvolution for comprehensive metabolome analysis. *Nature Methods* **12**: 523–526. https://doi.org/10.1038/nmeth.3393

Tsugawa H, Kind T, Nakabayashi R, Yukihira D, Tanaka W, Cajka T, Saito K, Fiehn O, Arita M, 2016. Hydrogen Rearrangement Rules: Computational MS/MS Fragmentation and Structure Elucidation Using MS-FINDER Software. *Analytical Chemistry* **88**: 7946–7958. https://doi.org/10.1021/acs.analchem.6b00770

Wang W-X, Kusari S, Sezgin S, Lamshöft M, Kusari P, Kayser O, Spiteller M, 2015. Hexacyclopeptides secreted by an endophytic fungus Fusarium solani N06 act as crosstalk molecules in Narcissus tazetta. *Applied Microbiology and Biotechnology* **99**: 7651–7662. https://doi.org/10.1007/s00253-015-6653-7

Wang X, Lin M, Xu D, Lai D, Zhou L, 2017. Structural Diversity and Biological Activities of Fungal Cyclic Peptides, Excluding Cyclodipeptides. *Molecules* **22**: 2069. https://doi.org/10.3390/molecules22122069

Welch TR, Williams RM, 2014. Epidithiodioxopiperazines. occurrence, synthesis and biogenesis. *Natural Product Reports* **31**: 1376–1404. https://doi.org/10.1039/c3np70097f

Yu Z, Fischer R, 2019. Light sensing and responses in fungi. *Nature Reviews Microbiology* **17**: 25–36. https://doi.org/10.1038/s41579-018-0109-x

Zhao Q, Zhang J Le, Li F, 2018. Application of Metabolomics in the Study of Natural Products. *Natural Products and Bioprospecting* **8**: 321–334. https://doi.org/10.1007/s13659-018-0175-9

Zheng R, Li S, Zhang X, Zhao C, 2021. Biological activities of some new secondary metabolites isolated from endophytic fungi: A review study. *International Journal of Molecular Sciences* **22**: 1–75. https://doi.org/10.3390/ijms22020959

INTRODUCTION

Natural products have been historically used for the development of drugs and drug leads. Currently, nearly 50% of the total small molecules approved as drugs, between 1981 and 2019, are derived from natural products or from their synthetic variations (Newman & Cragg 2020). Most of the clinically relevant drugs are derived from microorganisms, including bacteria, actinomycetes and fungi (Hutchings *et al.* 2019) with fungal species accounting for 45% of the microbial metabolite production (Bérdy 2012). This highlights the importance of microbial natural products even nowadays in 2021.

However, the arsenal of drugs with antimicrobial activity are becoming very limited while the increasing emergence of microbial resistant strains lead us to alarming predictions of 10 million of deaths by 2050 along with an enormous economic burden for the health care systems around the world (Browne *et al.* 2020). In addition to this, the World Health Organization (WHO), reported only 6 drugs in clinical development, addressed to the list of priority pathogens that were considered innovative. In order to face this problematic, new drugs with novel structural scaffolds and/or new mechanisms of action are needed, and they can potentially be found in unusual sources as in little explored or unexplored environments such as endophytes (Challinor & Bode 2015).

Endophytes are a group of microorganisms that successfully colonize internal plant tissues without generating visible harmful effects. This occurs as a result of multiple compatible interactions before, during and after invasion of the host plant, involving cross-talk signal molecules with the plant itself and its microbiome (Khare *et al.* 2018). It is considered that almost all plants on Earth are in constant and close interaction with endophytes (Arnold 2007). Despite of this, only 1-2% of all the known plants have been studied for their endophyte composition (Strobel 2018).

Most of the isolated and studied endophytes correspond to endophytic fungi which are capable of producing chemically diverse compounds (Gao *et al.* 2018; Zheng *et al.* 2021) with antibacterial, antifungal, anti-parasitic, antiviral, anticancer, antioxidant, immunosuppressive and antidiabetic properties (Manganyi & Ateba 2020; Adeleke & Babalola 2021). Many of these compounds represent potential applications in various areas such as public health, agriculture and pharmaceutical industries (Gupta *et al.* 2020a) with a total of 245 patent applications reported, between 2001 and 2019, involving secondary metabolites production and biotransformation processes (Torres-Mendoza *et al.* 2020). In this regard, endophytic fungi represent a renewable and effective source of natural products.

In this study, we focused on an endophytic fungal strain of *Cophinforma mamane* (D.E. Gardner) A. J. L. Phillips & A. Alves (Botryosphaeriaceae) isolated from the leaves of the medicinal plant *Bixa orellana* (Bixaceae). The collection of the leaves samples was carried out in the Amazonian forest of Peru allowing the isolation of 17 endophytic fungal strains belonging to the following genera: *Diaporthe*, *Nigrospora*, *Phyllosticta*, *Endomelanconiopsis*, *Sporothrix*, *Xylaria*, and *Cophinforma*

(unpublished data). A crude extract of the strain E224 (*Cophinforma mamane*) showed *in vitro* antileishmanial activity against *Leishmania infantum* (IC_{50} value of 1.96 µg/mL) and led to the isolation of four novel thiodiketopiperazines (TDKPs) alkaloids, botryosulfuranols A, B, C and D (Barakat 2018). These compounds present sulfur atoms on α- and β-positions of the phenylalanine residues and two unprecedented spirocyclic centers at C-4 and C-2 (**Figure 1**). Antileishmanial activity of all the TDKPs were evaluated *in vitro* against the axenic amastigotes of *Leishmania infantum*. Botryosulfuranol D exhibited the strongest antileishmanial activity with an IC_{50} value of 0.03 µM and a selective index (SI) of 190 followed by botryosulfuranol C (IC_{50} = 0.44 µM); botryosulfuranol A (IC_{50} = 0.69 µM) and botryosulfuranol B (IC_{50} = 3.87 µM) (unpublished data). Botryosulfuranol A, B and C exhibited weak to moderate cytotoxic activity (GI_{50} = 8.0 – 115.7 µM) against 4 cancer lines (Barakat *et al.* 2019). Although these new compounds presented interesting antileishmanial activity, the small isolated quantities did not allow a deeper investigation of their biological activity.

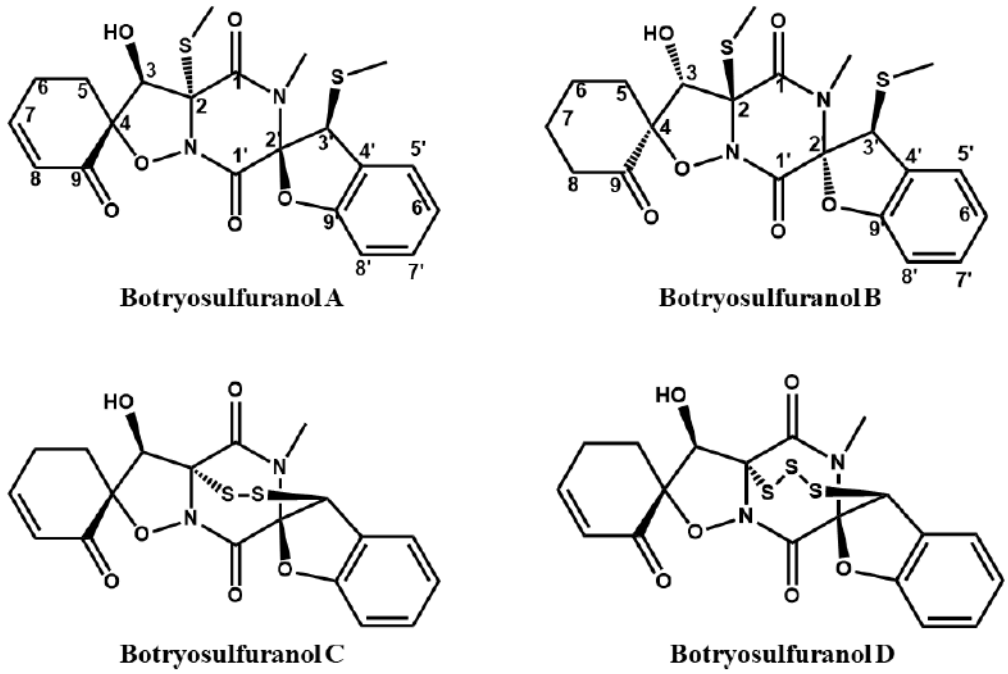

Figure 1. Chemical structure of thiodiketopiperazines, botryosulfuranols A - D

A pre-maturation project, financially supported by the Occitanie region, has been launched with the objective to continue on further research on biological activity through *in vivo* assays. This is performed through a collaboration with Critt Bioindustries who will take over the fermentation of the fungus on a large scale. In parallel to this project in which I took part, especially for the extraction and isolation of

the botryosulfuranols, a study on the metabolism changes under different culture conditions of this fungal endophyte has been performed as my doctoral research work.

Although the isolated compounds mentioned above have been obtained by cultivating the E224 strain of *C. mamane* under standard culture conditions, it is known that in fungi, the number of gene clusters is greatly superior to the number of gene clusters known from the isolated secondary metabolites (Pettit 2011) due to the presence of silent or lowly-expressed genes (Brakhage & Schroeckh 2011). Considering this, different approaches have been applied for the induction of the secondary metabolite in fungi, such as cultivation-based methodologies including OSMAC approach, co-culture with other microorganisms and the addition of chemical elicitors to the culture media, including epigenetic modifiers. In this regard, the metabolism of *C. mamane* E224 has been previously studied under the influence of two epigenetic modifiers (suberoylanilide hydroxamic acid and sodium valproate) (Triastuti *et al*. 2019) and in co-culture with *Fusarium solani* (Triastuti, 2021), identifying in both cases metabolites induced *de novo*.

In order to avoid the bottleneck of re-isolation of known compounds, metabolomics is a powerful tool for the analysis, identification and quantification of small metabolites (Zhao *et al.* 2018). Mass Spectrometry (MS) is the most widely used technique due to its high sensibility, small samples volume, the possibility of coupling with chromatographic techniques, acquisition of MS/MS fragmentation data for structural elucidation followed by a comparison with specific databases. Additionally, the association with computational and statistical tools can offer a better view that simplifies the vast data analyses (Demarque *et al.* 2020). Specifically, Untargeted Metabolomics, focuses on the detection of as many metabolites as possible to elaborate a comprehensive data set in order to better understand the metabolome of the object under study.

After a literature review prepared for the present doctoral thesis in **Chapter 1**, we applied different culture-based and epigenetic approaches (detailed in **Chapter 2**) to alter the secondary metabolism of an endophytic fungal strain of *Cophinforma mamane* (Botryosphaeriaceae) isolated from the medicinal plan *Bixa orellana* (Bixaceae). Special importance has been given to the 4 bioactive thiodiketopiperazines previously isolated in our team by F. Barakat (Barakat *et al.* 2019). The two main goals of this study are:

1. A better understanding of the production of the botryosulfuranols previously isolated and more generally, the induction of diketopiperazines and other alkaloids through kinetic and OSMAC approach including the use of epigenetic modifiers and biosynthetic precursors (**Chapter 3** and **Chapter 4**).
2. The production of new compounds, especially anti-infective metabolites through the co-culture of *C. mamane* with pathogenic bacterial strains, and the culture with inactivated parasites (**Chapter 5**).

UHPLC – Mass Spectrometry analysis and untargeted metabolomics tools have been used in order to reach our goals and they will be detailed and explained in **Chapter 2**, corresponding to materials and methods.

In order to respond to our first objective, a time-variations study of secondary metabolite production was carried out. This analysis was followed by the application of the OSMAC approach consisting in using different culture media and different light conditions as factors that may induce the secondary metabolism of this endophytic fungus. These results will be detailed and discussed in **Chapter 3**. Moreover, the induction of secondary metabolism under the treatment with chemical elicitors such as epigenetic modifiers to stimulate the transcription of lowly-expressed or silenced genes has been performed, as well as the addition of amino acids in the culture to stimulate specific biosynthetic pathways that utilize these building blocks for the production of secondary metabolites. These results will be detailed and discussed in **Chapter 4**.

Finally, to respond our second objective, heat-killed leishmanial parasites were added to the culture of the endophytic fungus in an attempt to simulate the presence of other microorganism that might induce the production of antiparasitic secondary metabolites. Co-cultures of *C. mamane* with living pathogenic bacterial strains have also been performed in order to induce the production of antibacterial metabolites. These results will be detailed and discussed in **Chapter 5**.

CHAPTER 1 LITERATURE REVIEW

1.1 Natural product research

1.1.1 Implications of antibiotic resistance in natural product research

The use of natural products as medicinal agents can be traced back to the records found in Mesopotamia (2600 BCE) where several substances derived from plants, used even today for many ailments, were described. The best known Egyptian record, the Ebers papyrus (1500 BCE), describes also several natural drugs and their usage (Newman *et al.* 2000) while traditional medicine from China (1100 BCE) (Petrovska 2012) and India (1000 BCE) (Dev 1999) are the best documented records, mentioning also hundreds of herbal drugs and prescriptions. Anthropological studies have proven that antibiotic exposure started before the antibiotic era due to the findings of tetracycline traces in human skeletal remains of ancient populations from Sudanese Nubia (350 – 550 CE) (Nelson *et al.* 2010). This was possible because tetracyclines, naturally produced by *Streptomyces* spp. (Actinomycetes), are potent chelators. Therefore they can bind to the bones and teeth and act as permanent markers, unlike other antibiotics that are difficult to trace (Aminov 2010).

Another known event is the first hospital use of a drug called Pyocyanase, prepared as an extract of *Pseudomonas aeruginosa*, active against different pathogenic bacteria but with inconsistent results and toxic effects (Emmerich & Löw 1899). In the early 1900s, Paul Ehrlich began to screen systematically a treatment for syphilis and several years later, a drug sold under the name of Salvarsan (later Neosalvarsan) showed great success treating this disease and it became frequently prescribed (Ehrlich & Hata 1910). Close to this date and thanks to the systematic approach introduced by Ehrlich, a new drug called Prontosil (sulfa drug) possessing a sulfanilamide active moiety, already used in the dye industry, was synthesized by Bayer chemists. The massive production of sulfonamide derivatives made these drugs the oldest antibiotics on the market (Domagk 1935). In 1928, the discovery of penicillin took place, considering that the antimicrobial activity of the mold was previously observed (Fleming 1929). Despite the difficulties that Alexander Flemming found in the purification and stability of the active substance, its production and distribution was finally achieved in 1945. Thanks to the sufficient quantities of penicillin obtained by Howard Florey and Ernest Chain and to the screening method using inhibition zones applied by Flemming, this antibiotic became widely used in academia and industry (Chain *et al.* 2005).

Between the early 1930s and late 1960s, most of the new classes of drugs were discovered, corresponding to the golden era of antibiotics (**Figure 1.1**). This period was followed by an important decline in drug discovery rate along with the increase and emergence of resistant pathogens (Aminov 2009). Four years before the introduction of penicillin as a therapeutic agent, a bacterial enzyme called

penicillinase (β-lactamases) was identified (Abraham & Chain 1988), an event that led the resistant strains to become prevalent by the time. In 1960, this situation became a pandemic problem and despite the introduction of new drugs, new resistant strains continued to appear, in addition to the first reported cases of methicillin-resistant *Staphylococcus aureus* (MRSA) in 1961 in UK and in 1968 in US (Johnson 2011). The antibiotic vancomycin was introduced in 1958 but the first cases of resistance to this antibiotic were reported for the first time in 1979 and in 1983 (Srinivasan *et al.* 2002). Similarly, antibiotic resistance to other antimicrobials was detected for the first time for enteric bacteria such as *Salmonella*, *Shigella* and *Escherichia coli*, as well as for the strains of *Mycobacterium tuberculosis* resistant to streptomycin, strains of *Neisseria gonorrhoeae* and *Haemophilus influenzae* resistant to ampicillin, tetracycline and chloramphenicol, among many other cases (Aslam *et al.* 2018).

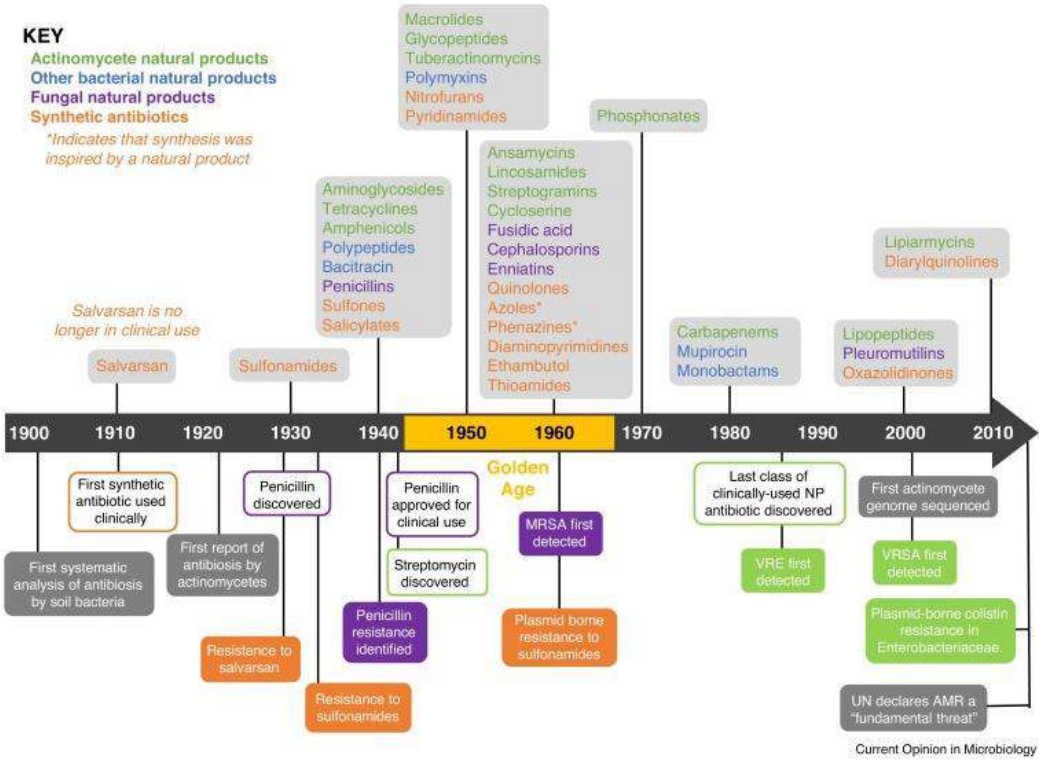

Figure 1.1 Timeline of antibiotics discovery and antimicrobial resistance reports, classified by their source in colors: bacterial, fungi and synthetic (Hutchings et al., 2019)

Resistant phenotypes existed before the introduction of antibiotics in clinical treatments due to the finding that most of the antibiotic-producing strains carry the genes encoding resistance to the antibiotic produced (Hopwood 2007). This means that most of the microbial strains able to produce antibiotics, possess genes that confers them the resistance to the produced antibiotic. However, anthropogenic activity, such as agriculture and industry, caused the massive use of lethal concentrations of antibiotics and contributed to the rapid dissemination of resistant pathogens in a shorter period of time (**Figure 1.2**)

(Davies & Davies 2010). It is important to mention that antibiotic resistance occurring in nature and that one inflicted by human activity possess different dynamics due to the multiple microbial interactions occurring in natural microenvironments (Chait *et al.* 2012). On the other hand, pathogens are also exposed to sub lethal concentrations of antibiotics in clinical situations when the treatment has not been completed or due to low drug availability in tissues while during human activity, the use of animal manure containing sub lethal concentrations of antibiotics are released to the soil and water. Low levels of antibiotics also contribute to the dissemination of resistance, demonstrated by different studies carried out in bacteria (Sengupta *et al.* 2013).

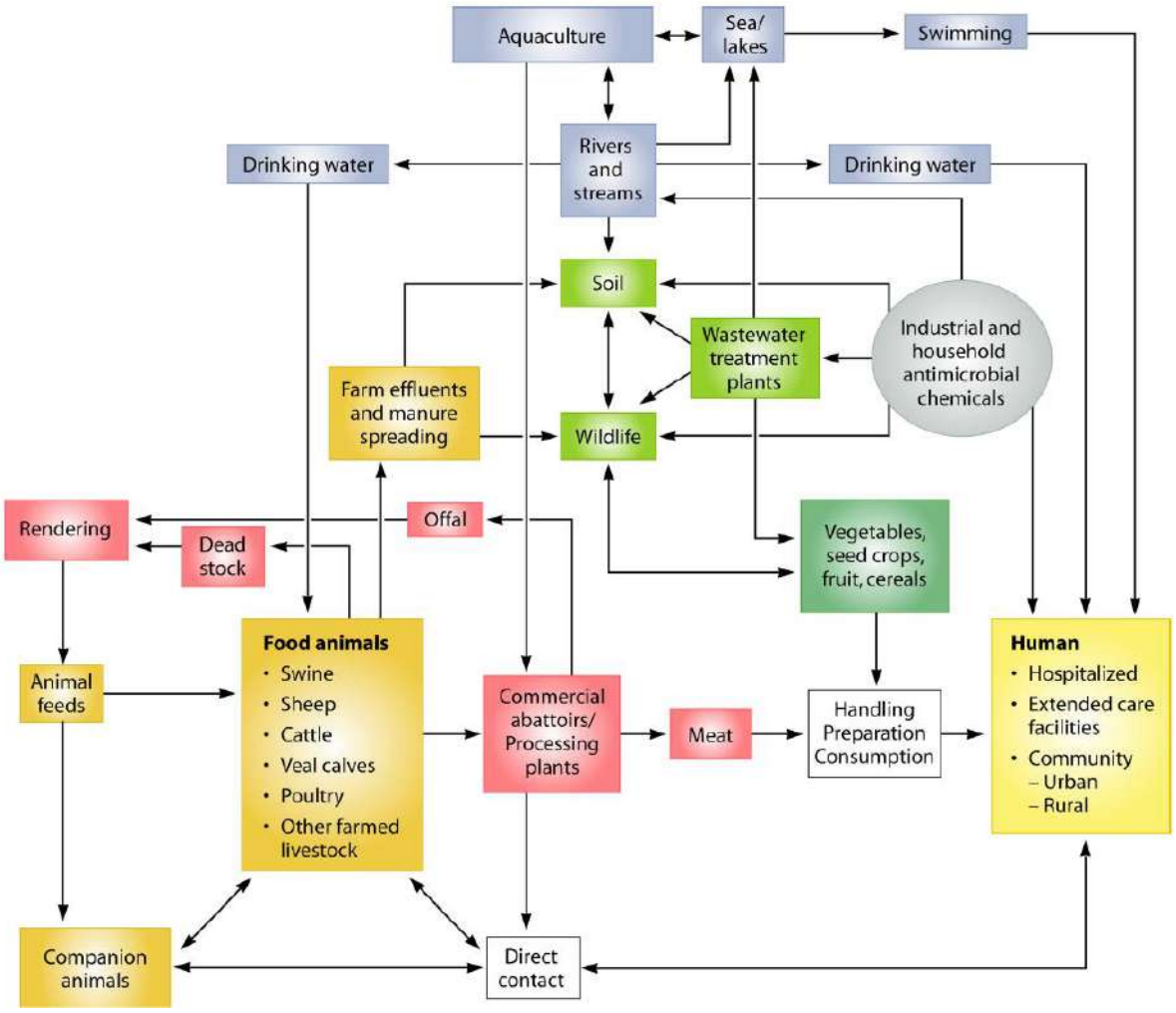

Figure 1.2. Human dissemination pathways of antibiotics contributing to antibiotic resistance (Davies et al., 2010)

Several investigations have shown us the biological properties that natural products possess and the useful applications in health and industry they can confer (Khan 2018). As these compounds are mainly produced in the late stationary growth phases, they have been called secondary metabolites, however the investigations about their different roles in biology and ecology are rare and remain largely unknown

(Davies & Davies 2010). In addition to their inhibitory activity, antibiotics might also act as signaling molecules in interspecies competition or in host-parasite interactions (Aminov 2009) and therefore they might help us to understand the complex interactions occurring in different ecological niches.

The discovery of antibiotics unquestionably revolutionized human history saving countless lives, allowing also its current use in animals and plants. Human exposure to antibiotics through history added to the extensive use of antimicrobials and the intrinsic resistance found in microbial genomes, lead us to alarming predictions of 10 million of deaths by 2050 with an enormous economic burden caused by antibiotic resistance (Browne *et al.* 2020). Most of the current new drugs for clinical use are based on semisynthetic modifications of existing chemical scaffolds due to the decline of drug development (Genilloud 2014). The urgent need for new antibiotics with novel structural scaffolds can be found in natural products produced by unusual sources in little explored or unexplored environments (Challinor & Bode 2015).

It is known that the major examples of antimicrobial resistance concern bacterial infections, but, what about the resistance cases occurring in protozoal diseases? Protozoal diseases such as malaria (caused by *Plasmodium* spp.) (**Figure 1.3**), leishmaniasis (caused by *Leishmania* spp.) (**Figure 1.4**), and trypanosomiasis (caused by *Trypanosoma* spp.) (**Figure 1.5**) affect mainly tropical and subtropical regions with great health and economic impacts worldwide. Antibiotic resistance involves natural environmental changes and proliferation of infections occurs mainly due to human activities. The absence of effective vaccines and the development of resistance to the current drugs situates these infections as major problems in endemic countries and highlight the need of novel molecules acting on new targets.

In the case of malaria, *Plasmodium falciparum* and *Plasmodium vivax* are responsible for most severe infections and most cases of antibiotic resistance (Tjitra *et al.* 2008). The first line recommended by the World Health Organization (WHO) is the Artemisinin Combination Therapy (ACT), which acts against the intraerythrocytic stages of *Plasmodium* parasites however it presents most of the cases of antibiotic resistance. Other drugs corresponding to the classes of naphthoquinones (atovaquone), quinolines (chloroquine), endoperoxides (artemisinin) and antifolates (pyrimethamine, sulfadoxine) present mutations in specific genes of the parasite that are responsible for antibiotic resistance (Capela *et al.* 2019).

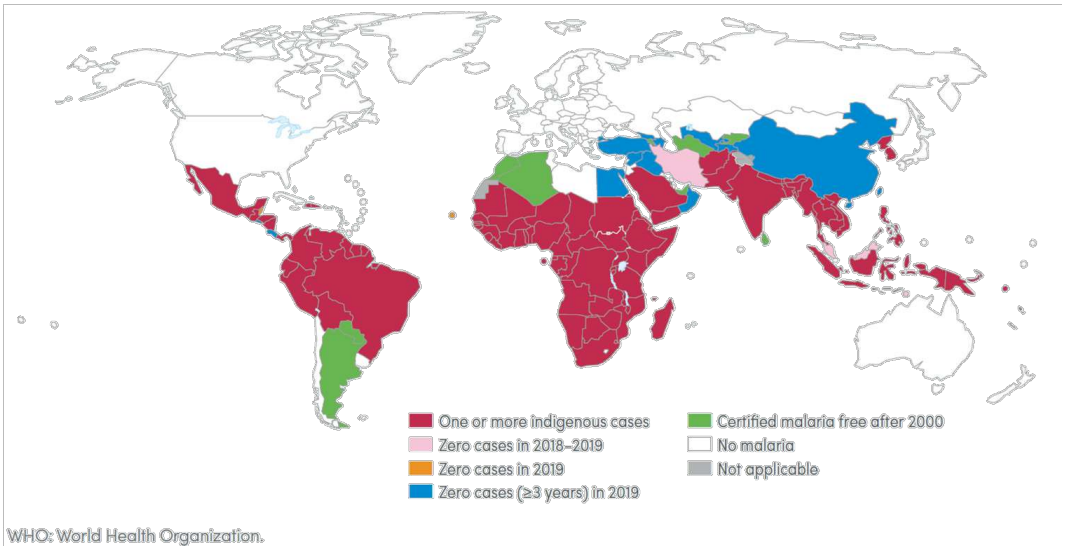

Figure 1.3. Countries with indigenous cases of malaria in 2000 and their status by 2019 (World Malaria Report 2020)

Leishmaniasis is a complex disease endemic in more than 98 countries (**Figure 1.4**) caused by more than 50 species from the *Leishmania* genus, causing visceral (VL), cutaneous (CL) or mucocutaneous leishmaniasis (MCL). VL is a form of infection that can remain in the skin for a lifetime and therefore act as a reservoir for a potential relapse. If this occurs in a person with a compromised immune system, the reactivation can be fulminant (Burza *et al.* 2018). For this disease, pentavalent antimonials are the standard treatment, currently compromised by antibiotic resistance while second-line (pentamidine and amphotericine B) and third-line (miltefosine) drugs are showing emerging resistance and toxicity (Capela *et al.* 2019).

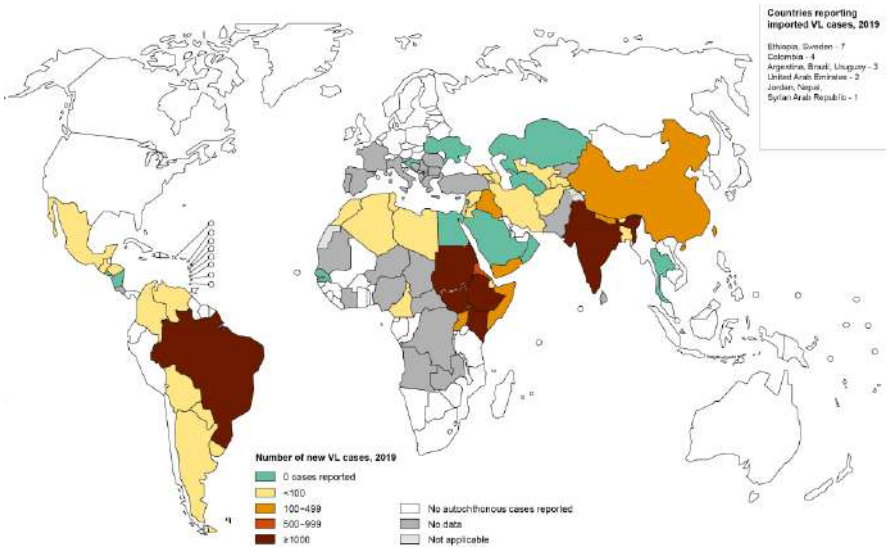

Figure 1.4. Status of endemicity of visceral leishmaniasis wordwide in 2019 (WHO Control of Neglected Tropical Diseases, 2021)

African trypanosomiasis is caused by two clinical variants *Trypanosoma brucei gambiense* (West and Central Africa) and *Trypanosoma brucei rhodesiense* (Eastern and Southern Africa) whose burden has currently decreased due to the efforts of various organizations (Barrett 2018). Parasite *T. b. rhodesiense* causes a more aggressive disease while *T. b. gambiense* develops a slower disease however, both parasites develop bloodstream and lymphatic stages and they are able to cross the blood-brain barrier into the central nervous system. For this reason, pentamidine and suramin (low toxicity) are drugs recommended on the first stage of infection while melarsoprol (high toxicity) is recommended for the second stage of infection due to its capacity to cross the blood-brain barrier. Despite the low rate of drug resistance in trypanosomiasis, compared to other infectious diseases, pentamidine and melarsoprol have shown increased emergence resistance and there is an urgent need for new treatments.

American trypanosomiasis or Chagas disease, on the other side, is caused by *Trypanosoma cruzi*, being endemic in Latin America (**Figure 1.5**) but infecting animals from central Argentina to the southern United States. In this case, most mechanisms of resistance of *T. cruzi* involve the immune system evasion, establishing a persistent infection with low parasite levels in the host referred as disease tolerance (Chevillard *et al.* 2018). In addition to this, resistance to nifurtimox has been also observed for Chagas' disease while the effects of fexinidazole as a new treatment have been recently evaluated (Deeks 2019).

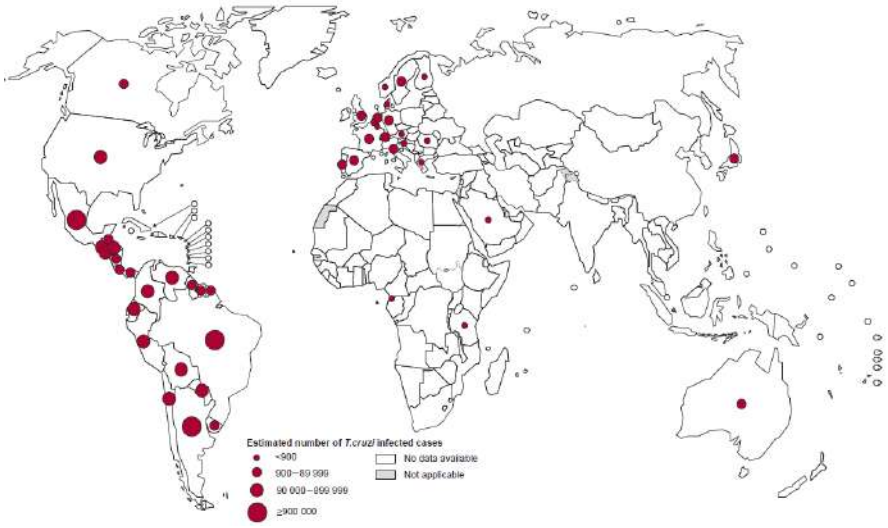

Figure 1.5. Global distribution of cases of Chagas disease worldwide in 2018 (WHO Control of Neglected Tropical Diseases, 2018)

To overcome the resistance problem for tropical parasitic diseases, especially in endemic countries but also for looking for eradication, different approaches are needed. Besides better understanding the mechanisms of action and resistance of drugs in order to design more appropriate alternatives, new

molecules that focus on new targets have to be investigated in order to increase the chemotherapeutic options with less undesirable effects.

1.1.2 Natural products as the main source of novel chemical structure

Natural products have been traditionally used throughout human history for treating illnesses and diseases and even nowadays, they continue to be lead compounds for drug discovery despite the fewer interest shown by the pharmaceutical industry due to the challenges found on their development, the increasing rediscovery of compounds, among other reasons (Molinski 2014). Some specific attributes of the chemical structure of natural products are the higher number of stereochemical centers and the fewer aromatic rings, compared to the drug leads provided by robotic and combinatorial chemistry providing structural analogues. In addition to this, more than 80% of the core ring scaffolds present in natural products were not present in molecules deriving from screening libraries or in those commercially active (Hert *et al.* 2009). These attributes of natural products provide the molecular complexity that has shown to be more successful in clinical trials, specifically with anticancer and antimicrobials properties (Dias *et al.* 2012). The latter may be also due to their capacity of acting as substrates or transporters therefore, inherently falling in the biological relevant space compared to the libraries of synthetic compounds that may possess appropriate physicochemical properties, such as permeability and bioavailability, but not necessarily be biologically active over the target (Kellenberger *et al.* 2011).

To have a better visualization of the importance of natural products in the development of new drugs, a follow-up study has shown the main sources of the approved drugs since 1981 until 2019 (Newman & Cragg 2020). The most interesting result is that the use of natural products or synthetic variations using their novel structures represent 50% of the total small molecules approved as drugs (n=1394), corresponding to: N: unaltered natural product (5.1%); NB: botanical drug (1%); ND: natural product derivative (27.5%); S*: synthetic with natural product pharmacophore (4.7%) and S* with NM: mimic of natural product (14.8%) (**Figure 1.6**).

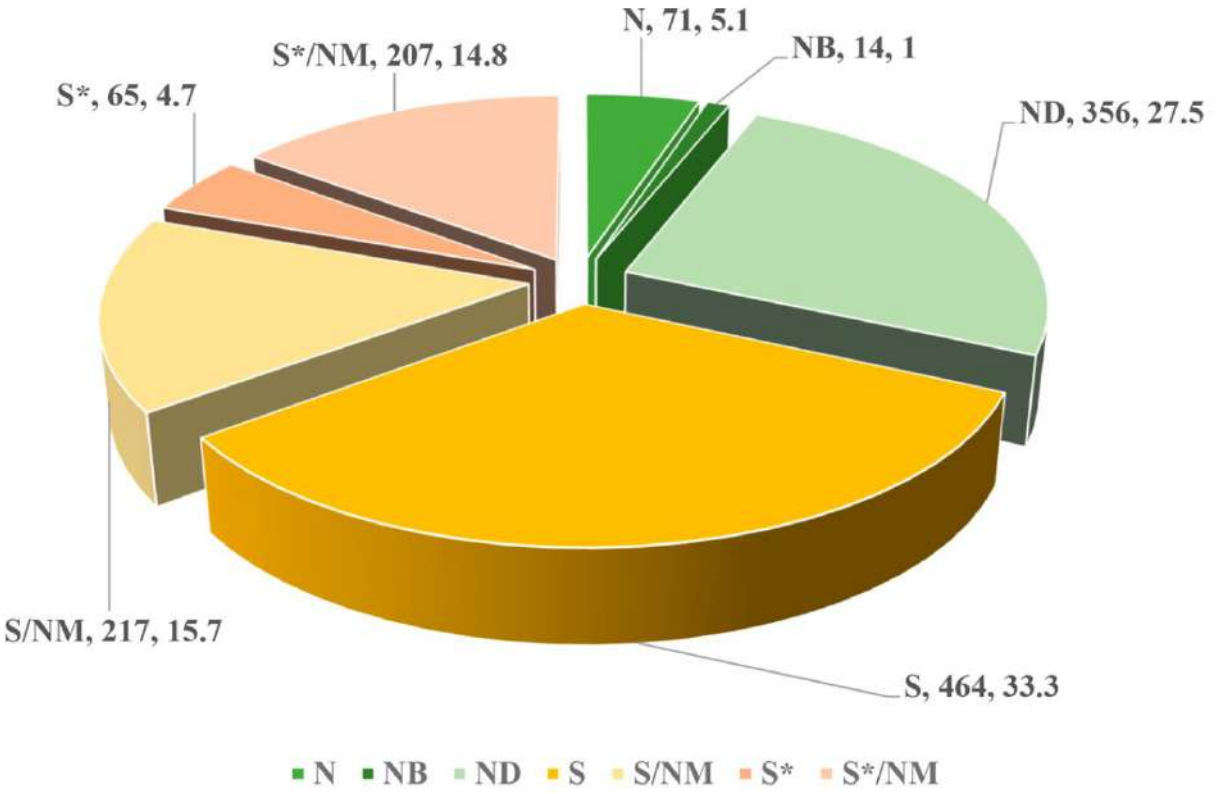

Figure 1.6. Small molecules approved as drugs from 1981 until 2019 from all source categories, n=1394. N: unaltered natural product; NB: botanical drug; ND: natural product derivative; S: synthetic; S*: synthetic with natural product pharmacophore; NM: mimic of natural product (Newman & Cragg, 2020)

As a result of the use and research of natural products, there are also important contributions in different aspects and disciplines such as the development of economies from resource-rich nations and the implementation of alternative medicines, elaboration of consumables (dyes, essential oils), production of fibers and polymers and the development of different other areas of health sciences (Khan 2018). As a consequence, human activities have endangered natural resources due to the ecological contamination and environmental alterations, which at the same time, have increased the concerns about resources protection from different points of view. In this regard, it is worth mentioning the regulations to international access to natural products arising from the United Nations Convention on Biological Diversity (CBD) and the Nagoya Protocol. Together, they seek to implement suitable laws and regulations and to suggest the practices to adopt in regards to the biodiversity and the traditional knowledge of the countries that are involved (Harvey *et al.* 2015).

1.1.3 Medicinal plants as a source of natural products

The most documented traditional medicine is the one from China which has been used for thousands of years and it remains as part of the current healthcare in China. Studying and isolating secondary

metabolites from medicinal plants have shown the enormous potential of finding drug-like or lead-like compounds for modern medicinal chemistry (Boufridi & Quinn 2018). For instance, the medicinal plant *Artemisia annua* (Asteraceae), used for treating malaria, led to the isolation of artemisinin; the potent anti-cancer drug paclitaxel was discovered thanks to the plant *Taxus brevifolia* [1] (Taxaceae) while the widely used drug aspirin was obtained from the medicinal plant *Filipendula ulmaria* [2] (Rosaceae) (Anand *et al.* 2019). Approximately only 15 % of the species from the plant kingdom have been investigated from which only 6% have been screened for biological activity. Around 80% of the population, particularly those in developing countries, continue using plant extracts as traditional medicine or even as the most affordable treatment available (Alvin *et al.* 2014). In developed countries, such as Australia, Canada or France, 48%, 70% and 75% of their population, respectively, have used the medicinal plants as alternative medicine at least once (Bussmann 2013).

Besides all the benefits, important uses and applications of medicinal plants, they have also shown some limitations such as the large quantities of plant needed to obtain sufficient bioactive compounds for clinical use. Another limitation are the compounds with biological activity isolated from plants that are endangered or highly endemic, raising concerns about their conservation. Although culture of plant tissue is an alternative, their costs are still elevated. For these reasons microorganisms, including micromycetes and bacteria might represent an easier way of scaling-up the production process of active compounds (Alvin *et al.* 2014).

[1] Also known as the Western yew whose principal toxic constituents are the diterpenoid derivatives termed taxanes
[2] Also known as Meadowsweet

1.2 Fungal secondary metabolites

Microorganisms produce compounds as a response to environmental factors or to stressful situations which provides them better survival mechanisms. This response will also depend on the genetic diversity of these microbial strains and therefore, this will maximize and diversify the natural products produced. Samples collected from diverse environments for the isolation of novel microorganisms, especially those with high biodiversity (hot spots) (**Figure 1.7**) or under-represented ecosystems, will potentially provide novel compounds (Knight *et al.* 2003). Collaborative work of microbiologists, ecologists and botanists to collect as many samples as possible from one hot-spot area will maximize the probabilities of finding novel species with unique metabolic pathways.

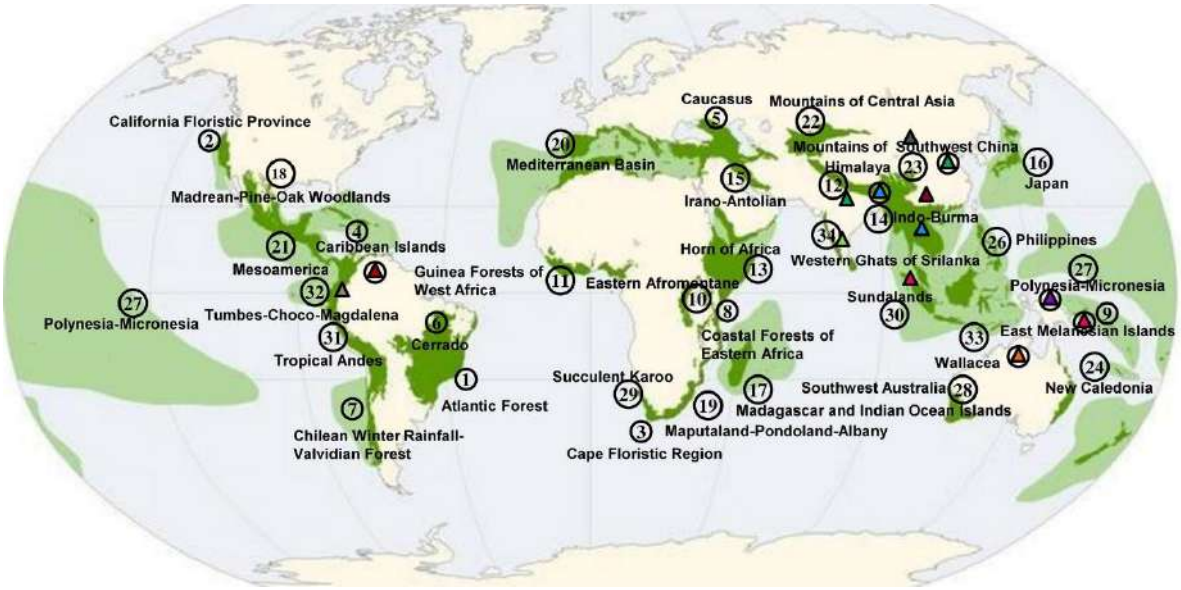

Figure 1.7. Biodiversity map representing 34 "hot-spot" areas of plant diversity and medicinal plants for microorganisms' isolation and diversity studies (numbered from 1 to 34) as recognized by Conservation International (Nalini & Prakash 2017)

Plants represent niches for microorganism interaction and many natural products isolated from plants were, in fact, produced by bacteria or fungi symbionts living within their tissues (Aly *et al.* 2013). Prokaryotes and eukaryotes have existed on earth for over billions of years but only around 1% of them have been cultured under laboratory conditions and studied for their secondary metabolite production (Demain 2014). However, massive whole-genome sequencing has exposed the great capacity of microbes to produce secondary metabolites (Genilloud 2014). The challenge is to access the biosynthetic pathways that are not expressed under standard laboratory conditions from culturable microorganisms and from those that are difficult to culture, called also 'unculturable' (Challinor & Bode 2015). Natural products obtained from bacteria and fungi have shown to have diverse activities such as antibacterial, antiviral, antiprotozoal, antifungal, anticancer, anti-inflammatory and many other biological activities

important for the pharmaceutical industry (Pham *et al.* 2019), corresponding to different chemical classesError! Reference source not found.. As they play a significant role in human activities, research nitiatives are focusing towards fungi and bacteria isolated from high biodiversity areas or from marine ecosystems using novel approaches of culture to activate cryptic metabolic pathways (Abdel-Razek *et al.* 2020).

1.2.1 Biosynthesis and classification of fungal secondary metabolites

The systematic study of secondary metabolites started with the characterization of over 200 mold metabolites by Harold Raistrick in 1922 but it was not until the discovery of penicillin that this area of investigation gained more attention. In the case of fungi, secondary metabolites are low molecular compounds usually correlated with morphological differentiation stages. It is also known that synthesizer strains can grow without producing them, unlike primary metabolites, and they have restricted taxonomic distribution (Keller *et al.* 2005). Species from fungal kingdom are responsible for 45% of the production of microbial metabolites, belonging mainly to the species of *Penicillium*, *Aspergillus* and *Trichoderma,* while yeasts produce around 1% of all microbial metabolites (Bérdy 2012).

Although secondary metabolites are chemically very diverse, they are synthesized from a few building blocks or precursors derived from primary metabolism (**Figure 1.8**) (King *et al.* 2016). Most of the genes involved in the biosynthesis of secondary metabolites in fungi are organized in clusters and they encode multi-domain and multi-modular enzymes such as the polyketide synthases (PKSs) and non-ribosomal peptide synthetases (NRPSs), besides other additional enzymes needed for transportation, regulation or used for specific modifications (Keller 2019). According to the class of enzyme that is involved in their biosynthesis, fungal secondary metabolites can be classified as polyketides, non-ribosomal peptides, terpenes or hybrid products (Keller *et al.* 2005).

Generally in fungi, polyketides are synthesized by type I PKSs, condensing acetyl coenzyme A and malonyl coenzyme A to form carbon chains of varying lengths. Non-ribosomal peptides are produced from amino acids (proteinogenic or non-proteinogenic) and synthesized by NRPSs. Terpenes are produced from activated isoprene units and synthesized by terpene cyclases and terpene synthases. Dimethylallyl diphosphate and isopentenyl diphosphate, products of the mevalonate pathway, act as building blocks for the production of indole alkaloids, monoterpenes, sesquiterpenes and diterpenes. Some secondary metabolites are synthetized by other enzymes encoded by different genes such as for the biosynthesis of gibberellin in *Fusarium fujikuroi* (Tudzynski *et al.* 1998) or they are hybrid products from NRPS-PKS systems and many other hybrid pathways, such as the case of aspyridones produced

by *Aspergillus* spp. (Theobald *et al.* 2019). Fungal secondary metabolites can be synthesized by diverse and complex pathways different from those mentioned here, which are not yet well elucidated.

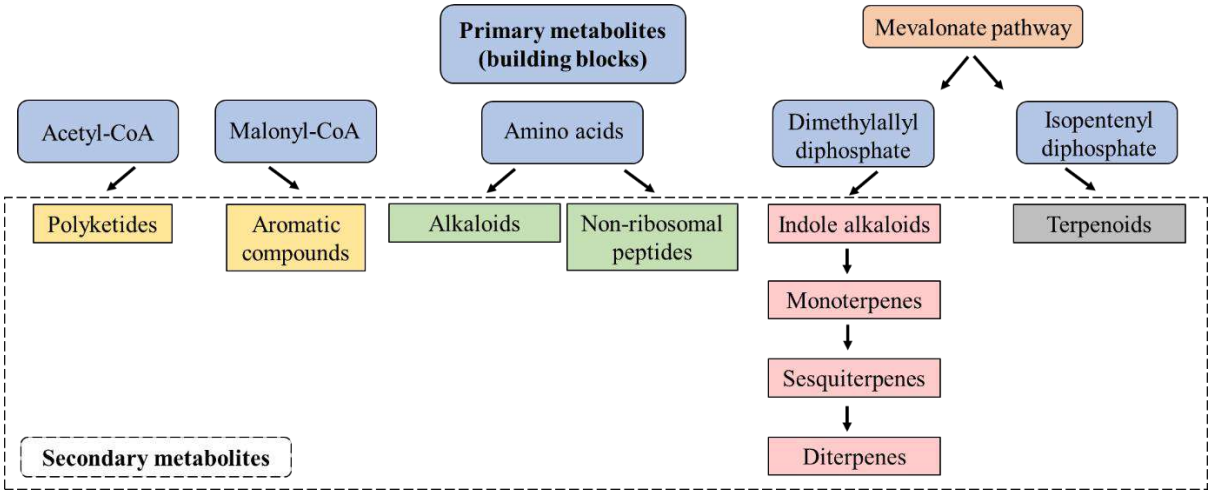

Figure 1.8. Main building blocks of fungal secondary metabolites (own diagram with information obtained from (King et al. 2016)

Some initial limitations for the study of the biochemical pathways in fungi were the short presence (minute scale) of enzymes involved in the biosynthesis of secondary metabolites and the lack of sexual stages in many species, needed for genetic studies. Later, thanks to gene cloning studies, many fungal gene clusters were characterized, such as for the aflatoxins, cephalosporin, penicillin, gibberellins, etc. (Keller *et al.* 2005).

Fungal secondary metabolites can also be grouped by chemical relationships (**Table 1.1**), as it is shown in the handbook elaborated by Cole and colleagues (2003) that summarizes and classifies most of the fungal secondary metabolites, including their biological activity information. Fungal natural products have exhibited a broad spectrum of biological activities such as antibiotic, anticancer, immunosuppressant drugs, hypocholesterolemic agents, mycotoxins, enzyme inhibitors, pigments, natural sweeteners, industrial enzymes and biofuels (Sanchez & Demain 2017). As previously mentioned, natural products from fungi possess high chemical originality, especially from those species isolated from high biodiversity areas (endophytes or marine organisms). A review covering 230 fungal compounds published between 2009 and 2013, highlighted novel structures and important bioactivities, showing the increasing interest of fungal natural products in drug discovery considering also innovative approaches (Schueffler & Anke 2014). Among these, cytospolides A-Q, decytospolides A and B, benzophomopsin A, xanalteric acids I and II, epicoccolides A and B and trichodermanin A were new compounds isolated from endophytic fungi.

Table 1.1 Main chemical groups of fungal secondary metabolites according to Cole *et al*. 2003

Classification of fungal secondary metabolites

1	Aflatoxins	**34**	Hebevinosides and Hebelomic acids
2	Aflavinines and related indoles	**35**	Helminthosporols
3	Alliacolide and related metabolites	**36**	Herbarin and related metabolites
4	Altenuene and related metabolites	**37**	Hericenes and Hericenones
5	Altertoxins	**38**	Indole alkaloids
6	Altranones	**39**	Indole metabolites
7	Antheridiols and Oogoniols	**40**	Janthitrems
8	Aphidicolins	**41**	LL-Z1271 antibiotics and related metabolites
9	Arcyroxepin A and related Bisindoles	**42**	LL-Z1272 antibiotics and related metabolites
10	Arugosins	**43**	Loline alkaloids
11	Austalides	**44**	Lucidenic acids
12	Azasterols	**45**	Lucidones
13	Baccharinoids	**46**	Macrocyclic trichothecenes and related metabolites
14	Botrydial and related metabolites	**47**	Memnobotrins
15	Boviquinones and related metabolites	**48**	Miotoxins
16	Cercophorins	**49**	Myrotoxins and Myotoxins
17	Cercosporin and related metabolites	**50**	Neovasinins
18	Chaetoglobosins/Cytochalasins	**51**	Ochratoxins and related metabolites
19	Chokols	**52**	Palmarumycins
20	Curvularins	**53**	Paspaline and related metabolites
21	Cyathanes	**54**	Penitrems/Lolitrems
22	Diketopiperazines	**55**	Phomosines
23	Enaminomycins and related metabolites	**56**	Radicinins
24	Fasciculols	**57**	Roritoxins
25	Fiscalins	**58**	Siccanochromenes and Grifolins
26	Fumiquinazolines	**59**	Stachybotrylactone and related metabolites
27	Fumonisins and related metabolites	**60**	Sterigmatocystin and related metabolites
28	Fusarochromanones	**61**	Sterols
29	Fusicoccins	**62**	Trichothecenes and related metabolites
30	Fusidanes and Protostanes	**63**	Tryptoquivalines
31	Ganoderic acids	**64**	Tsugicolines
32	Ganoderiols	**65**	Versicolorins
33	Ganomastenols	**66**	Viridin and related metabolites

Among the fungal metabolites, the smallest cyclic peptides that are built from two amino acids are named diketopiperazines (DPKs), where the thiodiketopiperazines (TDKPs) are higher functionalized analogs that possess a broad bioactivity such as cytotoxic, antibacterial, antifungal or anti-inflamatory properties. They have been isolated from fungi species corresponding mainly to the genera *Aspergillus*, *Candida*, *Chaetonium*, *Gliocladium*, *Penicillium* and *Verticillium* (Bräse *et al.* 2013), but also from the species *Cophinforma mamane*, which is the object of study of this thesis. Natural thiodiketopiperazines

alkaloids are characterized by the presence of a diketopiperazine core with thiomethyl groups and/or sulfide bridges. According to the position of the sulfur linkages, they can be classified in 1,4-bridged epipolythioxopiperazines (ETPs), derivatives with sulfur bridge outside the 2,5-DKP ring, nonbridged dimethylthio derivatives and others cyclodipeptides containing sulfur (Wang *et al.* 2017a). Biogenetically, DKPs are derived from at least one aromatic amino acid and in fungi, the diverse scaffolds arise from the formation of a wide variety of amino acids and different sulfur bridges which directly affect their bioactivity (Niu *et al.* 2017). The major catalysts of the peptide bond formations are the nonribosomal peptides synthetases (NRPS) and cyclodipeptide synthases (CDP) (Borgman *et al.* 2019).

Regarding the 1,4-ETPs, their observed toxicity is due to the presence of a disulfide bridge, which inactivates proteins through the reaction with thiol groups and by the generation of reactive oxygen species (Borthwick 2012). The most known example is gliotoxin, which in the case of the marine-derived fungus *Penicillium* sp., seven gliotoxin analogues with cytotoxic effects were isolated while compounds with a disulfide bridge exhibited histone methyltransferase inhibitory activities (Sun *et al.* 2012). Recently, 4 new thiodiketopiperazines alkaloids were isolated from the endophytic fungus *Phaeosphaeria fuckelii* called phaeosphaeones A – D, while phaeosphaeone D exhibited mushroom tyrosinase inhibitory activity (Zhai *et al.* 2020). Regarding the sulfur-bridged derivatives outside the 2,5-DKP ring, epicoccins A – F have been isolated from fungus *Epicoccum nigrum* and they present unusual sulfur bridges and one of these compounds exhibited moderate antimicrobial activity (Zhang *et al.* 2007).

1.2.2 What are the roles of fungal secondary metabolites?

Metabolites produced during the secondary metabolism of fungi, called also specialized metabolism, are not essential for their growth or survival but they have been widely used for different human activities, as it has been previously mentioned. However, the role of these metabolites in their natural environment during their interaction with other microorganisms or during their own development are still under investigation with some findings that help us to understand their ecological functions besides their utility. Some secondary metabolites might be useful for their interaction with other microorganisms in their ecological niches, for protection or defense against competitors or against other environmental factors such as light. They can also serve as virulence factors during infections or during symbiotic interactions with plants and pathogens.

Interaction with other microorganisms

The role of secondary metabolites during microbial interactions is still not well understood, however some studies have shown their importance during these interactions. Quorum sensing (QS) is the communication process between bacteria largely studied in gram-positive and gram-negative bacteria. This process occurs mainly during biofilm formation, regulation of cell densities or secretion of virulence factors (Grandclément *et al.* 2015), while this communication process is less known in eukariotes. For example, it has been recently reported the production of a small peptide Qsp1 by *Cryptococcus neoformans* that acts as a quorum sensing regulator involved in its own virulence and morphology (Homer *et al.* 2016). Additionally, *Penicillium sclerotiorum* produces the molecule sclerotiorin, whose production is related to derivatives of a QS molecule that contains the signaling molecule gamma-butyrolactone. While in *Aspergillus terreus*, butyrolactone I might act in the regulation of lovastatin production as a QS molecule, stimulating its biosynthesis (Macheleidt *et al.* 2016). Regarding microbial communication, induction of new secondary metabolites due to intimate or physical interaction between fungi and bacteria might indicate the use of compounds to communicate that they are sharing the same habitat and nutrients, which will trigger different signaling pathways and responses.

Virulence factors during interactions with plants and pathogens

These types of interactions occur during symbiotic interactions with the host plant and the pathogens harbored within its tissues such as insects, other fungi and bacteria, parasites, etc. Some species are host-specific and they produce different types of infection and therefore different secondary metabolites. In the case of *Alternaria alternata*, while the AM toxin is produced during the infection of apples (*Alternaria mali*), the AF toxin is produced during infection of strawberries (*Alternaria alternata* f. sp. Fragariae), causing black spots and therefore showing their host and target site specificity (Tsuge *et al.* 2013). Additionally, *Botrytis cinerea* produces botrydial and botcinic acid on plants, which play a role in its pathogenicity. If one of the genes that encodes for these compounds is deleted, the fungal pathogenicity does not change but when both genes are deleted, the infection continues but with no visible symptoms of infection (Dalmais *et al.* 2011).

Another situation is for example the entomopathogenic fungus *Beauveria bassiana*, which expresses beauvericin and other secondary metabolites as virulence factors during the infection of the insect *Triatoma infestans*. Interestingly, this entomopathogenic fungus also secretes antimicrobial metabolites to the dead insect to limit competition for nutrients. Similarly, the fungus *Metarhizium robertsii* produces the secondary metabolite destruxin as a virulence factor during infection of the insect larva of *Spodoptera exigua* (Macheleidt *et al.* 2016).

Protection from toxic natural products and environmental conditions

Among all the bioactivities of fungal natural products, several possess antifungal activity. Fungi protect themselves from these toxic compounds using different mechanisms encoded in their biosynthetic gene clusters. It should be noted that the toxic concentrations under laboratory conditions are not the same to the physiologically relevant concentrations, making secondary metabolites more of a signal rather than a toxin in natural conditions. It is known that it exists mainly 3 fungal strategies to avoid toxicity from natural products: efflux transporters or pumps, intermediate transporters or translocators, detoxifying enzymes that reduce the target binding properties and duplicated copies of the target protein to recover from the toxic effect (Keller 2019).

Regarding environmental conditions, the production of melanin in fungi represents an evolutionary and important mechanism of adaptation against difficult conditions. This metabolite is a hydrophobic pigment formed by the oxidative polymerization of indolic or phenolic compounds produced in plants, animals and fungi. In fungi, melanin is produced after the active growth stage and therefore it is considered as a secondary metabolite that confers UV light protection thanks to its photochemical properties, transforming UV radiation into harmless amounts of energy. Moreover, it has been postulated that melanin possesses other roles such as fungal protection against toxins, hydrolytic enzymes, redox buffering, among others functions, providing them defense mechanisms and helping fungi to survive (Cordero & Casadevall 2017).

Fungal development processes

Fungal secondary metabolites are also produced as signals to initiate developmental programs or morphological changes such as protection of sexual structures, formation of fruiting bodies, spore germination or pigmentation. In *Aspergillus nidulans* the production of linoleic acid is associated with the sporulation induction, as it occurs in *Fusarium graminearum* and in *Aspergillus terreus* with the production of zearalenone and butyrolactone I, respectively. Also, the production of mycotoxins in *Aspergillus* spp. and the production of patulin in *Penicillium urticae* are induced after the sporulation process (Calvo *et al.* 2002).

1.2.3 Regulation of secondary metabolism in fungi

Interactions of microorganisms in natural environments are very complex due to the multiple chemical signals used for communication, competition or defense between fungi, bacteria, plants, protozoa or even metazoa (Brakhage 2013). Secondary metabolite production can also respond to various environmental signals such as nutritional sources, temperature, light, pH or the presence of other microorganisms (**Figure 1.9**). This process does not follow a hierarchical scheme as it is regulated at different levels within different cellular processes, including development and transcription and it can vary between different fungal species.

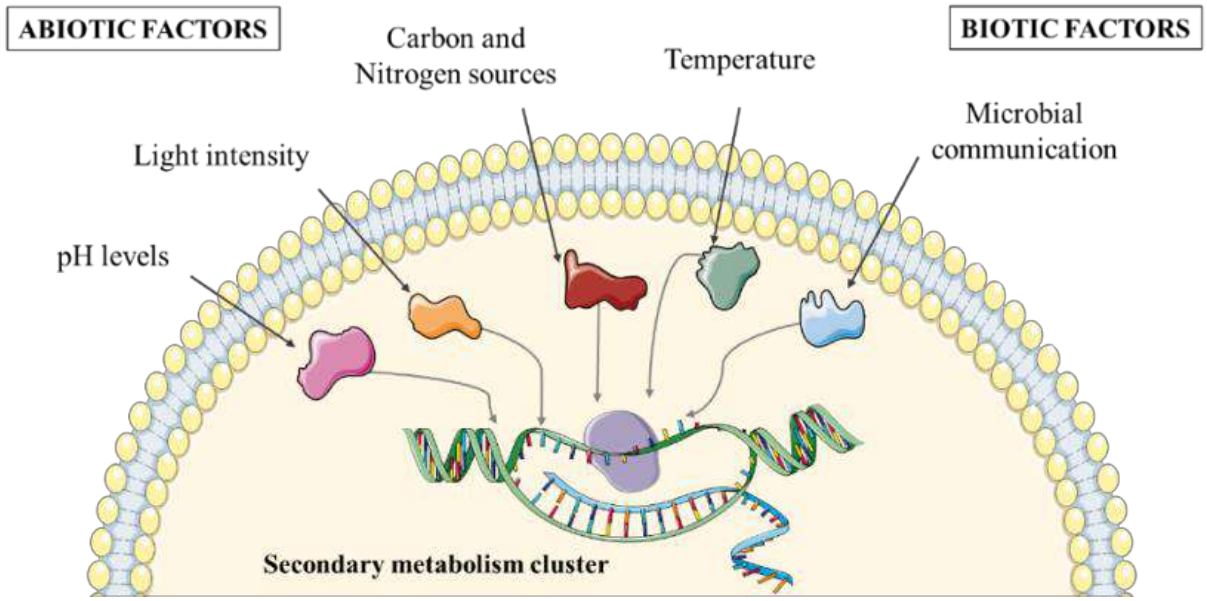

Figure 1.9. Environmental signals (biotic and abiotic) that influence the regulation of secondary metabolism clusters in fungi (Own diagram using smart.servier.com)

Transcriptional regulation

The regulation of a specific gene cluster by transcription factors occurs for instance in the biosynthesis of the mycotoxin gliotoxin regulated by the Zn-finger. This regulation has shown to be affected by pH, temperature, aeration or even the presence of gliotoxin itself in *Aspergillus fumigatus* (Scharf *et al.* 2012). In this case, if the unique gene of the cluster encoding for the Zn-finger is deleted, the gliotoxin production does not occur. Specific regulators can be encoded by genes found inside or outside the cluster they regulate. Interaction between gene clusters through cross-talk regulation may highlight the need of a deeper understanding of these regulatory networks.

On the other hand, different stimuli can induce distinct global regulatory proteins, showing a greater level of regulatory networks. Approximately, half of the currently known secondary metabolite gene clusters in fungi do not encode regulatory proteins, therefore they respond to a global regulation. Some of these global regulators have been identified: PacC for pH levels, AreA for nitrogen sources, CreA for carbon sources and the velvet complex for light intensity (Macheleidt *et al.* 2016). Light stimuli is involved in secondary metabolism, sporulation and development in fungi. For instance, the velvet complex coordinates filamentous fungal development in response to light and the nuclear protein LaeA, which is part of this complex, acts as a regulator at the chromatin level (Bayram & Braus 2012). Another example is the transcription factor PacC that activates penicillin biosynthesis in pH alkaline but represses aflatoxin production in *Aspergillus parasiticus* (Keller & Hohn 1997). Temperature also influences metabolite production as in *Aspergillus flavus*, whose optimal growth is 37°C but aflatoxin production occurs only at 30°C yet no global regulator has been identified.

Signaling pathways

In addition to this, highly conserved signaling pathways are also involved in the activation of secondary metabolism in fungi through regulation of gene expression. Fungal development and secondary metabolite production have been associated mainly during sporulation, pathogenicity or pigmentation (Keller *et al.* 2005). Cyclic adenosine monophosphate (cAMP)/protein kinase A (PKA) and mitogen-activated protein kinase (MAPK) are among the most investigated signaling pathways associated with the production of secondary metabolites. For instance, overexpression of one catalytic subunit of PKA induced the expression of a melanin gene cluster in *Aspergillus fumigatus* while PKA phosphorylation led to the enhanced production of the polyketide sterigmatocystin in *Aspergillus nidulans*. MAPK pathways possess 3 signaling cascades which are involved in cell wall repair (CW1), in the osmolarity stress (HOG) and in the sexual crossing and pseudohyphal formation (pheromone pathway). Inhibition of the pheromone pathway and repression of CW1 pathway generated lower levels of sterigmatocystin and penicillin production in *Aspergillus nidulans* (Macheleidt *et al.* 2016).

Epigenetic regulation

In eukaryotic cells, transcription is performed by RNA polymerase II and its access to the DNA depends on the chromatin state, composed by DNA and histone protein complexes assembled in nucleosomes. Biosynthetic gene clusters in fungi are often found in the distal telomeric regions of the chromosome (Williams *et al.* 2008), which are transcriptionally controlled by epigenetic regulation, mainly histone acetylation and methylation (Brakhage 2013). When fungal DNA is organized into histone proteins and is densely packed into heterochromatin, it becomes transcriptionally silent (Okada & Seyedsayamdost

2017). When DNA is loosely packed into euchromatin, it becomes transcriptionally active mainly due to the presence of highly acetylated histones (Cichewicz 2010). By contrast, when histones are methylated, genes are found to be silenced (Suzuki & Bird 2008) (**Figure 1.10**).

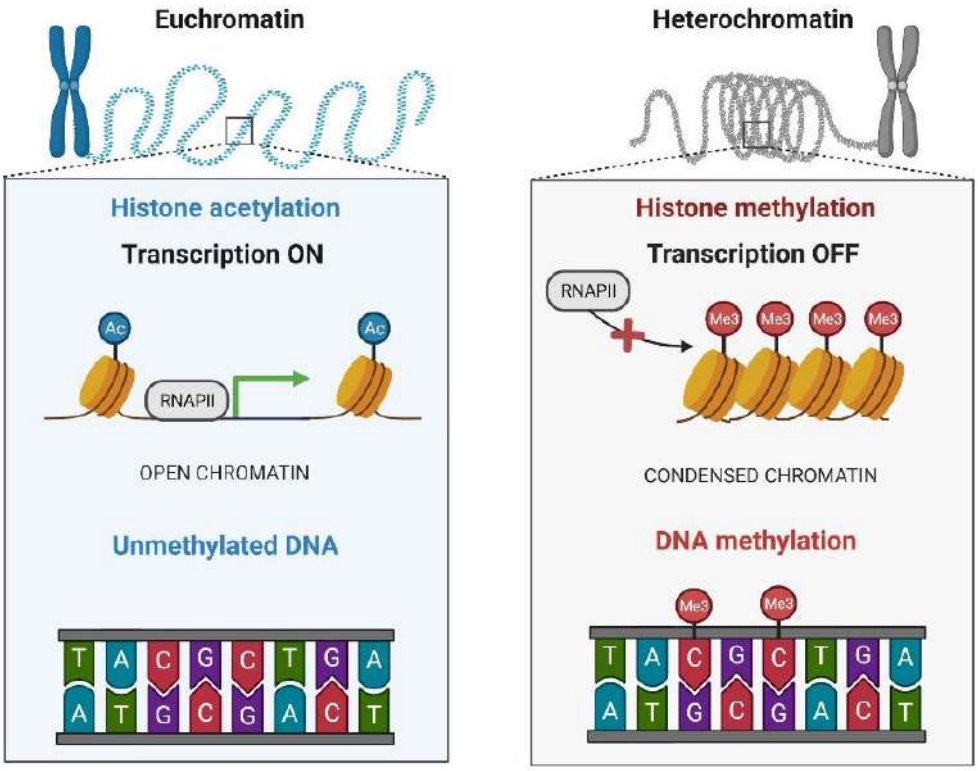

Figure 1.10. Epigenetic modifications of chromatin by DNA methylation and histone acetylation. RNAPII: RNA polymerase II (own creation using biorender.com)

Histone acetylation and methylation are catalyzed by histone acetyl transferases (HATs) and by histone methyltransferases (HMTs), respectively while the removal of acetyl and methyl groups are catalyzed by histone deacetylases (HDACs) and histone demethylases (HDMs), respectively. Similarly, DNA methylation also plays an important role in the regulation of gene expression, despite the low abundance of this modification found in fungal genomes. In this case, the transfer of the methyl group to the DNA is catalyzed by DNA methyltransferases (DNMTs).

It was observed that during the early-phase growth of *Aspergillus nidulans*, some methylation marks on histone protein H3 were reversed by the nuclear protein LaeA when the fungus changed to a stationary phase of growth. Additionally, when studying the effects of epigenetic manipulation by deleting a histone deacetylase gene (*hdaA*) in *Aspergillus nidulans*, it resulted in a transcriptional activation of multiple biosynthetic gene clusters (Shwab *et al.* 2007). Moreover, production of aflatoxin was reduced when a DNA methyltransferase gene (*dmtA*) was deleted in *Aspergillus flavus*, indicating its role in gene

activation rather than in gene repression. These findings allowed the expansion of additional studies on this subject, by either activating or silencing chromatin regions or by treating fungi with epigenetic modifier chemical inhibitors (Keller 2019).

However, besides histone acetylation and methylation, other post-transcriptional modifications have been observed in fungi such as butyrylation, propionylation, phosphorylation, sumoylation and ubiquitination. The relative number of modifications predicted in *Aspergillus nidulans* based on similarity shows that 46% correspond to methylation, 36% to acetylation, 10% to sumoylation, 5% to phosphorylation and 3% to ubiquitination (Collemare & Seidl 2019), indicating the potential influence of additional transcriptional regulations involved in secondary metabolism in fungi.

1.3 Endophytes as a source of new drugs

The term "endophyte" was first described in 1886 by Anton de Bary, and was broadly used to refer to any organism living within plant tissues however, this term has undergone various redefinitions through time. A widely accepted definition describes endophytes as any organism that colonizes internal plant tissues such as branches, stems, roots, petioles, leaves, fruits or seeds, without generally producing signs of its presence or showing harmful effects to the host plant. These microorganisms can spend all their life cycle or part of it within inter or intracellular spaces of the plant cells and the symbiotic interactions can vary from mutualist, antagonist or even parasitism, corresponding to obligate or facultative endophytes (Gouda *et al.* 2016). The latter also depends on the environmental and physiological conditions of the host plant.

Endophytic microorganisms have been descr in almost all plant families found in different environments and climates around the world. Most of the endophytic microorganisms isolated from plants correspond to fungal species from the Ascomycota and Basidiomycota phyla and to bacterial species from the Actinobacteria, Bacteroidetes, Firmicutes and Proteobacteria phyla (Martinez-Klimova *et al.* 2017). Only 1-2% of all the known plants have been studied for their endophyte composition (Strobel 2018), of which more than 34 plant families have been used for the isolation of endophytes, corresponding, for instance, to the Araceae, Asteraceae, Fabaceae or Lamiaceae families from different collection sites (**Figure 1.11**). Considering current environmental problems such as contamination, deforestation or biodiversity losses, many of these endophytic species will be lost before their value is explored. Therefore, the need to preserve and explore these natural reservoirs of biological agents is urgent.

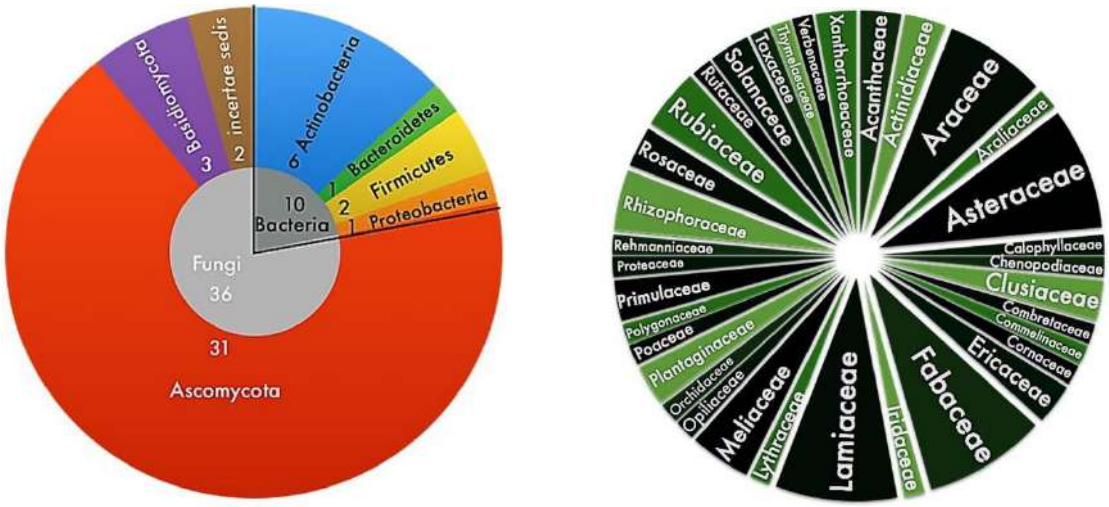

Figure 1.11. Taxonomic classification of isolated endophytes (left) from different plant families (right) (Martinez-Klimova et al. 2017)

Although endophytes were first described in 1904 from *Lolium temulentum* (Poaceae) grains, it was not until the isolation of paclitaxel in 1993 from the fungal endophyte *Taxomyces andreanae* that these microorganisms started to gain more attention for the study of new potential sources of novel natural products. This discovery also prompted the study of other plants able to host different endophytes capable of producing secondary metabolites with important pharmacological uses (Strobel & Daisy 2003).

1.3.1 Bacterial endophytes

Bacterial endophytes include more than 200 genera from 16 phyla of gram-positive and gram-negative bacterial species, considering actinobacteria and mycoplasma. They possess a capacity for colonizing root surfaces in the rhizosphere that actively switches to endophytic lifestyles to colonize stems, leaves and other host tissues. The diversity of bacterial endophytes include species from *Achromobacter*, *Acinetobacter*, *Agrobacterium*, *Bacillus*, *Brevibacterium*, *Pseudomonas* genera, being *Streptomyces* one of the most promising and dominant genera in endophytic actinomycetes (Gouda *et al.* 2016). Additionally, the most characterized genera are *Bacillus* and *Pseudomonas* while the less studied are the mycoplasma species, known to have a symbiotic relationship with some red algae.

In the context of plant-bacteria interactions, production of toxins, virulence factors, biofilm formation agents and plant hormones or their structural analogues have been reported. The endophytic actinobacterium *Pseudonocardia* sp., for instance, enhanced artemisinin production in the host plant *Artemisia annua* while the production of the cardiotoxin pavettamine is due to a bilateral biosynthesis of South African Rubiaceae and their bacterial endophytes (Brader *et al.* 2014). However, a large plethora of metabolites found in endophytic actinobacteria and in other phyla remain to be discovered.

1.3.2 Fungal Endophytes

Fungal endophytes represent the majority of endophytes isolated from different plant families. Similar to the results found by Martinez-Klimova and colleagues (Martinez-Klimova *et al.* 2017), a more recent analysis of diversity and distribution of endophytes including almost 600 published studies between 2016 - 2019, revealed that fungal endophyte diversity has been characterized in at least one host plant of the embryophyte families (**Figure 1.12)** however, most the host phylogeny remains unsampled (Harrison & Griffin 2020).

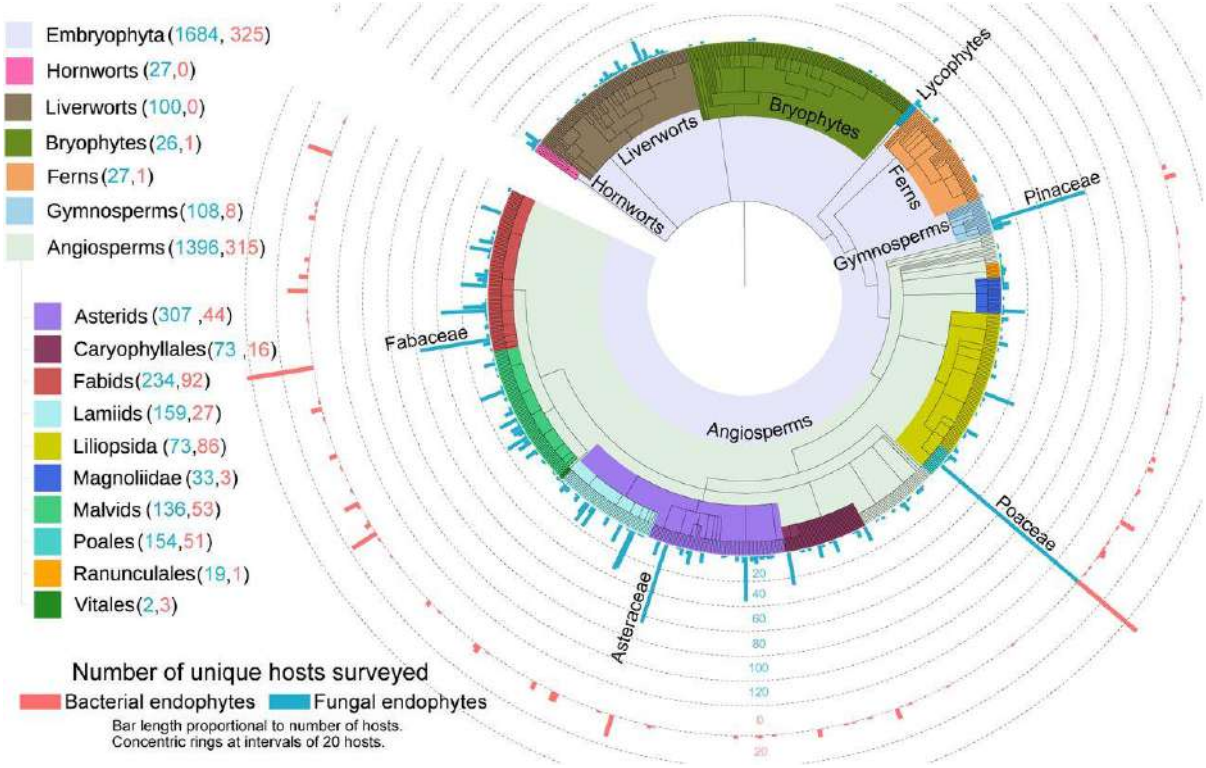

Figure 1.12. Number of studies between 2016-2019 surveying fungal (blue bars) and bacterial (red bars) endophytes from Embryophyta (Land plants) with main taxa labeled on the left including the number of unique host surveyed in parentheses (Harrison & Griffin 2020)

Taxonomic diversity of endophytic fungi is very vast and therefore these communities can be grouped under different criteria, based on their ecological or symbiotic function in relationship with the host plants. They can be classified based on the mode of transmission, mode of reproduction, expression of the infection, source of nutrition or type of tissue colonized within the plant (Bamisile *et al.* 2018). Besides this, two major groups of fungal endophytes are also distinguished: clavicipitaceous endophytes that occupy grasses as host plants while non-clavicipitaceous colonize vascular and nonvascular plants, among other considerations based on their phylogeny and life history traits (Rodriguez *et al.* 2009).

On the other hand, a total of 185 patents related to endophytic fungi applications were recorded for the period 1988-2019, of which 88 correspond to stress tolerance and growth promoters, 90 patents correspond to biocontrol of plant pathogens and 7 patents correspond to bioremediation and phytoremediation and the most representative fungi belong to the genera *Alternaria*, *Aspergillus*, *Chaetomium*, *Fusarium*, *Penicillium* and *Muscodor* (Ortega *et al.* 2020). However, commercial exploitation and application remains a big challenge due to the low biomass generated by fermentation or the low stability of axenic endophytes culture over time (Venugopalan & Srivastava 2015). Many strategies are being developed in order to explore the potential of endophytic fungi and enhance their productivity of bioactive secondary metabolites.

Considering the importance of fungal endophytes, being the representative group of endophytes in comparison to the bacterial endophytes, the following sections will be focused on fungal endophytes, regarding their relationship with their hosts, their isolation for laboratory studies, and the novel bioactive natural products obtained from these microorganisms.

1.3.3 The special relationship between endophytic fungi and their host plants

Over long periods of evolution, endophytes have formed a special symbiotic relationship with their host plant. They can act as a biological defense for the plant against phytopathogens and produce the same or similar secondary metabolites as their host (Alvin *et al.* 2014), with approximately 18% of plant metabolites that can be produced by associated fungi. Endophytes can alter the quantity and quality of drugs derived from medicinal plants due to their capacity to increase their fitness and their growth, improving their tolerance to biotic or abiotic stress factors as well as inducing the accumulation of bioactive secondary metabolites. In this regard, the endophyte population is also indirectly affected by environmental conditions such as temperature, humidity, soil nutrients, sunlight hours, etc., therefore the same host plant species from different regions can exhibit different endophytic populations (Jia *et al.* 2016).

In general, the interactions between endophytic fungi and their host plant occurs in different forms at a metabolic level: endophytes can induce plant metabolism, plants can induce endophyte metabolism, both contribute and share metabolic pathways, plants metabolize products from their endophytes or endophytes synthesize secondary metabolites (or similar) of the plant host (Cabezas Gómez & Hortolan Luiz 2018).

The study of plants for the isolation of fungal endophytes and further research of novel natural products represents a promising approach that has already shown positive results. A review study analyzed several investigations of endophytic fungi and medicinal plants covering a period of 30 years (1986 - 2016). A total of 46 families and 96 species of plants showed a mutualistic relationship with their endophytes, used either as part of traditional medicine or through the consumption of the extracted bioactive compound. Additionally, they were distributed in temperate, tropical, subtropical or extreme environments (savanna deserts and high altitude conditions) (Jia *et al.* 2016). Of the multiple ecosystems on Earth, those having the greatest biodiversity can also hold the greatest number of biodiverse endophytes, including also high endemic plants which harbor several species of endophytes that have evolved along with their hosts.

A study on the identification of endophytic fungi communities from the medicinal plant *Withania somnifera* (Solanaceae), led to the isolation of 33 fungal strains corresponding to 24 species from the Ascomycota and Deuteromycetes classes. Another study of the endophytic fungi residing in the endemic

medicinal plants from India *Artocarpus hirsutus* (Moraceae) and *Vateria indica* (Dipterocarpaceae), recovered a total of 106 strains belonging to diverse genera such as *Coniothyrium*, *Trichoderma*, *Mortierella*, *Phyllostica* and *Acremonium* (Nisa *et al.* 2015). Endophytic fungi associated with the medicinal Amazonian plant *Carapa guianensis* (Meliaceae) were classified into 35 different taxa in the genera *Colletotrichum*, *Diaporthe* and *Pestalopsis* as the most frequent endophytes while the rest correspond to the genera *Aspergillus*, *Botryosphaeria*, *Fusarium*, *Phomopsis*, among others. Many of these fungi presented antibacterial, antiparasitic and antiviral activities (Ferreira *et al.* 2015).

Potential role of fungal endophytes in agriculture

The relationship between host plants and their endophytes are very complex due to all the biotic and abiotic factors that can influence (**Figure 1.13**). Generally, the presence of endophytes is beneficial for the host plant since they positively influence plant growth under different active or passive mechanisms, which might have useful applications for sustainable agriculture (Fadiji & Babalola 2020). In this sense, endophytes could help cultivate crops with less fertilizers or pesticides and chemicals, making crop plant management a more parsimonious process with the environment (White *et al.* 2019).

Endophytes enhance a plant's ability to survive under stress for example by increasing nutrient availability. The endophytic fungus *Cladosporium sphaerospermum* isolated from the roots of *Glycin max* (*Fabaceae*) improved the growth of its host by the production of bioactive compounds gibberellin (GA) GA4 and GA7 (Hamayun *et al.* 2009). Also root growth and elongation were observed under the presence of endophytic fungi *Penicillium chrysogenum* and *Alternaria alternata* isolated from *Asclepias sinaica* (*Apocynaceae*) due to the production of ammonia and indole acetic acid (IAA) (Fouda *et al.* 2015). They have also shown to enhance plant tolerance against cold or drought stress through the induction of photosynthesis by enhancing phytohormones, chlorophyll and gaseous exchange, maintenance of osmosis, reduction of reactive oxygen species generation and increasing the production of IAA and GA.

As part of their capacity to produce bioactive natural products against microorganisms, endophytic fungi can be used as potential biocontrol agents for plant diseases. They can suppress plant pathogens by releasing toxins or antibiotics, competing for nutrients and space or inducing plant defense systems. Endophytic fungi *Penicillium* sp. and *Hypocrea* sp., isolated from different healthy chinese plants, could effectively inhibit mycelial colony growth of *Fusarium oxysporum* f. sp. *cucumerinum* causing wilt in cucumber (Abro *et al.* 2019).

In addition to this, endophytic fungi play an important role in the production of volatile organic compounds (VOCs) which can be bioactive against pathogenic microbes such as those produced by the endophytic fungus *Muscodor* sp. considered as a biological control agent (Zhang *et al.* 2010) or by

Nodulisporium sp. isolated from *Myroxylon balsamum* (*Fabaceae*) producing VOCs with also biofuel potential (Tess Mends & Yu 2012).

It is known that endophytic fungi have the potential to decompose organic matter such as lignin or cellulose, helping in the balance of nutrients present in the ecosystem and making them available. However, they can also be involved in bioremediation processes to remove waste and pollutants from the environment. For instance, two strains of the endophytic fungus *Pestalotiopsis microspora* were able to use polymer polyester polyurethane as their only source of carbon under aerobic and anaerobic conditions probably due to the enzyme serine hydrolase found in a molecular characterization analysis (Russell *et al.* 2011).

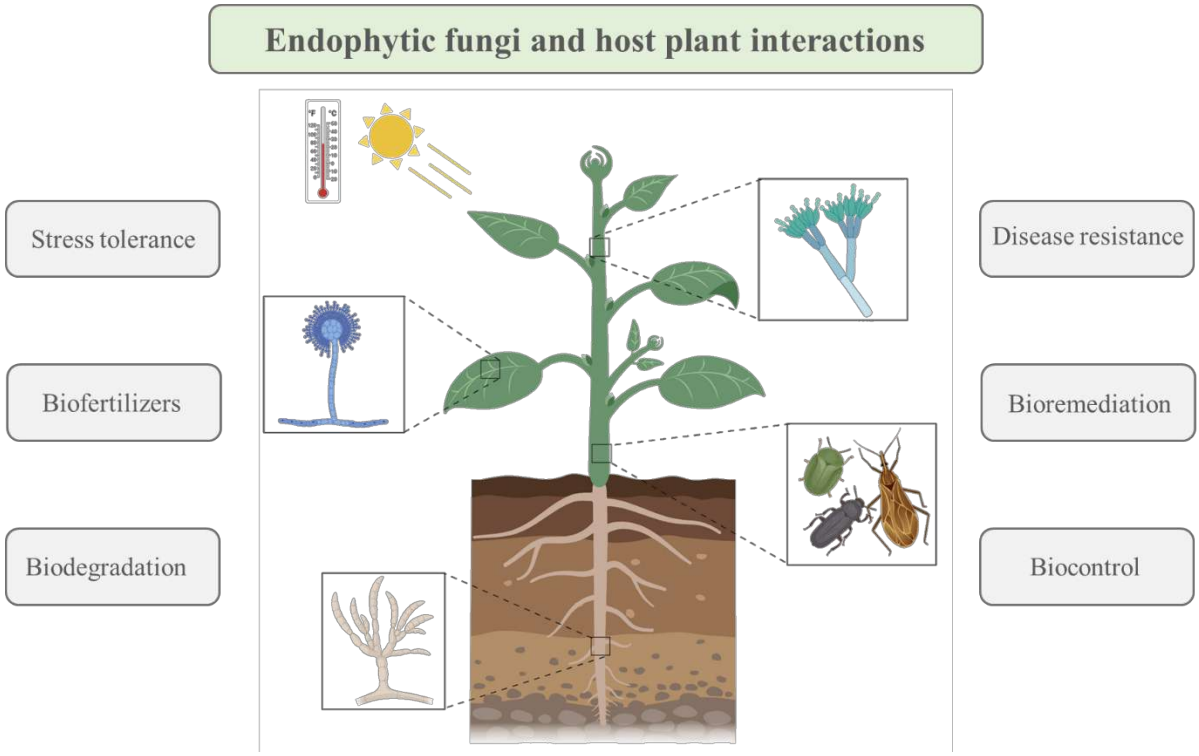

Figure 1.13. Plant growth promotion by endophytic fungi through different mechanisms (own creation using biorender.com)

Plant secondary metabolites produced by endophytic fungi

Some bioactive secondary metabolites produced by plants can also be produced by endophytic fungi besides all the interactions between the host plant and their endophytic fungi mentioned before. The most known example is the production of the anticancer compound paclitaxel by *Taxus brevifolia* (Taxaceae) but also produced by its endophytic fungus *Taxomyces andreanae*. Moreover, at least 20 genera of endophytic fungi have been screened for their ability to produce paclitaxel or its analogues,

isolated from different plant families such as *Spindaceae*, *Rutaceae*, *Cupressaceae*, *Ginkgoaceae*, *Malvaceae*, *Podocarpaceae*, *Taxodiaceae* and *Combretaceae* (Zhao *et al.* 2011). Another example is the production of the anticancer compound camptothecin by *Camptotheca acuminata* (Nyssaceae) and *Nothapodytes foetida* (Icacinaceae) but also by different endophytic fungi belonging to the genera *Botryosphaeria*, *Entrophospora*, *Fusarium*, *Phomopsis*, *Neurospora*, *Trichoderma* and *Alternaria* (Uzma *et al.* 2018).

In addition to these compounds, there are many other plant-derived bioactive secondary metabolites that are produced by endophytic fungi such as piperine (alkaloid), marmesin (coumarin), kaempferol (flavonoid), pinselin (xanthone) and many others, including lignans and saponins (Singh *et al.* 2021).

1.3.4 Procedures for the isolation and identification of fungal endophytes

There are mainly two methodologies for studying endophytes, cultivation-based and cultivation-independent techniques. For recovering isolates on solid culture media, there are no standardized steps for surface sterilization because the solutions and the time of exposure might vary depending on the type of the sampled tissue. In addition to this, the endophyte community present on the plant can be altered depending on the sampling season, the environmental conditions, the growth stage and physiological state of the plant and the genotype of the plant, besides all the culture conditions applied for their recovery (Gouda *et al.* 2016). In this regard, there is a set of steps with important considerations to be taken into account. For instance, it is essential to select a healthy plant tissue to avoid the isolation of pathogen microorganisms and to collect fresh plant material to be used within 24 hours of harvesting to prevent death of endophytes. The surface sterilization is necessary to ensure the isolation of endophytes and not of external contaminants, such as epiphytes or roots actinomycetes.

Washing plant tissues under tap water before sterilization will help to reduce soil particles but also Tween 20 (0.1%) has been used for rinsing. For surface sterilization, strong oxidant or general disinfectant followed by a sterile rinses is the most common procedure. Among the most used solutions for surface sterilization are sodium hypochlorite solution between 2-10%, hydrogen peroxide at 3% or potassium permanganate at 2%, combined with ethanol (70-95%) washing steps and rinses with sterile distilled water (Martinez-Klimova *et al.* 2017). Sterilized surface is aseptically cut into small fragments, between 3 to 5 mm long, to maximize surface exposure to the solid media. Different tissue segments are cut, rinsed and dried under a laminar flow hood and placed over the agar, incubated during 2-4 weeks for posterior isolation (**Figure 1.14**). Generally, plates are discarded after 4 weeks since contaminants are more likely to grow after this time, however certain endophytic fungi might take longer incubation times thus it is important to corroborate this using the control plates containing culture media with water samples.

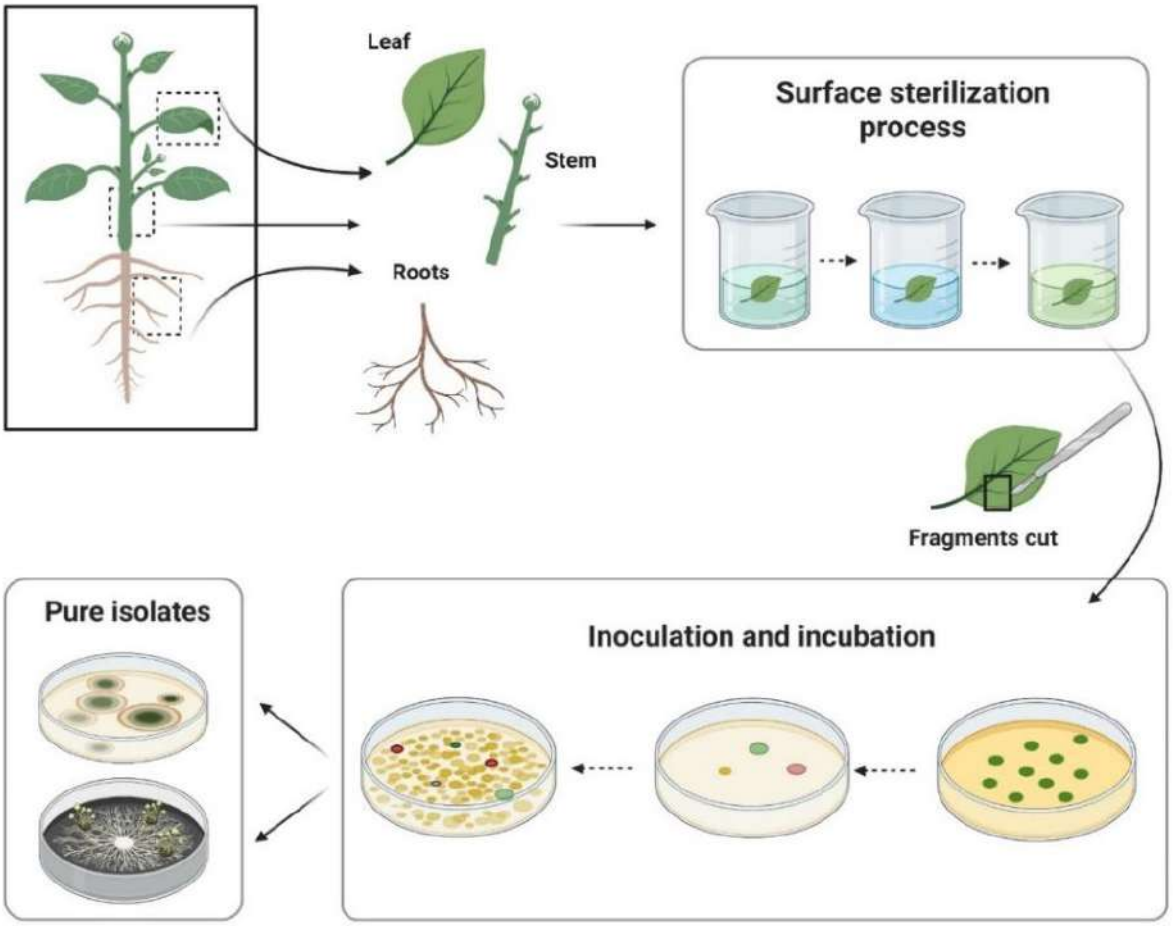

Figure 1.14. Sample preparation for endophyte isolation (own creation using biorender.com)

It is important to mention that several endophytes are not readily cultivable, go undetected or are under-represented. Faddetta and colleagues have observed the occurrence of endophytes through laser scanning microscopy with fluorescence *in situ* (Faddetta *et al.* 2021). For identification of isolates, combinations of microscopic and molecular methods are recommended. For fungi, after the morphology identification, sequence comparisons of 18S rDNA, internal transcriber spacer (ITS1 and ITS2), 5.8S rDNA or 28S subunit of rDNA are done (Zhang *et al.* 2006). Almost 70% of the currently isolated endophytes from different plant tissues are fungi of which 81% are culturable and 19% are considered unculturable. The other 30% of endophytes correspond to bacteria of which 65% are culturable and 45% are considered unculturable, according to the nucleotide database from the National Center for Biotechnology Information (NCBI) (Manias *et al.* 2020).

1.3.5 Novel bioactive compounds from fungal endophytes

As previously mentioned, fungal species have been one of the main sources of bioactive natural products while endophytic fungi represent a promising source of novel and different bioactive secondary metabolites due to their physiological and ecological roles as part of the complex interaction with the host plant and with other microorganisms and pathogens that harbor these types of unexplored niche areas. Recently, 449 new secondary metabolites obtained from endophytic fungi were reported between 2017 and 2019 from 134 journal articles described in a review study (**Figure 1.15**), highlighting that a large percentage correspond to terpenoids and polyketones, followed by alkaloids, steroids and other compounds (Zheng *et al.* 2021). Additionally, many of these secondary metabolites possess structurally diverse new carbon skeletons, unusual ring systems or rare and unique structural moieties biosynthesized by different pathways corresponding to the polyketides, non-ribosomal peptides, and isoprenoids and hybrid products. The last originating from the PKS-NRPS, NRPS-Terpene, PKS-Terpene or PKS-NRPS-Terpene pathways (Gao *et al.* 2018).

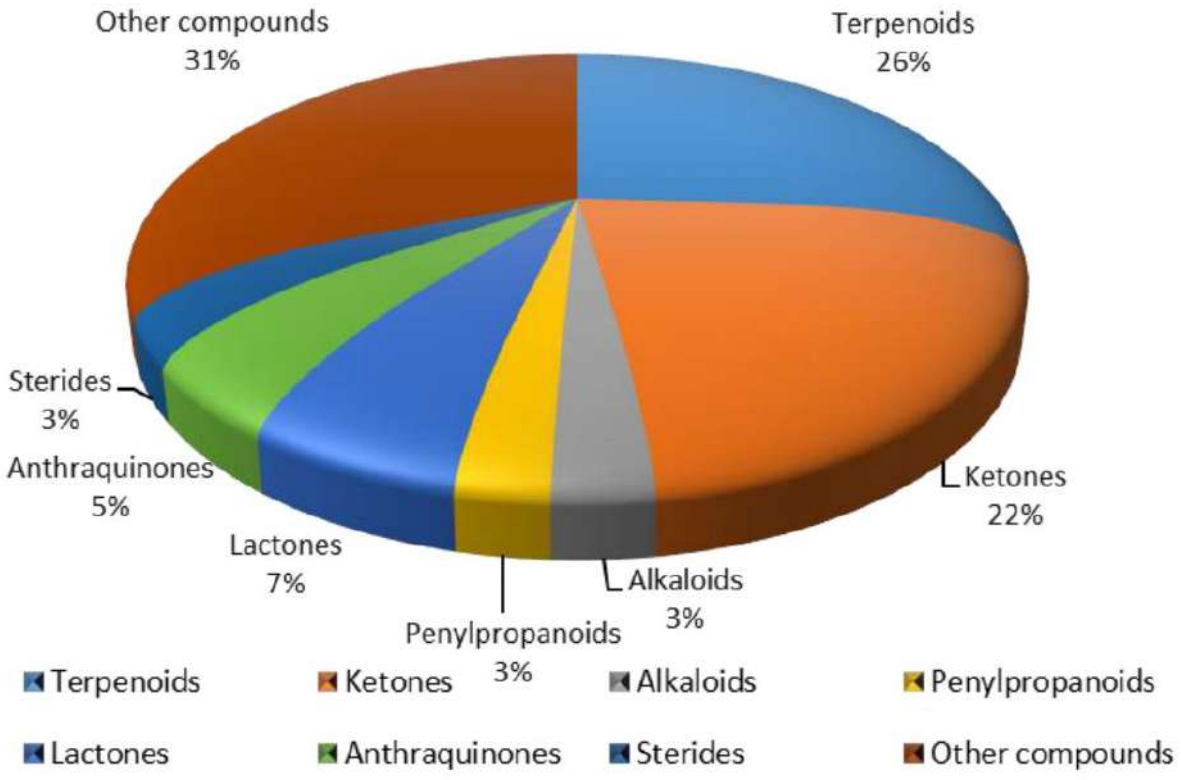

Figure 1.15. Percentage of new secondary metabolites synthesized by endophytic fungi reported from 2017-2019 (*n*=449) (Zheng et al., 2021)

A recent review study analyzed the patent applications made between 2001 and 2019 that were related to the production of secondary metabolites and biotransformation processes by using endophytic fungi. Interestingly, 224 patents correspond to secondary metabolite production while 21 are related to the biotechnological processes such as biotransformation, being *Aspergillus*, *Fusarium*, *Penicillium*, *Trichoderma* and *Phomopsis* the most patented fungi genera (Torres-Mendoza *et al.* 2020).

Endophytic fungi are able to produce chemically diverse bioactive compounds (**Figure 1.16**) that can be renewable and more affordable than the current antimicrobials. Many of these compounds have shown antibacterial, antifungal, anti-parasitic, antiviral, anticancer, antioxidant, immunosuppressive and antidiabetic properties (Manganyi & Ateba 2020; Adeleke & Babalola 2021) important for public health, agriculture, pharmaceutical industries and many other areas (Gupta *et al.* 2020a) and some of them will be mentioned in the following paragraphs.

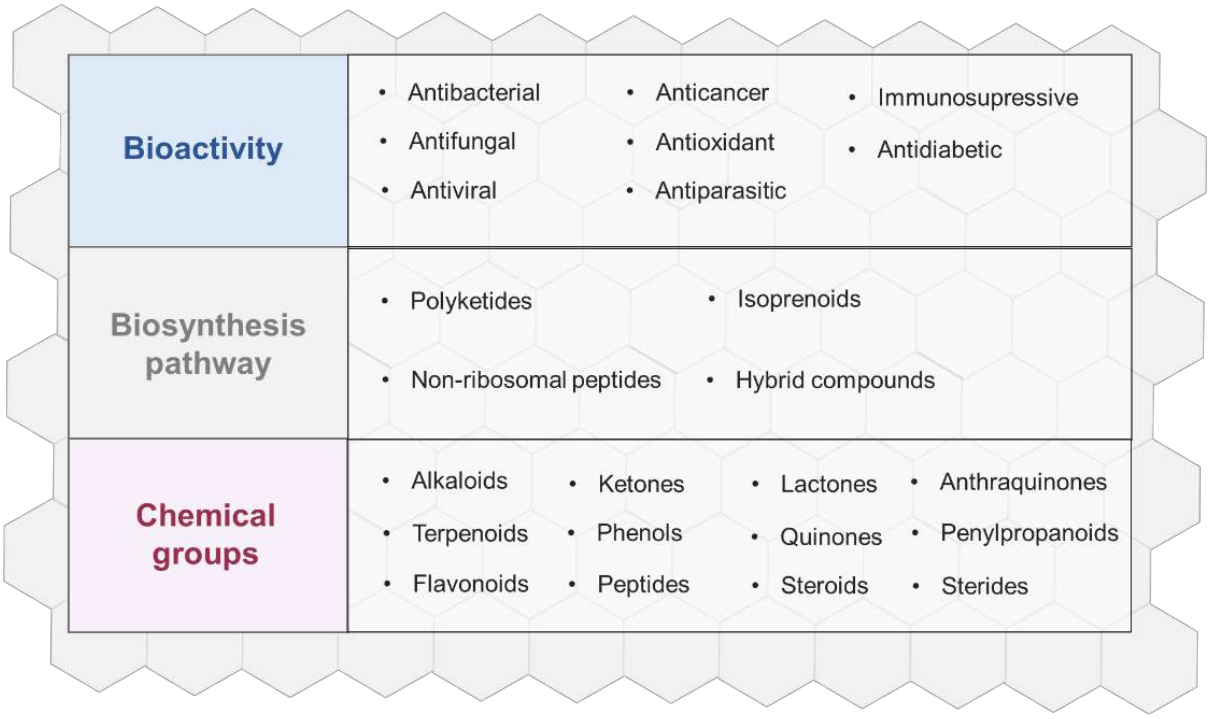

Figure 1.16. Classification of secondary metabolites from fungal endophytes by bioactivity, biosynthetic pathway and chemical group (own creation)

The book chapter entitled "Fungal endophytes: a source of anti-infectives", wrote with my colleagues (Pacheco *et al*., in Press) summarize the antibacterial and antiparasitic compounds isolated from endophytic fungi are largely discussed, specifically those isolated from medicinal plants from areas with great biodiversity (**Annexe**s). In the following, some examples of bioactive compounds isolated from endophytic fungi will be mentioned.

Antibacterial

According to the World Health Organization (WHO), antibiotic resistance is one of the major global health problems with increasing cases of resistance in bacteria such as *Klebsiella pneumoniae*, *Escherichia coli*, *Staphylococcus aureus* (MRSA), *Neisseria gonorrohoeae* and *Mycobacterium tuberculosis*. Two new compounds, xanalteric acid I and II, were isolated from *Alternaria* sp., an endophytic fungus isolated from chinese mangrove plant *Sonneratia alba* (Lythraceae). The 10-oxo-10*H*-phenalenon[1,2,3-*de*]chromene skeleton of these compounds was for the first time reported in fungi. These new carboxylic acids exhibited antibacterial activity against multidrug-resistant *Staphylococcus aureus* (Kjer *et al.* 2009). Another life-threatening disease is tuberculosis caused by *Mycobacterium turberculosis* and commonly associated with compromised human immune systems. Several antitubercular compounds corresponding to different chemical classes such as amides, peptides, polyketides and terpenes have been obtained from endophytic fungi (Alvin *et al.* 2014). For example, endophytic fungus *Fusarium solani* isolated from the medicinal plant *Glycyrrhiza glabra* (Fabaceae) was able to produce a new compound, fusarubin and other known compounds with antimicrobial activity, being fusarubin the compound that showed a good activity against *M. tuberculosis* (Shah *et al.* 2017). In addition to these compounds, three novel aminolipopeptides, trichoderins A, A1 and B were obtained from the endophytic fungus *Trichoderma* sp. isolated from an unidentified marine sponge. These compounds exhibited potent activity against *M. smegmatis*, *M. bovis* and *M. tuberculosis* (Pruksakorn *et al.* 2010). The structures of these compounds are shown in **Figure 1.17**.

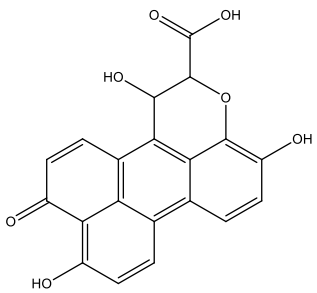

Xaltaneric acid I

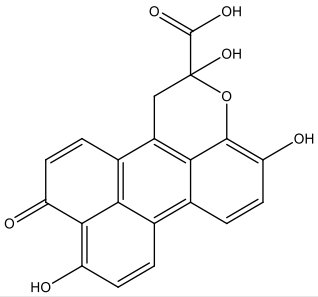

Xaltaneric acid II

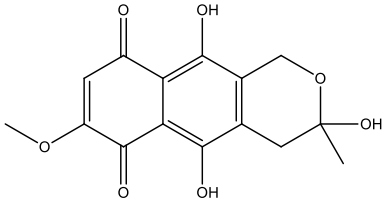

Fusarubin

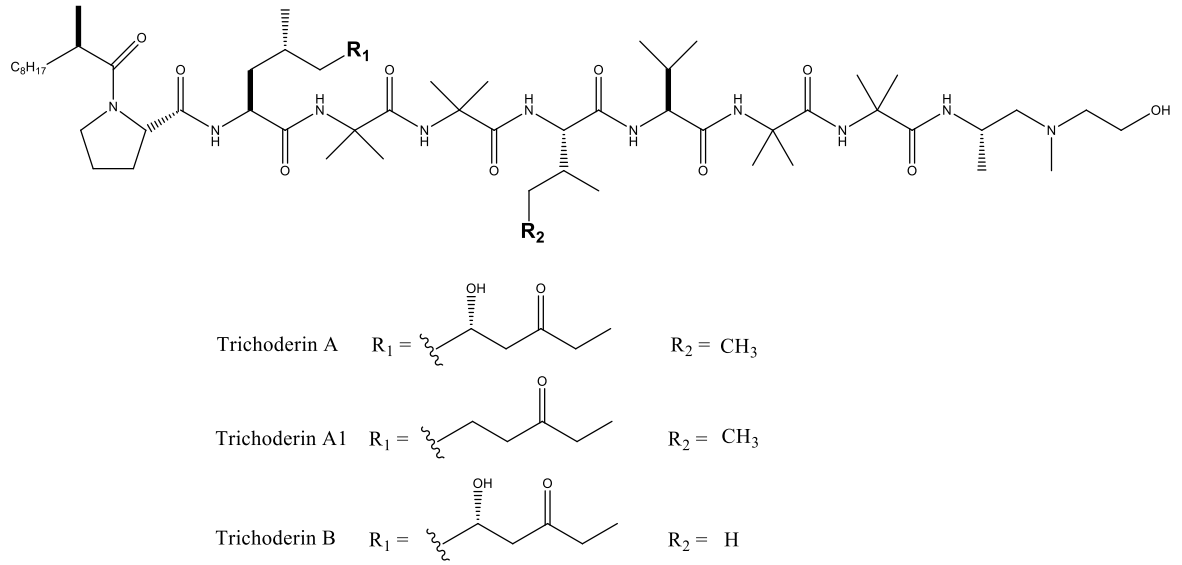

Trichoderin A, Trichoderin A1, Trichoderin B

Figure 1.17 Examples of novel compounds isolated from endophytic fungi with antibacterial activity

Antifungal

Fungal diseases cause 6 millions of human deaths per year while in the agricultural sector, they generate many economic losses, threatening the food security and production. Antibiotic resistance in fungi are dramatically increasing mainly in immunocompromised individuals, posing a serious burden on healthcare systems. Endophytic fungi isolated from medicinal plants have shown to produce chemically diverse secondary metabolites with antifungal activity (Deshmukh *et al.* 2018). Endophytic fungus *Pestalotiopsis adusta*, isolated from the stem of an unidentified chinese tree, produced three new chlorinated benzophenone derivatives, pestalachlorides A-C, which exhibited significant antifungal activity against 3 plant pathogenic fungi, *Fusarium culmorum*, *Gibberella zeae* and *Verticillium albo-atrum* (Li *et al.* 2008). The structures of these compounds are shown in **Figure 1.18**.

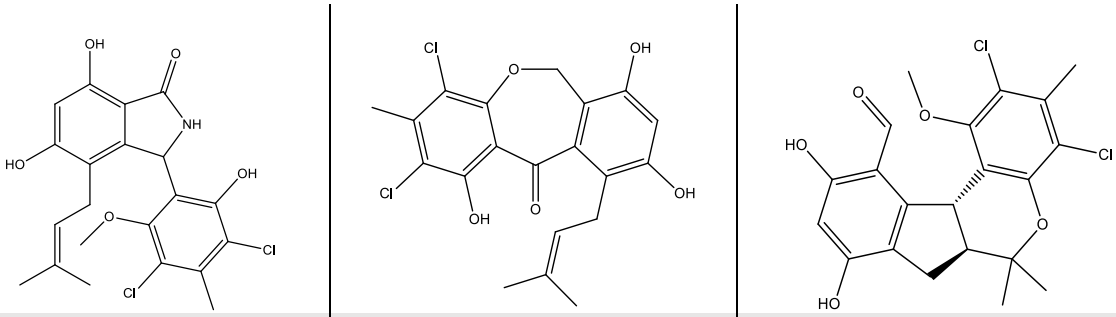

Pestalachloride A	**Pestalachloride B**	**Pestalachloride C**

Figure 1.18. Examples of novel compounds isolated from endophytic fungi with antifungal activity

Antiparasitic

In the research of new drugs for treating tropical diseases such as leishmaniasis (caused by *Leishmania* spp.) or malaria (caused by *Plasmodium* spp.), endophytes have shown to harbor novel metabolites with biological activity. During a 15-year project, more than 2700 isolates were obtained from the fresh leaves of 3198 healthy plant samples (232 different genera) located in different National Parks of Panama possessing high biodiversity. The crude extracts of these endophytic fungi were tested for anti-parasitic activity showing that 16.6% of the isolates were highly active against *P. falciparum*, 15.4% were highly active against *L. donovani* while 4.1% of them were highly active against *T. cruzi* (Higginbotham *et al.* 2013).

The new ergochrome, purpureone was obtained from the endophytic fungus *Purpureocillium lilacinum* isolated from the roots of the medicinal plant *Rauvolfia macrophylla* (Apocynaceae). This compound exhibited a potent activity against the amastigotes of *Leishmania donovani* with a good selectivity index and antimicrobial activity (MIC=62.6 μg mL^{-1}), signaling the promising future investigations for drug development (Lenta *et al.* 2016). Additionally, two novel xanthone dimers, Phomoxanthone A and B, were obtained from the fungal endophyte *Phomopsis sp.* isolated from the leaves of *Tectona crispa* (Lamiaceae). They exhibited activity against *Plasmodium falciparum* K1 (IC_{50}=0.11 - 0.33 μg mL^{-1}) and cytotoxicity (IC_{50}=0.51 - 4.1 μg mL^{-1}) against 3 different cancer cell lines (Isaka *et al.* 2001). The structures of these compounds are shown in **Figure 1.19**.

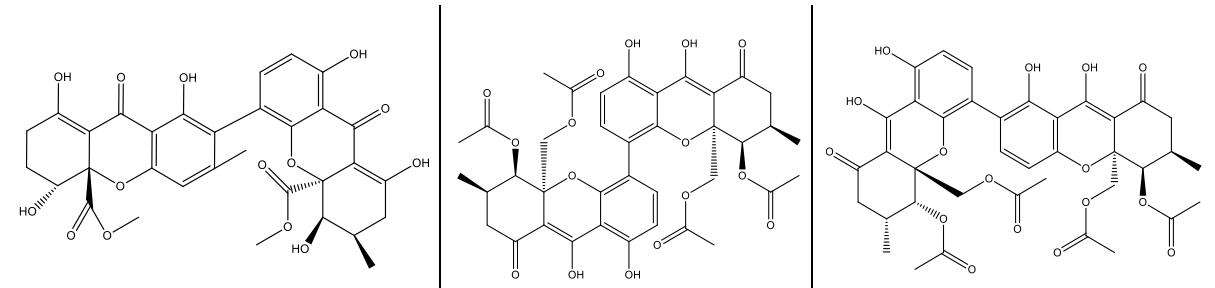

Purpureone	Phomoxanthone A	Phomoxanthone B

Figure 1.19. Examples of novel compounds isolated from endophytic fungi with antiparasitic activity

Antiviral

Viruses are a leading cause of mortality and morbidity. Current antivirals usually target viral proteins or host cellular factors used to reproduce and gain control of host cell processes, however the increasing emergence of resistance of viruses represents an important global public health problem. Some examples have shown that endophytic fungi are able to produce compounds active against some viruses. For

instance, a new rare sesquiterpenoid, phomanolide was recently isolated from the endophytic fungus *Phoma* sp. isolated from the roots of the plant *Aconitum vilmorinianum* (Ranunculaceae). This compound exhibited antiviral activities against influenza A virus (Liu *et al.* 2019). Also, a new hydroanthraquinone derivative, 6-O-demethyl-4-dehydroxyaltersolanol A, exhibited inhibitory effects on an influenza viral strain. This compound was isolated from the endophytic strain of *Nigrospora sp*. obtained from the roots of *Aconitum carmichaeli* (Ranunculaceae) (Zhang *et al.* 2016). The structures of these compounds are shown in **Figure 1.20**.

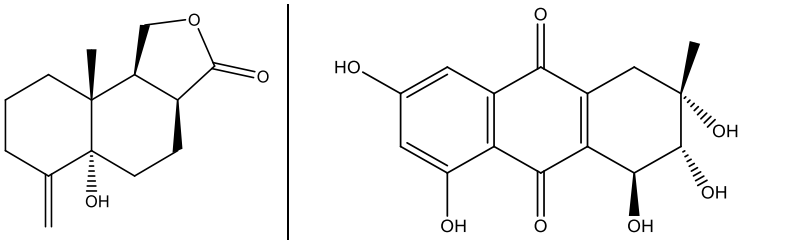

Phomanolide	6-O-demethyl-4-dehydroxyaltersolanol A

Figure 1.20. Examples of novel compounds isolated from endophytic fungi with antiviral activity

Anticancer

Despite all the efforts in developing new chemotherapies, cancer remains a major disease with high human mortality rates. Only in 2018, more than 18 million cancer incidences with almost 10 million of deaths were reported by the WHO. Considering the prolonged use of anticancer drugs and the several threatening side effects, many other sources were evaluated, including endophytic fungi (Li *et al.* 2018) after the discovery of taxol obtained from the endophytic fungus *Taxomyces andreanae*. Three novel azaphilone alkaloids, chaetomugilides A-C, produced by endophytic fungus *Chaetomium globosum,* isolated from the healthy barks of the medicinal plant *Ginkgo biloba* (Ginkgoaceae), exhibited high cytotoxicity against human cancer cell line HePG2 (hepatoblastoma) (Li *et al.* 2013). Other novel compounds were obtained from endophytic fungus *C. globosum* isolated from the fresh tissue of marine green alga *Ulva peftusa* (Ulvaceae). The novel alkaloids, cytoglobosins C and D exhibited cytotoxic activity against A-549 tumor cell line (adenocarcinoma human alveolar basal epithelial cells) (Cui *et al.* 2010). The structures of these compounds are shown in **Figure 1.21**.

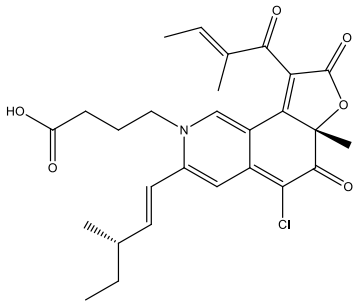

Chaetomugilide A

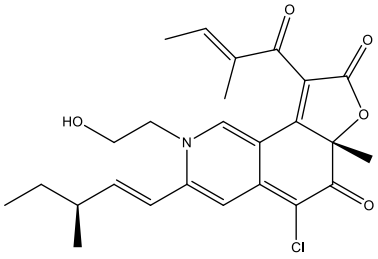

Chaetomugilide B

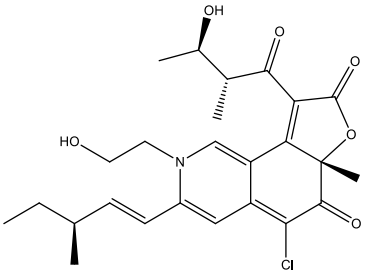

Chaetomugilide C

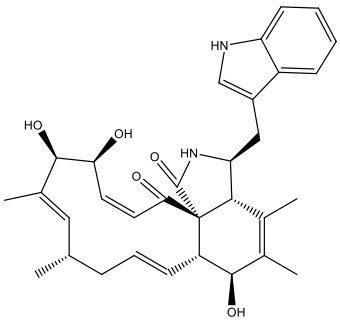

Cytoglobosin C

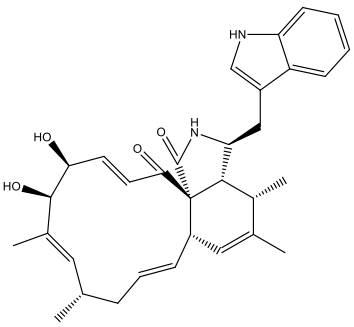

Cytoglobosin D

Figure 1.21. Examples of novel compounds isolated from endophytic fungi with anticancer activity

Antioxidant

Many studies have shown that phenolic acids, phenylpropanoids, flavonoids, melanin and tannins exhibit antioxidant activity. Endophytic fungi are known to produce these types of compounds to confer stress tolerance to the plant under oxidative stress. Additionally, in the human body, free radicals cause cell damage and contribute to cellular degeneration as in Alzheimer's disease, Parkinson's disease, Crohn's disease, atherosclerosis, hepatic and kidney damage, among other disorders influenced by oxidative stress. Extracts and compounds with strong antioxidant activities have been isolated from endophytic fungi colonizing medicinal plants from diverse environments (Kouipou Toghueo & Boyom 2019). Isopestacin is a new isobenzofuranone with a unique core, obtained from endophytic fungus *Pestalotiopsis microspora* isolated from the tropical plant *Terminalia morobensis* (Combretaceae). Besides its antifungal activity, it behaves as an antioxidant against superoxide and hydroxyl free radicals (Strobel *et al.* 2002). Moreover, a total of 42 endophytic fungi were isolated from *Nerium oleander* (Apocynaceae) and tested for their antioxidant activity, of which one strain of *Chaetomium* sp. showed the strongest antioxidant capacity, probably due to the high levels of phenolic acids and their derivatives and flavonoids detected in the fungal cultures (Huang *et al.* 2007). The structures of these compounds are shown in **Figure 1.22**.

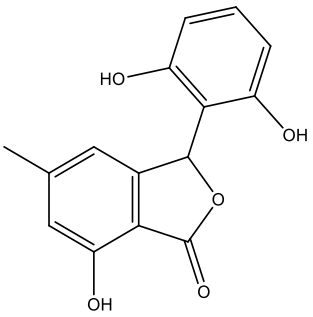

Isopestacin

Figure 1.22. Example of a novel compound isolated from endophytic fungi with antioxidant activity

Immunosuppressive

Immunosuppressive drugs are important for treating autoimmune disorders or during organ transplants to suppress or reduce rejection. Fungal endophytes have shown to produce secondary metabolites with immunomodulatory activity and immunosuppressive action with low cytotoxicity and high selectivity. For instance, the endophytic fungus *Mycosphaerella nawae* isolated from the leaves of the medicinal plant *Smilax china* (Smilacaceae) produced a novel amide derivative, (-)mycousnine enamine that selectively inhibited the proliferation of T cells through the inhibition of the expression of antigens CD25 and CD29 (Wang *et al.* 2017b). Moreover, the endophytic fungus *Penicillium* sp. isolated from the leaves of the mangrove plant *Sonneratia apetala* (Lythraceae), produced 9 polyketides including 2 novel benzophenone derivatives, peniphenone and methyl peniphenone, with immunosuppressive properties (Liu *et al.* 2016). The structures of these compounds are shown in **Figure 1.23**.

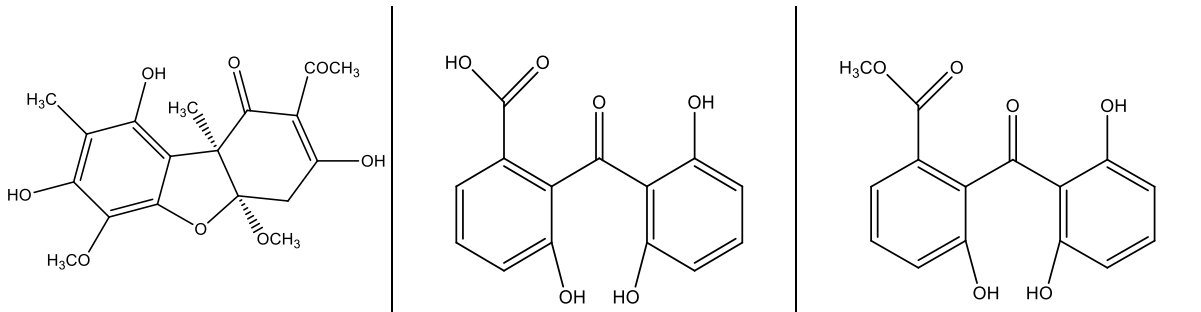

Mycousnine | **Peniphenone** | **Methyl peniphenone**

Figure 1.23. Examples of novel compounds isolated from endophytic fungi with immunosuppressive activity

Among the fungal endophytes, Dothideomycetes is one of the largest and most diverse class in Ascomycete fungi (Schoch *et al.* 2009). Among them, the Botryosphaeriales order contains the Botryosphaeria family and the species Cophinforma mamane, the object of this thesis. The following sections will give a special focus on this order and family, as well as the current knowledge about this fungus.

1.4 Botryosphaeriales order (Dothideomycetes)

There is an increased interest in the study of the Botryosphaeriales order and especially in the species within the Botryosphaeriaceae family which is evidenced by the number of publications found on SciFinder over the last years containing "Botryosphaeriales" and "Botryosphaeriaceae" (**Figure 1.24**). This increase is related to the continuous efforts for a better taxonomic classification of the diverse fungal species but also due to their ecological importance as pathogens of important plant families and to their linkage to climate and anthropogenic changes to the environment (Slippers *et al.* 2017).

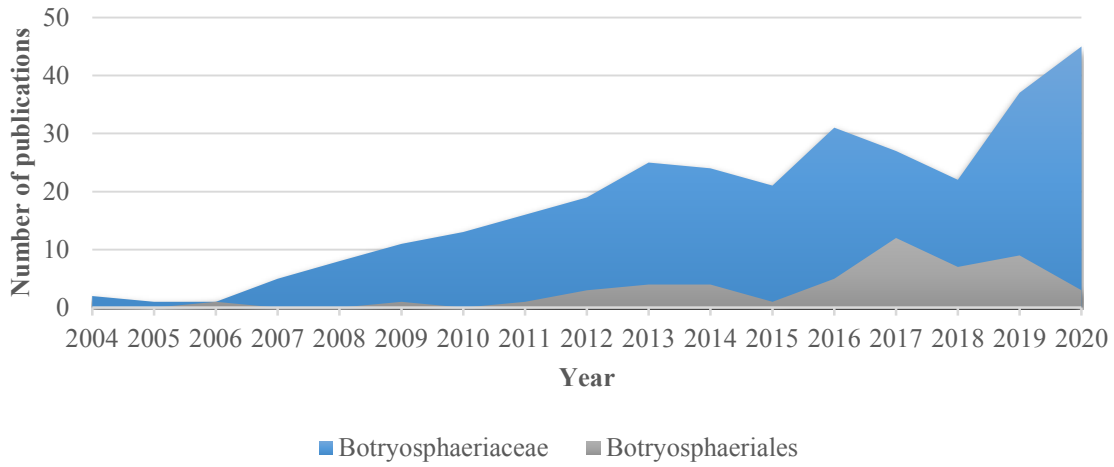

Figure 1.24. Number of Journal publications and patents including "Botryosphaeriales" or "Botryosphaeriaceae" over the last years according to SciFinder

The Botryosphaeriales order includes endophytic and saprophytic fungal species but most commonly pathogenic species associated with branches, leaves, fruits or seeds of woody plants distributed worldwide (Slippers *et al.* 2017). In 2006, the Botryosphaeriales order was introduced for the Botryosphaeriaceae family and since then, the number of families residing in this order has been increasing (Slippers *et al.* 2013). Many of the re-assignations of the taxonomic groups based on DNA sequence data did not find a consensus due to the different genes or loci used for the phylogenetic reconstructions.

One of the last re-assessment of this order in terms of morphology, phylogenetic relationships based on ITS (Internal transcribed spacer) and LSU (large-subunit rRNA) sequences and evolutionary divergence allowed to consider 6 linages that represent the families in the Botryosphaeriales (**Table 1.2**): *Aplosporellaceae*, *Botryosphaeriaceae*, *Melanopsaceae*, *Phyllostictaceae*, *Planistromellaceae* and *Saccharataceae* (Phillips *et al.* 2019). However, in a precedent study, 8 families were recognized as part of the Botryosphaeriales order in addition to the newly described families, *Endomelanconiopsisaceae* and *Pseudofusicoccumaceae* (Yang *et al.* 2017). This family went under dramatic taxonomic changes

mainly at the family level, besides the definition for the recognition of cryptic and hybrid species, essential for the understanding of the Botryosphaeriales diversity (Slippers *et al.* 2017). More recently, a multigene phylogenetic analysis was performed using the sequences of ITS, LSU, *tef1* (translation elongation factor 1-alpha gene), *tub2* (beta-tubulin gene) and *rpb2* (RNA polymerase II second largest subunit gene) for 230 fungal isolates, where 8 novel species were described within a total of 33 genera recognized for the Botryosphaeriales order, of which the majority belong to the Botryosphaeriaceae family (Zhang *et al.* 2021).

Table 1.2. Families and genera described in the Botryosphaeriales by different authors

Family	Genus	Author		
		Yang et al., 2017	**Slippers et al., 2017**	**Phillips et al., 2019**
Aplosporellaceae	*Aplosporella*	X	X	X
	Bagnisiella	X	X	X
	Alanomyces	-	-	X
Botryosphaeriaceae	*Alanphillipsia*	X	X	X
	Bahusutrabeeja	-	X	-
	Barriopsis	X	X	X
	Botryobambusa	-	X	X
	Botryosphaeria	X	X	X
	Cophinforma	X	X	X
	Diplodia	X	X	X
	Dothiorella	X	X	X
	Endomelanconiopsis	-	Other family	X
	Eutiarospella	X	X	-
	Lasiodiplodia	X	X	X
	Macrophomina	X	X	X
	Marasasiomyces	X	X	-
	Mucoharknessia	-	X	-
	Neodeightonia	X	X	X
	Neofusicoccum	X	X	X
	Neoscytalidium	X	X	X
	Oblomgocollomyces	X	X	X
	Otthia	-	X	-
	Phaeobotryon	X	X	X
	Pseodofusicoccum	-	Other family	X
	Sakireeta	X	X	-
	Sardiniella	-	X	-
	Spencermartinsia	(=Dothiorella)	(=Dothiorella)	-
	Sphaeropsis	-	X	X
	Tiarosporella	X	X	X

Endomelanopsisaceae	*Endomelanconiopsis*	X	X	Other family
Melanopsaceae	*Melanops*	X	X	X
Phyllostictaceae	*Phyllosticta*	-	X	X
	Pseudofusicoccum	Other family	Other family	X
Planistromellaceae	*Kellermania*	X	X	X
	Umthunziomyces	-	X	X
Pseudofusicoccumaceae	*Pseudofusicoccum*	X	X	Other family
	Saccharata	Other family	X	Other family
Saccharataceae	*Saccharata*	X	Other family	X
	Neoseptorioides	-	-	X
	Septorioides	Other family	Other family	X
Septorioideaceae	*Septorioides*	X	X	Other family

1.4.1 Botryosphaeriaceae family

Botryosphaeriaceae is the largest family within the Botryosphaeriales order, generally existing as hemibiotrophic [3] in healthy plant tissues but also as endophytes or saprobes. They possess a cosmopolitan distribution and a diverse morphology, where the conidial features are the most informative characters for differentiation such as pigmentation, wall thickness and septation. Despite the efforts for a better taxonomic classification and the gained knowledge about their phylogenetic divergence, there are still some differences in the consensus about the number of genera belonging to this family. Besides the genera shown in **Table 1.2** for Botryosphaeriaceae, two other studies recognize a total of 24 well-defined genera with more than 200 species (Burgess *et al.* 2019; Garcia *et al.* 2021). In general, the ecology of the taxa from Botryosphaeriaceae is complex added to the fact that some fungi have been considered as pathogenic species but later, they have been found during their endophytic phase and reported as such.

In the case of infection of horticultural crops, ecological genomic comparisons of isolates originating from different symptomatic crops showed that gene expansion falls mainly into lytic capabilities and putative transporters, which are related to pathogenicity. The genome sequences of 17 species representing 6 genera of these family, indicated that species with gene families in expansion, encoding for secreted cell wall degrading enzymes, secondary metabolism and transporters, are the most virulent ones such as species from the genera *Lasiodiplodia*, *Botryosphaeria* and *Neofusicoccum* (Garcia *et al.* 2021).

Considering climate change, mainly the increase of temperature, environmental conditions have shown to modify symbiotic or commensal interactions into pathogenic interactions. Under this scenario,

[3] Hemibiotrophic: group of plant pathogens that require living plant tissue to survive and complete their life cycle

frequent extreme temperatures and prolonged droughts can make this transit of interactions easier. For example, filtrates of 5 species of Botryosphaeriaceae showed to be dramatically more phytotoxic and cytotoxic when the temperature of culture changed from 25 to 37°C, indicating that in during a global increase of temperature, this species might contribute to plant and even to human infections (Nazar Pour *et al.* 2020).

A diverse range of bioactive secondary metabolites are produced by members of the Botryosphaeriaceae family, of which most of them are associated with plant host diseases, however further studies are needed to understand whether or not these metabolites are related with their virulence. It is known that during their endophytic life, they do not cause apparent damage to the host cell and do not generate a host response. Despite this, when the host gets subjected to different stress factors, they might become latent pathogens. In this regard, it is suggested that climate change will continue to trigger stress on plant species and this will indirectly affect the interactions between the plant and their fungal communities.

Most of the bioactive secondary metabolites reported in the literature produced by members of the Botryosphaeriaceae family were isolated from species belonging to the genera *Botryosphaeria*, *Diplodia*, *Dothiorella*, *Lasiodiplodia*, *Neofusicoccum* and *Sphaeropsis* (Kumar 2020) and they are shown in **Table 1.3**.

Table 1.3. Main bioactive compounds from the Botryosphaeriaceae Family

Genus	Species	Compound	Bioactivity	Reference
Botryosphaeria	*rhodina*	Botryorhodine A-D	Antifungal, cytotoxic	Abdou (2010)
	species	Botryosphaerin H	Antifungal, nematicidal	Chen (2015)
	obtusa	(3R,4R)-4,7-dihydroxymellein	Phytotoxins	Djoukeng (2009)
	species	Botryoisocoumarin A	COX-2 inhibitor	Ju (2015)
	species	Botryosphaerin B	COX-2 inhibitor	Ju (2016)
	rhodina	Botryosphaerilactone A-C	Antibacterial	Rukachaisirikul (2009)
	rhodina	Botryosphaeridione	Antibacterial	Rukachaisirikul (2009)
	rhodina	Botryosphaerihydrofuran	Antibacterial	Rukachaisirikul (2009)
	rhodina	Botryosphaerinone	Antibacterial	Rukachaisirikul (2009)
	rhodina	Botryosphaeriodiplodin	Antibacterial	Rukachaisirikul (2009)
	obtusa	Melleins	Phytotoxins	Venkatasubbaiah (1991)
	obtusa	Tyrosol	Phytotoxins	Venkatasubbaiah (1991)
	obtusa	4-hydroxymellein	Phytotoxins	Venkatasubbaiah (1991)
	obtusa	5-hydroxymellein	Phytotoxins	Venkatasubbaiah (1991)
	obtusa	4-hydroxybenzaldehyde	Phytotoxins	Venkatasubbaiah (1991)
	rhodina	Botryosphaeran	Immunomodulatory, antioxidant, antitumor, hypoglycemic, hypocholesterolemic	Weng (2011)

	dothidea	3-Hydroxy-2-methoxy-5-methylpyridin-2(1H)-one	Antimicrobial, antioxidant, cytotoxic	Xiao (2014)
	dothidea	Pycnophorin	Antimicrobial	Xiao (2014)
	dothidea	Stemphyperylenol	Antifungal	Xiao (2014)
	dothidea	Altenuene	Cytotoxic	Xiao (2014)
	dothidea	Altenusin	Antioxidant	Xiao (2014)
	dothidea	Djalonensone	Antioxidant	Xiao (2014)
	australis	6-Ethyl-2,7-dimethoxyjuglon	Phytotoxic	Xu (2011)
	australis	6-Ethyl-2,7-dimethoxyjuglon derivative	Cytotoxic, antimicrobial	Xu (2011)
	species	Botryosphaerin A-E	Antibacterial	Yuan (2009)
Diplodia	*quercivora*	Diplopimarane	Phytotoxic	Andolfi (2014b)
	quercivora	Sphaeropsidin A	Antifungal	Andolfi (2014b)
	corticola	Diorcinol	Phytotoxic	Cimmino (2016b)
	mutila	Diplopyrone	Phytotoxic	Evidente (2003)
	corticola	Diplofuranone A	Phytotoxic	Evidente (2007)
	cupressi	Sphaeropsidone	Phytotoxic	Evidente (2011a)
	cupressi	Sphaeropsidin A	Phytotoxic	Evidente (2011b)
	africana	Afritoxinone A	Phytotoxic	Evidente (2012)
	mutila	Diploquinone A-B	Phytotoxic	Reveglia (2018a)
	mutila	Vanillic acid	Phytotoxic	Reveglia (2018a)
Dothiorella	*vidmadera*	Resorcinol	Phytotoxic	Reveglia (2018b)
	vidmadera	Protocatechuic alcohol isopropyl ether	Phytotoxic	Reveglia (2018b)
	vidmadera	Benzene-1,2,4-triol	Phytotoxic	Reveglia (2018b)
	vidmadera	3-Hydroxymethyl phenol	Phytotoxic	Reveglia (2018b)
	vidmadera	Protocatechuic alcohol	Phytotoxic	Reveglia (2018b)
	vidmadera	Tyrosol	Phytotoxic	Reveglia (2020)
Lasiodiplodia	*pseudotheobromae*	Mellein	Bioherbicidal	Adetunji (2018)
	theobromae	Jasmonic acid	Plant growth inhibitor	Alridge (1971)
	Species	Lasiojasmonate A	Phytotoxic	Andolfi (2014a)
	Mediterranea	Lasiolactol A-B	Phytotoxic	Andolfi (2016)
	species	Lasicicol	Alfa-glucosidase inhibitory activity	Chen (2015)
	theobromae	Chloropreussomerin A-B	Cytotoxic, Antibacterial	Chen (2016b)
	theobromae	Preussomerin A, F, G, H	Antibacterial	Chen (2016b)
	brasiliense	(3R,4S)-(−)-4-Hydroxymellein	Phytotoxic	Cimmino (2017)
	theobromae	3-Indolecarboxylic acid	Phytotoxic	Felix (2018b)
	species	Adeninealkylresorcinol	Antioxidant	Gao (2016)
	species	Lasiosan	Antimicrobial, anti-biofilm, antioxidant, immunomodulatory	Kumar (2018)
	species	7-Oxolasiodiplodin	Cytotoxic	Li (2016)
	species	Ethyl-2,4-Dihydroxy-6-nonylbenzoate	Cytotoxic	Li (2016)
	pseudotheobromae	Palmarumycin LP1	Cytotoxic	Lü (2014)

	pseudotheobromae	Cladospirone B	Cytotoxic	Lü (2014)
	theobromae	(R)-(−)-2-Octeno-δ-lactone	Insect attractant	Matsumoto and Nago (1994)
	theobromae	Cyclohexenone derivatives	Phytotoxic	Matsuura (1998b)
	theobromae	Lasiodiplodin	Cytotoxic	Sultan (2014)
	theobromae	Ethyl linoleate	Plant growth regulator	Uranga (2016)
	theobromae	Ethyl palmitate	Plant growth regulator	Uranga (2016)
	theobromae	Ethyl stereate	Plant growth regulator	Uranga (2016)
	pseudotheobromae	Lasiodipline A-F	Antibacterial	Wei (2014)
	theobromae	Maculosin	Antibacterial	Zaher (2015)
Neofusicoccum	*parvum*	(+)-Epi-sphaeropsidone	Phytotoxic	Abou-Mansour (2015)
	australe	Cyclobotryoxide	Phytotoxic	Andolfi (2012)
	parvum	Botryosphaerone D	Phytotoxic	Burruano (2016)
	parvum	Exopolysaccharide	Phytotoxic	Cimmino (2016a)
	luteum	Exopolysaccharide	Phytotoxic	Martos (2008)
Spencermartinsia	*viticola*	Spencertoxin	Phytotoxic	Reveglia (2020)
	viticola	p-Hydroxybenzaldehyde	Phytotoxic	Reveglia (2020)
	viticola	2-(4-Hydroxyphenyl) acetic acid	Phytotoxic	Reveglia (2020)
Sphaeropsis	*sapinea*	R-(−)-Mellein	Phytotoxic	Cabras (2006)
	sapinea	(3R,4R)-4-hydroxymellein	Phytotoxic	Cabras (2006)
	sapinea	(3R,4S)-4-hydroxymellein	Phytotoxic	Cabras (2006)
	sapinea	Sphaeropsidin A - C	Phytotoxic	Evidente (1997)

1.4.2 *Cophinforma mamane* (*Botryosphaeria mamane* D.E. Gardner) A. J. L. Phillips & A. Alves

Botryosphaeria mamane was first described in an endemic Hawaiian tree, *Sophora chrysophylla* (Fabaceae), associated with witches' broom disease (Gardner 1997). Unfortunately, the ex-type cultures of this strain no longer exist and no other sequences were generated after the ones published in Genbank under the codes AF246929 and AF246930. Later, this endophyte was described in other plants such in *Garcinia mangostana* (Clusiaceae) (Pongcharoen *et al.* 2007), in the medicinal Amazonian plants *Carapa guianensis* (Meliaceae) (Ferreira *et al.* 2015) and in *Bixa orellana* (Bixaceae) (Barakat *et al.* 2019). A similar species was also found in *Acacia*, *Eucalyptus* and *Pinus* species from Venezuela (Mohali *et al.* 2007) but it was later considered to represent *Cophinforma atrovirens* (Phillips *et al.* 2013). Additionally, the genus *Cophinforma* was introduced in 2012 to better accommodate the species

C. eucalypti (Liu *et al.* 2012) while in 2013, the species *Botryosphaeria mamane* was recognized as a basionym of *Cophinforma mamane* (Phillips *et al.* 2013).

Few chemical studies have been performed on *C. mamane*. Currently, only 17 compounds have been isolated from different strains of this species. One new dihydrobenzofuran derivative, botryomaman and six other known compounds were obtained from *Botryosphaeria mamane* isolated from *Garcinia mangostana* (Clusiaceae). All these compounds were tested for antibacterial activity, primin being the one that exhibited bioactivity (MIC 8µg/mL) against two strains of *Staphylococcus aureus* (Pongcharoen *et al.* 2007). Moreover, volatile organic compounds (VOCs) were obtained from different endophytic fungi of the Botryosphaeriaceae family, including 6 VOCs isolated from one strain of *Botryosphaeria mamane* isolated from diverse brazilian plants (species not specified) (Oliveira *et al.* 2015). Also, three novel thiodiketopiperazines were isolated from the endophytic fungus *Botryosphaeria mamane* isolated from the healthy leaves of *Bixa orellana* (Bixaceae). These compounds present sulfur atoms on rarely described –α and –β positions of phenylalanine derived residues and also two unprecedented spirocyclic centers at C4 and C2'. Botryosulfuranols A-C exhibited cytotoxic activity against 4 different cancer cell lines (Barakat *et al.* 2019). A fourth thiodiketopiperazine, botryosulfuranol D, has also been isolated from this strain (unpublished data). These compounds are listed in **Table 1.4** and their respective structures are shown in **Figure 1.25**.

Table 1.4. Compounds isolated from *Cophinforma mamane* (*Botryosphaeria mamane*)

N°	Compound	Bioactivity	Reference
1	Botryomaman	>128µg/mL against SA and MRSA	Pongcharoen (2007)
2	2,4-dimethoxy-6-pentylphenol	>128µg/mL against SA and MRSA	Pongcharoen (2007)
3	(R)-(-)-mellein	>128µg/mL against SA and MRSA	Pongcharoen (2007)
4	cis-4-hydroxymellein	>128µg/mL against SA and MRSA	Pongcharoen (2007)
5	trans-4-hydroxymellein	>128µg/mL against SA and MRSA	Pongcharoen (2007)
6	4,5-dihydroxy-2-hexenoic acid	>128µg/mL against SA and MRSA	Pongcharoen (2007)
7	Primin	8 µg/mL against SA and MRSA	Pongcharoen (2007)
8	Isobutanol	-	Oliveira (2015)
9	Isopentyl alcohol	-	Oliveira (2015)
10	2-Methylbutan-1-ol	-	Oliveira (2015)
11	Phenylethyl alcohol	-	Oliveira (2015)
12	Aristolene	-	Oliveira (2015)
13	α-Selinene	-	Oliveira (2015)
14	Botryosulfuranol A	Antiparasitic (IC_{50}=0.69 µM) against *L. infantum* amastigotes; Cytotoxic (CC_{50} 8 - 23.5 µM) against 4 cancer cell lines	Barakat (2019)
15	Botryosulfuranol B	Antiparasitic (IC_{50}=3.87 µM) against *L. infantum* amastigotes Cytotoxic (CC_{50} 49.9 - >100 µM) against 4 cancer cell lines	Barakat (2019)

16	Botryosulfuranol C	Antiparasitic (IC_{50}=0.44 µM) against *L. infantum* amastigotes Cytotoxic (CC_{50} 15.9 - >100 µM) against 4 cancer cell lines	Barakat (2019)
17	Botryosulfuranol D	Antiparasitic (IC_{50}=0.03 µM) against *L. infantum* amastigotes	Barakat (2019)

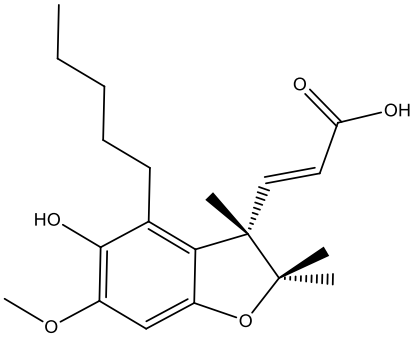

(1) Botryomaman

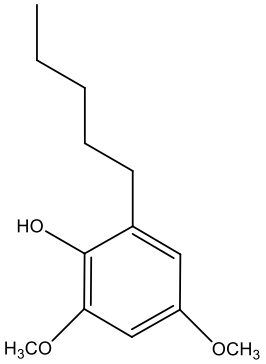

(2) 2,4-dimethoxy-6-pentylphenol

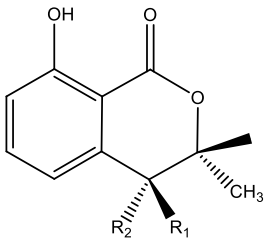

(3) (R)-(-)-mellein; $R_1 = R_2 = H$
(4) *cis*-4-hydroxymellein; $R_1 = H$, $R_2 = OH$
(5) trans-4-hydroxymellein; $R_1 = OH$, $R_2 = H$

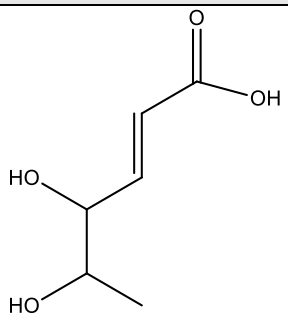

(6) 4,5-dihydroxy-2-hexenoic acid

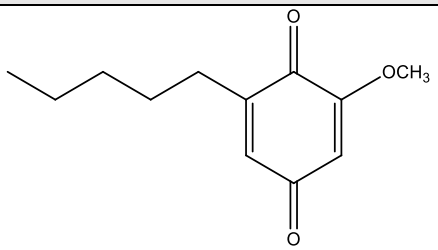

(7) Primin

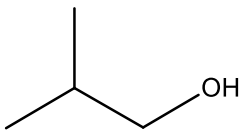

(8) Isobutanol

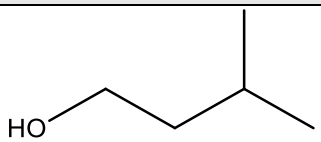

(9) Isopentyl alcohol

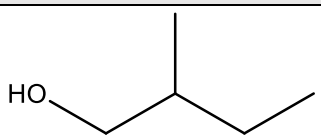

(10) 2-Methylbutan-1-ol

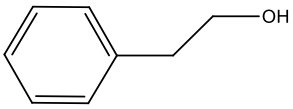

(11) Phenylethyl alcohol

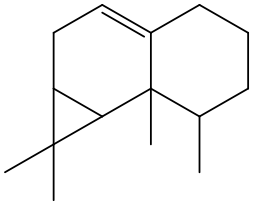

(12) Aristolene

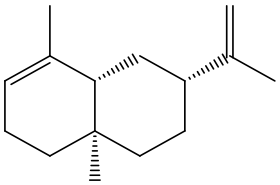

(13) α-Selinene

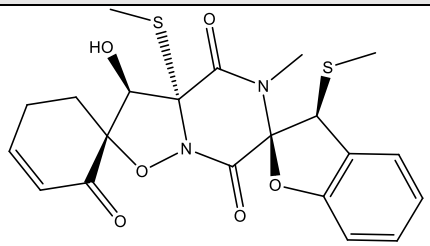

(14) Botryosulfuranol A

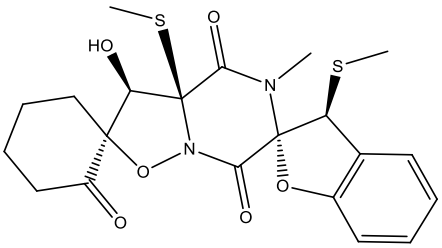

(15) Botryosulfuranol B

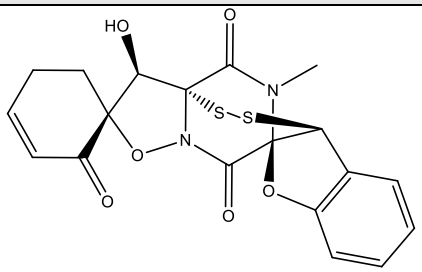

(16) Botryosulfuranol C

Figure 1.25. Structures of compounds isolated from *Cophinforma mamane* (*Botryosphaeria mamane*)

Regarding the plants used in traditional medicine and also used for the isolation of endophytic fungi, the following section will focus on the plant *Bixa orellana*, from which the fungus *Cophinforma mamane* E224 and other endophytes were isolated.

Bixa orellana L. (Bixaceae) as a source of endophytes

Bixa orellana L. is a tropical tree from the Bixaceae family (**Figure 1.26**), native from the Central and South American rainforests known under the common names of annatto, achiote, urucum, urucu or roucou. One of the main uses by the Amazonian tribes is the colored ink of the seeds for body painting. Traditionally, it is used to treat various diseases and ailments such as fevers, inflammatory conditions, parasitic diseases, dysentery, vomiting, heartburn, prostate, urinary difficulties and stomach problems (Giorgi *et al.* 2013). It also has a commercial use for food industry, textiles, dye manufacturing and printing industry due to its high content of the red-colored carotenoid, bixin (Vilar *et al.* 2014).

Figure 1.26. Plant of *Bixa orellana* (a) with their fruits (b, c) and seeds (d) (Raddatz-Mota *et al*., 2017)

Several studies have shown the different biological activities of the leaves, seeds and roots of *B. orellana* while some the findings are in accordance with the traditional use. For instance, the ethanolic extract of the plant seeds showed significant activity against promastigotes and amastigotes of *Leishmania amazonensis* (García *et al.* 2011). Similarly, the hairy root culture of *B. orellana* was extracted with ethyl acetate for the isolation of major compounds. Both crude extract and isolated compounds exhibited activity against *Plasmodium falciparum* (Zhai *et al.* 2014). Regarding its antimicrobial activity, the methanolic extracts of the seeds and leaves of *B. orellana* showed significant activity against bacteria such as *Staphylococcus aureus, Salmonella typhi, Klebsiella pneumoniae*, *Pseudomonas aeruginosa, Enterococcus faecalis, Vibrio cholera, Moraxella catarrhalis, Acinetobacter* sp.*, Brucella* sp. and against fungi such as *Trichophyton mentagrophytes* and *Trichophyton rubrum* (Tamil Selvi *et al.* 2011). The hydroalcoholic and ethyl acetate fractions of the leaves exhibited also antimicrobial activity against *Mycobacterium abscessus* accompanied by anti-inflammatory activity in a peritonitis model induced in mice by *M. abscessus* (Lima Viana *et al.* 2018). Additionally, the aqueous extract of the seeds from a plant collected in the northeast of Brazil was capable of reversing the hypertriglyceridemia induced in mice (Ferreira *et al.* 2013) while the aqueous extract of the leaves from *B. orellana* collected in Malaysia showed anti-inflammatory activity produced by histamine in rats (Yong *et al.* 2013).

Compounds isolated from different parts of this plant are chemically diverse, such as carotenoids, apocarotenoids, sterols, aliphatic compounds, terpenoids and terpenes, volatile compounds (essential oils) and many others have been described from all the plant parts from *Bixa orellana* (Giorgi *et al.* 2013; Vilar *et al.* 2014; Shahid-ul-Islam *et al.* 2016).

Regarding the use of the plant for the isolation of endophytes, different parts of a healthy plant of *B. orellana* growing in an Indian forest were collected for the isolation of fungal endophytes (Kannan 2017). This was the first report on endophytic fungi documented from this medicinal plant, where 300 segments of stem cuttings, leaves and roots were used. The identification was based on morphology of the isolates. Isolates from the leaves were identified as *Pestalotiopsis* sp., *Phoma* sp., *Phyllosticta* sp. and *Alternaria* sp., *Colletotrichum* sp. and *Nigrospora* sp. Stem was dominated by *Pestalotiopsis* sp. *Chaetomium* sp. and *Nigrospora* sp. Recently, a novel lactone was obtained as a red pigment from the endophytic fungus *Fusarium verticillioides,* isolated from the leaves of *Bixa orellana* (Bixaceae) (Vijayakumar *et al.* 2021). Additionally, a harvest of *Bixa orellana* leaves from the Amazonian forest of Peru led to the isolation of 17 fungal endophytes including a strain of *Cophinforma mamane* (E224) from which the antileishmanial botryosulfuranols had been isolated (Triastuti *et al.* 2019; Barakat *et al.* 2019). Other strains were also isolated in this study belong to the genera *Diaporthe* spp., *Nigrospora* spp., *Phyllosticta* spp., *Endomelanconiopsis* spp., *Sporothrix* spp. and *Xylaria* spp. (unpublished data).

1.5 Different methodologies for metabolite induction in endophytic fungi

The number of gene clusters found in fungi is greatly superior to the number of gene clusters known from the isolated secondary metabolites (Pettit 2011). Conditions for gene expression are not fully understood and the presence of silent or lowly-expressed genes represent one of the main challenges for the isolation of novel secondary metabolites under laboratory conditions (Brakhage & Schroeckh 2011). Different approaches are proposed for the activation of cryptic gene clusters in endophytic fungi, broadly divided into methods based on genetic engineering techniques, in order to express biosynthetic gene clusters, and methods based on modifying the cultivation conditions to provide a better environment to trigger the expression of these gene clusters. The variations of the culture conditions known as OSMAC approach (Pan *et al.* 2019), the co-cultivation with other microorganisms (Chagas & Pupo 2018) and the addition of chemical elicitors and epigenetic modifiers, have shown to be rapid and useful techniques for the induction of cryptic genes in fungi (Zutz *et al.* 2014).

1.5.1 One Strain - Many Compounds (OSMAC)

The different methodologies that aim to modify the growth parameters are known as the OSMAC approach (One Strain - Many Compounds) which is based on the potential of one single strain to produce different compounds under small changes in the culture conditions (Bode *et al.* 2002; Romano *et al.* 2018). Under this approach, many endophytic fungi have been able to expand their chemical diversity in culture producing new metabolites with biological activity (Ariantari *et al.* 2019; Tran-Cong *et al.* 2019; Fan *et al.* 2019). Regarding the changes in nutrient regimes, the types of carbon, nitrogen, sulfur and phosphorus sources, the presence of trace elements and the culture on solid or liquid media can elicit a differential production of secondary metabolites besides its influence on growth. Also, the change of physical parameters such as temperature, aeration and shaking conditions, salinity, pH levels and osmotic stress are considered for the optimization of culture conditions as well as for the metabolite induction (Pan *et al.* 2019).

Fungi use light as a source of information to anticipate conditions for vegetative growth, conidia production, sexual development and circadian rhythms (Tisch & Schmoll 2010). Quantity, direction, wavelength and quality of light are used as a signal to induce these adaptive responses and to control development which can also affect their interaction with the plant hosts (Schumacher 2017). A large proportion of the fungal genome is regulated by light which encodes a photosensory system capable of responding to different intensities and wavelengths of light (Yu & Fischer 2019). For instance, aflatoxin production by *Aspergillus flavus* is influenced by light (Joffe & Lisker 1969) as well as the compounds ochratoxin 1 (Aziz & Moussa 1997), averufin or versicolorin A and C (Bennett *et al.* 1981). In addition

to this, bioactive compounds such as anthraquinone and griseofulvin have exhibited an enhanced production under red, blue or green light conditions compared to dark conditions, showing the importance of light in metabolite production (Zhang *et al.* 2017).

The time for growth and development of each fungal strain is another important factor to consider for the discovery of new metabolites or for monitoring specific compounds behavior (Peters *et al.* 2010). The metabolome of microorganisms is constantly changing due to all the dynamic processes involved during development (Roullier *et al.* 2016). Some studies have shown the potential novelty hidden when considering the time frame in fungi culture for natural product discovery (Choi *et al.* 2010; Bertrand *et al.* 2014). For example, the metabolome of the endophytic fungus *Cophinforma mamane* was studied in a time-scale revealing the presence of 3 *de novo* compounds with different emergence periods induced in co-culture with *Fusarium solani* (Triastuti *et al.* 2021).

1.5.2 Chemical elicitation

Several small molecules possessing diverse chemical structures are reported to act as histone deacetylase (HDAC) inhibitors or DNA methyltransferase (DNMT) inhibitors which possess diverse chemical structures and have been used for the induction of cryptic genes in fungal endophytes (**Figure 1.27**). The HDAC family can be divided into four major classes, I, II, III and IV. Among the HDAC inhibitors, the organic compounds suberoylanilide hydroxamic acid (SAHA), suberohydroxamic acid (SBHA), sodium butyrate, valproic acid and trichostatin A inhibit HDAC classes I and II, while nicotinamide and quercetin inhibit HDAC class III (Gupta *et al.* 2020b). Among the DNMT inhibitors, 5-azacytidine (AZA), hydralazine, procainamide and procaine have been reported (Toghueo *et al.* 2020). For instance, the compound piperine showed an enhanced production when the endophytic fungi, *Diaporthe* sp. was treated with suberohydroxamic acid and valproic acid (Jasim *et al.* 2019). Similarly, the addition of 5-azacytidine enhanced the production of camptothecin in *Botryosphaeria rhodina* (Vasanthakumari *et al.* 2015) while the addition of nicotinamide to the culture of the endophytic fungus *Graphiopsis chlorocephala*, led to a general enrichment in secondary metabolite production, allowing the isolation of new benzophenones and cephalanones (Asai *et al.* 2013). The treatment with epigenetic modifiers for the induction of secondary metabolites in endophytic fungi has the advantage of not requiring genetic manipulation, allowing the identification of new compounds and the enhancement of the synthesis of low-yield metabolites (Deshmukh *et al.* 2018).

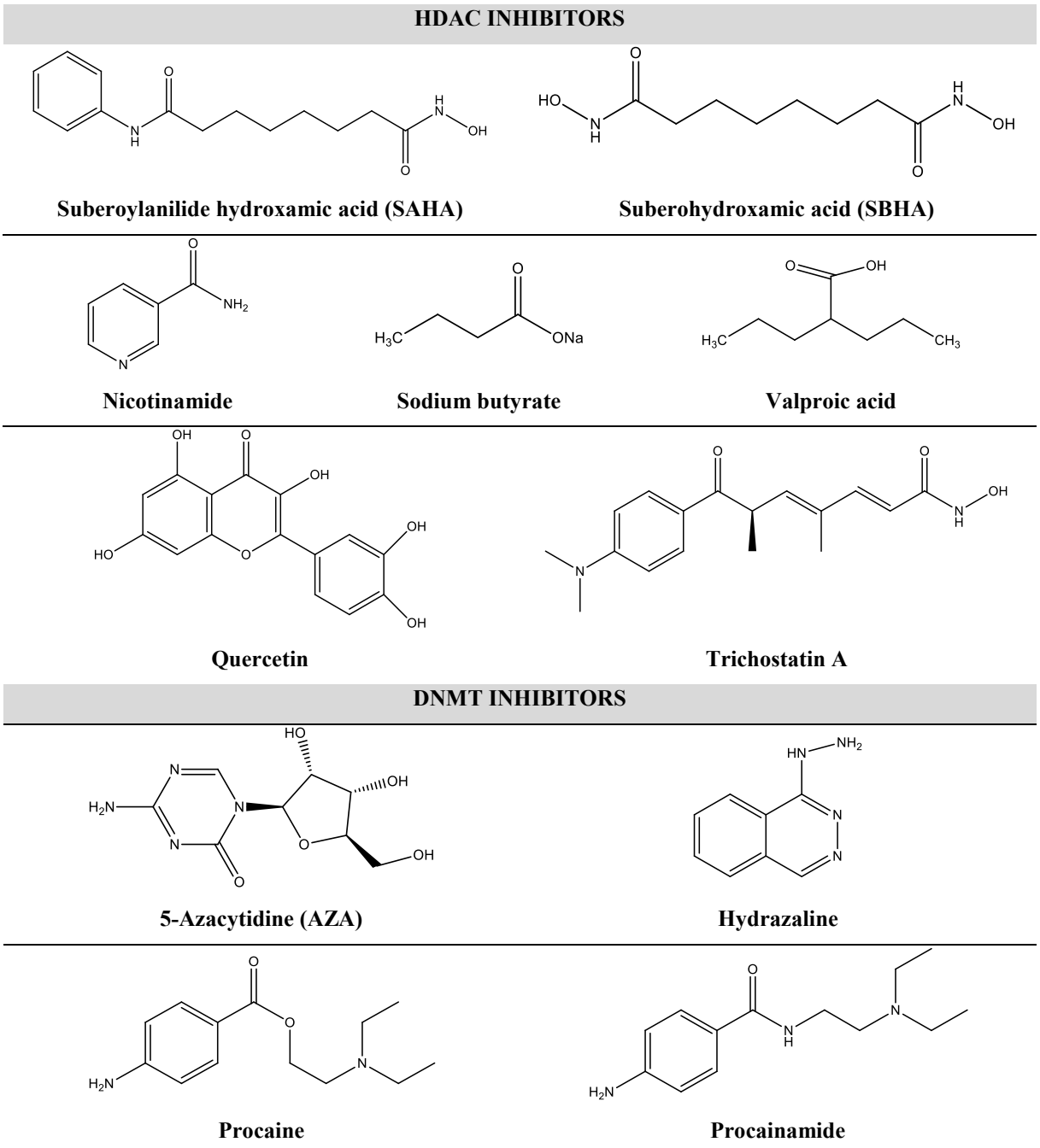

Figure 1.27. Structure of some HDAC and DNMT inhibitors used for metabolite induction

Solvents and heavy metals have also shown to disturb the secondary metabolism; however, the mechanisms are not well understood. For example, the addition of 6% of ethanol or 3% of dimethylsulfoxide (DMSO) to the culture might cause mistranslation and induction of the stress response (Pettit 2011). The addition of methanol, acetone, acetonitrile, 1-butanol and chloroform have also shown to change the profile of the metabolites produced by endophytic fungi (Toghueo *et al.* 2018). Similarly, fungi cultured in presence of enzyme inhibitors such as metyrapone (cytochrome P-450 inhibitor) or jasplakinolide (F-actin inhibitor) were able to synthesize new compounds (Pan *et al.* 2019).

Moreover, the addition of plant products in fungi culture have also been reported. For example, nitric oxide is a phytohormone that has shown to influence the secondary metabolite production in *Hypocrea koningii* (*Trichoderma koningii*) and *Penicillium miczynskii* (Zutz *et al.* 2014). In addition to this, the supplementation of the endophytic fungi culture medium with leaves, barks, roots and other plant parts or extracts can induce or maintain the production of secondary metabolites. Finally, metal ions such as Mn^{2+}, La^{3+}, Ce^{3+} and Nd^{3+} are involved in the stimulation of carotenoids synthesis while Cd^{2+}, Cu^{2+} and Cr^{3+} have been used for the induction of secondary metabolites in fungi (Toghueo *et al.* 2020).

1.5.3 Addition of biosynthetic precursors

Some studies have recently applied the amino-acid directed strategy for the induction of cryptic biosynthetic pathways in fungi. The addition of phenylalanine, methionine, tryptophan, lysine, and threonine to the culture of fungus *Pseudallescheria boydii* induced the production of 25 compounds corresponding to diverse chemical structures comprising alkaloids, diketopiperazines, sesquiterpenoids and polyketides (Lan *et al.* 2016). In another study, novel compounds corresponding to amides, polyketides and diketopiperazines were obtained from the marine-derived fungus *Dichotomomyces* when the culture was supplemented with L-tryptophan and L-phenylalanine (Chen *et al.* 2017). Continuing the research of this endophytic strain by the addition of the same amino acids, 7 additional compounds were discovered: 2 new polyketides, 2 new alkaloids and 3 known fumiquinazolines indicating the enhanced the production of nitrogen-containing compounds in this fungus under the addition of these amino acids (Wu *et al.* 2018). Likewise, other studies were able to isolate novel bioactive alkaloids from marine-derived fungi using this same strategy (Huang *et al.* 2017; Yuan *et al.* 2019; Qiu *et al.* 2020; Guo *et al.* 2020).

1.5.4 Co-cultivation

Endophytic fungi coexist with other microorganisms in their natural environment and co-culturing fungus-fungus, fungus-bacteria or bacteria-bacteria under laboratory conditions has shown to naturally enhance the production of cryptic compounds that were not detected in axenic culture. This increased production might be the result of competition for nutrients or antagonism in their development between microorganisms sharing the same niche (Deshmukh *et al.* 2018). The endophytic fungus *Paraconiothyrium variabile* was able to induce its metabolite production and to negatively modulate the production of the mycotoxin beauvericin of the phytopathogen *Fusarium oxysporum* when they were co-cultured in PDA medium (Combès *et al.* 2012). Also, endophytic fungus *Fusarium tricinctum* was co-cultured with *Bacillus subtilis*, leading to the accumulation of secondary metabolites and to the production of 3 new natural products including macrocarpon C, (−)-citreoisocoumarin and 2-

(carboxymethylamino) benzoic acid (Ola *et al.* 2013). Co-cultivation is an emerging tool and several studies have been applying this approach in terrestrial and marine-derived fungi and bacteria (Marmann *et al.* 2014) including many endophytic fungi (Chagas & Pupo 2018; Pan *et al.* 2019).

1.6 Applying Metabolomics to natural products research

1.6.1 Study of the Metabolome with Mass Spectrometry

The classical approach for the discovery of natural products with biological activity starts with the biological screening of crude extracts and the posterior fractionation, isolation and identification of the bioactive compounds. To complement this approach and to avoid the bottleneck of re-isolation of known compounds, metabolomics is a powerful tool for the analysis, identification and quantification of small metabolites, usually molecular weights less than 1000 Da, with biological activities. This approach studies a biological system at a specific time for measuring their changes that captures the final alteration of endogenous metabolites which at the same time facilitates the search for novel bioactive compounds (Zhao *et al.* 2018). The most common analytical techniques used for this purpose are Mass Spectrometry (MS) and Nuclear Magnetic Resonance (NMR). The first technique is the most widely used and possess some advantages over NMR, including high sensibility, small samples volume, acquisition of MS/MS fragmentation data for structural elucidation followed by a comparison with databases. Additionally, the association with computational and statistical tools can offer a better view that simplifies the vast data analyses (Demarque *et al.* 2020).

Depending on the research discipline, the specific objectives and the equipment used, the general analytical strategies can be divided in four: Targeted metabolomics and Metabolic profiling, in order to perform validations (quantification of one or a few metabolites) and Metabolic Fingerprinting (identification of metabolite patterns) and Untargeted Metabolomics, in order to discover fingerprints or patterns in a biological process to identify metabolites of interest. Specifically, untargeted metabolomics focuses on the detection of as many metabolites as possible to elaborate a comprehensive data set due to the little or no information available about the metabolome under study. It is important to mention that any strategy covers only a part of the real metabolome (Uthe *et al.* 2021).

1.6.2 Data processing software

For data processing, there are many bioinformatics tools that enable the obtention of a data matrix with the intensities or abundances of peaks from raw data of each sample. For this purpose, bioinformatical operations such as peak detection, retention time shift correction and peak alignment are the typical steps performed by bioinformatics tools, including MZmine (Pluskal *et al.* 2010), MS-DIAL (Tsugawa *et al.* 2015), along with MS-FINDER (Tsugawa *et al.* 2016) and MS-CleanR package (Fraisier-Vannier *et al.* 2020), and XCMS (Domingo-Almenara & Siuzdak 2020) as the most popular open-source software.

1.6.3 Databases for annotation

Published chemical structures available in chemical databases indicate that the most abundant natural products are derived from plants (about 70%), followed by animal-derived, fungi-derived and bacteria-derived natural products (Ntie-Kang & Svozil 2020). Currently, there is no open database that gathers all natural products produced by microbes besides the fact that many of the predictions of fragmentation patterns from mass spectrometry depend on the availability of known compounds found in databases for comparison with the experimental data. Commercial databases, such as Antibase or The Dictionary of Natural Products, and open databases have some difficulties including limited information, not downloadable or overly specific compounds (**Figure 1.28**). Recently, a new automated curation platform followed by manually curation, was created to identify microbial-derived natural products found in scientific literature and patents. The Natural Products Atlas (https://www.npatlas.org/) currently contains more than 29, 000 natural product structures and is linked to the GNPS database (Van Santen *et al.* 2019).

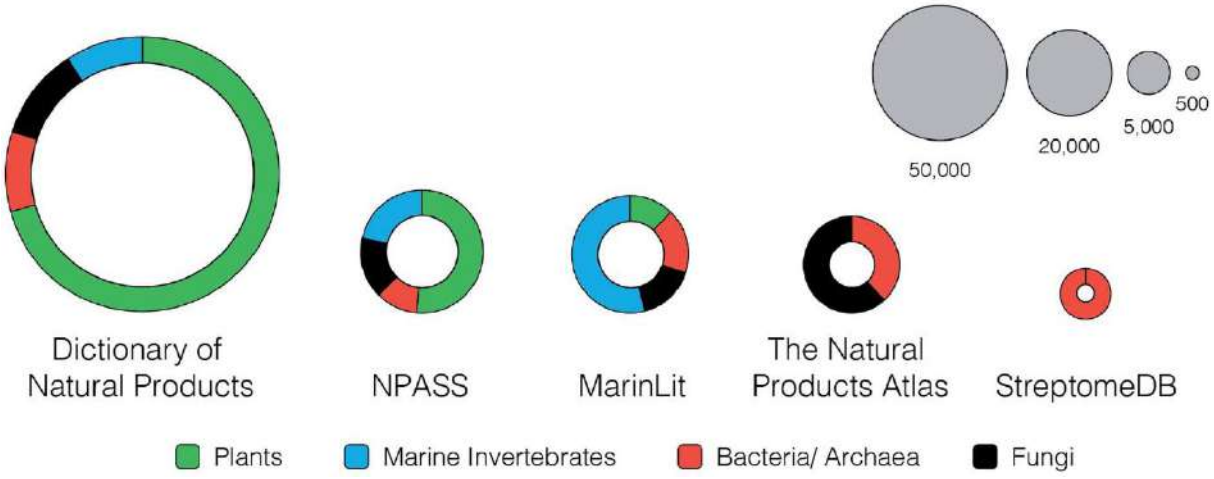

Figure 1.28. Distribution of compound source in some natural products databases (van Santen et al., 2020)

1.6.4 Statistical analysis and data visualization for further interpretation

The data matrix obtained from the data processing software can be used for statistical analyses or uploaded to data repositories and libraries for the scientific community. Untargeted metabolomics usually provides thousands of features that require multivariate analysis such as unsupervised and supervised methods for pattern recognition among different groups. Online platforms, such as Workflow4Metabolomics and Galaxy workflow (https://workflow4metabolomics.usegalaxy.fr/) or

Metaboanalyst (https://www.metaboanalyst.ca/) can cover data processing entirely from the feature table to perform statistical analysis.

In addition to this, molecular networking is a tool that facilitates the mapping of chemical diversity observed in an untargeted mass spectrometry experiment, being the GNPS platform (https://gnps.ucsd.edu/) and MetGem software (Olivon *et al.* 2018) the main methodologies used for this purpose. Molecular networking compares and aligns ion fragmentation patterns and structurally related molecules are assigned with a cosine score. Molecules are represented by a node and can be related to others forming a cluster according to the similarity of the fragment ions. Cytoscape® (Shannon 2003) is another software that helps to better visualize the clustered data in the molecular network produced either by GNPS or MetGem. In the case of GNPS, public information provided by the scientific community is searched against spectral libraries allowing the annotation of high confidence spectral matches (Aron *et al.* 2020). To complement the information given by this online platform, it exists many other annotation and classification tools that either use fragmentation libraries or *in silico* tools that predict fragmentation (da Silva *et al.* 2018).

CHAPTER 2 MATERIALS AND METHODS

The general steps of the methodology, from fungal isolation to metabolomics analysis, performed during this doctoral work is summarized in the following schema (**Figure 2.1**).

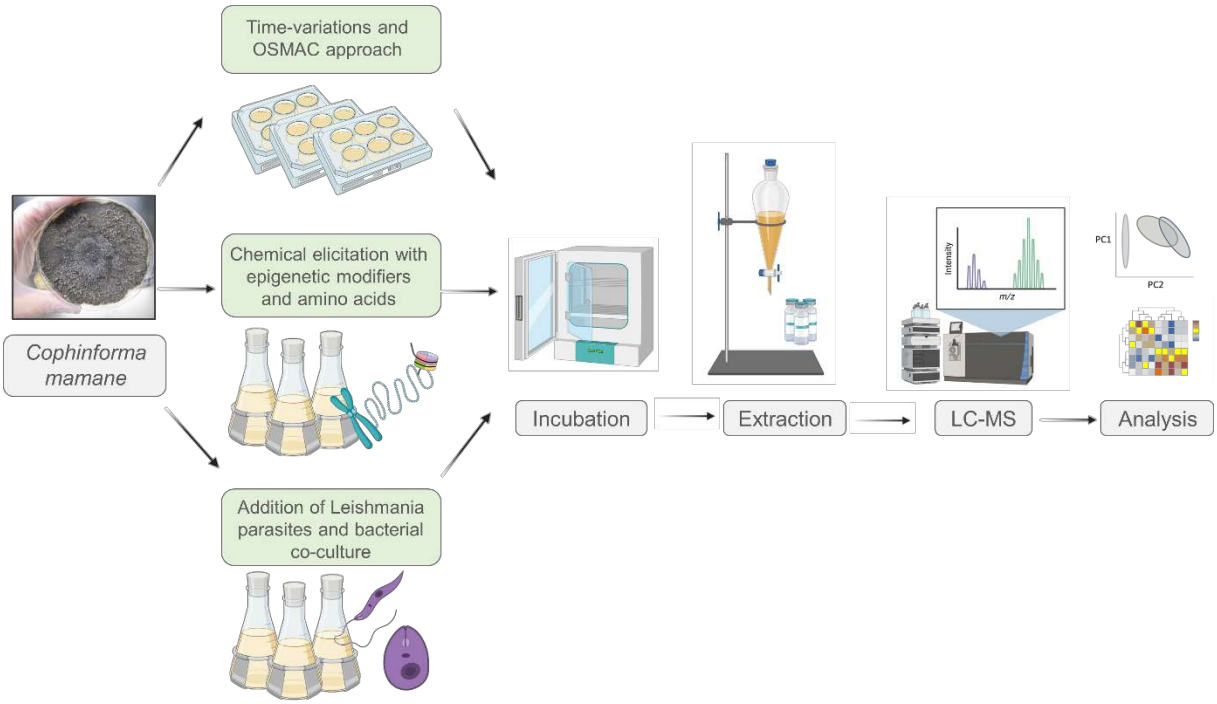

Figure 2.1. General methodology steps: the different approaches for secondary metabolite induction in *C. mamane* (own creation with biorender.com)

2.1 Materials and reagents

2.1.1 Culture media

The culture media used for the different experiments are the following:

- Trypticase Soy Agar (TSA, BD – BBL) containing 15 g of pancreatic digest of casein, 5 g of papaic digest of soybean meal and 5 g of sodium chloride for 1L of distilled water.
- Malt extract broth or agar (MEB / MEA) containing malt extract 20g, dextrose 20g, peptone 1g, copper sulfate pentahydrate 0.005g, zinc sulfate heptahydrate 0.01g in 1 L of distilled water. MEA contains 20 g/L of agar-agar.
- LB broth (BD – Difco™) containing 10 g of tryptone, 10 g of yeast extract and 10 g of sodium chloride for 1L of distilled water.

- Czapek solution agar (Difco™) containing saccharose 30 g, sodium nitrate 2 g, dipotassium phosphate 1 g, magnesium sulfate 0.5 g, potassium chloride 0.5 g, and ferrous sulfate 0.01 g for 1 L of distilled water.
- Yeast malt extract agar or ISP2 containing malt extract 10 g, dextrose 4 g, and yeast extract 4 g for 1L of distilled water (Shirling & Gottlieb 1966).
- Potato dextrose broth or agar (PDB / PDA) (Difco™) containing 4g of potato extract and 20g of glucose for 1L of distilled water. PDA contains 15 g/L of agar-agar.
- RPMI 1640 containing L-glutamine and phenol red.

2.1.2 Reagents and solvents

The different reagents and chemical solvents used for the experiments are the following:

- Dimethyl sulfoxide (DMSO, Sigma Aldrich)
- Glycerol 99% extra pure (ACROS Organics™)
- Nicotinamide (NIC, Sigma)
- Sodium butyrate (SB, Sigma)
- Butyryl-DL-homoserine (HSL, Sigma)
- 5-azacytidine (AZA, Sigma)
- L-Phenylalanine (L-Phe, Sigma)
- L-Tryptophan (L-Trp, Sigma)
- Formic acid (FA, Sigma)
- Methanol HPLC grade (Fisher chemical)
- Ethyl acetate HPLC grade (Fisher chemical)
- Acetonitrile HPLC grade (Fisher chemical)
- Dichloromethane HPLC grade (Fisher chemical)

2.1.3 Fungal material

The strain E224 of *Cophinforma mamane* (D.E. Gardner) A. J. L. Phillips & A. Alves was isolated from the fresh leaves of *Bixa orellana* L. collected in November 2013 by Carlos Amasifuen and Mohamed Haddad in the National Reserve of Allpahuayo Mishana in the Amazonian forest of Iquitos, Peru (GPS coordinates: 3°58’2.3’’ S, 73°25’3.9’’ W). The isolation, identification and storage processes performed for this strain have been previously described in the literature (Triastuti *et al.* 2019; Barakat *et al.* 2019).

Briefly, the collected tissues were sterilized with 5% sodium hypochlorite, 70% ethanol (2 times) and rinsed with distilled water. Sterilized surfaces were cut into small fragments (5x5 mm) and placed on a Petri dish containing MEA and chloramphenicol (100 mg/L). The pure isolates were identified using internal transcriber spacer (ITS1 and ITS2) sequences which are available in the GenBank database under the accession number MG457709.1. The cryotubes are conserved at -80 °C in 30% of glycerol in the fungal collection of the UMR 152 laboratory.

2.1.4 Bacterial material

For the co-culture experiments three different strains from the American Type Culture Collection (ATCC) were used: *Escherichia coli* ATCC® 25922™; *Pseudomonas aeruginosa* ATCC® 27853™ and *Staphylococcus aureus* ATCC® 25923™.

2.1.5 Leishmanial parasites

For the culture of *C. mamane* and for the biological tests of its crude extracts, *Leishmania infantum* parasites expressing luciferase activity (MHOM/MA/67/ITMAP-263, CNR Leishmania, Montpellier, France) were used.

2.2 Culture conditions and extraction procedures

2.2.1 Time-variations study and OSMAC approach

Culture media and conditions

For the time-variations study, *C. mamane* was incubated in 6-well plates containing 4 mL of MEA during 28 days at 27°C under natural light. At the end of each culture day, a culture plate and a control plate were placed at -80°C until extraction with solvents.

Concerning the OSMAC approach, *C. mamane* was incubated in 6-well plates containing CZA and ISP2 during 6 and 10 days at 27 °C under presence or absence of natural light in a 24 h dark regime. At the end of each incubation time, the culture plates and control plates were placed at -80 °C until extraction with solvents.

Extraction and preparation of crude extracts

For time-variations experiment, each culture (biomass and medium) was freeze-dried. The dry material was transferred into a glass tube with 10 mL of solvent. The extraction was performed using a freshly prepared dichloromethane-methanol-water mixture 64:36:8 (v/v/v) (Bertrand *et al.* 2014).

For OSMAC-based experiment, each culture was directly transferred to a glass tube containing 10 mL of ethyl acetate. The medium and mycelia were crushed in the solvent and taken under ultrasound treatment over 60 minutes.

In both experiments, the supernatants were filtered through glass cotton then dehydrated on magnesium sulfate and filtered using filter paper. Finally, all the extracts were evaporated to dryness under reduced pressure (KNF rotary evaporator RC 600) at 40°C.

2.2.2 Chemical elicitation with epigenetic modifiers and addition of amino acids

Culture media and conditions

The endophyte *C. mamane* was cultured in PDB and PDA. First, the fungus was grown on PDA during 7 days to inoculate the seed culture in 50 mL of PDB during 3 days at 27°C. Two mL of seed culture were used to inoculate 250mL Erlenmeyer flasks containing 50 mL of PDB. The fungus culture was treated with 4 different epigenetic modulators, NIC, SB, AZA and HSL, dissolved in DMSO and added to the 50 mL of PDB. NIC and SB were added at 1 µM, AZA was added at 25 µM and HSL was added at 100 µM as final concentrations. Fermentation was carried out during 2 weeks at 27°C under static conditions. All conditions, including negative controls, were done in triplicate.

For the addition of amino acids, *C. mamane* was cultured in MEB and supplemented MEB with 2 mg/L of L-Trp and L-Phe. Fermentation was carried out in 250mL Erlenmeyer flasks during 2 weeks at 27°C under constant agitation containing 50 mL of MEB and 50 mL of supplemented MEB. All conditions and negative controls were done in triplicate.

Extraction and preparation of crude extracts

After 2 weeks of incubation, the whole culture broths (including mycelium) were extracted with 50mL of ethyl acetate under 60 minutes of ultrasound treatment. Mycelia were removed from the culture supernatant through filtration with glass cotton. Organic phases were then dehydrated on magnesium

sulfate and filtered with filter paper. Finally, they were evaporated to dryness under reduced pressure (KNF rotary evaporator RC 600) at 40°C.

2.2.3 Addition of heat-killed leishmanial parasites

Culture media and conditions

Heat-killed *Leishmania* parasites were added into the culture of *C. mamane*. For this, fresh cultures of promastigotes and amastigotes of *Leishmania infantum* were first centrifuged at 2100 RPM during 10 minutes to remove the supernatant. Each pellet was resuspended in distilled water and autoclaved at 121°C during 15 min for parasite inactivation.

Following this procedure, *C mamane* was cultured in MEB in the presence of three different concentrations of heat–killed amastigotes: C1=5.2 x 10^5, C2=1.06 x 10^6 and C3=2.12 x 10^6 parasites / mL. Fermentation was carried out in 250mL Erlenmeyer flasks containing 50 mL of MEB during 2 weeks at 27 °C under constant agitation. All conditions, including negative controls, were done in triplicate.

Extraction and preparation of crude extracts

After 2 weeks of incubation under constant agitation, the whole culture broths (including mycelium) were extracted with 50mL of ethyl acetate under 60 minutes of ultrasound treatment. Mycelia were removed from the culture supernatant through filtration with glass cotton. Supernatant was filtered using regenerated cellulose acetate membranes (0.45 µm) to remove the cellular debris. Organic phases were then dehydrated on magnesium sulfate and filtered with filter paper. Finally, they were evaporated to dryness under reduced pressure (KNF rotary evaporator RC 600) at 40°C.

2.2.4 Co-culture of *C. mamane* with pathogenic bacteria

Culture media and conditions

Escherichia coli ATCC® 25922™; *Pseudomonas aeruginosa* ATCC® 27853™ and *Staphylococcus aureus* ATCC® 29923™ were first seeded in TSA and incubated at 30°C during 24 h. One colony of each strain was later cultivated in LB broth at 30°C during 48 h at 150 RPM.

C. mamane was grown on PDA during 7 days to inoculate the seed culture in 50 mL of PDB during 3 days at 27°C. 1 mL of seed culture were used to inoculate 250mL Erlenmeyer flasks containing 50 mL of PDB.

For the co-culture experiments, each flask containing 50 mL of PDB was inoculated with 1 mL of seed culture from *C. mamane* and 200 µL of the 48 h LB broth from each bacterial strain and then incubated at 27°C during 10 days.

Extraction and preparation of crude extracts

After incubation time, whole culture broths were extracted with 50mL of ethyl acetate under 60 minutes of ultrasound treatment. Mycelia were removed from the culture supernatant through filtration with glass cotton. Organic phases were then dehydrated on magnesium sulfate and filtered with filter paper. Finally, they were evaporated to dryness under reduced pressure.

The different culture conditions used in this doctoral thesis have been summarized in **Table 2.1**.

Table 2.1. Summary of culture conditions for the induction of *C. mamane* metabolites

Study	Culture medium	Time of incubation	Other conditions
Time variations	MEA	28 days	27ºC
OSMAC	ISP2, CZA	6 and 10 days	27ºC, 24h of natural light and 24 h of darkness
Epigenetic modifiers	PDB	14 days	27ºC, no agitation
Amino acids	MEB	14 days	27ºC, 120 RPM
Heat-killed *Leishmania*	MEB	14 days	27ºC, 120 RPM
Co-culture	PDB	10 days	27ºC, no agitation

2.3 Evaluation of the biological activity

Anti-parasitic activity assay was performed for the crude extracts obtained from the culture of *C. mamane* in presence of the thermally inactivated amastigotes of *L. infantum*. For this, *L. infantum* promastigotes were cultivated in RPMI 1640 medium supplemented with 10% foetal calf serum (FCS), 2 mM L-glutamine and antibiotics (100 U/mL penicillin and 100 µg/mL streptomycin) and harvested in logarithmic phase of growth by centrifugation at 900 g for 10 min. The supernatant was removed

carefully and was replaced by the same volume of RPMI 1640 complete medium at pH 5.4 and incubated for 24 h at 24°C. The acidified promastigotes were then incubated for 24 h at 37°C in a ventilated flask to transform acidified promastigotes into axenic amastigotes (Sereno & Lemesre 1997). The effects of the extracts on the growth of *L. infantum* axenic amastigotes were assessed as follows: *L. infantum* amastigotes were incubated (2×10^6 parasites/mL) in sterile 96-well plates with each samples dissolved in MeOH (final concentration 0.5% v/v), in duplicate. Appropriate controls, DMSO or MeOH and amphotericin B, were added to each set of experiments.

After a 48 h incubation period at 37°C, each plate-well was then microscopically-examined to detect any precipitate formation. To estimate the luciferase activity of axenic amastigotes, 80 µL of each well were transferred to white 96-well plates, Steady Glow® reagent (Promega) was added according to manufacturer's instructions, and plates were incubated for 2 min. The luminescence was measured in Microbeta Luminescence Counter (PerkinElmer). Efficient concentration 50% (EC_{50}) was defined as the concentration of drug required to inhibit by 50% the metabolic activity of *L. infantum* amastigotes compared to control. EC_{50} values were calculated by non-linear regression analysis processed on dose response curves, using TableCurve 2D (version 5.0) software.

2.4 UHPLC-Mass spectrometry analysis

Methanolic solutions at 2 mg/mL of all extracts were prepared for Ultra-High Performance Liquid Chromatography - MS analysis. Quality control (QC) samples were prepared by pooling an aliquot of all extracts for each experiment. Analyses were performed on a UHPLC Ultimate 3000 system (Dionex) coupled with an LTQ Orbitrap XL mass spectrometer (Thermo Fisher Scientific, Hemel Hempstead, UK). Samples were separated on a C18 Acquity column (100 × 2.1 mm i.d, 1.7 µm, Waters, MA, USA) equipped with a guard column. The mobile phase A was ultrapure water acidified with 0.1% FA and mobile phase B was acetonitrile acidified with 0.1% FA. The solvent gradient was: 0 min, 95% A; 10 min, 95% B; 12.5 min, 95% B. The flow rate was 0.45 mL/min, the column temperature was set to 40°C, the autosampler temperature was set to 15°C and injection volume fixed to 5 µL for extracts. Mass detection was performed using an electrospray source (ESI) in positive ionization (PI) mode at 15,000 resolving power [full width at half maximum (FWHM)) at 400 *m/z*]. The mass scanning range was *m/z* 100-2000 for all samples. Ionization spray voltage was set to 3.5 kV and the capillary temperature was set to 300°C. Each full MS scan was followed by data-dependent acquisition of MS/MS spectra for the three most intense ions using stepped collision-induced dissociation (CID) at 35 arbitrary energy units.

2.5 Data treatment and statistical analysis

2.5.1 Data processing

LC-MS data from each experiment were separately processed with MS-DIAL version 4.7 (Tsugawa *et al.* 2015) for mass signal extraction between 100 and 1500 Da from 0.5 to 12.5 min. MS1 and MS2 tolerances were set to 0.01 and 0.025 Da, respectively, in centroid mode for each dataset. Peaks were aligned on a QC reference file with a retention time (RT) tolerance of 0.05 min and a mass tolerance of 0.025 Da. Minimum peak height was set to 70% below the observed total ion chromatogram (TIC) baseline for blank samples. MS-DIAL data was cleaned with MS-CleanR workflow using default parameters (Fraisier-Vannier *et al.* 2020): all filters with a minimum blank ratio set to 0.8, a maximum relative standard deviation (RSD) set to 30 and a relative mass defect (RMD) ranging from 50 - 3000. The maximum mass difference for feature relationships detection was set to 0.005 Da and maximum RT difference was set to 0.025 min. The Pearson correlation links were considered with correlation ≥0.8 and statistically significant $\alpha = 0.05$. Two peaks were kept in each cluster: the most intense and the most connected to other ions. The kept features were annotated with MS-FINDER version 3.5 (Tsugawa *et al.* 2016). The MS1 and MS2 tolerances were set to 0.005 and 0.05 Da, respectively. Formula finder were processed with C, H, O, N, P and S atoms. Annotation was done with the use of internal generic databases from MS-FINDER: LipidMaps, YMDB, ChEBI, NPA, NANPDB, COCONUT, KNApsacK and UNPD. Only annotations with a score greater than 5 were retained throughout the analysis while unannotated features are referred to as “unknown”. Data were finally exported as .msp file for MSMS spectral information and .csv files for metadata information (peak area, retention times, annotation results, etc.).

The MSP and metadata files generated after the MS-CleanR workflow were imported into MetGem (version 1.3.4) (Olivon *et al.* 2018). The data was filtered by removing all MS/MS peaks within ±17 Da of the precursor *m/z*. MS/MS spectra were window filtered by using the top 6 peaks in the ±50 Da window throughout the spectrum. MS/MS fragment ion tolerance was set to 0.2 Da. A mass spectral similarity network was created where edges were filtered to have a cosine score above 0.7 and at least six matched peaks. Further edges between two nodes were kept in the similarity network only if each of the nodes appeared on each other’s top 10 most similar nodes. The resulting network was then imported into Cytoscape (version 3.8.2, Institute for Systems Biology, Seattle,WA, USA) to improve visualization (Shannon 2003). Nodes were colored according to their culture conditions and the node sizes indicate their normalized total peak area.

2.5.2 Statistical analysis

Statistical analysis were done by uploading the CSV file to the Metaboanalyst platform version 5.0 (https://www.metaboanalyst.ca/) (Chong *et al.* 2019). The data were pre-processed, first by normalization (by median) of the samples, then the variables were weighted by auto scale (mean-centered and divided by the square root of the standard deviation of each variable). A Principal Component Analysis (PCA) then a Partial Least Squares Discriminant Analysis (PLS-DA) were carried out. Finally, the *m/z* and the retention time of the top features associated to their normalized peak area were plotted on a heat map (hierarchical clustering) using ANOVA.

CHAPTER 3 TIME-VARIATIONS STUDY AND OSMAC APPROACH

3.1 Introduction

The OSMAC (One Strain - Many Compounds) approach is based on the potential of microorganisms to produce different compounds under specific conditions (Bode et al., 2002; Romano et al., 2018), focusing on the modification of the growth parameters for the induction of metabolites. This methodology has allowed the expansion of the chemical diversity of endophytic fungi, which are able to produce new metabolites with biological activity (Ariantari et al., 2019; Fan et al., 2019; Tran-Cong et al., 2019).

Among these growth parameters, the nutrient content, the time of incubation, the light conditions and other physicochemical parameters can be easily modified. As previously described as part of the strategies for metabolite induction (**Section 1.5.1**), a large proportion of the fungal genome can be regulated by light (Schumacher, 2017) including its different wavelengths (Yu and Fischer, 2019). The time for incubation is intimately related to the growth and development of each fungal strain, which is important to consider for the discovery of new metabolites and for monitoring specific compounds behavior (Peters et al., 2010). Taking into consideration the time-frame production for metabolite production has allowed the discovery of the potential novelty hidden in fungi for natural product discovery (Bertrand et al., 2014; Choi et al., 2010).

Under these concepts, this work has two main objectives: to study the metabolome changes of the endophytic fungus *C. mamane* during 28 days of culture and to evaluate its response when using two different culture media and light *versus* dark conditions at 2 different incubation times under the OSMAC approach. A special focus was given to the previously isolated thiodiketopiperazines (TDKPs), botryosulfuranols A, B, C (Barakat et al., 2019) and D.

3.2 Results

3.2.1 Time-variations of the metabolome of *C. mamane*

General observations

During the first 24 and 48 hours of culture of *C. mamane* in 6-well plates containing MEA, the colonies started to growth as a white mycelium, as observed in **Figure 3.1.**

***C. mamane* at day 1** ***C. mamane* at day 2**

Figure 3.1. Closer view of the mycelium growth of *C. mamane* during the first 2 days of growing in 6-well plates containing MEA (upper view with stereoscope)

After 28 days of incubation in MEA, most of the colonies presented white mycelia with black spots, mainly observed from the bottom view (**Figure 3.2**), indicating a potential production of pigments.

Upper view **Bottom view**

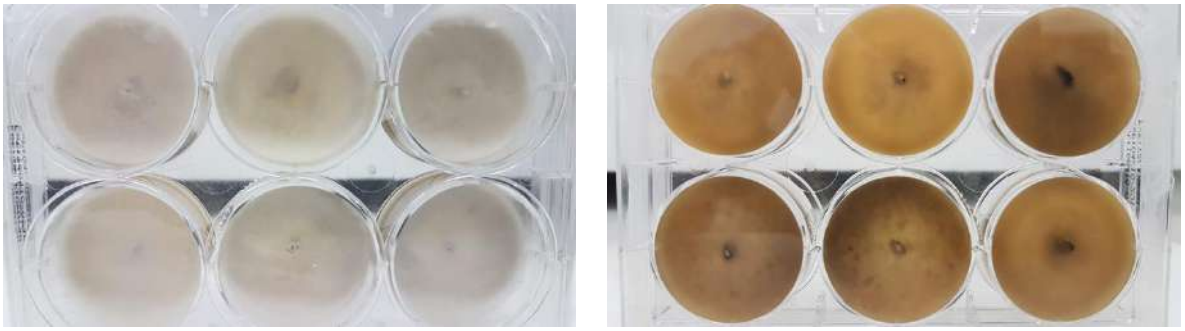

***C. mamane* at day 28**

Figure 3.2. Growth of *C. mamane* after 28 days of incubation showing surface (upper view) and reverse appearance (bottom view) of the white mycelium with some black sports in MEA

Preliminary results of the general chemical profiling using quality controls (QC) samples (pool sample of replicates), allowed us to select some time-points (4, 8, 12, 16, 20, 24 and 28 days) for the metabolomics analysis. An overview of the chromatograms corresponding to the day 4 (D4), 8 (D8), 12 (D12), 16 (D16), 20 (D20), 24 (D24) and 28 (D28) days of culture indicate the general variations in the metabolome with major and minor peaks appearing at different culture times. For example, feature *m/z* 230.1383 at 4.58 min corresponds to a minor peak that appeared between D24 and D28; *m/z* 292.1536 at 5.12 min corresponds to a major peak that was detected during the whole culture while *m/z* 442.2441 at 6.85 min corresponds to a minor peak that appeared between D20 and D28 while the feature *m/z* 230.138 at 4.83 that appeared between D20 and D28 (**Figure 3.3**).

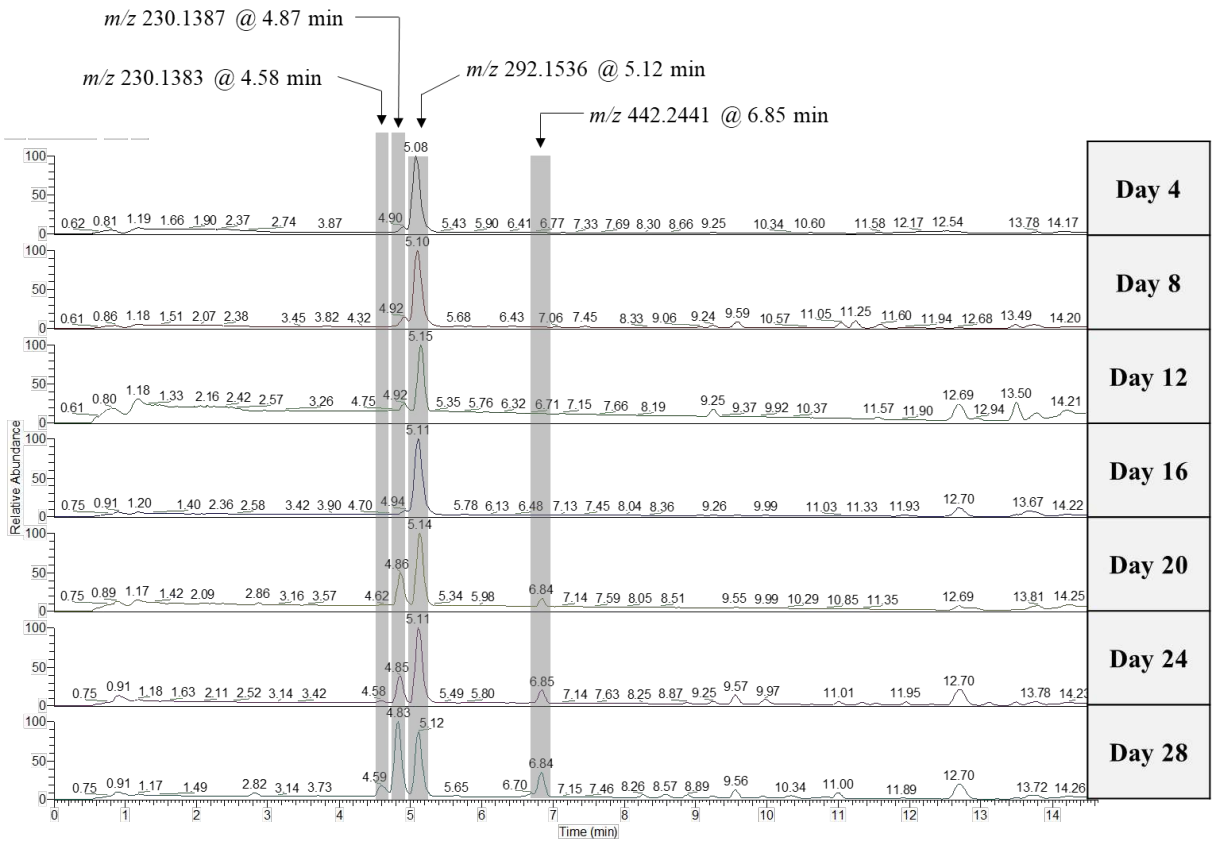

Figure 3.3. (+)ESI-HRMS base peak chromatograms from crude extracts of *C. mamane* cultivated at day 4, 8, 12, 16, 20, 24 and 28 in MEA

LC-MS profiles of all the 28 crude extracts from the time-series study afforded 303 features (*m/z*-RT pairs) in positive ionization (PI) mode, which were considered for the metabolomics and statistical analysis. Fifteen percent of these features (45 out of 303) were putatively annotated, corresponding to different chemical classes such as diketopiperazines (DKPs), cyclic peptides, fatty acids, phosphoethanolamines, phosphocholines (**Annexes 1**).

Multivariate classification (PLS-DA)

A supervised PLS-DA analysis was carried out on these data which indicated the evolution of metabolites of *C. mamane* through 28 days of culture (**Figure 3.4**). Separate clusters appear on the PLS-DA score plot (26 % of total variability). The component 1 (X-axis) explained 16.9 % of the variability, allowing the discrimination of the different clusters, mainly between D4-D8, D12-D16 and D20-D28. While in the component 2 (9.1%), we can observe a slight differentiation following a semicircle trajectory which represents the apparition and disappearance of the compounds found in crude extracts from D4 to D28.

The **Figure 3.4** presents the top 15 features that contributed to the differences between these clusters while some of them were putatively identified. Among them, we can find tiglylcarnitine, a type of acylcarnitine known to be involved in acyl-groups transport for mitochondrial normal functions and in lipid metabolism in mycorrhizal fungi (Laparre et al., 2014) which was detected during D28. A 1,3-dicarbonyl compound, previously isolated from a marine-derived strain of *Penicillium citrinum* (Pimenta et al., 2010) was also detected mainly during D28. The sugar alcohol derived from galactose, galacticol, found in different microorganisms including yeast and fungi (Jagtap et al., 2019), was mainly detected during D4 as well as a putatively identified cyclopentapeptide, previously isolated from a endophytic fungal strain of *Fusarium decemcellulare* (Li et al., 2016). These metabolites are detailed in

Table *3.1*.

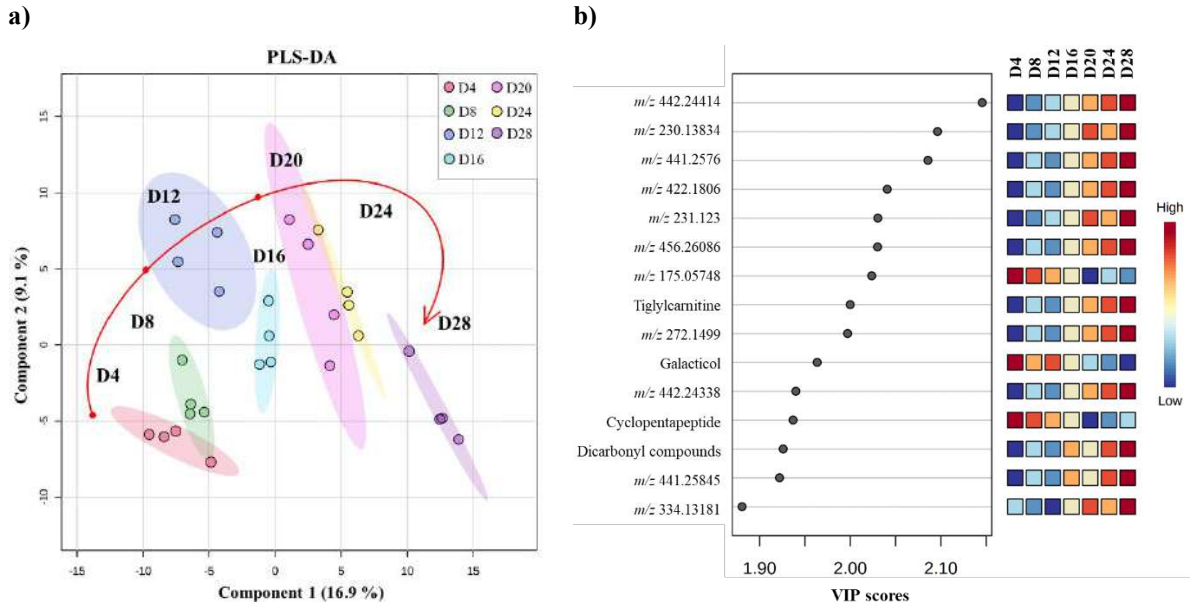

Figure 3.4. (a) Partial least squares discriminant analysis (PLS-DA) obtained from LC-(+)ESI-HRMS profiles corresponding to the extracts of *C. mamane* cultivated in MEA during 4, 8, 12, 16, 20, 24 and 28 days (4 replicates per day) based on features (*m/z* at Rt to its normalized peak area) detected in LC-MS chromatograms; (b) Variable importance in projection (VIP) score of the top 15 compounds from the PLS-DA analysis corresponding to each group (D4, D8, D12, D16, D20, D24, D28

Table 3.1. Top 15 features that significantly contribute to the difference in the PLS-DA analysis from LC-HRMS/MS data corresponding to the time-series study of *C. mamane*

ID	Rt (min)	*m/z*	Adduct	Formula	Δ mass (ppm)	Putative identification	Ontology	VIP scores
109	6.84	442.2441	$[M+H]^+$	$C_{23}H_{31}N_5O_4$	1.67	Unknown	Unknown	2.1457
240	4.58	230.1383	$[M+H]^+$	$C_{11}H_{19}NO_4$	1.49	Unknown	Unknown	2.0965
105	8.26	441.258	$[M+NH_4]^+$	$C_{22}H_{33}NO_7$	4.37	Unknown	Unknown	2.0858
96	5.86	422.1806	$[M+H]^+$	$C_{22}H_{23}N_5O_4$	3.98	Unknown	Unknown	2.0409
262	5.653	231.1230	$[M+H]^+$	$C_{11}H_{18}O_5$	1.29	Unknown	Unknown	2.0305
116	7.32	456.2609	$[M+H]^+$	$C_{24}H_{33}N_5O_4$	0.72	Unknown	Unknown	2.0302
160	0.88	175.0575	$[M+H]^+$	$C_3H_6N_6O_3$	0.37	Unknown	Unknown	2.0238
252	5.42	244.1539	$[M+H]^+$	$C_{12}H_{21}NO_4$	1.45	Tiglylcarnitine	Fatty acyls	2.0001
276	5.70	272.1499	$[M+H]^+$	$C_{14}H_{17}N_5O$	2.52	Unknown	Unknown	1.9972
286	0.88	205.0683	$[M+Na]^+$	$C_6H_{14}O_6$	0.39	Galactitol	Sugar alcohols	1.9636
107	6.70	442.2434	$[M+H]^+$	$C_{22}H_{35}NO_8$	0.37	Unknown	Unknown	1.9401
174	9.37	583.4518	$[M+NH_4]^+$	$C_{30}H_{55}N_5O_5$	3.95	Cyclo-(L-Ile-L-Leu-L-Leu-L-Leu-L-Leu)*	Cyclopeptides	1.937
265	3.90	250.1800	$[M+H]^+$	$C_{15}H_{23}NO_2$	0.45	(E)-1-(2,3-dihydro-1H-pyrrol-1-yl)-2-methyldec-8-ene-1,3-dione	1,3-dicarbonyl compounds	1.9261
106	8.05	441.2585	$[M+NH_4]^+$	$C_{22}H_{33}NO_7$	2.44	Unknown	Unknown	1.9221
39	5.26	334.1318	$[M+H]^+$	$C_{14}H_{23}NO_6S$	0.22	Unknown	Unknown	1.8807

*unknown amino acids sequence

Hierarchical clustering analysis (Heat map)

Out of the 303 features, 156 showed a significant change over time (p-value < 0.05) using the analysis of variance (one-way ANOVA). The top 50 features with significant changes were plotted in the hierarchical clustering analysis (heat map) where three main clusters of metabolite behaviors are observed (**Figure 3.5**): a cluster of metabolites that appeared in the early days of culture, between D4 and D8; a cluster of metabolites that started to be produced during a middle stage, mainly between D8 and D12 and that were not observed after D16; and a cluster of metabolites that started to be produced at a late stage from D20 until D28. These results are consistent with PLS-DA analysis observed above.

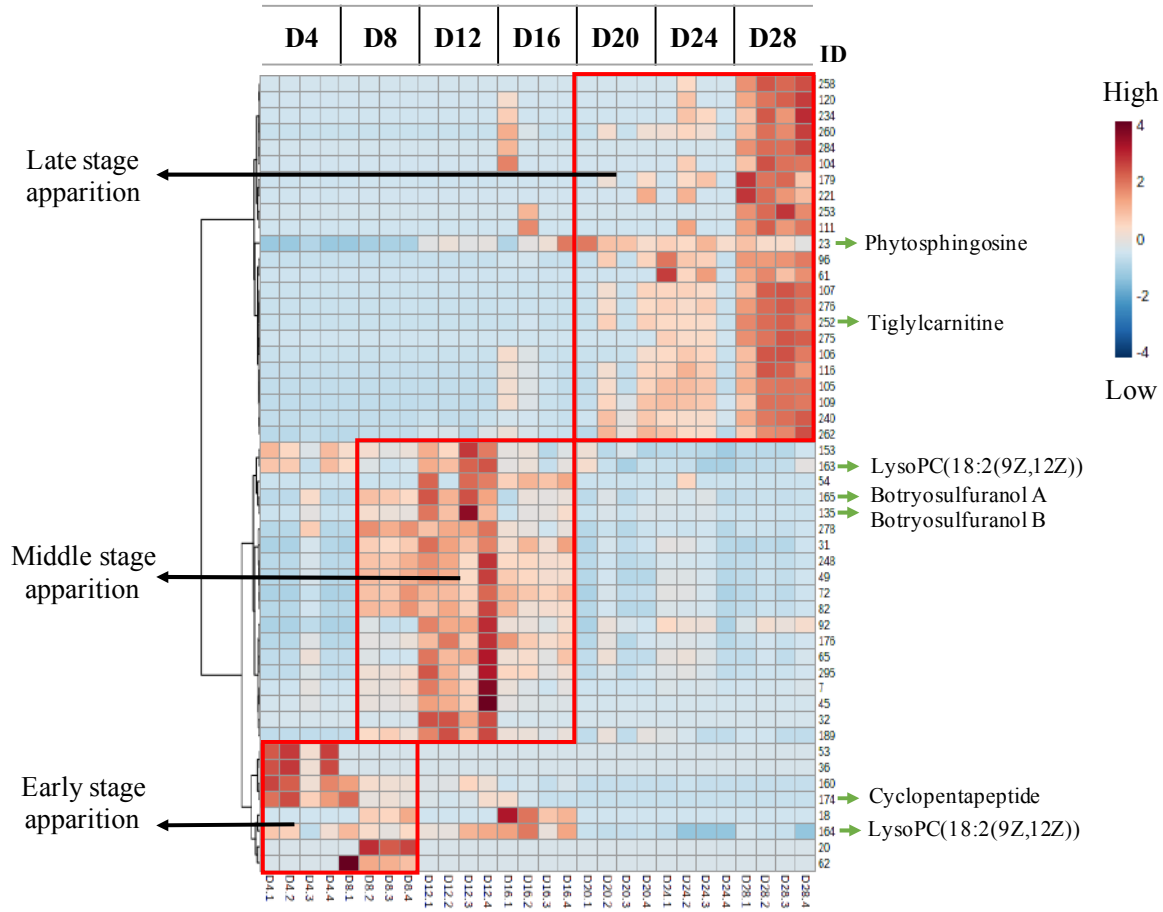

Figure 3.5. Hierarchical clustering of the top 50 features observed from day 4 (D4) to day 28 (D28) in *C. mamane*

Two metabolites putatively identified as glycerophoshocholines were produced during the early stage and middle stage while a cyclopentapeptide, mentioned above as part of top 15 features from the PLS-DA in **Figure 3.4**, was produced during the early stage. During the middle stage, we observed the production of the previously isolated TDKPs, botryosulfuranols A and B (Barakat et al., 2019) while a

tiglylcarnitine and a phytosphingosine, previously isolated from an unidentified fungus (Reindel et al., 1940), were produced during the late stage of *C. mamane* culture.

Thiodiketopiperazines evolution over time

Taking a closer look to the production of the TDKPs, botryosulfuranols A and B exhibited a significant change over time, being produced along the 28 days of culture with a maximum detection at D12 (**Figure 3.6**) while botryosulfuranol C presented a short time-frame production, being lowly detected between D6 and D9 (**Figure 3.6)**. Different adducts were detected along the time-series study for the TDKPs, being $[M+NH_4]^+$ the major adduct, followed by $[M+Na]^+$ and $[M+H]^+$, except for botryosulfuranol C. Botryosulfuranol D was not detected in this study. The error bars also indicates us that these experiments need to be repeated in order to confirm our hypothesis, however this trend give us insights of their behavior over time.

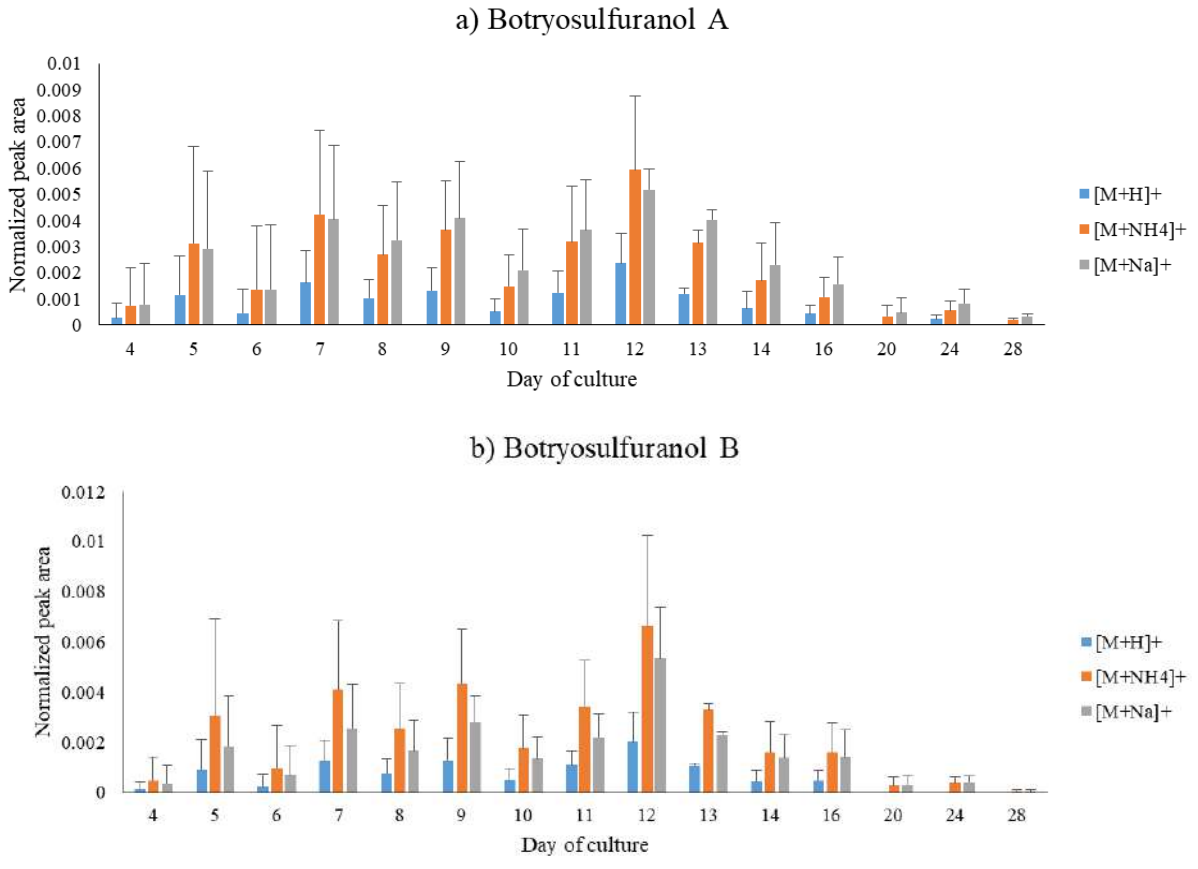

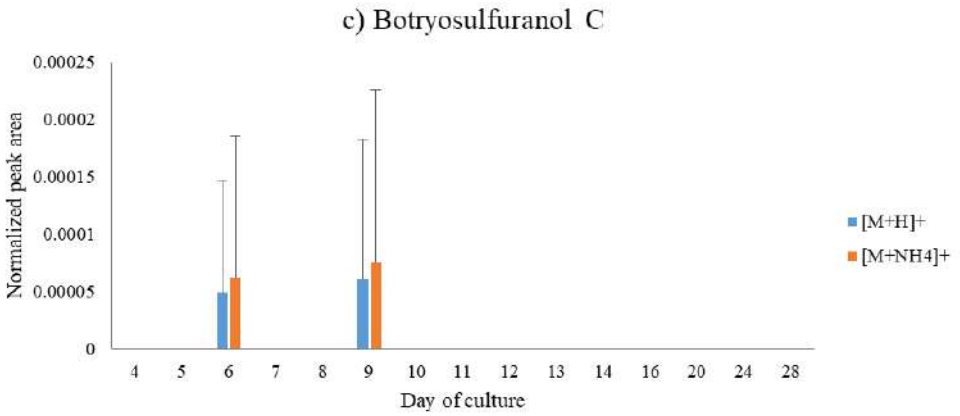

Figure 3.6. Normalized peak areas of the TDKPs (a) botryosulfuranols A, (b) B and (c) C under different incubation times observed for each detected adduct ($[M+H]^+$; $[M+NH_4]^+$ and $[M+Na]^+$)

Comparing and overlapping the production trends of the three TDKPs (**Figure 3.7**) considering the major adduct detected ($[M+NH_4]^+$), botryosulfuranols A and B present a similar pattern in contrast to botryosulfuranol C, which is almost not visible due to its lowly production and detection during the 28 days of culture. Moreover, their production tend to increase until D12 with a clear decrease from that day on.

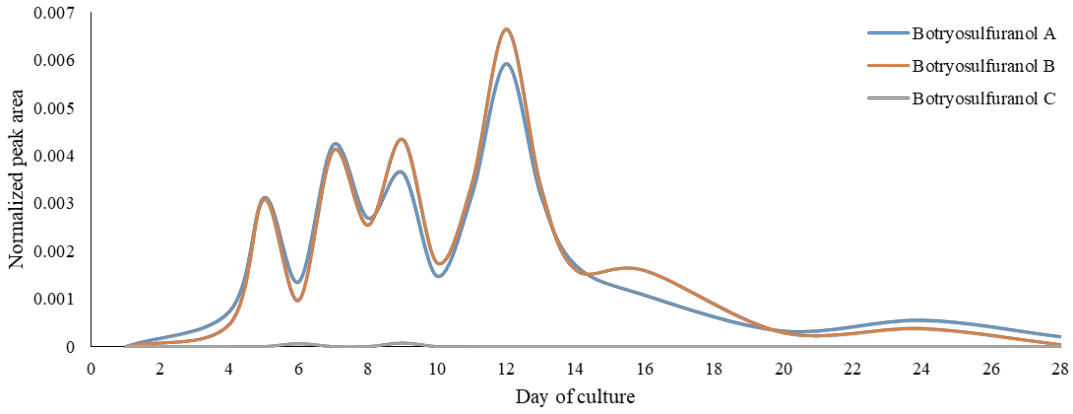

Figure 3.7. Production trend of TDKPs based on their normalized peak area

Molecular network analysis

To better visualize chemical relationships based on acquired MS-MS data, and to focus on the general chemical diversity based on annotated metabolites, a molecular networking was performed. Our analysis displayed a molecular network that contained 303 nodes and 29 spectral families with 161 connected

nodes while the rest of the nodes showed no link to others (self-loop). The size of the nodes represents VIP scores obtained for each feature (a bigger size, a higher VIP score) (**Figure 3.8**).

We observed the presence of chemical families such as the cluster containing long-chain fatty acids with the highest number of nodes possessing the highest VIP scores (bigger node sizes). Moreover, we can also observe the other clusters corresponding to phosphoethanolamines, phosphocholines, fatty amides, fatty acyls, steroid derivatives, amines, hybrid peptides, cyclopeptides and the cluster of TDKPs, botryosulfuranol A and B (**Figure 3.8**). The putatively identified metabolites found in the clusters within the molecular networking are detailed in **Table 3.2**.

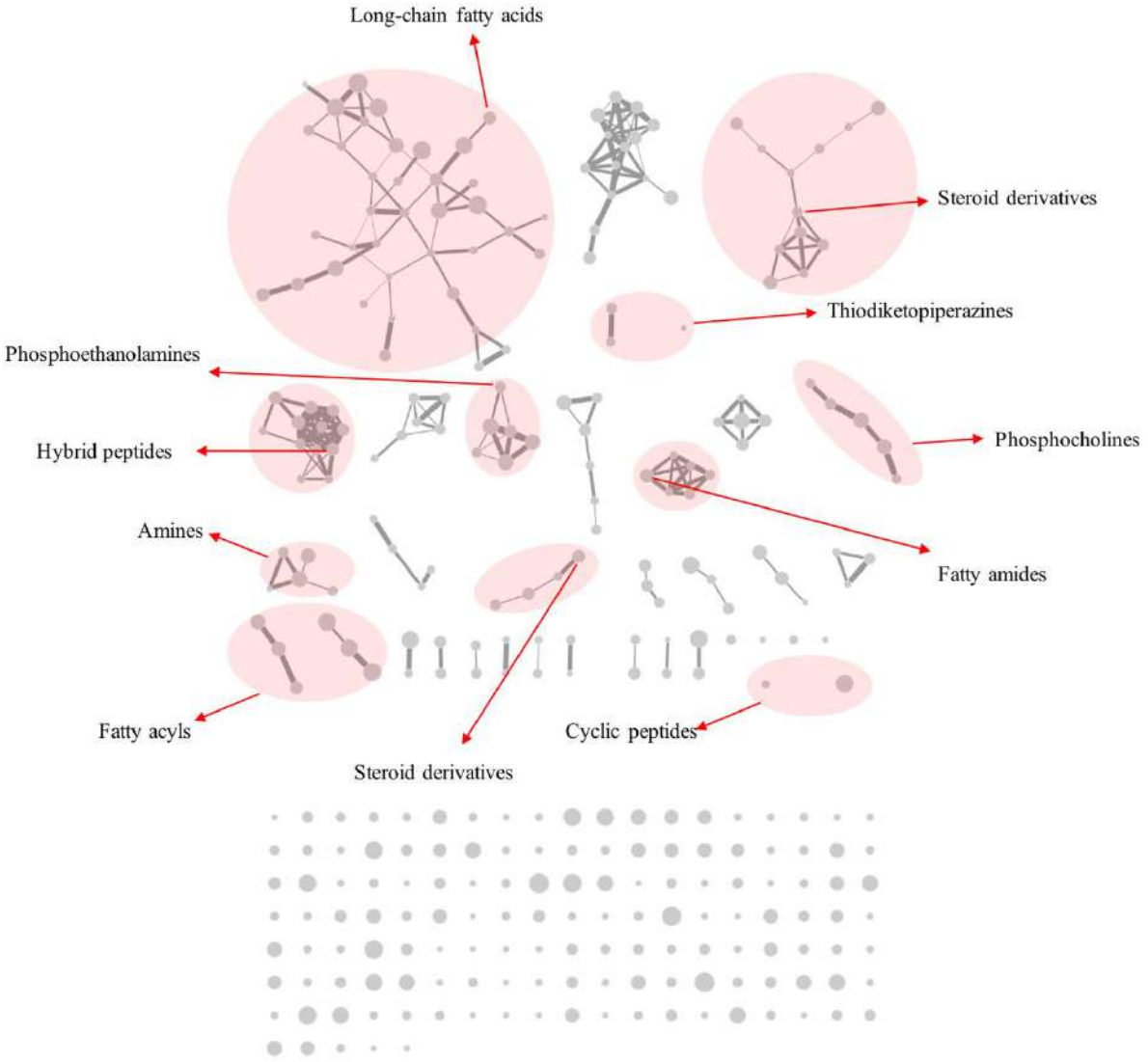

Figure 3.8. Molecular network showing the chemical families of the nodes corresponding to putatively annotated compounds clustered due to fragmentation pattern similarity

Table 3.2. Putative identification of metabolites detected during the time-series study of *C. mamane*

ID	Rt (min)	*m/z*	Adduct	Formula	Δ mass (ppm)	Putative identification	Ontology
23	8.39	318.2999	$[M+H]^+$	$C_{18}H_{39}NO_3$	4.70	Phytosphingosine	Sphingolipids
265	3.90	250.1800	$[M+H]^+$	$C_{15}H_{23}NO_2$	4.84	(E)-1-(2,3-dihydro-1H-pyrrol-1-yl)-2-methyldec-8-ene-1,3-dione	1,3-dicarbonyl compounds
252	5.42	244.1539	$[M+H]^+$	$C_{12}H_{21}NO_4$	5.94	Tiglylcarnitine	Fatty acyls
163	9.25	542.3193	$[M+Na]^+$	$C_{26}H_{50}NO_7P$	6.52	LysoPC(18:2(9Z,12Z))	Glycerophosphocholines
164	9.06	520.3383	$[M+H]^+$	$C_{26}H_{50}NO_7P$	5.00	LysoPC(18:2(9Z,12Z))	Glycerophosphocholines
112	7.50	450.0783	$[M+NH_4]^+$	$C_{19}H_{16}N_2O_6S_2$	3.46	Botryosulfuranol C	Thiodiketopiperazines
165	7.05	485.0816	$[M+Na]^+$	$C_{21}H_{22}N_2O_6S_2$	1.39	Botryosulfuranol A	Thiodiketopiperazines
135	7.32	487.0961	$[M+Na]^+$	$C_{21}H_{24}N_2O_6S_2$	3.68	Botryosulfuranol B	Thiodiketopiperazines
172	9.03	552.4119	$[M+H]^+$	$C_{29}H_{53}N_5O_5$	2.12	Cyclo-(L-Leu-L-Leu-D-Leu-L-Leu-L-Val)*	Cyclic peptides
174	9.37	583.4518	$[M+NH_4]^+$	$C_{30}H_{55}N_5O_5$	5.83	Cyclo-(L-Ile-L-Leu-L-Leu-L-Leu-L-Leu)*	Cyclic peptides
58	11.93	339.3256	$[M+H-H_2O]^+$	$C_{22}H_{44}O_3$	3.72	22-Hydroxydocosanoic acid	Long-chain fatty acids
127	9.03	478.2936	$[M+H]^+$	$C_{23}H_{44}NO_7P$	0.69	LysoPE(18:2(9Z,12Z)/0:0)	Phosphoethanolamines
202	11.19	799.5190	$[M+H]^+$	$C_{43}H_{70}N_6O_6S$	3.64	Symplostatin 1	Hybrid peptides
291	12.43	284.2949	$[M+H]^+$	$C_{18}H_{37}NO$	3.61	Octadecanamide	Fatty amides

*unknown amino acids sequence

3.2.2 *C. mamane* culture under the OSMAC approach

General observations

The endophytic fungus *C. mamane* was cultivated in 6-well plates containing Czapek (CZA) and ISP2 (see **Chapter 2** for methodoloy) during 6 and 10 days at 27 ºC. To observe the influence of light on the metabolism, *C. mamane* was cultured under natural light (L) and total darkness (D) (**Figure 3.9**). At first sight, colonies presented white mycelium with bigger black spot areas than those observed in the colonies grown on MEA under the time-series study (shown above in **Figure 3.2**), which might indicate the production of pigments except when *C. mamane* was cultured in ISP2 during 6 days at dark conditions, suggesting a probable influence of light for mycelium coloration under this culture medium.

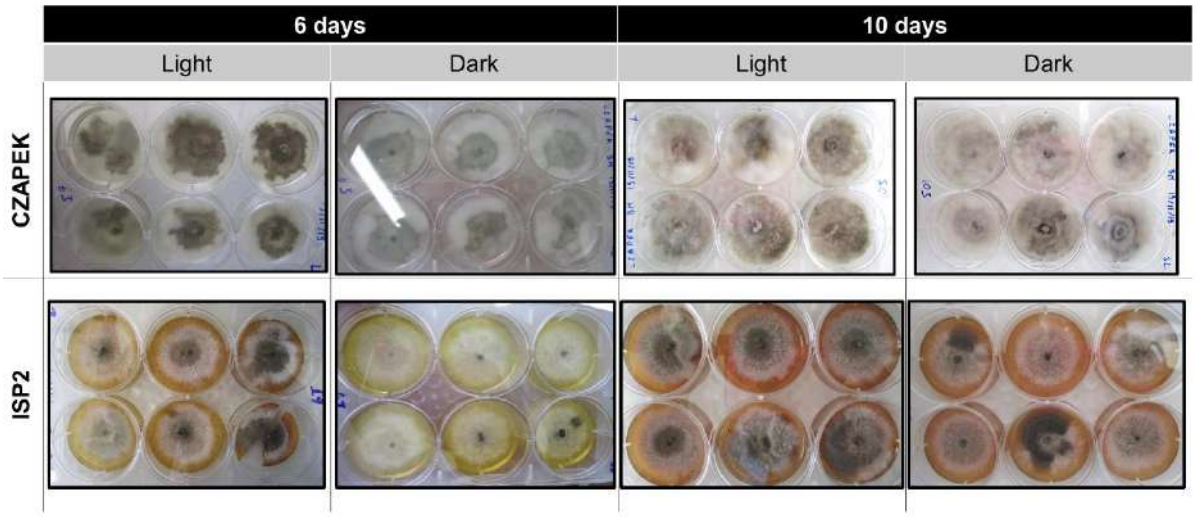

Figure 3.9. Morphological changes of *C. mamane* (upper view) cultivated in CZA and ISP2 media during 6 and 10 days under natural light and dark conditions

LC-(+)ESI-HRMS profiles of all the 48 extracts from the OSMAC experiment afforded 456 features (*m/z*-RT pairs) in PI mode, which were considered for the metabolomics and statistical analysis. A total of 16% of these features were putatively annotated (73 out of 456), corresponding to different chemical classes such as DKPs, cyclic peptides, fatty acids, fatty amides, flavonoids (**Annexes 2**).

Multivariate classification (PLS-DA)

A supervised PLS-DA analysis was carried out on these data indicating the different responses of *C. mamane* when cultured in ISP2 or CZA during 6 and 10 days under light or total darkness (**Figure 3.10**).

Separate clusters appear on the PLS-DA score plot (31 % of total variability). The component 1 (X-axis) explained 22.1 % of the variability, allowing the discrimination of the clusters corresponding to CZA and ISP2. While in the component 2 (9.9%), we can observe the influence of 6 and 10 days of culture and a slight differentiation between the clusters of light (L) and total darkness (D).

The **Figure 3.10** presents the top 15 features that contributed to the differences between these clusters. Among them, a metabolite mainly detected in ISP2, was putatively identified as 3-formylindole, a compound previously isolated from the endophytic fungus *Nigrospora* sp. (Kjer, 2009). Another compounds, mainly detected in CZA, was identified as botryosulfuranol C. The top 15 metabolites are detailed in **Table 3.3.**

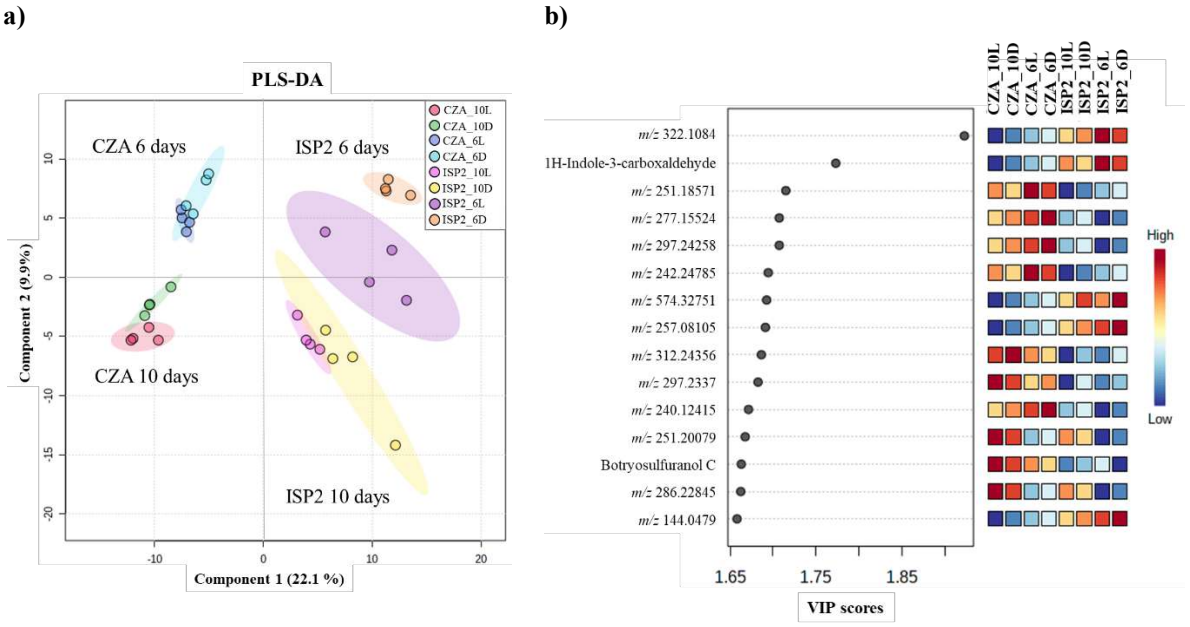

Figure 3.10. (a) Partial least squares discriminant analysis (PLS-DA) obtained from LC-MS profiles corresponding to the extracts of *C. mamane* cultivated in Czapek (CZA) and ISP2 during 6 and 10 days based on features (*m/z* at Rt to its normalized peak area), (b) Variable importance in projection (VIP) score of the top 15 compounds from the PLS-DA analysis corresponding to each condition of culture

Table 3.3. Top compounds that significantly contribute to the difference in the PLS-DA analysis from LC-HRMS/MS data corresponding to the OSMAC approach of *C. mamane* culture

ID	Rt (min)	*m/z*	Adduct	Formula	Δ mass (ppm)	Putative identification	Ontology	VIP scores
182	3.69	322.1084	$[M+H]^+$	$C_{11}H_{19}N_3O_6S$	3.15	Unknown	Unknown	1.9221
208	3.34	146.0604	$[M+H]^+$	C_9H_7NO	2.46	3-formylindole	Indoles	1.7728
75	5.70	251.1857	$[M+H]^+$	$C_{12}H_{26}O_5$	1.59	Unknown	Unknown	1.7148
88	4.25	277.1552	$[M+H]^+$	$C_{15}H_{20}N_2O_3$	1.91	Unknown	Unknown	1.7072
131	10.10	297.2425	$[M+NH_4]^+$	$C_{11}H_{37}NS_3$	0.46	Unknown	Unknown	1.7072
43	10.97	242.2478	$[M+H]^+$	$C_{15}H_{31}NO$	0.16	Unknown	Unknown	1.6944
344	9.43	574.3275	$[M+H-H_2O]^+$	$C_{34}H_{45}N_3O_6$	0.08	Unknown	Unknown	1.6925
61	5.64	257.0810	$[M+H-H_2O]^+$	$C_{15}H_{14}O_5$	0.64	Unknown	Unknown	1.6911
163	9.16	312.2435	$[M+H]^+$	$C_{20}H_{29}N_3$	0.24	Unknown	Unknown	1.6864
128	7.29	297.2337	$[M+H]^+$	$C_{20}H_{28}N_2$	3.9	Unknown	Unknown	1.6826
38	5.36	240.1241	$[M+H]^+$	$C_{12}H_{17}NO_4$	4.40	Unknown	Unknown	1.6715
132	8.47	251.2007	$[M+H]^+$	$C_{16}H_{26}O_2$	0.56	Unknown	Unknown	1.6676
287	7.67	455.0363	$[M+Na]^+$	$C_{19}H_{16}N_2O_6S_2$	4.60	Botryosulfuranol C	Thiodiketopiperazines	1.6631
102	8.48	286.2284	$[M+NH_4]^+$	$C18H_{24}N_2$	2.18	Unknown	Unknown	1.6625
196	1.80	144.0479	$[M+H]^+$	C_6H_9NOS	0.96	Unknown	Unknown	1.6582

Hierarchical clustering analysis (Heat map)

Out of the 456 features, 253 showed a significant change over time (p-value < 0.05) using the analysis of variance (one-way ANOVA) and Fisher test (F-test). The top 50 features with significant changes were plotted in the hierarchical clustering analysis (heat map) where four main clusters of metabolite behaviors are observed (**Figure 3.11**): (**a**) a cluster of metabolites induced in CZA regardless of the culture time or light condition; (**b**) a cluster of metabolites induced in CZA at day 10 regardless the light condition, (**c**) a cluster of metabolites induced in ISP2 at day 6 under dark conditions, (**d**) a cluster of metabolites induced in ISP2 at day 6, (**e**) a cluster of metabolites induced in ISP2 at day 10 under light conditions and (**f**) a cluster of metabolites induced in ISP2 at day 10.

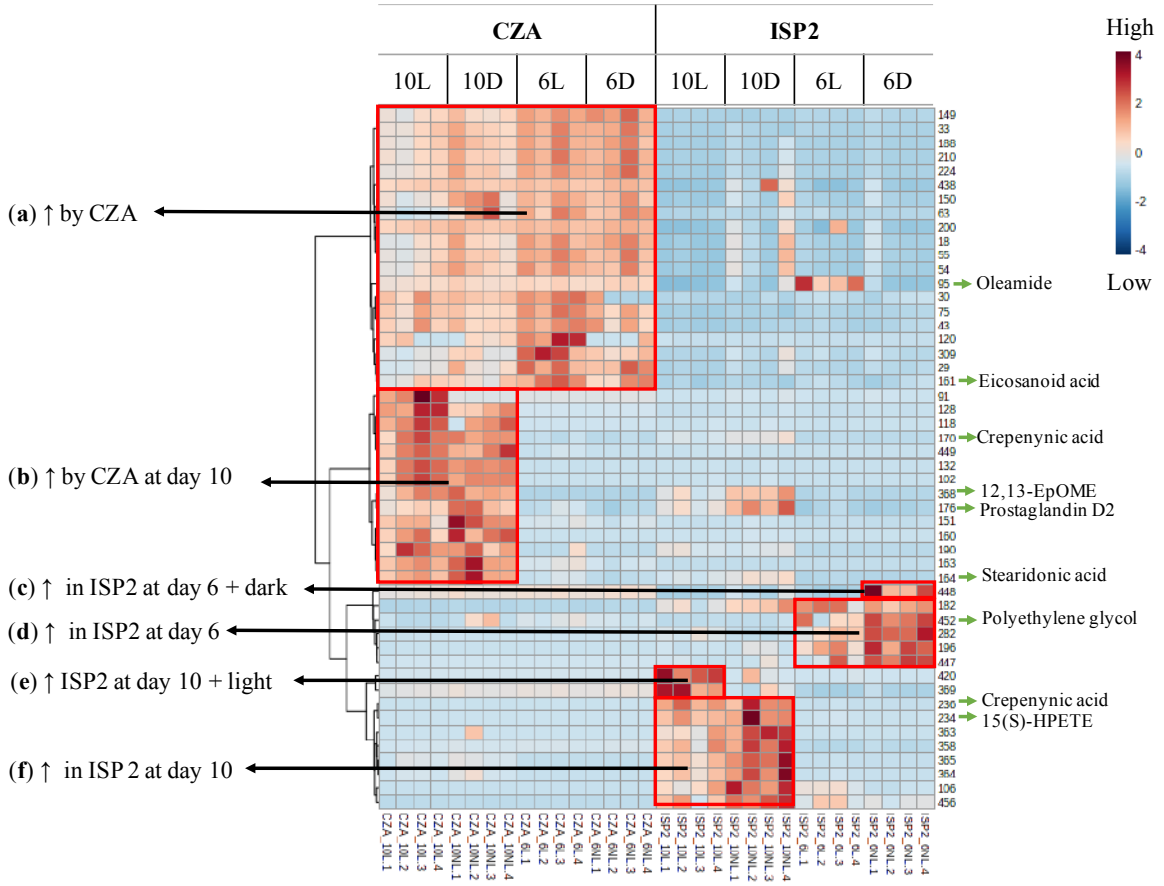

Figure 3.11. Hierarchical clustering of the top 50 features observed in *C. mamane* cultured under the OSMAC approach

Most of the putatively identified metabolites from the top 50 correspond to fatty acids, fatty acyl, fatty amides and prostaglandins such as oleamide, eicosanoid acid, 12,13-EpOME, prostaglandin D2.

Differential production of metabolites (Volcano plot analysis)

Regarding the influence of light more in details as shown in the Volcano plot representations (**Figure 3.12**), a total of 14, 38, 6 and 10 features were up-regulated when *C. mamane* was cultivated under light conditions in ISP2 during 6 days (**Figure 3.12a**) and 10 days (**Figure 3.12c**) and in CZA during 6 days (**Figure 3.12b**) and 10 days (**Figure 3.12d**), respectively. Notably, culturing *C. mamane* in ISP2 medium during 10 days was the condition that induced the highest number of metabolites. Moreover, some metabolites were down-regulated when *C. mamane* was cultivated under light conditions, meaning that total darkness was a suitable condition for the production of these metabolites. However, due to the low annotation rate, metabolites with the most important significant changes could not be putatively annotated.

a) CM grown on ISP2 during 6 days

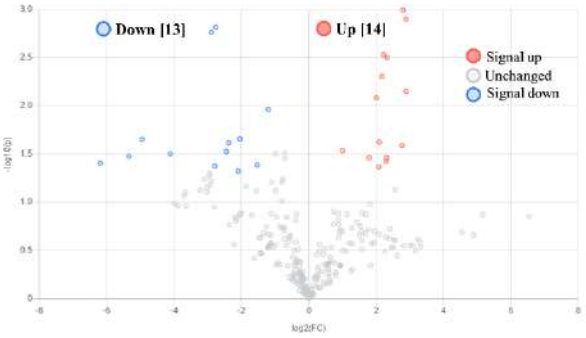

b) CM grown on Czapek during 6 days

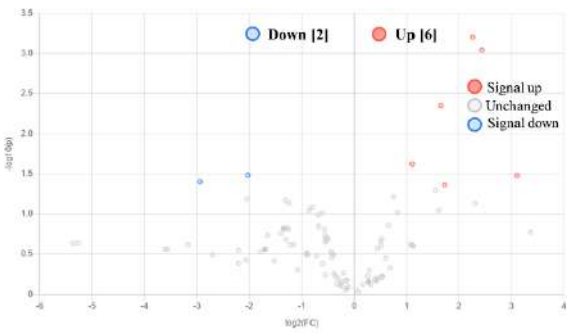

c) CM grown on ISP2 during 10 days

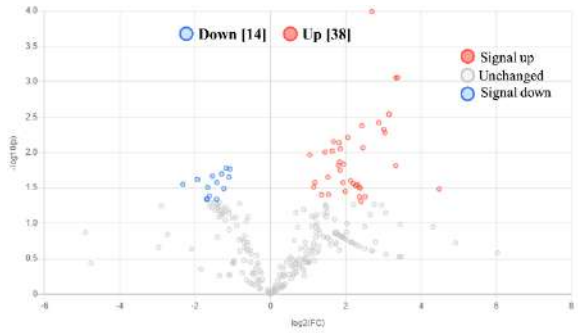

d) CM grown on Czapek during 10 days

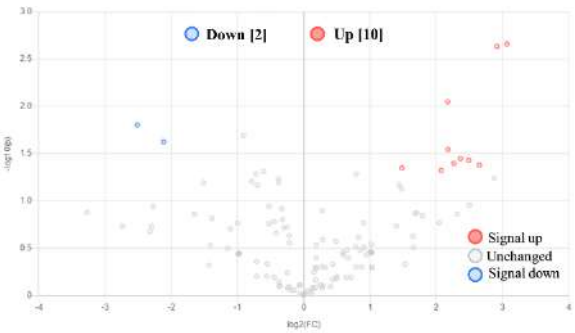

Figure 3.12. Volcano plot representations of *C. mamane* response to light conditions in ISP2 (a, c) and CZA (b, d) during 6 (a, b) and 10 days of incubation (c, d). Each dot represents a feature (*m/z* at Rt), the red and blue colors indicate a significant change (*p*-value < 0.05 and fold-change ratio > 2) of the features under the light influence in up-regulating (red) or down-regulating (blue) their production while the numbers in brackets indicate the number of significant features observed.

Focusing on the TDKPs, we can observe that no TDKP was detected when *C. mamane* was growth on ISP2 during 6 days under dark conditions (ISP2_6D), indicating that under these conditions, the presence of light was crucial for their production or that their production was delayed as it is observed during 10 days under dark conditions. Besides this, the production of botryosulfuranol C was

significantly different (p-value < 0.05) between CZA and ISP2 media, between 6 and 10 days of culture. Botryosulfuranol D was not detected in this study. Despite the high variability observed (error bars), this indicates that TDKPs production by *C. mamane* tend to be higher in CZA than in ISP2, specifically during 10 days under light conditions (**Figure 3.13**).

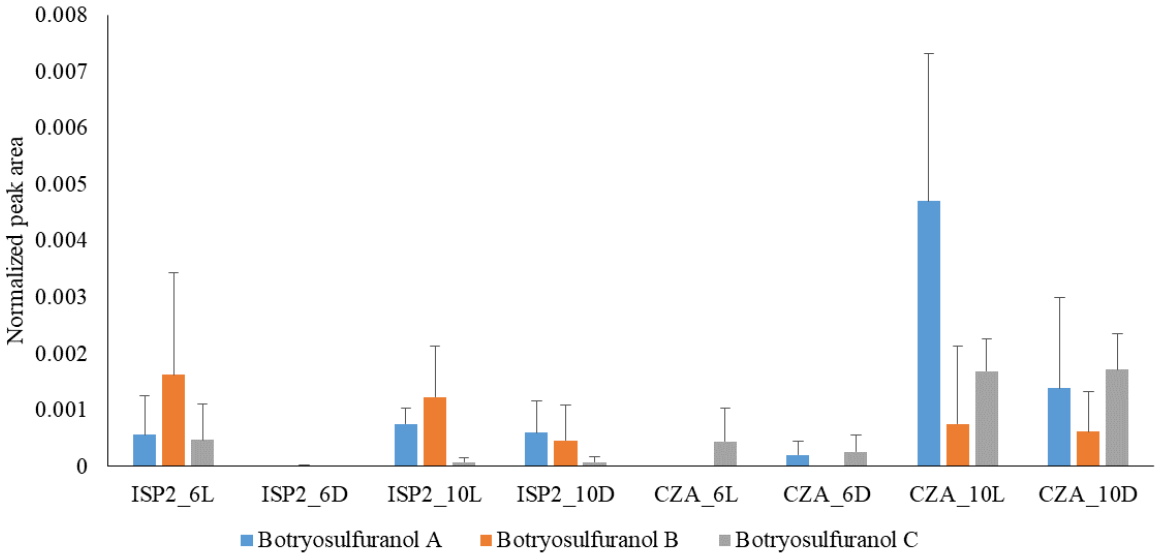

Figure 3.13. Normalized peak areas of TDKPs botryosulfuranols A, B and C when culturing *C. mamane* in ISP2 and CZA media during 6 and 10 days under light (L) and dark (D) conditions

Molecular network analysis

To better visualize chemical relationships based on acquired MS-MS data, and to focus on potential derivatives of annotated metabolites, a molecular networking was performed. Our analysis displayed a molecular network that contained 456 nodes and 38 spectral families with 252 connected nodes while the rest of the nodes showed no link to others (self-loop). The size of the nodes represents the total average of the detected peak areas for each compound in all the conditions while the colors depend on their detection in CZA and/or ISP2 medium (**Figure 3.14**). A cluster containing metabolites mostly produced in ISP2 was observed with no putatively annotated features.

The putatively annotated DKP, brevianamide F, was previously isolated from *Penicillium brevi-compactum* (Birch and Russell, 1972), also from an endophytic fungal strain of *Aspergillus fumigatus* cultured in three different culture media under the OSMAC approach (Zhang et al., 2013) and more recently, from an endophytic fungal strain of *Colletotrichum gloeosporioides* (Yang et al., 2019). This DKP was found to be linked to two unknown metabolites with *m/z* 288.0716 at 3.8 min ($C_7H_{14}N_2O_5S_2$) and with *m/z* 300.1708 at 5.4 min ($C_{17}H_{21}N_3O_2$). Regarding the nodes corresponding to the TDKPs,

botryosulfuranols A, B and C were not linked to each other, contrary to what expected and observed in the time-series study.

Another DKP, cordycedipeptide A, previously isolated from the fungus *Cordyceps sinensis* (Jia et al., 2005) was found to be linked to one unknown metabolite with *m/z* 228.1341 at 2.95 min ($C_{10}H_{14}N_2O_3$). Moreover, the molecular network highlighted the presence of a cluster corresponding to cyclic peptides, containing putatively annotated metabolites previously isolated from a endophytic fungal strain of *Fusarium decemcellulare* with *m/z* 552.4145 at 9.176 min ($C_{29}H_{53}N_5O_5$), *m/z* 588.4099 at 9.504 min ($C_{30}H_{55}N_5O_5$) (Li et al., 2016) and *m/z* 600.4117 at 9.491 min ($C_{33}H_{53}N_5O_5$) from a non-identified endophytic fungal strain (Li et al., 2004). However, the order of the amino acids within the structure are not known and cannot be determined by this methodology.

Four metabolites were annotated as long-chain fatty acids such as the eicosanoid OPC-8:0, previously isolated from the fungus *Fusarium oxysporum* (Miersch et al., 1999), one eicosanoid acid; one sphingolipid phytosphingosine, previously isolated from an unknown fungus (Reindel et al., 1940), a prostaglandine D2, fatty acids crepenynic acid and 12-13-EpOME. These metabolites are detailed in **Table 3.4**.

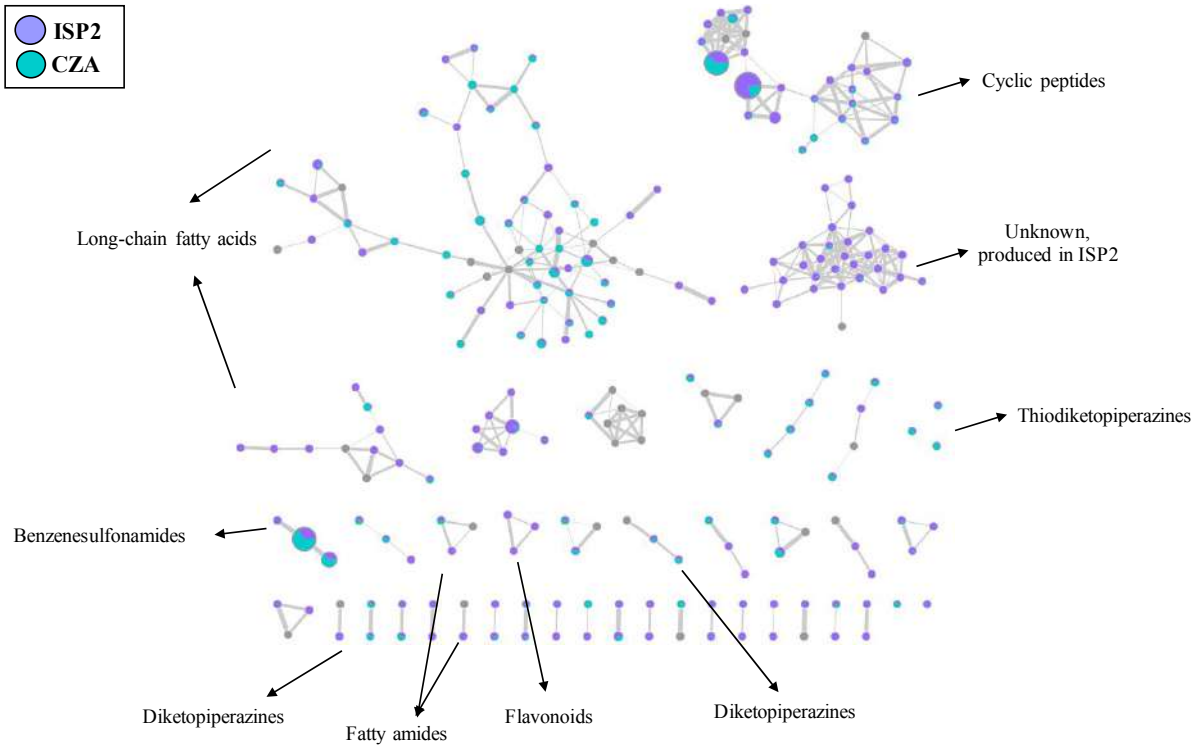

Figure 3.14. Molecular networking showing the chemical families of putatively annotated compounds detected under ISP2 and/or CZA

Table 3.4. Putative identified compounds detected in the OSMAC approach

ID	Rt (min)	*m/z*	Adduct	Formula	Δ mass (ppm)	Putative identification	Ontology
95	11.55	282.2793	$[M+H]^+$	$C_{18}H_{35}NO$	0.56	Oleamide	Fatty amides
161	11.20	311.2945	$[M+H]^+$	$C_{20}H_{38}O_2$	0.13	Eicosenoic acid	Eicosanoids
170	9.64	279.2323	$[M+H]^+$	$C_{18}H_{30}O_2$	1.58	Crepenynic acid	Long-chain fatty acids
368	9.64	319.2244	[M+Na]+	$C_{18}H_{32}O_3$	0.11	12,13-EpOME	Long-chain fatty acids
176	9.06	317.2098	$[M+H-2H_2O]^+$	$C_{20}H_{32}O_5$	4.16	Prostaglandin D2	Prostaglandins and related compounds
164	9.06	277.2174	$[M+H]^+$	$C_{18}H_{28}O_2$	4.30	Stearidonic acid	Lineolic acids and derivatives
452	4.39	188.1288	$[M+H]^+$	$C_9H_{17}NO_3$	3.61	Polyethylene glycol	Medium-chain fatty acids
236	10.73	279.2322	$[M+H]^+$	$C_{18}H_{30}O_2$	1.22	Crepenynic acid	Long-chain fatty acids
234	10.21	359.2195	$[M+Na]^+$	$C_{20}H_{32}O_4$	0.60	15(S)-HPETE	Fatty acyls
208	3.34	146.0604	$[M+H]^+$	C_9H_7NO	2.46	1H-Indole-3-carboxaldehyde	Indoles
301	7.19	463.0989	$[M+H]^+$	$C_{21}H_{22}N_2O_6S_2$	0.50	Botryosulfuranol A	Thiodiketopiperazines
305	7.44	487.0989	$[M+Na]^+$	$C_{21}H_{24}N_2O_6S_2$	4.33	Botryosulfuranol B	Thiodiketopiperazines
287	7.67	455.0363	$[M+Na]^+$	$C_{19}H_{16}N_2O_6S_2$	4.60	Botryosulfuranol C	Thiodiketopiperazines
98	4.82	284.1395	$[M+H]^+$	$C_{16}H_{17}N_3O_2$	0.62	Brevianamide F	Diketopiperazines
166	9.76	295.2267	$[M+H]^+$	$C_{18}H_{30}O_3$	0.24	3-Oxo-2-(2-entenyl)cyclopentaneoctanoic acid;OPC-8:0	Eicosanoids
351	9.50	588.4099	$[M+Na]^+$	$C_{30}H_{55}N_5O_5$	0.73	Cyclo-(L-Ile-L-Leu-L-Leu-L-Leu-L-Leu)*	Cyclic peptides
332	9.17	552.4144	$[M+H]^+$	$C_{29}H_{53}N_5O_5$	4.60	Cyclo-(L-Leu-L-Leu-D-Leu-L-Leu-L-Val)*	Cyclic peptides
360	9.49	600.4118	$[M+H]^+$	$C_{33}H_{53}N_5O_5$	0.13	Cyclo-(L-Phe-L-Leu1-L-Leu2-L-Leu3-L-Ile)*	Cyclic peptides
28	3.17	228.1345	$[M+H]^+$	$C_{10}H_{17}N_3O_3$	1.23	Cordycedipeptide A;(-)-Cordycedipeptide A	Diketopiperazines
178	9.98	318.3002	$[M+H]^+$	$C_{18}H_{39}NO_3$	0.22	Phytosphingosine	Sphingolipids

*unknown amino acids sequence

3.3 Discussion

3.3.1 General morphological observations

Morphological changes were observed under both methodologies, mainly the darkening of mycelium pigmentation. Over 28 days of culture in MEA, most of the colonies maintained a white pigmentation while only some of them showed dark spots on their mycelium (**Figure 3.2**). In a previous study, *C. mamane* colonies showed a dark pigmentation of their mycelium when it was cultured in MEA during 10 days (Triastuti et al., 2021), probably indicating the aging of the strain, a different inoculation method or different light conditions in comparison to our study. Also, the first morphological descriptions of this species indicate a rapid change of mycelium color from medium to dark gray when the culture was exposed to natural light (Gardner, 1997). Similarly, another member of the Botryosphaeriaceae family, *Botryosphaeria dothidea*, showed initially colorless colonies that changed to dark with age (Phillips et al., 2005). Under the OSMAC approach, most of the colonies grown on ISP2 and CZA showed a darkening of their mycelium at day 6 and 10 of culture, except in ISP2 at day 6 under dark conditions (**Figure 3.9**).

Light can influence visible changes such as the mycelium growth (Kim et al., 2005) as observed with *C. mamane* when white colonies were produced on ISP2 during 6 days under dark conditions. Also, the correlation between mycelium color changes and metabolite production has been previously reported in, for example, the fungus *Menisporopsis theobromae* (Madla et al., 2006) but no pigments could be identified in this study. In general, fungi produce a wide array of pigments corresponding to different chemical classes such as melanins, carotenoids and quinones (Kalra et al., 2020) which possess many pharmacological activities that help the fungi to protect against biotic and abiotic stress (Berthelot et al., 2017; Dufossé et al., 2014).

3.3.2 Time-series study

Variations in the metabolome of *C. mamane* across the 28 days of culture in MEA allowed us to identify three main metabolite behaviors: early, middle and late stage (**Figure 3.5**). In agreement with our findings, similar patterns were observed in the metabolome of the fungus *Colletotrichum sublineolum* corresponding to 3 time periods: early adaptation, transition and stationery. It is postulated that in the transition period, the fungus can respond to environmental signals for a better adaptation to decreasing nutrient conditions (Tugizimana et al., 2019). Similarly, a time-variations study of the metabolome of two marine-derived fungal strains, *Penicillium canescens* and *Penicillium* sp., indicates three phases according the morphological changes and six groups of compounds with different behaviors according to their apparition or disappearance during the whole culture time (Roullier et al., 2016).

Among the metabolites that contributed to the cluster differentiation in the multivariate analysis (PLS-DA), we found a cyclic pentapeptide, which exhibited an early-stage apparition between D4 and D8 and a rapid decrease, being almost undetected after this period. Cyclic peptides produced by fungi have been reviewed elsewhere, indicating their important biological activities and potential applications (Wang et al., 2017b), however, their ecological roles have been very less discussed. Their relevance in interspecies interactions as crosstalk communication molecules has been proposed as for example for the hexocyclopeptides produced by the endophytic fungus *Fusarium solani* due to their accumulation under the co-culture with an endophytic bacterium (Wang et al., 2015). Also, cyclic pentapeptides produced by the endophytic fungus *Fusarium decemcellulare* exhibited a weak antimicrobial activity against another fungal endophyte in co-culture (Li et al., 2016), showing their role in microbial neighbor communication and in proving certain benefits in colonization. This might explain the rapid decrease in the production of the cyclic pentapeptide along the 28 days of culture of *C. mamane*, considering also that secondary metabolites stop being produced over time or after many subculture generations under axenic conditions (Kusari et al., 2014) in the absence of signals from their natural environment.

Other metabolites also showed a change in their production over time, including two glycerophoshocholines that were produced during the early stage and middle stage, which is consistent with a lipidomic study of *Trichoderma brevicompactum*, where the glycerophosholipids were found to be significantly altered at the early phase of a 15-day culture (Bai et al., 2019). Also, a phytosphingosine was produced during a late stage. Fungal sphingolipids have shown to possess antifungal activity, playing important functions in cell differentiation and pathogen recognition and virulence (Mota Fernandes and Del Poeta, 2020) such as two new sphingolipids with antifungal activity, previously isolated from the marine algous endophytic fungus *Aspergillus niger* (Zhang et al., 2007). Besides the reports showing their potent and novel antimicrobial activities (Barthélemy et al., 2019), it is known that lipids possess important functions in fungi, especially in the pathogen recognition by the host and signaling between cells during infection or during nutrient exchange (Siebers et al., 2016). In general, lipids are known to be important metabolites as signaling molecules during development and pathogenicity in fungi (Shea and Del Poeta, 2006) and in this case, their induction in CZA or ISP2 appeared to be significantly different. Moreover, molecular network analysis allowed us to observe the presence of many other fatty acids contained in one of the clusters from our molecular network analysis, as well as other chemical families based on the putatively annotated metabolites.

3.3.3 OSMAC approach

Among culture media used to cultivate *C. mamane* according to literature, ISP2 and CZA were not previously reported (Barakat et al., 2019; Gardner, 1997; Pongcharoen et al., 2007). CZA medium contains 3 salts as source of ions, being sodium nitrate the unique source of inorganic nitrogen (St-

Germain and Summerbell, 2003). Metal ions have demonstrated to have a physiological influence on microorganisms (Thorneley, 1990), triggering the synthesis of new compounds (Jiang et al., 2014). CZA medium could be considered as an oligotrophic medium, which could be favorable for the activation of some gene clusters, which may remain silent when fungi are cultured in eutrophic media such as MEA or ISP2. This might explain the cluster of metabolites induced when *C. mamane* was cultured in CZA but not by ISP2 (**Figure 3.11**). Although ISP2 medium does not contain any source of ions or supplements, it has been useful for the discovery of new metabolites and the induction of other known compounds in fungi (Wakefield et al., 2017) as also observed with the cluster of metabolites induced when *C. mamane* was cultured in ISP2 but in CZA (**Figure 3.11**).

On the other side, the influence of light seemed to be more important when culturing *C. mamane* in ISP2 during 10 days given the number of metabolites induced under natural light conditions (**Figure 3.12**) in comparison to the other conditions. In general, fungal endophytes have a prominent dark habitat in the internal host plant tissues and this condition has shown a great impact in, for example, taxol production by *Paraconiothyrium* spp. as this endophytic fungus is mainly found in the deep vascular system of the host plant (Soliman and Raizada, 2018). By contrast, *C. mamane* was isolated from the leaves of *Bixa orellana*, a plant that grows in tropical regions (Vilar et al., 2014) with natural light conditions varying from full sunlight to partial shade, since light quality is also important for the secondary metabolism of the host plant (Faria et al., 2019).

We were not able to determine the chemical classes of the metabolites that might be specifically induced by each culture media or the different light conditions. However, molecular networking showed us a cluster of metabolites that was mostly produced by *C. mamane* in ISP2 (**Figure 3.14**) but no metabolite belonging to this cluster could be putatively annotated either. Similar chemical families observed in the time-series study were observed under the OSMAC approach, including the fatty acids, fatty amides, cyclic peptides and TDKPs. Moreover, the presence of two DKPs, putatively annotated as brevianamide F and cordycedipeptide A linked with other metabolites in different clusters could indicate the presence of their derivatives or similar compounds that will need further future investigations.

3.3.4 Special focus on the TDKPs

We observed the production of botryosulfuranols A and B (**Figure 3.6**) during the whole culture period of 28 days with a significant higher production during the middle stage at D12 (**Figure 3.7**) while botrysulfuranol D was undetected in both studies, indicating its production is less constant or in undetected quantities. In contrast, botryosulfuranol C was only detected between D6 and D9, highlighting the short time frame for its detection. This TDKP possesses a di-sulfur bridge, which plays an important role in biological activity (Barakat et al., 2019; Jiang and Guo, 2011). In addition to this,

di-sulfur bridge might represent certain toxicity to the producer organism, which activates defense mechanisms involving the opening of the di-sulfur bridge as it was observed for the biosynthesis of the DKP gliotoxin produced by *Aspergillus fumigatus* (Scharf et al., 2014). This situation might explain the short time-frame production of botryosulfuranol C by *C. mamane*.

In this study, we also observed that the presence of light was important to avoid the production delay of the TDKPs when growing *C. mamane* in ISP2 during 6 days. It is known that for the biosynthesis of DKPs, two main enzymes are needed, nonribosomal peptide synthetases (NRPSs) and cyclodipeptide synthases (CDPSs) (Borgman et al., 2019) whose coding gene clusters have shown to respond to environmental signals such as light and nutrient sources (Brakhage, 2013), which can explain our observations of the influence of light over the TDKPs production. Moreover, culturing *C. mamane* in CZA during 10 days under light conditions allowed a higher production of the TDKPs, specifically a significant induction of botryosulfuranol C, in comparison to the other conditions used under the OSMAC approach. Similarly, the endophytic fungus *Penicillium brocae* produced four new TDKPs when cultured in CZA (Meng et al., 2017). Also, the fungus *Aspergillus sydowii* allowed the isolation of four bioactive DKPs when cultured in three different culture media under the OSMAC approach (da Silva Lima et al., 2018).

Our interest in understanding the production trend over time of the TDKPs and their production patterns under different culture conditions lies on their biological activity as cytotoxic (Barakat et al., 2019) and as antileishmanial metabolites (unpublished data) as well as in the different biological activities reported in the literature for these type of metabolites (Song et al., 2021; Wang et al., 2017a). Their ecological roles in fungi are still not fully understood, however DKPs might act as quorum sensing (QS) molecules, a mechanism that is observed in yeast and filamentous fungi through the production of tyrosol, farnesol (Mondal and Majumdar, 2019) and mycotoxins (Venkatesh and Keller, 2019). This role has been recently reported for DKP-producing bacteria (Bofinger et al., 2017; Zhu et al., 2019) and in *Aspergillus fumigatus*, where the production of DKPs emestrins A and B were induced in presence of bacterial QS molecules, probably acting as QS inhibitors to modulate or attenuate bacterial populations (Rateb et al., 2013).

3.4 Conclusions

During the time variations study, we observed that a cyclopentapeptide appeared significantly produced during the early stage of *C. mamane*. This metabolite is probably involved in QS mechanisms as reported for other fungi and the absence of other signals might have cause the decline of its production in later stages. Moreover, the production of the TDKPs, botryosulfuranols A and B showed a significant increase during the middle stage at day 12 while botryolsulfuranol C exhibited a short time frame

production, probably due to the toxicity that the di-sulfur bridge might generate in *C. mamane* as reported for other DKPs such as the gliotoxin.

The OSMAC approach allowed us to observe the different cluster of metabolites that were induced under CZA and ISP2, the latter being the culture medium that induced most of the metabolites under light conditions. Interestingly, TDKPs were not detected in ISP2 during 6 days of culture under dark conditions, indicating the importance of light for an ealier production. The culture of *C. mamane* in CZA during 10 days under natural light conditions allowed a higher production (6 times higher) of the TDKPs in comparison to the other conditions. Different light wavelengths will be contemplated for future studies involving the influence of light, as it has been shown that light influence the secondary metabolism in fungi. In order to better understand the biological activities and the ecological roles of botryosulfuranols A, B and C, optimal culture conditions for their production are needed where different physicochemical conditions have to be followed up. This will allow us to obtain significant quantities of TDKPs for future experiments under different approaches and to discover new bioactive metabolites that this endophyte might produce.

Molecular network analysis allowed us to identified different chemical classes produced under the time variations study and OSMAC approach. Despite the low percentage of putative annotation in this study and in other untargeted metabolomics studies using mass spectrometry databases, some of the putatively annotated metabolites gave us insights about the chemical diversity produced by *C. mamane* under different conditions.

CHAPTER 4 ADDITION OF EPIGENETIC MODIFIERS AND AMINO ACIDS

This Chapter has been prepared from the submitted original research article

Chemical modulation of the metabolism of an endophytic fungal strain of *Cophinforma mamane* using epigenetic modifiers and amino-acids

R. Pacheco[a,b*], P. Vásquez-Ocmín[a], S. Duthen[a], S. Ortiz[a,4], P. Jargeat[c], C. Amasifuen[d], M. Haddad[a*], M. Vansteelandt[a]

[a]UMR 152 Pharma Dev, Université de Toulouse, IRD, UPS, France

[b]Laboratorios de Investigación y Desarrollo, Facultad de Ciencias y Filosofía, Universidad Peruana Cayetano Heredia, Lima, Perú

[c]Laboratoire Evolution et Diversité Biologique UMR 5174, Université de Toulouse, CNRS, IRD, France

[d]Instituto Nacional de Innovación Agraria, Dirección de Recursos Genéticos y Biotecnología, Avenida La Molina 1981, La Molina, Lima 15024, Perú

Abstract

Endophytic fungi are capable of producing a great diversity bioactive metabolites. However, the presence of silent and lowly expressed genes represents a main challenge for the discovery of novel secondary metabolites with different potential uses. Epigenetic modifiers have shown to perturb the production of fungal metabolites through the induction of silent biosynthetic pathways leading to an enhanced chemical diversity. Moreover, the addition of bioprecursors to the culture medium has been described as a useful strategy to induce specific biosynthetic pathways. The aim of this study was to assess the effects of different chemical modulators on the metabolic profiles of an endophytic fungal strain of *Cophinforma mamane* (Botryosphaeriaceae), known to produce 3 bioactive thiodiketopiperazine (TDKPs) alkaloids (botryosulfuranols A-D). Four epigenetic modifiers, 5-azacytidine (AZA), sodium butyrate (SB), nicotinamide (NIC), homoserin lactone (HSL) and 2 amino acids, L-phenylalanine and L-tryptophan, as bioprecursors of diketopiperazines, were used. The metabolic profiles were analysed by UHPLC-HRMS/MS under an untargeted metabolomics approach. Our results show that the addition of the two amino acids in *C. mamane* culture and the treatment with AZA significantly reduced the production of botryosulfuranols A, B and C. Interestingly, the treatment with HSL significantly induced the production of different classes of DKPs. The treatment with AZA resulted as the most effective epigenetic modifier for the alteration of the secondary metabolite profile of *C. mamane* by promoting the expression of cryptic genes.

Keywords: endophytic fungi, *Cophinforma mamane*, epigenetic modifiers, metabolomics, diketopiperazines

[4]Present address: Pharmacognosy Research Group, Louvain Drug Research Institute, Université Catholique de Louvain, Bruxelles, Belgium.

4.1 Introduction

Microorganisms such as bacteria, filamentous actinomycetes and fungi, have produced most of the known antibiotics due to the large chemical diversity and biological activities of their metabolites (Boufridi & Quinn 2018; Abdel-Razek *et al.* 2020). Among them, endophytic fungi are considered as a goldmine of secondary metabolites (Strobel & Daisy 2003), represented by little explored and characterized microorganisms capable of produce compounds with potential for pharmaceutical and commercial uses (Strobel 2018; Deshmukh *et al.* 2018; White *et al.* 2019). However, the conditions for gene expression in fungi are not fully understood and the presence of silent or lowly-expressed genes represent one of the main challenges for the isolation of novel secondary metabolites (Brakhage & Schroeckh 2011). Biosynthetic gene clusters in fungi are often found in the distal telomeric regions of the chromosome (Shwab *et al.* 2007; Williams *et al.* 2008), which are transcriptionally controlled by epigenetic regulation, specifically histone acetylation and methylation (Brakhage 2013; Pfannenstiel & Keller 2019). When fungal DNA is organized onto histone proteins and is densely packed into heterochromatin, it becomes transcriptionally silent (Okada & Seyedsayamdost 2017). In this regard, highly acetylated histones are generally loosely packed into euchromatin and therefore genes are considered as transcriptionally active (Cichewicz 2010) while methylation of histones often results in gene silencing (Suzuki & Bird 2008).

Recently, a very well-reviewed strategy to induce cryptic genes has consisted in the treatment of fungal endophytes with epigenetic modifiers such as histone deacetylase inhibitors (HDACi) and DNA methyltransferase inhibitors (DNMTi) (Toghueo *et al.* 2020; Gupta *et al.* 2020). For instance, the addition of 5-azacytidine, a DNMTi, enhanced the production of the alkaloid camptothecine in *Botryosphaeria rhodina* (Botryosphaeriaceae), a finding that could give insights of the signaling mechanisms between the host plant and its endophytic fungus (Vasanthakumari *et al.* 2015). Similarly, metabolite production in *Diaporthe* sp. (Diaporthaceae) was enhanced when it was subjected to epigenetic treatment with the HDACi suberohydroxamic acid and valproic acid (Jasim *et al.* 2019). The addition of the HDACi nicotinamide to the culture of the endophytic fungus *Graphiopsis chlorocephala* (Cladosporiaceae), led to a notable enrichment in secondary metabolite production and also allowed the isolation of new benzophenones and cephalanones (Asai *et al.* 2013). A clear advantage of using epigenetic-based methods is that they do not require genetic manipulation and they can be applied to any fungal strain, potentially allowing the annotation of new secondary metabolites and the enhancement of the synthesis of low-yield metabolites.

Based on these promising results, we decided to use epigenetic modifiers for the induction of cryptic genes of an endophytic fungal strain of *Cophinforma mamane* (D.E. Gardner) A. J. L. Phillips & A. Alves (Botryosphaeriaceae) isolated from the leaves of *Bixa orellana* (Bixaceae) (Barakat *et al.* 2019). The first attempt to induce the metabolite production of *C. mamane* using epigenetic modifiers allowed

the detection of 8 metabolites produced *de novo* (Triastuti *et al.* 2019). Additionally, to date, 10 compounds have been isolated from *C. mamane*, including 3 new thiodiketopiperazines alkaloids, botryosulfuranols A, B and C isolated by our team, exhibiting cytotoxic activity against different cancer cell lines (Barakat *et al.* 2019). This class of diketopiperazines (DKPs) are derived from two phenylalanines residues and present an unprecedented skeleton with two spirocyclic centers which are currently under biological investigation to go further in elucidation of their mechanism of action. Moreover, as described in Welch and Williams (2014) (Welch & Williams 2014), thiodiketopiperazines are biogenetically derived from at least one aromatic amino acid (phenylalanine, tyrosine and/or tryptophan), therefore the addition of these type of bioprecursors into the culture media might induce their biosynthetic pathway. The amino-acid directed strategy has shown to induce cryptic biosynthetic pathways, allowing the isolation of many novel fungal bioactive compounds in fungi, specifically alkaloids (Huang *et al.* 2017; Yuan *et al.* 2019; Qiu *et al.* 2020; Guo *et al.* 2020). Other molecules previously isolated from *C. mamane* include a new dihydrobenzofuran derivative, botryomaman and a known molecule, primin (Pongcharoen *et al.* 2007).

In the present study, the effects on secondary metabolism of *C. mamane* through the addition of four different epigenetic modifiers to the culture medium were investigated. Two HDACi, sodium butyrate (SB) and nicotinamide (NIC), one DNMTi, 5-azacytidine (AZA) and one bacterial *quorum-sensing* (QS) molecule, N-Butyryl-DL-homoserine lactone (HSL), were used for this purpose. In a separated experiment, culture medium was supplemented with 2 amino acids, L-phenylalanine and L-tryptophan, precursors of nitrogenous compounds such as DKPs, to evaluate their influence on the metabolism of this strain, especially on the production of the three known phenylalanine-derived DKPs previously isolated. This work presents two final objectives: to assess the effects of chemical elicitors on the secondary metabolites profile of *C. mamane* by promoting the expression of cryptic genes, and 2) to obtain a better yield of botryosulfuranols A, B and C needed for further biological investigations in future research.

4.2 Results and Discussion

4.2.1 General observations

The general overview of the chromatograms of the experiment carried out with the epigenetic modifiers show five main peaks produced in all the conditions, including the control (untreated *C. mamane*) corresponding to the three TDKPs, botryosulfuranol A, botryosulfuranol B, botryosulfuranol C and two cyclopentapeptides (**Figure 4.1**). Endophytic fungi have shown a great potential to produce diverse

DKPs and cyclopeptides under standard culture conditions, which possess interesting biological activities reported in the literature (Wang *et al.* 2017a,b).

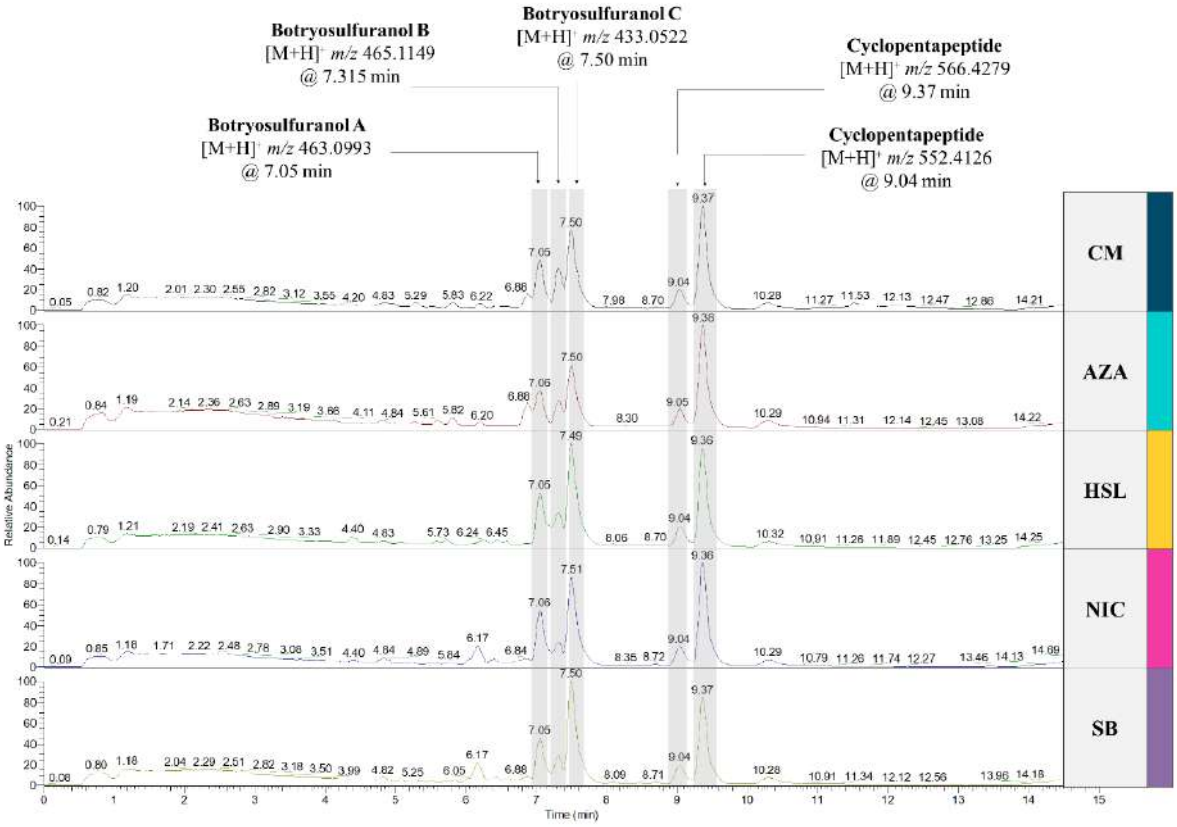

Figure 4.1. UHPLC-(+)ESI-HRMS (total ion chromatogram) from crude extracts of *C. mamane* (CM) cultivated in PDB and treated with 5-azacytidine (AZA), homoserine-lactone (HSL), nicotinamide (NIC) and sodium butyrate (SB).

A metabolomic profile of 20 extracts used in the epigenetic modifier treatment obtained by UHPLC-(+)HRMS afforded 294 features (*m/z*-RT pairs), which were considered for the metabolomics and statistical analysis. Twenty percent of these features were putatively annotated, corresponding to metabolites belonging to different chemical classes such as diketopiperazines, cyclic peptides, fatty acyls, phosphoethanolamines, and ubiquinones (**Annexes 3**).

4.2.2 Multivariate classification (PLS-DA)

As a first step, a PCA was applied as an unsupervised overview of the general LC-MS profile (data not shown). This analysis clustered all independent biological replicates from the same conditions. Then, a supervised PLS-DA analysis was carried out on these same data which indicated the different responses of *C. mamane* (CM) when treated with the HDACi (NIC and SB), the DNMTi (AZA) and the QS

molecule (HSL) in comparison to the untreated culture of *C. mamane* (**Figure 4.2**). Separate clusters appear on the PLS-DA score plot (65.3% of total variability). The component 1 (X-axis) explained 56.2% of the variability, allowing the discrimination of the AZA cluster. While in the component 2 (9.1%), we can observed two clusters: NIC/SB and CM/HSL, however a slight differentiation can be observed between CM and HSL.

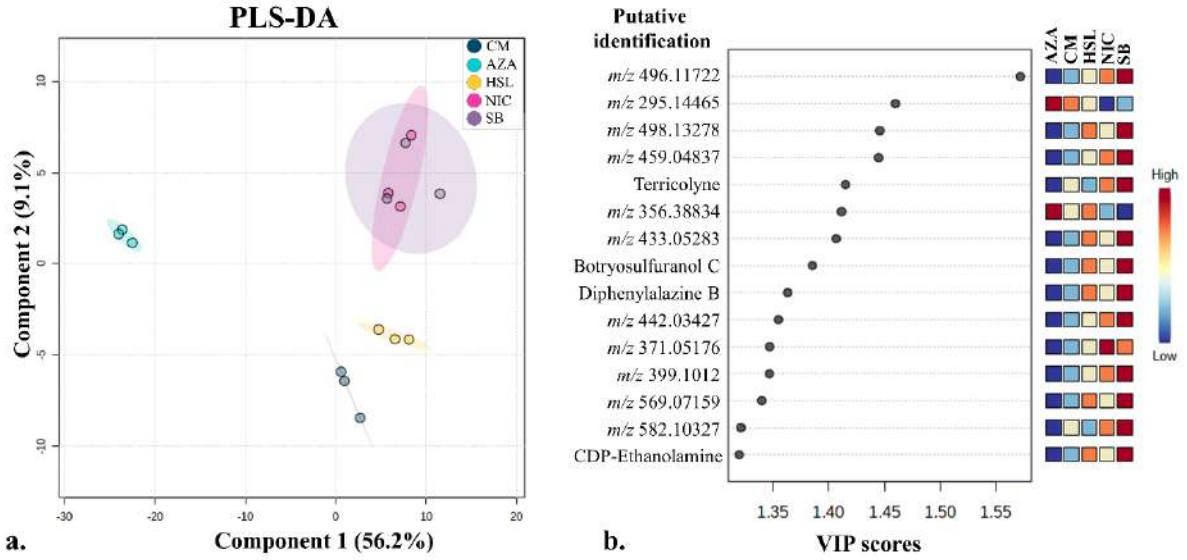

Figure 4.2. a) PLS-DA corresponding to the extracts of *C. mamane* cultivated in PDB (CM) and treated with nicotinamide (NIC), sodium butyrate (SB), 5-azacytidine (AZA) and homoserin lactone (HSL), based on features (*m/z* at Rt to its normalized peak area) detected in LC-MS chromatograms; (b) PLS-DA-VIP projection for the top 15 features corresponding to each group (AZA, CM, HSL, NIC, SB).

The **Figure 4.2** presents the top 15 features that contributed to the differences between the treatments while some of them were putatively identified. Among them, a metabolite was annotated as fatty acyl terrycoline, a metabolite that was previously isolated from an endophytic fungal strain of *Neurospora terricola* (Sordariaceae) isolated from a lichen, therefore categorized as an endolichenic fungus (Zhang *et al.* 2009). Another annotated metabolite was the phospholipid cytidine diphosphate ethanolamine (CDP-ethanolamine) which has previously shown to be critical for mycelial growth and whose biosynthesis is involved in the mycotoxin production and virulence in *Fusarium graminearum* (Nectriaceae) (Wang *et al.* 2019). The annotated DKP diphenylalazine B was previously isolated from *Epicoccum nigrum* (Didymellaceae) which colonized *Cordyceps sinensis* (Cordycipitaceae) (Guo *et al.* 2009) and the TDKP, botryosulfuranol C, previously isolated from the strain of *C. mamane* (Barakat *et al.* 2019) used in this study. The aforementioned metabolites are detailed in **Table 4.1**

Table 4.1. Top 15 features that significantly contribute to the difference in the PLS-DA analysis from LC-MS data under the treatment with epigenetic modifiers in *C. mamane* culture

ID	Rt (min)	*m/z*	Adduct	Formula	Δ mass (ppm)	Putative identification	Ontology	VIP scores
7	5.49	193.0857	$[M+H]^+$	$C_{11}H_{12}O_3$	0.73	Terricolyne	Fatty acyls	1.415
99	5.81	295.1446	$[M+H]^+$	$C_{18}H_{18}N_2O_2$	1.84	Unknown	Unknown	1.46
125	6.90	323.1393	$[M+H]^+$	$C_{19}H_{18}N_2O_3$	1.08	Diphenylalazine B;(+)-Diphenylalazine B	Diketopiperazines	1.3631
148	10.80	356.3883	$[M+H]^+$	$C_{23}H_{49}NO$	0.98	Unknown	Unknown	1.4116
155	7.44	371.0517	$[M+H]^+$	$C_{18}H_{14}N_2O_3S_2$	0.26	Unknown	Unknown	1.3469
168	7.83	399.1012	$[M+H]^+$	$C_{20}H_{18}N_2O_5S$	0.7	Unknown	Unknown	1.3467
181	6.62	433.0528	$[M+H]^+$	$C_{23}H_{12}O_9$	5.95	Unknown	Unknown	1.4068
189	4.79	442.0342	$[M+H]^+$	$C_{14}H_{16}N_7O_2PS_3$	1.06	Unknown	Unknown	1.355
191	7.07	447.0678	$[M+H]^+$	$C_{11}H_{20}N_4O_{11}P_2$	0.34	CDP-Ethanolamine	Phosphoethanolamine	1.3198
198	6.43	459.0483	$[M+H]^+$	$C_{15}H_{19}N_6O_3PS_3$	1.62	Unknown	Unknown	1.4449
222	5.76	496.1172	$[M+H]^+$	$C_{21}H_{25}N_3O_7S_2$	6.94	Unknown	Unknown	1.5721
224	6.06	498.1327	$[M+H]^+$	$C_{24}H_{23}N_3O_7S$	0.33	Unknown	Unknown	1.4459
255	6.01	569.0715	$[M+H]^+$	$C_{30}H_{16}O_{12}$	0.24	Unknown	Unknown	1.3399
261	6.96	582.1032	$[M+NH_4]^+$	$C_{27}H_{20}N_2O_8S_2$	5.7	Unknown	Unknown	1.3212
278	7.49	433.0521	$[M+H]^+$	$C_{19}H_{16}N_2O_6S_2$	0.24	Botryosulfuranol C	Thiodiketopiperazines	1.3854

4.2.3 Hierarchical clustering analysis (Heat-map)

Out of the 294 features, 221 showed significant changes under the treatment with epigenetic modifiers (p-value < 0.05) using the analysis of variance (one way ANOVA) and Fisher test (F-test). The top 150 features with significant changes were plotted in the hierarchical clustering analysis (heat map) where five main clusters of metabolite behaviors are detected (**Figure 4.3**): a cluster corresponding to the up-regulation with AZA treatment, a cluster corresponding to the up-regulation with NIC and SB treatment, a cluster corresponding to the up-regulation with HSL treatment and a cluster corresponding to the down-regulation with the 4 epigenetic modifiers treatment. These results are consistent with PLS-DA analysis observed above.

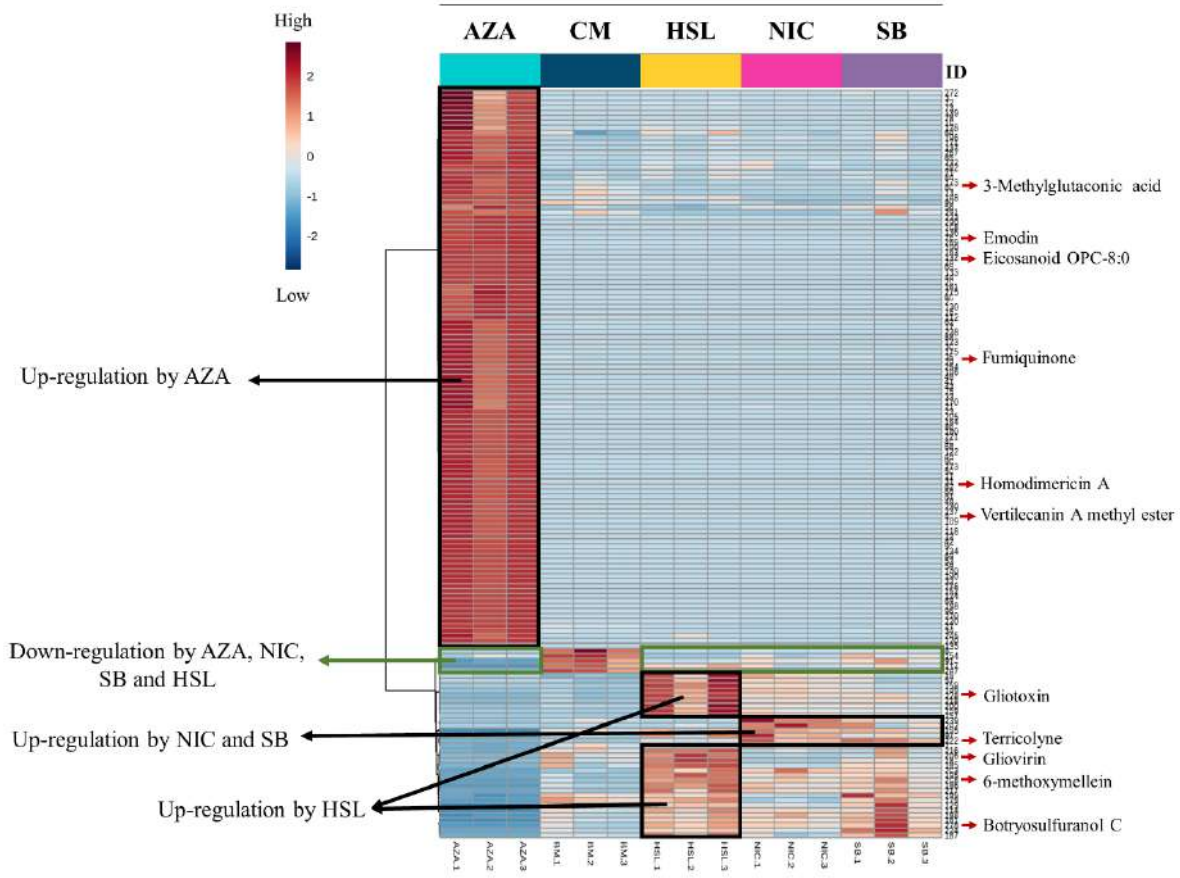

Figure 4.3. Hierarchical clustering of the main features observed in *C. mamane* in the positive mode after the treatment with the epigenetic modifiers

AZA significantly induced 113 metabolites among the top 150, initially lowly produced by *C. mamane*, highlighting the great capacity of this epigenetic modifier to alter the gene expression through the induction of DNA demethylation in the endophytic fungus. An analysis of the differential expression of endophytic fungi under the treatment with 7 different HDACi and DNMTi (including AZA, NIC and

SB) published in 2016 showed that AZA was the epigenetic modifier that induced most of the changes in the secondary metabolite profile of the ascomycete *Dothiora* sp. (Dothioraceae) (González-Menéndez *et al.* 2016), which is consistent with our results. Metabolites annotated as 3-methylglutanonic acid, eicoisanoid, emodin, fumiquinone A, homodimericin A and vertilecanin A methyl ester were also induced under the treatment with AZA as observed in **Figure 4.3**.

Interestingly, the metabolites identified as DKPs gliotoxin, gliovirin and botryosulfuranol C were up-regulated under the treatment with HSL, indicating that the recognition of a bacterial QS molecule by *C. mamane* triggered a signal that induced the production of these type of metabolites. Similarly, the metabolite annotated as isocoumarin 6-methoxymellein was also up-regulated by HSL, first isolated from the fungus *Preussia bipartis* (Sporormiaceae) while different isocoumarin derivatives have been also isolated from Botryosphaeriaceae family members, including *Botryosphaeria mamane*, *B. obtusa* and *B. rhodina* (Reveglia *et al.* 2020). Moreover, the fatty acyl terricolyne was up-regulated by NIC and SB but not by AZA or HSL (**Figure 4.3**), suggesting that NIC and SB might trigger similar effects as they both are HDACi.

4.2.4 Differential production of metabolites (Volcano plot analysis)

Regarding the influence of the epigenetic modifiers more in details as shown in the Volcano plot representations (**Figure 4.4**), a total of 113, 46, 39 and 18 metabolites were up-regulated when *C. mamane* culture was treated with AZA (**Figure 4.4a**), HSL (**Figure 4.4b**), NIC (**Figure 4.4c**) and SB (**Figure 4.4d**), respectively. Notably, as observed above in the heat map, AZA was the epigenetic modifier that induced and down-regulated the highest number of metabolites. On the contrary, SB is the one that alters the metabolism the least, inducing and down-regulating the smallest number of metabolites.

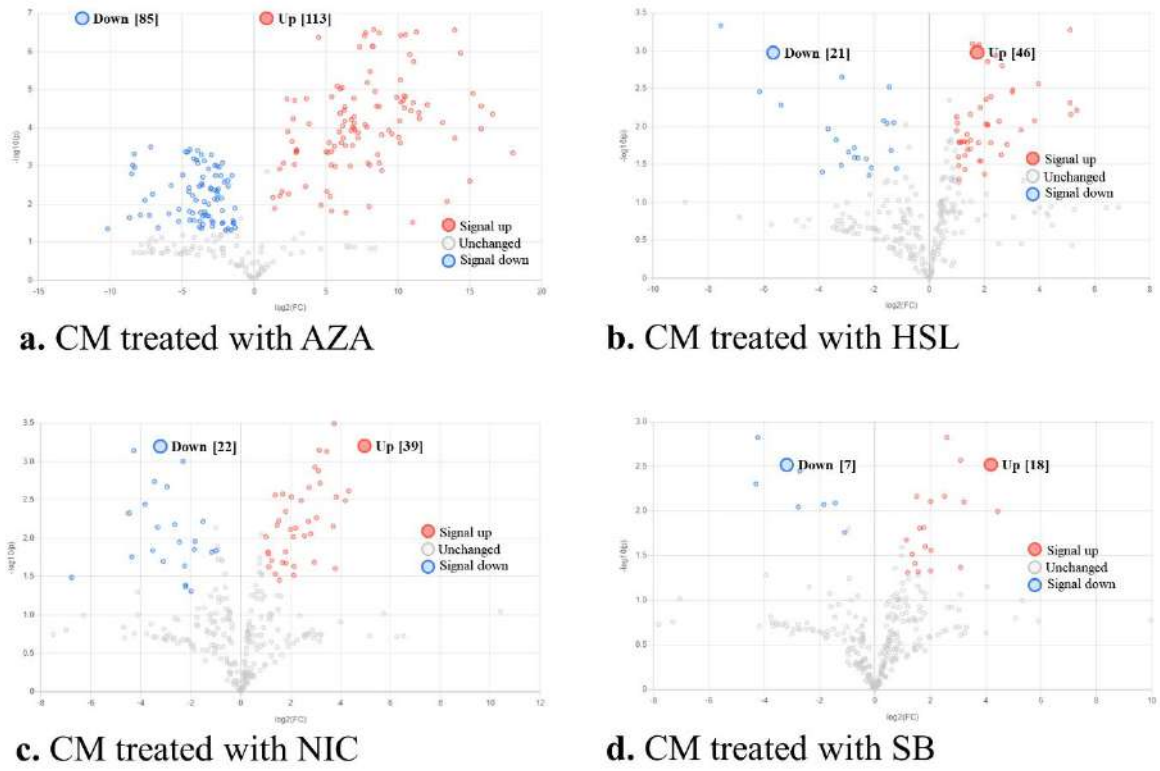

Figure 4.4. Volcano plot representations of *C. mamane* response to the treatment with epigenetic modifiers (a) azacytidine (AZA), (b) homoserin lactone (HSL), (c) nicotinamide (NIC) and (d) sodium butyrate (SB). Each dot represents a feature (m/z at Rt), the red and blue colors indicate a significant change (p-value < 0.05 and fold-change ratio > 2) of the features under treatment in up-regulating (red) or down-regulating (blue) their production in comparison with the untreated culture of CM, while the numbers in brackets indicate the number of significant features observed.

Among the metabolites with the highest significant changes (p-value < 0.05 and fold-change ratio > 2) shown in

Table 4.2, the metabolite annotated as vertilecanin A methyl ester was significantly up-regulated by the addition of AZA but also by NIC. This phenopicolinic acid derivative was previously isolated from the entomopathogenic fungus *Verticillium lecanii* (Soman *et al.* 2001), a species that is currently classified within the genus *Lecanicillium* (Nicoletti & Becchimanzi 2020).

The metabolite annotated as fumiquinone A, previously isolated from *Aspergillus fumigatus* (Hayashi *et al.* 2007) was significantly up-regulated by AZA. Another ubiquinone, fumiquinone B, was isolated from the endophytic fungus *Neopestalotiopsis* sp. (Grigoletto *et al.* 2019). AZA, NIC and HSL significantly up-regulated the metabolite annotated as hydroxyanthrequinone emodin, a compound known to be produced by different fungal species as a pigmented metabolite (Wells *et al.* 1975). Emodin has also been described in different endophytic fungal species including *Aspergillus versicolor* (Hawas *et al.* 2012), *Alternaria* sp., *Epicoccum nigrum* (Vigneshwari *et al.* 2019) and an endophytic strain of *Penicillium citrinum* isolated from a medicinal plant (Luo *et al.* 2019).

The metabolite annotated as homodimericin, significantly up-regulated by AZA and SB, has been described as a complex fungal polyketide isolated from *Trichoderma harzianum*, whose biosynthesis occurs in a similar manner to an epicolactone produced by an endophytic fungal strain of *Epicoccum* sp. ((Mevers *et al.* 2016; Long *et al.* 2018).

Although both NIC and SB inhibit the deacetylation of histones (HDACi), they differently induce the production of compounds in *C. mamane*, probably because each of these HDACi interacts in different manner with different histone deacetylases. As described in the literature, SB inhibits HDAC class I and II, while NIC inhibits HDAC class III (Harrison *et al.* 2019). In agreement with these observations, El-Hawary *et al*., (2018) observed that when the marine-derived fungus *Penicillium brevicompactum* is treated with NIC and SB, different compounds were induced, obtaining more phenolic metabolites with NIC than with SB (El-Hawary *et al.* 2018).

While the majority of compounds produced by *C. mamane* were up-regulated with AZA treatment, many other compounds were down-regulated. Similar results were reported in the literature. As an example, when the endophytic fungus *Diaporthe* sp. is treated with AZA, Deepika *et al*., (2020) demonstrated a significant increase in most metabolites, specifically in colchicine production, while a negative regulation in the production of other metabolites in the presence of demethylating agents was observed (Deepika *et al.* 2020).

Table 4.2. Most significant metabolites up-regulated by the treatment with epigenetic modifiers in *C. mamane* culture based on volcano plot analysis. Up-regulation is shown with a significant (*) or not significant (N.S.) fold-change (FC) value. Significant values with *p*-value < 0.05 and fold-change ratio > 2

ID	Rt (min)	*m/z*	Adduct	Formula	Δ mass (ppm)	Putative identification	Ontology	*C. mamane* and AZA	*C. mamane* and NIC	*C. mamane* and SB	*C. mamane* and HSL
								Log2 (FC)	Log2 (FC)	Log2 (FC)	Log2 (FC)
45	6.57	244.0967	$[M+H]^+$	$C_{14}H_{13}NO_3$	0.49	Vertilecanin A methyl ester	Phenopicolinic acid derivatives	16.58*	4.18*	N.S.	4.41
60	5.30	255.0864	$[M+H]^+$	$C_{12}H_{14}O_6$	0.45	Fumiquinone A	Ubiquinones	10.43*	N.S.	N.S.	N.S.
76	6.11	271.060	$[M+H]^+$	$C_{15}H_{10}O_5$	0.36	Emodin	Hydroxyanthraquinones	13.95*	3.8*	N.S.	3.82*
107	6.41	300.1439	$[M+H]^+$	$C_{14}H_{21}NO_6$	0.87	Unknown	Unknown	6.62*	6.54	N.S.	5.35*
124	9.12	320.2221	$[M+H]^+$	$C_{19}H_{29}NO_3$	0.24	Unknown	Unknown	15.22*	N.S.	1.18	2.52
148	10.81	356.3883	$[M+H]^+$	$C_{23}H_{49}NO$	1.09	Unknown	Unknown	2.26*	N.S.	2.02*	N.S.
149	4.39	357.0904	$[M+H]^+$	$C_{15}H_{20}N_2O_4S_2$	9.2	Bisdethiobis (methylthio)gliotoxin	Epipolythiodiketopiperazine	N.S.	3.16*	1.4	3.97*
156	4.13	375.0678	$[M+H]^+$	$C_{15}H_{14}N_6O_2S_2$	3.84	Unknown	Unknown	N.S.	1.18	3.22*	N.S.
157	5.59	375.1009	$[M+H]^+$	$C_{18}H_{18}N_2O_5S$	0.05	Unknown	Unknown	N.S.	3.83*	2.52	5.13*
158	4.09	375.1012	$[M+H]^+$	$C_{18}H_{18}N_2O_5S$	0.79	Unknown	Unknown	N.S.	3.75*	3.1	5.11*
159	5.73	375.1014	$[M+H]^+$	$C_{18}H_{18}N_2O_5S$	1.28	Unknown	Unknown	N.S.	3.72*	N.S.	5.11*
161	5.77	378.1189	$[M+H]^+$	$C_{18}H_{19}NO_8$	1.47	Unknown	Unknown	15.78*	3.18	N.S.	4.26
175	4.06	417.1186	$[2M+H]^+$	$C_{11}H_{12}O_2S$	0.66	Unknown	Unknown	17.99*	N.S.	1.24	N.S.
190	4.39	446.1968	$[M+H]^+$	$C_{20}H_{27}N_7O_3S$	0.19	Unknown	Unknown	15.78*	2.54	N.S.	N.S.
221	9.76	491.1675	$[M+H]^+$	$C_{28}H_{26}O_8$	5.17	Homodimericin A	Diterpenoids	6.95*	N.S.	2.61*	N.S.
227	9.88	498.3788	$[M+H]^+$	$C_{28}H_{51}NO_6$	0.23	Unknown	Unknown	N.S.	N.S.	2*	N.S.
242	5.73	530.1049	$[M+H]^+$	$C_{18}H_{24}N_7O_6PS_2$	1.72	Unknown	Unknown	N.S.	4.32*	N.S.	N.S.
271	9.52	681.4417	$[M+H]^+$	$C_{34}H_{64}O_{13}$	0.39	Unknown	Unknown	N.S.	N.S.	3.09*	N.S.

Focusing on the three novel DKPs previously isolated from *C. mamane* (Barakat *et al.* 2019), botryosulfuranols A, B and C were significantly down-regulated by AZA (**Figure 4.5a,b**), while only botryosulfuranol C showed a significant up-regulation by HSL (**Figure 4.5c**). The HDACi SB had no influence on their production, contrary to the results of a previous study, where the 3 botryosulfuranols were found to be induced when *C. mamane* culture was treated with the HDACi sodium valproate (Triastuti *et al.* 2019). This could have been explained by an interaction of the HDACi with different histone deacetylases, however, sodium valproate and SB belong to the same class of HDACi (Shukla & Tekwani 2020) and they were expected to present the same effect on *C. mamane* metabolism.

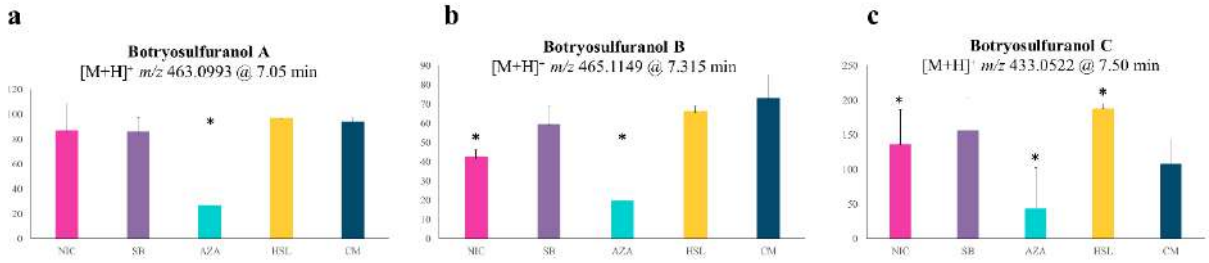

Figure 4.5. Normalized peak area of the TDKPs (a) botryosulfuranol A, (b) botryosulfuranol B and (c) botryosulfuranol C detected under the treatment with the epigenetic modifiers nicotinamide (NIC), sodium butyrate (SB), 5-azacytidine (AZA) and homoserin lactone (HSL) in comparison to the untreated culture of *C. mamane* (CM).

Homoserin lactones are well-known molecules involved in QS in bacterial communities and their role in gram-negative bacteria has already been reported, indicating their modulatory activity in regulatory proteins for gene expression (Fuqua & Greenberg 2002). The roles of DKPs in QS have also been reported during bacterial interactions (Bofinger *et al.* 2017), suggesting a similar role of botryosulfuranols in *C. mamane* when treated with HSL. Moreover, mechanisms of QS are also observed in yeast and filamentous fungi through the production of tyrosol, farnesol (Mondal & Majumdar 2019) and mycotoxins (Venkatesh & Keller 2019). As observed with the up-regulation of botryosulfuranol C by HSL, QS are molecules known to be capable of inducing the production of cyclic DKPs, such as emestrin A and emestrin B, produced by *Aspergillus fumigatus* in presence of HSL. In spite of their lack of *in vitro* activity against bacteria, it was hypothesized that these DKPs could act as QS inhibitors to modulate or attenuate bacterial populations (Rateb *et al.* 2013).

In our study, the metabolite annotated as DKP diphenylalazine B was also significantly up-regulated by HSL. A similar compound, diphenylalazine C, has been isolated from the fungus *Schizophyllum commune* (Chunyu *et al.* 2017), recently described as an endophytic fungus isolated from the medicinal plant *Alchornea glandulosa* (Euphorbiaceae), being a source of many other DKPs (Rabal Biasetto *et al.* 2019). Furthermore, the metabolite annotated as DKP bisdethiobis (methylthio)-gliotoxin was

significantly up-regulated by HSL and NIC. In a previous work, this metabolite was isolated from an endophytic fungal strain of *Aspergillus fumigatus* isolated from a Chinese medicinal plant (Zhang *et al.* 2018).

4.2.5 Molecular network analysis

To better visualize chemical relationships based on acquired MS-MS data, and to focus on derivatives of annotated metabolites, a molecular networking was performed. Our analysis displayed a molecular network that contained 294 nodes and 26 spectral families with 109 connected nodes while the rest of the nodes showed no link to others (self-loop). The size of the nodes represents the total average of the detected peak areas for each compound in all the conditions while the colors depend on their detection under the treatment with each epigenetic modifier (**Figure 4.6**).

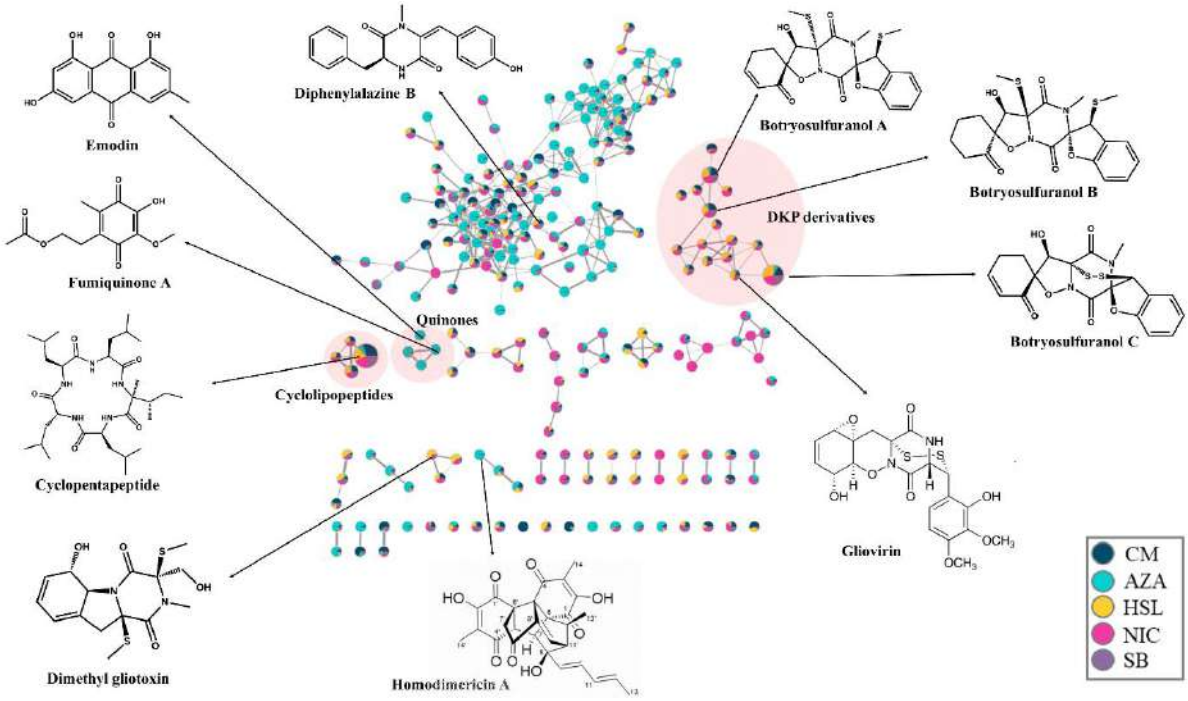

Figure 4.6. Molecular networking corresponding to the extracts of *C. mamane* treated with 4 epigenetic modifiers based on features (*m/z* at Rt to its normalized peak area) detected in LC-MS chromatograms.

The metabolite annotated as gliovirin, an epidithiodiketopiperazine obtained from the marine-derived fungus *Trichoderma* sp. isolated from a red alga (Yamazaki *et al.* 2015), was up-regulated by SB and appeared within the cluster containing the 3 TDKPs, botryosulfuranols A, B and C. Additionally, in the same cluster of DKP derivatives, a feature with *m/z* 463.0991 at 6.272 min was found to possess the

same molecular formula than botryosulfuranol A, linked with a cosine value of 0.89 (data not shown), possibly indicating an isomer of this metabolite. The metabolite annotated as bisdethiobis (methylthio)-gliotoxin was found in a different cluster linked to two unknown metabolites (**Figure 4.6**). Moreover, the molecular network highlighted the presence of another cyclopentapeptide linked to the two main cyclopentapeptides observed above in the LC-MS chromatograms (**Figure 4.1**). In the cluster of quinones, we observed two metabolites annotated as fumiquinone A and emodin linked to two other metabolites: one annotated as chrysophanol, previously isolated from marine fungus *Aspergillus* sp. (Qian *et al.* 2011) and a metabolite with *m/z* 285.0763 at 5.56 min ($C_{16}H_{12}O_5$) that did not show any putative annotation. The metabolite annotated as homodimericin A was also linked to two unidentified metabolites with *m/z* 505.1832 at 10.04 min ($C_{24}H_{28}N_2O_{10}$) and *m/z* 519.1989 at 10.01 min ($C_{30}H_{30}O_8$).

The putatively annotated metabolites mentioned above are listed in **Table 4.3**.

4.2.6 Addition of amino acids for DKPs induction

Regarding the experiment with amino acids, our hypothesis consisted of an increase in the production of botryosulfuranols and other DKPs after the addition of the bioprecursors L-phe and L-trp to the culture medium. Some studies have shown that the addition of different amino acids in the culture of fungi led to the induction of different metabolites, including new compounds such as bioactive alkaloids, in, for example, the fungus *Pseudallescheria boydii* (Microascaceae) (Huang *et al.* 2017) and in the marine fungus *Aspergillus* sp. (Qiu *et al.* 2020). However, contrary to what was expected, botryosulfuranol A, B and C showed a significant down-regulation under the addition of L-phe and L-trp (p-value < 0.05 and fold-change ratio >2) in comparison to the untreated culture of *C. mamane* (**Figure 4.7**). Other metabolites, including alkaloids, might have been induced but not detected (data not shown). Different concentrations of other amino acids as well as different culture media and incubation times will be contemplated for future experiments.

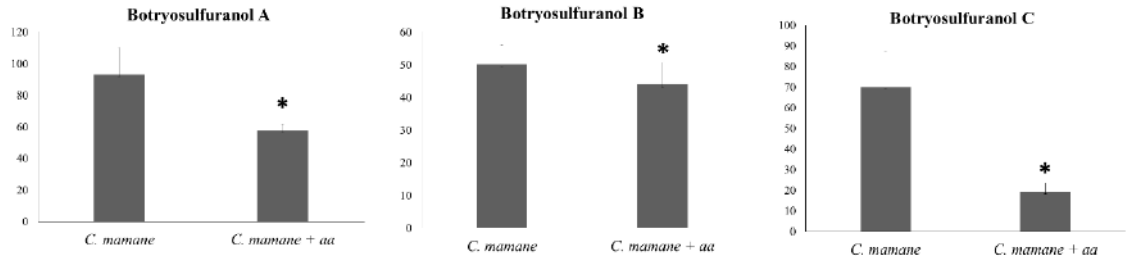

Figure 4.7. Normalized peak area of botryosulfuranols A, B and C detected under the addition of amino acids (*C.mamane* + aa) in comparison to the untreated culture of *C. mamane*.

Table 4.3. List of putative identified compounds detected under the treatment with epigenetic modifiers when culturing *C. mamane*

ID	Rt (min)	*m/z*	Adduct	Formula	Δ mass (ppm)	Putative identification	Ontology
262	9.36	566.4279	$[M+H]^+$	$C_{30}H_{55}N_5O_5$	0.67	Cyclo-(L-Ile-L-Leu-L-Leu-L-Leu-L-Leu)*	Cyclopentapeptides
257	9.03	552.4126	$[M+H]^+$	$C_{29}H_{53}N_5O_5$	1.18	Cyclo-(L-Leu-L-Leu-D-Leu-L-Leu-L-Val)*	Cyclopentapeptides
263	9.25	600.4108	$[M+H]^+$	$C_{33}H_{53}N_5O_5$	1.75	Cyclo-(L-Phe-L-Leu-L-Leu-L-Leu-L-Ile)*	Cyclopentapeptides
283	7.31	465.1149	$[M+H]^+$	$C_{21}H_{24}N_2O_6S_2$	0.22	Botryosulfuranol B	Thiodiketopiperazines
215	7.04	463.0992	$[M+H]^+$	$C_{21}H_{22}N_2O_6S_2$	0.14	Botryosulfuranol A	Thiodiketopiperazines
278	7.49	433.0521	$[M+H]^+$	$C_{19}H_{16}N_2O_6S_2$	0.24	Botryosulfuranol C	Thiodiketopiperazines
216	6.51	481.0734	$[M+H]^+$	$C_{20}H_{20}N_2O_8S_2$	0.22	Gliovirin	Epidithiodiketopiperazines
201	6.27	463.0990	$[M+H]^+$	$C_{21}H_{22}N_2O_6S_2$	0.24	Botryosulfuranol A derivative	Thiodiketopiperazines
125	6.90	323.1393	$[M+H]^+$	$C_{19}H_{18}N_2O_3$	1.08	Diphenylalazine B;(+)-Diphenylalazine B	Diketopiperazines
149	4.39	357.0904	$[M+H]^+$	$C_{15}H_{20}N_2O_4S_2$	9.3	Bisdethiobis (methylthio)-gliotoxin	Epipolythiodiketopiperazines
45	6.57	244.0967	$[M+H]^+$	$C_{14}H_{13}NO_3$	0.49	Vertilecanin A methyl ester	Phenopicolinic acid derivatives
60	5.30	255.0864	$[M+H]^+$	$C_{12}H_{14}O_6$	0.45	Fumiquinone A	Ubiquinones
76	6.11	271.0600	$[M+H]^+$	$C_{15}H_{10}O_5$	0.36	Emodin	Hydroxyanthraquinones
221	9.76	491.1675	$[M+H]^+$	$C_{28}H_{26}O_8$	5.17	Homodimericin A	Diterpenoids
191	7.07	447.0678	$[M+H]^+$	$C_{11}H_{20}N_4O_{11}P_2$	0.34	CDP-Ethanolamine	Phosphoethanolamines
7	5.49	193.0857	$[M+H]^+$	$C_{11}H_{12}O_3$	0.73	Terricolyne	Fatty acyls
18	6.92	209.0809	$[M+H]^+$	$C_{11}H_{12}O_4$	0.41	6-Methoxymellein	2-benzopyrans
173	1.76	145.0493	$[M+H]^+$	$C_6H_8O_4$	1.21	3-Methylglutaconic acid	Methyl-branched fatty acids
100	9.81	295.2268	$[M+H]^+$	$C_{18}H_{30}O_3$	0.23	3-Oxo-2-(2-entenyl)cyclopentaneoctanoic acid;OPC-8:0	Eicosanoids

*unknown amino acids sequence

4.3 Additional information

The following results have not been included in the draft article and they correspond to the addition of L-Trp and L-Phe into the culture of *C. mamane* in order to evaluate additional results besides the observed for the TDKPs botryosulfuranols A, B and C.

4.3.1 General observations

The general overview of the chromatograms (**Figure 4.8**) shows five main metabolites produced in all conditions: botryosulfuranol A, botryosulfuranol B, botryosulfuranol C and two others putatively identified as cyclopeptides (*m/z* 566.4279 and *m/z* 552.4126). In this chromatogram, the peak corresponding to botryosulfuranol C appears to be less intense in the presence of amino acids.

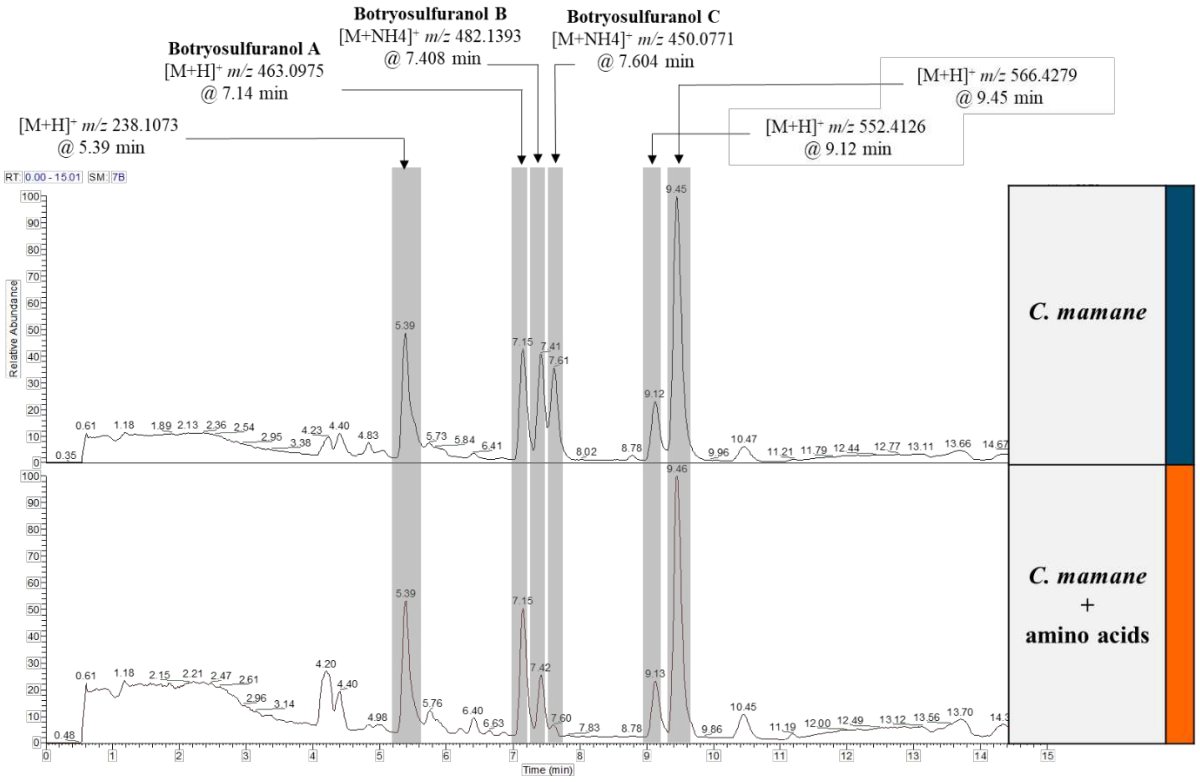

Figure 4.8. UHPLC-(+)ESI-HRMS base peak chromatograms from crude extracts of *C. mamane* cultivated in MEA with the addition of L-phenylalanine and L-tryptophan

A metabolic profile of the 7 extracts obtained by UHPLC-(+)ESI-HRMS afforded 132 features (m/z-Rt pairs), which were considered for the metabolomics and statistical analysis. 20% of these features (23 out of 132) were putatively annotated (**Annexes 4**).

4.3.1 Multivariate classification (PLS-DA)

A supervised PLS-DA analysis was carried out on these data which indicated the different responses of *C. mamane* when cultivated in a medium supplemented with two amino acids (CM + aa) in comparison to the untreated culture of *C. mamane* (CM) (**Figure 4.9**). Separate clusters appear on the PLS-DA score plot (80.5% of total variability). The component 1 (X-axis) explained 60.9% of the variability, allowing the discrimination of the CM and CM+aa cluster.

The **Figure 4.9** presents the top 15 features (**Table 4.4**) that contributed to the differences between the treatments. Among them, the features *m/z* 566.4270 at 9.448 min and *m/z* 574.3937 at 9.125 min were putatively identified as cyclic pentapeptides while similar metabolites were previously isolated from an endophytic fungal strain of *Fusarium decemcellulare* (Li *et al.* 2016). Feature *m/z* 299.1385 at 4.637 min was putatively identified as a prenylated tryptophan derivative called luteoride A, first isolated from an entomopathogenic fungus *Torrubiella luteorostrata* (Asai *et al.* 2013) while another derivative, luteoride E was isolated from a marine-derived fungus *Aspergillus terreus* (Liu *et al.* 2018). Moreover, feature *m/z* 176.0704 at 1.852 min was putatively identified as 7-amino-4-methylcoumarin, first isolated from endophytic fungus *Xylaria* sp. (Liu *et al.* 2008).

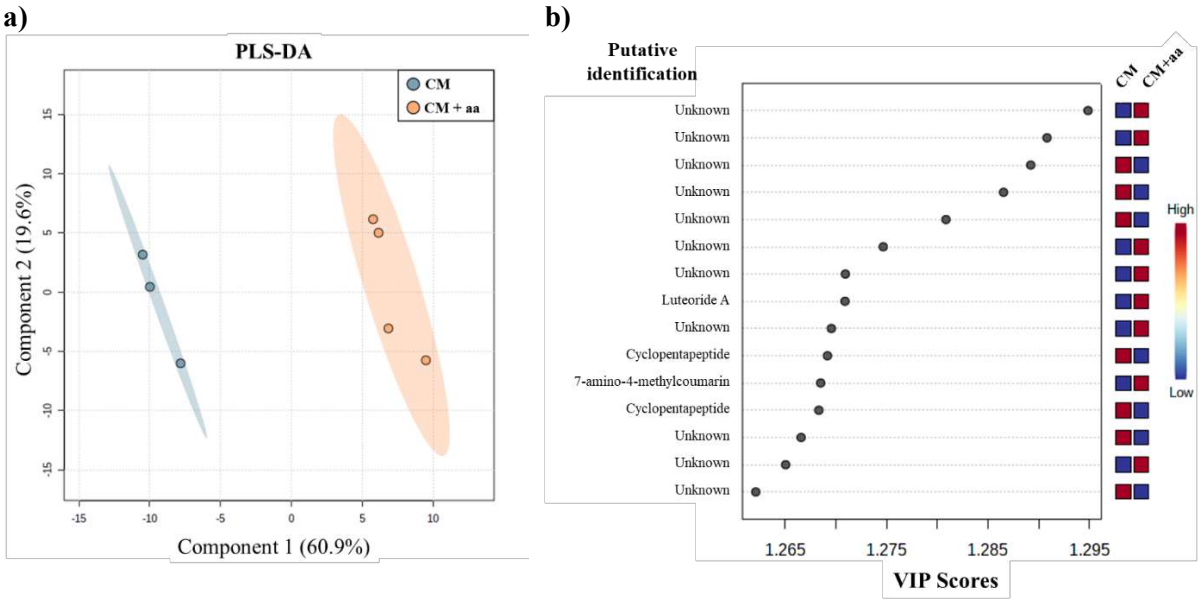

Figure 4.9. a) Partial least squares discriminant analysis (PLS-DA) obtained from LC-(+)ESI-HRMS profiles corresponding to the extracts of *C. mamane* cultivated in MEB (CM) and under the addition of L-phe and L-trp (CM+aa); based on features (*m/z* at Rt to its normalized peak area) detected in LC-MS chromatograms; (b) Variable importance in projection (VIP) score of the top 15 compounds from the PLS-DA analysis corresponding to each condition

Table 4.4. Top 15 features that significantly contribute to the difference in the PLS-DA analysis from LC-HRMS/MS data under the addition of amino acids in *C. mamane* culture

ID	Rt (min)	*m/z*	Adduct	Formula	Δ mass (ppm)	Putative identification	Ontology
118	4.80	285.1228	$[M+H]^+$	$C_{16}H_{16}N_2O_3$	1.99	Unknown	Unknown
127	4.17	301.1176	$[M+H]^+$	$C_{16}H_{16}N_2O_4$	2.26	Unknown	Unknown
44	5.06	501.0752	$[M+Na]^+$	$C_{12}H_{24}N_4O_{12}P_2$	1.22	Unknown	Unknown
62	7.60	903.0509	$[M+H]^+$	$C_{38}H_{26}N_6O_{13}S_4$	0.49	Unknown	Unknown
75	2.57	220.1180	$[M+H]^+$	$C_9H_{17}NO_5$	0.23	Unknown	Unknown
100	10.14	253.1336	$[M+H]^+$	$C_{16}H_{16}N_2O$	0.23	Unknown	Unknown
117	4.69	285.1228	$[M+H]^+$	$C_{16}H_{16}N_2O_3$	1.99	Unknown	Unknown
125	4.63	299.1385	$[M+H]^+$	$C_{17}H_{18}N_2O_3$	1.73	Luteoride A	Indolyl carboxylic acids and derivatives
18	1.85	176.0704	$[M+H]^+$	$C_{10}H_9NO_2$	1.16	7-Amino-4-methylcoumarin	Coumarins and derivatives
35	7.14	480.0511	$[M+H]^+$	$C_{22}H_{13}N_3O_8S$	3.09	Unknown	Unknown
51	9.44	566.4270	$[M+H]^+$	$C_{30}H_{55}N_5O_5$	1.05	Cyclo-(L-Ile-L-Leu-L-Leu-L-Leu-L-Leu)*	Oligopeptides
56	9.12	574.3938	$[M+Na]^+$	$C_{29}H_{53}N_5O_5$	0.15	Cyclo-(L-Leu-L-Leu-D-Leu-L-Leu-L-Val)*	Oligopeptides
110	6.63	269.0918	$[M+H-H_2O]^+$	$C_{15}H_{14}N_2O_4$	0.99	Unknown	Unknown
116	5.83	284.1180	$[M+H]^+$	$C_{19}H_{13}N_3$	0.78	Unknown	Unknown

*amino acids sequence not known

4.3.1 Differential production of metabolites (Volcano plot analysis)

Out of the 132 features, 81 showed significant changes under the treatment with amino acids (p-value < 0.05) using the analysis of variance (one way ANOVA) and Fisher test (F-test). Regarding the influence of the amino acids more in details as shown in the Volcano plot representations (**Figure 4.10**), a total of 41 metabolites were down-regulated and 23 were up-regulated.

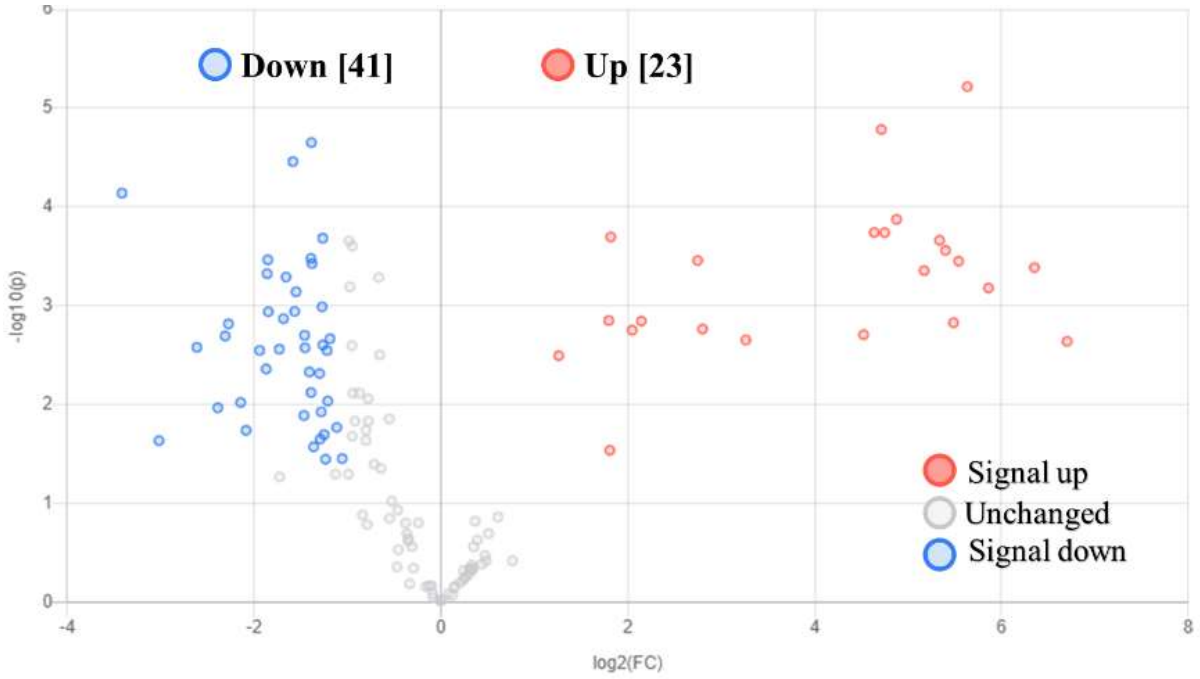

Figure 4.10. Volcano plot representations of *C. mamane* response to the addition of amino acids L-phenylalanine and L-tryptophan. Each dot represents a feature (*m/z* at Rt), the red and blue colors indicate a significant change (p-value < 0.05 and fold-change ratio > 2) of the features under treatment in up-regulating (red) or down-regulating (blue) their production in comparison with the untreated culture of CM, while the numbers in brackets indicate the number of significant features observed.

Among the metabolites with the highest significant changes (**Table 4.5**) (p-value < 0.05 and fold-change ratio > 2), considering their up-regulation under the addition of the amino acids based on the Volcano plot analysis, feature *m/z* 178.0863 at 4.315 min, putatively identified as (-)-3a-hydroxyfuroindoline, was first isolated from an endophytic fungal strain of *Fusarium incarnatum* (Li *et al.* 2008) while feature *m/z* 210.0759 at 3.837 min, putatively identified as penidilamine, was isolated from *Penicillium* sp. (Kimura *et al.* 2000). Feature *m/z* 241.0966 at 6.175 was also significantly up-regulated under the presence of the amino acids and it was putatively identified as 1,2,3,11b-tetrahydroquinolactacide, which was first isolated from an endophytic fungal strain of *Penicillium citrinum* (El-Neketi *et al.* 2013).

Table 4.5. Most important compounds up-regulated by the treatment with epigenetic modifiers in *C. mamane* culture. Up-regulation is shown with a significant (*) or not significant (N.S.) fold-change (FC) value. Significant values with *p*-value < 0.05 and fold-change ratio > 2

ID	Rt (min)	*m/z*	Adduct	Formula	Δ mass (ppm)	Putative identification	Ontology	Log2 (FC)
2	6.25	313.0812	$[M+H]^+$	$C_{16}H_{12}N_2O_5$	2.22	Unknown	Unknown	5.86*
14	1.38	174.0546	$[M+H]^+$	$C_{10}H_7NO_2$	2.03	Unknown	Unknown	2.8*
17	3.07	176.0704	$[M+H]^+$	$C_{10}H_9NO_2$	1.16	Unknown	Unknown	3.26*
20	4.31	178.0863	$[M+H]^+$	$C_{10}H_{11}NO_2$	0.25	(-)-3a-Hydroxyfuroindoline	Indolines	4.52*
28	6.75	440.2170	$[M+H]^+$	$C_{24}H_{29}N_3O_5$	2.26	Unknown	Unknown	5.17*
68	3.83	210.0759	$[M+H]^+$	$C_{10}H_{11}NO_4$	0.87	Penidilamine;(+)-Penidilamine	Alpha amino acids and derivatives	1.26*
76	5.05	221.0706	$[M+H]^+$	$C_{14}H_8N_2O$	1.53	Unknown	Unknown	6.35*
79	5.34	227.0808	$[M+H]^+$	$C_{13}H_{10}N_2O_2$	3.1	Unknown	Unknown	2.14*
89	6.17	241.0966	$[M+H]^+$	$C_{14}H_{12}N_2O_2$	2.29	1,2,3,11b-tetrahydroquinolactacide	Hydroquinolones	5.54*
98	9.64	253.1334	$[M+H]^+$	$C_{16}H_{16}N_2O$	0.55	Unknown	Unknown	5.48*
105	5.63	259.1227	$[M+H]^+$	$C_{18}H_{14}N_2$	1.06	Unknown	Unknown	1.8*
124	8.38	297.1225	$[M+H]^+$	$C_{17}H_{16}N_2O_3$	2.92	Unknown	Unknown	1.79*
128	4.73	301.1185	$[M+Na]^+$	$C_{11}H_{22}N_2O_4S$	2.48	Unknown	Unknown	2.74*
130	5.20	307.1286	$[M+H]^+$	$C_{15}H_{18}N_2O_5$	0.8	Unknown	Unknown	6.7*

4.3.1 Molecular network analysis

To better visualize chemical relationships based on acquired MS-MS data, and to focus on derivatives of annotated metabolites, a molecular networking was performed. Our analysis displayed a molecular network that contained 132 nodes and 10 spectral families with 86 connected nodes while the rest of the nodes showed no link to others (self-loop). The size of the nodes represents the total average of the detected peak areas for each compound in all the conditions while the colors depend on their detection under the treatment with each epigenetic modifier (**Figure 4.11**).

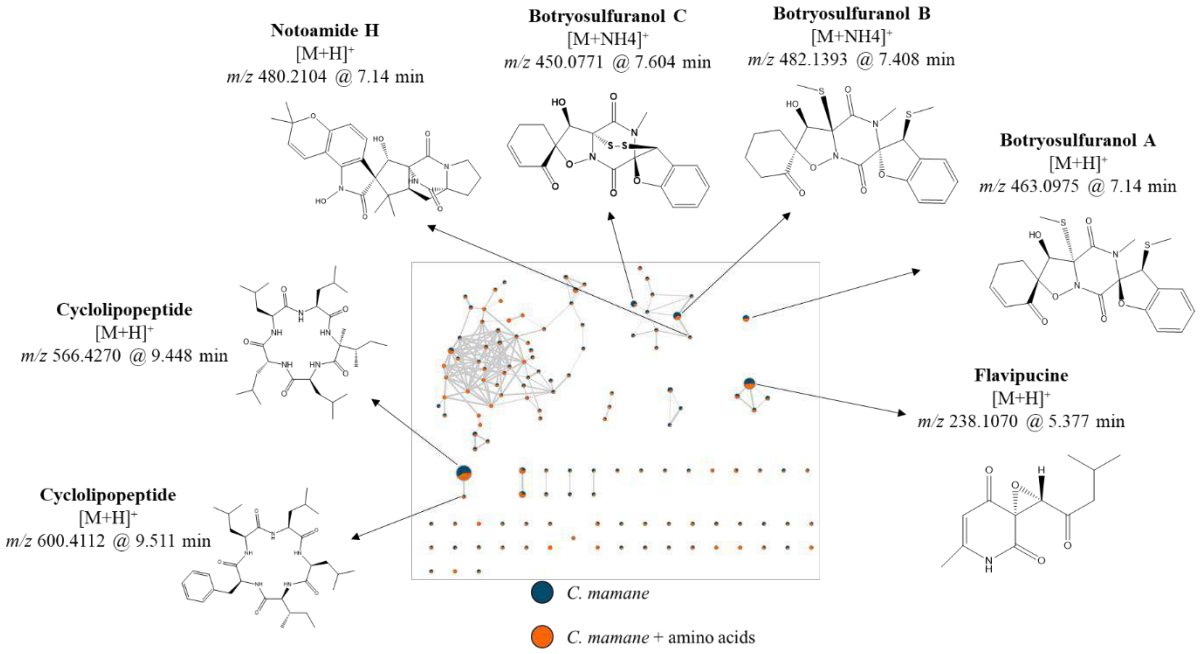

Figure 4.11. Molecular networking corresponding to the extracts of *C. mamane* treated with amino acids based on features (*m/z* at Rt to its normalized peak area) detected in LC-MS chromatograms.

Focusing on the cluster containing the thiodiketopiperazines botryosulfuranols B and C, feature *m/z* 480.21042 at 7.14 min was putatively identified as a diketopiperazine alkaloid analogue, notoamide H, isolated from the marine-derived endophytic fungus *Aspergillus* sp. (Yang *et al.* 2021) linked to the node corresponding to botryosulfuranol B with a cosine value of 0.97. Moreover, 4 other features linked in the same cluster were putatively identified as flavipucine (or isomers), a compound isolated from an endophytic fungal strain of *Phoma* sp. (Loesgen *et al.* 2011) (**Figure 4.11**). Feature *m/z* 600.4112 at 9.51 min, putatively identified as a cyclic pentapeptide previously isolated from a non-identified endophytic fungal strain (Li *et al.* 2004) was found to be linked to cyclic pentapeptide (*m/z* 566.4270 at 9.448 min). The list of putatively identified compounds for this experiment is detailed in **Table 4.6.**

Table 4.6. List of putative identified compounds detected under the addition of amino acids in the culture of *C. mamane*

ID	Rt (min)	*m/z*	Adduct	Formula	Δ mass (ppm)	Putative identification	Ontology
60	9.51	600.4112	$[M+H]^+$	$C_{33}H_{53}N_5O_5$	1.25	Cyclo-(L-Phe-L-Leu1-L-Leu2-L-Leu3-L-Ile)*	Cyclopentapeptides
51	9.44	566.4270	$[M+H]^+$	$C_{30}H_{55}N_5O_5$	1.05	Cyclo-(L-Ile-L-Leu-L-Leu-L-Leu-L-Leu)*	Cyclopentapeptides
56	9.12	574.3938	$[M+Na]^+$	$C_{29}H_{53}N_5O_5$	0.15	Cyclo-(L-Leu-L-Leu-D-Leu-L-Leu-L-Val)*	Cyclopentapeptides
103	5.38	238.1071	$[M+H]^+$	$C_{12}H_{15}NO_4$	1.06	(±)-Flavipucine**	Tetrahydropyridines
109	5.75	238.1069	$[M+H]^+$	$C_{12}H_{15}NO_4$	1.94	(±)-Flavipucine**	Tetrahydropyridines
86	6.41	238.1069	$[M+H]^+$	$C_{12}H_{15}NO_4$	1.9	(±)-Flavipucine**	Tetrahydropyridines
87	5.96	238.1071	$[M+H]^+$	$C_{12}H_{15}NO_4$	1.31	(±)-Flavipucine**	Tetrahydropyridines
36	7.14	463.0975	$[M+H]^+$	$C_{21}H_{22}N_2O_6S_2$	3.61	Botryosulfuranol A	Thiodiketopiperazines
39	7.41	482.1393	$[M+NH_4]^+$	$C_{21}H_{24}N_2O_6S_2$	4.27	Botryosulfuranol B	Thiodiketopiperazines
30	7.60	450.0771	$[M+NH_4]^+$	$C_{19}H_{16}N_2O_6S_2$	3.8	Botryosulfuranol C	Thiodiketopiperazines
37	7.14	480.2104	$[M+H]^+$	$C_{26}H_{29}N_3O_6$	5.18	Notoamide H;(-)-Notoamide H	Diketopiperazines
125	4.64	299.1385	$[M+H]^+$	$C_{17}H_{18}N_2O_3$	1.73	Luteoride A	Indolyl carboxylic acids and derivatives
68	3.84	210.0759	$[M+H]^+$	$C_{10}H_{11}NO_4$	0.87	Penidilamine;(+)-Penidilamine	Alpha amino acids and derivatives
18	1.85	176.0704	$[M+H]^+$	$C_{10}H_9NO_2$	1.16	7-Amino-4-methylcoumarin	Coumarins and derivatives
20	4.32	178.0863	$[M+H]^+$	$C_{10}H_{11}NO_2$	0.25	(-)-3a-Hydroxyfuroindoline	Indolines
89	6.17	241.0966	$[M+H]^+$	$C_{14}H_{12}N_2O_2$	2.29	1,2,3,11b-tetrahydroquinolactacide	Hydroquinolones

*Amino acid sequence not known

*Isomers of this metabolite could also correspond to this putatively annotation

4.3.1 Discussions

Acoording to the literature, amino acid – directed strategy has shown to promote nitrogen-containing compounds, such as alkaloid production in *Dichotomomyces cejpii* when the culture medium was supplemented with L-tryptophan and L-phenylalanine (2 g/L), obtaining new aliphatic amides, polyketides and (Chen *et al.* 2017; Wu *et al.* 2018) or the 22 diverse alkaloids, including 14 new compounds of which 12 are fumiquinazoline analogues produced by the fungus *Scedosporium apiospermum* when the culture medium was supplemented with L-tryptophan, L-phenylalanine, L-threonine and D-L-methionine (2 g/L) (Huang *et al.* 2017).

Surprisingly, this experiment did not lead to an increase in the production of the botryosulfuranols, nor to the detection and identification of new diketopiperazines or more generally other alkaloids.

One possible explanation for our unexpected results is the low rate in compound annotation, due to a lack of data in the databases used, or a non-detection due to a low level of production, or their absence in the molecular network because of a lack of fragmentation due the methodology used.

Another explanation is the probable elevated and toxic intracellular levels of specific amino acids previously observed in prokaryotic and eukaryotic cells. For instance, *Saccharomyces cerevisiae* is capable to synthesize all amino acids de novo or to obtain them from the environment using plasma membrane transporters, however, the addition of high levels of amino acids (0.5-5 mM) in culture media induce growth inhibition and growth defects (Ruiz *et al.* 2020).

4.4 Conclusions

Our results show that treatment with HDACi and DNMTi effectively activated biosynthetic pathway due to the induction of lowly produced metabolites when *C. mamane* was grown without any treatment. This indicates that methylation and deacetylation are mechanisms that regulates expression in the endophytic fungus, specifically the up-regulation obtained with the treatment with the DNMTi AZA. Meanwhile, deacetylation or methylation of histones were necessary for those compounds that were down-regulated in presence of the epigenetic modifiers. The induction different classes of DKPs by the treatment with the QS molecule HSL represents a promising result for future experiments involving a different induction approach such as the co-culture of this endophytic fungus with bacteria. This also suggests a possible role of DKPs as QS molecules in *C. mamane* as this potential role is suggested for other DKPs in other fungi and bacteria. Possible analogues or derivatives of putatively identified metabolites were indeed uncovered thanks to the molecular networking which can be improved by a better adapted LC-MS methodology for a larger diversity of metabolites, including the DKPs.

This work consisted in a preliminary step to modulate the culture of *C. mamane* in order to find better conditions to induce the production of botryosulfuranols A, B and C and new metabolites. In view of these results, further experiments will consist in performing large-scale cultures of *C. mamane* with AZA, in order to isolate and to structurally characterize compounds induced by this epigenetic modifier.

CHAPTER 5 - ADDITION OF HEAT-KILLED PARASITES AND CO-CULTURE WITH BACTERIA

5.1 Introduction

Fungal endophytes represent an important reservoir of metabolites presenting antibacterial (Deshmukh *et al.* 2014), antifungal (Deshmukh *et al.* 2018) and anti-parasitic activity (Hzounda Fokou *et al.* 2021), offering a great opportunity to search for novel compounds with bioactivity against diverse microorganisms. Neglected tropical diseases, including leishmaniasis caused by *Leishmania* spp., collectively affect approximately 2 billion people located mainly in tropical and subtropical regions (Engels & Zhou 2020). Moreover, multi-drug resistance in bacteria is a global health and development threat, specifically the ESKAPE pathogens (*Enterococcus faecium*, *Staphylococcus aureus*, *Klebsiella pneumoniae*, *Acinetobacter baumannii*, *Pseudomonas aeruginosa*, and *Enterobacter* spp.) which are the leading cause of nosocomial infections throughout the world and one of the greatest challenges in clinical practice (Santajit & Indrawattana 2016). Currently, the absence of effective vaccines and the development of resistance to the current drugs make these infections a major problem in endemic or developing countries and highlight the need for novel molecules acting on new targets.

Besides all the new bioactive compounds isolated from endophytes under standard culture conditions, new methodologies have been applied for the induction of novel metabolites such as co-culturing fungi with other fungi or bacteria, which has shown to naturally enhance the production of cryptic compounds that were not detected in axenic culture or that were lowly produced (Kamdem *et al.* 2018). This increased production might be the result of competition for nutrients or antagonism in their development between microorganisms sharing the same environment (Deshmukh *et al.* 2018).

A study on the fungal diversity associated to medicinal plants conducted in our laboratory led to the isolation of more than 400 endophytic fungal strains from twenty South American plants used in traditional medicine for their anti-parasitic activities (unpublished data). Among these strains, the ethyl acetate extract of an endophytic fungal strain of *Cophinforma mamane* (Botryosphaeriaceae), isolated from the leaves of the medicinal plant *Bixa orellana* (Bixaceae) collected in Peruvian amazon, exhibited antileishmanial activity against the axenic amastigotes of *Leishmania infantum* (Triastuti *et al.* 2016). Three thiodiketopiperazines (TDKPs), botryosulfuranols A, B and C presenting cytotoxic activity against four cancer lines were isolated from *C. mamane* (Barakat *et al.* 2019), along with a fourth TDKP, botryosulfuranol D (unpublished data). All the TDKPs were tested *in vitro* against axenic amastigotes of *Leishmania infantum*. Botryosulfuranol D exhibited the strongest activity with an IC_{50} value of 0.03 µM and a selective index (SI) of 190 followed by botryosulfuranol C (IC_{50} = 0.44 µM); botryosulfuranol A (IC_{50} = 0.69 µM) and botryosulfuranol B (IC_{50} = 3.87 µM) (unpublished data).

As *C. mamane* produces antileishmanial metabolites, we hypothesized that a co-culture between these two microorganisms could enhance the production of these bioactive compounds. However, *Leishmania* spp. and filamentous micromycetes need very different culture media and conditions to grow, therefore a way to allow biochemical interactions, involving the recognition of cell surface components with no biological interactions is using heat-killed cells (thermal inactivation) (Liang *et al.* 2019). In this case, we cultivated *C. mamane* in presence of heat-killed *Leishmania* parasites. To the best of our knowledge, the use of heat-killed inducers to reveal cryptic pathways has been described in the literature only for bacteria and fungi (Fourati-Ben Fguira *et al.* 2008; Liang *et al.* 2019, 2020) but not for parasites.

Furthermore, in a previous study performed in our team, *C. mamane* was confronted with *Fusarium solani* allowing the detection of 5 *de* novo compounds produced only under co-culture but not detected in mono-culture (Triastuti *et al.* 2021). This result highlighted that *C. mamane* is sensitive to the presence of another microorganism in its own culture medium, and can modulate its metabolome in response to this presence. Additionally, the experiment using epigenetic modifiers (see **Chapter 4**) has shown that the production of botryosulfuranol C was up-regulated when *C. mamane* was cultivated in presence of N-butyryl-DL-homoserine lactone (HSL), a main *quorum*-sensing molecule in gram-negative bacteria.

In the present study, two strategies to induce the production of potential antimicrobial metabolites were followed: the co-culture of *C. mamane* with three pathogenic bacterial strains (two gram-negative bacteria, *Escherichia coli* ATCC® 25922™ and *Pseudomonas aeruginosa* ATCC® 27853™ and a gram-positive bacterium, *Staphylococcus aureus* ATCC® 25923™) and the culture of *C. mamane* with thermally inactivated parasites of *Leishmania infantum* as a heat-killed inducer. The global chemical response of *C. mamane* was evaluated, with a focus on the production of TDKPs.

5.2 Results

5.2.1 Addition of heat-killed leishmanial parasites

Preliminary results

In a preliminary analysis, in order to compare the global chemical profile alteration and to observe if the production of the TDKPs responded differently to different parasitic forms, two developmental stages of *L. infantum* were used, promastigotes and amastigotes (**Figure 5.1**), at an unknown concentration of parasites/mL of culture medium. The intracellular *Leishmania* amastigote replicates within macrophages of the host while the extracellular promastigote develops within the insect vector.

a. Addition of heat-killed promastigotes of *L. infantum* into *C. mamane* culture

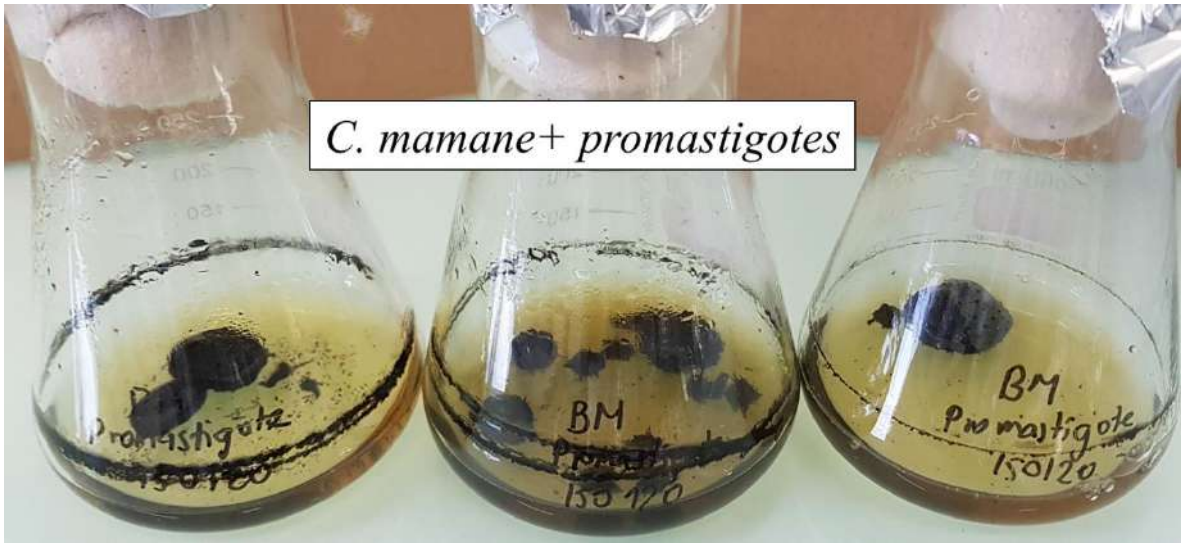

b. Addition of heat-killed amastigotes of *L. infantum* into *C. mamane* culture

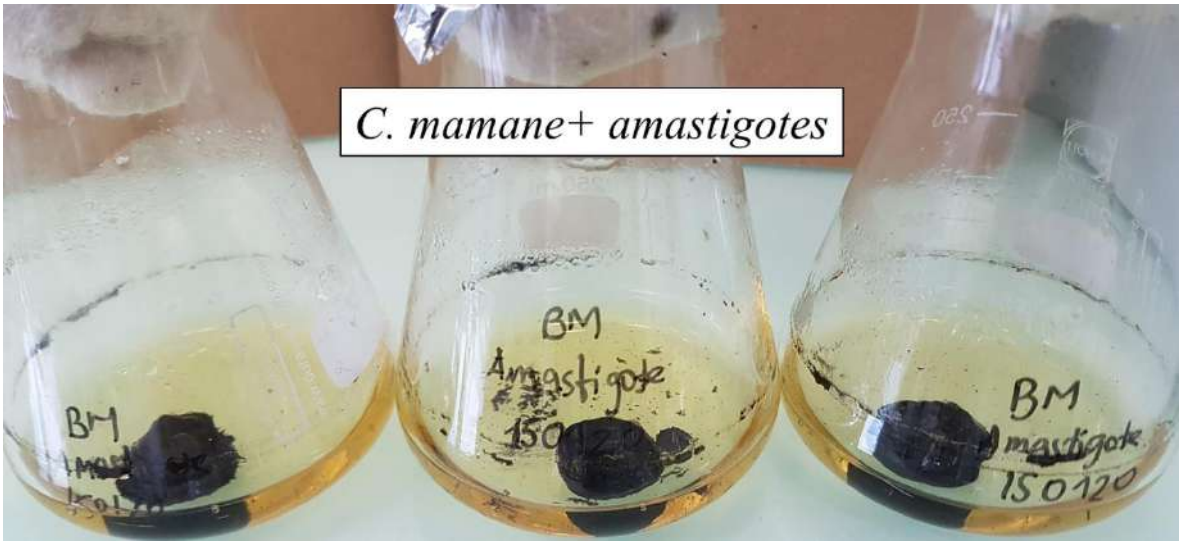

Figure 5.1. Culture of *C. mamane* in presence of heat-killed promastigotes and amastigotes of *L. infantum*

UHPLC-(+)ESI-HRMS chromatograms of extracts from the 3 groups (control, *C. mamane* + promastigotes and *C. mamane* + amastigotes) were compared. At a first look, we can observe that untreated *C. mamane* and *C. mamane* + amastigotes present a qualitatively quite similar global chemical profile, with 5 major peaks corresponding to the TDKPs, botryosulfuranols A, B and C and to two cyclopentapeptides (*m/z* 552.4164 at 8.69 min and *m/z* 566.4324 at 9.35 min) previously annotated. On the contrary, the extract of *C. mamane* cultured with promastigotes of *Leishmania infantum* present a different chemical profile, with only 2 major peaks corresponding to the cyclopentapeptides while botryosulfuranols are almost undetectable in the chromatogram under this culture condition (**Figure 5.2**).

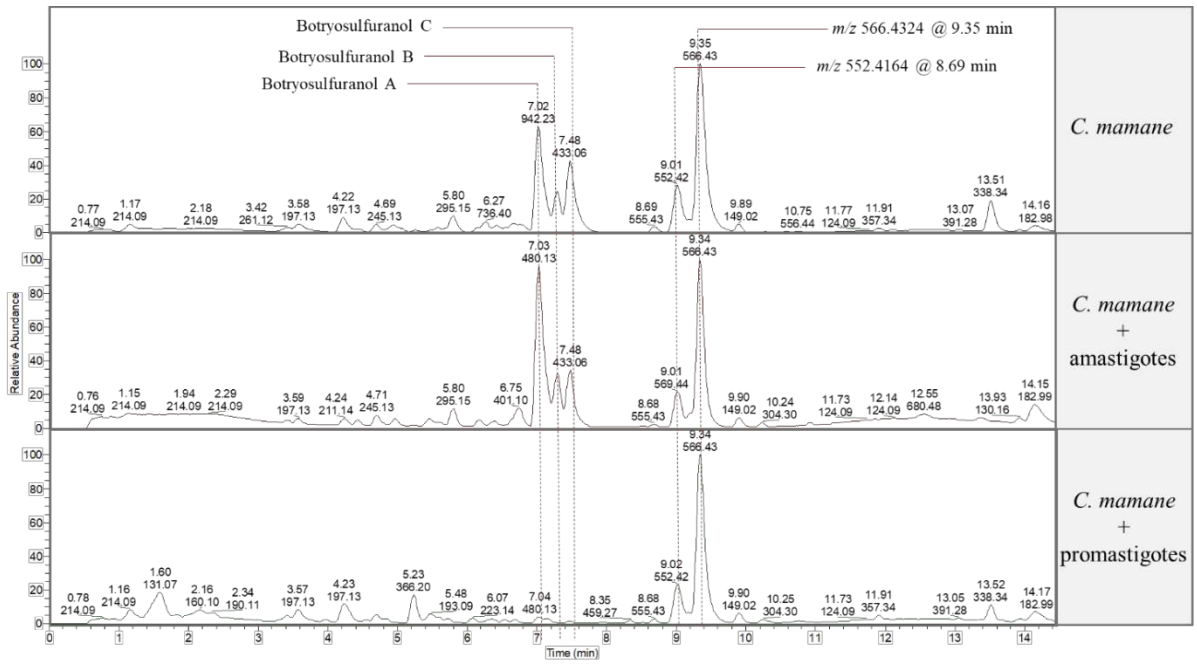

Figure 5.2. UHPLC-(+)ESI-HRMS base peak chromatograms of crude extracts of *C. mamane* treated with heat-killed promastigotes and amastigotes of *Leishmania infantum* in comparison to the control of *C. mamane*

Therefore, to repeat the experiment with more replicates and known concentrations of heat-killed parasites to be able to do statistical analyses, we decided to work only with amastigotes of *Leishmania infantum*. We also expected that the higher the concentration of parasites, the greater the induction of TDKPs will be.

General observations: Culture of C. mamane with known concentrations of heat-killed amastigotes of Leishmania infantum

Three different concentrations of *L. infantum* amastigotes were evaluated: C1=5.2 x 10^5, C2=1.06 x 10^6 and C4=2.12 x 10^6 parasites/mL (C1 < C2 < C4) to observe additional alterations of the metabolome. The general overview of the chromatograms is presented in **Figure 5.3,** slightly different from the previous chromatogram (**Figure 5.2**) probably due to the different concentrations used. At a first look, we can observe peaks corresponding to the TDKPs, botryosulfuranols A and B in all conditions, while botryosulfuranol C seems to be less present under the presence of heat-killed parasites. The feature *m/z* 255.1318 at 5.192 min (not detected in any control or blank sample) appears to be induced under the presence of heat-killed parasites in comparison to the untreated culture of *C. mamane* (**Figure 5.3**).

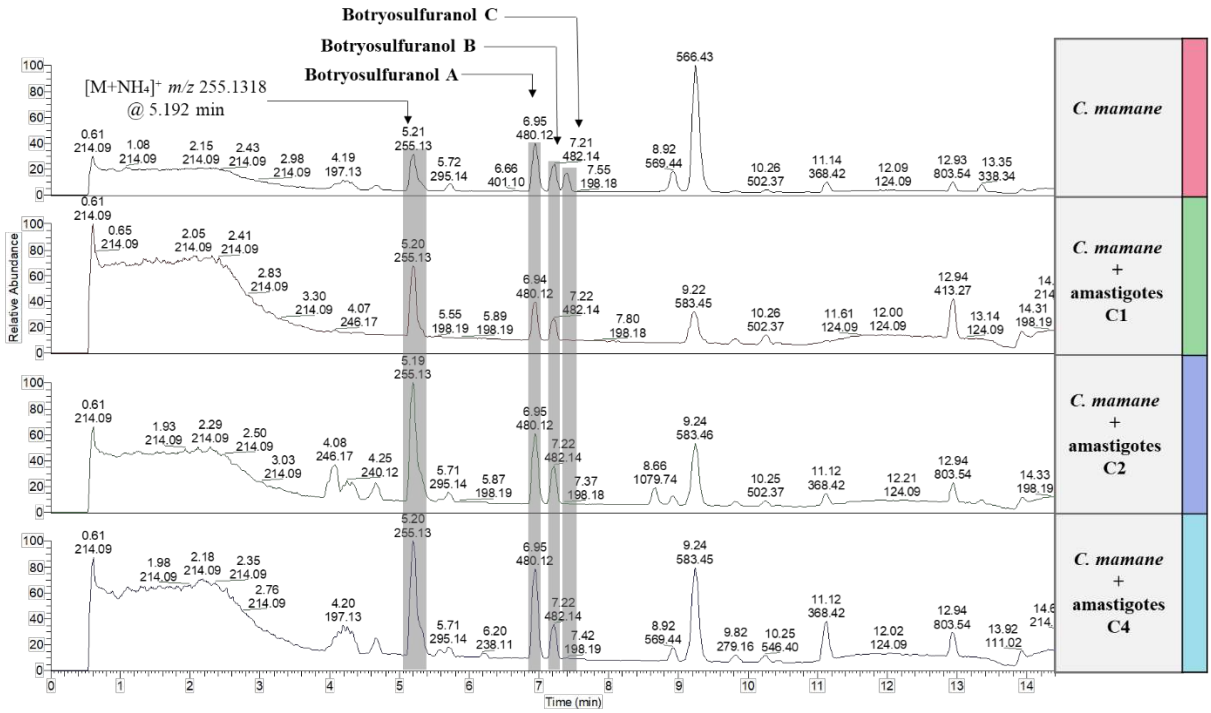

Figure 5.3. UHPLC-(+)ESI-HRMS base peak chromatograms from crude extracts of *C. mamane* treated with heat-killed amastigotes of *Leishmania infantum* at 3 different concentrations: C1, C2 and C4

UHPLC-(+)ESI-HRMS profiles of all the 12 crude extracts from this study afforded 93 features (m/z-RT pairs), which were considered for the metabolomics and statistical analysis. Thirty-three percent of these features (27 out of 93) were putatively annotated, corresponding to diketopiperazines (DKPs), cyclic peptides, tetrahydropyridines, eicosanoids etc (**Annexes 5**).

Multivariate classification (PLS-DA)

A supervised PLS-DA analysis was carried out on these data which indicated the response of *C. mamane* to the different concentrations of heat-killed amastigotes of *L. infantum* (**Figure 5.4**). Separate clusters appear on the PLS-DA score plot (37.3 % of total variability). The component 1 (X-axis) explained 18.5 % of the variability, allowing a slight the discrimination of the different clusters, mainly between the untreated *C. mamane* (CM) culture, CM+C1 - CM+C2 culture and CM+C4 culture. Component 2 (Y-axis) explained 18.8% of the variability with overlapping clusters, reflecting the few changes of the general metabolome of *C. mamane* when cultured in presence of heat-killed parasites.

The **Figure 5.4** also presents the top 15 compounds that contribute to the differences between these clusters while some of them were putatively identified. For instance, TDKPs botryosulfuranols A and C, which seems to have a lower detection under the addition of the parasites compared to the control. On the contrary, (±)flavipucine or its isomers ((±)isoflavipucine, fruit rot toxin A, sapinopyridion),

compounds isolated from an endophytic fungal strain of *Phoma* sp. (Loesgen *et al.* 2011), appear to have a higher detection under the addition of the parasites (CM+C4), along with other 5 other unidentified features (**Figure 5.4**).

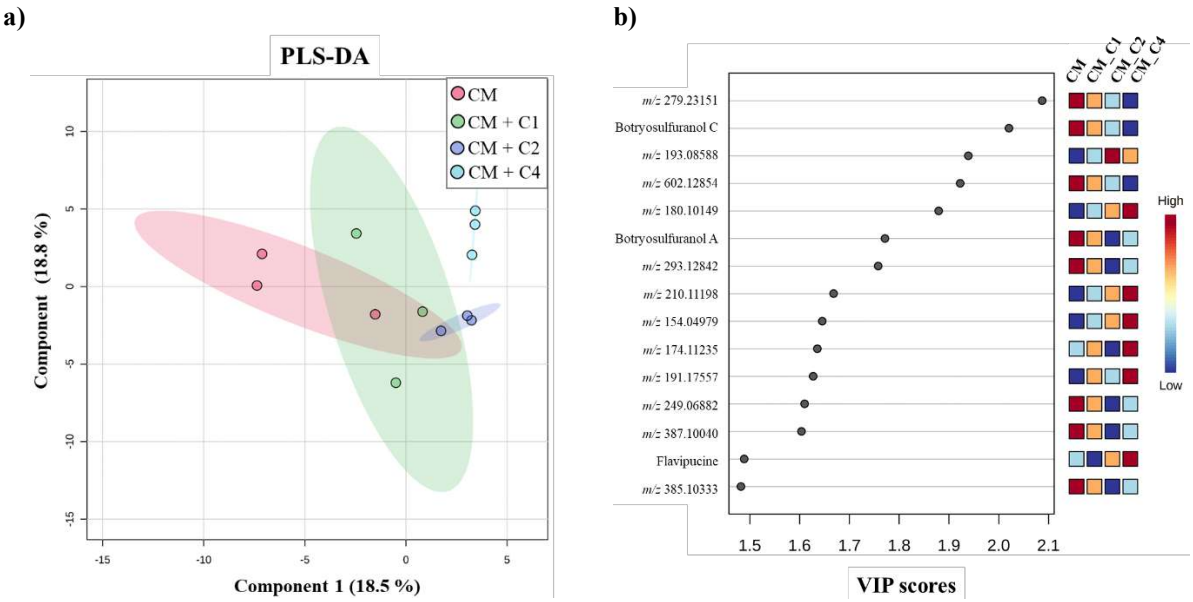

Figure 5.4. a) Partial least squares discriminant analysis (PLS-DA) obtained from UHPLC-(+)ESI-HRMS profiles corresponding to the extracts of *C. mamane* (CM) cultivated under the addition of heat-killed *Leishmania* parasites at 3 different concentrations (C1, C2 and C4); based on features (m/z at Rt to its normalized peak area) detected in LC-MS chromatograms; (b) Variable importance in projection (VIP) score of the top 15 compounds from the PLS-DA analysis corresponding to each condition

Table 5.1. Top 15 features that significantly contribute to the difference in the PLS-DA analysis from LC-HRMS/MS data under the addition of heat-killed parasites in *C. mamane* culture

ID	Rt (min)	Observed *m/z*	Adduct	Formula	Δ mass (ppm)	Putative identification	Ontology	VIP scores
69	9.37	279.2315	$[M+H]^+$	$C_{18}H_{30}O_2$	1.24	Unknown	Unknown	2.09
16	7.39	455.0332	$[M+Na]^+$	$C_{19}H_{16}N_2O_6S_2$	2.12	Botryosulfuranol C	Thiodiketopiperazines	2.02
38	5.40	193.0858	$[M+H]^+$	$C_{11}H_{12}O_3$	0.21	Unknown	Unknown	1.94
31	6.59	602.1285	$[M+NH_4]^+$	$C_{31}H_{20}O_{12}$	1.26	Unknown	Unknown	1.92
12	3.90	180.1014	$[M+H]^+$	$C_{10}H_{13}NO_2$	2.3	Unknown	Unknown	1.88
21	6.94	480.1244	$[M+NH_4]^+$	$C_{21}H_{22}N_2O_6S_2$	2.65	Botryosulfuranol A	Thiodiketopiperazines	1.77
76	6.11	293.1284	$[M+H]^+$	$C_{18}H_{16}N_2O_2$	0.11	Unknown	Unknown	1.76
45	6.81	210.1119	$[M+H]^+$	$C_{11}H_{15}NO_3$	2.33	Unknown	Unknown	1.67
80	3.68	154.0497	$[M+Na]^+$	$C_5H_9NO_3$	7.97	Unknown	Unknown	1.65
8	3.72	174.1123	$[M+H]^+$	$C_8H_{15}NO_3$	0.68	Unknown	Unknown	1.64
33	2.14	191.1755	$[M+H]^+$	$C_9H_{22}N_2O_2$	0.86	Unknown	Unknown	1.63
53	6.43	249.0688	$[M+H]^+$	$C_{12}H_{12}N_2O_2S$	1.62	Unknown	Unknown	1.61
3	6.94	387.1004	$[M+H]^+$	$C_{19}H_{18}N_2O_5S$	1.34	Unknown	Unknown	1.60
49	6.22	238.1069	$[M+H]^+$	$C_{12}H_{15}NO_6$	1.9	(±)-Flavipucine	Tetrahydropyridines	1.49
2	7.42	385.1033	$[M+H]^+$	$C_{19}H_{16}N_2O_7$	0.78	Unknown	Unknown	1.48

Differential production of metabolites (Volcano plot analysis)

Regarding the influence of heat-killed amastigotes more in details as shown in the Volcano plot representations (**Figure 5.5**), only 3, 3 and 1 features were up-regulated when *C. mamane* was cultivated with C1 (**Figure 5.5a**), C2 (**Figure 5.5b**) and C4 (**Figure 5.5c**), respectively, indicating the few significantly up-regulated metabolites regardless the concentration used which is in line with the PLS-DA results (**Figure 5.4**). However, due to the low annotation rate, metabolites with the most important significant changes could not be putatively annotated.

Among the most significantly induced metabolites (**Table 5.2**), unknown features, at *m/z* 461.3239 at 11.468 min ($C_{26}H_{46}O_5$) and at *m/z* 174.1124 at 3.726 min ($C_8H_{15}NO_3$) were significantly up-regulated under concentration C1 and C4 of amastigotes, respectively. Similarly, the metabolite annotated as (±)-flavipucine was significantly up-regulated by concentration C2 of amastigotes. On the other side, the putatively annotated cyclic pentapeptide, previously isolated from a non-identified endophytic fungal strain (Li *et al.* 2004), was significantly down-regulated under concentration C1 and C2 of amastigotes

a) Volcano plot of treatment with C1 of amastigotes

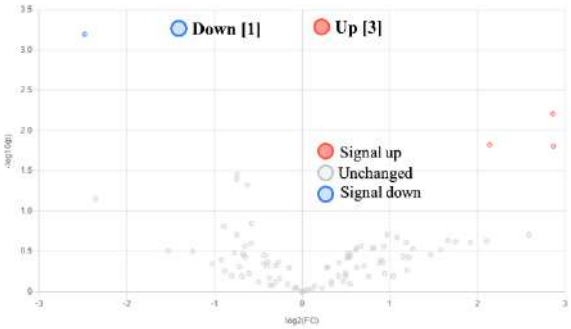

b) Volcano plot of treatment with C2 of amastigotes

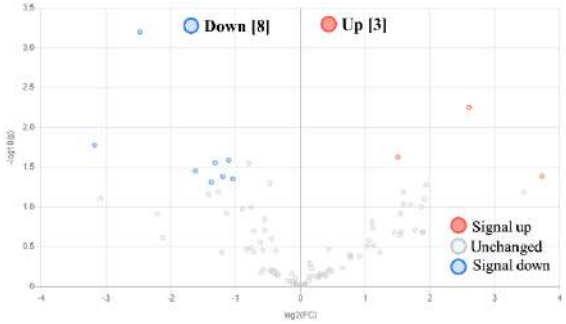

c) Volcano plot of treatment with C4 of amastigotes

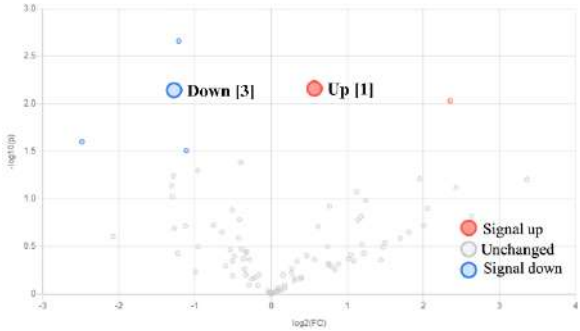

Figure 5.5. Volcano plot representations of *C. mamane* response to the treatment with heat-killed parasites at 3 different concentrations (C1, C2 and C4). Each dot represents a feature (*m/z* at Rt), the red and blue colors indicate a significant change (p-value < 0.05 and fold-change ratio > 2) of the features under treatment in up-regulating (red) or down-regulating (blue) their production in comparison with the untreated culture of *C. mamane*, while the numbers in brackets indicate the number of significant features observed.

Focusing on the TDKPs, the addition of the heat-killed parasites did not significantly induce the production of TDKPs, on the contrary, botryosulfuranol C was significantly down-regulated by concentration C1, C2 and C4 of amastigotes (**Figure 5.6**) while botryosylfuranol A was significantly down-regulated by concentration C4, both compared to the untreated culture of *C. mamane*. The TDKP botryosulfuranol D was almost undetectable as shown in **Figure 5.6**.

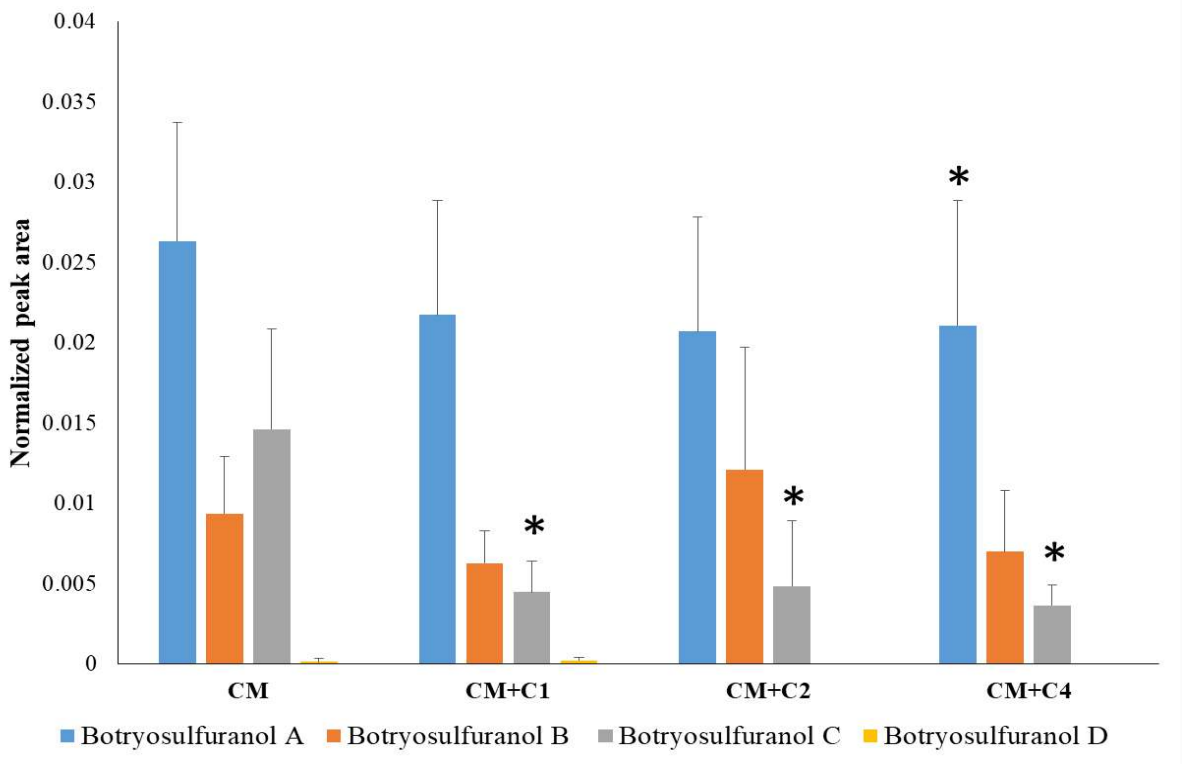

Figure 5.6. Normalized peak area of the TDKPs botryosulfuranols A, B, C and D detected under the addition of heat-killed *Leishmania* amastigotes at 3 different concentrations (C1, C2 and C4) in comparison to the untreated culture of *C. mamane* (CM). Significant changes (T-test with $p<0.05$) are shown (*)

Table 5.2. Most important compounds up-regulated (↑) or down-regulated (↓) by the treatment heat-killed parasites in *C. mamane* culture. Up-regulation or down-regulation is shown with a significant (*) or not significant (N.S.) fold-change (FC) value. Significant values with *p*-value < 0.05 and fold-change ratio > 2

ID	Rt min	Observed *m/z*	Adduct	Formula	Δ mass (ppm)	Putative identification	Ontology	***C. mamane* and C1 amastigotes**		***C. mamane* and C2 amastigotes**		***C. mamane* and C4 amastigotes**	
								Log2 (FC)	**Trend**	**Log2 (FC)**	**Trend**	**Log2 (FC)**	**Trend**
2	7.42	385.1033	[M+H]+	$C_{19}H_{16}N_2O_7$	0.78	Unknown	Unknown	N.S.		-3.1775	↓*	-1.2925	↓
4	6.07	392.2272	[M+H]+	$C_{22}H_{33}NO_3S$	4.61	Unknown	Unknown	2.8625	↑*	1.2277	↑	2.0559	↑
7	11.47	461.3239	[M+Na]+	$C_{26}H_{46}O_5$	0.33	Unknown	Unknown	2.8714	↑*	3.4472	↑	3.3639	↑
8	3.73	174.1124	[M+H]+	$C_8H_{15}NO_3$	0.68	Unknown	Unknown	N.S.		-1.2187	↓	2.353	↑ *
16	7.39	455.0332	[M+Na]+	$C_{19}H_{16}N_2O_6S_2$	2.12	Botryosulfuranol C	Thiodiketopiperazines	N.S.		N.S.		-1.2105	↓*
31	6.59	602.1285	[M+NH4]+	$C_{31}H_{20}O_{12}$	1.26	Unknown	Unknown	N.S.		-1.1415	↓	-2.4837	↓*
36	9.31	600.4116	[M+H]+	$C_{33}H_{53}N_5O_5$	0.54	Cyclo-(L-Phe-L-Leu1-L-Leu2-L-Leu3-L-Ile)*	Cyclopeptides	-2.4823	↓*	-2.4747	↓*	-1.3075	↓
38	5.40	193.0859	[M+H]+	$C_{11}H_{12}O_3$	0.21	Unknown	Unknown	N.S.		1.5046	↑*	1.2445	↑
50	5.68	238.1071	[M+H]+	$C_{12}H_{15}NO_4$	1.19	(±)-Flavipucine	Tetrahydropyridines	1.2189	↑	3.7314	↑*	N.S.	
57	0.88	256.1182	[M+H]+	$C_{12}H_{17}NO_5$	0.98	Unknown	Unknown	2.5871	↑	2.6041	↑*	1.2185	↑
69	9.37	279.2315	[M+H]+	$C_{18}H_{30}O_2$	1.24	Unknown	Unknown	N.S.		N.S.		-1.1146	↓*
71	7.36	285.1698	[M+H]+	$C_{15}H_{24}O_5$	0.52	Unknown	Unknown	2.1424	↑*	1.5908	↑	1.4941	↑

*unknown amino acids sequence

Molecular network analysis

To better visualize chemical relationships based on acquired MS-MS data, and to focus on derivatives of annotated metabolites, a molecular networking was performed. Our analysis displayed a molecular network that contained 93 nodes and 12 spectral families with 31 connected nodes while the rest of the nodes showed no link to others (self-loop). The size of the nodes represents the total average of the detected peak areas for each compound in all the conditions while the colors depend on their detection in each condition (**Figure 5.7**).

The metabolite annotated as flavipucine (or isomers), which corresponds to one of the peaks induced by the addition of the parasites, was found to be linked to other two isomers. Moreover, two clusters were observed containing metabolites putatively annotated as cyclopentapeptides (**Figure 5.7**).

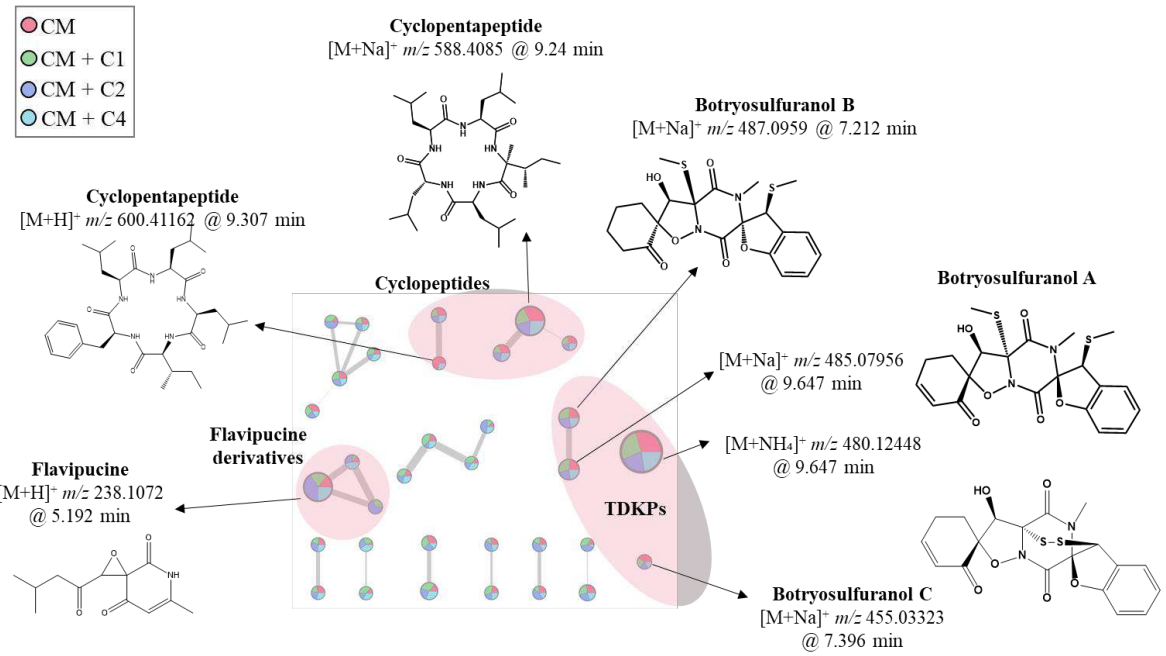

Figure 5.7. Molecular networking corresponding to the extracts of *C. mamane* treated with heat-killed parasites at 3 different concentrations (C1, C2, C4) based on features (*m/z* at Rt to its normalized peak area) detected in LC-MS chromatograms. Visualization of botryosulfuranols A, B and C and major peaks flavipucine and a cyclic peptide

Focusing on the cluster containing the thiodiketopiperazines, botryosulfuranol A and B were linked with a cosine value of 0.9 (data not shown) (**Figure 5.7**) but no other metabolites appeared to be linked in the same cluster. In another cluster, two metabolites putatively annotated as eicosanoids (*m/z* 295.22626 at 7.313 min and *m/z* 295.22632 at 7.719 min) were previously found to be produced by *Fusarium oxysporum* along with other jasmonates and related compounds (Miersch *et al.* 1999). This fungal

species has also been described in the literature as an endophyte isolated from different plants, including medicinal ones (do Nascimento *et al.* 2012; Ben Rhouma *et al.* 2020).

All putatively identified compounds are detailed in **Table 5.3**. The TDKP botryosulfuranol D does not possess an ID number because it was not considered for the metabolomics analyses due to its low detection.

Table 5.3. Putative identified compounds detected under the addition of heat-killed parasites in the culture of *C. mamane*

ID	Rt (min)	*m/z*	Adduct	Formula	Δ mass (ppm)	Putative identification	Ontology
49	6.22	238.1069	[M+H]+	$C_{12}H_{15}NO_6$	1.9	(±)-Flavipucine	Tetrahydropyridines
61	5.19	238.1072	[M+H]+	$C_{12}H_{15}NO_6$	0.77	(±)-Flavipucine	Tetrahydropyridines
50	5.68	238.1071	[M+H]+	$C_{12}H_{15}NO_6$	1.19	(±)-Flavipucine	Tetrahydropyridines
43	8.92	574.3934	[M+Na]+	$C_{29}H_{53}N_5O_5$	0.8	Cyclo-(L-Leu-L-Leu-D-Leu-L-Leu-L-Val)*	Cyclopeptides
26	9.24	588.4085	[M+Na]+	$C_{30}H_{55}N_5O_5$	1.75	Cyclo-(L-Ile-L-Leu-L-Leu-L-Leu-L-Leu)*	Cyclopeptides
27	9.07	566.4275	[M+H]+	$C_{30}H_{55}N_5O_5$	0.17	Cyclo-(L-Ile-L-Leu-L-Leu-L-Leu-L-Leu)*	Cyclopeptides
36	9.30	600.4116	[M+H]+	$C_{33}H_{53}N_5O_5$	0.54	Cyclo-(L-Phe-L-Leu1-L-Leu2-L-Leu3-L-Ile)*	Cyclopeptides
78	7.31	295.2262	[M+H]+	$C_{18}H_{30}O_3$	1.73	3-Oxo-2-(2-entenyl)cyclopentaneoctanoic acid;OPC-8:0	Eicosanoids
79	7.71	295.2263	[M+H]+	$C_{18}H_{30}O_3$	1.52	3-Oxo-2-(2-entenyl)cyclopentaneoctanoic acid;OPC-8:0	Eicosanoids
18	7.21	487.0959	[M+Na]+	$C_{21}H_{24}N_2O_6S_2$	1.8	Botryosulfuranol B	Thiodiketopiperazines
16	7.39	455.0332	[M+Na]+	$C_{19}H_{16}N_2O_6S_2$	2.12	Botryosulfuranol C	Thiodiketopiperazines
21	6.94	480.1244	[M+NH4]+	$C_{21}H_{22}N_2O_6S_2$	2.65	Botryosulfuranol A	Thiodiketopiperazines
-	7.09	465.0231	[M+H]+	$C_{19}H_{16}N_2O_6S_3$	2.56	Botryosulfuranol D	Thiodiketopiperazines

*amino acid sequence not known

Antileishmanial activity of crude extracts against amastigotes of L. infantum

In order to know if there is a correlation between the concentration of TDKPs in the ethyl acetate extracts of the *C. mamane* culture and their antileishmanial activity, *in vitro* assays were performed on axenic amastigotes of *L. infantum* and the half-maximal effective concentration *Leishmania* growth (EC_{50}) was calculated for each extract while the IC_{50} value for the amphotericin B is 0.06 µM (**Table 5.4)**.

As observed in the chemical profiles (**Figure 5.3**) and the down-regulation of TDKPs when *C. mamane* was cultivated with heat-killed *Leishmania* (**Figure 5.6**), the crude extracts of the untreated culture of *C. mamane* present the best activity, being twice as high as the most active crude extract of the culture treated with *L. infantum* at concentration C2 (CM+C2) (EC_{50}=0.807 µg/mL). Thus, these results tend to show a correlation between the concentration of TDKPs and the antileishmanial activity, but also that no other antileishmanial compounds appear to have been induced by the heat-killed parasites.

Table 5.4. Antileishmanial activity of the crude extracts of *C. mamane* (CM) cultivated under the addition of heat-killed leishmanial parasites at 3 different concentrations (C1, C2 and C4)

Samples	**EC_{50} (µg/mL)**		
CM	0.423	±	0.04
CM + C1	1.217	±	0.79
CM + C2	0.807	±	0.10
CM + C4	1.193	±	0.89
Amphotericin B	0.06	**µM**	

5.2.2 Co-culture with pathogen bacteria

General observations

We have previously observed that the addition of the *quorum*-sensing molecule N-butyryl-DL-homoserine lactone (HSL) into *C. mamane* culture, induced the production of the TDKPs botryosulfuranol C (see **Chapter 4**). In addition to the previous experiment with heat-killed *Leishmania* parasites and to hopefully increase antimicrobial metabolites and TDKPs production, living pathogenic bacteria were added into *C. mamane* culture. Two gram-negative bacteria, *P. aeruginosa* and *E. coli* and one gram-positive bacterium, *S. aureus*, were used for this purpose as observed in **Figure 5.8**. Also, as in this experiment the incubation was performed without agitation, the mycelium covers the surface of the culture media, contrary to what observed in **Figure 5.1,** where the mycelium has a rond shape due to the agitation during the incubation.

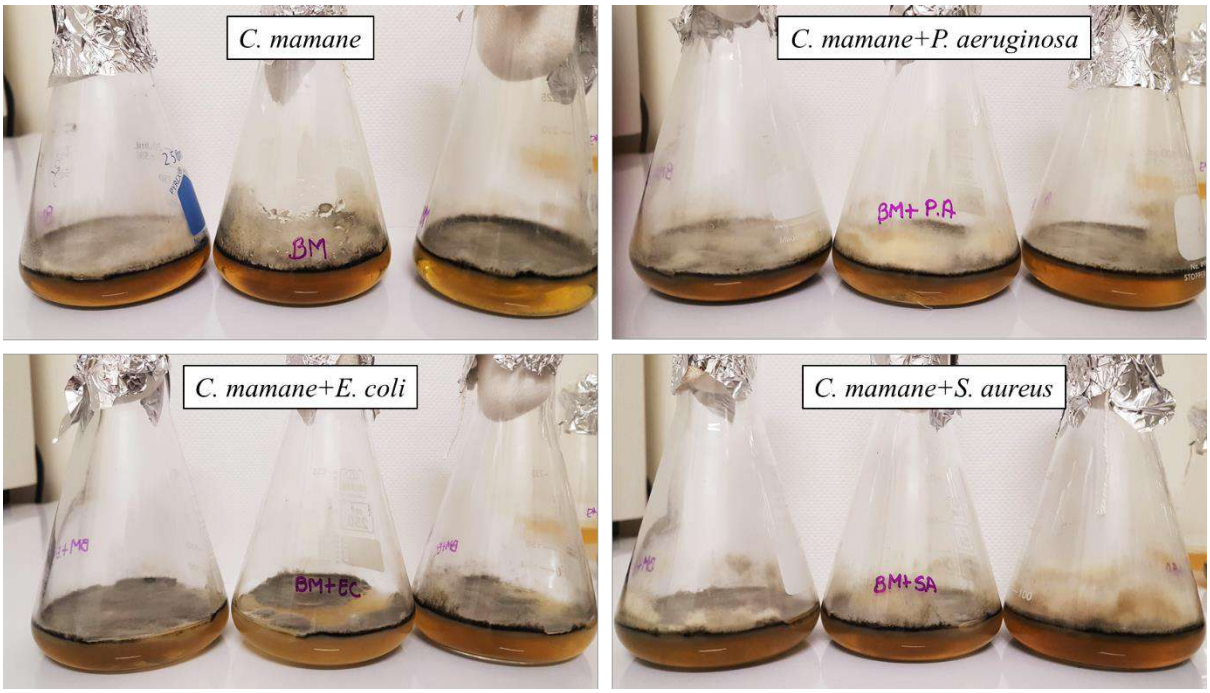

Figure 5.8. Culture of *C. mamane* in axenic conditions and in co-culture with pathogenic gram-negative bacteria, *E. coli* and *P. aeruginosa*, and gram-positive bacterium, *S. aureus*

The general chemical profiles of the axenic culture of *C. mamane* exhibit the presence of the TDKPs, whose extracted-ion chromatograms (XIC) are shown in **Figure 5.9**. To compare the general chemical profiles of the axenic culture of *C. mamani* and the ones of the axenic culture of each pathogenic bacteria against their respective co-culture, their chromatograms are shown in **Figure 5.10**, **Figure 5.11** and **Figure 5.12**.

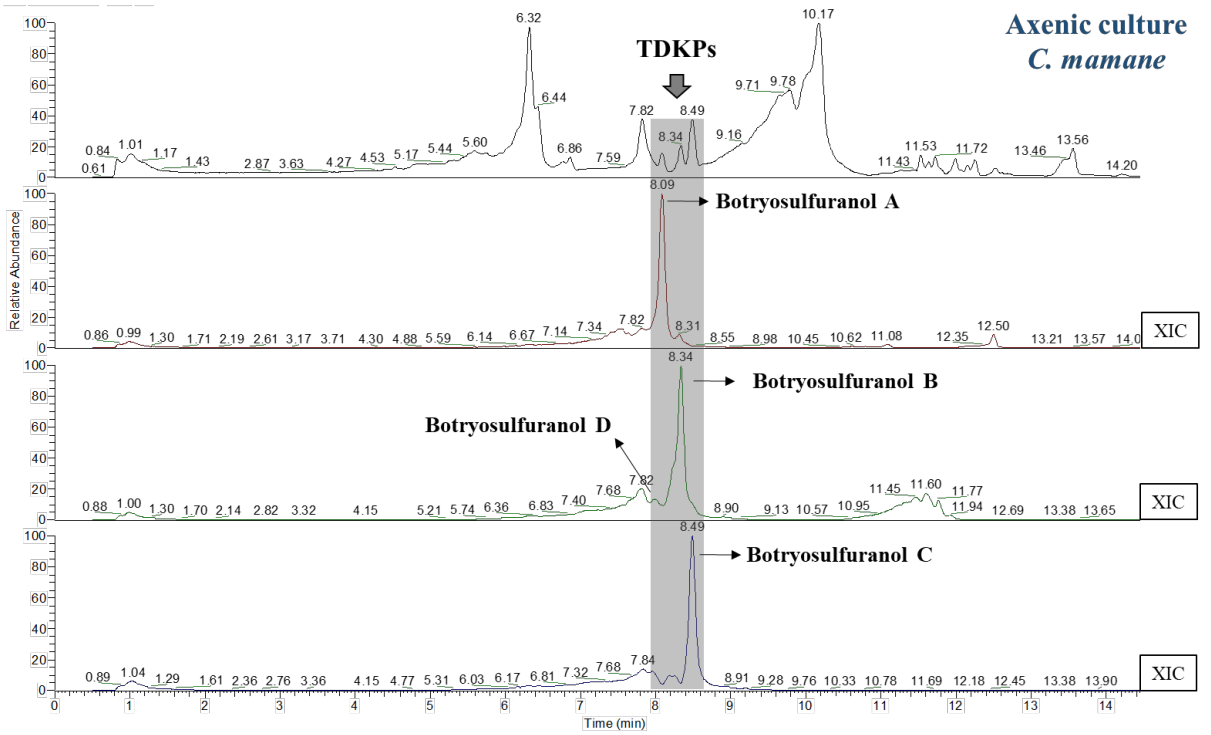

Figure 5.9. UHPLC-(+)ESI-HRMS base peak chromatograms from crude extracts of *C. mamane* culture with extracted-ion chromatograms showing the presence of TDKPs, botryosulfuranols A, B, C and D

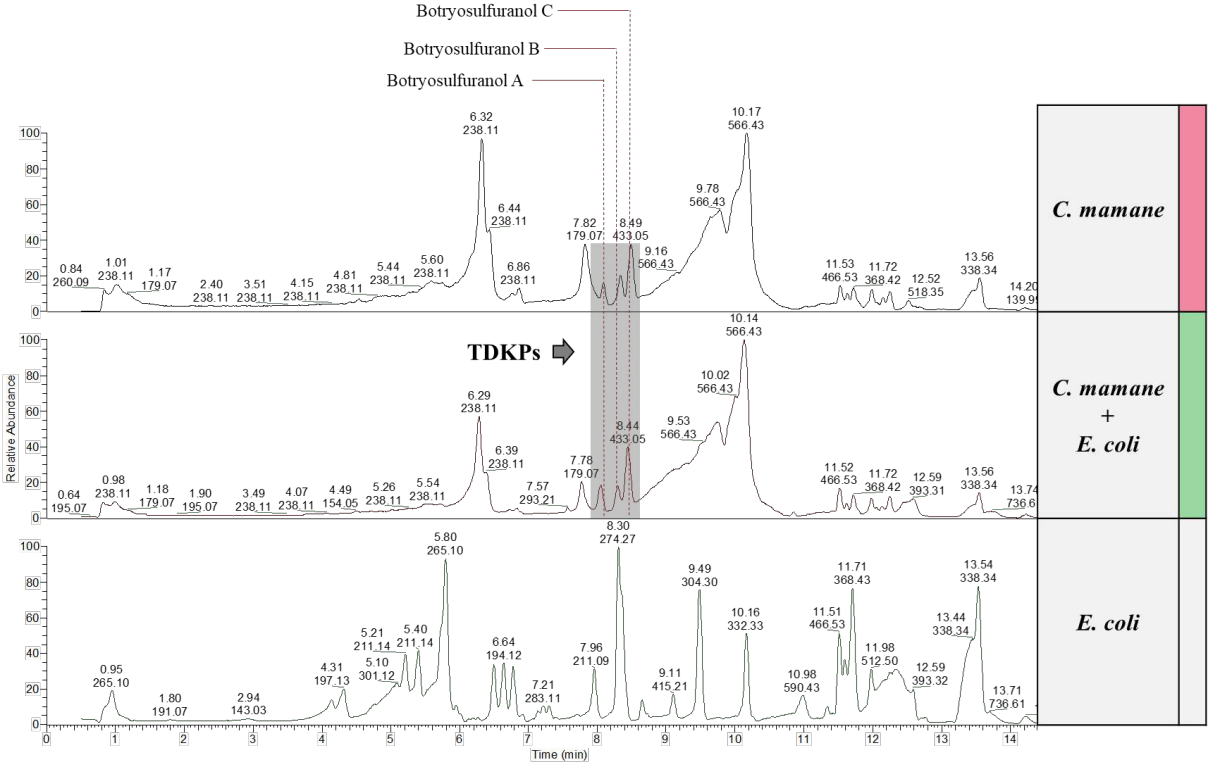

Figure 5.10. UHPLC-(+)ESI-HRMS base peak chromatograms of crude extracts of *C. mamane* and *E. coli* culture in axenic and co-culture conditions, showing the presence of the TDKPs

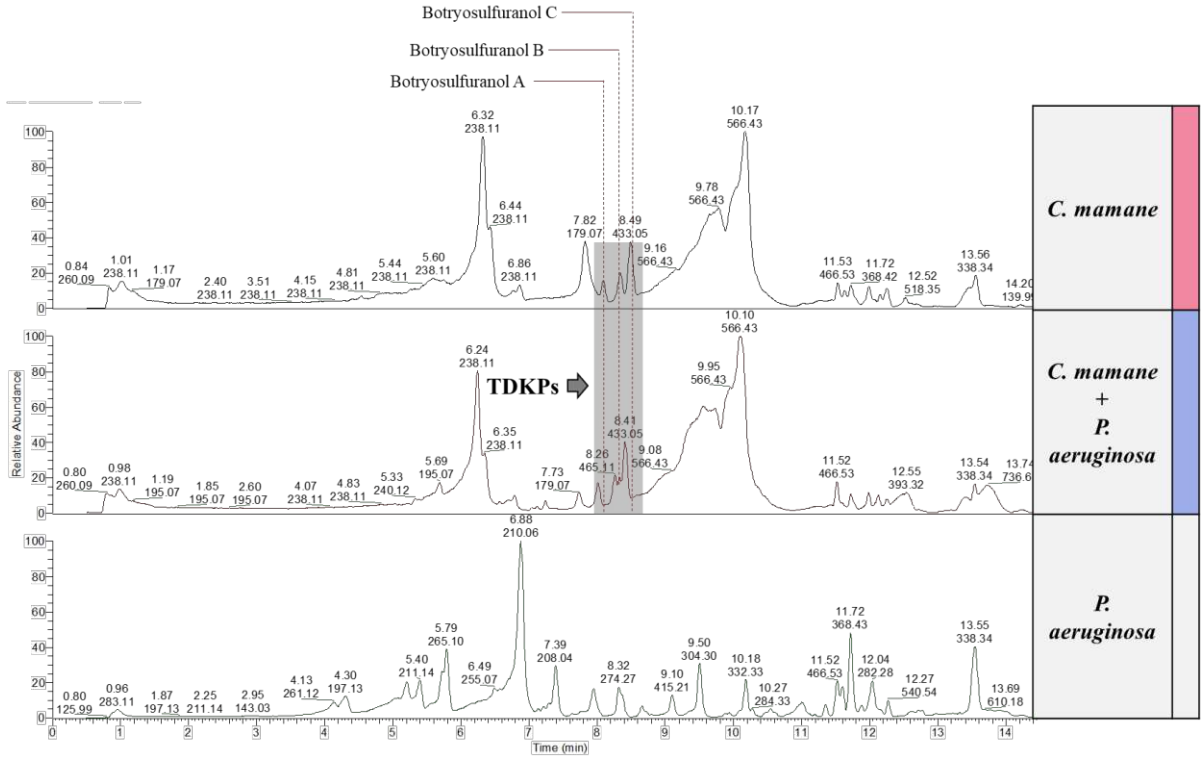

Figure 5.11. UHPLC-(+)ESI-HRMS base peak chromatograms of crude extracts of *C. mamane* and *P. aeruginosa* culture in axenic and co-culture conditions, showing the presence of the TDKPs

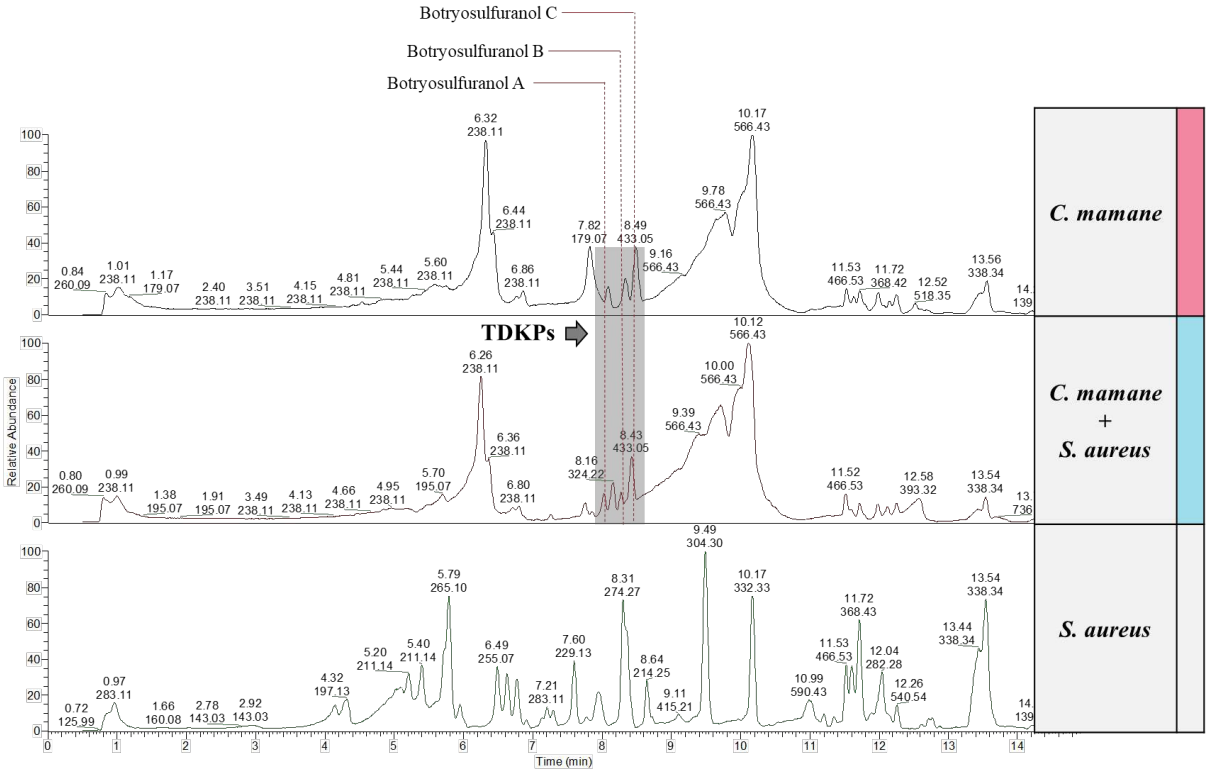

Figure 5.12. UHPLC-(+)ESI-HRMS base peak chromatograms of crude extracts of *C. mamane* and *S. aureus* culture in axenic and co-culture conditions, showing the presence of the TDKPs

UHLC-(+)ESI-HRMS profiles of all the 12 crude extracts from this study afforded 328 features (*m/z*-RT pairs) in PI mode, which were considered for the metabolomics and statistical analysis. Some of the putatively annotated metabolites correspond to diketopiperazines (DKPs), cyclic peptides, cyclohexenones, benzenoids, hydropyridines, etc.

Multivariate classification (PLS-DA)

A supervised PLS-DA analysis carried out on these data indicated the response of *C. mamane* in presence of the 3 living pathogenic bacteria, *E. coli* (EC), *P. aeruginosa* (PA) and *S. aureus* (SA) (**Figure 5.13**). Separate clusters appear on the PLS-DA score plot (32.4 % of total variability). The component 1 (X-axis) explained 20 % of the variability, allowing a slight discrimination mainly of the cluster corresponding to the co-culture of *C. mamane* with *S. aureus* from the rest conditions. Component 2 (Y-axis) explained 12.4 % of the variability with overlapping clusters, reflecting the few changes of the general metabolome of *C. mamane* when co-cultured with these pathogenic bacteria.

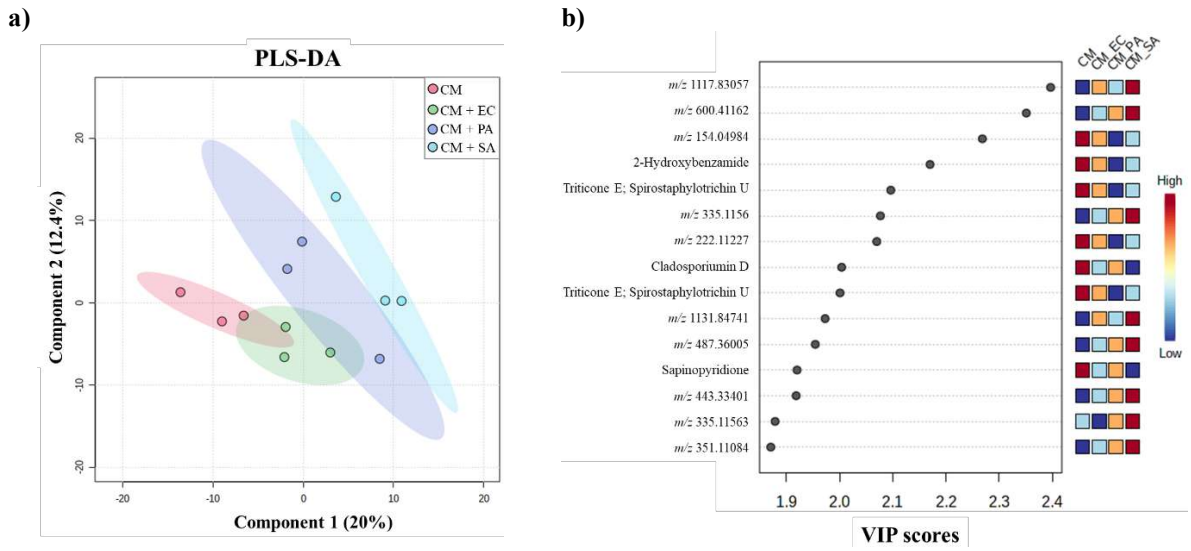

Figure 5.13. a) Partial least squares discriminant analysis (PLS-DA) obtained from LC-(+)ESI-HRMS profiles corresponding to the extracts of *C. mamane* (CM) co-cultivated with *E. coli* (EC), *P. aeruginosa* (PA) and *S. aureus* (SA); based on features (*m/z* at Rt to its normalized peak area) detected in LC-MS chromatograms; (b) Variable importance in projection (VIP) score of the top 15 compounds from the PLS-DA analysis corresponding to each condition

The **Figure 5.13 also** presents the top 15 compounds that contribute to the differences between these clusters while some of them were putatively identified. For instance, feature *m/z* 238.1069 at 7.28 min was putatively identified as sapinopyridione, a structurally closely compound related to flavipucine, both isolated from an endophytic fungal strain of *Phoma* sp. (Loesgen *et al.* 2011). The metabolite annotated as 2-hydroxybenzamide was previously isolated from a strain of *Streptomyces* sp. (Shaaban

et al. 2017) while the metabolite annotated as 4-hydroxybenzamide was previously isolated from an endophytic fungal strain of *Colletotrichum gloeosporioides*, which exhibited a potent antifungal activity against two pathogenic strains of *Cladosporium sp* (Chapla *et al.* 2014).

Moreover, the metabolite annotated as cladiosporumin D, is a tetramic acid derivative previously isolated from a deep-sea derived strain of *Cladosporium* sp. with no reported biological activity (Huang *et al.* 2018). Features *m/z* 298.1287 at 5.7 and 6.8 min were putatively identified as spirostaphylotrichin U, one of the three major compounds obtained from an endophytic fungal strain of *Bipolaris* sp., whose crude extract exhibited a weak antileishmanial activity (de Almeida *et al.* 2018). One of these two metabolites could also correspond to triticone E, a compound previously isolated from an endophytic fungal strain of *Curvularia lunata* which exhibited a good antibacterial activity against *E. coli*. Both molecules have previously shown to be inseparable by chromatographic methods (Hilario *et al.* 2020). These metabolites are detailed in **Table 5.5**.

Table 5.5. Top 15 features that significantly contribute to the difference in the PLS-DA analysis from LC-HRMS/MS data in *C. mamane* co-culture with *E. coli*, *P. aeruginosa* and *S. aureus*

ID	Rt (min)	*m/z*	Adduct	Formula	Δ mass (ppm)	Putative identification	Ontology	VIP scores
632	9.82	1117.8306	$[M+H]^+$	$C_{56}H_{100}N_{20}O_4$	0.31	Unknown	Unknown	2.397
551	10.20	600.4116	$[M+NH_4]^+$	$C_{33}H_{50}N_4O_5$	0.54	Unknown	Unknown	2.351
26	6.87	154.0498	$[M+H]^+$	$C_7H_7NO_3$	0.19	Unknown	Unknown	2.268
11	5.81	138.0549	$[M+H]^+$	$C_7H_7NO_2$	0.25	2-Hydroxybenzamide	Benzenoids	2.170
241	5.77	298.1283	$[M+H]^+$	$C_{14}H_{19}NO_6$	0.82	Triticone E; Spirostaphylotrichin U	Cyclohexenones	2.096
292	7.06	335.1156	$[M+H]^+$	$C_{15}H_{18}N_4O_3S$	4.89	Unknown	Unknown	2.077
113	5.82	222.1123	$[M+H]^+$	$C_{12}H_{15}NO_3$	0.9	Unknown	Unknown	2.070
169	5.81	254.1385	$[M+H]^+$	$C_{13}H_{19}NO_4$	0.85	Cladosporium in D	Carbonyl compounds	2.004
240	6.88	298.1283	$[M+H]^+$	$C_{14}H_{19}NO_6$	0.82	Triticone E; Spirostaphylotrichin U	Cyclohexenones	2.001
635	10.12	1131.8474	$[M+H]^+$	$C_{50}H_{102}N_{26}O_2S$	0.14	Unknown	Unknown	1.973
451	11.59	487.3601	$[M+Na]^+$	$C_{25}H_{52}O_7$	0.97	Unknown	Unknown	1.954
150	7.28	238.1074	$[M+H]^+$	$C_{12}H_{15}NO_4$	0.11	Sapinopyridione	Hydropyridines	1.920
407	11.60	443.3340	$[M+Na]^+$	$C_{24}H_{44}N_4O_2$	3.69	Unknown	Unknown	1.918
293	7.26	335.1156	$[M+H]^+$	$C_{15}H_{18}N_4O_3S$	4.79	Unknown	Unknown	1.879
306	6.68	351.1108	$[M+H]^+$	$C_{15}H_{18}N_4O_4S$	3.74	Unknown	Unknown	1.871

Differential production of metabolites (Volcano plot analysis)

Regarding more in details the metabolome changes of *C. mamane* in co-culture with bacteria, as shown in the Volcano plot representations (**Figure 5.14**), a total of 4, 5 and 6 features were up-regulated when *C. mamane* was co-cultivated with *E. coli* (**Figure 5.14a**), *P. aeruginosa* (**Figure 5.14b**) and *S. aureus* (**Figure 5.14c**), respectively, indicating the few significantly up-regulated metabolites which is in line with the PLS-DA results while a higher number of significantly down-regulated metabolites were observed (**Figure 5.14**). However, not all the metabolites with the most important significant changes could not be putatively annotated (**Table 5.6**).

a) Volcano plot of co-culture with *E. coli*

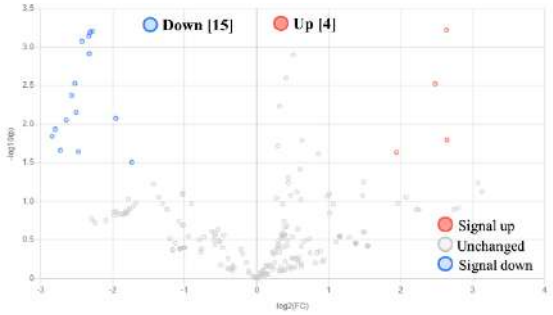

b) Volcano plot of co-culture with *P. aeruginosa*

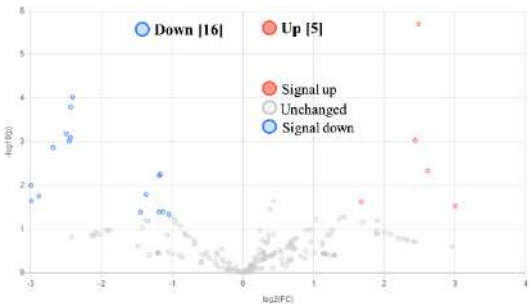

c) Volcano plot of co-culture with *S. aureus*

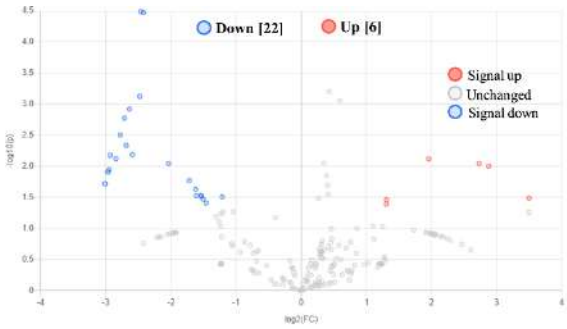

Figure 5.14. Volcano plot representations of co-culture of *C. mamane* with 3 different pathogenic bacteria (*E. coli, P. aeruginosa* and *S. aureus*). Each dot represents a feature (*m/z* at Rt), the red and blue colors indicate a significant change (*p*-value < 0.05 and fold-change ratio > 2) of the features under treatment in up-regulating (red) or down-regulating (blue) their production in comparison with the axenic culture of *C. mamane*, while the numbers in brackets indicate the number of significant features observed.

Among the most significantly induced compounds under co-culture with *E. coli*, we observed putatively identified diketopiperazine diphenylalazine B, previously isolated from entomopathogenic fungus *Epicoccum nigrum* (Guo *et al.* 2009). Two metabolites that were significantly up-regulated under the co-culture with *P. aeruginosa* and *S. aureus* were putatively identified as cyclic pentapeptides previously isolated from an endophytic fungal strain of *Cryptosporiopsis sp.,* which exhibited antifungal activity (Talontsi *et al.* 2012).

Moreover, of the 126 metabolites that were induced under the co-culture but lowly produced and undetected in the fungal or bacterial axenic cultures, were mainly produced under the co-culture with *E. coli*. Among these metabolites, two features (*m/z* 262.1436 at 5.99 min and *m/z* 262.1437 at 5.93 min) were putatively identified as bassiatin, a metabolite previously isolated from endophytic fungus *Fusarium proliferatum*, which exhibited moderate antibacterial activity (Jiang *et al.* 2019) (**Table 5.7**).

Regarding the TDKPs, the co-culture of *C. mamane* with *E. coli*, *P. aeruginosa* and *S. aureus* did not significantly alter their production (**Figure 5.15**) as it was also observed above in the chromatograms (**Figure 5.10**, **Figure 5.11** and **Figure 5.12**). The TDKP botryosulfuranol D was almost undetectable as shown in **Figure 5.15**. Interestingly, the production of a metabolite, possessing the same chemical formula as botryosulfuranol C (*m/z* 433.05219 at 7.91 min), was significantly up-regulated under the co-culture with *E. coli* and *P. aeruginosa* while the production of a metabolite, possessing the same chemical formula as botryosulfuranol A (*m/z* 485.08069 at 7.95 min), was significantly up-regulated under the co-culture with *S. aureus*.

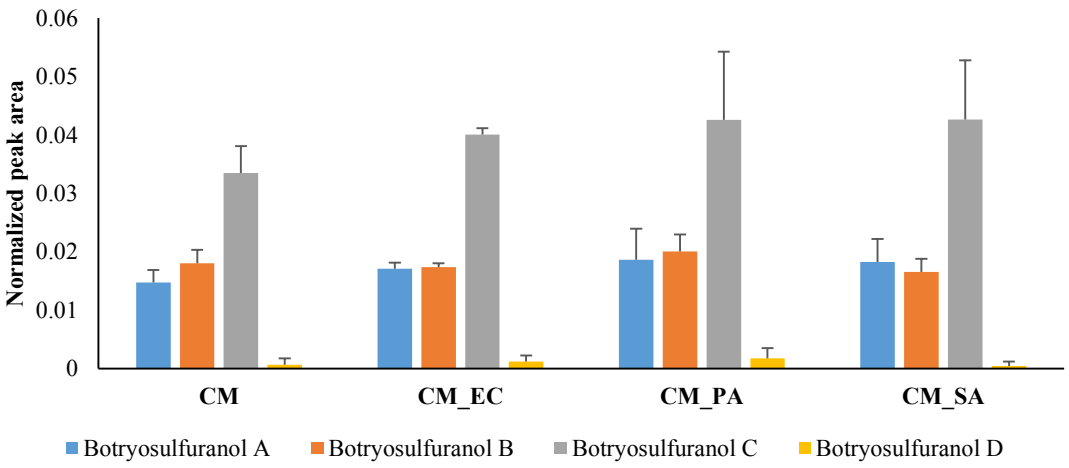

Figure 5.15. Normalized peak area of the TDKPs botryosulfuranol A, botryosulfuranol B, botryosulfuranol C and botryosulfuranol D detected under the co-culture with *E. coli* (EC), *P. aeruginosa* (PA) and *S. aureus* (SA) in comparison to the axenic culture of *C. mamane* (CM)

The most significantly induced metabolites produced under co-culture are detailed in **Table 5.6**.

Table 5.6. Metabolites up-regulated under the co-culture of *C. mamane* with *E. coli*, *P. aeruginosa* and *S. aureus* with significant values with *p*-value < 0.05 and fold-change (FC) ratio > 2 and compounds with not significant (N.S.) FC ratio.

ID	Rt (min)	*m/z*	Adduct	Formula	Δ mass (ppm)	Putative identification	Ontology	*C. mamane and E. coli*	*C. mamane* and *P. aeruginosa*	*C. mamane* and *S. aureus*
								Log2 (FC)	Log2 (FC)	Log2 (FC)
165	7.74	247.0534	$[M+H]^+$	$C_{12}H_{10}N_2O_2S$	0.55	Unknown	Unknown	2,48	N.S.	N.S.
277	7.88	323.1386	$[M+H]^+$	$C_{19}H_{18}N_2O_3$	1.17	Diphenylalazine B;(+)-Diphenylalazine B	Diketopiperazines	1,94	N.S.	N.S.
292	7.06	335.1156	$[M+H]^+$	$C_{15}H_{18}N_4O_3S$	4.89	Unknown	Unknown	N.S.	N.S.	2,73
293	7.26	335.1156	$[M+H]^+$	$C_{15}H_{18}N_4O_3S$	4.79	Unknown	Unknown	N.S.	N.S.	1,31
306	6.67	351.1108	$[M+H]^+$	$C_{15}H_{18}N_4O_4S$	3.74	Unknown	Unknown	N.S.	N.S.	2,88
395	7.91	433.0521	$[M+H]^+$	$C_{19}H_{16}N_2O_6S_2$	0.15	Unknown	Unknown	2,64	3,01	N.S.
445	7.95	485.0806	$[M+Na]^+$	$C_{21}H_{22}N_2O_6S_2$	0.95	Unknown	Unknown	N.S.	N.S.	3,50
456	6.84	496.1167	$[M+H]^+$	$C_{24}H_{21}N_3O_7S$	1.2	Unknown	Unknown	N.S.	2,49	N.S.
468	7.83	509.1046	$[M+H]^+$	$C_{22}H_{24}N_2O_8S_2$	0.09	Unknown	Unknown	N.S.	2,62	N.S.
513	8.19	566.4273	$[M+H]^+$	$C_{30}H_{55}N_5O_5$	0.55	Cyclo-(L-Ile-L-Leu-L-Leu-L-Leu-L-Leu)*	Cyclic peptides	N.S.	N.S.	1,31
517	9.96	566.4275	$[M+H]^+$	$C_{30}H_{55}N_5O_5$	0.08	Cyclo-(L-Ile-L-Leu-L-Leu-L-Leu-L-Leu)*	Cyclic peptides	N.S.	2,44	N.S.
551	10.19	600.4116	$[M+NH_4]^+$	$C_{33}H_{50}N_4O_5$	0.54	Unknown	Unknown	N.S.	1,67	1,96
606	8.36	849.1001	$[M+H]^+$	$C_{32}H_{41}N_4O_9PS_6$	0.77	Unknown	Unknown	2,63	N.S.	N.S.

*Unknown amino acids sequence of cyclic peptides

The mentioned putative identified metabolites are detailed in **Table 5.7** and in **Figure 5.16**.

Table 5.7. Putative identified compounds detected under the co-culture of *C. mamane* with *E. coli*, *P. aeruginosa* and *S. aureus*

ID	Rt (min)	*m/z*	Adduct	Formula	Δ mass (ppm)	Putative identification	Ontology
277	7.88	323.1386	$[M+H]^+$	$C_{19}H_{18}N_2O_3$	1.17	Diphenylalazine B	Diketopiperazines
421	8.03	463.0989	$[M+H]^+$	$C_{21}H_{22}N_2O_6S_2$	0.63	Botryosulfuranol A	Thiodiketopiperazines
445	7.95	485.0806	$[M+Na]^+$	$C_{21}H_{22}N_2O_6S_2$	0.95	Unknown	Unknown
426	8.28	465.1141	$[M+H]^+$	$C_{21}H_{24}N_2O_6S_2$	1.47	Botryosulfuranol B	Thiodiketopiperazines
391	8.43	433.0516	$[M+H]^+$	$C_{19}H_{16}N_2O_6S_2$	1.35	Botryosulfuranol C	Thiodiketopiperazines
395	7.91	433.0521	$[M+H]^+$	$C_{19}H_{16}N_2O_6S_2$	0.15	Unknown	Unknown
425	8.17	465.0235	$[M+H]^+$	$C_{19}H_{16}N_2O_6S_3$	1.77	Botryosulfuranol D	Thiodiketopiperazines
513	8.19	566.4273	$[M+H]^+$	$C_{30}H_{55}N_5O_5$	0.55	Cyclo-(L-Ile-L-Leu-L-Leu-L-Leu-L-Leu)*	Cyclic peptides
517	9.97	566.4275	$[M+H]^+$	$C_{30}H_{55}N_5O_5$	0.08	Cyclo-(L-Ile-L-Leu-L-Leu-L-Leu-L-Leu)*	Cyclic peptides
11	5.81	138.0549	$[M+H]^+$	$C_7H_7NO_2$	0.25	2-Hydroxybenzamide	Benzenoids
150	7.28	238.1074	$[M+H]^+$	$C_{12}H_{15}NO_4$	0.11	Sapinopyridione	Hydropyridines
169	5.81	254.1384	$[M+H]^+$	$C_{13}H_{19}NO_4$	0.85	Cladosporiumin D	Carbonyl compounds
240	6.88	298.1282	$[M+H]^+$	$C_{14}H_{19}NO_6$	0.82	Triticone E; Spirostaphylotrichin U	Cyclohexenones
241	5.77	298.1282	$[M+H]^+$	$C_{14}H_{19}NO_6$	0.82	Triticone E; Spirostaphylotrichin U	Cyclohexenones
187	5.99	262.1436	$[M+H]^+$	$C_{15}H_{19}NO_3$	0.45	Bassiatin	Alkaloids
188	5.93	262.1437	$[M+H]^+$	$C_{15}H_{19}NO_3$	0.23	Bassiatin	Alkaloids

*Unknown amino acids sequence of cyclic peptides

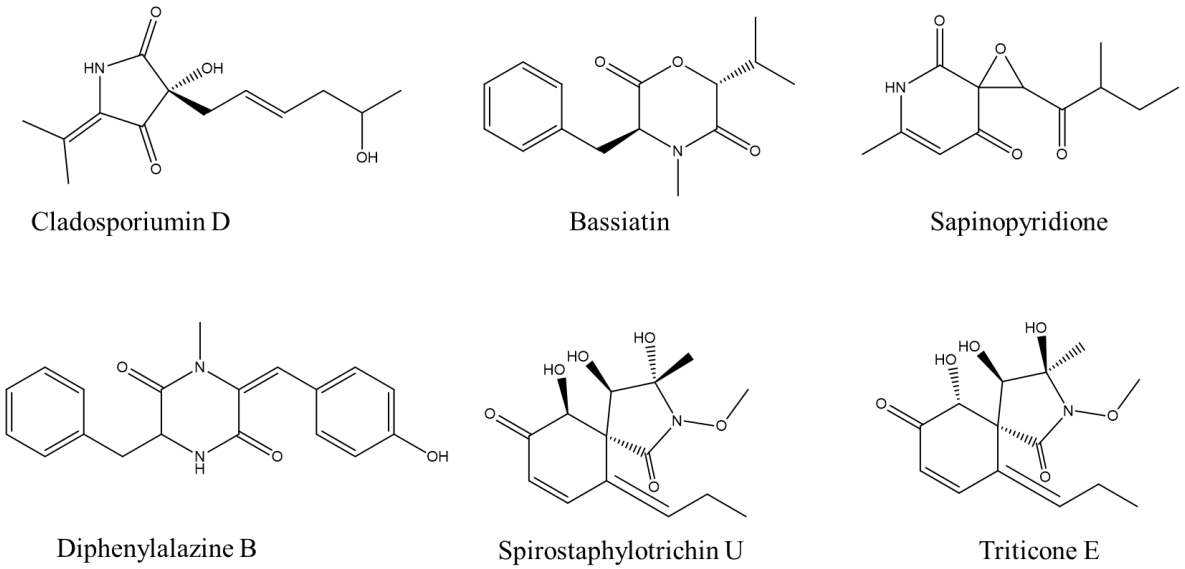

Figure 5.16. Chemical structure of some of the putatively identified compounds shown in Table 5.7

5.3 Discussions

5.3.1 Addition of thermally inactivated leishmanial parasites

Endophytic fungi have shown to naturally produce bioactive metabolites under standard laboratory culture conditions, representing an important resource of new drugs to combat antimicrobial resistance, including parasites (Hzounda Fokou *et al.* 2021) and bacteria (Deshmukh *et al.* 2014). Previously isolated TDKPs from *C. mamane* have shown a potent antileishmanial activity (unpublished data) and in order to induce their production and the production of other antiparasitic metabolites focusing on *Leishmania* parasites, we added heat-killed amastigotes of *Leishmania infantum* into the culture of *C. mamane*. It is important to mention that co-culture was not possible due to the very different culture conditions (culture media, temperature, oxygen levels, etc.) used for growing Leishmanial parasites and fungi. A preliminary work comparing the effects of heat-killed amastigotes versus promastigotes on *C. mamane* metabolism showed that the use of heat-killed amastigotes was more interesting in terms of production of TDKPs. Moreover, the difference observed between the addition of heat-killed promastigotes and amastigotes might be due to the expression of stage-specific molecules such as virulence factors expressed on the surface of the promastigotes of *Leishmania* species but minimally expressed in amastigotes forms, causing also different responses in the mammalian cells (Kima 2007).

In this study, the production of 12 metabolites were significantly influenced by the addition of heat-killed amastigotes of *L. infantum* at three different concentrations, with 7 of them showing an up-regulation, including flavipucine (and/or its isomers), while 5 metabolites showed a down-regulation, including a cyclic pentapeptide and a TDKP, botryosulfuranol C (**Table 5.2**). It has been described that during heat inactivation of cells, some cellular components might be exposed or solubilized, acting as inducers of antimicrobials compounds (Benitez *et al.* 2011; Liang *et al.* 2019). Specifically during wet heat inactivation, protein denaturation and membrane damage plays an important role (Smelt & Brul 2014). These exposed cellular components might have been recognized by *C. mamane*, triggering a response that induced the production of these 7 metabolites that included flavipucine (or isomers). Flavipucine has shown to be a cytotoxic compound, potent bactericide and strong antifungal (Loesgen *et al.* 2011; Kusakabe *et al.* 2019). This same metabolite was present in a fraction obtained from the crude extract of a *Botryosphaeria dothidea* strain, which exhibited cytoxicity but no antiplasmodial activity (Kumarihamy *et al.* 2020). In the case of the down-regulated cyclopentapeptide, similar molecules have been observed to be used as chemical communication molecules between neighboring endophytic fungi and bacteria, highlighting a possible ecological function of these molecules (Wang *et al.* 2015) besides their different biological activities (Wang *et al.* 2017).

Moreover, the decrease in the production of botryosulfuranol C under the addition of heat-killed amastigotes in comparison to the untreated culture of *C. mamane* suggests that its production might be influenced by the cellular components from the living *Leishmania* parasites (degraded by temperature) or that their presence at different concentrations somehow represses the biosynthetic pathway of the TDKPs. This is reflected in the bioactivity results obtained against *L. infantum*, where the EC_{50} values of the crude extracts of *C. mamane* cultivated with C1, C2 and C4 are higher (0.8 – 1.2 µg/mL) than the EC_{50} value of the crude extract of the untreated culture of *C. mamane* (0.4 µg/mL).

Furthermore, molecular networking allowed to identify a cluster containing two eicosanoids, which have been reported to possess putative signaling functions in fungi, related to quorum sensing processes especially in pathogenic fungi (Shea & Del Poeta 2006).

Although our results show the down-regulation of the TKDPs, meaning the contrary to what we expected, and that no other antileshmanial metabolites might have been produced, considering the weaker bioactivity observed for the extract of the *C. mamane* culture with the heat-killed parasites, we might consider the addition of living parasites in conditions that favor the growth of the fungus but not the parasite.

5.3.2 Co-culture with pathogenic bacteria

Our second strategy used to induce the production of antimicrobial compounds consisted in co-cultivation of *C. mamane* with living pathogenic bacteria. These co-cultures led to the detection of 126 metabolites in co-culture conditions (undetected in axenic conditions) as well as the significant up-regulation of a few metabolites produced by *C. mamane*. In natural environments, the coexistence of different endophytic strain communities can be explained by the maintenance of low population densities through the production of metabolites that inhibit microbial growth without generating damage to the host plant (Chagas & Pupo 2018).

Among the metabolites induced under co-culture conditions, the production of metabolite bassiatin could suggest that this metabolite could play a role in regulating *E. coli* density due to the low detection of this compound. The diketopiperazine, diphenylalazine B and two metabolites possessing the same chemical formula as botrysulfuranol A and C, were the most significantly up-regulated in comparison to the axenic culture of *C. mamane*. In a study, 9 known diketopiperazines that were lowly produced by *Penicillium* sp. under axenic conditions were induced under the co-culture with *Bacillus* sp. (Yu *et al.* 2017). Similarly, glionitrin B appeared to be produced by *Aspergillus fumigatus* as a minor diketopiperazine, whose production was dramatically increased during long-term co-culture with *Sphingomonas sp.* (Park *et al.* 2011). Despite the fact that TDKPs botryosulfuranols A, B, C and D did

not show significant variations in their production during co-culture with *E. coli*, *P. aeruginosa* and *S. aureus*, co-culture with other microorganisms might be an interesting and promising method in the context of the search for this chemical class of compounds.

Moreover, the production of a cyclopentapeptide, a metabolite that is probably involved in chemical communication between neighboring microorganisms as mentioned before, was up-regulated in *C. mamane* when co-cultured with *P. aeruginosa* and *S. aureus*. Along with this, a cyclotetrapeptide was previously obtained from the co-culture of two marine mangrove fungi, *Phomopsis* sp. and *Alternaria* sp., exhibiting moderate antifungal activities (Huang *et al.* 2014).

It has been described in the literature that the *quorum*-sensing mechanisms differ between gram-negative and gram-positive bacteria: the acyl-homoserin lactones are predominantly involved in the communication processes within the gram-negative bacteria while modified oligopeptides are mainly use by gram-positive bacteria (Verbeke *et al.* 2017). Therefore, this might explain the different metabolites significantly induced in *C. mamane* under co-culture with gram-negative bacteria, *E. coli* and *P. aeruginosa* or with gram-positive bacterium, *S. aureus*. These results set a depart for further experiments of co-culture between *C. mamane* and these 3 bacteria, taking also into consideration other culture parameters, such as time of incubation and microorganisms concentrations. In addition, the biological test for the extracts will be performed against these same pathogenic bacterial strains.

5.4 Conclusions

The culture of *C. mamane* in presence of heat-killed promastigotes of *Leishmania infantum* attenuated the production of the TDKPs by this fungus. The addition of heat-killed amastigotes at different concentrations did not induce their production either. We can hypothesize that this might be due to heat degradation of the cellular components of the amastigotes of *Leishmania*. Moreover, the down-regulation of botryosulfuranol C was reflected in the bioactivity test against the amastigotes of *L. infantum*. The crude extract of the untreated culture of *C. mamane* exhibited a lower EC_{50} value than the treated one, confirming that TDKPs are responsible of the antileishmanial activity of *C. mamane*.

Interestingly, cyclopentapeptides were down-regulated by heat-killed amastigotes of *L. infantum* but up-regulated in co-culture with *P. aeruginosa* and *S. aureus*, highlighting its possible role in chemical communication between neighboring living microorganisms.

Co-culture of *C. mamane* with pathogenic gram-negative bacterium, *E. coli*, also resulted in the up-regulation of diketopiperazines diphenylalazine B as also observed in other fungi-bacteria co-culture experiments. Similarly, the co-culture of *C. mamane* with *E. coli* led to the induction of bassiatin production, not detected under axenic conditions. Other parameters not analyzed in this study might have affected to the metabolites productions, such as the growing rate, development of the endophytic fungus or population density that induced specific metabolites.

Finally, the addition of heat-killed parasites or co-culture with living bacteria might results in the activation of other cryptic genes in *C. mamane* considering the potential of this endophytic fungi to produce bioactive compounds such as the TDKPs. Co-culture of *C. mamane* with heat-killed bacteria and the evaluation of antibacterial activity of the crude extracts will complement the results obtained with these experiments.

GENERAL DISCUSIONS, CONCLUSIONS AND PERSPECTIVES OF THE THESIS

This work focused on the study of the metabolome variations under different culture-based approaches of an endophytic fungal strain of *Cophinforma mamane* (Botryosphaeriaceaee), isolated from *Bixa orellana* (Bixaceae), a medicinal plant from Peru. This doctoral thesis is a work that continues the research carried out by Ph.D. Fatima Barakat and Ph.D. Asih Triastuti in the framework of their doctoral work, which allowed the study of the metabolome of this fungus (Triastuti *et al.* 2019, 2021) and led to the isolation of 4 antiparasitic compounds, botryosulfuranols A, B, C (Barakat *et al.* 2019) and D (Barakat 2018) (unpublished data).

Our main objectives were: 1) to achieve a better understanding about the production of the TDKP botryosulfuranols A-D and other DKPs and 2) to induce the production of anti-infective metabolites.

In order to carry out this work, different approaches were followed. A time-series study was performed to analysis the metabolome changes over time while the OSMAC approach was applied in order to observe the influence of the culture media and the presence of light on the global chemical profile of *C. mamane*. In an attempt to induce lowly-expressed of silenced genes, different chemical elicitors were added into the fungal culture, including 3 epigenetic modifiers that act at the chromosome level (histone proteins) and a *quorum*-sensing (QS) molecule (homoserin lactone). Moreover, to specifically stimulate the biosynthetic pathways of alkaloids, including the TDKPs botryosulfuranols A-D, the amino acids L-tryptophan and L-phenylalanine were added as biosynthetic precursors into the fungal culture. Finally, in the context of the search for new anti-infectives, *C. mamane* was co-cultured with 3 different pathogenic bacterial strains. Also, a methodology using heat-killed *Leishmania* parasites for culturing *C. mamane* was developed in order to induce the production of antileishmanial metabolites, including the TDKPs, botryosulfuranols A-D.

General modulation of the chemical diversity of *C. mamane*

The methodologies used allowed us to identify different chemical groups produced by *C. mamane* in mostly all the conditions such as diketopiperazines, cyclic peptides, long and medium-chain fatty acids, eicosanoids, followed by sphingolipids, terpenoids, quinones, coumarins, hydropyridines and benzenoids as the least frequent ones. Among the applied methodologies, the addition of epigenetic modifiers was the one that most altered the general metabolism of *C. mamane*, specifically the addition of 5-azacytidine (a DNA methyltransferase inhibitor) both in the up- and down-regulation of metabolites. Also, culturing *C. mamane* in ISP2 culture medium during 10 days under light conditions seemed to alter the general metabolism, both in the up-regulation and down-regulation of many metabolites, in comparison to the other methodologies used.

Besides the approaches regarding the variations of the culture media and culture conditions, the addition of dried host plant parts or crude extracts of the host plant to the culture medium of the endophytic fungi, may be another interesting method for simulating natural environment conditions that might trigger different biosynthetic pathways. Preliminary studies of the addition of crude extracts of *Bixa orella* and dried and ground leaves in the culture medium of *C. mamane* were carried out but they need to be further investigated, which will be also considered for future experiments.

One of the main results, focusing on putatively annotated metabolites, led us to the finding that this endophytic fungus produces a group of metabolites identified as cyclopentapeptides. These metabolites were observed, in most conditions, as the major peaks in the chemical chromatograms, appearing during an early stage (D4-D8) and decreasing rapidly after this period, as observed during the time-variations study. However, in a previous study of the dynamics in co-culture between *C. mamane* and *Fusarium solani*, the production of cyclopentapeptides by both fungi was maintained over time after 10 days of co-culture in MEA (Triastuti *et al.* 2021). Moreover, the cyclopentapeptides production was down-regulated under the presence of heat-killed *Leishmania* amastigotes but significantly induced under the presence of living bacteria, including *P. aeruginosa* and *S. aureus*. In previous studies, fungal cyclopentaptides have exhibited diverse biological activities against other fungi, bacteria, virus and parasites with potential applications (Wang *et al.* 2017). However, their ecological role have been less discussed and in this regard, some authors have suggested their role in interspecies communication, such as in the case of the cyclopentapeptides produced by the endophytic fungus *Fusarium decemcellulare* (Li *et al.* 2016) or the hexocyclopeptides produced by endophytic fungus *Fusarium solani* (Wang *et al.* 2015). The down-regulation of the cyclopentapeptides production in *C. mamane* under the presence of heat-killed parasites but their up-regulation under the presence of living bacteria, reinforces their potential role as communication molecules between different microbial species but further research is needed in order to understand the triggering mechanisms as it is known for bacterial *quorum*-sensing process.

Modulation of the production of TDKPs botryosulfuranols A-D

The methodologies applied in this doctoral thesis had also the objective to induce the production of 4 TDKPs, previously isolated from *C. mamane* (Barakat *et al.* 2019). One interesting result is the short-time frame production observed during the time-variations study for botryosulfuranol C, a TDKP that possesses a di-sulfur bridge on its structure that might play an important role on its biological activity (Jiang & Guo 2011; Barakat *et al.* 2019). It is suggested that the producer organism could activate defense mechanisms that involves the opening of the di-sulfur bridge to avoid its toxicity as observed for the biosynthesis of the DKP gliotoxin produced by *Aspergillus fumigatus* (Scharf *et al.* 2014) which might explain the short time-frame production of botryosulfuranol C observed in *C. mamane*. Regarding

botryosulfuranol D, which is one of the most active TDKPs in comparison to botryosulfuranols A-C, exhibited a low production under the different methodologies and that was mostly undetected, indicating a different production pattern with a crucial step on its biosynthetic pathway influenced by the culture conditions and other factors.

Moreover, culturing *C. mamane* in ISP2 during 6 days in dark conditions seemed to exert a delaying effect on TDKPs production during the OSMAC approach study. It is known that the coding genes of these type of compounds respond to different environmental signals including light (Brakhage 2013) while a large proportion of the fungal genome respond to different light intensities and wavelengths (Yu & Fischer 2019). This finding highlights that light can influence the production of these metabolites in *C. mamane* and that it is an important factor to consider when culturing in laboratory conditions and during large-scale fermentations in bioreactors at the industrial level. Further experiments involving different light wavelengths when culturing *C. mamane* will be considered.

Regarding the addition of chemical modulators, the DNMTi AZA down-regulated the production of botryosulfuranols A, B and C, indicating that the inhibition of the DNA methylation has a negative effect on their production, either directly or indirectly along their biosynthetic pathway. However, the addition of HSL, which is a QS molecule involved in the communication of gram-negative bacteria with other species, significantly induced the production of botryosulfuranol C. It is also important to mention that HSL not only significantly induced the production of this TDKP but also the production of other putatively identified DKPs, including diphenylalazine B and bisdethiobis(methylthio)gliotoxin, highlighting that these types of metabolites might be involved in interspecies communication. Their role as QS molecules was also suggested for the DKPs produced during bacterial interactions between *Cronobacter sakazakii* and *Bacillus cereus* (Bofinger *et al.* 2017) but also for the DKPs, emestrin A and B, produced by *Aspergillus fumigatus* in presence of HSL and during co-culture with *Streptomyces bulli* (Rateb *et al.* 2013). In addition to this, the addition of heat-killed parasites into *C. mamane* culture significantly down-regulated the production of botryosulfuranol C while the addition of living bacteria did not significantly affect its production under the tested conditions. Longer fermentation periods and other bacterial and fungal species will be performed for the co-culture experiments in order to verify the influence of living microorganism on TDKPs production, considering the results obtained under the addition of the QS molecule, HSL and their potential role in microbial communication.

Furthermore, contrary to what was expected with the addition of two DKPs bioprecursors, L-phe and L-trp, the production of botryosulfuranols A-D was down-regulated in comparison to the untreated culture, even though these metabolites are biogenetically derived from two phenylalanine residues (Barakat *et al.* 2019). More generally, the addition of these two amino acids did not seem to induce other DKPs derived from at least one phenylalanine, tyrosine or tryptophan (Welch & Williams 2014). Further investigations are needed in order to understand the negative effects that these amino acids exert on the

production of TDKPs while the addition of different amino acids at different concentrations will be also tested.

Induction of the production of anti-infective metabolites

The general alteration of the *C. mamane* metabolome observed under the addition of heat-killed parasites and the co-culture with living pathogenic bacteria seemed to significantly up- and down-regulate metabolites but no chemical family of metabolites could be identified to be specifically influenced under each condition. However, co-culturing fungus-fungus or fungus-bacterium has previously shown to induce metabolites that are not produced under axenic conditions or that are lowly detected (Kamdem *et al.* 2018) as a results of the diverse complex interactions regarding the competition for nutrients or antagonistic interactions in shared environments (Deshmukh *et al.* 2018). Different pathogenic bacterial strains with different resistant profiles as well as the co-culture with previously isolated endophytes from *Bixa orellana*, kept in the fungal collection of the UMR 152 laboratory, will be considered for future co-culture experiments.

Furthermore, we will contemplate the addition of living *Leishmania* parasites into the culture of *C. mamane* in order to evaluate the difference with heat-killed parasites, where mutual responses can potentially induce the production of anti-infective metabolites. The main limitations of this methodology will include the pH and the nutrients of the culture medium and the temperature and time of incubation, which will might need an appropriate culture chamber or a different dispositive to carry it out.

Moreover, metabolomics itself represents a strategy that facilitates and accelerates the laborious processes of natural product isolation and helps to avoid the re-isolation of known compounds by providing MS/MS information useful for structural elucidation and comparison with available databases (Demarque *et al.* 2020). However, it presents some limitations and challenges due to its inherent complexity, from samples preparation and data acquisition to reproducibility and interpretation issues (Marshall & Powers 2017). Furthermore, the absence of a consensus in structural data from different platforms and the low availability of free databases can generate low putative annotation rates (Van Santen *et al.* 2019), therefore, dereplication studies continue to be a very important part to complement this type of work. Despite of the limitations, metabolomics has unveiled information that otherwise would have remained hidden and this relatively novel approach used in the discovery of natural products has shown to effectively reduce large data sets into much smaller ones that potentially contain novel or active metabolites (Caesar *et al.* 2019). Different and better methodologies regarding the UHPL-HRMS analysis when considering specific metabolites as well as more replicates will be considered for future experiments with *C. mamane* and the metabolites produced by this this endophytic strain.

Conclusions

The results obtained under an untargeted metabolomics analysis provide us direct and useful information about what is being produced by cells during their metabolism, in this case, what *C. mamane* is producing at a specific time under a specific culture condition, giving us insights about its physiological status and cellular activity.

Integrating this information with other omics techniques such as genomics, proteomics and transcriptomics, which falls on the systems biology research field, will offer a more holistic understanding about microorganisms and even communities, especially for endophytic microorganism, representing at the same time an ongoing challenge (Pinu *et al.* 2019). In this sense, understanding the physiological responses of *C. mamane* to environmental changes and different culture conditions can lead to specific pathway activation or manipulation. This is useful for the search of specific metabolites, mainly to determine the optimal cultures conditions, including the optimal incubation time for their production and extraction, as is the case with the TDKPs.

In addition to this and besides the further experiments needed, the isolation of the most significant induced metabolites and the metabolites chemically related to the known TDKPs revealed by the molecular networking, will also be the focus of future work, as well as the understanding of their biological mechanisms and potential ecological roles in nature. Thanks to a pre-maturation project, financially supported by the Occitanie region, a highly concentrated TDKP fraction has been obtained as a result of a collaboration with Critt Bioindustries, who took over the cultivation of the fungus on a larger scale. This will allow further investigation for the *in vivo* biological activity of the TDKPs.

REFERENCES

Chapter 1

Abdel-Razek AS, El-Naggar ME, Allam A, Morsy OM, Othman SI, 2020. Microbial natural products in drug discovery. *Processes* **8**: 1–19. https://doi.org/10.3390/PR8040470

Abraham EP, Chain E, 1988. An enzyme from bacteria able to destroy penicillin. 1940. *Reviews of infectious diseases* **10**: 677–8.

Abro MA, Sun X, Li X, Jatoi GH, Guo L-D, 2019. Biocontrol Potential of Fungal Endophytes against Fusarium oxysporum f. sp. cucumerinum Causing Wilt in Cucumber. *The Plant Pathology Journal* **35**: 598–608. https://doi.org/10.5423/PPJ.OA.05.2019.0129

Adeleke B, Babalola O, 2021. Pharmacological Potential of Fungal Endophytes Associated with Medicinal Plants: A Review. *Journal of Fungi* **7**: 147. https://doi.org/10.3390/jof7020147

Alvin A, Miller KI, Neilan BA, 2014. Exploring the potential of endophytes from medicinal plants as sources of antimycobacterial compounds. *Microbiological Research* **169**: 483–495. https://doi.org/10.1016/j.micres.2013.12.009

Aly AH, Debbab A, Proksch P, 2013. Fungal endophytes - secret producers of bioactive plant metabolites. *Die Pharmazie* **68**: 499–505.

Aminov RI, 2009. The role of antibiotics and antibiotic resistance in nature. *Environmental Microbiology* **11**: 2970–2988. https://doi.org/10.1111/j.1462-2920.2009.01972.x

Aminov RI, 2010. A brief history of the antibiotic era: Lessons learned and challenges for the future. *Frontiers in Microbiology* **1**: 1–7. https://doi.org/10.3389/fmicb.2010.00134

Anand U, Jacobo-Herrera N, Altemimi A, Lakhssassi N, 2019. A Comprehensive Review on Medicinal Plants as Antimicrobial Therapeutics: Potential Avenues of Biocompatible Drug Discovery. *Metabolites* **9**: 258. https://doi.org/10.3390/metabo9110258

Ariantari NP, Daletos G, Mándi A, Kurtán T, Müller WEG, Lin W, Ancheeva E, Proksch P, 2019. Expanding the chemical diversity of an endophytic fungus Bulgaria inquinans , an ascomycete associated with mistletoe, through an OSMAC approach. *RSC Advances* **9**: 25119–25132. https://doi.org/10.1039/C9RA03678D

Arnold AE, 2007. Understanding the diversity of foliar endophytic fungi: progress, challenges, and frontiers. *Fungal Biology Reviews* **21**: 51–66. https://doi.org/10.1016/j.fbr.2007.05.003

Aron AT, Gentry EC, McPhail KL, Nothias LF, Nothias-Esposito M, Bouslimani A, Petras D, Gauglitz JM, Sikora N, Vargas F, van der Hooft JJJ, Ernst M, Kang K Bin, Aceves CM, Caraballo-Rodríguez AM, Koester I, Weldon KC, Bertrand S, Roullier C, Sun K, Tehan RM, Boya P CA, Christian MH, Gutiérrez M, Ulloa AM, Tejeda Mora JA, Mojica-Flores R, Lakey-Beitia J, Vásquez-Chaves V, Zhang Y, Calderón AI, Tayler N, Keyzers RA, Tugizimana F, Ndlovu N, Aksenov AA, Jarmusch AK, Schmid R, Truman AW, Bandeira N, Wang M,

Dorrestein PC, 2020. Reproducible molecular networking of untargeted mass spectrometry data using GNPS. *Nature Protocols* **15**: 1954–1991. https://doi.org/10.1038/s41596-020-0317-5

Asai T, Otsuki S, Sakurai H, Yamashita K, Ozeki T, Oshima Y, 2013. Benzophenones from an endophytic fungus, graphiopsis chlorocephala, from Paeonia lactiflora cultivated in the presence of an NAD+-dependent HDAC inhibitor. *Organic Letters* **15**: 2058–2061. https://doi.org/10.1021/ol400781b

Aslam B, Wang W, Arshad MI, Khurshid M, Muzammil S, Rasool MH, Nisar MA, Alvi RF, Aslam MA, Qamar MU, Salamat MKF, Baloch Z, 2018. Antibiotic resistance: a rundown of a global crisis. *Infection and drug resistance* **11**: 1645–1658. https://doi.org/10.2147/IDR.S173867

Aziz NH, Moussa LAE, 1997. Influence of white light, near-UV irradiation and other environmental conditions on production of aflatoxin B1 byAspergillus flavus and ochratoxin A byAspergillus ochraceus. *Food / Nahrung* **41**: 150–154. https://doi.org/10.1002/food.19970410307

Bamisile BS, Dash CK, Akutse KS, Keppanan R, Wang L, 2018. Fungal Endophytes: Beyond Herbivore Management. *Frontiers in Microbiology* **9**: 1–11. https://doi.org/10.3389/fmicb.2018.00544

Barakat F, Vansteelandt M, Triastuti A, Jargeat P, Jacquemin D, Graton J, Mejia K, Cabanillas B, Vendier L, Stigliani J-L, Haddad M, Fabre N, 2019. Thiodiketopiperazines with two spirocyclic centers extracted from Botryosphaeria mamane, an endophytic fungus isolated from Bixa orellana L. *Phytochemistry* **158**: 142–148. https://doi.org/10.1016/j.phytochem.2018.11.007

Barrett MP, 2018. The elimination of human African trypanosomiasis is in sight: Report from the third WHO stakeholders meeting on elimination of gambiense human African trypanosomiasis. *PLoS Neglected Tropical Diseases* **12**: 10–13. https://doi.org/10.1371/journal.pntd.0006925

Bayram Ö, Braus GH, 2012. Coordination of secondary metabolism and development in fungi: The velvet family of regulatory proteins. *FEMS Microbiology Reviews* **36**: 1–24. https://doi.org/10.1111/j.1574-6976.2011.00285.x

Bennett JW, Dunn JJ, Goldsman CL, 1981. Influence of white light on production of aflatoxins and anthraquinones in Aspergillus parasiticus. *Applied and Environmental Microbiology* **41**: 488–491. https://doi.org/10.1128/aem.41.2.488-491.1981

Bérdy J, 2012. Thoughts and facts about antibiotics: Where we are now and where we are heading. *Journal of Antibiotics* **65**: 385–395. https://doi.org/10.1038/ja.2012.27

Bertrand S, Azzollini A, Schumpp O, Bohni N, Schrenzel J, Monod M, Gindro K, Wolfender J, 2014. Multi-well fungal co-culture for de novo metabolite-induction in time-series studies based on untargeted metabolomics. *Mol. BioSyst.* **10**: 2289–2298. https://doi.org/10.1039/C4MB00223G

Bode HB, Bethe B, Höfs R, Zeeck A, 2002. Big Effects from Small Changes: Possible Ways to Explore Nature's Chemical Diversity. *ChemBioChem* **3**: 619. https://doi.org/10.1002/1439-7633(20020703)3:7<619::AID-CBIC619>3.0.CO;2-9

Borgman P, Lopez RD, Lane AL, 2019. The expanding spectrum of diketopiperazine natural product

biosynthetic pathways containing cyclodipeptide synthases. *Organic and Biomolecular Chemistry* **17**: 2305–2314. https://doi.org/10.1039/c8ob03063d

Borthwick AD, 2012. 2,5-diketopiperazines: Synthesis, reactions, medicinal chemistry, and bioactive natural products. *Chemical Reviews* **112**: 3641–3716. https://doi.org/10.1021/cr200398y

Boufridi A, Quinn RJ, 2018. Harnessing the Properties of Natural Products. *Annual Review of Pharmacology and Toxicology* **58**: 451–470. https://doi.org/10.1146/annurev-pharmtox-010716-105029

Brader G, Compant S, Mitter B, Trognitz F, Sessitsch A, 2014. Metabolic potential of endophytic bacteria. *Current Opinion in Biotechnology* **27**: 30–37. https://doi.org/10.1016/j.copbio.2013.09.012

Brakhage AA, 2013. Regulation of fungal secondary metabolism. *Nature Reviews Microbiology* **11**: 21–32. https://doi.org/10.1038/nrmicro2916

Brakhage AA, Schroeckh V, 2011. Fungal secondary metabolites – Strategies to activate silent gene clusters. *Fungal Genetics and Biology* **48**: 15–22. https://doi.org/10.1016/j.fgb.2010.04.004

Bräse S, Gläser F, Kramer C, Lindner S, Linsenmeier AM, Masters K-S, Meister AC, Ruff BM, Zhong S, 2013. The Chemistry of Mycotoxins. In: *The chemistry of mycotoxins*. Progress in the Chemistry of Organic Natural Products. Springer Vienna, Vienna, pp. 91–108.

Browne K, Chakraborty S, Chen R, Willcox MDP, Black DS, Walsh WR, Kumar N, 2020. A new era of antibiotics: The clinical potential of antimicrobial peptides. *International Journal of Molecular Sciences* **21**: 1–23. https://doi.org/10.3390/ijms21197047

Burgess TI, Tan YP, Garnas J, Edwards J, Scarlett KA, Shuttleworth LA, Daniel R, Dann EK, Parkinson LE, Dinh Q, Shivas RG, Jami F, 2019. Current status of the Botryosphaeriaceae in Australia. *Australasian Plant Pathology* **48**: 35–44. https://doi.org/10.1007/s13313-018-0577-5

Burza S, Croft SL, Boelaert M, 2018. Leishmaniasis. *The Lancet* **392**: 951–970. https://doi.org/10.1016/S0140-6736(18)31204-2

Bussmann RW, 2013. The Globalization of Traditional Medicine in Northern Peru: From Shamanism to Molecules. *Evidence-Based Complementary and Alternative Medicine* **2013**: 1–46. https://doi.org/10.1155/2013/291903

Cabezas Gómez O, Hortolan Luiz JH, 2018. Endophytic fungi isolated from medicinal plants: future prospects of bioactive natural products from Tabebuia/Handroanthus endophytes. *Applied Microbiology and Biotechnology* **102**: 9105–9119. https://doi.org/10.1007/s00253-018-9344-3

Calvo AM, Wilson RA, Bok JW, Keller NP, 2002. Relationship between Secondary Metabolism and Fungal Development. *Microbiology and Molecular Biology Reviews* **66**: 447–459. https://doi.org/10.1128/MMBR.66.3.447-459.2002

Capela R, Moreira R, Lopes F, 2019. An overview of drug resistance in protozoal diseases. *International Journal of Molecular Sciences* **20**. https://doi.org/10.3390/ijms20225748

Chagas FO, Pupo MT, 2018. Chemical interaction of endophytic fungi and actinobacteria from

Lychnophora ericoides in co-cultures. *Microbiological Research* **212**–**213**: 10–16. https://doi.org/10.1016/j.micres.2018.04.005

Chain E, Florey HW, Gardner AD, Heatley NG, Jennings MA, Orr-Ewing J, Sanders AG, Peltier LF, 2005. The Classic: Penicillin as a Chemotherapeutic Agent. *Clinical Orthopaedics and Related Research* **439**: 23–26. https://doi.org/10.1097/01.blo.0000183429.83168.07

Chait R, Vetsigian K, Kishony R, 2012. What counters antibiotic resistance in nature? *Nature Chemical Biology* **8**: 2–5. https://doi.org/10.1038/nchembio.745

Challinor VL, Bode HB, 2015. Bioactive natural products from novel microbial sources. *Annals of the New York Academy of Sciences* **1354**: 82–97. https://doi.org/10.1111/nyas.12954

Chen Y-X, Xu M-Y, Li H-J, Zeng K-J, Ma W-Z, Tian G-B, Xu J, Yang D-P, Lan W-J, 2017. Diverse Secondary Metabolites from the Marine-Derived Fungus Dichotomomyces cejpii F31-1. *Marine Drugs* **15**: 339. https://doi.org/10.3390/md15110339

Chevillard C, Nunes JPS, Frade AF, Almeida RR, Pandey RP, Nascimento MS, Kalil J, Cunha-Neto E, 2018. Disease Tolerance and Pathogen Resistance Genes May Underlie Trypanosoma cruzi Persistence and Differential Progression to Chagas Disease Cardiomyopathy. *Frontiers in Immunology* **9**. https://doi.org/10.3389/fimmu.2018.02791

Choi JN, Kim J, Lee MY, Park DK, Hong YS, Lee CH, 2010. Metabolomics revealed novel isoflavones and optimal cultivation time of cordyceps militaris fermentation. *Journal of Agricultural and Food Chemistry* **58**: 4258–4267. https://doi.org/10.1021/jf903822e

Cichewicz RH, 2010. Epigenome manipulation as a pathway to new natural product scaffolds and their congeners. *Nat. Prod. Rep.* **27**: 11–22. https://doi.org/10.1039/B920860G

Cole R, Schweikert M, Jarvis B, 2003. Handbook of Secondary Fungal Metabolites. In: *Handbook of Secondary Fungal Metabolites*. Elsevier, p. iii.

Collemare J, Seidl MF, 2019. Chromatin-dependent regulation of secondary metabolite biosynthesis in fungi: Is the picture complete? *FEMS Microbiology Reviews* **43**: 591–607. https://doi.org/10.1093/femsre/fuz018

Combès A, Ndoye I, Bance C, Bruzaud J, Djediat C, Dupont J, Nay B, Prado S, 2012. Chemical Communication between the Endophytic Fungus Paraconiothyrium Variabile and the Phytopathogen Fusarium oxysporum (V Chaturvedi, Ed,). *PLoS ONE* **7**: e47313. https://doi.org/10.1371/journal.pone.0047313

Cordero RJB, Casadevall A, 2017. Functions of fungal melanin beyond virulence. *Fungal Biology Reviews* **31**: 99–112. https://doi.org/10.1016/j.fbr.2016.12.003

Cui CM, Li XM, Li CS, Proksch P, Wang BG, 2010. Cytoglobosins A-G, cytochalasans from a marine-derived endophytic Fungus, chaetomium globosum QEN-14. *Journal of Natural Products* **73**: 729–733. https://doi.org/10.1021/np900569t

Dalmais B, Schumacher J, Moraga J, Le Pêcheur P, Tudzynski B, Collado IG, Viaud M, 2011. The Botrytis cinerea phytotoxin botcinic acid requires two polyketide synthases for production and

has a redundant role in virulence with botrydial. *Molecular Plant Pathology* **12**: 564–579. https://doi.org/10.1111/j.1364-3703.2010.00692.x

Davies J, Davies D, 2010. Origins and Evolution of Antibiotic Resistance. *Microbiology and Molecular Biology Reviews* **74**: 417–433. https://doi.org/10.1128/MMBR.00016-10

Deeks ED, 2019. Fexinidazole: First Global Approval. *Drugs* **79**: 215–220. https://doi.org/10.1007/s40265-019-1051-6

Demain AL, 2014. Importance of microbial natural products and the need to revitalize their discovery. *Journal of Industrial Microbiology and Biotechnology* **41**: 185–201. https://doi.org/10.1007/s10295-013-1325-z

Demarque DP, Dusi RG, de Sousa FDM, Grossi SM, Silvério MRS, Lopes NP, Espindola LS, 2020. Mass spectrometry-based metabolomics approach in the isolation of bioactive natural products. *Scientific Reports* **10**: 1–9. https://doi.org/10.1038/s41598-020-58046-y

Deshmukh S, Gupta M, Prakash V, Saxena S, 2018. Endophytic Fungi: A Source of Potential Antifungal Compounds. *Journal of Fungi* **4**: 77. https://doi.org/10.3390/jof4030077

Dev S, 1999. Ancient-modern concordance in Ayurvedic plants: some examples. *Environmental Health Perspectives* **107**: 783–789. https://doi.org/10.1289/ehp.99107783

Dias DA, Urban S, Roessner U, 2012. A Historical overview of natural products in drug discovery. *Metabolites* **2**: 303–336. https://doi.org/10.3390/metabo2020303

Domagk G, 1935. Chemotherapie der bakteriellen Infektionen. *Angewandte Chemie* **48**: 657–667. https://doi.org/10.1002/ange.19350484202

Domingo-Almenara X, Siuzdak G, 2020. Metabolomics Data Processing Using XCMS. In: pp. 11–24.

Ehrlich P, Hata S, 1910. *Die experimentelle Chemotherapie der Spirillosen*. Springer Berlin Heidelberg, Berlin, Heidelberg.

Emmerich R, Löw O, 1899. Bakteriolytische Enzyme als Ursache der erworbenen Immunität und die Heilung von Infectionskrankheiten durch dieselben. *Zeitschrift für Hygiene und Infectionskrankheiten* **31**: 1–65. https://doi.org/10.1007/BF02206499

Faddetta T, Abbate L, Alibrandi P, Arancio W, Siino D, Strati F, De Filippo C, Fatta Del Bosco S, Carimi F, Puglia AM, Cardinale M, Gallo G, Mercati F, 2021. The endophytic microbiota of Citrus limon is transmitted from seed to shoot highlighting differences of bacterial and fungal community structures. *Scientific Reports* **11**: 7078. https://doi.org/10.1038/s41598-021-86399-5

Fadiji AE, Babalola OO, 2020. Exploring the potentialities of beneficial endophytes for improved plant growth. *Saudi Journal of Biological Sciences* **27**: 3622–3633. https://doi.org/10.1016/j.sjbs.2020.08.002

Fan B, Parrot D, Blümel M, Labes A, Tasdemir D, 2019. Influence of OSMAC-Based Cultivation in Metabolome and Anticancer Activity of Fungi Associated with the Brown Alga Fucus vesiculosus. *Marine Drugs* **17**: 67. https://doi.org/10.3390/md17010067

Ferreira JM, Sousa DF, Dantas MB, Fonseca SGC, Menezes DB, Martins AMC, De Queiroz MGR,

2013. Effects of Bixa orellana L. seeds on hyperlipidemia. *Phytotherapy Research* **27**: 144–147. https://doi.org/10.1002/ptr.4675

Ferreira MC, Vieira M de LA, Zani CL, Alves TM de A, Junior PAS, Murta SMF, Romanha AJ, Gil LHVG, Carvalho AG de O, Zilli JE, Vital MJS, Rosa CA, Rosa LH, 2015. Molecular phylogeny, diversity, symbiosis and discover of bioactive compounds of endophytic fungi associated with the medicinal Amazonian plant Carapa guianensis Aublet (Meliaceae). *Biochemical Systematics and Ecology* **59**: 36–44. https://doi.org/10.1016/j.bse.2014.12.017

Fleming A, 1929. On the Antibacterial Action of Cultures of a Penicillium, with Special Reference to their Use in the Isolation of B. influenzæ. *British journal of experimental pathology* **10**: 226–236.

Fouda AH, Hassan SED, Eid AM, Ewais EED, 2015. Biotechnological applications of fungal endophytes associated with medicinal plant Asclepias sinaica (Bioss.). *Annals of Agricultural Sciences* **60**: 95–104. https://doi.org/10.1016/j.aoas.2015.04.001

Fraisier-Vannier O, Chervin J, Cabanac G, Puech V, Fournier S, Durand V, Amiel A, André O, Benamar OA, Dumas B, Tsugawa H, Marti G, 2020. MS-CleanR: A Feature-Filtering Workflow for Untargeted LC–MS Based Metabolomics. *Analytical Chemistry* **92**: 9971–9981. https://doi.org/10.1021/acs.analchem.0c01594

Gao H, Li G, Lou H-X, 2018. Structural Diversity and Biological Activities of Novel Secondary Metabolites from Endophytes. *Molecules* **23**: 646. https://doi.org/10.3390/molecules23030646

Garcia JF, Lawrence DP, Morales-Cruz A, Travadon R, Minio A, Hernandez-Martinez R, Rolshausen PE, Baumgartner K, Cantu D, 2021. Phylogenomics of Plant-Associated Botryosphaeriaceae Species. *Frontiers in Microbiology* **12**: 1–18. https://doi.org/10.3389/fmicb.2021.652802

García M, Monzote L, Montalvo AM, Scull R, 2011. Effect of Bixa orellana against Leishmania amazonensis. *Forschende Komplementarmedizin* **18**: 351–353. https://doi.org/10.1159/000335280

Gardner DE, 1997. Botryosphaeria mamane sp. nov. associated with witches'-brooms on the endemic forest tree Sophora chrysophylla in Hawaii. *Mycologia* **89**: 298–303. https://doi.org/10.1080/00275514.1997.12026785

Genilloud O, 2014. The re-emerging role of microbial natural products in antibiotic discovery. *Antonie van Leeuwenhoek, International Journal of General and Molecular Microbiology* **106**: 173–188. https://doi.org/10.1007/s10482-014-0204-6

Giorgi A, De Marinis P, Granelli G, Chiesa LM, Panseri S, 2013. Secondary metabolite profile, antioxidant capacity, and mosquito repellent activity of Bixa orellana from Brazilian Amazon region. *Journal of Chemistry* **2013**. https://doi.org/10.1155/2013/409826

Gouda S, Das G, Sen SK, Shin HS, Patra JK, 2016. Endophytes: A treasure house of bioactive compounds of medicinal importance. *Frontiers in Microbiology* **7**: 1–8. https://doi.org/10.3389/fmicb.2016.01538

Grandclément C, Tannières M, Moréra S, Dessaux Y, Faure D, 2015. Quorum quenching: Role in

nature and applied developments. *FEMS Microbiology Reviews* **40**: 86–116. https://doi.org/10.1093/femsre/fuv038

Guo Y-W, Liu X-J, Yuan J, Li H-J, Mahmud T, Hong M-J, Yu J-C, Lan W-J, 2020. L -Tryptophan Induces a Marine-Derived Fusarium sp. to Produce Indole Alkaloids with Activity against the Zika Virus. *Journal of Natural Products* **83**: 3372–3380. https://doi.org/10.1021/acs.jnatprod.0c00717

Gupta S, Chaturvedi P, Kulkarni MG, Van Staden J, 2020a. A critical review on exploiting the pharmaceutical potential of plant endophytic fungi. *Biotechnology Advances* **39**: 107462. https://doi.org/10.1016/j.biotechadv.2019.107462

Gupta S, Kulkarni MG, White JF, Van Staden J, 2020b. Epigenetic-based developments in the field of plant endophytic fungi. *South African Journal of Botany* **134**: 394–400. https://doi.org/10.1016/j.sajb.2020.07.019

Hamayun M, Afzal Khan S, Ahmad N, Tang DS, Kang SM, Na CI, Sohn EY, Hwang YH, Shin DH, Lee BH, Kim JG, Lee IJ, 2009. Cladosporium sphaerospermum as a new plant growth-promoting endophyte from the roots of Glycine max (L.) Merr. *World Journal of Microbiology and Biotechnology* **25**: 627–632. https://doi.org/10.1007/s11274-009-9982-9

Harrison JG, Griffin EA, 2020. The diversity and distribution of endophytes across biomes, plant phylogeny and host tissues: how far have we come and where do we go from here? *Environmental Microbiology* **22**: 2107–2123. https://doi.org/10.1111/1462-2920.14968

Harvey AL, Edrada-Ebel R, Quinn RJ, 2015. The re-emergence of natural products for drug discovery in the genomics era. *Nature Reviews Drug Discovery* **14**: 111–129. https://doi.org/10.1038/nrd4510

Hert J, Irwin JJ, Laggner C, Keiser MJ, Shoichet BK, 2009. Quantifying biogenic bias in screening libraries. *Nature Chemical Biology* **5**: 479–483. https://doi.org/10.1038/nchembio.180

Higginbotham SJ, Arnold AE, Ibañez A, Spadafora C, Coley PD, Kursar TA, 2013. Bioactivity of Fungal Endophytes as a Function of Endophyte Taxonomy and the Taxonomy and Distribution of Their Host Plants (JE Stajich, Ed,). *PLoS ONE* **8**: e73192. https://doi.org/10.1371/journal.pone.0073192

Homer CM, Summers DK, Goranov AI, Clarke SC, Wiesner DL, Diedrich JK, Moresco JJ, Toffaletti D, Upadhya R, Caradonna I, Petnic S, Pessino V, Cuomo CA, Lodge JK, Perfect J, Yates JR, Nielsen K, Craik CS, Madhani HD, 2016. Intracellular Action of a Secreted Peptide Required for Fungal Virulence. *Cell Host and Microbe* **19**: 849–864. https://doi.org/10.1016/j.chom.2016.05.001

Hopwood DA, 2007. How do antibiotic-producing bacteria ensure their self-resistance before antibiotic biosynthesis incapacitates them? *Molecular Microbiology* **63**: 937–940. https://doi.org/10.1111/j.1365-2958.2006.05584.x

Huang WY, Cai YZ, Hyde KD, Corke H, Sun M, 2007. Endophytic fungi from Nerium oleander L

(Apocynaceae): Main constituents and antioxidant activity. *World Journal of Microbiology and Biotechnology* **23**: 1253–1263. https://doi.org/10.1007/s11274-007-9357-z

Huang L-H, Xu M-Y, Li H-J, Li J-Q, Chen Y-X, Ma W-Z, Li Y-P, Xu J, Yang D-P, Lan W-J, 2017. Amino Acid-Directed Strategy for Inducing the Marine-Derived Fungus Scedosporium apiospermum F41–1 to Maximize Alkaloid Diversity. *Organic Letters* **19**: 4888–4891. https://doi.org/10.1021/acs.orglett.7b02238

Hutchings MI, Truman AW, Wilkinson B, 2019. Antibiotics: past, present and future. *Current Opinion in Microbiology* **51**: 72–80. https://doi.org/10.1016/j.mib.2019.10.008

Isaka M, Jaturapat A, Rukseree K, Danwisetkanjana K, Tanticharoen M, Thebtaranonth Y, 2001. Phomoxanthones A and B, Novel Xanthone Dimers from the Endophytic Fungus Phomopsis Species. *Journal of Natural Products* **64**: 1015–1018. https://doi.org/10.1021/np010006h

Jasim B, Sahadevan N, Chithra S, Mathew J, Radhakrishnan EK, 2019. Epigenetic Modifier Based Enhancement of Piperine Production in Endophytic Diaporthe sp. PF20. *Proceedings of the National Academy of Sciences India Section B - Biological Sciences* **89**: 671–677. https://doi.org/10.1007/s40011-018-0982-0

Jia M, Chen L, Xin H-L, Zheng C-J, Rahman K, Han T, Qin L-P, 2016. A Friendly Relationship between Endophytic Fungi and Medicinal Plants: A Systematic Review. *Frontiers in Microbiology* **7**: 1–14. https://doi.org/10.3389/fmicb.2016.00906

Joffe AZ, Lisker N, 1969. Effects of light, temperature, and pH value on aflatoxin production in vitro. *Applied microbiology* **18**: 517–8. https://doi.org/10.1128/am.18.3.517-518.1969

Johnson AP, 2011. Methicillin-resistant Staphylococcus aureus: the European landscape. *Journal of Antimicrobial Chemotherapy* **66**: iv43–iv48. https://doi.org/10.1093/jac/dkr076

Kannan K, 2017. Investigation of Endophytic Fungi Associated with Bixa orellana L., a Medicinal Plant Collected from Western Ghats of Sathyamangalam - A First Report. *Journal of Bacteriology & Mycology: Open Access* **5**: 381–385. https://doi.org/10.15406/jbmoa.2017.05.00150

Kellenberger E, Hofmann A, Quinn RJ, 2011. Similar interactions of natural products with biosynthetic enzymes and therapeutic targets could explain why nature produces such a large proportion of existing drugs. *Natural Product Reports* **28**: 1483. https://doi.org/10.1039/c1np00026h

Keller NP, 2019. Fungal secondary metabolism: regulation, function and drug discovery. *Nature Reviews Microbiology* **17**: 167–180. https://doi.org/10.1038/s41579-018-0121-1

Keller NP, Hohn TM, 1997. Metabolic Pathway Gene Clusters in Filamentous Fungi. *Fungal Genetics and Biology* **21**: 17–29. https://doi.org/10.1006/fgbi.1997.0970

Keller NP, Turner G, Bennett JW, 2005. Fungal secondary metabolism - From biochemistry to genomics. *Nature Reviews Microbiology* **3**: 937–947. https://doi.org/10.1038/nrmicro1286

Khan RA, 2018. Natural products chemistry: The emerging trends and prospective goals. *Saudi*

Pharmaceutical Journal **26**: 739–753. https://doi.org/10.1016/j.jsps.2018.02.015

Khare E, Mishra J, Arora NK, 2018. Multifaceted Interactions Between Endophytes and Plant: Developments and Prospects. *Frontiers in Microbiology* **9**. https://doi.org/10.3389/fmicb.2018.02732

King JR, Edgar S, Qiao K, Stephanopoulos G, 2016. Accessing Nature ' s diversity through metabolic engineering and synthetic biology [version 1 ; referees : 2 approved] Referee Status : *F1000Research* **5**: 1–11.

Kjer J, Wray V, Edrada-Ebel RA, Ebel R, Pretsch A, Lin W, Proksch P, 2009. Xanalteric acids I and II and related phenolic compounds from an endophytic Alternaria sp. isolated from the Mangrove plant Sonneratia alba. *Journal of Natural Products* **72**: 2053–2057. https://doi.org/10.1021/np900417g

Knight V, Sanglier JJ, DiTullio D, Braccili S, Bonner P, Waters J, Hughes D, Zhang L, 2003. Diversifying microbial natural products for drug discovery. *Applied Microbiology and Biotechnology* **62**: 446–458. https://doi.org/10.1007/s00253-003-1381-9

Kouipou Toghueo RM, Boyom FF, 2019. Endophytes from ethno-pharmacological plants: Sources of novel antioxidants- A systematic review. *Biocatalysis and Agricultural Biotechnology* **22**: 101430. https://doi.org/10.1016/j.bcab.2019.101430

Kumar CG, 2020. Bioprospecting for secondary metabolites of family Botryosphaeriaceae from a biotechnological perspective. In: *New and Future Developments in Microbial Biotechnology and Bioengineering*. Elsevier, pp. 167–286.

Lan W-J, Wang K-T, Xu M-Y, Zhang J-J, Lam C-K, Zhong G-H, Xu J, Yang D-P, Li H-J, Wang L-Y, 2016. Secondary metabolites with chemical diversity from the marine-derived fungus Pseudallescheria boydii F19-1 and their cytotoxic activity. *RSC Advances* **6**: 76206–76213. https://doi.org/10.1039/C6RA06661E

Lenta BN, Ngatchou J, Frese M, Ladoh-Yemeda F, Voundi S, Nardella F, Michalek C, Wibberg D, Ngouela S, Tsamo E, Kaiser M, Kalinowski J, Sewald N, 2016. Purpureone, an antileishmanial ergochrome from the endophytic fungus Purpureocillium lilacinum. *Zeitschrift für Naturforschung B* **71**: 1159–1167. https://doi.org/10.1515/znb-2016-0128

Li E, Jiang L, Guo L, Zhang H, Che Y, 2008. Pestalachlorides A-C, antifungal metabolites from the plant endophytic fungus Pestalotiopsis adusta. *Bioorganic and Medicinal Chemistry* **16**: 7894–7899. https://doi.org/10.1016/j.bmc.2008.07.075

Li X, Tian Y, Yang SX, Zhang YM, Qin JC, 2013. Cytotoxic azaphilone alkaloids from Chaetomium globosum TY1. *Bioorganic and Medicinal Chemistry Letters* **23**: 2945–2947. https://doi.org/10.1016/j.bmcl.2013.03.044

Li SJ, Zhang X, Wang XH, Zhao CQ, 2018. Novel natural compounds from endophytic fungi with anticancer activity. *European Journal of Medicinal Chemistry* **156**: 316–343. https://doi.org/10.1016/j.ejmech.2018.07.015

Lima Viana J, Zagmignan A, Lima Lobato LF, Gomes Abreu A, Da Silva LCN, De Sá JC, Monteiro CDA, Lago JHG, Gonçalves LM, Carvalho RC, Neto LGL, De Sousa EM, 2018. Hydroalcoholic Extract and Ethyl Acetate Fraction of Bixa orellana Leaves Decrease the Inflammatory Response to Mycobacterium abscessus Subsp. massiliense. *Evidence-based Complementary and Alternative Medicine* **2018**. https://doi.org/10.1155/2018/6091934

Liu H, Chen S, Liu W, Liu Y, Huang X, She Z, 2016. Polyketides with immunosuppressive activities from mangrove endophytic fungus penicillium sp. ZJ-SY2. *Marine Drugs* **14**: 1–7. https://doi.org/10.3390/md14120217

Liu SS, Jiang JX, Huang R, Wang YT, Jiang BG, Zheng KX, Wu SH, 2019. A new antiviral 14-nordrimane sesquiterpenoid from an endophytic fungus Phoma sp. *Phytochemistry Letters* **29**: 75–78. https://doi.org/10.1016/j.phytol.2018.11.005

Liu JK, Phookamsak R, Doilom M, Wikee S, Li YM, Ariyawansha H, Boonmee S, Chomnunti P, Dai DQ, Bhat JD, Romero AI, Zhuang WY, Monkai J, Jones EBG, Chukeatirote E, Ko Ko TW, Zhao YC, Wang Y, Hyde KD, 2012. Towards a natural classification of Botryosphaeriales. *Fungal Diversity* **57**: 149–210. https://doi.org/10.1007/s13225-012-0207-4

Macheleidt J, Mattern DJ, Fischer J, Netzker T, Weber J, Schroeckh V, Valiante V, Brakhage AA, 2016. Regulation and Role of Fungal Secondary Metabolites. *Annual Review of Genetics* **50**: 371–392. https://doi.org/10.1146/annurev-genet-120215-035203

Manganyi MC, Ateba CN, 2020. Untapped potentials of endophytic fungi: A review of novel bioactive compounds with biological applications. *Microorganisms* **8**: 1–25. https://doi.org/10.3390/microorganisms8121934

Manias D, Verma A, Soni DK, 2020. Isolation and characterization of endophytes: Biochemical and molecular approach. In: *Microbial Endophytes*. Elsevier, pp. 1–14.

Marmann A, Aly AH, Lin W, Wang B, Proksch P, 2014. Co-cultivation - A powerful emerging tool for enhancing the chemical diversity of microorganisms. *Marine Drugs* **12**: 1043–1065. https://doi.org/10.3390/md12021043

Martinez-Klimova E, Rodríguez-Peña K, Sánchez S, 2017. Endophytes as sources of antibiotics. *Biochemical Pharmacology* **134**: 1–17. https://doi.org/10.1016/j.bcp.2016.10.010

Mohali SR, Slippers B, Wingfield MJ, 2007. Identification of Botryosphaeriaceae from Eucalyptus, Acacia and Pinus in Venezuela. *Fungal Diversity* **25**: 103–125.

Molinski TF, 2014. All Natural: The Renaissance of Natural Products Chemistry. *The Journal of Organic Chemistry* **79**: 6765–6765. https://doi.org/10.1021/jo501288m

Nalini MS, Prakash HS, 2017. Diversity and bioprospecting of actinomycete endophytes from the medicinal plants. *Letters in Applied Microbiology* **64**: 261–270. https://doi.org/10.1111/lam.12718

Nazar Pour F, Ferreira V, Félix C, Serôdio J, Alves A, Duarte AS, Esteves AC, 2020. Effect of temperature on the phytotoxicity and cytotoxicity of Botryosphaeriaceae fungi. *Fungal Biology*

124: 571–578. https://doi.org/10.1016/j.funbio.2020.02.012

Nelson ML, Dinardo A, Hochberg J, Armelagos GJ, 2010. Brief communication: Mass spectroscopic characterization of tetracycline in the skeletal remains of an ancient population from Sudanese Nubia 350-550 CE. *American Journal of Physical Anthropology* **143**: 151–154. https://doi.org/10.1002/ajpa.21340

Newman DJ, Cragg GM, 2020. Natural Products as Sources of New Drugs over the Nearly Four Decades from 01/1981 to 09/2019. *Journal of Natural Products* **83**: 770–803. https://doi.org/10.1021/acs.jnatprod.9b01285

Newman DJ, Cragg GM, Snader KM, 2000. The influence of natural products upon drug discovery. *Natural Product Reports* **17**: 215–234. https://doi.org/10.1039/a902202c

Nisa H, Kamili AN, Nawchoo IA, Shafi S, Shameem N, Bandh SA, 2015. Fungal endophytes as prolific source of phytochemicals and other bioactive natural products: A review. *Microbial Pathogenesis* **82**: 50–59. https://doi.org/10.1016/j.micpath.2015.04.001

Niu S, Liu D, Shao Z, Proksch P, Lin W, 2017. Eutypellazines N−S, new thiodiketopiperazines from a deep sea sediment derived fungus Eutypella sp. with anti-VRE activities. *Tetrahedron Letters* **58**: 3695–3699. https://doi.org/10.1016/j.tetlet.2017.08.015

Ntie-Kang F, Svozil D, 2020. An enumeration of natural products from microbial, marine and terrestrial sources. *Physical Sciences Reviews* **5**. https://doi.org/10.1515/psr-2018-0121

Okada BK, Seyedsayamdost MR, 2017. Antibiotic dialogues: induction of silent biosynthetic gene clusters by exogenous small molecules (A Shen, Ed,). *FEMS Microbiology Reviews* **41**: 19–33. https://doi.org/10.1093/femsre/fuw035

Ola ARB, Thomy D, Lai D, Brötz-Oesterhelt H, Proksch P, 2013. Inducing Secondary Metabolite Production by the Endophytic Fungus Fusarium tricinctum through Coculture with Bacillus subtilis. *Journal of Natural Products* **76**: 2094–2099. https://doi.org/10.1021/np400589h

Oliveira FC, Barbosa FG, Mafezoli J, Oliveira MCF, Camelo ALM, Longhinotti E, Lima ACA, Câmara MPS, Gonçalves FJT, Freire FCO, 2015. Volatile organic compounds from filamentous fungi: A chemotaxonomic tool of the Botryosphaeriaceae family. *Journal of the Brazilian Chemical Society* **26**: 2189–2194. https://doi.org/10.5935/0103-5053.20150204

Olivon F, Elie N, Grelier G, Roussi F, Litaudon M, Touboul D, 2018. MetGem Software for the Generation of Molecular Networks Based on the t-SNE Algorithm. *Analytical Chemistry* **90**: 13900–13908. https://doi.org/10.1021/acs.analchem.8b03099

Ortega HE, Torres-Mendoza D, Cubilla-Rios L, 2020. Patents on endophytic fungi for agriculture and bio-and phytoremediation applications. *Microorganisms* **8**: 1–26. https://doi.org/10.3390/microorganisms8081237

Pan R, Bai X, Chen J, Zhang H, Wang H, 2019. Exploring Structural Diversity of Microbe Secondary Metabolites Using OSMAC Strategy: A Literature Review. *Frontiers in Microbiology* **10**: 1–20. https://doi.org/10.3389/fmicb.2019.00294

Peters S, Janssen H-G, Vivó-Truyols G, 2010. Trend analysis of time-series data: A novel method for untargeted metabolite discovery. *Analytica Chimica Acta* **663**: 98–104. https://doi.org/10.1016/j.aca.2010.01.038

Petrovska B, 2012. Historical review of medicinal plants′ usage. *Pharmacognosy Reviews* **6**: 1. https://doi.org/10.4103/0973-7847.95849

Pettit RK, 2011. Small-molecule elicitation of microbial secondary metabolites. *Microbial Biotechnology* **4**: 471–478. https://doi.org/10.1111/j.1751-7915.2010.00196.x

Pham J V., Yilma MA, Feliz A, Majid MT, Maffetone N, Walker JR, Kim E, Cho HJ, Reynolds JM, Song MC, Park SR, Yoon YJ, 2019. A review of the microbial production of bioactive natural products and biologics. *Frontiers in Microbiology* **10**: 1–27. https://doi.org/10.3389/fmicb.2019.01404

Phillips AJL, Alves A, Abdollahzadeh J, Slippers B, Wingfield MJ, Groenewald JZ, Crous PW, 2013. The Botryosphaeriaceae: Genera and species known from culture. *Studies in Mycology* **76**: 51–167. https://doi.org/10.3114/sim0021

Phillips AJL, Hyde KD, Alves A, Liu JK (Jack), 2019. Families in Botryosphaeriales: a phylogenetic, morphological and evolutionary perspective. *Fungal Diversity* **94**: 1–22. https://doi.org/10.1007/s13225-018-0416-6

Pluskal T, Castillo S, Villar-Briones A, Orešič M, 2010. MZmine 2: Modular framework for processing, visualizing, and analyzing mass spectrometry-based molecular profile data. *BMC Bioinformatics* **11**: 395. https://doi.org/10.1186/1471-2105-11-395

Pongcharoen W, Rukachaisirikul V, Phongpaichit S, Sakayaroj J, 2007. A new dihydrobenzofuran derivative from the endophytic fungus Botryosphaeria mamane PSU-M76. *Chemical and Pharmaceutical Bulletin* **55**: 1404–1405. https://doi.org/10.1248/cpb.55.1404

Pruksakorn P, Arai M, Kotoku N, Vilchze C, Baughn AD, Moodley P, Jacobs WR, Kobayashi M, 2010. Trichoderins, novel aminolipopeptides from a marine sponge-derived Trichoderma sp., are active against dormant mycobacteria. *Bioorganic and Medicinal Chemistry Letters* **20**: 3658–3663. https://doi.org/10.1016/j.bmcl.2010.04.100

Qiu Y, Guo Q, Ran Y-Q, Lan W-J, Lam C-K, Feng G-K, Deng R, Zhu X-F, Li H-J, Chen L-P, 2020. Cytotoxic alkaloids from the marine shellfish-associated fungus Aspergillus sp. XBB-4 induced by an amino acid-directed strategy. *RSC Advances* **10**: 4243–4250. https://doi.org/10.1039/C9RA10306F

Rodriguez RJ, White JF, Arnold AE, Redman RS, 2009. Fungal endophytes: Diversity and functional roles: Tansley review. *New Phytologist* **182**: 314–330. https://doi.org/10.1111/j.1469-8137.2009.02773.x

Romano S, Jackson S, Patry S, Dobson A, 2018. Extending the "One Strain Many Compounds" (OSMAC) Principle to Marine Microorganisms. *Marine Drugs* **16**: 244. https://doi.org/10.3390/md16070244

Roullier C, Bertrand S, Blanchet E, Peigné M, Robiou du Pont T, Guitton Y, Pouchus Y, Grovel O, 2016. Time Dependency of Chemodiversity and Biosynthetic Pathways: An LC-MS Metabolomic Study of Marine-Sourced Penicillium. *Marine Drugs* **14**: 103. https://doi.org/10.3390/md14050103

Russell JR, Huang J, Anand P, Kucera K, Sandoval AG, Dantzler KW, Hickman DS, Jee J, Kimovec FM, Koppstein D, Marks DH, Mittermiller PA, Núñez SJ, Santiago M, Townes MA, Vishnevetsky M, Williams NE, Vargas MPN, Boulanger LA, Bascom-Slack C, Strobel SA, 2011. Biodegradation of polyester polyurethane by endophytic fungi. *Applied and Environmental Microbiology* **77**: 6076–6084. https://doi.org/10.1128/AEM.00521-11

Sanchez S, Demain AL, 2017. Bioactive Products from Fungi. In: *Food Bioactives*. Springer International Publishing, Cham, pp. 59–87.

Van Santen JA, Jacob G, Singh AL, Aniebok V, Balunas MJ, Bunsko D, Neto FC, Castaño-Espriu L, Chang C, Clark TN, Cleary Little JL, Delgadillo DA, Dorrestein PC, Duncan KR, Egan JM, Galey MM, Haeckl FPJ, Hua A, Hughes AH, Iskakova D, Khadilkar A, Lee JH, Lee S, Legrow N, Liu DY, Macho JM, McCaughey CS, Medema MH, Neupane RP, O'Donnell TJ, Paula JS, Sanchez LM, Shaikh AF, Soldatou S, Terlouw BR, Tran TA, Valentine M, Van Der Hooft JJJ, Vo DA, Wang M, Wilson D, Zink KE, Linington RG, 2019. The Natural Products Atlas: An Open Access Knowledge Base for Microbial Natural Products Discovery. *ACS Central Science* **5**: 1824–1833. https://doi.org/10.1021/acscentsci.9b00806

Scharf DH, Heinekamp T, Remme N, Hortschansky P, Brakhage AA, Hertweck C, 2012. Biosynthesis and function of gliotoxin in Aspergillus fumigatus. *Applied Microbiology and Biotechnology* **93**: 467–472. https://doi.org/10.1007/s00253-011-3689-1

Schoch CL, Crous PW, Groenewald JZ, Boehm EWA, Burgess TI, de Gruyter J, de Hoog GS, Dixon LJ, Grube M, Gueidan C, Harada Y, Hatakeyama S, Hirayama K, Hosoya T, Huhndorf SM, Hyde KD, Jones EBG, Kohlmeyer J, Kruys Å, Li YM, Lücking R, Lumbsch HT, Marvanová L, Mbatchou JS, McVay AH, Miller AN, Mugambi GK, Muggia L, Nelsen MP, Nelson P, Owensby CA, Phillips AJL, Phongpaichit S, Pointing SB, Pujade-Renaud V, Raja HA, Plata ER, Robbertse B, Ruibal C, Sakayaroj J, Sano T, Selbmann L, Shearer CA, Shirouzu T, Slippers B, Suetrong S, Tanaka K, Volkmann-Kohlmeyer B, Wingfield MJ, Wood AR, Woudenberg JHC, Yonezawa H, Zhang Y, Spatafora JW, 2009. A class-wide phylogenetic assessment of Dothideomycetes. *Studies in Mycology* **64**: 1–15. https://doi.org/10.3114/sim.2009.64.01

Schueffler A, Anke T, 2014. Fungal natural products in research and development. *Nat. Prod. Rep.* **31**: 1425–1448. https://doi.org/10.1039/C4NP00060A

Schumacher J, 2017. How light affects the life of Botrytis. *Fungal Genetics and Biology* **106**: 26–41. https://doi.org/10.1016/j.fgb.2017.06.002

Sengupta S, Chattopadhyay MK, Grossart HP, 2013. The multifaceted roles of antibiotics and antibiotic resistance in nature. *Frontiers in Microbiology* **4**: 1–13.

https://doi.org/10.3389/fmicb.2013.00047

Shah A, Rather MA, Hassan QP, Aga MA, Mushtaq S, Shah AM, Hussain A, Baba SA, Ahmad Z, 2017. Discovery of anti-microbial and anti-tubercular molecules from Fusarium solani : an endophyte of Glycyrrhiza glabra. *Journal of Applied Microbiology* **122**: 1168–1176. https://doi.org/10.1111/jam.13410

Shahid-ul-Islam, Rather LJ, Mohammad F, 2016. Phytochemistry, biological activities and potential of annatto in natural colorant production for industrial applications - A review. *Journal of Advanced Research* **7**: 499–514. https://doi.org/10.1016/j.jare.2015.11.002

Shannon P, 2003. Cytoscape: A Software Environment for Integrated Models of Biomolecular Interaction Networks. *Genome Research* **13**: 2498–2504. https://doi.org/10.1101/gr.1239303

Shwab EK, Bok JW, Tribus M, Galehr J, Graessle S, Keller NP, 2007. Histone Deacetylase Activity Regulates Chemical Diversity in Aspergillus. *Eukaryotic Cell* **6**: 1656–1664. https://doi.org/10.1128/EC.00186-07

da Silva RR, Wang M, Nothias LF, van der Hooft JJJ, Caraballo-Rodríguez AM, Fox E, Balunas MJ, Klassen JL, Lopes NP, Dorrestein PC, 2018. Propagating annotations of molecular networks using in silico fragmentation. *PLoS Computational Biology* **14**: 1–26. https://doi.org/10.1371/journal.pcbi.1006089

Singh A, Singh DK, Kharwar RN, White JF, Gond SK, 2021. Fungal endophytes as efficient sources of plant-derived bioactive compounds and their prospective applications in natural product drug discovery: Insights, avenues, and challenges. *Microorganisms* **9**: 1–42. https://doi.org/10.3390/microorganisms9010197

Slippers B, Boissin E, Phillips AJL, Groenewald JZ, Lombard L, Wingfield MJ, Postma A, Burgess T, Crous PW, 2013. Phylogenetic lineages in the botryosphaeriales: A systematic and evolutionary framework. *Studies in Mycology* **76**: 31–49. https://doi.org/10.3114/sim0020

Slippers B, Crous PW, Jami F, Groenewald JZ, Wingfield MJ, 2017. Diversity in the Botryosphaeriales: Looking back, looking forward. *Fungal Biology* **121**: 307–321. https://doi.org/10.1016/j.funbio.2017.02.002

Srinivasan A, Dick JD, Perl TM, 2002. Vancomycin Resistance in Staphylococci. *Clinical Microbiology Reviews* **15**: 430–438. https://doi.org/10.1128/CMR.15.3.430-438.2002

Strobel G, 2018. The emergence of endophytic microbes and their biological promise. *Journal of Fungi* **4**. https://doi.org/10.3390/jof4020057

Strobel G, Daisy B, 2003. Bioprospecting for Microbial Endophytes and Their Natural Products. *Microbiology and Molecular Biology Reviews* **67**: 491–502. https://doi.org/10.1128/MMBR.67.4.491-502.2003

Strobel G, Ford E, Worapong J, Harper JK, Arif AM, Grant DM, Fung PCW, Ming Wah Chau R, 2002. Isopestacin, an isobenzofuranone from Pestalotiopsis microspora, possessing antifungal and antioxidant activities. *Phytochemistry* **60**: 179–183. https://doi.org/10.1016/S0031-

9422(02)00062-6

Sun Y, Takada K, Takemoto Y, Yoshida M, Nogi Y, Okada S, Matsunaga S, 2012. Gliotoxin analogues from a marine-derived fungus, penicillium sp., and their cytotoxic and histone methyltransferase inhibitory activities. *Journal of Natural Products* **75**: 111–114. https://doi.org/10.1021/np200740e

Suzuki MM, Bird A, 2008. DNA methylation landscapes: provocative insights from epigenomics. *Nature Reviews Genetics* **9**: 465–476. https://doi.org/10.1038/nrg2341

Tamil Selvi A, Dinesh MG, Satyan RS, Chandrasekaran B, Rose C, 2011. Leaf and Seed extracts of Bixa orellana L. exert anti-microbial activity against bacterial pathogens. *Journal of Applied Pharmaceutical Science* **1**: 116–120.

Tess Mends M, Yu E, 2012. An Endophytic Nodulisporium Sp. Producing Volatile Organic Compounds Having Bioactivity and Fuel Potential. *Journal of Petroleum & Environmental Biotechnology* **03**. https://doi.org/10.4172/2157-7463.1000117

Theobald S, Vesth TC, Andersen MR, 2019. Genus level analysis of PKS-NRPS and NRPS-PKS hybrids reveals their origin in Aspergilli. *BMC Genomics* **20**: 1–12. https://doi.org/10.1186/s12864-019-6114-2

Tisch D, Schmoll M, 2010. Light regulation of metabolic pathways in fungi. *Applied Microbiology and Biotechnology* **85**: 1259–1277. https://doi.org/10.1007/s00253-009-2320-1

Tjitra E, Anstey NM, Sugiarto P, Warikar N, Kenangalem E, Karyana M, Lampah DA, Price RN, 2008. Multidrug-Resistant Plasmodium vivax Associated with Severe and Fatal Malaria: A Prospective Study in Papua, Indonesia (S Rogerson, Ed,). *PLoS Medicine* **5**: e128. https://doi.org/10.1371/journal.pmed.0050128

Toghueo RMK, Sahal D, Boyom FF, 2020. Recent advances in inducing endophytic fungal specialized metabolites using small molecule elicitors including epigenetic modifiers. *Phytochemistry* **174**: 112338. https://doi.org/10.1016/j.phytochem.2020.112338

Toghueo RMK, Sahal D, Zabalgogeazcoa Í, Baker B, Boyom FF, 2018. Conditioned media and organic elicitors underpin the production of potent antiplasmodial metabolites by endophytic fungi from Cameroonian medicinal plants. *Parasitology Research* **117**: 2473–2485. https://doi.org/10.1007/s00436-018-5936-1

Torres-Mendoza D, Ortega HE, Cubilla-Rios L, 2020. Patents on endophytic fungi related to secondary metabolites and biotransformation applications. *Journal of Fungi* **6**. https://doi.org/10.3390/jof6020058

Tran-Cong NM, Mándi A, Kurtán T, Müller WEG, Kalscheuer R, Lin W, Liu Z, Proksch P, 2019. Induction of cryptic metabolites of the endophytic fungus: Trichocladium sp. through OSMAC and co-cultivation. *RSC Advances* **9**: 27279–27288. https://doi.org/10.1039/c9ra05469c

Triastuti A, Haddad M, Barakat F, Mejia K, Rabouille G, Fabre N, Amasifuen C, Jargeat P, Vansteelandt M, 2021. Dynamics of Chemical Diversity during Co-Cultures: An Integrative

Time-Scale Metabolomics Study of Fungal Endophytes Cophinforma mamane and Fusarium solani. *Chemistry & Biodiversity* **18**. https://doi.org/10.1002/cbdv.202000672

Triastuti A, Vansteelandt M, Barakat F, Trinel M, Jargeat P, Fabre N, Amasifuen Guerra CA, Mejia K, Valentin A, Haddad M, 2019. How Histone Deacetylase Inhibitors Alter the Secondary Metabolites of Botryosphaeria mamane, an Endophytic Fungus Isolated from Bixa orellana. *Chemistry and Biodiversity* **16**. https://doi.org/10.1002/cbdv.201800485

Tsugawa H, Cajka T, Kind T, Ma Y, Higgins B, Ikeda K, Kanazawa M, VanderGheynst J, Fiehn O, Arita M, 2015. MS-DIAL: data-independent MS/MS deconvolution for comprehensive metabolome analysis. *Nature Methods* **12**: 523–526. https://doi.org/10.1038/nmeth.3393

Tsugawa H, Kind T, Nakabayashi R, Yukihira D, Tanaka W, Cajka T, Saito K, Fiehn O, Arita M, 2016. Hydrogen Rearrangement Rules: Computational MS/MS Fragmentation and Structure Elucidation Using MS-FINDER Software. *Analytical Chemistry* **88**: 7946–7958. https://doi.org/10.1021/acs.analchem.6b00770

Tsuge T, Harimoto Y, Akimitsu K, Ohtani K, Kodama M, Akagi Y, Egusa M, Yamamoto M, Otani H, 2013. Host-selective toxins produced by the plant pathogenic fungus Alternaria alternata. *FEMS Microbiology Reviews* **37**: 44–66. https://doi.org/10.1111/j.1574-6976.2012.00350.x

Tudzynski B, Kawaide H, Kamiya Y, 1998. Gibberellin biosynthesis in Gibberella fujikuroi: Cloning and characterization of the copalyl diphosphate synthase gene. *Current Genetics* **34**: 234–240. https://doi.org/10.1007/s002940050392

Uthe H, van Dam NM, Hervé MR, Sorokina M, Peters K, Weinhold A, 2021. *A practical guide to implementing metabolomics in plant ecology and biodiversity research*. Elsevier Ltd.

Uzma F, Mohan CD, Hashem A, Konappa NM, Rangappa S, Kamath P V., Singh BP, Mudili V, Gupta VK, Siddaiah CN, Chowdappa S, Alqarawi AA, Abd_Allah EF, 2018. Endophytic Fungi—Alternative Sources of Cytotoxic Compounds: A Review. *Frontiers in Pharmacology* **9**: 1–37. https://doi.org/10.3389/fphar.2018.00309

Vasanthakumari MM, Jadhav SS, Sachin N, Vinod G, Shweta S, Manjunatha BL, Kumara PM, Ravikanth G, Nataraja KN, Uma Shaanker R, 2015. Restoration of camptothecine production in attenuated endophytic fungus on re-inoculation into host plant and treatment with DNA methyltransferase inhibitor. *World Journal of Microbiology and Biotechnology* **31**: 1629–1639. https://doi.org/10.1007/s11274-015-1916-0

Venugopalan A, Srivastava S, 2015. Endophytes as in vitro production platforms of high value plant secondary metabolites. *Biotechnology Advances* **33**: 873–887. https://doi.org/10.1016/j.biotechadv.2015.07.004

Vijayakumar S, Raj R, Shaanker U, Sivaramakrishna A, Ramamoorthy S, 2021. Mycosynthesis of novel lactone in foliar endophytic fungus isolated from Bixa orellana L. *3 Biotech* **11**: 33. https://doi.org/10.1007/s13205-020-02566-x

Vilar DDA, Vilar MSDA, Moura TFADLE, Raffin FN, Oliveira MR De, Franco CFDO, De Athayde-

Filho PF, Diniz MDFFM, Barbosa-Filho JM, 2014. Traditional Uses, chemical constituents, and biological activities of Bixa Orellana L.: A review. *Scientific World Journal* **2014**. https://doi.org/10.1155/2014/857292

Wang X, Lin M, Xu D, Lai D, Zhou L, 2017a. Structural Diversity and Biological Activities of Fungal Cyclic Peptides, Excluding Cyclodipeptides. *Molecules* **22**: 2069. https://doi.org/10.3390/molecules22122069

Wang LW, Wang JL, Chen J, Chen JJ, Shen JW, Feng XX, Kubicek CP, Lin FC, Zhang CL, Chen FY, 2017b. A novel derivative of (-)mycousnine produced by the endophytic fungus Mycosphaerella nawae, exhibits high and selective immunosuppressive activity on T cells. *Frontiers in Microbiology* **8**: 1–14. https://doi.org/10.3389/fmicb.2017.01251

White JF, Kingsley KL, Zhang Q, Verma R, Obi N, Dvinskikh S, Elmore MT, Verma SK, Gond SK, Kowalski KP, 2019. Review: Endophytic microbes and their potential applications in crop management. *Pest Management Science* **75**: 2558–2565. https://doi.org/10.1002/ps.5527

Williams RB, Henrikson JC, Hoover AR, Lee AE, Cichewicz RH, 2008. Epigenetic remodeling of the fungal secondary metabolome. *Organic & Biomolecular Chemistry* **6**: 1895. https://doi.org/10.1039/b804701d

Wu DL, Li HJ, Smith DR, Jaratsittisin J, Xia-Ke-Er XFKT, Ma WZ, Guo YW, Dong J, Shen J, Yang DP, Lan WJ, 2018. Polyketides and alkaloids from the marine-derived fungus Dichotomomyces cejpii F31-1 and the antiviral activity of scequinadoline A against dengue virus. *Marine Drugs* **16**: 1–10. https://doi.org/10.3390/md16070229

Yang T, Groenewald JZ, Cheewangkoon R, Jami F, Abdollahzadeh J, Lombard L, Crous PW, 2017. Families, genera, and species of Botryosphaeriales. *Fungal Biology* **121**: 322–346. https://doi.org/10.1016/j.funbio.2016.11.001

Yong YK, Zakaria ZA, Kadir AA, Somchit MN, Ee Cheng Lian G, Ahmad Z, 2013. Chemical constituents and antihistamine activity of Bixa orellana leaf extract. *BMC Complementary and Alternative Medicine* **13**: 1–7. https://doi.org/10.1186/1472-6882-13-32

Yu Z, Fischer R, 2019. Light sensing and responses in fungi. *Nature Reviews Microbiology* **17**: 25–36. https://doi.org/10.1038/s41579-018-0109-x

Yuan M-X, Qiu Y, Ran Y-Q, Feng G-K, Deng R, Zhu X-F, Lan W-J, Li H-J, 2019. Exploration of Indole Alkaloids from Marine Fungus Pseudallescheria boydii F44-1 Using an Amino Acid-Directed Strategy. *Marine Drugs* **17**: 77. https://doi.org/10.3390/md17020077

Zhai B, Clark J, Ling T, Connelly M, Medina-Bolivar F, Rivas F, 2014. Antimalarial evaluation of the chemical constituents of hairy root culture of bixa orellana l. *Molecules* **19**: 756–766. https://doi.org/10.3390/molecules19010756

Zhai Y-J, Huo G-M, Zhang Q, Li D, Wang D-C, Qi J-Z, Han W-B, Gao J-M, 2020. Phaeosphaones: Tyrosinase Inhibitory Thiodiketopiperazines from an Endophytic Phaeosphaeria fuckelii. *Journal of Natural Products* **83**: 1592–1597. https://doi.org/10.1021/acs.jnatprod.0c00046

Zhang X, Gao Y, Yin Y, Cai M, Zhou X, Zhang Y, 2017. Regulation of different polyketide biosynthesis by green light in an endophytic fungus of mangrove leaf. *3 Biotech* **7**: 363. https://doi.org/10.1007/s13205-017-0996-y

Zhang W, Groenewald JZ, Lombard L, Schumacher RK, Phillips AJL, Crous PW, 2021. Evaluating species in Botryosphaeriales. *Persoonia - Molecular Phylogeny and Evolution of Fungi*: 63–115. https://doi.org/10.3767/persoonia.2021.46.03

Zhang SP, Huang R, Li FF, Wei HX, Fang XW, Xie XS, Lin DG, Wu SH, He J, 2016. Antiviral anthraquinones and azaphilones produced by an endophytic fungus Nigrospora sp. from Aconitum carmichaeli. *Fitoterapia* **112**: 85–89. https://doi.org/10.1016/j.fitote.2016.05.013

Zhang HW, Song YC, Tan RX, 2006. Biology and chemistry of endophytes. *Natural Product Reports* **23**: 753–771. https://doi.org/10.1039/b609472b

Zhang Y, Wang S, Li X-M, Cui C-M, Feng C, Wang B-G, 2007. New Sphingolipids with a Previously Unreported 9-Methyl-C20-sphingosine Moiety from a Marine Algous Endophytic Fungus Aspergillus niger EN-13. *Lipids* **42**: 759–764. https://doi.org/10.1007/s11745-007-3079-8

Zhang C-L, Wang G-P, Mao L-J, Komon-Zelazowska M, Yuan Z-L, Lin F-C, Druzhinina IS, Kubicek CP, 2010. Muscodor fengyangensis sp. nov. from southeast China: morphology, physiology and production of volatile compounds. *Fungal Biology* **114**: 797–808. https://doi.org/10.1016/j.funbio.2010.07.006

Zhao J, Shan T, Mou Y, Zhou L, 2011. Plant-Derived Bioactive Compounds Produced by Endophytic Fungi. *Mini-Reviews in Medicinal Chemistry* **11**: 159–168. https://doi.org/10.2174/138955711794519492

Zhao Q, Zhang J Le, Li F, 2018. Application of Metabolomics in the Study of Natural Products. *Natural Products and Bioprospecting* **8**: 321–334. https://doi.org/10.1007/s13659-018-0175-9

Zheng R, Li S, Zhang X, Zhao C, 2021. Biological activities of some new secondary metabolites isolated from endophytic fungi: A review study. *International Journal of Molecular Sciences* **22**: 1–75. https://doi.org/10.3390/ijms22020959

Zutz C, Bandian D, Neumayer B, Speringer F, Gorfer M, Wagner M, Strauss J, Rychli K, 2014. Fungi treated with small chemicals exhibit increased antimicrobial activity against facultative bacterial and yeast pathogens. *BioMed Research International* **2014**. https://doi.org/10.1155/2014/540292

Chapter 2

Barakat F, Vansteelandt M, Triastuti A, Jargeat P, Jacquemin D, Graton J, Mejia K, Cabanillas B, Vendier L, Stigliani J-LL, Haddad M, Fabre N, 2019. Thiodiketopiperazines with two spirocyclic centers extracted from Botryosphaeria mamane, an endophytic fungus isolated from Bixa orellana L. *Phytochemistry* **158**: 142–148. https://doi.org/10.1016/j.phytochem.2018.11.007

Bertrand S, Azzollini A, Schumpp O, Bohni N, Schrenzel J, Monod M, Gindro K, Wolfender JL, 2014. Multi-well fungal co-culture for de novo metabolite-induction in time-series studies based on untargeted metabolomics. *Molecular BioSystems* **10**: 2289–2298. https://doi.org/10.1039/c4mb00223g

Chong J, Wishart DS, Xia J, 2019. Using MetaboAnalyst 4.0 for Comprehensive and Integrative Metabolomics Data Analysis. *Current Protocols in Bioinformatics* **68**. https://doi.org/10.1002/cpbi.86

Fraisier-Vannier O, Chervin J, Cabanac G, Puech V, Fournier S, Durand V, Amiel A, André O, Benamar OA, Dumas B, Tsugawa H, Marti G, 2020. MS-CleanR: A Feature-Filtering Workflow for Untargeted LC–MS Based Metabolomics. *Analytical Chemistry* **92**: 9971–9981. https://doi.org/10.1021/acs.analchem.0c01594

Olivon F, Elie N, Grelier G, Roussi F, Litaudon M, Touboul D, 2018. MetGem Software for the Generation of Molecular Networks Based on the t-SNE Algorithm. *Analytical Chemistry* **90**: 13900–13908. https://doi.org/10.1021/acs.analchem.8b03099

Sereno D, Lemesre JL, 1997. Axenically cultured amastigote forms as an in vitro model for investigation of antileishmanial agents. *Antimicrobial Agents and Chemotherapy* **41**: 972–976. https://doi.org/10.1128/AAC.41.5.972

Shannon P, 2003. Cytoscape: A Software Environment for Integrated Models of Biomolecular Interaction Networks. *Genome Research* **13**: 2498–2504. https://doi.org/10.1101/gr.1239303

Shirling EB, Gottlieb D, 1966. Methods for characterization of Streptomyces species. *International Journal of Systematic Bacteriology* **16**: 313–340. https://doi.org/10.1099/00207713-16-3-313

Triastuti A, Vansteelandt M, Barakat F, Trinel M, Jargeat P, Fabre N, Amasifuen Guerra CA, Mejia K, Valentin A, Haddad M, 2019. How Histone Deacetylase Inhibitors Alter the Secondary Metabolites of Botryosphaeria mamane, an Endophytic Fungus Isolated from Bixa orellana. *Chemistry and Biodiversity* **16**. https://doi.org/10.1002/cbdv.201800485

Tsugawa H, Cajka T, Kind T, Ma Y, Higgins B, Ikeda K, Kanazawa M, VanderGheynst J, Fiehn O, Arita M, 2015. MS-DIAL: data-independent MS/MS deconvolution for comprehensive metabolome analysis. *Nature Methods* **12**: 523–526. https://doi.org/10.1038/nmeth.3393

Tsugawa H, Kind T, Nakabayashi R, Yukihira D, Tanaka W, Cajka T, Saito K, Fiehn O, Arita M, 2016. Hydrogen Rearrangement Rules: Computational MS/MS Fragmentation and Structure Elucidation Using MS-FINDER Software. *Analytical Chemistry* **88**: 7946–7958. https://doi.org/10.1021/acs.analchem.6b00770

Chapter 3

Ariantari, N.P., Daletos, G., Mándi, A., Kurtán, T., Müller, W.E.G., Lin, W., Ancheeva, E., Proksch, P., 2019. Expanding the chemical diversity of an endophytic fungus Bulgaria inquinans , an ascomycete associated with mistletoe, through an OSMAC approach. RSC Adv. 9, 25119–25132. https://doi.org/10.1039/C9RA03678D

Bai, Y., Gao, Y., Lu, X., Wang, H., 2019. Lipidomics characterization of the alterations of Trichoderma brevicompactum membrane glycerophospholipids during the fermentation phase. J. Ind. Microbiol. Biotechnol. 46, 809–818. https://doi.org/10.1007/s10295-019-02152-y

Barakat, F., Vansteelandt, M., Triastuti, A., Jargeat, P., Jacquemin, D., Graton, J., Mejia, K., Cabanillas, B., Vendier, L., Stigliani, J.-L., Haddad, M., Fabre, N., 2019. Thiodiketopiperazines with two spirocyclic centers extracted from Botryosphaeria mamane, an endophytic fungus isolated from Bixa orellana L. Phytochemistry 158, 142–148. https://doi.org/10.1016/j.phytochem.2018.11.007

Barthélemy, M., Elie, N., Pellissier, L., Wolfender, J.-L., Stien, D., Touboul, D., Eparvier, V., 2019. Structural Identification of Antibacterial Lipids from Amazonian Palm Tree Endophytes through the Molecular Network Approach. Int. J. Mol. Sci. 20, 2006. https://doi.org/10.3390/ijms20082006

Berthelot, C., Perrin, Y., Leyval, C., Blaudez, D., 2017. Melanization and ageing are not drawbacks for successful agro-transformation of dark septate endophytes. Fungal Biol. 121, 652–663. https://doi.org/10.1016/j.funbio.2017.04.004

Bertrand, S., Azzollini, A., Schumpp, O., Bohni, N., Schrenzel, J., Monod, M., Gindro, K., Wolfender, J., 2014. Multi-well fungal co-culture for de novo metabolite-induction in time-series studies based on untargeted metabolomics. Mol. BioSyst. 10, 2289–2298. https://doi.org/10.1039/C4MB00223G

Birch, A.J., Russell, R.A., 1972. Studies in relation to biosynthesis—XLIV. Tetrahedron 28, 2999–3008. https://doi.org/10.1016/0040-4020(72)80014-0

Bode, H.B., Bethe, B., Höfs, R., Zeeck, A., 2002. Big Effects from Small Changes: Possible Ways to Explore Nature's Chemical Diversity. ChemBioChem 3, 619. https://doi.org/10.1002/1439-7633(20020703)3:7<619::AID-CBIC619>3.0.CO;2-9

Bofinger, M.R., de Sousa, L.S., Fontes, J.E.N., Marsaioli, A.J., 2017. Diketopiperazines as Cross-Communication Quorum - Sensing Signals between Cronobacter sakazakii and Bacillus cereus. ACS Omega 2, 1003–1008. https://doi.org/10.1021/acsomega.6b00513

Borgman, P., Lopez, R.D., Lane, A.L., 2019. The expanding spectrum of diketopiperazine natural product biosynthetic pathways containing cyclodipeptide synthases. Org. Biomol. Chem. 17, 2305–2314. https://doi.org/10.1039/C8OB03063D

Brakhage, A.A., 2013. Regulation of fungal secondary metabolism. Nat. Rev. Microbiol. 11, 21–32.

https://doi.org/10.1038/nrmicro2916

Choi, J.N., Kim, J., Lee, M.Y., Park, D.K., Hong, Y.S., Lee, C.H., 2010. Metabolomics revealed novel isoflavones and optimal cultivation time of cordyceps militaris fermentation. J. Agric. Food Chem. 58, 4258–4267. https://doi.org/10.1021/jf903822e

da Silva Lima, G., da Rocha, A.M., dos Santos, G.F., D'Silva, A.F., Marriel, I.E., Takahashi, J.A., 2018. Metabolic response of Aspergillus sydowii to OSMAC modulation produces acetylcholinesterase inhibitors. Phytochem. Lett. 24, 39–45. https://doi.org/10.1016/j.phytol.2018.01.007

Dufossé, L., Fouillaud, M., Caro, Y., Mapari, S.A.S., Sutthiwong, N., 2014. Filamentous fungi are large-scale producers of pigments and colorants for the food industry. Curr. Opin. Biotechnol. 26, 56–61. https://doi.org/10.1016/j.copbio.2013.09.007

Fan, B., Parrot, D., Blümel, M., Labes, A., Tasdemir, D., 2019. Influence of OSMAC-Based Cultivation in Metabolome and Anticancer Activity of Fungi Associated with the Brown Alga Fucus vesiculosus. Mar. Drugs 17, 67. https://doi.org/10.3390/md17010067

Faria, D.V., Correia, L.N. de F., Souza, M.V.C., Ríos-Ríos, A.M., Vital, C.E., Batista, D.S., Costa, M.G.C., Otoni, W.C., 2019. Irradiance and light quality affect two annatto (Bixa orellana L.) cultivars with contrasting bixin production. J. Photochem. Photobiol. B Biol. 197, 111549. https://doi.org/10.1016/j.jphotobiol.2019.111549

Gardner, D.E., 1997. Botryosphaeria mamane sp. nov. associated with witches'-brooms on the endemic forest tree Sophora chrysophylla in Hawaii. Mycologia 89, 298–303. https://doi.org/10.1080/00275514.1997.12026785

Jagtap, S.S., Bedekar, A.A., Liu, J.-J., Jin, Y.-S., Rao, C. V., 2019. Production of galactitol from galactose by the oleaginous yeast Rhodosporidium toruloides IFO0880. Biotechnol. Biofuels 12, 250. https://doi.org/10.1186/s13068-019-1586-5

Jia, J.-M., Ma, X.-C., Wu, C.-F., Wu, L.-J., Hu, G., 2005. Cordycedipeptide A, a New Cyclodipeptide from the Culture Liquid of Cordyceps sinensis (BERK.) SACC. Chem. Pharm. Bull. 53, 582–583. https://doi.org/10.1248/cpb.53.582

Jiang, C.-S., Guo, Y.-W., 2011. Epipolythiodioxopiperazines from Fungi: Chemistry and Bioactivities. Mini-Reviews Med. Chem. 11, 728–745. https://doi.org/10.2174/138955711796355276

Jiang, W., Zhong, Y., Shen, L., Wu, X., Ye, Y., Chen, C.-T., Wu, B., 2014. Stress-driven Discovery of Natural Products from Extreme Marine Environment- Kueishantao Hydrothermal Vent, a Case Study of Metal Switch Valve. Curr. Org. Chem. 18, 925–934. https://doi.org/10.2174/1385272818071405151557O5

Kalra, R., Conlan, X.A., Goel, M., 2020. Fungi as a Potential Source of Pigments: Harnessing Filamentous Fungi. Front. Chem. 8, 1–23. https://doi.org/10.3389/fchem.2020.00369

Kim, S.-B., Kim, S.-H., Lee, K.-R., Shim, J.-O., Lee, M.-W., Shim, M.-J., Lee, U.-Y., Lee, T.-S., 2005. The Optimal Culture Conditions for the Mycelial Growth of Oudemansiella radicata.

Mycobiology 33, 230. https://doi.org/10.4489/MYCO.2005.33.4.230

Kjer, J., 2009. New Natural Products from Endophytic Fungi from Mangrove Plants – Structure Elucidation and Biological Screening. Heinrich-Heine-Universität Düsseldorf.

Kusari, S., Singh, S., Jayabaskaran, C., 2014. Biotechnological potential of plant-associated endophytic fungi: hope versus hype. Trends Biotechnol. 32, 297–303. https://doi.org/10.1016/j.tibtech.2014.03.009

Laparre, J., Malbreil, M., Letisse, F., Portais, J.C., Roux, C., Bécard, G., Puech-Pagès, V., 2014. Combining Metabolomics and Gene Expression Analysis Reveals that Propionyl- and Butyryl-Carnitines Are Involved in Late Stages of Arbuscular Mycorrhizal Symbiosis. Mol. Plant 7, 554–566. https://doi.org/10.1093/mp/sst136

Li, G., Kusari, S., Golz, C., Strohmann, C., Spiteller, M., 2016. Three cyclic pentapeptides and a cyclic lipopeptide produced by endophytic Fusarium decemcellulare LG53. RSC Adv. 6, 54092–54098. https://doi.org/10.1039/C6RA10905E

Li, H.-J., Lin, Y.-C., Yao, J.-H., Vrijmoed, L.L.P., Jones, E.B.G., 2004. Two new metabolites from the mangrove endophytic fungus No. 2524. J. Asian Nat. Prod. Res. 6, 185–191. https://doi.org/10.1080/102860201653237

Madla, S., Kittakoop, P., Wongsa, P., 2006. Optimization of culture conditions for production of antimalarial menisporopsin A by the seed fungus Menisporopsis theobromae BCC 4162. Lett. Appl. Microbiol. 43, 548–553. https://doi.org/10.1111/j.1472-765X.2006.01994.x

Meng, L.H., Li, X.M., Liu, Y., Xu, G.M., Wang, B.G., 2017. Antimicrobial alkaloids produced by the mangrove endophyte Penicillium brocae MA-231 using the OSMAC approach. RSC Adv. 7, 55026–55033. https://doi.org/10.1039/c7ra12081h

Miersch, O., Bohlmann, H., Wasternack, C., 1999. Jasmonates and related compounds from Fusarium oxysporum. Phytochemistry 50, 517–523. https://doi.org/10.1016/S0031-9422(98)00596-2

Mondal, S., Majumdar, S., 2019. The Bull Effect of Endophytic Fungi: An Approach with Quorum Sensing, in: Advances in Endophytic Fungal Research. pp. 171–181. https://doi.org/10.1007/978-3-030-03589-1_8

Mota Fernandes, C., Del Poeta, M., 2020. Fungal sphingolipids: role in the regulation of virulence and potential as targets for future antifungal therapies. Expert Rev. Anti. Infect. Ther. 18, 1083–1092. https://doi.org/10.1080/14787210.2020.1792288

Peters, S., Janssen, H.-G., Vivó-Truyols, G., 2010. Trend analysis of time-series data: A novel method for untargeted metabolite discovery. Anal. Chim. Acta 663, 98–104. https://doi.org/10.1016/j.aca.2010.01.038

Phillips, A.J.L., Rumbos, I.C., Alves, A., Correia, A., 2005. Morphology and phylogeny of Botryosphaeria dothidea causing fruit rot of olives. Mycopathologia 159, 433–439. https://doi.org/10.1007/s11046-005-0256-2

Pimenta, E.F., Vita-Marques, A.M., Tininis, A., Seleghim, M.H.R., Sette, L.D., Veloso, K., Ferreira,

A.G., Williams, D.E., Patrick, B.O., Dalisay, D.S., Andersen, R.J., Berlinck, R.G.S., 2010. Use of Experimental Design for the Optimization of the Production of New Secondary Metabolites by Two Penicillium Species. J. Nat. Prod. 73, 1821–1832. https://doi.org/10.1021/np100470h

Pongcharoen, W., Rukachaisirikul, V., Phongpaichit, S., Sakayaroj, J., 2007. A new dihydrobenzofuran derivative from the endophytic fungus Botryosphaeria mamane PSU-M76. Chem. Pharm. Bull. 55, 1404–1405. https://doi.org/10.1248/cpb.55.1404

Rateb, M.E., Hallyburton, I., Houssen, W.E., Bull, A.T., Goodfellow, M., Santhanam, R., Jaspars, M., Ebel, R., 2013. Induction of diverse secondary metabolites in Aspergillus fumigatus by microbial co-culture. RSC Adv. 3, 14444. https://doi.org/10.1039/c3ra42378f

Reindel, F., Weickmann, A., Picard, S., Luber, K., Turula, P., 1940. Über Pilzcerebrin. II. Justus Liebig's Ann. der Chemie 544, 116–137. https://doi.org/10.1002/jlac.19405440108

Romano, S., Jackson, S., Patry, S., Dobson, A., 2018. Extending the "One Strain Many Compounds" (OSMAC) Principle to Marine Microorganisms. Mar. Drugs 16, 244. https://doi.org/10.3390/md16070244

Roullier, C., Bertrand, S., Blanchet, E., Peigné, M., Robiou du Pont, T., Guitton, Y., Pouchus, Y., Grovel, O., 2016. Time Dependency of Chemodiversity and Biosynthetic Pathways: An LC-MS Metabolomic Study of Marine-Sourced Penicillium. Mar. Drugs 14, 103. https://doi.org/10.3390/md14050103

Scharf, D.H., Habel, A., Heinekamp, T., Brakhage, A.A., Hertweck, C., 2014. Opposed effects of enzymatic gliotoxin N - And S -methylations. J. Am. Chem. Soc. 136, 11674–11679. https://doi.org/10.1021/ja5033106

Schumacher, J., 2017. How light affects the life of Botrytis. Fungal Genet. Biol. 106, 26–41. https://doi.org/10.1016/j.fgb.2017.06.002

Shea, J.M., Del Poeta, M., 2006. Lipid signaling in pathogenic fungi. Curr. Opin. Microbiol. 9, 352–358. https://doi.org/10.1016/j.mib.2006.06.003

Siebers, M., Brands, M., Wewer, V., Duan, Y., Hölzl, G., Dörmann, P., 2016. Lipids in plant–microbe interactions. Biochim. Biophys. Acta - Mol. Cell Biol. Lipids 1861, 1379–1395. https://doi.org/10.1016/j.bbalip.2016.02.021

Soliman, S.S.M., Raizada, M.N., 2018. Darkness: A crucial factor in Fungal Taxol production. Front. Microbiol. 9, 1–7. https://doi.org/10.3389/fmicb.2018.00353

Song, Z., Hou, Y., Yang, Q., Li, X., Wu, S., 2021. Structures and Biological Activities of Diketopiperazines from Marine Organisms: A Review. Mar. Drugs 19, 403. https://doi.org/10.3390/md19080403

St-Germain, G., Summerbell, R., 2003. Identifying filamentous fungi: a clinical laboratory handbook.

Thorneley, R., 1990. Metal ions and bacteria. Trends Biotechnol. 8, 298–299. https://doi.org/10.1016/0167-7799(90)90204-B

Tran-Cong, N.M., Mándi, A., Kurtán, T., Müller, W.E.G., Kalscheuer, R., Lin, W., Liu, Z., Proksch,

P., 2019. Induction of cryptic metabolites of the endophytic fungus: Trichocladium sp. through OSMAC and co-cultivation. RSC Adv. 9, 27279–27288. https://doi.org/10.1039/c9ra05469c

Triastuti, A., Haddad, M., Barakat, F., Mejia, K., Rabouille, G., Fabre, N., Amasifuen, C., Jargeat, P., Vansteelandt, M., 2021. Dynamics of Chemical Diversity during Co-Cultures: An Integrative Time-Scale Metabolomics Study of Fungal Endophytes Cophinforma mamane and Fusarium solani. Chem. Biodivers. 18. https://doi.org/10.1002/cbdv.202000672

Tugizimana, F., Djami-Tchatchou, A.T., Fahrmann, J.F., Steenkamp, P.A., Piater, L.A., Dubery, I.A., 2019. Time-resolved decoding of metabolic signatures of in vitro growth of the hemibiotrophic pathogen Colletotrichum sublineolum. Sci. Rep. 9, 1–12. https://doi.org/10.1038/s41598-019-38692-7

Venkatesh, N., Keller, N.P., 2019. Mycotoxins in Conversation With Bacteria and Fungi. Front. Microbiol. 10, 1–10. https://doi.org/10.3389/fmicb.2019.00403

Vilar, D.D.A., Vilar, M.S.D.A., Moura, T.F.A.D.L.E., Raffin, F.N., Oliveira, M.R. De, Franco, C.F.D.O., De Athayde-Filho, P.F., Diniz, M.D.F.F.M., Barbosa-Filho, J.M., 2014. Traditional Uses, chemical constituents, and biological activities of Bixa Orellana L.: A review. Sci. World J. 2014. https://doi.org/10.1155/2014/857292

Wakefield, J., Hassan, H.M., Jaspars, M., Ebel, R., Rateb, M.E., 2017. Dual Induction of New Microbial Secondary Metabolites by Fungal Bacterial Co-cultivation. Front. Microbiol. 8, 1–10. https://doi.org/10.3389/fmicb.2017.01284

Wang, W.-X., Kusari, S., Sezgin, S., Lamshöft, M., Kusari, P., Kayser, O., Spiteller, M., 2015. Hexacyclopeptides secreted by an endophytic fungus Fusarium solani N06 act as crosstalk molecules in Narcissus tazetta. Appl. Microbiol. Biotechnol. 99, 7651–7662. https://doi.org/10.1007/s00253-015-6653-7

Wang, X., Li, Y., Zhang, X., Lai, D., Zhou, L., 2017a. Structural Diversity and Biological Activities of the Cyclodipeptides from Fungi. Molecules 22, 2026. https://doi.org/10.3390/molecules22122026

Wang, X., Lin, M., Xu, D., Lai, D., Zhou, L., 2017b. Structural Diversity and Biological Activities of Fungal Cyclic Peptides, Excluding Cyclodipeptides. Molecules 22, 2069. https://doi.org/10.3390/molecules22122069

Yang, Z.-D., Li, Z.-J., Zhao, J.-W., Sun, J.-H., Yang, L.-J., Shu, Z.-M., 2019. Secondary Metabolites and PI3K Inhibitory Activity of Colletotrichum gloeosporioides, a Fungal Endophyte of Uncaria rhynchophylla. Curr. Microbiol. 76, 904–908. https://doi.org/10.1007/s00284-019-01707-7

Yu, Z., Fischer, R., 2019. Light sensing and responses in fungi. Nat. Rev. Microbiol. 17, 25–36. https://doi.org/10.1038/s41579-018-0109-x

Zhang, Q., Wang, S.Q., Tang, H.Y., Li, X.J., Zhang, L., Xiao, J., Gao, Y.Q., Zhang, A.L., Gao, J.M., 2013. Potential allelopathic indole diketopiperazines produced by the plant endophytic Aspergillus fumigatus using the one strain-many compounds method. J. Agric. Food Chem. 61,

11447–11452. https://doi.org/10.1021/jf403200g

Zhang, Y., Wang, S., Li, X.-M., Cui, C.-M., Feng, C., Wang, B.-G., 2007. New Sphingolipids with a Previously Unreported 9-Methyl-C20-sphingosine Moiety from a Marine Algous Endophytic Fungus Aspergillus niger EN-13. Lipids 42, 759–764. https://doi.org/10.1007/s11745-007-3079-8

Zhu, J., Zhang, Y., Deng, J., Jiang, H., Zhuang, L., Ye, W., Ma, J., Jiang, J., Feng, L., 2019. Diketopiperazines Synthesis Gene in Shewanella baltica and Roles of Diketopiperazines and Resveratrol in Quorum Sensing. J. Agric. Food Chem. 67, 12013–12025. https://doi.org/10.1021/acs.jafc.9b04620

Chapter 4 – Submitted article

Abdel-Razek AS, El-Naggar ME, Allam A, Morsy OM, Othman SI, 2020. Microbial natural products in drug discovery. *Processes* **8**: 1–19. https://doi.org/10.3390/PR8040470

Asai T, Otsuki S, Sakurai H, Yamashita K, Ozeki T, Oshima Y, 2013. Benzophenones from an endophytic fungus, graphiopsis chlorocephala, from Paeonia lactiflora cultivated in the presence of an NAD+-dependent HDAC inhibitor. *Organic Letters* **15**: 2058–2061. https://doi.org/10.1021/ol400781b

Baccile JA, Le HH, Pfannenstiel BT, Bok JW, Gomez C, Brandenburger E, Hoffmeister D, Keller NP, Schroeder FC, 2019. Diketopiperazine Formation in Fungi Requires Dedicated Cyclization and Thiolation Domains. *Angewandte Chemie* **131**: 14731–14735. https://doi.org/10.1002/ange.201909052

Barakat F, Vansteelandt M, Triastuti A, Jargeat P, Jacquemin D, Graton J, Mejia K, Cabanillas B, Vendier L, Stigliani J-LL, Haddad M, Fabre N, 2019. Thiodiketopiperazines with two spirocyclic centers extracted from Botryosphaeria mamane, an endophytic fungus isolated from Bixa orellana L. *Phytochemistry* **158**: 142–148. https://doi.org/10.1016/j.phytochem.2018.11.007

Bofinger MR, de Sousa LS, Fontes JEN, Marsaioli AJ, 2017. Diketopiperazines as Cross-Communication Quorum - Sensing Signals between Cronobacter sakazakii and Bacillus cereus. *ACS Omega* **2**: 1003–1008. https://doi.org/10.1021/acsomega.6b00513

Boufridi A, Quinn RJ, 2018. Harnessing the Properties of Natural Products. *Annual Review of Pharmacology and Toxicology* **58**: 451–470. https://doi.org/10.1146/annurev-pharmtox-010716-105029

Brakhage AA, 2013. Regulation of fungal secondary metabolism. *Nature Reviews Microbiology* **11**: 21–32. https://doi.org/10.1038/nrmicro2916

Brakhage AA, Schroeckh V, 2011. Fungal secondary metabolites – Strategies to activate silent gene clusters. *Fungal Genetics and Biology* **48**: 15–22. https://doi.org/10.1016/j.fgb.2010.04.004

Chen Y-X, Xu M-Y, Li H-J, Zeng K-J, Ma W-Z, Tian G-B, Xu J, Yang D-P, Lan W-J, 2017. Diverse Secondary Metabolites from the Marine-Derived Fungus Dichotomomyces cejpii F31-1. *Marine Drugs* **15**: 339. https://doi.org/10.3390/md15110339

Chong J, Wishart DS, Xia J, 2019. Using MetaboAnalyst 4.0 for Comprehensive and Integrative Metabolomics Data Analysis. *Current Protocols in Bioinformatics* **68**. https://doi.org/10.1002/cpbi.86

Chunyu W-X, Ding Z-G, Zhao J-Y, Wang Y-X, Han X-L, Li M-G, Wen M-L, 2017. Two new diketopiperazines from the tin mine tailings-derived fungus Schizophyllum commune YIM DT 10058. *Natural Product Research* **31**: 1566–1572. https://doi.org/10.1080/14786419.2016.1274894

Cichewicz RH, 2010. Epigenome manipulation as a pathway to new natural product scaffolds and their congeners. *Nat. Prod. Rep.* **27**: 11–22. https://doi.org/10.1039/B920860G

Deepika VB, Vohra M, Mishra S, Dorai K, Rai P, Satyamoorthy K, Murali TS, 2020. DNA demethylation overcomes attenuation of colchicine biosynthesis in an endophytic fungus Diaporthe. *Journal of Biotechnology* **323**: 33–41. https://doi.org/10.1016/j.jbiotec.2020.07.019

Deshmukh S, Gupta M, Prakash V, Saxena S, 2018. Endophytic Fungi: A Source of Potential Antifungal Compounds. *Journal of Fungi* **4**: 77. https://doi.org/10.3390/jof4030077

El-Hawary S, Sayed A, Mohammed R, Hassan H, Zaki M, Rateb M, Mohammed T, Amin E, Abdelmohsen U, 2018. Epigenetic Modifiers Induce Bioactive Phenolic Metabolites in the Marine-Derived Fungus Penicillium brevicompactum. *Marine Drugs* **16**: 253. https://doi.org/10.3390/md16080253

El-Neketi M, Ebrahim W, Lin W, Gedara S, Badria F, Saad H-EA, Lai D, Proksch P, 2013. Alkaloids and Polyketides from Penicillium citrinum , an Endophyte Isolated from the Moroccan Plant Ceratonia siliqua. *Journal of Natural Products* **76**: 1099–1104. https://doi.org/10.1021/np4001366

Fraisier-Vannier O, Chervin J, Cabanac G, Puech V, Fournier S, Durand V, Amiel A, André O, Benamar OA, Dumas B, Tsugawa H, Marti G, 2020. MS-CleanR: A Feature-Filtering Workflow for Untargeted LC–MS Based Metabolomics. *Analytical Chemistry* **92**: 9971–9981. https://doi.org/10.1021/acs.analchem.0c01594

Fuqua C, Greenberg EP, 2002. Listening in on bacteria: acyl-homoserine lactone signalling. *Nature Reviews Molecular Cell Biology* **3**: 685–695. https://doi.org/10.1038/nrm907

González-Menéndez V, Pérez-Bonilla M, Pérez-Victoria I, Martín J, Muñoz F, Reyes F, Tormo J, Genilloud O, 2016. Multicomponent Analysis of the Differential Induction of Secondary Metabolite Profiles in Fungal Endophytes. *Molecules* **21**: 234. https://doi.org/10.3390/molecules21020234

Grigoletto DF, Correia AML, Abraham W-R, Rodrigues A, Assis MA, Ferreira AG, Massaroli M, Lira SP de, 2019. Secondary metabolites produced by endophytic fungi: novel antifungal activity

of fumiquinone B. *Acta Scientiarum. Biological Sciences* **41**: e48785. https://doi.org/10.4025/actascibiolsci.v41i1.48785

Guo Y-W, Liu X-J, Yuan J, Li H-J, Mahmud T, Hong M-J, Yu J-C, Lan W-J, 2020. L -Tryptophan Induces a Marine-Derived Fusarium sp. to Produce Indole Alkaloids with Activity against the Zika Virus. *Journal of Natural Products* **83**: 3372–3380. https://doi.org/10.1021/acs.jnatprod.0c00717

Guo H, Sun B, Gao H, Chen X, Liu S, Yao X, Liu X, Che Y, 2009. Diketopiperazines from the Cordyceps -Colonizing Fungus Epicoccum nigrum. *Journal of Natural Products* **72**: 2115–2119. https://doi.org/10.1021/np900654a

Gupta S, Kulkarni MG, White JF, Van Staden J, 2020. Epigenetic-based developments in the field of plant endophytic fungi. *South African Journal of Botany* **134**: 394–400. https://doi.org/10.1016/j.sajb.2020.07.019

Harrison IF, Powell NM, Dexter DT, 2019. The histone deacetylase inhibitor nicotinamide exacerbates neurodegeneration in the lactacystin rat model of Parkinson's disease. *Journal of Neurochemistry* **148**: 136–156. https://doi.org/10.1111/jnc.14599

Hawas UW, El-Beih AA, El-Halawany AM, 2012. Bioactive anthraquinones from endophytic fungus Aspergillus versicolor isolated from red sea algae. *Archives of Pharmacal Research* **35**: 1749–1756. https://doi.org/10.1007/s12272-012-1006-x

Hayashi A, Fujioka S, Nukina M, Kawano T, Shimada A, Kimura Y, 2007. Fumiquinones A and B, nematicidal quinones produced by Aspergillus fumigatus. *Bioscience, Biotechnology and Biochemistry* **71**: 1697–1702. https://doi.org/10.1271/bbb.70110

Huang L-H, Xu M-Y, Li H-J, Li J-Q, Chen Y-X, Ma W-Z, Li Y-P, Xu J, Yang D-P, Lan W-J, 2017. Amino Acid-Directed Strategy for Inducing the Marine-Derived Fungus Scedosporium apiospermum F41–1 to Maximize Alkaloid Diversity. *Organic Letters* **19**: 4888–4891. https://doi.org/10.1021/acs.orglett.7b02238

Jasim B, Sahadevan N, Chithra S, Mathew J, Radhakrishnan EK, 2019. Epigenetic Modifier Based Enhancement of Piperine Production in Endophytic Diaporthe sp. PF20. *Proceedings of the National Academy of Sciences India Section B - Biological Sciences* **89**: 671–677. https://doi.org/10.1007/s40011-018-0982-0

Kimura Y, Mizuno T, Kawano T, Okada K, Shimada A, 2000. Peniamidienone and penidilamine, plant growth regulators produced by the fungus Penicillium sp. No. 13. *Phytochemistry* **53**: 829–831. https://doi.org/10.1016/S0031-9422(99)00492-6

Li G, Kusari S, Golz C, Strohmann C, Spiteller M, 2016. Three cyclic pentapeptides and a cyclic lipopeptide produced by endophytic Fusarium decemcellulare LG53. *RSC Advances* **6**: 54092–54098. https://doi.org/10.1039/C6RA10905E

Li H-J, Lin Y-C, Yao J-H, Vrijmoed LLP, Jones EBG, 2004. Two new metabolites from the mangrove endophytic fungus No. 2524. *Journal of Asian Natural Products Research* **6**: 185–191.

https://doi.org/10.1080/102860201653237

Li L-Y, Ding Y, Groth I, Menzel K-D, Peschel G, Voigt K, Deng Z-W, Sattler I, Lin W-H, 2008. Pyrrole and indole alkaloids from an endophytic Fusarium incarnatum (HKI00504) isolated from the mangrove plant Aegiceras corniculatum. *Journal of Asian Natural Products Research* **10**: 765–770. https://doi.org/10.1080/10286020802031106

Liu X, Dong M, Chen X, Jiang M, Lv X, Zhou J, 2008. Antimicrobial activity of an endophytic Xylaria sp.YX-28 and identification of its antimicrobial compound 7-amino-4-methylcoumarin. *Applied Microbiology and Biotechnology* **78**: 241–247. https://doi.org/10.1007/s00253-007-1305-1

Liu M, Sun W, Wang J, He Y, Zhang J, Li F, Qi C, Zhu H, Xue Y, Hu Z, Zhang Y, 2018. Bioactive secondary metabolites from the marine-associated fungus Aspergillus terreus. *Bioorganic Chemistry* **80**: 525–530. https://doi.org/10.1016/j.bioorg.2018.06.029

Loesgen S, Bruhn T, Meindl K, Dix I, Schulz B, Zeeck A, Bringmann G, 2011. (+)-Flavipucine, the Missing Member of the Pyridione Epoxide Family of Fungal Antibiotics. *European Journal of Organic Chemistry* **2011**: 5156–5162. https://doi.org/10.1002/ejoc.201100284

Long X, Huang Y, Long Y, Deng J, 2018. Biomimetic total synthesis of homodimericin A. *Organic Chemistry Frontiers* **5**: 1152–1154. https://doi.org/10.1039/C7QO01161J

Luo H, Qing Z, Deng Y, Deng Z, Tang X, Feng B, Lin W, 2019. Two Polyketides Produced by Endophytic Penicillium citrinum DBR-9 From Medicinal Plant Stephania kwangsiensis and Their Antifungal Activity Against Plant Pathogenic Fungi. *Natural Product Communications* **14**: 1934578X1984679. https://doi.org/10.1177/1934578X19846795

Mevers E, Saurí J, Liu Y, Moser A, Ramadhar TR, Varlan M, Williamson RT, Martin GE, Clardy J, 2016. Homodimericin A: A Complex Hexacyclic Fungal Metabolite. *Journal of the American Chemical Society* **138**: 12324–12327. https://doi.org/10.1021/jacs.6b07588

Mondal S, Majumdar S, 2019. The Bull Effect of Endophytic Fungi: An Approach with Quorum Sensing. In: *Advances in Endophytic Fungal Research*. pp. 171–181.

Nicoletti R, Becchimanzi A, 2020. Endophytism of Lecanicillium and Akanthomyces. *Agriculture* **10**: 205. https://doi.org/10.3390/agriculture10060205

Okada BK, Seyedsayamdost MR, 2017. Antibiotic dialogues: induction of silent biosynthetic gene clusters by exogenous small molecules (A Shen, Ed,). *FEMS Microbiology Reviews* **41**: 19–33. https://doi.org/10.1093/femsre/fuw035

Olivon F, Elie N, Grelier G, Roussi F, Litaudon M, Touboul D, 2018. MetGem Software for the Generation of Molecular Networks Based on the t-SNE Algorithm. *Analytical Chemistry* **90**: 13900–13908. https://doi.org/10.1021/acs.analchem.8b03099

Pfannenstiel BT, Keller NP, 2019. On top of biosynthetic gene clusters: How epigenetic machinery influences secondary metabolism in fungi. *Biotechnology Advances* **37**: 107345. https://doi.org/10.1016/j.biotechadv.2019.02.001

Pongcharoen W, Rukachaisirikul V, Phongpaichit S, Sakayaroj J, 2007. A new dihydrobenzofuran derivative from the endophytic fungus Botryosphaeria mamane PSU-M76. *Chemical and Pharmaceutical Bulletin* **55**: 1404–1405. https://doi.org/10.1248/cpb.55.1404

Qian Z-J, Zhang C, Li Y-X, Je J-Y, Kim S-K, Jung W-K, 2011. Protective Effects of Emodin and Chrysophanol Isolated from Marine Fungus Aspergillus sp. on Ethanol-Induced Toxicity in HepG2/CYP2E1 Cells. *Evidence-Based Complementary and Alternative Medicine* **2011**: 1–7. https://doi.org/10.1155/2011/452621

Qiu Y, Guo Q, Ran Y-Q, Lan W-J, Lam C-K, Feng G-K, Deng R, Zhu X-F, Li H-J, Chen L-P, 2020. Cytotoxic alkaloids from the marine shellfish-associated fungus Aspergillus sp. XBB-4 induced by an amino acid-directed strategy. *RSC Advances* **10**: 4243–4250. https://doi.org/10.1039/C9RA10306F

Rabal Biasetto C, Somensi A, Sales Figueiro F, Beraldo de Moraes LA, Silva GH, Marx Young MC, Da Silva Bolzani V, Araújo AR, 2019. Diketopiperazines and arylethylamides produced by Schizophyllum commune, an endophytic fungus in Alchornea glandulosa. *Eclética Química Journal* **44**: 36–42. https://doi.org/10.26850/1678-4618eqj.v44.3.2019.p36-42

Rateb ME, Hallyburton I, Houssen WE, Bull AT, Goodfellow M, Santhanam R, Jaspars M, Ebel R, 2013. Induction of diverse secondary metabolites in Aspergillus fumigatus by microbial co-culture. *RSC Advances* **3**: 14444. https://doi.org/10.1039/c3ra42378f

Reveglia P, Masi M, Evidente A, 2020. Melleins—Intriguing Natural Compounds. *Biomolecules* **10**: 772. https://doi.org/10.3390/biom10050772

Ruiz SJ, van 't Klooster JS, Bianchi F, Poolman B, 2020. Growth Inhibition by Amino Acids in Saccharomyces cerevisiae. *Microorganisms* **9**: 7. https://doi.org/10.3390/microorganisms9010007

Shannon P, 2003. Cytoscape: A Software Environment for Integrated Models of Biomolecular Interaction Networks. *Genome Research* **13**: 2498–2504. https://doi.org/10.1101/gr.1239303

Shukla S, Tekwani BL, 2020. Histone Deacetylases Inhibitors in Neurodegenerative Diseases, Neuroprotection and Neuronal Differentiation. *Frontiers in Pharmacology* **11**. https://doi.org/10.3389/fphar.2020.00537

Shwab EK, Bok JW, Tribus M, Galehr J, Graessle S, Keller NP, 2007. Histone Deacetylase Activity Regulates Chemical Diversity in Aspergillus. *Eukaryotic Cell* **6**: 1656–1664. https://doi.org/10.1128/EC.00186-07

Soman AG, Gloer JB, Angawi RF, Wicklow DT, Dowd PF, 2001. Vertilecanins: New Phenopicolinic Acid Analogues from Verticillium l ecanii. *Journal of Natural Products* **64**: 189–192. https://doi.org/10.1021/np000094q

Strobel G, 2018. The emergence of endophytic microbes and their biological promise. *Journal of Fungi* **4**. https://doi.org/10.3390/jof4020057

Strobel G, Daisy B, 2003. Bioprospecting for Microbial Endophytes and Their Natural Products.

Microbiology and Molecular Biology Reviews **67**: 491–502. https://doi.org/10.1128/MMBR.67.4.491-502.2003

Suzuki MM, Bird A, 2008. DNA methylation landscapes: provocative insights from epigenomics. *Nature Reviews Genetics* **9**: 465–476. https://doi.org/10.1038/nrg2341

Toghueo RMK, Sahal D, Boyom FF, 2020. Recent advances in inducing endophytic fungal specialized metabolites using small molecule elicitors including epigenetic modifiers. *Phytochemistry* **174**: 112338. https://doi.org/10.1016/j.phytochem.2020.112338

Triastuti A, Vansteelandt M, Barakat F, Trinel M, Jargeat P, Fabre N, Amasifuen Guerra CA, Mejia K, Valentin A, Haddad M, 2019. How Histone Deacetylase Inhibitors Alter the Secondary Metabolites of Botryosphaeria mamane, an Endophytic Fungus Isolated from Bixa orellana. *Chemistry and Biodiversity* **16**. https://doi.org/10.1002/cbdv.201800485

Tsugawa H, Cajka T, Kind T, Ma Y, Higgins B, Ikeda K, Kanazawa M, VanderGheynst J, Fiehn O, Arita M, 2015. MS-DIAL: data-independent MS/MS deconvolution for comprehensive metabolome analysis. *Nature Methods* **12**: 523–526. https://doi.org/10.1038/nmeth.3393

Vasanthakumari MM, Jadhav SS, Sachin N, Vinod G, Shweta S, Manjunatha BL, Kumara PM, Ravikanth G, Nataraja KN, Uma Shaanker R, 2015. Restoration of camptothecine production in attenuated endophytic fungus on re-inoculation into host plant and treatment with DNA methyltransferase inhibitor. *World Journal of Microbiology and Biotechnology* **31**: 1629–1639. https://doi.org/10.1007/s11274-015-1916-0

Venkatesh N, Keller NP, 2019. Mycotoxins in Conversation With Bacteria and Fungi. *Frontiers in Microbiology* **10**: 1–10. https://doi.org/10.3389/fmicb.2019.00403

Vigneshwari A, Rakk D, Németh A, Kocsubé S, Kiss N, Csupor D, Papp T, Škrbić B, Vágvölgyi C, Szekeres A, 2019. Host metabolite producing endophytic fungi isolated from Hypericum perforatum (V Gupta, Ed,). *PLOS ONE* **14**: e0217060. https://doi.org/10.1371/journal.pone.0217060

Wang X, Li Y, Zhang X, Lai D, Zhou L, 2017a. Structural Diversity and Biological Activities of the Cyclodipeptides from Fungi. *Molecules* **22**: 2026. https://doi.org/10.3390/molecules22122026

Wang X, Lin M, Xu D, Lai D, Zhou L, 2017b. Structural Diversity and Biological Activities of Fungal Cyclic Peptides, Excluding Cyclodipeptides. *Molecules* **22**: 2069. https://doi.org/10.3390/molecules22122069

Wang J, Wang H, Zhang C, Wu T, Ma Z, Chen Y, 2019. Phospholipid homeostasis plays an important role in fungal development, fungicide resistance and virulence in Fusarium graminearum. *Phytopathology Research* **1**: 16. https://doi.org/10.1186/s42483-019-0023-9

Welch TR, Williams RM, 2014. Epidithiodioxopiperazines. occurrence, synthesis and biogenesis. *Natural Product Reports* **31**: 1376–1404. https://doi.org/10.1039/c3np70097f

Wells JM, Cole RJ, Kirksey JW, 1975. Emodin, a Toxic Metabolite of Aspergillus wentii Isolated from Weevil-Damaged Chestnuts. *Applied Microbiology* **30**: 26–28.

https://doi.org/10.1128/am.30.1.26-28.1975

White JF, Kingsley KL, Zhang Q, Verma R, Obi N, Dvinskikh S, Elmore MT, Verma SK, Gond SK, Kowalski KP, 2019. Review: Endophytic microbes and their potential applications in crop management. *Pest Management Science* **75**: 2558–2565. https://doi.org/10.1002/ps.5527

Williams RB, Henrikson JC, Hoover AR, Lee AE, Cichewicz RH, 2008. Epigenetic remodeling of the fungal secondary metabolome. *Organic & Biomolecular Chemistry* **6**: 1895. https://doi.org/10.1039/b804701d

Wu DL, Li HJ, Smith DR, Jaratsittisin J, Xia-Ke-Er XFKT, Ma WZ, Guo YW, Dong J, Shen J, Yang DP, Lan WJ, 2018. Polyketides and alkaloids from the marine-derived fungus Dichotomomyces cejpii F31-1 and the antiviral activity of scequinadoline A against dengue virus. *Marine Drugs* **16**: 1–10. https://doi.org/10.3390/md16070229

Yang J, Gong L, Guo M, Jiang Y, Ding Y, Wang Z, Xin X, An F, 2021. Bioactive Indole Diketopiperazine Alkaloids from the Marine Endophytic Fungus Aspergillus sp. YJ191021. *Marine Drugs* **19**: 157. https://doi.org/10.3390/md19030157

Yamazaki H, Rotinsulu H, Narita R, Takahashi R, Namikoshi M, 2015. Induced Production of Halogenated Epidithiodiketopiperazines by a Marine-Derived Trichoderma cf. brevicompactum with Sodium Halides. *Journal of Natural Products* **78**: 2319–2321. https://doi.org/10.1021/acs.jnatprod.5b00669

Yuan M-X, Qiu Y, Ran Y-Q, Feng G-K, Deng R, Zhu X-F, Lan W-J, Li H-J, 2019. Exploration of Indole Alkaloids from Marine Fungus Pseudallescheria boydii F44-1 Using an Amino Acid-Directed Strategy. *Marine Drugs* **17**: 77. https://doi.org/10.3390/md17020077

Zhang F, Liu S, Lu X, Guo L, Zhang H, Che Y, 2009. Allenyl and Alkynyl Phenyl Ethers from the Endolichenic Fungus Neurospora terricola. *Journal of Natural Products* **72**: 1782–1785. https://doi.org/10.1021/np900512k

Zhang H, Ruan C, Bai X, Chen J, Wang H, 2018. Heterocyclic Alkaloids as Antimicrobial Agents of Aspergillus fumigatus D Endophytic on Edgeworthia chrysantha. *Chemistry of Natural Compounds* **54**: 411–414. https://doi.org/10.1007/s10600-018-2365-4

Chapter 4 – Additional information

Asai T, Otsuki S, Sakurai H, Yamashita K, Ozeki T, Oshima Y, 2013. Benzophenones from an endophytic fungus, graphiopsis chlorocephala, from Paeonia lactiflora cultivated in the presence of an NAD+-dependent HDAC inhibitor. *Organic Letters* **15**: 2058–2061. https://doi.org/10.1021/ol400781b

Chen Y-X, Xu M-Y, Li H-J, Zeng K-J, Ma W-Z, Tian G-B, Xu J, Yang D-P, Lan W-J, 2017. Diverse

Secondary Metabolites from the Marine-Derived Fungus Dichotomomyces cejpii F31-1. *Marine Drugs* **15**: 339. https://doi.org/10.3390/md15110339

El-Neketi M, Ebrahim W, Lin W, Gedara S, Badria F, Saad H-EA, Lai D, Proksch P, 2013. Alkaloids and Polyketides from Penicillium citrinum , an Endophyte Isolated from the Moroccan Plant Ceratonia siliqua. *Journal of Natural Products* **76**: 1099–1104. https://doi.org/10.1021/np4001366

Huang L-H, Xu M-Y, Li H-J, Li J-Q, Chen Y-X, Ma W-Z, Li Y-P, Xu J, Yang D-P, Lan W-J, 2017. Amino Acid-Directed Strategy for Inducing the Marine-Derived Fungus Scedosporium apiospermum F41–1 to Maximize Alkaloid Diversity. *Organic Letters* **19**: 4888–4891. https://doi.org/10.1021/acs.orglett.7b02238

Kimura Y, Mizuno T, Kawano T, Okada K, Shimada A, 2000. Peniamidienone and penidilamine, plant growth regulators produced by the fungus Penicillium sp. No. 13. *Phytochemistry* **53**: 829–831. https://doi.org/10.1016/S0031-9422(99)00492-6

Li L-Y, Ding Y, Groth I, Menzel K-D, Peschel G, Voigt K, Deng Z-W, Sattler I, Lin W-H, 2008. Pyrrole and indole alkaloids from an endophytic Fusarium incarnatum (HKI00504) isolated from the mangrove plant Aegiceras corniculatum. *Journal of Asian Natural Products Research* **10**: 765–770. https://doi.org/10.1080/10286020802031106

Li G, Kusari S, Golz C, Strohmann C, Spiteller M, 2016. Three cyclic pentapeptides and a cyclic lipopeptide produced by endophytic Fusarium decemcellulare LG53. *RSC Advances* **6**: 54092–54098. https://doi.org/10.1039/C6RA10905E

Li H-J, Lin Y-C, Yao J-H, Vrijmoed LLP, Jones EBG, 2004. Two new metabolites from the mangrove endophytic fungus No. 2524. *Journal of Asian Natural Products Research* **6**: 185–191. https://doi.org/10.1080/102860201653237

Liu X, Dong M, Chen X, Jiang M, Lv X, Zhou J, 2008. Antimicrobial activity of an endophytic Xylaria sp.YX-28 and identification of its antimicrobial compound 7-amino-4-methylcoumarin. *Applied Microbiology and Biotechnology* **78**: 241–247. https://doi.org/10.1007/s00253-007-1305-1

Liu M, Sun W, Wang J, He Y, Zhang J, Li F, Qi C, Zhu H, Xue Y, Hu Z, Zhang Y, 2018. Bioactive secondary metabolites from the marine-associated fungus Aspergillus terreus. *Bioorganic Chemistry* **80**: 525–530. https://doi.org/10.1016/j.bioorg.2018.06.029

Loesgen S, Bruhn T, Meindl K, Dix I, Schulz B, Zeeck A, Bringmann G, 2011. (+)-Flavipucine, the Missing Member of the Pyridione Epoxide Family of Fungal Antibiotics. *European Journal of Organic Chemistry* **2011**: 5156–5162. https://doi.org/10.1002/ejoc.201100284

Ruiz SJ, van 't Klooster JS, Bianchi F, Poolman B, 2020. Growth Inhibition by Amino Acids in Saccharomyces cerevisiae. *Microorganisms* **9**: 7. https://doi.org/10.3390/microorganisms9010007

Wu DL, Li HJ, Smith DR, Jaratsittisin J, Xia-Ke-Er XFKT, Ma WZ, Guo YW, Dong J, Shen J, Yang

DP, Lan WJ, 2018. Polyketides and alkaloids from the marine-derived fungus Dichotomomyces cejpii F31-1 and the antiviral activity of scequinadoline A against dengue virus. *Marine Drugs* **16**: 1–10. https://doi.org/10.3390/md16070229

Yang J, Gong L, Guo M, Jiang Y, Ding Y, Wang Z, Xin X, An F, 2021. Bioactive Indole Diketopiperazine Alkaloids from the Marine Endophytic Fungus Aspergillus sp. YJ191021. *Marine Drugs* **19**: 157. https://doi.org/10.3390/md19030157

Chapter 5

de Almeida TT, Ribeiro MA dos S, Polonio JC, Garcia FP, Nakamura CV, Meurer EC, Sarragiotto MH, Baldoqui DC, Azevedo JL, Pamphile JA, 2018. Curvulin and spirostaphylotrichins R and U from extracts produced by two endophytic Bipolaris sp. associated to aquatic macrophytes with antileishmanial activity. *Natural Product Research* **32**: 2783–2790. https://doi.org/10.1080/14786419.2017.1380011

Barakat F, Vansteelandt M, Triastuti A, Jargeat P, Jacquemin D, Graton J, Mejia K, Cabanillas B, Vendier L, Stigliani J-LL, Haddad M, Fabre N, 2019. Thiodiketopiperazines with two spirocyclic centers extracted from Botryosphaeria mamane, an endophytic fungus isolated from Bixa orellana L. *Phytochemistry* **158**: 142–148. https://doi.org/10.1016/j.phytochem.2018.11.007

Benitez L, Correa A, Daroit D, Brandelli A, 2011. Antimicrobial Activity of Bacillus amyloliquefaciens LBM 5006 is Enhanced in the Presence of Escherichia coli. *Current Microbiology* **62**: 1017–1022. https://doi.org/10.1007/s00284-010-9814-z

Chagas FO, Pupo MT, 2018. Chemical interaction of endophytic fungi and actinobacteria from Lychnophora ericoides in co-cultures. *Microbiological Research* **212**–**213**: 10–16. https://doi.org/10.1016/j.micres.2018.04.005

Chapla V, Zeraik M, Leptokarydis I, Silva G, Bolzani V, Young M, Pfenning L, Araújo A, 2014. Antifungal Compounds Produced by Colletotrichum gloeosporioides, an Endophytic Fungus from Michelia champaca. *Molecules* **19**: 19243–19252. https://doi.org/10.3390/molecules191119243

Deshmukh S, Gupta M, Prakash V, Saxena S, 2018. Endophytic Fungi: A Source of Potential Antifungal Compounds. *Journal of Fungi* **4**: 77. https://doi.org/10.3390/jof4030077

Deshmukh SK, Verekar SA, Bhave S V., 2014. Endophytic fungi: A reservoir of antibacterials. *Frontiers in Microbiology* **5**: 1–43. https://doi.org/10.3389/fmicb.2014.00715

Engels D, Zhou XN, 2020. Neglected tropical diseases: An effective global response to local poverty-related disease priorities. *Infectious Diseases of Poverty* **9**: 1–9. https://doi.org/10.1186/s40249-020-0630-9

Fourati-Ben Fguira L, Smaoui S, Karray-Rebai I, Bejar S, Mellouli L, 2008. The antifungal activity of

the terrestrial Streptomyces US80 strain is induced by heat-killed fungi. *Biotechnology Journal* **3**: 1058–1066. https://doi.org/10.1002/biot.200700155

Guo H, Sun B, Gao H, Chen X, Liu S, Yao X, Liu X, Che Y, 2009. Diketopiperazines from the Cordyceps -Colonizing Fungus Epicoccum nigrum. *Journal of Natural Products* **72**: 2115–2119. https://doi.org/10.1021/np900654a

Hilario F, Polinário G, de Amorim MR, de Sousa Batista V, do Nascimento Júnior NM, Araújo AR, Bauab TM, dos Santos LC, 2020. Spirocyclic lactams and curvulinic acid derivatives from the endophytic fungus Curvularia lunata and their antibacterial and antifungal activities. *Fitoterapia* **141**: 104466. https://doi.org/10.1016/j.fitote.2019.104466

Huang S, Ding W, Li C, Cox DG, 2014. Two new cyclopeptides from the co-culture broth of two marine mangrove fungi and their antifungal activity. *Pharmacognosy Magazine* **10**: 410. https://doi.org/10.4103/0973-1296.141781

Huang Z, Nong X, Liang X, Qi S, 2018. New tetramic acid derivatives from the deep-sea-derived fungus Cladosporium sp. SCSIO z0025. *Tetrahedron* **74**: 2620–2626. https://doi.org/10.1016/j.tet.2018.04.010

Hzounda Fokou JB, Dize D, Etame Loe GM, Nko'o MHJ, Ngene JP, Ngoule CC, Boyom FF, 2021. Anti-leishmanial and anti-trypanosomal natural products from endophytes. *Parasitology Research* **120**: 785–796. https://doi.org/10.1007/s00436-020-07035-1

Jiang C-X, Li J, Zhang J-M, Jin X-J, Yu B, Fang J-G, Wu Q-X, 2019. Isolation, Identification, and Activity Evaluation of Chemical Constituents from Soil Fungus Fusarium avenaceum SF-1502 and Endophytic Fungus Fusarium proliferatum AF-04. *Journal of Agricultural and Food Chemistry* **67**: 1839–1846. https://doi.org/10.1021/acs.jafc.8b05576

Kamdem RST, Wang H, Wafo P, Ebrahim W, Özkaya FC, Makhloufi G, Janiak C, Sureechatchaiyan P, Kassack MU, Lin W, Liu Z, Proksch P, 2018. Induction of new metabolites from the endophytic fungus Bionectria sp. through bacterial co-culture. *Fitoterapia* **124**: 132–136. https://doi.org/10.1016/j.fitote.2017.10.021

Kima PE, 2007. The amastigote forms of Leishmania are experts at exploiting host cell processes to establish infection and persist. *International Journal for Parasitology* **37**: 1087–1096. https://doi.org/10.1016/j.ijpara.2007.04.007

Kumarihamy M, Rosa LH, Techen N, Ferreira D, Croom EM, Duke SO, Tekwani BL, Khan S, Nanayakkara NPD, 2020. Antimalarials and Phytotoxins from Botryosphaeria dothidea Identified from a Seed of Diseased Torreya taxifolia. *Molecules* **26**: 59. https://doi.org/10.3390/molecules26010059

Kusakabe Y, Mizutani S, Kamo S, Yoshimoto T, Tomoshige S, Kawasaki T, Takasawa R, Tsubaki K, Kuramochi K, 2019. Synthesis, antibacterial and cytotoxic evaluation of flavipucine and its derivatives. *Bioorganic & Medicinal Chemistry Letters* **29**: 1390–1394. https://doi.org/10.1016/j.bmcl.2019.03.034

Li H-J, Lin Y-C, Yao J-H, Vrijmoed LLP, Jones EBG, 2004. Two new metabolites from the mangrove endophytic fungus No. 2524. *Journal of Asian Natural Products Research* **6**: 185–191. https://doi.org/10.1080/102860201653237

Liang L, Sproule A, Haltli B, Marchbank DH, Berrué F, Overy DP, McQuillan K, Lanteigne M, Duncan N, Correa H, Kerr RG, 2019. Discovery of a New Natural Product and a Deactivation of a Quorum Sensing System by Culturing a "Producer" Bacterium With a Heat-Killed "Inducer" Culture. *Frontiers in Microbiology* **9**. https://doi.org/10.3389/fmicb.2018.03351

Liang L, Wang G, Haltli B, Marchbank DH, Stryhn H, Correa H, Kerr RG, 2020. Metabolomic Comparison and Assessment of Co-cultivation and a Heat-Killed Inducer Strategy in Activation of Cryptic Biosynthetic Pathways. *Journal of Natural Products* **83**: 2696–2705. https://doi.org/10.1021/acs.jnatprod.0c00621

Loesgen S, Bruhn T, Meindl K, Dix I, Schulz B, Zeeck A, Bringmann G, 2011. (+)-Flavipucine, the Missing Member of the Pyridione Epoxide Family of Fungal Antibiotics. *European Journal of Organic Chemistry* **2011**: 5156–5162. https://doi.org/10.1002/ejoc.201100284

Miersch O, Bohlmann H, Wasternack C, 1999. Jasmonates and related compounds from Fusarium oxysporum. *Phytochemistry* **50**: 517–523. https://doi.org/10.1016/S0031-9422(98)00596-2

do Nascimento AM, Conti R, Turatti ICC, Cavalcanti BC, Costa-Lotufo L V., Pessoa C, de Moraes MO, Manfrim V, Toledo JS, Cruz AK, Pupo MT, 2012. Bioactive extracts and chemical constituents of two endophytic strains of Fusarium oxysporum. *Revista Brasileira de Farmacognosia* **22**: 1276–1281. https://doi.org/10.1590/S0102-695X2012005000106

Park HB, Kim YJ, Park JS, Yang HO, Lee KR, Kwon HC, 2011. Glionitrin B, a cancer invasion inhibitory diketopiperazine produced by microbial coculture. *Journal of Natural Products* **74**: 2309–2312. https://doi.org/10.1021/np200563x

Ben Rhouma M, Kriaa M, Ben Nasr Y, Mellouli L, Kammoun R, 2020. A New Endophytic Fusarium Oxysporum Gibberellic Acid: Optimization of Production Using Combined Strategies of Experimental Designs and Potency on Tomato Growth under Stress Condition. *BioMed Research International* **2020**: 1–14. https://doi.org/10.1155/2020/4587148

Santajit S, Indrawattana N, 2016. Mechanisms of Antimicrobial Resistance in ESKAPE Pathogens. *BioMed Research International* **2016**: 1–8. https://doi.org/10.1155/2016/2475067

Shaaban KA, Saunders MA, Zhang Y, Tran T, Elshahawi SI, Ponomareva L V., Wang X, Zhang J, Copley GC, Sunkara M, Kharel MK, Morris AJ, Hower JC, Tremblay MS, Prendergast MA, Thorson JS, 2017. Spoxazomicin D and Oxachelin C, Potent Neuroprotective Carboxamides from the Appalachian Coal Fire-Associated Isolate Streptomyces sp. RM-14-6. *Journal of Natural Products* **80**: 2–11. https://doi.org/10.1021/acs.jnatprod.6b00948

Shea JM, Del Poeta M, 2006. Lipid signaling in pathogenic fungi. *Current Opinion in Microbiology* **9**: 352–358. https://doi.org/10.1016/j.mib.2006.06.003

Smelt JPPM, Brul S, 2014. Thermal Inactivation of Microorganisms. *Critical Reviews in Food Science*

and Nutrition **54**: 1371–1385. https://doi.org/10.1080/10408398.2011.637645

Talontsi FM, Facey P, Tatong MDK, Tofazzal Islam M, Frauendorf H, Draeger S, Tiedemann A Von, Laatsch H, 2012. Zoosporicidal metabolites from an endophytic fungus Cryptosporiopsis sp. of Zanthoxylum leprieurii. *Phytochemistry* **83**: 87–94. https://doi.org/10.1016/j.phytochem.2012.06.006

Triastuti A, Haddad M, Barakat F, Mejia K, Rabouille G, Fabre N, Amasifuen C, Jargeat P, Vansteelandt M, 2021. Dynamics of Chemical Diversity during Co-Cultures: An Integrative Time-Scale Metabolomics Study of Fungal Endophytes Cophinforma mamane and Fusarium solani. *Chemistry & Biodiversity* **18**. https://doi.org/10.1002/cbdv.202000672

Triastuti A, Vansteelandt M, Barakat F, Jargeat P, Rieusset L, Fabre N, Amasifuen C, Valentin A, Haddad M, 2016. Search for novel metabolites in fungal endophytes: study of Phomopsis sp. and Colletotrichum sp. co-cultivation and Botryosphaeria mamane epigenetic modification. *Planta Medica* **81**: S1–S381.

Verbeke F, De Craemer S, Debunne N, Janssens Y, Wynendaele E, Van de Wiele C, De Spiegeleer B, 2017. Peptides as Quorum Sensing Molecules: Measurement Techniques and Obtained Levels In vitro and In vivo. *Frontiers in Neuroscience* **11**. https://doi.org/10.3389/fnins.2017.00183

Wang W-X, Kusari S, Sezgin S, Lamshöft M, Kusari P, Kayser O, Spiteller M, 2015. Hexacyclopeptides secreted by an endophytic fungus Fusarium solani N06 act as crosstalk molecules in Narcissus tazetta. *Applied Microbiology and Biotechnology* **99**: 7651–7662. https://doi.org/10.1007/s00253-015-6653-7

Wang X, Li Y, Zhang X, Lai D, Zhou L, 2017. Structural Diversity and Biological Activities of the Cyclodipeptides from Fungi. *Molecules* **22**: 2026. https://doi.org/10.3390/molecules22122026

Yu L, Ding W, Wang Q, Ma Z, Xu X, Zhao X, Chen Z, 2017. Induction of cryptic bioactive 2,5-diketopiperazines in fungus Penicillium sp. DT-F29 by microbial co-culture. *Tetrahedron* **73**: 907–914. https://doi.org/10.1016/j.tet.2016.12.077

de Almeida TT, Ribeiro MA dos S, Polonio JC, Garcia FP, Nakamura CV, Meurer EC, Sarragiotto MH, Baldoqui DC, Azevedo JL, Pamphile JA, 2018. Curvulin and spirostaphylotrichins R and U from extracts produced by two endophytic Bipolaris sp. associated to aquatic macrophytes with antileishmanial activity. *Natural Product Research* **32**: 2783–2790. https://doi.org/10.1080/14786419.2017.1380011

Barakat F, Vansteelandt M, Triastuti A, Jargeat P, Jacquemin D, Graton J, Mejia K, Cabanillas B, Vendier L, Stigliani J-LL, Haddad M, Fabre N, 2019. Thiodiketopiperazines with two spirocyclic centers extracted from Botryosphaeria mamane, an endophytic fungus isolated from Bixa orellana L. *Phytochemistry* **158**: 142–148. https://doi.org/10.1016/j.phytochem.2018.11.007

Benitez L, Correa A, Daroit D, Brandelli A, 2011. Antimicrobial Activity of Bacillus amyloliquefaciens LBM 5006 is Enhanced in the Presence of Escherichia coli. *Current Microbiology* **62**: 1017–1022. https://doi.org/10.1007/s00284-010-9814-z

Chagas FO, Pupo MT, 2018. Chemical interaction of endophytic fungi and actinobacteria from Lychnophora ericoides in co-cultures. *Microbiological Research* **212**–**213**: 10–16. https://doi.org/10.1016/j.micres.2018.04.005

Chapla V, Zeraik M, Leptokarydis I, Silva G, Bolzani V, Young M, Pfenning L, Araújo A, 2014. Antifungal Compounds Produced by Colletotrichum gloeosporioides, an Endophytic Fungus from Michelia champaca. *Molecules* **19**: 19243–19252. https://doi.org/10.3390/molecules191119243

Deshmukh S, Gupta M, Prakash V, Saxena S, 2018. Endophytic Fungi: A Source of Potential Antifungal Compounds. *Journal of Fungi* **4**: 77. https://doi.org/10.3390/jof4030077

Deshmukh SK, Verekar SA, Bhave S V., 2014. Endophytic fungi: A reservoir of antibacterials. *Frontiers in Microbiology* **5**: 1–43. https://doi.org/10.3389/fmicb.2014.00715

Engels D, Zhou XN, 2020. Neglected tropical diseases: An effective global response to local poverty-related disease priorities. *Infectious Diseases of Poverty* **9**: 1–9. https://doi.org/10.1186/s40249-020-0630-9

Fourati-Ben Fguira L, Smaoui S, Karray-Rebai I, Bejar S, Mellouli L, 2008. The antifungal activity of the terrestrial Streptomyces US80 strain is induced by heat-killed fungi. *Biotechnology Journal* **3**: 1058–1066. https://doi.org/10.1002/biot.200700155

Guo H, Sun B, Gao H, Chen X, Liu S, Yao X, Liu X, Che Y, 2009. Diketopiperazines from the Cordyceps -Colonizing Fungus Epicoccum nigrum. *Journal of Natural Products* **72**: 2115–2119. https://doi.org/10.1021/np900654a

Hilario F, Polinário G, de Amorim MR, de Sousa Batista V, do Nascimento Júnior NM, Araújo AR, Bauab TM, dos Santos LC, 2020. Spirocyclic lactams and curvulinic acid derivatives from the endophytic fungus Curvularia lunata and their antibacterial and antifungal activities. *Fitoterapia* **141**: 104466. https://doi.org/10.1016/j.fitote.2019.104466

Huang S, Ding W, Li C, Cox DG, 2014. Two new cyclopeptides from the co-culture broth of two marine mangrove fungi and their antifungal activity. *Pharmacognosy Magazine* **10**: 410. https://doi.org/10.4103/0973-1296.141781

Huang Z, Nong X, Liang X, Qi S, 2018. New tetramic acid derivatives from the deep-sea-derived fungus Cladosporium sp. SCSIO z0025. *Tetrahedron* **74**: 2620–2626. https://doi.org/10.1016/j.tet.2018.04.010

Hzounda Fokou JB, Dize D, Etame Loe GM, Nko'o MHJ, Ngene JP, Ngoule CC, Boyom FF, 2021. Anti-leishmanial and anti-trypanosomal natural products from endophytes. *Parasitology Research* **120**: 785–796. https://doi.org/10.1007/s00436-020-07035-1

Jiang C-X, Li J, Zhang J-M, Jin X-J, Yu B, Fang J-G, Wu Q-X, 2019. Isolation, Identification, and Activity Evaluation of Chemical Constituents from Soil Fungus Fusarium avenaceum SF-1502 and Endophytic Fungus Fusarium proliferatum AF-04. *Journal of Agricultural and Food Chemistry* **67**: 1839–1846. https://doi.org/10.1021/acs.jafc.8b05576

Kamdem RST, Wang H, Wafo P, Ebrahim W, Özkaya FC, Makhloufi G, Janiak C, Sureechatchaiyan P, Kassack MU, Lin W, Liu Z, Proksch P, 2018. Induction of new metabolites from the endophytic fungus Bionectria sp. through bacterial co-culture. *Fitoterapia* **124**: 132–136. https://doi.org/10.1016/j.fitote.2017.10.021

Kima PE, 2007. The amastigote forms of Leishmania are experts at exploiting host cell processes to establish infection and persist. *International Journal for Parasitology* **37**: 1087–1096. https://doi.org/10.1016/j.ijpara.2007.04.007

Kumarihamy M, Rosa LH, Techen N, Ferreira D, Croom EM, Duke SO, Tekwani BL, Khan S, Nanayakkara NPD, 2020. Antimalarials and Phytotoxins from Botryosphaeria dothidea Identified from a Seed of Diseased Torreya taxifolia. *Molecules* **26**: 59. https://doi.org/10.3390/molecules26010059

Kusakabe Y, Mizutani S, Kamo S, Yoshimoto T, Tomoshige S, Kawasaki T, Takasawa R, Tsubaki K, Kuramochi K, 2019. Synthesis, antibacterial and cytotoxic evaluation of flavipucine and its derivatives. *Bioorganic & Medicinal Chemistry Letters* **29**: 1390–1394. https://doi.org/10.1016/j.bmcl.2019.03.034

Li H-J, Lin Y-C, Yao J-H, Vrijmoed LLP, Jones EBG, 2004. Two new metabolites from the mangrove endophytic fungus No. 2524. *Journal of Asian Natural Products Research* **6**: 185–191. https://doi.org/10.1080/102860201653237

Liang L, Sproule A, Haltli B, Marchbank DH, Berrué F, Overy DP, McQuillan K, Lanteigne M, Duncan N, Correa H, Kerr RG, 2019. Discovery of a New Natural Product and a Deactivation of a Quorum Sensing System by Culturing a "Producer" Bacterium With a Heat-Killed "Inducer" Culture. *Frontiers in Microbiology* **9**. https://doi.org/10.3389/fmicb.2018.03351

Liang L, Wang G, Haltli B, Marchbank DH, Stryhn H, Correa H, Kerr RG, 2020. Metabolomic Comparison and Assessment of Co-cultivation and a Heat-Killed Inducer Strategy in Activation of Cryptic Biosynthetic Pathways. *Journal of Natural Products* **83**: 2696–2705. https://doi.org/10.1021/acs.jnatprod.0c00621

Loesgen S, Bruhn T, Meindl K, Dix I, Schulz B, Zeeck A, Bringmann G, 2011. (+)-Flavipucine, the Missing Member of the Pyridione Epoxide Family of Fungal Antibiotics. *European Journal of Organic Chemistry* **2011**: 5156–5162. https://doi.org/10.1002/ejoc.201100284

Miersch O, Bohlmann H, Wasternack C, 1999. Jasmonates and related compounds from Fusarium oxysporum. *Phytochemistry* **50**: 517–523. https://doi.org/10.1016/S0031-9422(98)00596-2

do Nascimento AM, Conti R, Turatti ICC, Cavalcanti BC, Costa-Lotufo L V., Pessoa C, de Moraes MO, Manfrim V, Toledo JS, Cruz AK, Pupo MT, 2012. Bioactive extracts and chemical constituents of two endophytic strains of Fusarium oxysporum. *Revista Brasileira de Farmacognosia* **22**: 1276–1281. https://doi.org/10.1590/S0102-695X2012005000106

Park HB, Kim YJ, Park JS, Yang HO, Lee KR, Kwon HC, 2011. Glionitrin B, a cancer invasion inhibitory diketopiperazine produced by microbial coculture. *Journal of Natural Products* **74**:

2309–2312. https://doi.org/10.1021/np200563x

Ben Rhouma M, Kriaa M, Ben Nasr Y, Mellouli L, Kammoun R, 2020. A New Endophytic Fusarium Oxysporum Gibberellic Acid: Optimization of Production Using Combined Strategies of Experimental Designs and Potency on Tomato Growth under Stress Condition. *BioMed Research International* **2020**: 1–14. https://doi.org/10.1155/2020/4587148

Santajit S, Indrawattana N, 2016. Mechanisms of Antimicrobial Resistance in ESKAPE Pathogens. *BioMed Research International* **2016**: 1–8. https://doi.org/10.1155/2016/2475067

Shaaban KA, Saunders MA, Zhang Y, Tran T, Elshahawi SI, Ponomareva L V., Wang X, Zhang J, Copley GC, Sunkara M, Kharel MK, Morris AJ, Hower JC, Tremblay MS, Prendergast MA, Thorson JS, 2017. Spoxazomicin D and Oxachelin C, Potent Neuroprotective Carboxamides from the Appalachian Coal Fire-Associated Isolate Streptomyces sp. RM-14-6. *Journal of Natural Products* **80**: 2–11. https://doi.org/10.1021/acs.jnatprod.6b00948

Shea JM, Del Poeta M, 2006. Lipid signaling in pathogenic fungi. *Current Opinion in Microbiology* **9**: 352–358. https://doi.org/10.1016/j.mib.2006.06.003

Smelt JPPM, Brul S, 2014. Thermal Inactivation of Microorganisms. *Critical Reviews in Food Science and Nutrition* **54**: 1371–1385. https://doi.org/10.1080/10408398.2011.637645

Talontsi FM, Facey P, Tatong MDK, Tofazzal Islam M, Frauendorf H, Draeger S, Tiedemann A Von, Laatsch H, 2012. Zoosporicidal metabolites from an endophytic fungus Cryptosporiopsis sp. of Zanthoxylum leprieurii. *Phytochemistry* **83**: 87–94. https://doi.org/10.1016/j.phytochem.2012.06.006

Triastuti A, Haddad M, Barakat F, Mejia K, Rabouille G, Fabre N, Amasifuen C, Jargeat P, Vansteelandt M, 2021. Dynamics of Chemical Diversity during Co-Cultures: An Integrative Time-Scale Metabolomics Study of Fungal Endophytes Cophinforma mamane and Fusarium solani. *Chemistry & Biodiversity* **18**. https://doi.org/10.1002/cbdv.202000672

Triastuti A, Vansteelandt M, Barakat F, Jargeat P, Rieusset L, Fabre N, Amasifuen C, Valentin A, Haddad M, 2016. Search for novel metabolites in fungal endophytes: study of Phomopsis sp. and Colletotrichum sp. co-cultivation and Botryosphaeria mamane epigenetic modification. *Planta Medica* **81**: S1–S381.

Verbeke F, De Craemer S, Debunne N, Janssens Y, Wynendaele E, Van de Wiele C, De Spiegeleer B, 2017. Peptides as Quorum Sensing Molecules: Measurement Techniques and Obtained Levels In vitro and In vivo. *Frontiers in Neuroscience* **11**. https://doi.org/10.3389/fnins.2017.00183

Wang W-X, Kusari S, Sezgin S, Lamshöft M, Kusari P, Kayser O, Spiteller M, 2015. Hexacyclopeptides secreted by an endophytic fungus Fusarium solani N06 act as crosstalk molecules in Narcissus tazetta. *Applied Microbiology and Biotechnology* **99**: 7651–7662. https://doi.org/10.1007/s00253-015-6653-7

Wang X, Li Y, Zhang X, Lai D, Zhou L, 2017. Structural Diversity and Biological Activities of the Cyclodipeptides from Fungi. *Molecules* **22**: 2026. https://doi.org/10.3390/molecules22122026

Yu L, Ding W, Wang Q, Ma Z, Xu X, Zhao X, Chen Z, 2017. Induction of cryptic bioactive 2,5-diketopiperazines in fungus Penicillium sp. DT-F29 by microbial co-culture. *Tetrahedron* **73**: 907–914. https://doi.org/10.1016/j.tet.2016.12.077

General Discussions

Barakat F, 2018. Etude mycochimique et activités leishmanicides de composés issus de Botryosphaeria mamane, un champignon endophyte isolé de Bixa orellana L. Université Paul Sabatier Toulouse III.

Barakat F, Vansteelandt M, Triastuti A, Jargeat P, Jacquemin D, Graton J, Mejia K, Cabanillas B, Vendier L, Stigliani J-LL, Haddad M, Fabre N, 2019. Thiodiketopiperazines with two spirocyclic centers extracted from Botryosphaeria mamane, an endophytic fungus isolated from Bixa orellana L. *Phytochemistry* **158**: 142–148. https://doi.org/10.1016/j.phytochem.2018.11.007

Bofinger MR, de Sousa LS, Fontes JEN, Marsaioli AJ, 2017. Diketopiperazines as Cross-Communication Quorum - Sensing Signals between Cronobacter sakazakii and Bacillus cereus. *ACS Omega* **2**: 1003–1008. https://doi.org/10.1021/acsomega.6b00513

Brakhage AA, 2013. Regulation of fungal secondary metabolism. *Nature Reviews Microbiology* **11**: 21–32. https://doi.org/10.1038/nrmicro2916

Caesar LK, Kellogg JJ, Kvalheim OM, Cech NB, 2019. Opportunities and Limitations for Untargeted Mass Spectrometry Metabolomics to Identify Biologically Active Constituents in Complex Natural Product Mixtures. *Journal of Natural Products* **82**: 469–484. https://doi.org/10.1021/acs.jnatprod.9b00176

Demarque DP, Dusi RG, de Sousa FDM, Grossi SM, Silvério MRS, Lopes NP, Espindola LS, 2020. Mass spectrometry-based metabolomics approach in the isolation of bioactive natural products. *Scientific Reports* **10**: 1–9. https://doi.org/10.1038/s41598-020-58046-y

Deshmukh S, Gupta M, Prakash V, Saxena S, 2018. Endophytic Fungi: A Source of Potential Antifungal Compounds. *Journal of Fungi* **4**: 77. https://doi.org/10.3390/jof4030077

Jiang C-S, Guo Y-W, 2011. Epipolythiodioxopiperazines from Fungi: Chemistry and Bioactivities. *Mini-Reviews in Medicinal Chemistry* **11**: 728–745. https://doi.org/10.2174/138955711796355276

Kamdem RST, Wang H, Wafo P, Ebrahim W, Özkaya FC, Makhloufi G, Janiak C, Sureechatchaiyan P, Kassack MU, Lin W, Liu Z, Proksch P, 2018. Induction of new metabolites from the endophytic fungus Bionectria sp. through bacterial co-culture. *Fitoterapia* **124**: 132–136. https://doi.org/10.1016/j.fitote.2017.10.021

Li G, Kusari S, Golz C, Strohmann C, Spiteller M, 2016. Three cyclic pentapeptides and a cyclic

lipopeptide produced by endophytic Fusarium decemcellulare LG53. *RSC Advances* **6**: 54092–54098. https://doi.org/10.1039/C6RA10905E

Marshall DD, Powers R, 2017. Beyond the paradigm: Combining mass spectrometry and nuclear magnetic resonance for metabolomics. *Progress in Nuclear Magnetic Resonance Spectroscopy* **100**: 1–16. https://doi.org/10.1016/j.pnmrs.2017.01.001

Pinu FR, Beale DJ, Paten AM, Kouremenos K, Swarup S, Schirra HJ, Wishart D, 2019. Systems Biology and Multi-Omics Integration: Viewpoints from the Metabolomics Research Community. *Metabolites* **9**: 76. https://doi.org/10.3390/metabo9040076

Rateb ME, Hallyburton I, Houssen WE, Bull AT, Goodfellow M, Santhanam R, Jaspars M, Ebel R, 2013. Induction of diverse secondary metabolites in Aspergillus fumigatus by microbial co-culture. *RSC Advances* **3**: 14444. https://doi.org/10.1039/c3ra42378f

Van Santen JA, Jacob G, Singh AL, Aniebok V, Balunas MJ, Bunsko D, Neto FC, Castaño-Espriu L, Chang C, Clark TN, Cleary Little JL, Delgadillo DA, Dorrestein PC, Duncan KR, Egan JM, Galey MM, Haeckl FPJ, Hua A, Hughes AH, Iskakova D, Khadilkar A, Lee JH, Lee S, Legrow N, Liu DY, Macho JM, McCaughey CS, Medema MH, Neupane RP, O'Donnell TJ, Paula JS, Sanchez LM, Shaikh AF, Soldatou S, Terlouw BR, Tran TA, Valentine M, Van Der Hooft JJJ, Vo DA, Wang M, Wilson D, Zink KE, Linington RG, 2019. The Natural Products Atlas: An Open Access Knowledge Base for Microbial Natural Products Discovery. *ACS Central Science* **5**: 1824–1833. https://doi.org/10.1021/acscentsci.9b00806

Scharf DH, Habel A, Heinekamp T, Brakhage AA, Hertweck C, 2014. Opposed effects of enzymatic gliotoxin N - And S -methylations. *Journal of the American Chemical Society* **136**: 11674–11679. https://doi.org/10.1021/ja5033106

Triastuti A, Haddad M, Barakat F, Mejia K, Rabouille G, Fabre N, Amasifuen C, Jargeat P, Vansteelandt M, 2021. Dynamics of Chemical Diversity during Co-Cultures: An Integrative Time-Scale Metabolomics Study of Fungal Endophytes Cophinforma mamane and Fusarium solani. *Chemistry & Biodiversity* **18**. https://doi.org/10.1002/cbdv.202000672

Triastuti A, Vansteelandt M, Barakat F, Trinel M, Jargeat P, Fabre N, Amasifuen Guerra CA, Mejia K, Valentin A, Haddad M, 2019. How Histone Deacetylase Inhibitors Alter the Secondary Metabolites of Botryosphaeria mamane, an Endophytic Fungus Isolated from Bixa orellana. *Chemistry and Biodiversity* **16**. https://doi.org/10.1002/cbdv.201800485

Wang W-X, Kusari S, Sezgin S, Lamshöft M, Kusari P, Kayser O, Spiteller M, 2015. Hexacyclopeptides secreted by an endophytic fungus Fusarium solani N06 act as crosstalk molecules in Narcissus tazetta. *Applied Microbiology and Biotechnology* **99**: 7651–7662. https://doi.org/10.1007/s00253-015-6653-7

Wang X, Lin M, Xu D, Lai D, Zhou L, 2017. Structural Diversity and Biological Activities of Fungal Cyclic Peptides, Excluding Cyclodipeptides. *Molecules* **22**: 2069. https://doi.org/10.3390/molecules22122069

Welch TR, Williams RM, 2014. Epidithiodioxopiperazines. occurrence, synthesis and biogenesis. *Natural Product Reports* **31**: 1376–1404. https://doi.org/10.1039/c3np70097f

Yu Z, Fischer R, 2019. Light sensing and responses in fungi. *Nature Reviews Microbiology* **17**: 25–36. https://doi.org/10.1038/s41579-018-0109-x

ANNEXE 1 - TIME-SERIES STUDY

ID	Alignment	Average.Rt.min	Average.Mz	Adduct.type	Formula	Structure	Total.score	Theoretical.mass	Mass.error
1	1006	5.082	297.18481	[M+H]+	C20H24O2	17a-Ethynylestradiol	5.2195	296.17763	0.0001065
2	101	3.117	135.1012	[M+H]+	C6H14O3			134.0942943	0.0003708
3	1010	8.379	297.24203	[M+H-H2O]+	C18H34O4	Octadecanedioic acid	5.1112	314.2457096	0.0004213
4	1032	5.2	300.17975	[M+H]+	C15H25NO5			299.1732729	0.0008494
5	1036	3.437	300.20148	[M+NH4]+	C12H26O7			282.1678532	0.0001787
6	1041	7.447	301.28476	[M+H]+	C17H36N2O2			300.2776784	0.0001548
7	1044	5.092	302.15915	[M+H]+	C14H23NO6			301.1525375	0.0007139
8	1055	8.734	304.2988	[M+H]+					
9	1072	0.946	308.14929	[M+H]+	C16H21NO5			307.1419728	-5.08E-05
10	1073	5.578	308.14932	[M+H]+	C16H21NO5			307.1419728	-5.08E-05
11	108	0.879	140.06798	[M+Na]+	C5H11NO2	L-Valine	5.4877	117.0789786	0.0001993
12	1081	5.735	309.08722	[M+H]+	C17H12N2O4			308.0797069	-0.0002167
13	1086	8.875	309.24249	[M+H]+	C19H32O3	androstane-3beta,6alpha,17b	5.035	308.2351449	-7.87E-05
14	1094	5.962	310.22198	[M+NH4]+	C14H28O6			292.1885886	0.0004142
15	1102	11.079	311.16382	[M+H]+	C20H22O3			310.1568946	0.000371
16	1111	9.248	312.22198	[M+H]+					
17	1114	10.195	312.35995	[M+H]+					
18	1335	2.83	344.17001	[M+H]+	C16H25NO7			343.1631021	0.0003786
19	1121	8.34	313.32172	[M+H]+	C19H40N2O			312.3140639	-0.0003596
20	1138	4.357	315.19589	[M+H]+	C20H26O3	4-oxo-Retinoic acid	5.3372	314.1881947	-0.0004289
21	1139	3.811	315.19604	[M+H]+	C20H26O3	4-oxo-Retinoic acid	5.1338	314.1881947	-0.0005289
22	1160	5.002	318.15482	[M+H-H2O]+	C15H21N5O4			335.1593542	0.0012659
23	1162	8.39	318.29987	[M+H]+	C18H39NO3	Phytosphingosine	5.1831	317.2929941	0.0003706
24	1169	5.219	319.66742	[M+2H]2+					
25	1183	5.526	322.16431	[M+H-H2O]+	C17H25NO6			339.1681875	0.0005993
26	1808	4.829	428.16754	[M+H]+	C18H25N3O9			427.1590794	-0.0011442
27	1194	4.452	324.1806	[M+H]+	C17H25NO5			323.1732729	-5.06E-05
28	1075	5.298	308.14941	[M+H-H2O]+	C16H23NO6			325.1525375	-0.0001508
29	1085	5.403	309.22675	[M+H]+	C15H32O6			308.2198887	0.0004652
30	1220	5.456	327.15518	[M+H]+	C15H22N2O6			326.1477864	-0.0001371
31	1231	5.102	328.1745	[M+H]+	C16H25NO6			327.1681875	0.000964
32	1233	4.978	328.1756	[M+H]+	C16H25NO6			327.1681875	-0.000136
33	1245	8.343	329.31604	[M+H]+					
34	125	0.903	147.07593	[M+NH4]+	C5H7NO3	Pyroglutamic acid	5.0851	129.0425931	0.0005186
35	1250	8.907	330.29791	[M+H]+					
36	1253	9.091	330.33633	[M+H]+	C20H43NO2			329.3293796	0.0003561
37	1262	6.481	332.15277	[M+H]+					
38	1267	8.472	332.27905	[M+H]+	C18H37NO4			331.2722587	0.0004351
39	1277	5.263	334.13181	[M+H]+	C14H23NO6S			333.1246085	8.49E-05
40	1289	5.199	336.14355	[M+H]+	C17H21NO6			335.1368874	0.0005638
41	1293	10.706	336.32571	[M+H-H2O]+	C22H43NO2			353.3293796	0.0003914
42	1294	8.6	337.10425	[M+Na]+	C18H18O5			314.1154237	0.0004444

43	1310	10.657	340.39404	[M+H]+					
44	1313	5.639	341.17093	[M+H]+	C16H24N2O6			340.1634365	-0.0001871
45	1324	6.071	342.15482	[M+H]+	C16H23NO7			341.1474521	-7.15E-05
46	1325	5.881	342.15509	[M+H]+	C16H23NO7			341.1474521	-0.0003715
47	1334	4.991	344.16977	[M+H]+	C16H25NO7			343.1631021	0.0005786
48	1338	5.429	344.20663	[M+Na]+	C16H27N5O2			321.2164751	-0.0009042
49	1340	5.714	344.20688	[M+H]+	C17H29NO6			343.1994876	-0.0001359
50	1341	3.674	344.228	[M+H]+					
51	1347	4.525	345.20178	[M+H]+	C16H28N2O6			344.1947366	0.0002131
52	1352	4.056	346.186	[M+H]+	C16H27NO7			345.1787522	2.87E-05
53	1354	9.127	346.33084	[M+H]+					
54	1363	4.724	350.17105	[M+H]+	C17H23N3O5			349.1637708	-5.27E-05
55	1378	6.024	352.14249	[M+H]+	C14H25NO7S			351.1351731	-5.04E-05
56	1379	6.228	352.14276	[M+NH4]+	C15H18N4O3S			334.1099614	0.000987
57	139	1.192	151.09625	[M+H]+	C6H14O4			150.0892089	0.0001854
58	1303	11.938	339.32559	[M+H-H2O]+	C22H44O3	22-Hydroxydocosanoic acid	5.1297	356.3290453	0.000157
59	1422	3.966	358.26956	[2M+H]+					
60	1432	4.277	359.21732	[M+H]+	C17H30N2O6			358.2103867	0.0003631
61	1436	7.062	360.15591	[M+NH4]+	C18H18N2O5			342.1215717	-0.0005028
62	144	1.182	153.0753	[M+H]+	C5H12O5			152.0684735	0.0004499
63	1463	9.647	365.13528	[M+Na]+	C20H22O5			342.1467238	0.0006445
64	1465	4.102	366.12152	[M+H]+	C18H15N5O4			365.112404	-0.0018196
65	1474	4.548	368.181	[M+H]+	C17H25N3O6			367.1743355	0.000612
66	1477	11.043	368.42523	[M+H]+					
67	1479	5.202	369.21307	[M+NH4]+	C17H25N3O5			351.1794209	0.0001465
68	1509	10.947	374.30295	[M+Na]+	C22H41NO2			351.3137296	5.03E-05
69	1514	8.111	375.19843	[M+H]+	C22H30O3S			374.1915658	0.0004423
70	1521	8.515	376.30508	[M+NH4]+	C20H38O5			358.2719243	0.0006499
71	1531	10.566	377.32059	[M+H]+	C28H40			376.3130013	-0.0003223
72	1538	6.089	378.19098	[M+H-2H2O]+	C20H31NO8			413.204967	0.000114
73	1539	5.811	378.19113	[M+H]+	C20H27NO6			377.1838376	1.40E-05
74	1548	4.531	380.18088	[M+H]+	C18H25N3O6			379.1743355	0.000712
75	1563	5.021	382.1853	[M+H]+	C19H27NO7			381.1787522	0.0007287
76	1566	4.892	383.08353	[M+H]+	C15H18N4O4S2			382.0769471	0.0007235
77	1567	9.947	383.20413	[M+Na]+	C18H32O7			360.2148034	-7.59E-05
78	1596	4.352	387.224	[2M+Na]+	C8H14N4O			182.1167611	-0.0009029
79	1603	3.867	388.25351	[M+H]+	C21H33N5S			387.2456671	-0.0005565
80	1618	4.804	392.19128	[M+H]+	C17H29NO9			391.1842315	0.000208
81	1620	10.146	392.328	[M+H]+	C23H41N3O2			391.3198776	-0.000846
82	1632	5.496	394.18604	[M+H]+	C20H27NO7			393.1787522	2.87E-05
83	1642	11.644	395.3306	[M+H]+	C28H42O	sta-5,7,22,24(28)-tetraen-3be	5.2604	394.323566	0.0002424
84	1656	4.896	398.18042	[M+H]+	C19H27NO8			397.1736668	0.0005433
85	1658	10.972	398.233	[M+H]+	C24H31NO4			397.2253085	-0.0004151
86	1679	9.483	402.35648	[M+H]+	C23H47NO4			401.350509	0.0012854
87	1681	5.006	403.20697	[M+H]+	C22H30N2O3S			402.1977138	-0.0020097

88	1597	7.605	387.27371	[M+H]+	C21H38O6	6-deoxyerythronolide B	5.3016	386.2668389	0.0004154
89	1692	11.063	407.27158	[M+H]+	C23H38N2O2S			406.2653995	0.0010759
90	1502	7.98	373.25739	[2M+H]+	C10H18O3			186.1255944	0.0002584
91	1713	12.03	409.30969	[M+H]+	C28H40O2			408.3028305	0.000407
92	1718	4.645	410.2287	[M+H]+	C21H27N7O2			409.2226231	0.0011996
93	1724	12.363	411.32523	[M+H]+	C28H42O2	Gamma-Tocotrienol	5.5606	410.3184806	0.000557
94	1726	5.351	412.20715	[M+H]+	C23H29N3O2S		5.0592	411.1980482	-0.0018754
95	1742	4.74	415.25558	[M+H]+	C19H34N4O6			414.2478348	-0.0004887
96	1771	5.863	422.1806	[M+H]+	C22H23N5O4			421.1750042	0.0016807
97	1683	10.553	403.23276	[M+H]+	C20H34O8			402.225368	-0.0001555
98	1803	11.394	427.3208	[M+H]+	C28H42O3			426.3133952	-0.0001283
99	1817	11.528	429.26062	[M+Na]+	C24H38O5	7-Ketodeoxycholic acid	5.0478	406.2719243	0.000545
100	1837	8.263	432.23782	[M+NH4]+	C24H30O6			414.2042387	0.0002642
101	1838	4.031	432.27994	[M+H]+	C19H37N5O6			431.2743839	0.0017604
102	1850	10.009	436.35751	[M+H]+	C30H45NO			435.3501151	-0.0001085
103	1855	8.266	437.19345	[M+Na]+	C24H30O6			414.2042387	-4.06E-05
104	1873	6.564	440.22745	[M+H]+	C22H33NO8			439.220617	0.0004935
105	1878	8.267	441.2576	[M+NH4]+	C22H33NO7			423.2257024	0.0019279
106	1879	8.051	441.25845	[M+NH4]+	C22H33NO7			423.2257024	0.0010279
107	1891	6.701	442.24338	[M+H]+	C22H35NO8			441.2362671	0.0001435
108	1893	6.611	442.24362	[2M+NH4]+	C11H16O4			212.104859	-0.0003025
109	1895	6.847	442.24414	[M+H]+	C23H31N5O4			441.2376045	0.0007809
110	1901	11.542	443.20456	[M+Na]+	C23H32O7			420.2148034	-0.0005759
111	1934	12.117	449.30225	[M+H-2H2O]+					
112	1937	7.505	450.07834	[M+NH4]+	C19H16N2O6S2	Botryosulfuranol C			
113	490	6.279	225.08673	[M+H]+	C10H12N2O4	Hydroxykynurenine	5.4224	224.0797069	0.0002833
114	1948	9.471	452.32147	[M+NH4]+	C23H38N4O4			434.2893057	0.0016312
115	1961	9.672	454.29193	[M+H]+	C21H44NO7P			453.2855394	0.0009158
116	1970	7.324	456.26086	[M+H]+	C24H33N5O4			455.2532545	-0.000369
117	1972	11.813	456.31046	[M+H]+	C28H41NO4			455.3035588	0.0003352
118	1802	11.094	427.24567	[M+Na]+	C24H36O5	Lovastatin	6.0218	404.2562743	-0.000205
119	2017	11.949	463.28152	[M+Na]+	C28H40O4	chaxalactin A, (rel)-	5.1483	440.2926598	0.0003805
120	2005	4.85	460.25354	[M+H]+	C22H37NO9			459.2468318	0.0006082
121	2030	12.211	465.29791	[M+H]+	C30H40O4			464.2926598	0.0020362
122	2063	8.211	475.25754	[M+H]+	C29H34N2O4			474.2518576	0.001634
123	2064	7.686	475.25903	[M+H]+	C29H34N2O4			474.2518576	0.000134
124	2073	8.651	476.27695	[M+H]+	C23H42NO7P			475.2698893	0.0002658
125	1392	4.173	355.18668	[M+H]+	C15H31O7P			354.18074	0.0013164
126	2083	9.212	478.29099	[M+Na]+	C28H41NO4			455.3035588	0.0017795
127	2084	9.033	478.29358	[M+H]+	C23H44NO7P	LysoPE(18:2(9Z,12Z)/0:0)	5.0817	477.2855394	-0.0007842
128	2094	9.917	480.30856	[M+H]+	C23H46NO7P			479.3011894	-0.0001341
129	2095	9.719	480.30933	[M+H]+	C23H46NO7P			479.3011894	-0.0008341
130	210	5.471	171.14876	[M+H]+	C9H18N2O			170.1419132	0.0003896
131	2100	5.161	480.6525	[M+H]+					
132	1995	8.371	459.26364	[M+H]+	C29H34N2O3			458.2569429	0.0006194

133	2104	11.552	481.29141	[M+Na]+	C28H42O5	candelalide C	5.5591	458.3032244	0.0010451
134	2105	11.401	481.29199	[M+Na]+	C28H42O5			458.3032244	0.0004451
135	2143	7.325	487.0961	[M+Na]+	C21H24N2O6S2	Botryosulfuranol B		464.1067095	-0.0001698
136	2127	7.922	484.15665	[M+NH4]+	C21H26N2O6S2			466.1232286	0.0004541
137	2146	12.194	487.23059	[M+H]+	C27H34O8			486.225368	0.0020445
138	1520	4.877	376.19632	[M+H]+	C18H25N5O4			375.1906543	0.0016307
139	2175	11.775	494.56531	[M+H]+					
140	2177	12.195	495.30795	[M+Na]+	C29H44O5			472.3188745	9.52E-05
141	2180	9.704	496.33936	[M+H]+	C24H50NO7P	LysoPC(16:0)	5.1632	495.3324896	0.000366
142	2183	10.671	496.3938	[M+Na]+					
143	1481	11.924	369.29749	[M+Na]+	C20H42O4			346.3083098	3.05E-05
144	2223	10.619	506.39932	[M+H]+	C34H51NO2			505.3919799	-4.37E-05
145	2230	8.587	508.38324	[M+H]+	C26H53NO8			507.3771177	0.0011941
146	1106	9.451	311.25812	[M+H]+	C19H34O3			310.2507949	-2.86E-05
147	2237	9.528	510.35696	[M+H]+	C25H52NO7P			509.3481396	-0.0015839
148	2240	10.177	510.35889	[M+H]+	C32H47NO4			509.350509	-0.0011146
149	2247	10.639	512.37384	[M+H]+	C32H49NO4			511.366159	-0.0003645
150	1788	10.863	424.36337	[M+NH4]+	C22H46O6			406.3294392	-0.0001353
151	2253	10.605	514.38885	[M+H]+	C32H51NO4			513.3818091	0.0001856
152	2245	7.145	512.15302	[M+NH4]+	C26H22O10			494.1212969	0.0021225
153	2264	8.684	518.32184	[M+H]+	C26H48NO7P			517.3168395	0.002316
154	2265	8.516	518.32489	[M+H]+	C26H48NO7P			517.3168395	-0.000784
155	2274	4.297	520.33252	[M+H]+					
156	2282	9.945	522.35565	[M+H]+	C26H52NO7P			521.3481396	-0.0002839
157	2283	9.749	522.35583	[M+H]+	C26H52NO7P	LysoPC(18:1(9Z))	5.1043	521.3481396	-0.0003839
158	2284	12.14	522.59662	[M+H]+	C36H75N			521.5899514	0.0006279
159	2285	12.288	522.59662	[M+H]+	C36H75N			521.5899514	0.0006279
160	229	0.884	175.05748	[M+H]+	C3H6N6O3			174.0501381	-8.55E-05
161	2329	6.966	534.23651	[M+H-2H2O]+	C33H35N3O6			569.2525858	0.0022329
162	2085	10.956	479.27713	[M+H]+	C30H38O5			478.2719243	0.0021008
163	2351	9.25	542.31927	[M+Na]+	C26H50NO7P	LysoPC(18:2(9Z,12Z))	5.315	519.3324896	0.0024103
164	2276	9.066	520.33826	[M+H]+	C26H50NO7P	LysoPC(18:2(9Z,12Z))	5.2432	519.3324896	0.001466
165	2134	7.053	485.08157	[M+Na]+	C21H22N2O6S2	Botryosulfuranol A		462.0919284	-0.0004509
166	2391	11.735	554.17578	[M+NH4]+					
167	2400	10.796	556.44238	[M+NH4]+	C28H58O9			538.4080834	-0.000491
168	2411	9.606	559.38324	[M+H-H2O]+	C30H56O10			576.387348	0.0008598
169	242	1.471	179.0787	[M+Na]+	C7H12N2O2			156.0898776	0.0003983
170	2430	4.41	564.35864	[M+H]+					
171	244	4.248	179.11758	[M+H-H2O]+	C10H16N2O2			196.1211778	0.0002895
172	2385	9.038	552.41187	[M+H]+	C29H53N5O5	Cyclopentapeptide	4.6903	551.4046698	4.62E-05
173	2482	6.521	580.28528	[M+H]+	C32H41N3O5S			579.2766924	-0.0013311
174	2491	9.37	583.45184	[M+NH4]+	C30H55N5O5	Cyclopentapeptide	4.3852	565.4203199	0.0023454
175	2508	12.255	589.1792	[M+H]+	C31H28N2O10			588.1743951	0.0024715
176	1431	4.556	359.21725	[2M+H]+	C9H13N3O			179.105862	0.000576
177	2519	6.352	592.28479	[M+H]+					

178	2542	10.77	600.46887	[M+NH4]+	C30H62O10			582.4342982	-0.0007763
179	2556	10.686	604.43671	[M+H]+					
180	2609	6.432	622.3338	[M+H]+					
181	2627	11.813	628.49951	[M+NH4]+					
182	2042	10.758	467.31326	[M+Na]+	C28H44O4			444.3239599	-0.0001194
183	2704	11.098	658.51001	[M+H]+					
184	273	4.207	185.11708	[M+H]+	C10H16O3	Streptenol C	5.4658	184.1099444	0.0001208
185	2741	11.784	672.52515	[M+NH4]+					
186	2778	10.713	688.52112	[M+NH4]+					
187	2783	10.643	690.3974	[M+H]+	C41H55NO8			689.3927677	0.0026442
188	2785	10.462	690.39868	[M+H]+	C41H55NO8			689.3927677	0.0013442
189	2788	11.514	690.61444	[M+H]+					
190	2829	12.021	704.19318	[M+NH4]+	C31H30N2O16			686.1595329	0.0001584
191	2861	3.161	718.33728	[M+H]+	C28H47N9O13			717.3293326	-0.000691
192	2886	10.686	732.54749	[M+NH4]+	C49H66N2O2			714.5124294	-0.0012451
193	291	4.216	188.12796	[M+H]+	C9H17NO3	Polyethylene glycol	7.6645	187.1208434	0.0001199
194	2942	3.148	759.32196	[M+NH4]+	C40H43N3O11			741.2897592	0.0015847
195	2946	11.726	760.57776	[M+NH4]+					
196	296	3.361	190.04977	[M+H]+	C10H7NO3	Kynurenic acid	5.2595	189.0425931	6.95E-05
197	2978	10.658	776.57416	[M+NH4]+					
198	298	3.719	190.10757	[M+NH4]+	C8H12O4			172.0735589	-0.0002156
199	3007	10.75	785.50165	[M+Na]+	C40H74O13			762.5129424	0.0005631
200	3009	10.504	785.50232	[M+Na]+	C40H74O13			762.5129424	-0.0001369
201	2962	3.407	771.24805	[M+H]+	C38H42O17			770.2421999	0.0014763
202	3025	11.19	799.51904	[M+H]+	C43H70N6O6S	Symplostatin 1	5.3368	798.507755	-0.0039686
203	3029	9.776	801.49646	[M+Na]+	C40H74O14			778.507857	0.0005777
204	304	5.112	191.29794	[2M+Na]+					
205	3043	11.698	804.604	[M+H]+					
206	3056	11.494	813.53479	[2M+H]+	C23H38N2O2S			406.2653995	0.0013634
207	308	5.503	193.0858	[M+H]+	C11H12O3			192.0786442	0.0001207
208	3166	11.381	899.57178	[M+Na]+					
209	3230	11.074	943.59753	[M+Na]+					
210	3249	11.968	953.61761	[M+H]+	C52H88O15			952.6123221	0.0019986
211	3268	11.192	969.61432	[M+H]+	C53H84N4O12			968.6085741	0.0015506
212	3271	11.596	971.62817	[M+H]+	C53H86N4O12			970.6242242	0.0033006
213	3281	10.803	987.62225	[M+Na]+	C63H84N2O6			964.6329384	-0.0001409
214	3282	10.658	987.62299	[M+H]+	C53H86N4O13			986.6191388	0.0034153
215	2363	10.037	544.36346	[M+H]+	C32H49NO6			543.3559883	-0.0002353
216	370	2.89	201.07533	[M+H]+	C9H12O5			200.0684735	0.0004499
217	374	1.479	202.15491	[M+H]+	C9H19N3O2			201.1477268	0.0001033
218	378	4.078	203.12743	[M+H]+	C10H18O4			202.1205091	0.0003855
219	392	0.911	206.04558	[M+Na]+	C5H13NO4S			183.0565289	0.0001496
220	401	3.695	208.10773	[M+H]+	C10H13N3O2			207.1007767	0.0003531
221	407	1.794	210.07588	[M+H]+	C10H11NO4			209.0688078	0.0001843
222	410	3.958	210.1698	[M+NH4]+					

223	428	7.016	213.112	[M+H]+	C11H16O4			212.104859	0.0001354
224	429	5.244	213.11209	[M+H]+	C11H16O4			212.104859	3.54E-05
225	450	3.031	216.12267	[M+H]+	C10H17NO4			215.115758	0.0003345
226	451	5.372	216.15926	[M+H]+	C11H21NO3			215.1521435	0.00012
227	455	3.765	217.09698	[M+H]+	C12H12N2O2			216.0898776	0.0001541
228	456	0.979	217.10439	[M+H]+					
229	1080	0.834	309.05576	[M+H]+					
230	476	5.612	222.11243	[M+H]+	C12H15NO3			221.1051933	6.98E-05
231	481	3.515	223.15347	[M+H]+	C10H22O5			222.1467238	0.0005003
232	489	5.366	224.18565	[M+NH4]+	C10H22O4			206.1518092	-6.53E-05
233	400	4.268	208.09625	[M+H-H2O]+	C11H15NO4			225.100108	0.0005197
234	502	3.378	227.09137	[M+H]+	C11H14O5			226.0841235	0
235	504	2.325	227.10255	[M+H]+	C10H14N2O4	Porphobilinogen	5.1745	226.0953569	3.34E-05
236	505	6.592	227.10274	[M+H]+	C10H14N2O4	Porphobilinogen	5.3653	226.0953569	-6.66E-05
237	510	7.076	228.1954	[M+H]+	C13H25NO2			227.188529	0.0004055
238	513	10.264	228.23228	[M+H]+	C14H29NO			227.2249145	-0.000109
239	518	4.282	229.10693	[M+H]+	C11H16O5			228.0997736	0.0001501
240	535	4.58	230.13834	[M+H]+	C11H19NO4			229.1314081	0.0003845
241	539	5.895	230.17487	[M+H]+	C12H23NO3			229.1677936	0.00017
242	541	7.472	230.24719	[M+H]+	C14H31NO			229.2405646	0.0006411
243	542	7.896	230.24767	[M+H]+	C14H31NO			229.2405646	0.0001411
244	558	7.506	232.11191	[M+H-2H2O]+	C17H17NO2			267.1259288	0.0001759
245	561	2.857	232.15396	[M+H]+	C11H21NO4			231.1470582	0.0003346
246	563	1.004	232.15428	[M+H]+	C11H21NO4	Butyrylcarnitine	5.064	231.1470582	3.46E-05
247	599	3.369	240.18019	[M+NH4]+	C10H22O5			222.1467238	0.0003494
248	1249	5.381	330.19138	[M+H]+	C16H27NO6			329.1838376	-0.000286
249	612	10.653	242.24786	[M+H]+	C15H31NO			241.2405646	-5.89E-05
250	1429	4.965	359.18097	[M+H]+	C17H22N6O3			358.1753386	0.001615
251	501	4.351	227.09108	[M+H]+	C11H14O5			226.0841235	3.00E-04
252	627	5.427	244.15398	[M+H]+	C12H21NO4	Tiglylcarnitine	5.0592	243.1470582	0.0003346
253	628	4.946	244.15401	[M+H]+	C12H21NO4			243.1470582	0.0003346
254	497	6.391	226.17963	[M+H-H2O]+	C13H25NO3			243.1834437	0.0005554
255	1699	11.721	408.30835	[M+Na]+	C22H43NO4			385.3192089	0.0001296
256	631	11.854	244.19066	[M+NH4]+	C13H22O3			226.1568946	2.01E-05
257	632	4.897	244.25784	[M+H]+					
258	646	2.001	246.13303	[M+H]+	C11H19NO5			245.1263227	0.0005992
259	648	3.732	246.16965	[M+H]+	C12H23NO4			245.1627082	0.0003847
260	649	3.343	247.11732	[M+H]+	C11H18O6			246.1103383	0.0003147
261	791	1.273	270.09491	[M+Na]+	C10H17NO6			247.1055873	-9.20E-05
262	550	5.653	231.123	[M+H]+	C11H18O5			230.1154237	-0.0002999
263	659	0.985	249.08444	[M+Na]+	C10H14N2O4	Porphobilinogen	5.2977	226.0953569	0.0001776
264	662	7.049	250.17824	[M+H]+					
265	663	3.902	250.18004	[M+H]+	C15H23NO2	ɔ-1H-pyrrol-1-yl)-2-methyldec	5.0916	285.1940083	0.0001554
266	664	4.772	251.18512	[M+H]+	C12H26O5			250.1780239	0.0002004
267	689	3.111	256.17514	[M+NH4]+	C10H22O6			238.1416384	0.000364

268	690	11.333	256.26358	[M+H-H2O]+					
269	705	5.025	258.16992	[M+H]+	C13H23NO4			257.1627082	8.47E-05
270	623	2.021	244.11798	[M+H-H2O]+	C11H19NO6			261.1212373	-5.09E-05
271	747	3.568	264.1225	[M+H]+	C14H17NO4			263.115758	0.0005345
272	660	7.38	249.20563	[M+H]+	C13H28O4			248.1987594	0.0004358
273	384	0.937	204.12315	[M+H]+	C9H17NO4	L-Acetylcarnitine	5.3812	203.115758	-0.0001655
274	794	11.625	270.27914	[M+H]+	C17H35NO			269.2718647	4.12E-05
275	802	5.978	272.1492	[M+H]+	C13H21NO5			271.1419728	4.92E-05
276	803	5.706	272.1499	[M+H]+	C13H21NO5			271.1419728	-0.0006508
277	804	2.317	272.16043	[M+H]+	C12H21N3O4			271.1532062	8.26E-05
278	815	4.92	274.16464	[M+H]+	C13H23NO5			273.1576228	0.0002993
279	937	4.607	290.13904	[M+H]+	C16H19NO4			289.1314081	-0.0003155
280	818	7.424	274.27344	[M+H]+					
281	822	0.927	275.21188	[2M+H]+					
282	1279	6.407	334.27359	[M+H]+	C21H35NO2			333.2667794	0.0004558
283	841	11.247	278.21164	[M+H]+	C17H27NO2			277.2041791	-0.0001444
284	845	3.581	279.13367	[M+H]+	C14H18N2O4			278.1266571	0.0002335
285	846	9.962	279.1593	[M+H]+	C16H22O4	[1-hydroxy-1-methylethyl)-8-(	5.6263	278.1518092	-0.0002144
286	386	0.886	205.06834	[M+Na]+	C6H14O6	Galactitol	5.6241	182.0790382	-4.11E-05
287	864	11.681	282.22156	[M+H]+	C20H27N		5.315	281.2143499	2.63E-05
288	865	11.49	282.27933	[M+H]+	C18H35NO	Oleamide	5.0009	281.2718647	-0.0001588
289	871	8.06	283.19049	[M+H]+	C16H26O4			282.1831093	-0.0001142
290	882	4.902	284.14944	[M+H]+	C14H21NO5			283.1419728	-0.0001508
291	885	12.431	284.29486	[M+H]+	C18H37NO	Octadecanamide	5.0143	283.2875148	-0.0001087
292	886	12.314	284.29501	[M+H]+	C18H37NO			283.2875148	-0.0002087
293	1333	7.409	343.29544	[M+Na]+					
294	913	10.489	287.22189	[M+H]+	C16H30O4	Hexadecanedioic acid	5.1565	286.2144094	-0.0002141
295	1263	5.028	332.17004	[M+H]+	C15H25NO7			331.1631021	0.0003786
296	923	7.711	288.29123	[M+H]+					
297	938	6.935	290.15945	[M+H]+	C13H23NO6			289.1525375	0.0003139
298	1560	6.279	381.18106	[M+H-2H2O]+	C22H28N2O6			416.1947366	-0.0002163
299	96	10.724	134.04448	[M+H]+	C4H7NO4	L-Aspartic acid	5.1575	133.0375077	0.0002842
300	960	5.119	292.15359	[M+H]+	C16H21NO4			291.1470582	0.0007346
301	961	4.655	292.15393	[M+H-2H2O]+	C16H25NO6			327.1681875	0.0004346
302	962	4.924	292.15445	[M+H]+	C16H21NO4			291.1470582	-6.54E-05
303	993	7.837	295.22675	[M+H-H2O]+	C18H32O4	8,13-DiHODE	5.2437	312.2300595	7.13E-05

ANNEXE 2 - OSMAC APPROACH

ID	Alignment	Average.Rt.min.	Average.Mz	Adduct.type	Formula	Structure	Theoretical.mass	Mass.error
1	108	0.902	123.0555	[M+H]+	C6H6N2O	Niacinamide	122.0480128	-0.0002107
2	113	1.269	124.03941	[M+H]+	C6H5NO2	Nicotinic acid	123.0320284	-9.51E-05
3	114	1.051	124.0395	[M+H]+	C6H5NO2	Nicotinic acid	123.0320284	-0.0001951
4	1143	2.783	201.12352	[M+H]+	C9H16N2O3		200.1160924	-0.0001312
5	115	9.706	124.08679	[M+H]+	C6H9N3		123.0796473	0.0001237
6	1159	4.939	202.14467	[M+H]+	C10H19NO3		201.1364935	-0.0009301
7	1162	1.011	202.1803	[M+H]+	C11H23NO2		201.172879	-0.0001446
8	1189	5.323	204.11406	[M+H]+	C11H13N3O		203.105862	-0.0009615
9	1234	4.914	207.15929	[M+H]+	C10H22O4		206.1518092	-0.0002144
10	1241	4.595	208.097	[M+H]+	C11H13NO3	N-Acetyl-L-phenylalanine	207.0895433	-0.0001803
11	1300	5.447	211.05466	[M+H]+	C9H10N2O2S		210.0462986	-0.001125
12	1301	7.21	211.08641	[M+H]+	C13H10N2O		210.0793129	0.0001894
13	1307	4.409	211.14413	[M+NH4]+	C11H15NO2		193.1102787	4.30E-06
14	1309	1.055	211.14424	[M+NH4]+	C11H15NO2		193.1102787	-9.57E-05
15	1325	1.406	212.1032	[M+H]+	C9H13N3O3		211.0956913	-0.0002323
16	1358	2.328	214.08952	[M+H]+	C10H15NO2S		213.0823497	0.0001262
17	1359	0.824	214.08969	[M+H]+	C10H15NO2S	N-Butylbenzenesulfonamide	213.0823497	-7.38E-05
18	1394	6.55	216.15955	[M+H]+	C11H21NO3		215.1521435	-8.00E-05
19	1422	4.181	218.1297	[M+H]+	C12H15N3O		217.1215121	-0.0009114
20	1175	0.964	203.04686	[M+H]+	C7H10N2O3S		202.0412132	0.0015896
21	1456	2.619	220.1187	[M+H]+	C9H17NO5	Pantothenic acid	219.1106726	-0.0007509
22	1476	3.976	221.13161	[M+H]+	C12H16N2O2		220.1211778	-0.0031458
23	1550	4.658	227.05357	[2M+NH4]+				
24	1553	2.38	227.1032	[M+H]+	C10H14N2O4	Porphobilinogen	226.0953569	-0.0005666
25	1558	4.14	227.13882	[M+H]+	C11H18N2O3		226.1317424	0.0002189
26	1561	5.156	227.1393	[M+H]+	C11H18N2O3		226.1317424	-0.0002811
27	1577	2.948	228.13412	[M+NH4]+	C10H14N2O3		210.1004423	0.0001679
28	1578	3.171	228.13455	[M+H]+	C10H17N3O3	ycedipeptide A;(-)-Cordycedipept	227.1269914	-0.0003321
29	1582	7.216	228.18906	[M+H]+				
30	1586	10.899	228.23224	[M+H]+	C14H29NO		227.2249145	-9.00E-06
31	1610	6.017	230.17619	[M+H]+	C12H23NO3		229.1677936	-0.00113
32	1620	1.01	231.08386	[M+H-2H2O]+	C11H14N4O4		266.1015049	0.003752
33	1357	1.268	214.08939	[M+H]+	C10H15NO2S		213.0823497	0.0002262
34	1633	3.471	232.14743	[M+H]+	C13H17N3O		231.1371622	-0.0029614
35	1695	4.388	238.10045	[M+H]+	C11H15N3OS		237.0935831	0.0004596
36	1698	6.899	238.12596	[M+H]+	C9H19NO6		237.1212373	0.0025138
37	1699	5.494	238.14235	[M+Na]+	C11H21NO3		215.1521435	-0.0009358
38	1726	5.365	240.12415	[M+H]+	C12H17NO4		239.115758	-0.0010655
39	1727	6.256	240.12418	[M+H]+	C12H17NO4		239.115758	-0.0011655
40	1728	4.432	240.12427	[M+FA+H]+	C11H15NO2		193.1102787	-0.0012658
41	1730	2.404	240.18028	[M+H]+	C14H25NS		239.1707708	-0.0022527
42	1741	3.029	241.11806	[M+FA+H]+	C10H14N2O2		194.1055277	0.0001831

43	1763	10.972	242.24785	[M+H]+	C15H31NO		241.2405646	4.11E-05
44	1777	3.837	243.13385	[M+H]+	C11H18N2O4		242.1266571	3.35E-05
45	1778	4.206	243.13406	[M+H]+	C11H18N2O4		242.1266571	-0.0001665
46	1805	1.008	245.09517	[2M+H]+	C6H6N2O		122.0480128	0.0037767
47	1809	4.633	245.12862	[M+H]+	C14H16N2O2	ɘ-L-Pro);(-)-cyclo-(L-Phe-L-Pro); M	244.1211778	-0.0001458
48	181	1.727	131.07019	[M+H]+	C6H10O3	Ketoleucine	130.0629942	7.06E-05
49	1810	4.836	245.12866	[2M+Na]+	C6H9NO		111.0684139	-0.0016
50	1815	4.317	245.15002	[M+H]+	C11H20N2O4		244.1423071	-0.0004164
51	1830	4.221	246.16295	[M+H]+	C14H19N3O		245.1528122	-0.0028113
52	1257	4.809	209.11734	[M+H-H2O]+	C12H18O4	Tuberonic acid	226.1205091	-7.92E-05
53	1874	3.598	249.12344	[M+H-H2O]+	C13H18N2O4		266.1266571	-3.12E-05
54	1887	11.023	251.04663	[M+H]+	C11H10N2O3S		250.0412132	0.0018896
55	1890	4.899	251.18639	[M+H]+	C12H26O5		250.1780239	-0.0010996
56	1891	8.192	251.2005	[M+H]+	C16H26O2		250.1932801	5.65E-05
57	1898	6.578	252.06348	[M+H]+	C15H9NO3		251.0582431	0.0020196
58	1931	4.736	254.13995	[M+H-2H2O]+	C14H19N5O2		289.1538748	2.19E-05
59	1716	3.214	239.14981	[M+H]+	C11H18N4O2		238.1429758	0.0004523
60	1968	11.504	256.26346	[M+H]+	C16H33NO		255.2562147	-8.90E-06
61	1977	5.642	257.08105	[M+H-H2O]+	C15H14O5		274.0841235	-0.0002647
62	198	3.297	133.07629	[M+H]+	C8H8N2		132.0687483	-0.0002753
63	1793	6.514	244.19188	[M+H]+	C13H25NO3		243.1834437	-0.0011799
64	2020	0.64	259.14716	[M+H]+	C15H18N2O2		258.1368278	-0.0030957
65	2021	1.255	259.14725	[M+H]+	C15H18N2O2		258.1368278	-0.0030957
66	1946	5.569	255.0654	[M+H]+	C15H10O4	5,7-Dihydroxyflavone	254.0579088	-0.0002147
67	2035	4.913	260.11304	[M+H]+	C11H17NO6		259.1055873	-0.0001363
68	2050	5.696	261.15994	[2M+Na]+				
69	2063	3.408	262.11862	[M+NH4]+	C10H16N2O3S		244.0881634	0.0033889
70	2073	4.699	263.09497	[M+H-H2O]+	C14H16O6		280.0946882	-0.0036
71	2075	3.83	263.1026	[M+H]+	C13H14N2O4		262.0953569	3.34E-05
72	2106	4.797	265.09744	[M+FA+H]+	C15H10N2		218.0843983	-0.0002462
73	2147	1.279	268.1044	[2M+NH4]+				
74	2148	1.024	268.10443	[2M+NH4]+				
75	1889	5.701	251.18571	[M+H]+	C12H26O5		250.1780239	-0.0003996
76	2179	3.281	270.12576	[M+H]+	C15H15N3O2		269.1164267	-0.0020968
77	2184	11.802	270.27939	[M+H]+	C17H35NO		269.2718647	-0.0002588
78	2200	7.481	271.18848	[M+Na]+	C14H24N4		248.2000968	0.0008175
79	2213	3.126	272.14883	[M+H]+	C13H21NO5		271.1419728	0.0004492
80	2222	7.945	272.25833	[M+H]+	C16H33NO2		271.2511293	0.0001057
81	2238	5.269	273.18225	[M+H]+	C18H24O2		272.17763	0.0026065
82	2251	10.467	274.15094	[M+NH4]+	C10H16N4O4		256.117155	8.05E-05
83	2271	3.355	275.04855	[M+H]+	C13H10N2O3S		274.0412132	-0.0001104
84	2273	4.045	275.15244	[2M+H]+				
85	2291	4.849	276.12207	[M+Na]+	C13H19NO4		253.1314081	-0.0014712
86	2310	3.892	277.11804	[M+H]+	C9H16N4O6		276.1069842	-0.0037393
87	2313	4.162	277.15475	[M+H]+	C15H20N2O3		276.1473925	-0.000131

88	2314	4.255	277.15524	[M+H]+	C15H20N2O3		276.1473925	-0.000531
89	2320	6.95	277.21613	[M+H]+	C18H28O2	Stearidonic acid	276.2089301	0.0001066
90	2322	7.068	277.21622	[2M+H]+	C9H14O	2,4-Nonadienal	138.1044651	-0.000271
91	2363	7.3	279.22345	[M+H-H2O]+	C20H28N2		296.2252489	-0.0014393
92	2373	11.738	279.49023	[M+Na]+				
93	2397	4.588	281.06018	[M+H]+	C12H12N2O4S		280.0517779	-0.0011457
94	2421	1.629	282.12009	[M+H]+	C11H15N5O4		281.112404	-0.0004196
95	2424	11.553	282.2793	[M+H]+	C18H35NO	Oleamide	281.2718647	-0.0001588
96	2443	5.232	283.16556	[M+H]+	C14H22N2O4		282.1579572	-0.0003664
97	2449	7.876	283.22818	[2M+NH4]+				
98	2463	4.82	284.13953	[M+H]+	C16H17N3O2	amide F;L-Prolyl-L-tryptophan an	283.1320768	-0.0001468
99	2468	3.091	284.20679	[M+H]+	C13H25N5O2		283.200825	0.0013015
100	2470	12.432	284.29462	[M+H]+	C18H37NO		283.2875148	0.0001913
101	2490	5.625	285.07614	[M+H]+	C16H12O5	xy-2-(4-methoxyphenyl)-4H-chrc	284.0684735	-0.0003501
102	2511	8.487	286.22845	[M+NH4]+	C18H24N2		268.1939488	-0.0007257
103	2522	7.675	287.08673	[M+Na]+	C14H16O5		264.0997736	0.0022943
104	2524	5.752	287.09161	[M+H]+	C16H14O5	Sakuranetin	286.0841235	-2.00E-04
105	2526	4.123	287.1713	[M+H]+	C17H22N2O2		286.1681279	0.0041044
106	2528	6.032	287.19803	[M+H]+	C19H26O2		286.1932801	0.0025565
107	2533	6.287	287.22189	[M+H]+	C16H30O4	Hexadecanedioic acid	286.2144094	-0.0002141
108	2538	3.842	288.07162	[M+NH4]+	C7H14N2O5S2		270.0344135	-0.0033609
109	2076	3.996	263.13934	[M+H]+	C14H18N2O3		262.1317424	-0.0002811
110	2546	1.106	288.18036	[M+FA+H]+	C13H23NO3		241.1677936	0.000149
111	2547	0.636	288.18045	[M+FA+H]+	C13H23NO3		241.1677936	4.90E-05
112	2550	8.581	288.25351	[M+H]+	C16H33NO3		287.2460439	-0.0001796
113	2587	5.164	291.01718	[M+H]+	C14H10O3S2		290.0071362	-0.0027874
114	2618	6.075	292.14584	[M+H]+	C11H21N3O6		291.1430354	0.0045118
115	2632	5.977	293.06055	[M+H]+	C13H12N2O4S		292.0517779	-0.0014457
116	2634	3.294	293.11298	[M+H]+	C14H16N2O5		292.1059216	0.0001981
117	2645	7.934	293.21091	[M+H]+	C18H28O3	10,15-phytodienoic acid;2-Cyclo	292.2038448	0.0002212
118	2646	7.46	293.21094	[M+H-H2O]+	C18H30O4		310.2144094	0.0002212
119	2648	6.69	293.21158	[M+H]+	C18H28O3	10,15-phytodienoic acid;2-Cyclo	292.2038448	-0.0004788
120	2649	8.029	293.21222	[M+H]+	C18H28O3		292.2038448	-0.0010788
121	265	9.176	140.2084	[M+H]+				
122	1200	3.66	205.09691	[M+H]+	C11H12N2O2	L-Tryptophan	204.0898776	0.0002541
123	4114	5.92	379.09863	[M+H]+	C17H18N2O6S		378.0885573	-0.0027663
124	3060	7.786	313.23727	[M+H-H2O]+	C18H34O5	9,12,13-TriHOME	330.2406242	3.60E-05
125	2687	8.236	295.19067	[M+H]+	C17H26O4		294.1831093	-0.0003142
126	2697	6.546	295.22705	[M+H-H2O]+	C18H32O4	7S,8S-Dihydroxylinoleic acid	312.2300595	-0.0003287
127	2712	3.123	296.13513	[M+H]+	C11H21NO8		295.1267166	-0.0011069
128	2742	7.294	297.2337	[M+H]+	C20H28N2		296.2252489	-0.0011747
129	2747	10.425	297.24249	[M+NH4]+				
130	2748	10.278	297.24255	[M+H]+	C18H32O3	12,13-EpOME	296.2351449	-0.0001787
131	2749	10.101	297.24258	[M+NH4]+				
132	1892	8.475	251.20079	[M+H]+	C16H26O2		250.1932801	-0.0002435

133	2778	9.039	299.03537	[M+H]+	C16H10O4S		298.0299798	0.0018563
134	2806	5.44	300.17084	[M+H]+	C17H21N3O2		299.1633769	-0.0001466
135	1596	3.319	229.11824	[M+H]+	C10H16N2O4		228.111007	8.34E-05
136	2812	11.072	300.29013	[M+H]+	C18H37NO2	3-Dehydrosphinganine	299.2824294	-0.0003941
137	2824	4.207	301.11844	[M+H]+	C16H16N2O4		300.111007	-0.0001166
138	2826	10.066	301.14114	[M+Na]+	C16H22O4	Boropinol C	278.1518092	-7.01E-05
139	1772	5.132	243.08777	[M+H]+	C12H10N4O2		242.0803756	-0.000148
140	2872	7.541	304.17554	[M+Na]+	C18H23N3		281.1891977	0.0029184
141	2886	5.658	305.14957	[M+H]+	C16H20N2O4		304.1423071	-1.64E-05
142	2888	8.468	305.16916	[M+H]+	C14H20N6O2		304.1647739	0.0028503
143	2922	10.506	307.22659	[M+H]+	C19H30O3	ihydromonacolin L;Dihydromona	306.2194948	0.0001713
144	2925	9.108	307.22791	[M+H-H2O]+	C19H32O4		324.2300595	-0.0011287
145	2926	8.117	307.24841	[M+H]+	C17H30N4O		306.2419616	0.000838
146	2169	9.783	269.20844	[M+Na]+	C14H30O3		246.2194948	0.0003155
147	2946	11.847	308.29416	[M+H]+	C20H37NO		307.2875148	0.0005913
148	2954	5.21	309.11432	[M+H]+	C19H16O4		308.104859	-0.0021646
149	1737	0.909	241.06812	[M+Na]+	C9H14O6		218.0790382	0.0001589
150	2968	5.524	309.22733	[M+H]+	C16H28N4O2		308.2212261	0.0012026
151	2969	9.025	309.24274	[M+H]+	C19H32O3		308.2351449	-0.0002787
152	2980	4.95	310.15564	[M+H]+	C18H19N3O2		309.1477268	-0.0005967
153	2281	8.455	275.20059	[M+H-H2O]+	C18H28O3		292.2038448	-4.35E-05
154	2996	4.782	311.13907	[M+H]+	C18H18N2O3		310.1317424	-8.11E-05
155	2997	5.917	311.13956	[M+H]+	C18H18N2O3		310.1317424	-0.0005811
156	30	2.178	109.02826	[M+H-H2O]+	C6H6O3	1,2,3-Trihydroxybenzene	126.0316941	0.0001058
157	3001	8.006	311.18524	[M+FA+H]+	C16H24O3		264.1725446	0.0001001
158	3007	7.934	311.22122	[M+H]+	C18H30O4		310.2144094	0.0004859
159	2650	6.369	293.21255	[M+H-2H2O]+	C18H32O5	Corchorifatty acid F	328.2249741	-0.0014788
160	3010	9.605	311.2485	[M+H]+	C21H30N2		310.240899	-0.0003246
161	3011	11.204	311.29449	[M+H]+	C20H38O2	Eicosenoic acid	310.2871805	-4.31E-05
162	3025	5.813	312.23853	[M+H]+				
163	3026	9.165	312.24356	[M+H]+	C20H29N3		311.2361479	-0.0001756
164	2327	9.064	277.21744	[M+H]+	C18H28O2	Stearidonic acid	276.2089301	-0.0011934
165	3036	8.954	312.33459	[M+H]+	C19H41N3		311.3300483	0.0027248
166	2694	9.764	295.22678	[M+H]+	C18H30O3	-entenyl)cyclopentaneoctanoic ac	294.2194948	-2.87E-05
167	3061	5.839	313.23752	[M+H]+	C18H32O4	5(S),8(R)-DiHODE	312.2300595	-0.000164
168	3072	1.273	314.09198	[M+H]+	C11H15N5O4S		313.084475	-0.0002486
169	3074	5.891	314.1192	[M+H]2+	C32H37NO12		627.2315756	-9.65E-05
170	2370	9.641	279.23227	[M+H]+	C18H30O2	Crepenynic acid	278.2245802	-0.0004433
171	3099	8.439	315.19464	[M+H]+	C20H26O3		314.1881947	0.0008711
172	3105	8.424	315.25314	[M+H]+	C18H34O4	-Epoxy-18-hydroxy-octadecanoic	314.2457096	-0.000114
173	3106	8.115	315.25323	[M+H]+	C18H34O4	-Epoxy-18-hydroxy-octadecanoic	314.2457096	-0.000214
174	3111	4.598	316.12936	[M+H]+	C16H17N3O4		315.121906	-0.0002175
175	3133	9.745	317.20886	[M+Na]+	C18H30O3	-entenyl)cyclopentaneoctanoic ac	294.2194948	-0.0001845
176	3134	9.066	317.20984	[M+H-2H2O]+	C20H32O5	Prostaglandin D2	352.2249741	0.0013212
177	3136	9.027	317.26895	[2M+H]+	C9H18O2		158.1306798	-0.0004562

178	3142	9.989	318.3002	[M+H]+	C18H39NO3	Phytosphingosine	317.2929941	7.06E-05
179	3148	7.988	319.05911	[M+Na]+	C17H12O5		296.0684735	-0.0014058
180	3152	9.062	319.18497	[M+H]+	C15H22N6O2		318.1804239	0.0027004
181	3184	10.163	321.1666	[M+H]+	C18H24O5		320.1623739	0.0030503
182	3192	3.696	322.1084	[M+H]+	C11H19N3O6S		321.0994563	-0.0016672
183	3203	4.356	322.16608	[2M+NH4]+	C5H12O5		152.0684735	0.002062
184	3236	7.313	324.20779	[M+H]+	C20H25N3O		323.1997624	-0.0007611
185	3240	10.526	324.28967	[M+H]+	C20H37NO2		323.2824294	5.90E-06
186	3277	3.912	326.17255	[M+H]+	C15H23N3O5		325.1637708	-0.0014527
187	5519	11.219	528.24475	[M+NH4]+	C25H34O11		510.2101119	-0.0008625
188	3294	9.347	327.0784	[M+H]+	C13H14N2O8		326.0750154	0.0038919
189	3298	7.173	327.13373	[M+H]+	C13H18N4O6		326.1226343	-0.0037893
190	2280	7.156	275.20038	[M+H]+	C18H26O2		274.1932801	0.0001565
191	3322	12.077	328.32086	[M+H]+	C20H41NO2		327.3137296	0.000106
192	3370	6.948	331.18076	[M+H]+	C11H22N8O4		330.1764012	0.0028776
193	3374	7.429	331.18979	[M+Na]+	C18H28O4		308.1987594	-0.0018199
194	3379	5.495	331.21088	[M+Na]+	C21H28N2		308.2252489	0.0035696
195	3387	7.068	331.24973	[M+H]+	C18H34O5	9,12,13-TriHOME	330.2406242	-0.0017994
196	340	1.808	144.0479	[M+H]+	C6H9NOS		143.0404849	-0.0001386
197	3413	7.154	333.20343	[M+Na]+	C18H30O4		310.2144094	0.0002301
198	3419	8.427	333.20557	[M+H]+	C20H28O4		332.1987594	0.0004358
199	3422	8.101	333.26566	[M+H]+	C18H36O5		332.2562743	-0.0021493
200	2952	5.782	309.08728	[M+H]+	C17H12N2O4		308.0797069	-0.0003167
201	3432	8.776	334.23602	[M+NH4]+	C20H28O3		316.2038448	0.0016703
202	3442	6.001	335.16052	[M+H]+	C17H22N2O5		334.1528718	-0.0003517
203	3466	4.192	336.15674	[M+H]+	C21H21NO3		335.1521435	0.00272
204	3475	10.811	336.32596	[M+H-H2O]+	C22H43NO2		353.3293796	9.14E-05
205	3480	8.688	337.1066	[M+H]+	C20H16O5		336.0997736	0.0004501
206	3493	4.003	338.18298	[M+H]+	C15H23N5O4	Kyotorphin	337.1750042	-0.0007193
207	3529	4.413	340.18719	[M+NH4]+	C16H22N2O5		322.1528718	-0.0005026
208	354	3.347	146.06042	[M+H]+	C9H7NO	1H-Indole-3-carboxaldehyde	145.0527638	-0.0003597
209	3542	8.997	340.28519	[M+H]+	C20H37NO3		339.277344	-0.0005795
210	3548	9.774	341.09424	[M+H]+	C14H16N2O8		340.0906655	0.0037419
211	3563	5.066	342.15503	[M+H]+	C16H23NO7		341.1474521	-0.0002715
212	3564	4.607	342.20267	[M+H]+	C16H27N3O5		341.195071	-0.0003526
213	357	2.271	146.11732	[M+H]+	C7H15NO2		145.1102787	0.0002552
214	3576	4.143	343.13126	[M+Na]+	C21H20O3		320.1412445	-0.0008348
215	3595	6.319	344.06665	[M+H]+	C16H13N3O4S		343.0626769	0.0032533
216	478	3.73	154.0498	[M+H]+	C7H7NO3	3-Hydroxyanthranilic acid	153.0425931	6.95E-05
217	3648	10.533	347.21936	[M+Na]+	C19H32O4		324.2300595	-0.0001198
218	3660	6.678	348.27493	[M+NH4]+	C18H34O5	9,12,13-TriHOME	330.2406242	-0.0004503
219	3677	8.933	349.23547	[M+Na]+	C19H34O4		326.2457096	-0.0005697
220	3687	11.665	350.3056	[M+H]+	C22H39NO2		349.2980795	-0.0002441
221	3757	0.575	354.03375	[M+H]+				
222	3765	8.82	354.28537	[M+H]+	C23H35N3		353.2830981	0.0049746

223	3767	11.663	354.33728	[M+H]+	C22H43NO2		353.3293796	-0.0006439
224	3778	10.175	355.10962	[M+H]+	C19H18N2O3S		354.1038134	0.0014899
225	3787	11.39	355.28201	[M+Na]+	C19H40O4		332.2926598	-0.0001195
226	3799	5.021	356.21817	[M+H]+	C22H29NO3		355.2147438	0.0038202
227	3800	5.147	356.21841	[M+H]+	C22H29NO3		355.2147438	0.0036202
228	3811	4.437	357.08032	[M+H]+	C9H17N4O9P	nino-6-(5'-phosphoribitylamino)u	356.0733148	0.0002912
229	3822	12.119	357.33694	[M+H]+	C22H44O3	22-Hydroxydocosanoic acid	356.3290453	-0.0005783
230	3828	6.825	358.14145	[M+NH4]+	C15H20N2O5S		340.1092927	0.0017183
231	3830	4.238	358.19763	[M+H]+	C16H27N3O6		357.1899856	-0.000338
232	3834	6.668	358.29547	[M+H]+	C20H39NO4		357.2879087	-0.0003148
233	3845	5.273	359.18158	[M+H]+	C21H26O5		358.1780239	0.0037004
234	3846	10.212	359.21951	[M+Na]+	C20H32O4	15(S)-HPETE	336.2300595	-0.0002198
235	3848	8.826	359.24075	[M+H]+	C15H30N6O4		358.2328534	-0.0006701
236	2369	10.733	279.23218	[M+H]+	C18H30O2	Crepenynic acid	278.2245802	-0.0003433
237	3906	0.947	365.10635	[M+H-2H2O]+	C18H24O8S		400.1191887	-0.0010642
238	3908	9.788	365.13675	[M+Na]+	C20H22O5	Brosimacutin C	342.1467238	-0.0007555
239	395	9.88	149.01721	[M+H]+	C7H4N2S		148.0095191	-0.0004044
240	3952	5.4	369.20248	[M+H]+	C19H24N6O2		368.196074	0.0008505
241	3969	10.575	370.29538	[M+NH4]+	C21H36O4		352.2613596	-0.0002148
242	4010	7.925	373.25845	[2M+H]+	C10H18O3		186.1255944	-0.0002916
243	4011	7.713	373.25861	[M+H]+	C20H36O6	8,8a-Deoxyoleandolide	372.2511889	-0.0001347
244	4014	8.612	373.25873	[2M+H]+	C10H18O3		186.1255944	-0.0003916
245	2811	9.383	300.29013	[M+H]+	C18H37NO2	3-Dehydrosphinganine	299.2824294	-0.0003941
246	4031	10.13	375.1207	[M+Na]+	C21H20O5		352.1310737	-0.0004056
247	4034	8.175	375.19971	[M+H]+	C19H26N4O4		374.1954053	0.0029818
248	4084	11.093	377.07898	[M+Na]+	C15H18N2O6S		354.0885573	-0.001222
249	4104	11.57	378.21072	[M+H]+	C24H27NO3		377.1990937	-0.0043298
250	4107	11.395	378.22128	[M+H]+	C20H31N3O2S		377.2136982	-0.0003253
251	4118	9.662	379.2485	[M+Na]+	C20H36O5		356.2562743	-0.003005
252	1893	6.804	251.20102	[M+H]+	C16H26O2		250.1932801	-0.0004435
253	4156	10.054	383.2041	[M+Na]+	C18H32O7		360.2148034	-7.59E-05
254	4179	6.522	384.12085	[M+NH4]+	C16H18N2O6S		366.0885573	0.0015828
255	2231	6.101	273.07623	[M+H]+	C15H12O5	Naringenin	272.0684735	-0.0004501
256	3897	12.278	363.25323	[M+H]+	C22H34O4		362.2457096	-0.000214
257	4202	10.765	385.29224	[M+H]+	C22H40O5		384.2875744	0.0026508
258	4223	3.958	388.25531	[M+NH4]+	C16H34O9		370.2202827	-0.0011918
259	4244	5.421	390.20255	[M+H]+	C20H27N3O5		389.195071	-0.0001526
260	4305	7.789	395.28067	[M+H-H2O]+	C23H40O6		412.282489	-0.0014992
261	4307	11.796	395.33066	[M+NH4]+	C23H39NO3		377.2929941	-0.0038803
262	432	0.843	151.03549	[M+H]+	C8H6O3		150.0316941	0.0034705
263	4340	10.928	398.16537	[M+H]+	C16H23N5O7		397.1597481	0.0016245
264	4349	7.686	399.10123	[M+H]+	C20H18N2O5S		398.0936427	-0.0002809
265	4094	11.682	377.22998	[M+H]+	C22H32O5		376.2249741	0.0022506
266	6216	6.736	600.13391	[M+H]+	C28H25NO14		599.1275045	0.0008809
267	441	5.713	151.11162	[M+H-H2O]+	C10H16O2		168.1150298	0.0001415

268	4420	12.114	406.32959	[M+NH4]+	C25H40O3		388.2977451	0.0019707
269	4519	7.447	417.05743	[M+H]+	C23H12O8		416.0532173	0.0030938
270	4344	11.125	398.23254	[M+H]+	C24H31NO4		397.2253085	8.49E-05
271	4543	11.819	420.32501	[M+H]+	C24H41N3O3		419.3147922	-0.0029314
272	4576	8.545	421.25754	[M+Na]+	C22H38O6		398.2668389	-0.0014404
273	462	0.838	153.03275	[M+FA+H]+				
274	4640	11.369	427.32059	[M+H]+	C28H42O3		426.3133952	7.17E-05
275	465	4.493	153.05447	[M+Na]+	C6H10O3		130.0629942	-0.0022851
276	4653	5.305	429.2139	[M+FA+H]+	C20H30O7		382.1991533	-0.0019912
277	3159	11.049	319.2847	[M+H]+	C18H38O4		318.2770097	-0.0004139
278	4685	4.124	432.28	[M+NH4]+	C18H38O10		414.2464974	0.000323
279	4692	4.638	433.11285	[M+H]+	C21H20O10	6-[3,4,5-trihydroxy-6-(hydroxym	432.1056468	2.33E-05
280	4732	9.997	437.20865	[M+H]+	C25H28N2O5		436.199822	-0.0015016
281	4737	9.936	437.26855	[M+H-H2O]+	C28H38O5		454.2719243	3.61E-05
282	4787	10.244	441.37299	[M+H-H2O]+	C30H50O3		458.3759955	-0.0002928
283	4795	6.598	442.3381	[2M+NH4]+	C11H20N2O2		212.1524779	6.64E-05
284	4825	4.105	447.12918	[M+H]+	C22H22O10		446.1212969	-0.0006266
285	4839	6.332	448.10406	[M+NH4]+	C11H20N4O10P2		430.0654661	-0.0048083
286	4843	4.687	449.10339	[M+FA+H]+	C12H23N2O9PS		402.0861879	-0.0044566
287	4896	7.674	455.03632	[M+Na]+	C19H16N2O6S2	Botryosulfuranol C	432.0455	
288	4864	4.954	451.11911	[M+H]+	C21H22O11		450.1162115	0.004388
289	3287	12.31	326.30573	[M+H]+	C20H39NO2	miplenamide C;(-)-Semiplenamid	325.2980795	-0.0003441
290	488	1.527	155.08113	[M+H]+	C7H10N2O2		154.0742276	0.000404
291	4880	6.337	453.07443	[M+Na]+	C21H18O10		430.0899968	0.0048175
292	489	0.939	155.08136	[M+H-2H2O]+	C7H14N2O4		190.0953569	0.000104
293	4962	10.989	463.12997	[M+H]+	C25H22N2O5S		462.1249428	0.0022193
294	4966	12.078	463.28217	[M+Na]+	C28H40O4		440.2926598	-0.0003195
295	5004	11.661	465.29758	[M+H]+	C30H40O4		464.2926598	0.0023362
296	4863	6.516	451.06314	[M+FA+H]+	C18H16N2O5S2		404.0500636	-0.0002809
297	507	1.458	156.13872	[M+H]+	C9H17NO		155.1310142	-0.0004094
298	5070	12.371	471.36475	[M+Na]+	C32H48O		448.3705162	-0.0049631
299	5084	7.675	473.24554	[M+H]+	C21H36N4O6S		472.2355559	-0.0026677
300	5108	4.262	476.30917	[M+H]+	C21H41N5O7		475.3005987	-0.0013249
301	4961	7.191	463.09897	[M+H]+	C21H22N2O6S2	Botryosulfuranol A	462.092	
302	5155	8.451	481.24847	[M+H-2H2O]+	C31H36N2O5		516.2624223	6.93E-05
303	5157	11.493	481.2926	[M+Na]+	C28H42O5		458.3032244	-0.0001549
304	4817	11.628	445.33109	[M+H-2H2O]+	C28H48O6		480.3450893	0.0001363
305	5202	7.443	487.09891	[M+Na]+	C21H24N2O6S2	Botryosulfuranol B	464.1077	
306	5169	12.398	482.28357	[M+H]+	C19H39N5O9		481.2747778	-0.0015457
307	4358	11.334	399.30832	[M+Na]+	C22H40N4O		376.3202119	0.0011326
308	5236	10.206	490.20792	[M+H]+	C25H31NO9		489.1998816	-0.000742
309	525	7.393	158.15375	[M+H]+	C9H19NO		157.1466642	0.0002407
310	5274	5.873	496.11917	[M+H]+	C21H25N3O7S2		495.1133921	0.0014686
311	4673	5.105	431.09268	[M+FA+H]+	C20H16O8		384.0845175	0.0045729
312	5277	9.679	496.34018	[M+H]+	C24H50NO7P	LysoPC(16:0)	495.3324896	-0.000434

313	3946	5.415	369.09732	[M+H-H2O]+	C20H18O8		386.1001675	-0.0004207
314	5293	6.161	498.13516	[M+H]+	C24H23N3O7S		497.1256711	-0.0022525
315	5308	6.319	500.15057	[M+H]+	C24H25N3O7S		499.1413211	-0.0020024
316	5315	5.106	501.0784	[M+Na]+	C25H18O10		478.0899968	0.0008175
317	5320	12.007	501.37582	[M+Na]+	C27H50N4O3		478.3882915	0.0017122
318	5334	5.427	503.09399	[M+Na]+	C25H20O10		480.1056468	0.0008675
319	5387	11.971	510.43738	[M+H]+				
320	5474	9.913	522.3551	[M+H]+	C26H52NO7P		521.3481396	0.0003161
321	5493	8.38	524.38031	[M+H]+				
322	5510	11.284	526.43134	[M+NH4]+				
323	5518	11.419	528.22955	[M+NH4]+	C21H34O14		510.1948558	-0.0009187
324	5577	6.02	538.11572	[M+NH4]+	C23H20O14		520.0853053	0.0034309
325	5607	10.139	541.37335	[M+H-H2O]+	C31H50N4O5		558.3781207	0.0014325
326	5613	11.612	542.24475	[M+NH4]+	C27H32N4O5S		524.2093411	-0.0016333
327	5628	8.413	544.36353	[M+H]+	C32H49NO6		543.3559883	-0.0002353
328	5646	10.484	546.39984	[M+NH4]+	C29H52O8		528.3662186	0.0002442
329	5673	10.666	550.38348	[M+Na]+				
330	5694	9.027	552.30884	[M+H]+	C31H41N3O6		551.299536	-0.0019875
331	5695	9.305	552.39417	[M+H]+				
332	5698	9.176	552.41449	[M+H]+	C30H55N5O5	clo-(L-Leu-L-Leu-D-Leu-L-Leu-L-V	552.41449	
333	2983	12.331	310.3103	[M+H]+	C20H39NO		309.3031649	0.0001413
334	5583	8.782	538.39624	[M+H]+	C33H51N3O3		537.3930425	0.0041189
335	5735	11.663	556.27661	[M+NH4]+	C27H38O11		538.241412	-0.0013624
336	5738	10.902	556.44263	[M+NH4]+	C28H58O9		538.4080834	-0.000691
337	5851	9.173	566.42755	[M+H]+	C30H55N5O5		565.4203199	-3.70E-06
338	5879	6.172	568.10803	[M+H-H2O]+				
339	5955	9.118	574.39636	[M+H]+	C31H51N5O5		573.3890197	-0.0001038
340	5897	9.088	569.5553	[M+2H]2+				
341	5908	11.258	570.45654	[M+NH4]+	C36H56O4		552.4178603	-0.0048142
342	5915	8.005	571.42065	[M+NH4]+	C33H51N3O4		553.3879571	0.0010827
343	5924	9.723	572.43719	[M+NH4]+	C36H50N4O		554.3984622	-0.0049122
344	5953	9.435	574.32751	[M+H-H2O]+	C34H45N3O6		591.3308362	4.79E-05
345	5967	8.407	575.37909	[M+H-H2O]+	C30H56O11		592.3822626	-0.0001256
346	6022	8.36	582.4248	[2M+NH4]+	C20H26O		282.1983655	0.0026039
347	6024	8.309	582.42578	[M+H]+	C35H55N3O4		581.4192572	0.0007337
348	6057	11.953	584.47516	[M+NH4]+				
349	6074	9.036	586.39642	[M+H]+	C31H55NO9		585.3876823	-0.0014412
350	6112	11.62	588.40979	[M+H]+	C32H53N5O5		587.4046698	0.0021462
351	6113	9.509	588.40997	[M+Na]+	C30H55N5O5	yclo-(L-Ile-L-Leu-L-Leu-L-Leu-L-Le	565.4203199	-0.0004594
352	6138	10.453	590.42639	[M+NH4]+	C31H56O9		572.3924334	-0.0001411
353	6689	8.634	684.49341	[M+NH4]+	C35H62N4O8		666.4567649	-0.0028095
354	6192	8.948	597.36298	[M+Na]+	C31H50N4O6		574.3730353	-0.000744
355	6195	9.119	597.46997	[M+H]+	C35H64O7		596.4652044	0.0024808
356	6196	9.78	597.47241	[M+H]+	C35H64O7	Isoannonacin A	596.4652044	8.08E-05
357	1947	6.544	255.07693	[M+H-2H2O]+	C14H14N2O5	N-(1H-Indol-3-ylacetyl)aspartic ac	290.0902715	-0.0004814

358	6209	11.85	599.42877	[M+Na]+	C35H60O6		576.4389896	-0.0005897
359	6215	6.642	600.1156	[M+H]+				
360	6222	9.491	600.41187	[M+H]+	C33H53N4O5	lo-(L-Phe-L-Leu1-L-Leu2-L-Leu3-L	582.3781207	4.63E-05
361	6226	10.872	600.46863	[M+NH4]+	C30H62O10		582.4342982	-0.0004763
362	6262	5.789	606.06964	[M+H]+				
363	6291	11.36	609.41333	[M+Na]+	C36H58O6		586.4233396	-0.0007397
364	6309	11.822	611.42841	[2M+Na]+	C18H30O3		294.2194948	-0.0003691
365	6334	12.31	613.44336	[M+Na]+	C36H62O6		590.4546397	0.0004604
366	6345	11.37	614.48389	[M+NH4]+	C31H64O10		596.4499482	-0.0001262
367	635	4.135	169.07651	[M+H]+	C11H8N2		168.0687483	-0.0004753
368	3156	9.64	319.22437	[M+Na]+	C18H32O3	12,13-EpOME	296.2351449	-3.44E-05
369	6358	10.143	616.40588	[M+H]+	C33H53N5O6		615.3995844	0.0009609
370	636	2.11	169.0968	[M+H]+	C8H12N2O2	Pyridoxamine	168.0898776	0.0003541
371	6364	7.488	617.40875	[M+NH4]+	C37H49N3O4		599.372307	-0.0026674
372	2140	9.403	267.17209	[M+H-2H2O]+	C19H26O3		302.1881947	0.0022418
373	6219	7.796	600.38171	[M+H]+	C37H49N3O4		599.372307	-0.0021165
374	6403	9.491	622.39368	[M+Na]+	C33H53N5O5		599.4046698	0.0001905
375	6426	8.092	626.45209	[M+H]+	C37H59N3O5		625.445472	0.0006484
376	6432	10.433	627.42352	[M+Na]+	C36H60O7		604.4339043	-0.000375
377	6439	11.924	628.50037	[M+NH4]+				
378	6448	10.877	629.43903	[M+H]+	C34H56N6O5		628.4312189	-0.0005047
379	6473	10.418	634.45282	[M+NH4]+	C33H60O10		616.4186481	-0.0003263
380	5453	12.112	518.34778	[M+H]+	C30H47NO6		517.3403382	-0.0001853
381	2473	12.278	284.29468	[M+H]+	C18H37NO	Octadecanamide	283.2875148	9.13E-05
382	6517	10.844	644.49554	[M+NH4]+	C38H62N2O5		626.4658731	0.0041986
383	6539	10.7	648.46869	[M+NH4]+	C31H54N10O4		630.4329502	-0.0019242
384	5849	9.433	566.33722	[M+H]+	C30H47NO9		565.3250821	-0.0048415
385	6561	12.417	653.43866	[M+Na]+	C38H62O7		630.4495543	7.50E-05
386	6583	11.203	658.51031	[M+NH4]+	C33H68O11		640.476163	-0.0003115
387	659	3.038	171.11255	[M+H]+	C8H14N2O2		170.1055277	0.0003041
388	660	3.332	171.11267	[M+H]+	C8H14N2O2		170.1055277	0.0001041
389	661	5.599	171.14389	[M+NH4]+				
390	6633	11.607	671.45013	[M+H]+	C36H58N6O6		670.4417836	-0.00104
391	6658	11.89	677.48187	[M+Na]+				
392	6660	10.39	678.47961	[M+NH4]+	C41H60N2O5		660.450223	0.0044486
393	6694	12.172	685.4339	[M+Na]+	C42H63O4P		662.4463971	0.0017178
394	6707	10.81	688.52167	[M+NH4]+				
395	6725	12.395	691.49268	[M+Na]+				
396	5768	9.507	559.3844	[M+H-H2O]+	C30H56O10		576.387348	-0.0003402
397	6641	9.726	673.39301	[M+Na]+	C36H58O10		650.4029981	-0.0007812
398	6797	11.857	716.55249	[M+NH4]+	C42H70N2O6		698.523388	0.0047135
399	6811	10.362	722.5058	[2M+NH4]+	C24H32O2		352.2402303	0.0039687
400	6825	11.745	727.47375	[M+H]+	C46H66N2OS2		726.4616567	-0.0048668
401	6826	11.473	727.47595	[M+Na]+	C41H68O9		704.4863338	-0.0004455
402	6831	8.628	728.52075	[M+NH4]+	C42H66N2O7		710.4870025	2.80E-05

403	6837	12.351	730.56769	[M+NH4]+	C37H76O12		712.5336779	-0.0001966
404	6849	10.772	732.54779	[2M+NH4]+	C20H31N5O		357.2528606	-0.0044009
405	6880	11.106	743.47247	[M+Na]+	C41H68O10		720.4812484	-0.0020309
406	691	3.292	174.11212	[M+H]+	C8H15NO3		173.1051933	0.0003698
407	692	4.502	174.11235	[M+H]+	C8H15NO3	Swainsonine;(-)-Swainsonine	173.1051933	6.98E-05
408	6929	11.432	757.48816	[M+H]+	C45H64N4O6		756.4825858	0.0016622
409	694	4.337	174.11304	[M+H-2H2O]+	C9H15N5O		209.1276601	0.0008072
410	6942	11.827	760.58075	[M+NH4]+				
411	6946	9.518	761.50525	[M+H]+	C43H73N2O5PS		760.4977811	-0.0001425
412	695	3.696	174.11308	[M+H-2H2O]+	C9H15N5O		209.1276601	0.0007072
413	6954	10.336	766.53149	[M+NH4]+	C45H68N2O7		748.5026525	0.0049781
414	6962	11.263	767.49323	[M+Na]+	C46H68N2O6		744.5077379	0.0037586
415	698	10.003	174.12245	[M+H]+	C7H15N3O2		173.1164267	0.0012032
416	7001	10.679	780.54779	[M+NH4]+	C40H74O13		762.5129424	-0.001032
417	7010	10.202	783.48877	[M+Na]+	C43H73N2O5PS		760.4977811	-0.0017982
418	675	10.453	172.13318	[M+NH4]+	C9H14O2		154.0993797	5.20E-06
419	7016	10.693	785.5033	[M+Na]+	C40H74O13		762.5129424	-0.0011369
420	7050	7.135	795.3009	[M+Na]+				
421	7100	10.432	810.41052	[M+NH4]+	C45H52N4O9		792.3734292	-0.0032452
422	7102	10.308	810.55902	[M+Na]+	C43H82NO9P		787.5727198	0.0029405
423	7147	10.729	829.38354	[M+Na]+	C44H58N2O12		806.3989753	0.004696
424	7151	10.533	829.53046	[M+H-H2O]+				
425	7226	9.082	868.61835	[2M+H]+				
426	7234	11.28	871.39429	[M+Na]+	C49H52N8O6		848.4009814	-0.0040979
427	7266	7.69	883.50903	[M+H]+	C52H70N2O10		882.5030464	0.0013229
428	7279	9.378	884.64563	[M+H]+				
429	7280	9.526	884.64648	[M+Na]+				
430	7287	9.11	886.62878	[M+H]+	C52H88NO8P		885.6247554	0.0032319
431	7289	9.938	886.66052	[M+H]+				
432	729	7.775	177.0546	[M+H]+	C10H8O3	Herniarin	176.0473441	2.06E-05
433	7317	10.254	898.61163	[2M+Na]+				
434	1530	7.397	225.18933	[M+H]+	C14H24O2		224.17763	-0.0043935
435	7388	7.537	919.14746	[2M+H]+	C20H17N3O8S		459.0736355	0.0032494
436	745	4.774	179.06444	[M+NH4]+	C5H7NO5		161.0324223	0.0018479
437	7453	9.409	944.66229	[M+Na]+				
438	747	11.265	179.07018	[M+H]+	C10H10O3	4-hydroxy-3-methoxyphenyl)proı	178.0629942	7.06E-05
439	4846	11.193	449.30286	[M+H-2H2O]+	C30H44O5		484.3188745	0.0021216
440	7514	11.557	971.62823	[M+Na]+				
441	7539	10.559	987.62299	[M+Na]+	C63H84N2O6		964.6329384	-0.0008409
442	7540	10.745	987.62366	[M+Na]+	C63H84N2O6		964.6329384	-0.0015409
443	755	4.357	179.11789	[M+H-H2O]+	C10H16N2O2	cyclo(L-Pro-L-Val)	196.1211778	-1.05E-05
444	7553	10.022	1003.61829	[M+Na]+				
445	762	3.758	180.10234	[M+H]+	C10H13NO2		179.0946287	-0.0003949
446	763	4.056	180.10242	[M+H]+	C10H13NO2		179.0946287	-0.0004949
447	764	4.498	180.10249	[M+H]+	C10H13NO2		179.0946287	-0.0005949

448	1806	2.013	245.09537	[M+FA+H]+	C12H10N2O		198.0793129	-0.0033316
449	3056	7.007	313.22824	[M+H-H2O]+	C20H30N2O2		330.2307282	-0.00076
450	1849	5.257	247.1443	[M+H]+	C14H18N2O2		246.1368278	-0.0001957
451	874	6.192	187.13298	[M+H]+	C10H18O3		186.1255944	-0.0001291
452	892	4.397	188.12881	[M+H]+	C9H17NO3	Polyethylene glycol	187.1208434	-0.0006801
453	926	5.459	191.06464	[M+H]+	C6H10N2O5		190.0589714	0.0016479
454	2045	3.55	261.12344	[M+H]+	C14H16N2O3	ine-L-tyrosine anhydride;Cyclo(L-	260.1160924	-3.12E-05
455	928	5.691	191.08453	[M+Na]+	C13H12		168.0939004	-0.0013789
456	1378	5.629	215.06871	[M+Na]+	C11H12O3		192.0786442	-0.0008351

ANNEXE 3 - EPIGENETIC MODIFIERS

ID	Alignment	Average.Rt.min	Average.Mz	Adduct.type	Formula	Structure	Total.score	Theoretical.mas	Mass.error
1	101	3.671	180.10167	[M+H]+	C10H13NO2			179.0946287	0.0002051
2	103	4.535	182.02747	[M+H]+	C5H11NO2S2			181.0231206	0.002897
3	105	4.326	183.09195	[M+H]+	C7H10N4O2			182.0803756	-0.004248
4	107	3.916	185.12848	[M+H]+	C9H16N2O2			184.1211778	-4.58E-05
5	110	4.289	188.12839	[M+H]+	C9H17NO3	Polyethylene glycol	7.0045	187.1208434	-0.0002801
6	112	5.313	191.07054	[M+H]+	C11H10O3			190.0629942	-0.0002294
7	113	5.494	193.08578	[M+H]+	C11H12O3	Terricolyne	5.2244	192.0786442	0.0001207
8	139	6.877	200.28011	[M+H]+					
9	142	5.504	202.14395	[M+H]+	C10H19NO3			201.1364935	-0.0002301
10	143	3.361	204.12291	[M+H]+	C9H17NO4	acine B1;(1S,2R,3R,5R,7aR)-1,2-Dihydroxy-3,5	8.1144	203.115758	0.0001345
11	144	3.524	205.09708	[M+H]+	C11H12N2O2	L-Tryptophan	7.3486	204.0898776	5.41E-05
12	146	0.933	208.06393	[M+H]+	C10H9NO4			207.0531578	-0.0034658
13	147	4.624	208.09639	[M+H]+	C11H13NO3			207.0895433	0.0004197
14	148	5.535	208.09685	[M+H]+	C11H13NO3	(+)-Streptazolin	7.6517	207.0895433	1.97E-05
15	149	4.255	208.09695	[M+H-H2O]+	C11H15NO4			225.100108	-0.0001803
16	150	6.156	208.09697	[M+H]+	C11H13NO3	Thalifoline	6.9737	207.0895433	-0.0001803
17	151	6.366	208.13306	[M+H]+	C12H17NO2			207.1259288	0.0001052
18	152	6.923	209.08092	[M+H]+	C11H12O4	6-Methoxymellein	4.9472	208.0735589	-6.47E-05
19	154	4.092	209.08105	[M+H]+	C11H12O4			208.0735589	-0.0002647
20	160	7.13	211.08679	[M+H]+	C13H10N2O			210.0793129	-0.0002106
21	114	4.267	193.08595	[M+H-H2O]+	C11H14O4			210.0892089	-7.93E-05
22	164	4.431	211.1445	[M+H]+	C11H18N2O2	L,L-Cyclo(leucylprolyl)	6.1578	210.1368278	-0.0003957
23	171	4.899	213.1597	[M+H]+	C11H20N2O2			212.1524779	5.43E-05
24	183	6.884	222.11258	[M+H]+	C12H15NO3			221.1051933	-0.0001302
25	187	6.266	225.08711	[M+H]+	C10H12N2O4	Stavudine	6.6801	224.0797069	-0.0001167
26	188	5.556	225.11209	[M+H]+	C12H16O4			224.104859	3.54E-05
27	189	7.284	225.19597	[M+H]+	C13H24N2O			224.1888634	0.0001398
28	193	4.331	227.09178	[M+H]+	C11H14O5			226.0841235	-4.00E-04
29	195	7.677	227.12784	[M+H]+	C12H18O4			226.1205091	-1.45E-05
30	196	3.776	227.13875	[M+H]+	C11H18N2O3	Amobarbital	6.1565	226.1317424	0.0003189
31	197	5.156	227.13885	[M+H]+	C11H18N2O3			226.1317424	0.0001189
32	198	5.464	227.17537	[M+H]+	C12H22N2O2			226.1681279	4.40E-06
33	203	2.814	228.13431	[M+H]+	C10H17N3O3			227.1269914	-3.21E-05
34	207	7.764	229.14339	[M+H]+	C12H20O4			228.1361591	3.56E-05
35	208	6.842	229.14355	[M+H]+	C12H20O4			228.1361591	-0.0001644
36	21	4.196	122.05992	[M+H]+	C7H7NO			121.0527638	0.0001403
37	211	4.469	231.12236	[M+H]+	C12H14N4O			230.1167611	0.0016375
38	224	4.328	240.1234	[M+H]+	C12H17NO4			239.115758	-0.0003655
39	225	6.468	240.15939	[M+H]+	C13H21NO3			239.1521435	2.00E-05
40	226	0.873	242.10225	[M+H]+	C11H15NO5			241.0950226	9.90E-05
41	228	3.285	242.14995	[M+H]+	C11H19N3O3			241.1426415	1.79E-05
42	229	3.712	243.13336	[M+H]+	C16H18O2			242.1306798	0.0045563

43	23	1.209	123.05505	[M+H]+	C6H6N2O	Niacinamide	5.8124	122.0480128	0.0001893
44	230	4.092	243.13396	[M+H]+	C11H18N2O4			196.1211778	-6.68E-05
45	232	6.576	244.09666	[M+H]+	C9H13N3O5	Vertilecanin A methyl ester	5.2244	243.0855205	-0.003903
46	234	4.887	244.15408	[M+H]+	C12H21NO4			243.1470582	0.0002346
47	235	4.597	245.05583	[M+H]+	C9H12N2O4S			244.0517779	0.0032543
48	236	1.873	245.09558	[M+H]+	C10H16N2O3S	Biotin	7.5918	244.0881634	-0.0001602
49	238	4.507	245.12859	[M+H]+	C14H16N2O2	Limazepine F;(+)-Limazepine F	6.5852	244.1211778	-0.0001458
50	239	4.708	245.12877	[M+H]+	C14H16N2O2	Limazepine F;(+)-Limazepine F	6.9662	244.1211778	-0.0003458
51	244	5.679	247.05328	[M+H-H2O]+	C12H12N2O3S			264.0568632	0.000275
52	245	6.771	247.05367	[M+H]+	C12H10N2O2S			200.0408193	-0.0001253
53	248	5.147	247.14398	[M+H]+	C14H18N2O2			246.1368278	0.0001043
54	250	6.53	249.06929	[M+H]+	C12H12N2O2S			248.0619486	-7.49E-05
55	252	4.868	251.05513	[M+H]+	C12H10O6			250.047738	-8.55E-05
56	254	3.849	252.08658	[M+H]+	C12H13NO5			251.0793725	4.90E-05
57	255	4.67	252.09789	[M+H]+	C11H13N3O4			251.0906059	-1.77E-05
58	256	3.81	253.07056	[M+H]+	C12H12O6			252.0633881	6.46E-05
59	261	5.437	255.06551	[M+H]+	C15H10O4	Chrysophanol	6.4368	254.0579088	-0.0003147
60	263	5.305	255.08643	[M+H]+	C12H14O6	Fumiquinone A	6.3439	254.0790382	-8.54E-05
61	264	5.276	255.13429	[M+NH4]+	C12H15NO4			237.100108	-0.0003665
62	268	0.913	256.11823	[M+NH4]+	C12H14O5			238.0841235	-0.0002509
63	271	5.514	257.08063	[M+H]+	C15H12O4	(2S)-Liquiritigenin	7.6136	256.0735589	0.0002353
64	278	4.351	261.12323	[M+H]+	C14H16N2O3			260.1160924	0.0001688
65	182	5.608	222.11255	[M+H]+	C12H15NO3			221.1051933	-3.02E-05
66	286	3.886	263.13876	[M+H]+	C14H18N2O3			262.1317424	0.0002189
67	287	3.606	264.12308	[M+H]+	C14H17NO4			263.115758	-6.55E-05
68	288	6.955	264.15927	[M+H]+	C15H21NO3			263.1521435	0.00012
69	290	4.815	265.0976	[M+H]+	C13H16N2O2S			264.0932488	0.0029252
70	291	5.104	265.11813	[M+H]+	C13H16N2O4			264.111007	0.0001834
71	292	4.177	265.11832	[M+H]+	C13H16N2O4			264.111007	-1.66E-05
72	297	0.919	268.10425	[2M+NH4]+					
73	298	1.232	268.10431	[M+H]+	C10H13N5O4	Adenosine	9.2014	267.0967539	-0.0002697
74	301	3.746	269.06564	[M+H]+	C12H12O7			268.0583027	-2.08E-05
75	302	6.43	270.11267	[M+Na]+	C14H17NO3			247.1208434	-0.0026359
76	304	6.11	271.06003	[M+H]+	C15H10O5	Emodin	6.5017	270.0528234	9.99E-05
77	306	5.912	271.11795	[M+H]+	C13H18O6			270.1103383	-0.0003853
78	308	0.927	272.11301	[M+H-H2O]+	C12H19NO7			289.1161519	-0.0001363
79	314	4.763	276.12094	[M+Na]+	C13H19NO4			253.1314081	-0.0002712
80	317	4.34	277.11844	[M+H]+	C9H16N4O6			276.1069842	-0.0041393
81	163	4.264	211.14444	[M+H]+	C11H18N2O2	L,L-Cyclo(leucylprolyl)	6.1323	210.1368278	-0.0002957
82	319	4.03	277.155	[M+H]+	C15H20N2O3			276.1473925	-0.000331
83	320	8.906	277.21597	[M+H-H2O]+	C18H30O3	E,12Z,15Z)-9-Hydroxy-10,12,15-octadecatrien	6.6235	294.2194948	0.0002066
84	323	4.837	279.13385	[M+H]+	C14H18N2O4	1-(alpha-D-ribosyl)-5,6-dimethyl-benzimidazo	7.3687	278.1266571	3.35E-05
85	326	1.499	282.06436	[M+H]+	C12H11NO7			281.0535517	-0.0035719
86	329	4.366	283.10764	[M+H]+	C16H14N2O3			282.1004423	0.0001188
87	33	1.605	131.07024	[M+H]+	C6H10O3	Ketoleucine	5.4301	130.0629942	7.06E-05

88	332	4.469	283.10828	[M+H]+	C13H18N2O3S			282.1038134	0.0027899
89	336	5.563	285.07632	[M+H]+	C16H12O5			284.0684735	-0.0005501
90	337	0.87	285.10825	[M+H]+	C12H16N2O6			284.1008362	-8.73E-05
91	100	6.869	179.07039	[M+H]+	C10H10O3	Cinnamaldehyde	6.2215	132.0575149	-0.0001297
92	341	5.931	287.19659	[M+H]+	C19H26O2			286.1932801	0.0039565
93	347	4.68	290.13901	[M+H]+	C16H19NO4			289.1314081	-0.0003155
94	352	5.032	292.1546	[M+H]+	C16H21NO4			291.1470582	-0.0002654
95	353	5.245	292.15475	[M+H]+	C16H21NO4			291.1470582	-0.0004654
96	355	8.058	292.19116	[M+H]+	C17H25NO3			291.1834437	-0.0004799
97	357	5.841	293.0593	[M+H]+	C9H8N8O2S			292.0490925	-0.0029311
98	361	6.211	293.12866	[M+H]+	C18H16N2O2			292.1211778	-0.0002458
99	363	5.817	295.14465	[M+H]+	C18H18N2O2			294.1368278	-0.0005957
100	364	9.819	295.22684	[M+H]+	C18H30O3	o-2-(2-entenyl)cyclopentaneoctanoic acid;OP(	6.7468	294.2194948	-2.87E-05
101	366	5.019	297.18549	[M+H]+	C20H24O2	17a-Ethynylestradiol	6.5489	296.17763	-0.0005935
102	368	4.463	298.12869	[M+H]+	C14H19NO6	UNPD147549	6.7766	297.1212373	-0.0001862
103	369	5.454	298.16476	[M+H]+	C15H23NO5			297.1576228	9.93E-05
104	370	6.634	298.16476	[M+H]+	C15H23NO5			297.1576228	9.93E-05
105	371	5.62	298.16498	[M+H]+	C15H23NO5			297.1576228	-0.0001007
106	372	0.894	299.12433	[M+H]+	C18H18O4			298.1205091	0.0034855
107	374	6.412	300.14392	[M+H]+	C14H21NO6			299.134202	-0.0024215
108	376	5.348	300.17035	[M+H]+	C17H21N3O2			299.1633769	0.0003534
109	377	4.161	301.11859	[M+H]+	C16H16N2O4			300.111007	-0.0003166
110	386	5.986	306.17023	[M+H]+	C17H23NO4			305.1627082	-0.0002153
111	388	0.919	308.14969	[M+H]+	C16H21NO5			307.1419728	-0.0004508
112	389	5.73	309.08728	[M+H]+	C17H12N2O4			308.0797069	-0.0003167
113	390	5.082	309.12366	[M+H]+	C18H16N2O3			308.1160924	-0.0003312
114	391	5.613	309.12378	[M+H]+	C18H16N2O3			308.1160924	-0.0004312
115	392	3.835	310.16467	[M+H]+	C16H23NO5			309.1576228	0.0001993
116	394	5.499	311.13892	[M+H]+	C18H18N2O3			310.1317424	0.0001189
117	395	5.898	311.1391	[M+H]+	C18H18N2O3			310.1317424	-8.11E-05
118	396	4.658	311.13953	[M+H]+	C18H18N2O3			310.1317424	-0.0004811
119	397	5.701	311.15985	[M+H]+	C20H22O3			310.1568946	0.004271
120	399	11.016	311.29407	[M+H]+	C20H38O2	Eicosenoic acid	6.4012	310.2871805	0.0003569
121	403	2.801	313.18091	[M+H]+	C20H24O3			312.1725446	-0.0010789
122	404	4.375	315.13422	[M+H]+	C17H18N2O4			314.1266571	-0.0002665
123	405	4.46	315.13467	[M+H]+	C17H18N2O4			314.1266571	-0.0007665
124	409	9.121	320.22214	[M+H]+	C19H29NO3			319.2147438	-7.98E-05
125	414	6.906	323.13937	[M+H]+	C19H18N2O3	Diphenylalazine B;(+)-Diphenylalazine B	6.4654	322.1317424	-0.0003811
126	416	4.552	324.18127	[M+H]+	C17H25NO5			323.1732729	-0.0007506
127	418	6.791	326.23215	[M+H]+	C18H31NO4			325.2253085	0.0004849
128	419	11.091	326.37772	[M+H]+	C22H47N			325.3708505	0.000427
129	421	7.133	327.13397	[M+H]+	C18H18N2O4			280.117155	-0.0040896
130	426	9.049	331.24826	[M+H-H2O]+	C18H36O6			348.2511889	-0.0003994
131	427	8.46	332.27954	[M+NH4]+	C18H34O4	9,10-Epoxy-18-hydroxy-octadecanoic acid	5.8321	314.2457096	3.51E-05
132	430	6.031	335.16028	[M+H]+	C17H22N2O5			334.1528718	-0.0001517

133	431	4.623	336.16736	[M+H]+	C15H21N5O4			335.1593542	-0.0007694
134	432	8.585	337.10455	[M+H]+	C20H16O5			336.0997736	0.0024501
135	439	11.914	339.32611	[M+H]+	C22H42O2	Erucic acid	6.2462	338.3184806	-0.000343
136	44	3.09	141.0545	[M+H]+	C7H8O3			140.0473441	0.0001206
137	443	7.015	341.15942	[M+H]+	C17H24O7			340.1522031	7.96E-05
138	446	5.894	343.12894	[M+H]+	C18H18N2O5			342.1215717	-5.19E-05
139	447	3.967	345.14447	[M+H]+	C18H20N2O5			344.1372217	-1.80E-06
140	262	6.499	255.07651	[M+H]+	C14H10N2O3			254.0691422	-8.14E-05
141	453	4.506	350.16034	[M+H]+	C18H23NO6			349.1525375	-0.0004861
142	454	7.843	351.0972	[M+H]+	C16H18N2O5S			350.0936427	0.0037191
143	455	5.599	351.11118	[M+H]+	C15H18N4O4S			350.1048761	0.0009525
144	456	5.375	351.11139	[M+H]+	C17H18O8			350.1001675	-0.003956
145	428	6.211	335.11606	[M+H]+	C17H18O7			334.1052529	-0.0035706
146	429	6.018	335.11636	[M+H]+	C17H18O7			334.1052529	-0.0038706
147	460	7.762	353.14981	[M+H]+	C20H20N2O4			352.1423071	-0.0002164
148	462	10.806	356.38834	[M+H]+	C23H49NO				
149	464	4.399	357.09042	[M+H]+	C15H20N2O4S2	Bisdethiobis (methylthio)-gliotoxin	6.8552	356.0864491	0.0033256
150	466	6.021	357.10794	[M+H]+	C18H16N2O6			356.1008362	0.0002127
151	467	5.735	359.07312	[M+H]+	C18H14O8			358.0688674	0.0030439
152	471	9.611	365.13712	[M+H]+	C22H20O5			364.1310737	0.0012502
153	472	6.374	367.09293	[M+H]+	C16H18N2O6S			366.0885573	0.0029337
154	474	5.377	367.1062	[M+H]+	C15H18N4O5S			366.0997907	0.0008671
155	477	7.446	371.05176	[M+H]+	C18H14N2O3S2			370.0445843	6.08E-05
156	482	4.134	375.06784	[M+H]+	C15H14N6O2S2			374.063782	0.0032585
157	483	5.598	375.10089	[M+H]+	C18H18N2O5S			374.0936427	1.91E-05
158	484	4.095	375.1012	[M+H]+	C18H18N2O5S			374.0936427	-0.0002809
159	485	5.732	375.10135	[M+H]+	C18H18N2O5S			374.0936427	-0.0003809
160	486	8.53	376.30505	[M+H]+	C20H41NO5			375.2984734	0.0006499
161	488	5.774	378.11893	[M+H]+	C18H19NO8			377.1110666	-0.000557
162	489	6.676	379.14188	[M+H]+	C19H22O8			378.1314677	-0.0031559
163	493	5.893	384.21317	[M+H]+	C23H29NO4			383.2096584	0.0037349
164	502	5.391	390.20255	[M+H]+	C20H27N3O5			389.195071	-0.0001526
165	504	5.058	391.26895	[M+H]+	C20H38O7			390.2617536	3.00E-05
166	505	7.673	396.21707	[M+H]+	C24H29NO4	l-1-(2,4-dimethoxyphenyl)-decahydroisoquin	7.8266	395.2096584	-0.0001651
167	509	7.706	399.1011	[M+H]+	C17H22N2O5S2			398.0970138	0.0031903
168	510	7.833	399.1012	[M+H]+	C20H18N2O5S			398.0936427	-0.0002809
169	512	6.577	400.28067	[M+H]+	C25H37NO3			399.277344	0.0039205
170	520	6.182	408.27411	[M+H]+	C23H37NO5			407.2671733	0.0003497
171	524	6.615	412.21146	[2M+NH4]+	C7H11N5O2			197.0912746	0.0021631
172	529	7.394	417.05701	[M+H]+	C23H12O8			416.0532173	0.0034938
173	53	1.764	145.04936	[M+H]+	C6H8O4	3-Methylglutaconic acid	5.9764	144.0422587	0.0001352
174	530	5.974	417.11136	[M+H]+	C15H20N4O8S			416.1001846	-0.0039389
175	533	4.059	417.11856	[2M+H]+	C11H12O2S			208.0583027	0.0023667
176	536	6.374	419.12741	[M+H]+	C20H22N2O6S			418.1198574	-0.0002661
177	540	8.345	423.20093	[M+H]+	C22H30O8			422.1940679	0.0004444

178	541	10.536	425.21414	[M+Na]+	C20H34O8	UNPD173832	6.9284	402.225368	0.0004887
179	526	5.661	415.04208	[M+H-H2O]+	C23H12O9			432.048132	0.0027437
180	55	3.233	146.05971	[M+H]+	C9H7NO			145.0527638	0.0003403
181	550	6.625	433.05283	[M+H]+	C23H12O9			432.048132	0.0026084
182	552	6.272	433.10684	[M+H]+	C20H20N2O7S			432.099122	-0.0004016
183	554	7.366	434.08426	[M+H]+	C19H19N3O5S2			433.0766127	-0.0004108
184	531	6.13	417.11142	[M+H]+	C15H20N4O8S			416.1001846	-0.0039389
185	556	8.599	435.06665	[M+H]+	C22H14N2O6S			434.0572572	-0.0021664
186	557	6.93	435.06802	[M+H]+	C23H14O9			434.063782	0.0030585
187	194	6.578	227.1026	[M+H]+	C10H14N2O4	Porphobilinogen	6.3809	226.0953569	3.34E-05
188	56	5.027	146.05972	[M+H]+	C9H7NO			145.0527638	0.0003403
189	566	4.79	442.03427	[M+H]+	C14H16N7O2PS3				
190	567	4.397	446.19684	[M+H]+	C20H27N7O3S			445.188923	-0.0006006
191	569	7.076	447.06781	[M+H]+	C11H20N4O11P	CDP-Ethanolamine	6.176	446.0603807	-0.0001428
192	545	6.188	431.09149	[M+H]+	C17H22N2O7S2			430.086843	0.0026195
193	574	6.659	449.04733	[M+H]+					
194	580	4.383	450.13239	[M+H]+	C20H23N3O7S			449.1256711	0.0005475
195	583	6.837	451.06299	[M+H]+	C23H14O10			450.0586966	0.0029731
196	593	7.509	455.03375	[M+H]+	C14H14N8O4S3			454.0300139	0.0034904
197	594	4.265	457.20728	[2M+H]+	C11H16O5			228.0997736	-0.0005125
198	597	6.439	459.04837	[M+H]+					
199	598	7.757	459.26392	[M+H]+	C29H34N2O3			458.2569429	0.0003194
200	599	8.363	459.26431	[M+H]+	C29H34N2O3			458.2569429	-8.06E-05
201	602	6.272	463.09909	[M+H]+	C14H19N6O10P	Botryosulfuranol A isomer		462.0900274	-0.0017961
202	604	5.942	463.12332	[M+H]+	C22H22O11	6-Methoxyluteolin 7-rhamnoside	7.6539	462.1162115	0.000188
203	609	8.04	465.07861	[M+H]+	C24H16O10			464.0743467	0.0030232
204	614	3.719	466.12805	[M+H]+	C24H23N3O3S2			465.1180836	-0.00274
205	553	4.558	433.11356	[M+H]+	C21H20O10	henyl)-6-[3,4,5-trihydroxy-6-(hydroxymethyl)c	8.2188	432.1056468	-0.0006767
206	616	6.007	467.05765	[M+H]+					
207	648	7.917	489.11267	[M+Na]+	C25H22O9			466.1263823	0.002903
208	584	6.45	451.06308	[M+H]+	C23H14O10			450.0586966	0.0028731
209	581	4.815	450.13297	[M+H-H2O]+	C24H25N3O3S2			467.1337337	-0.0025546
210	620	4.021	468.14337	[M+H]+	C23H21N3O8			467.1328646	-0.0032589
211	621	9.578	473.36307	[M+H]+	C30H48O4	Ganodermanontriol	5.9807	472.35526	-0.0005635
212	624	7.575	478.10983	[M+H]+	C21H23N3O6S2			477.1028275	0.0003039
213	628	5.516	479.11847	[M+H]+	C22H22O12	yphenyl)-3-{[3,4,5-trihydroxy-6-(hydroxymetl	8.7521	478.1111261	-9.74E-05
214	595	9.583	457.27881	[M+H]+	C24H40O8			456.2723182	0.0007947
215	603	7.049	463.09927	[M+H]+	C25H18O9	Botryosulfuranol A		462.0950822	0.0030586
216	632	6.518	481.07349	[M+H]+	C20H20N2O8S2	Gliovirin	5.8412	480.0661076	-0.0001159
217	635	7.205	482.05057	[M+NH4]+					
218	641	6.648	483.03506	[M+H]+					
219	642	5.915	484.0849	[M+H]+	C17H18N5O10P			483.0791284	0.0015049
220	649	4.847	489.23529	[M+H]+	C29H32N2O5			488.2311221	0.0030986
221	650	9.76	491.16754	[M+H]+	C28H26O8	Homodimericin A	5.6618	490.1627678	0.0025442
222	653	5.761	496.11722	[M+H]+	C21H25N3O7S2			495.1133921	0.0034686

223	473	4.967	367.09338	[M+H-H2O]+	C19H16N2O7			384.0957509	-0.0009374
224	658	6.068	498.13278	[M+H]+	C24H23N3O7S			497.1256711	0.0001475
225	659	5.295	498.13614	[M+NH4]+	C24H20N2O7S			480.099122	-0.0031525
226	634	6.476	481.11002	[M+H]+	C25H20O10			480.1056468	0.0029233
227	662	9.886	498.37875	[M+H]+	C28H51NO6			497.3716384	0.0001148
228	663	6.52	500.06149	[M+NH4]+					
229	664	4.979	501.0755	[M+H]+	C14H22N4O12P2			500.0709454	0.0027219
230	667	10.042	505.1832	[M+H]+	C24H28N2O10			504.1743951	-0.0015285
231	668	7.181	507.08881	[M+H]+	C26H18O11			506.0849114	0.0033878
232	67	0.802	151.03505	[M+H]+	C8H6O3			150.0316941	0.0039705
233	519	6.095	407.18143	[M+H]+	C20H26N2O7			406.1740012	-0.0001224
234	677	6.794	513.04437	[M+H]+					
235	678	5.673	514.11017	[M+H]+	C28H19NO9			513.1059812	0.0030576
236	656	7.802	497.08688	[M+H]+	C28H16O9			496.0794321	-0.0001915
237	682	10.012	519.19891	[M+H]+	C30H30O8			518.1940679	0.0024444
238	280	3.428	261.12369	[M+H]+	C14H16N2O3			260.1160924	-0.0003312
239	689	5.218	524.11145	[M+H]+					
240	691	6.049	526.11005	[M+H]+	C18H23N9O4S3	Cefotiam	6.2597	525.1035132	0.0007897
241	693	6.012	528.12579	[M+H]+	C29H21NO9			527.1216313	0.0031077
242	696	5.734	530.10486	[M+H]+	C18H24N7O6PS2			529.1008958	0.0032723
243	698	5.944	538.13153	[M+NH4]+	C20H20N6O9S			520.1012472	0.0035728
244	684	6.328	521.10516	[M+H]+	C20H20N6O9S			520.1012472	0.0033237
245	1	2.987	102.0547	[M+H]+	C4H7NO2			101.0476785	0.0002549
246	417	7.181	324.21756	[M+H]+	C18H29NO4			323.2096584	-0.0006651
247	704	6.5	540.14697	[M+NH4]+	C19H22N8O6S2			522.1103724	-0.002802
248	705	6.055	542.14154	[M+H]+	C30H23NO9			541.1372813	0.0030578
249	708	6.172	544.12091	[M+H]+	C17H26N3O15P			543.1101538	-0.0034698
250	711	6.163	549.15088	[M+H]+	C28H24N2O10			548.143095	-0.0005286
251	714	4.78	551.13977	[2M+Na]+	C17H12O3			264.0786442	0.0030803
252	701	8.707	538.39587	[M+H]+	C33H51N3O3			537.3930425	0.0044189
253	718	5.84	560.15167	[M+H]+	C30H25NO10			559.147846	0.0034225
254	72	1.432	155.0815	[M+H]+	C7H10N2O2			154.0742276	4.00E-06
255	734	6.007	569.07159	[M+H]+	C30H16O12			568.064176	-0.0001476
256	735	6.292	569.35461	[M+H]+	C33H48N2O6			568.3512373	0.0039137
257	716	9.037	552.4126	[M+H]+	C29H53N5O5	Cyclo-(L-Leu-L-Leu-D-Leu-L-Leu-L-Val)	6.0255	551.4046698	-0.0006538
258	738	6.323	571.08716	[M+H]+	C30H18O12			570.079826	-9.75E-05
259	742	6.386	574.16791	[M+H]+	C31H27NO10			573.1634961	0.0028725
260	745	4.748	581.15155	[M+H]+	C26H28O15	Neocarlinoside	6.2047	580.1428202	-0.0015034
261	746	6.964	582.10327	[M+NH4]+	C27H20N2O8S2			564.0661076	-0.0033668
262	730	9.366	566.42798	[M+H]+	C30H55N5O5	Cyclo-(L-Ile-L-Leu-L-Leu-L-Leu-L-Leu)	5.9073	565.4203199	-0.0004037
263	761	9.252	600.41089	[M+H]+	C33H53N5O5	Cyclo-(L-Phe-L-Leu-L-Leu-L-Leu-L-Ile	5.9294	599.4046698	0.0010462
264	762	6.255	601.09735	[M+H]+	C24H28N2O10S3			600.0906081	0.0004845
265	763	6.693	602.1297	[M+H]+					
266	750	6.794	585.10376	[M+H]+	C24H28N2O9S3			584.0956935	-0.0008301
267	770	5.213	625.1767	[M+H]+	C28H32O16	Tamarixetin 3-robinobioside	6.3859	624.1690349	-0.0003886

268	771	5.105	631.12927	[M+H]+	C29H26O16			630.1220848	6.12E-05
269	330	6.254	283.10782	[M+H]+	C16H14N2O3			282.1004423	-8.12E-05
270	775	6.293	649.35559	[M+H]+	C35H52O11			648.3509625	0.0026389
271	781	9.523	681.44171	[M+H]+	C34H64O13			680.4346921	0.0002686
272	783	12.131	685.43445	[M+H]+	C34H60N4O10			684.4309441	0.0038206
273	791	5.714	747.37244	[M+H]+	C44H50N4O7	Pandicine	6.2146	746.3679499	0.0028264
274	793	11.516	758.59125	[M+H]+					
275	293	2.194	266.15485	[M+H]+	C18H19NO			265.1466642	-0.0008593
276	812	6.161	869.17889	[M+H]+					
277	813	12.11	871.57373	[M+H]+	C55H74N4O5	Pheophytin-a;Pheophytin a5	7.2856	870.5659215	-0.0005021
278	548	7.496	433.05215	[M+H]+	C23H12O9	Botryosulfuranol C		432.048132	0.0032084
279	83	5.566	166.12236	[M+H]+	C10H15NO	Pseudoephedrine	6.1942	165.1153641	0.0002406
280	834	7.47	919.14563	[M+Na]+					
281	839	7.095	931.14307	[M+H]+					
282	84	0.802	167.01257	[M+H]+	C4H7O5P			166.00311	-0.0022136
283	610	7.317	465.11496	[M+H]+	C25H20O9	Botryosulfuranol B		464.1107322	0.0030087
284	858	7.526	1014.14862	[M+H]+					
285	109	5.025	187.13281	[M+H]+	C10H18O3			186.1255944	7.09E-05
286	860	8.63	1049.6969	[M+H]+	C68H92N2O7			1048.690453	0.0007297
287	861	9.188	1053.72791	[M+H]+					
288	863	9.378	1079.74487	[M+H]+					
289	867	9.784	1093.75769	[M+H]+	C55H100N10O12			1092.752219	0.0014951
290	90	1.344	174.05482	[M+H]+	C10H7NO2			173.0476785	0.0001549
291	91	4.352	174.11247	[M+H]+	C8H15NO3			173.1051933	-3.02E-05
292	96	4.826	177.05453	[M+H]+	C10H8O3	10-Hydroxy-2,8-decadiene-4,6-diynoic acid	5.8021	176.0473441	0.0001206
293	98	5.301	177.05461	[M+H]+	C10H8O3	Herniarin	6.8944	176.0473441	2.06E-05
294	99	4.557	179.07024	[M+H-H2O]+	C10H12O4			196.0735589	7.06E-05

ANNEXE 4 - ADDITION OF AMINO ACIDS

ID	Alignment	Average.Rt.min.	Average.Mz	Adduct.type	Formula	Structure	Theoretical.mass	Mass.error
1	100	3.856	154.04971	[M+H]+	C7H7NO3	ıydroxyanthranilic a	153.0425931	0.0001695
2	1019	6.25	313.08124	[M+H]+				
3	1025	9.9	313.14404	[M+H]+	C19H20O4		312.1361591	
4	103	3.209	154.08612	[M+H]+	C8H11NO2		153.0789786	
5	106	0.581	158.02655	[M+NH4]+	C3H8O2S2		139.9965715	
6	1238	5.232	345.10742	[M+FA+H]+	C16H14N2O4		298.0953569	
7	1271	5.674	351.09702	[M+H]+	C16H18N2O5S		350.0936427	
8	1296	9.054	354.33679	[M+H]+	C22H43NO2		353.3293796	
9	1305	8.187	356.10223	[M+FA+H]+	C14H15NO7		309.0848518	
10	1306	5.454	356.13873	[M+H-2H2O]+	C19H25N3O4S		391.1565773	
11	1339	5.893	360.17987	[M+H]+	C20H25NO5		359.1732729	
12	1364	9.742	365.13605	[M+H]+	C22H20O5		364.1310737	
13	1449	5.889	382.16165	[M+FA+H]+	C16H21N3O5		335.1481208	
14	151	1.382	174.05469	[M+H]+	C10H7NO2		173.0476785	
15	1542	6.857	401.09784	[2M+H]+	C12H8O3		200.0473441	
16	1549	10.659	403.23297	[M+H]+	C20H34O8		402.225368	
17	155	3.073	176.07042	[M+H]+	C10H9NO2	Indoleacetic acid	175.0633285	0.000205
18	157	1.852	176.07047	[M+H]+	C10H9NO2	ıino-4-methylcoum	175.0633285	0.000105
19	1592	7.51	417.05621	[M+H]+				
20	162	4.315	178.08632	[M+H]+	C10H11NO2	3a-Hydroxyfuroindo	177.0789786	-4.50E-05
21	1628	11.006	424.30621	[M+NH4]+	C24H38O5		406.2719243	
22	1650	11.228	429.26089	[M+H]+	C26H36O5		428.2562743	
23	1651	10.998	429.26105	[M+Na]+	C24H38O5	3-Oxocholic acid	406.2719243	0.000145
24	1652	11.629	429.26196	[M+H]+	C26H36O5		428.2562743	
25	167	3.752	180.10172	[M+H]+	C10H13NO2		179.0946287	
26	168	4.079	180.10191	[M+H]+	C10H13NO2		179.0946287	
27	1692	8.311	438.24847	[M+H]+	C23H35NO7		437.2413525	
28	1702	6.756	440.21707	[M+H]+	C21H33N3O5S		439.2140922	
29	1734	6.275	448.11594	[M+NH4]+	C17H22N2O7S2		430.086843	
30	1742	7.604	450.07709	[M+NH4]+	C19H16N2O6S2	Botryosulfuranol C	432.04	
31	1745	6.593	450.13159	[M+H]+	C20H23N3O7S		449.1256711	
32	1757	6.277	453.07156	[M+Na]+	C17H22N2O7S2		430.086843	
33	1806	5.565	464.11197	[M+NH4]+				
34	1123	7.228	327.13315	[M+H]+	C13H18N4O6		326.1226343	
35	1884	7.144	480.05118	[M+H]+	C22H13N3O8S		479.0423354	
36	1784	7.14	463.09753	[M+H]+	C21H22N2O6S2	Botryosulfuranol A	462.0900274	
37	1891	7.14	480.21042	[M+H]+	C26H29N3O6	amide H;(-)-Notoam	479.2056356	0.0025121
38	1908	7.415	482.06784	[M+H]+				
39	1910	7.408	482.13934	[M+NH4]+	C21H24N2O6S2	Botryosulfuranol B	464.11	
40	1911	8.292	482.14224	[M+NH4]+	C25H20O9		464.1107322	
41	1871	6.858	478.14502	[M+NH4]+	C22H24N2O5S2		460.1126639	
42	1370	5.055	367.09192	[M+H-H2O]+	C19H16N2O7		384.0957509	

43	1970	6.552	498.13516	[M+NH4]+	C24H20N2O7S		480.099122	
44	1980	5.061	501.0752	[M+Na]+	C25H18O10		478.0899968	
45	199	1.583	192.12306	[M+H]+	C8H17NO4		191.115758	
46	2005	7.425	510.17102	[M+FA+H]+	C25H25N3O4S		463.1565773	
47	203	5.594	193.08574	[M+H-H2O]+	C11H14O4		210.0892089	
48	1718	8.384	445.23178	[M+H]+	C24H32N2O6		444.2260367	
49	2097	11.828	554.17615	[M+NH4]+				
50	2099	8.794	555.42218	[M+NH4]+	C33H51N3O3		537.3930425	
51	2131	9.448	566.427	[M+H]+	C30H55N5O5	-Ile-L-Leu-L-Leu-L-Le	565.4203199	0.0005963
52	2166	5.367	574.12628	[M+H]+	C19H24N7O12P		573.1220558	
53	2180	7.061	582.10187	[M+H]+				
54	2208	9.451	588.40869	[M+Na]+	C30H55N5O5		565.4203199	
55	2209	11.101	588.4101	[M+H]+	C32H53N5O5		587.4046698	
56	2170	9.125	574.39386	[M+Na]+	C29H53N5O5	Leu-L-Leu-D-Leu-L-L	551.4046698	-9.50E-06
57	2230	7.744	600.37756	[M+H]+	C31H53NO10		599.3669469	
58	2240	9.189	603.42151	[M+NH4]+	C31H55NO9		585.3876823	
59	2256	9.475	611.48566	[M+H]+				
60	2231	9.511	600.41119	[M+H]+	C33H53N5O5	-Phe-L-Leu-L-Leu-L-	599.4046698	0.0007462
61	238	4.371	202.14395	[M+H]+	C10H19NO3		201.1364935	
62	2397	7.607	903.0509	[M+H]+				
63	2398	7.461	903.14423	[M+H]+				
64	2409	7.591	919.14124	[M+Na]+				
65	2421	7.174	931.14014	[2M+Na]+	C13H19N4O12P		454.0737087	
66	2438	7.411	951.20111	[2M+Na]+	C21H24N2O6S2		464.11	
67	245	10.066	205.086	[M+H]+	C12H12O3		204.0786442	
68	273	3.837	210.07599	[M+H]+	C10H11NO4	lilamine;(+)-Penidila	209.0688078	8.43E-05
69	274	7.009	210.11195	[M+H]+	C11H15NO3		209.1051933	
70	283	4.548	211.08899	[M+H]+	C10H14N2OS		210.0826841	
71	284	6.421	211.09618	[M+H]+	C11H14O4		210.0892089	
72	293	0.583	212.07339	[M+H]+	C10H13NO2S		211.0666997	
73	311	0.597	214.08955	[M+H]+	C10H15NO2S		213.0823497	
74	312	1.184	214.08961	[M+H]+	C10H15NO2S		213.0823497	
75	340	2.573	220.118	[M+H]+	C9H17NO5		219.1106726	
76	347	5.055	221.07068	[M+H]+	C11H12N2OS		220.067034	
77	364	4.643	224.1281	[M+NH4]+	C12H14O3		206.0942943	
78	1367	5.333	366.15405	[M+H]+	C18H23NO7		365.1474521	
79	381	5.348	227.08084	[M+H]+	C8H10N4O4		226.0702048	
80	393	5.304	228.159	[M+H]+	C12H21NO3		227.1521435	
81	394	5.476	228.15903	[M+H]+	C12H21NO3		227.1521435	
82	395	5.163	228.15909	[M+H]+	C12H21NO3		227.1521435	
83	405	3.259	229.11809	[M+H]+	C10H16N2O4		228.111007	
84	41	1.675	131.06998	[2M+H]+				
85	413	4.295	230.13885	[M+H]+	C11H19NO4		229.1314081	
86	455	6.405	238.10693	[M+H]+	C12H15NO4	(+)-Flavipucine	237.100108	0.0004844
87	456	5.958	238.10707	[M+H]+	C12H15NO4	(+)-Flavipucine	237.100108	0.0002844

88	458	4.405	238.10724	[M+H]+	C12H15NO4		237.100108	
89	477	6.175	241.09668	[M+H]+	C14H12N2O2	.b-tetrahydroquinol	240.0898776	0.0004541
90	490	4.124	243.11374	[M+FA+H]+	C8H12N4O2		196.0960256	
91	499	4.98	244.1541	[M+H]+	C12H21NO4		243.1470582	
92	514	4.52	246.07339	[M+Na]+	C11H13NO4		223.0844579	
93	516	5.27	246.16963	[M+H]+	C12H23NO4		245.1627082	
94	517	3.562	246.17004	[M+H]+	C12H23NO4		245.1627082	
95	520	4.209	246.17024	[M+H]+	C12H23NO4		245.1627082	
96	521	4.22	246.22508	[M+H]+	C17H27N		245.2143499	
97	538	4.102	248.18547	[M+NH4]+	C12H22O4		230.1518092	
98	569	9.648	253.13345	[M+H]+	C16H16N2O		252.1262631	
99	57	2.178	140.07048	[M+H]+	C7H9NO2		139.0633285	
100	570	10.149	253.13368	[M+H]+	C16H16N2O		252.1262631	
101	578	4.83	254.13855	[M+H]+	C13H19NO4		253.1314081	
102	579	4.721	254.13873	[M+H]+	C13H19NO4		253.1314081	
103	457	5.379	238.10713	[M+H]+	C12H15NO4	(+)-Flavipucine	237.100108	0.0002844
104	599	3.945	256.11783	[M+H]+	C12H17NO5		255.1106726	
105	626	5.638	259.12277	[M+H]+	C13H14N4O2		258.1116757	
106	629	5.96	260.08865	[M+Na]+	C12H15NO4		237.100108	
107	644	4.384	262.10495	[M+Na]+	C12H17NO4		239.115758	
108	649	5.026	262.14352	[M+H]+	C15H19NO3	-methylethyl)-3-(ph	261.1364935	0.0002699
109	454	5.751	238.10692	[M+H]+	C12H15NO4	(+)-Flavipucine	237.100108	0.0004844
110	703	6.633	269.09183	[M+H-H2O]+	C15H14N2O4		286.0953569	
111	729	6.084	273.07507	[M+H]+	C15H12O5		272.0684735	
112	752	4.826	276.12036	[M+FA+H]+	C9H15N3O4		229.106256	
113	758	3.866	277.11813	[M+H]+	C9H16N4O6		276.1069842	
114	764	4.384	278.07883	[M+H]+	C9H15N3O5S		277.0732416	
115	779	10.05	279.15918	[M+H]+	C16H22O4		278.1518092	
116	810	5.831	284.11801	[M+H]+	C14H13N5O2		283.1069247	
117	824	4.697	285.12283	[M+H]+	C11H16N4O5		284.1120696	
118	825	4.804	285.12283	[M+H]+	C16H16N2O3		284.1160924	
119	835	5.726	287.09076	[M+H]+	C16H14O5		286.0841235	
120	869	4.828	292.09439	[2M+NH4]+	C7H7NS		137.0299202	
121	871	4.862	292.1539	[M+H]+	C16H21NO4		291.1470582	
122	874	5.941	293.05847	[M+H]+	C9H8N8O2S		292.0490925	
123	879	3.274	293.11301	[M+H]+	C14H16N2O5		292.1059216	
124	909	8.384	297.12256	[M+H]+	C17H16N2O3		296.1160924	
125	929	4.637	299.13858	[M+H]+	C17H18N2O3	Luteoride A	298.1317424	0.0004189
126	932	5.484	299.15918	[M+H]+	C19H22O3		298.1568946	
127	939	4.173	301.11761	[M+H]+	C14H21O5P		300.1126604	
128	941	4.735	301.11856	[M+Na]+	C11H22N2O4S		278.1300282	
129	95	1.549	153.06566	[M+H]+	C7H8N2O2		152.0585775	
130	975	5.202	307.1286	[M+H]+	C15H18N2O5		306.1215717	
131	98	5.963	154.04935	[M+H]+	C7H7NO3	łydroxyanthranilic a	153.0425931	0.0005695
132	99	4.647	154.0497	[M+H]+	C7H7NO3	łydroxyanthranilic a	153.0425931	0.0001695

ANNEXE 5 - HEAT-KILLED LEISHMANIA

ID	Alignment	Average.Rt.min	Average.Mz	Adduct.type	Formula	Structure	Theoretical.mas	Mass.error
1	1009	5.168	366.15494	[M+H]+	C18H23NO7		365.1474521	
2	1097	7.42	385.10333	[M+H]+	C19H16N2O7		384.0957509	
3	1108	6.946	387.1004	[M+H]+	C19H18N2O5S		386.0936427	
4	1119	6.067	392.2272	[M+H]+	C22H33NO3S		391.2181149	
5	1129	6.574	396.22192	[M+NH4]+	C24H26O4		378.1831093	
6	1134	10.857	398.23294	[M+H]+	C24H31NO4		397.2253085	
7	1332	11.468	461.32388	[M+Na]+	C26H46O5		438.3345246	
8	122	3.726	174.11235	[M+H]+	C8H15NO3	Swainsonine;(-)-Swainsonine	173.1051933	6.98E-05
9	1240	10.762	429.26041	[M+Na]+	C24H38O5	3-Oxocholic acid	406.2719243	0.000745
10	1295	6.09	448.11673	[M+NH4]+	C17H22N2O7S2		430.086843	
11	133	4.165	179.11769	[M+H]+	C10H14N2O	Nicotine-1'-N-oxide	178.1106131	0.0001895
12	136	3.908	180.10149	[M+H]+	C10H13NO2		179.0946287	
13	1367	6.981	469.04996	[M+H]+				
14	1292	7.603	447.10309	[M+H]+	C21H22N2O5S2		446.0970138	
15	138	3.59	180.10202	[M+H]+	C10H13NO2	(R)-Salsolinol	179.0946287	-9.49E-05
16	1315	7.396	455.03323	[M+Na]+	C19H16N2O6S2	Botryosulfuranol C	432.0455	
17	1390	6.67	478.14548	[M+NH4]+	C22H24N2O5S2		460.1126639	
18	1439	7.212	487.09592	[M+Na]+	C21H24N2O6S2	Botryosulfuranol B	464.1077	
19	1461	4.882	496.12042	[M+NH4]+	C25H18O10		478.0899968	
20	1467	5.208	498.13568	[M+NH4]+	C24H20N2O7S		480.099122	
21	1402	6.946	480.12448	[M+NH4]+	C21H22N2O6S2	Botryosulfuranol A	462.092	
22	150	1.647	184.09685	[M+H]+	C9H13NO3		183.0895433	
23	1528	5.857	538.13086	[M+NH4]+	C27H20O11		520.1005615	
24	1529	8.592	538.39722	[M+H]+	C33H51N3O3		537.3930425	
25	161	4.219	188.12782	[M+H]+	C9H17NO3	Polyethylene glycol	187.1208434	0.0003199
26	1637	9.244	588.40851	[M+Na]+	C30H55N5O5	Cyclo-(L-Ile-L-Leu-L-Leu-L-Leu-L-Leu)	565.4203199	0.0010406
27	1582	9.072	566.42725	[M+H]+	C30H55N5O5	Cyclo-(L-Ile-L-Leu-L-Leu-L-Leu-L-Leu)	565.4203199	0.0003963
28	1628	11.514	584.47296	[M+H]+				
29	163	2.215	190.10732	[M+H]+	C8H15NO4		189.100108	
30	165	5.229	191.07011	[M+H]+	C11H10O3		190.0629942	
31	1662	6.595	602.12854	[M+NH4]+	C31H20O12		584.0954761	
32	1664	9.245	604.38171	[M+FA+H]+	C33H51NO6		557.3716384	
33	167	2.141	191.17557	[M+H]+	C14H22		190.1721507	
34	1670	12.394	610.18408	[M+H]+				
35	168	1.461	192.12288	[M+H]+	C8H17NO4		191.115758	
36	1657	9.307	600.41162	[M+H]+	C33H53N5O5	yclo-(L-Phe-L-Leu1-L-Leu2-L-Leu3-L-Il	599.4046698	0.0003462
37	169	1.618	192.1232	[M+H]+	C8H17NO4		191.115758	
38	171	5.401	193.08588	[M+H]+	C11H12O3		192.0786442	
39	1745	7.216	729.2132	[M+H]+	C34H36N2O16		728.2064831	
40	1776	12.015	823.51117	[M+H]+	C48H66N6O6		822.5043838	
41	1429	6.947	485.07956	[M+Na]+	C14H19N6O10P	3'-L-aspartyl-AMP	462.092	-0.0003519
42	1829	7.209	949.19055	[M+H]+				

43	1601	8.925	574.39343	[M+Na]+	C29H53N5O5	Cyclo-(L-Leu-L-Leu-D-Leu-L-Leu-L-Val)	551.4046698	0.0004905
44	228	4.589	209.11719	[M+H]+	C12H16O3		208.1099444	
45	233	6.814	210.11198	[M+H]+	C11H15NO3		209.1051933	
46	240	9.12	211.10956	[M+H]+	C10H14N2O3		210.1004423	
47	287	2.326	220.11769	[M+H]+	C9H17NO5	Pantothenic acid	219.1106726	0.0002491
48	29	1.541	131.07004	[M+H]+	C6H10O3	Ketoleucine	130.0629942	0.0002706
49	372	6.22	238.10693	[M+H]+	C12H15NO4	(+)-Flavipucine	237.100108	0.0004844
50	375	5.681	238.10715	[M+H]+	C12H15NO4	(+)-Flavipucine	237.100108	0.0002844
51	384	4.235	240.12276	[M+FA+H]+	C11H15NO2		193.1102787	
52	430	5.088	246.1702	[M+H]+	C12H23NO4		245.1627082	
53	440	6.43	249.06882	[M+H]+	C12H12N2O2S		248.0619486	
54	459	3.757	253.07077	[M+H]+	C12H12O6		252.0633881	
55	463	4.572	254.1384	[M+H]+	C13H19NO4		253.1314081	
56	481	3.797	256.11804	[M+H]+	C12H17NO5		255.1106726	
57	482	0.884	256.11816	[M+H]+	C12H17NO5		255.1106726	
58	490	5.437	257.08087	[M+H]+	C15H12O4	(2S)-Liquiritigenin	256.0735589	-6.47E-05
59	493	7.503	257.17432	[M+H]+	C14H24O4		256.1674592	
60	505	6.764	259.1647	[M+H]+	C12H22N2O4		258.1579572	
61	376	5.192	238.10722	[M+H]+	C12H15NO4	(+)-Flavipucine	237.100108	0.0001844
62	522	4.229	262.10474	[M+FA+H]+	C8H13N3O4		215.0906059	
63	526	4.872	262.14374	[M+H]+	C15H19NO3	ethyl-6-(1-methylethyl)-3-(phenylmeth	261.1364935	6.99E-05
64	538	5.596	265.06384	[M+H]+	C15H8N2O3	4-oxo-1-cyclohexa-2,5-dienylidene)me	264.0534921	-0.0030314
65	573	2.93	272.14917	[M+H]+	C13H21NO5		271.1419728	
66	574	4.669	272.14951	[M+H]+	C13H21NO5		271.1419728	
67	590	8.198	275.20053	[M+FA+H]+	C17H24		228.1878008	
68	60	2.143	146.11751	[M+H]+	C7H15NO2		145.1102787	
69	613	9.371	279.23151	[M+H]+	C18H30O2	Crepenynic acid	278.2245802	0.0003567
70	627	5.196	283.16492	[2M+NH4]+				
71	641	7.36	285.16977	[M+H]+	C15H24O5		284.1623739	
72	648	5.555	287.09113	[M+H]+	C16H14O5	Sakuranetin	286.0841235	3.00E-04
73	651	6.466	288.17978	[M+H]+	C14H25NO5		287.1732729	
74	664	4.159	290.15958	[2M+NH4]+	C7H8N2O		136.0636629	
75	676	5.752	293.05927	[M+H]+	C13H12N2O4S		292.0517779	
76	679	6.117	293.12842	[M+H]+	C18H16N2O2	UNPD92998	292.1211778	5.42E-05
77	688	6.671	295.05655	[M+H]+	C17H10O5		294.0528234	
78	692	7.313	295.22626	[M+H]+	C18H30O3	(2-entenyl)cyclopentaneoctanoic acid	294.2194948	0.0004713
79	693	7.719	295.22632	[M+H]+	C18H30O3	(2-entenyl)cyclopentaneoctanoic acid	294.2194948	0.0004713
80	72	3.682	154.04979	[M+Na]+	C5H9NO3		131.0582431	
81	73	4.491	154.04991	[M+Na]+	C5H9NO3		131.0582431	
82	748	8.745	309.24274	[M+Na]+	C17H34O3		286.2507949	
83	752	8.199	310.23773	[M+H]+	C18H31NO3		309.2303939	
84	604	8.787	277.21631	[M+H]+	C18H28O2		276.2089301	
85	805	6.533	320.20627	[M+H]+	C16H25N5O2		319.200825	
86	806	5.588	320.20676	[M+H]+	C16H25N5O2		319.200825	
87	826	7.037	327.13339	[M+H]+	C13H18N4O6	cyclo(tyrosyl-tyrosyl)	326.1226343	-0.0034893

88	867	10.447	336.27484	[M+NH4]+	C17H34O5	318.2406242
89	878	4.239	340.18695	[M+H]+	C16H25N3O5	339.1794209
90	939	4.722	352.19669	[M+H]+	C19H29NO3S	351.1868148
91	982	5.746	360.1803	[M+H]+	C20H25NO5	359.1732729
92	992	8.545	362.21741	[M+H]+	C18H27N5O3	361.2113897
93	994	8.213	362.21793	[M+H]+	C18H27N5O3	361.2113897

ANNEXES

Fungal endophytes: a source of anti-parasitic and antibacterial compounds

Romina PACHECO[a], Sergio ORTIZ[a, b], Mohamed HADDAD[a], Marieke VANSTEELANDT[a*]

[a] UMR 152 Pharma Dev, Université de Toulouse, IRD, UPS, France

[b] Pharmacognosy Research Group, Louvain Drug Research Institute, Université Catholique de Louvain, Bruxelles, Belgium.

* Corresponding author. Tel. : +33(0)5 62 25 98 11.

E-mail address : marieke.vansteelandt@univ-tlse3.fr

Abstract

The increase and emergence of resistant microbes (bacteria, fungi, and parasites) have led researchers to search for new anti-infective drugs and to study new sources of bioactive compounds. Among them, endophytic fungi are attracting more and more attention because this source is still largely under-exploited and relatively little studied from a chemical point of view. Because of their specific environment, and especially their constant interactions with their host plant and its entire microbiome, they represent a huge reservoir of bioactive compounds. This review lists the most active antibacterial and antiparasitic compounds isolated from endophytic fungi over the past two decades (2000-2019). A discussion of the strains producing these compounds as well as their host plant is followed by a review of new methods used to induce or modify fungal metabolism to discover novel and bioactive compounds.

1. Introduction

1.1. Current situation of microbial infections

The golden era of the antibiotic occurred between the early 1930s and late 1960s, a period where most of the new classes of drugs were discovered. This period was followed by an important decline in drug discovery rate along with the increase and emergence of resistant microbes, including bacteria, viruses, fungi and parasites (Aminov, 2010). In 2019, the WHO listed 32 antibiotics in clinical development that were addressed to the list of priority pathogens, of which only 6 were considered innovative. Antimicrobial resistance affects health care systems from all countries found in any level of development, generating a great economic burden while other medical procedures become more risky.

Protozoal diseases such as Malaria (*Plasmodium* spp.), Leishmaniasis (*Leishmania* spp.), and Trypanosomiasis (*Trypanosoma* spp.) affect mainly tropical and subtropical regions with great health and economic impacts worldwide. These unicellular eukaryotic organisms are free-living organisms and their developmental stages include intracellular stages within the host cell or extracellular stages in body fluids, hollow organs or between

cells in the interstitial space. Additionally, they can possess dormant forms that help them to survive under extreme conditions over a long period of time. Their transmission is mainly vector-borne but also fecal-oral or predator-prey transmission.

According to the WHO, there are currently 20 diseases caused by bacteria, helminthes, protozoa or viruses considered as part of the neglected tropical diseases (NTDs), including Chagas disease, human African trypanosomiasis, leishmaniasis and many others. Individually, none of them represents a global priority however, counted together, they affect approximately 2 billion people with a collective number of people affected equivalent to HIV/AIDS, tuberculosis or malaria (Engels & Zhou, 2020).

In general, the arsenal of antimicrobial drugs are becoming very limited while the resistance development is rising against many of the main treatments. The problem of antibiotic resistance also involves natural environmental changes and proliferation of infections due to human activities. The absence of effective vaccines and the development of resistance to the current drugs situates these infections as major problems in endemic countries and highlight the need of novel molecules acting on new targets.

1.2. Microbial natural products as sources of new drugs

A significant number of compounds, including drugs and drug leads, are produced by microorganisms during the interaction with other microorganisms and with their environment. Almost 50% of the total small molecules approved as drugs between 1981 and 2019 are derived from natural products or from their synthetic variations (Newman & Cragg, 2020). In general, microorganisms respond to environmental signals which provide them better survival mechanisms and in this process, many secondary metabolites with different biological activities are produced. Most of the relevant classes that are currently clinically important are derived from fungi, actinomycetes and other bacteria, besides the compounds obtained from medicinal plants (Hutchings et al., 2019). Environments with high biodiversity will potentially harbor new species or strains of microorganisms capable of producing novel compounds. These environments are considered as hot spots, such as the tropical forests, where plants represent excellent niches for interactions between microorganisms, including fungi and bacteria (Knight et al., 2003).

Species from fungal kingdom, including basidiomycetes and filamentous fungi, are responsible for 45% of the microbial metabolites production, mainly from species corresponding to *Penicillium*, *Aspergillus* and *Trichoderma* genera (Berdy et al., 2012). Massive whole-genome sequencing has shown the excellent capacity of fungi to produce a variety of secondary metabolites, however, the current challenge is to access these biosynthetic pathways that are usually silenced under standard culture conditions (Challinor & Bode, 2015). Secondary metabolites produced by fungi are chemically diverse including polyketides, aromatic compounds, alkaloids or terpenoids, which are mainly synthesized by polyketide synthases and non-ribosomal peptide synthetases. Additionally, there are other biosynthetic systems, including hybrid pathways that give rise to a greater chemical diversity (Keller, 2019). They exhibit a broad spectrum of biological activities such as antifungal, antibacterial, antiviral, anti-parasitic, anticancer, immunosuppressant properties, and also possess high chemical originality, especially from fungal species obtained as endophytes or from marine ecosystems (Schueffler & Ankle, 2014).

1.3. Endophytic fungi

Endophytes are microorganisms, mainly bacteria and fungi that colonize internal plant tissues, including branches, leaves, seeds, roots, without generating visible harmful effects to the host plant. This successful endophyte colonization involves compatible interactions between the plant and its microbiome and the recognition of the endophyte during the invasion to the plant through the initiation of a cross-talk of signal molecules (Khare et al., 2018). It is important to consider that these interactions can be facultative or obligate which also depend on environmental conditions and on the physiological state of the plant, ranging from mutualism to commensalism and parasitism. Besides this, endophytic fungal communities can exhibit host plant species specificity and within the host plant, organ and tissue specificity (Aly et al., 2011).

It is considered that almost all plants on earth are in constant association and interaction with microorganisms, especially fungal endophytes (Arnold, 2007). This special relationship has evolved over long periods of time and approximately 18% of known plant metabolites can be produced by their associated fungi. The intrinsic relationships occur at different metabolic levels and have also shown to improve plant growth and tolerance to biotic and abiotic stress factors including resistance to environment, herbivores attacks, via the production of antimicrobials, insecticides and growth regulators while plants may provide them their nutrients and sugars. Specifically, a total of 46 families of medicinal plants distributed in tropical and subtropical or extreme environments, have shown to exhibit a mutualistic relationship with their endophytes (Jia et al., 2016).

Taken together, the rationale for studying endophytic microbes as potential sources of new drugs is related to the fact that they represent a relatively unexplored area of biochemical diversity. In particular, the protection provided by endophytes to the host plant by various bioactive compounds increases the attractiveness of these compounds in medical applications. Furthermore, since toxicity to higher organisms is a concern of any potential drug, natural products isolated from endophytes may be an attractive alternative, since these compounds are produced in an eukaryotic system without apparent damage. Therefore, the host plant itself has naturally served as a selection system for microbes producing bioactive compounds with reduced toxicity to higher organisms.

Given the number of existing plant species on the planet, what are the justifications for selecting a plant to be studied for its endophytes? It is noteworthy that each of the approximately 300,000 plant species that exist on our planet is a host for one or more endophytes (Strobel and Daisy 2003) and it is widely accepted that there are few plants without endophytes. It is estimated that there may be as many as 1 million different fungal species, only a few of which have been studied in detail (Ganley et al. 2004). The presence of plant-associated microorganisms detected in fossilized stem and leaf tissues indicates that endophyte-host associations may have evolved since the appearance of higher plants on earth (Strobel 2003, Andrzej 2002). Endophytes are detected in a wide variety of plant tissue types, such as seeds and ovules (Siegel et al. 1987), fruits (Schena et al. 2003), stems (Gutierrez-Zamora and Martínez-Romero, 2001), roots (Germida et al. 1998), leaves (Smith et al. 1996), tubers (Sturz et al. 1998), buds (Ragazzi et al. 1999), xylem (Hoff et al. 2004), rachis (Rodriguez and Samuels 1999) and bark (Raviraja 2005).

There are different ways to select plants to study their endophytes. The selection of a plant will be guided by different criteria ranging from random selection of a number of different plants in an ecosystem to the search for a useful plant in the hope of finding a useful molecule (e.g. medicinal plants). This selection rationale may be based on a particular morphology of the plant, its age, its ecological niche, its environment, and/or its ethnobotanical history (medicinal uses) (Strobel and Daisy 2003). For example, the research that led to the discovery of the Paclitaxel-producing endophyte followed an ethnomedical rationale (isolated from a tree known to have medicinal uses, due in part to the presence of Paclitaxel in its bark).

A total of 449 new secondary metabolites were isolated from endophytic fungi between 2017 and 2019, corresponding to terpenoids and polyketones, alkaloids, steroids and other compounds (Zheng et al., 2021). Many of these compounds exhibited biological activities (Manganyi et al., 2020) (Figure 1) important for public health, agriculture and pharmaceutical industries (Gupta et al., 2020). For instance, the *in vivo* and *in vitro* screening of griseofulvin isolated from different endophytic fungi from the genus *Xylaria* have revealed its microbicidal activity against plant pathogens allowing its potential use in the control of crop diseases. Also, the compound lectin produced by endophytic fungus *Alternaria* sp. has shown its antidiabetic activity in rats and *in vitro* with no harmful effects compared to the side effects observed with some antidiabetic drugs (Saanu Adeleke et al., 2021). In addition to this, 224 patents between 2001 and 2019 are related to secondary metabolite production and biotechnological processes involving endophytic fungi from *Aspergillus*, *Fusarium*, *Penicillium*, *Trichoderma* and *Phomopsis* genera. For example, one submitted patent of *Trichoderma* acid is involved with the preparation of antifungal agents, another patent is about obtaining three isopiramane diterpenoids compounds from *Xylaria* sp. with antifungal activity and with potential application in agriculture and medicine. Moreover, another patent is related to the production of antifungal and immunosuppressive compounds by endophytic fungus *Colletotrichum* sp. (Torres-Mendoza et al., 2020).

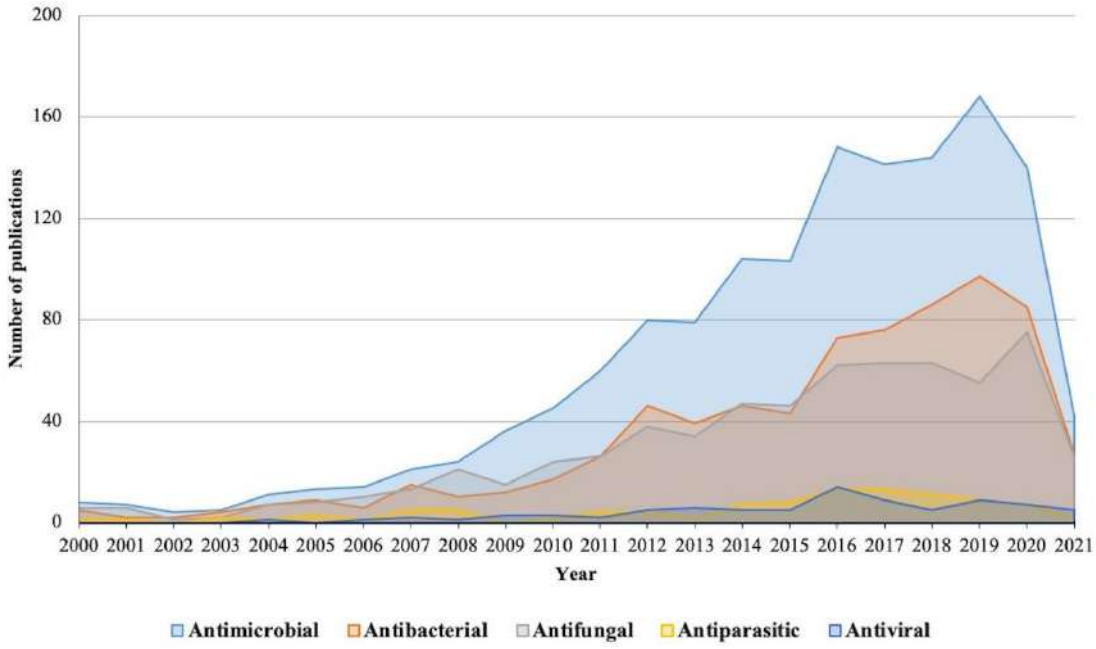

FIgure 1. Number of publications using the Search query: (“bioactivity”) AND (“endophytic fungi”) in PubMed.

The endophytic community present on the host plant is affected by different environmental factors such as the growth state and physiological conditions of the plant or the sampling season, while the culture conditions play an important role for their recovery (Gouda et al., 2016). For the isolation of endophytes, the selection of a healthy plant is mandatory to avoid the isolation of pathogenic fungi as well as the preservation of the tissue to be used within 24 hours of harvesting to prevent death of the endophytic community. This process is followed by a series of sterilization steps to ensure the isolation of endophytes instead of epiphytes or root actinomycetes. Before surface sterilization, washing plant tissues under tap water can help to reduce the soil particles. Among the most used solutions for the surface sterilization are 2-10% of hypochlorite solution, 3% of hydrogen peroxide or 2% of potassium permanganate combined with 70-96% of ethanol washing steps and rinses with sterile distilled water (Martínez-Klimova et al., 2017). Time in each bath depends on the plant material (leaves, roots, stems) especially their thickness. Sterilized tissues are cut in small fragments (3-5 mm) and dried under aseptically conditions to be later placed on solid agar media and incubated during 2 – 4 weeks. Usually, plates are discarded after this period of time to avoid the growth of contaminants. However, this can be corroborated with the control plates containing culture media with the sterile distilled water used for the surface sterilization. Some of the endophytes are not readily culturable or they are found to be under-represented in the selected tissue, therefore some culture-independent techniques are used for studying or identifying the unculturable endophytes. For the identification of pure isolates, sequencing of 18S rDNA, internal transcribed spacer (ITS1 and ITS2), 5.8S rDNA or 28S subunit of rDNA are usually done (Zhang et al., 2006).

2. Antimicrobial compounds from endophytic fungi

Endophytes are in close interaction with their host-plant but also with the entire microbiome of the plant. The microbiome can also change over time, becoming a dynamic interaction and a constant microbial competition which at the same time stimulates metabolite production. This trend of life is a huge opportunity for researchers looking for new anti-infectives compounds such as antibacterial or antifungal metabolites. Endophytes are not naturally in interaction with pathogens of animals, such as *Plasmodium*, *Leishmania* or other *Trypanosomatidae* parasites, however, their capacity to produce bioactive metabolites in answer to the presence of other microorganisms led the scientific community to screen fungal endophytes extracts for this kind of activity. Nowadays, there is an increasing interest for the research of anti-parasitic compounds from fungal endophytes although these organisms do not share the same biotopes.

This work aims at reviewing the most active antibacterial and antiparasitic compounds isolated from endophytic fungi, between 2000 and 2019.

2.1. Antibacterial compounds

As briefly introduced in point 1.1, drug and multi drug resistance in bacteria is a global health and development threat and is caused mainly by the large amounts of antibiotics used for human therapy, as well as for fish in aquaculture and for farm animals. The two principal mechanisms in the generation of drug resistance are the accumulation of resistance plasmids and the increase in the expression of the genes that code for drug efflux

pumps. These mechanisms have produced bacterial strains resistant to methicillin, aminoglycosides, macrolides, tetracyclines, chloramphenicol, lincosamides and/or penicilline agents. An important group of these drug/multidrug resistant bacteria are the ESKAPE pathogens (*Enterococcus faecium*, *Staphylococcus aureus*, *Klebsiella pneumoniae*, *Acinetobacter baumannii*, *Pseudomonas aeruginosa*, and *Enterobacter* spp.) which are the leading cause of nosocomial infections throughout the world and one of the greatest challenges in clinical practice.

The urgency of finding new agents to fight these pathogens or new antibacterial mechanisms of actions has been one of the most important focuses of science in the last decades. A special focus on natural products has been applied in the research for new antibacterial compounds with marine, plant or fungi origins. In the following section (Table 1), compounds with potent antibacterial activity isolated from endophytic fungi, obtained from mainly terrestrial but also some marine plants, have been listed. They exhibited activities with MIC values less than 20 µg/mL and/or with important inhibition zones (> 8 mm with at least 50 µg per disk).

In particular, the derivatives with MIC values lower than 10 µg/mL are described and discussed. Compounds are organized according to families of metabolites and the possible mechanisms of action proposed in the literature will be mentioned. Finally, we describe some cases of antivirulence compounds against different pathogens of human concern in order to evaluate new strategies to fight bacterial infections.

- Alkaloids

Pyrazin-2-one

Neoaspergillic acid (**6**), an alkaloid pyrazinoic derivative, was isolated from a co-culture of two *Aspergillus* strains (A. FSY-01 and A. FSW-02), which were isolated from the mangrove tree *Avicennia marina* (Acanthaceae) and showed antibacterial activity in a serial dilution assay with MIC values in 0.98 and 0.49 µg/mL against *Staphylococcus aureus* and *S. epidermidis* bacteria species (Zhu et al., 2011). In another study, neoaspergillic acid significantly inhibited the cell proliferation of SGC-7901 and K562 cancer cell lines with IC_{50} values of 8.24 and 7.99 µg/mL respectively, and moderate cytotoxicity to SPA-A-1 and BEL-7402 cell lines with IC_{50} values if 22.19 and 24.19 µg/mL, respectively.

Piperine

Piperine (**10**), a well-known plant-produced alkaloid, was found to be produced by an endophytic strain of *Periconia* sp. isolated from *Piper longum* L (Piperaceae). Additionally, piperine was reported to possess a MIC value of 1.74 µg/mL against a multi-drug resistance strain of *M. tuberculosis* (Verma et al., 2011). There are several reports in the literature that confirm the activity of piperine against *Mycobacterium* spp. and its role in the inhibition of Rv1258c, a putative multidrug efflux pump of *M. tuberculosis* (Sharma et al., 2010).

Pyrrocidines

The 13-member macrocycle alkaloids, pyrrocidine A (**12**)and B (**13**) were isolated for the first time from the endophytic fungi *Acremonium zeae* NRRL 13540, which was isolated from maize, and they showed MICs values of 0.25-2 and 4-8 µg/mL, respectively, against four strains of *Staphylococcus aureus* (including two piperacillin-

resistant strains); 0.25 and 8 µg/mL, respectively, against *S. haemolyticus* GC4546; 0.5 and 4-8 µg/mL against three strains of *Enterococcus faecalis* and 0.5-1 and 4-8 µg/mL, respectively, against three strains (including two vancomycin-resistant strains) of *Enterococcus faecium* (He et al., 2002; Wicklow and Poling, 2009). In addition, pyrrocidine A also exerted moderate antifungal activity against a strain of *Candida albicans* with a MIC value of 8 µg/mL. Another member of this family, pyrrocidine C (**14**) was isolated from the endophytic fungi *Lewia infectoria* SNB-GTC2402, which was obtained from the amazonian tree *Besleria insolita* (Gesneriaceae), and showed antibacterial activity against *S. aureus* ATCC 29213 with a MIC value of 2 µg/mL (Casella et al., 2013). In addition, pyrrocidine C showed cytotoxicicity activity against the cervical uterine cell line KB with an IC_{50} value of 10 µM, however it was inactive against MDA-MB-435 and MRC-5 cell lines.

Bisindoles

From the cultures of the same strain of *L. infectoria* described above, two bisindole alkaloids identified as semicochliodinol A (**15**) and cochliodinol (**3**) were also isolated and showed MICs values of 2 and 4 µg/mL, respectively, against *Staphylococcus aureus* ATCC 29213 strain. In addition, both derivatives showed cytotoxic activity against the KB cancer cell line with IC_{50} values of 0.31 and 0.53 µM respectively. Cochliodinol also showed antifungal activity against *Candida albicans* ATCC 10213 strain with a MIC value of 2 µg/mL. Semicochliodinol A has also been reported with anti-HIV activity by inhibiting the HIV-1 protease (IC_{50} of 0.37 µM) and as anticancer agent by inhibiting the epidermal growth factor receptor protein tyrosine kinase (IC_{50} of 20 µM). (Casella et al., 2013; Fredenhagen et al., 1997).

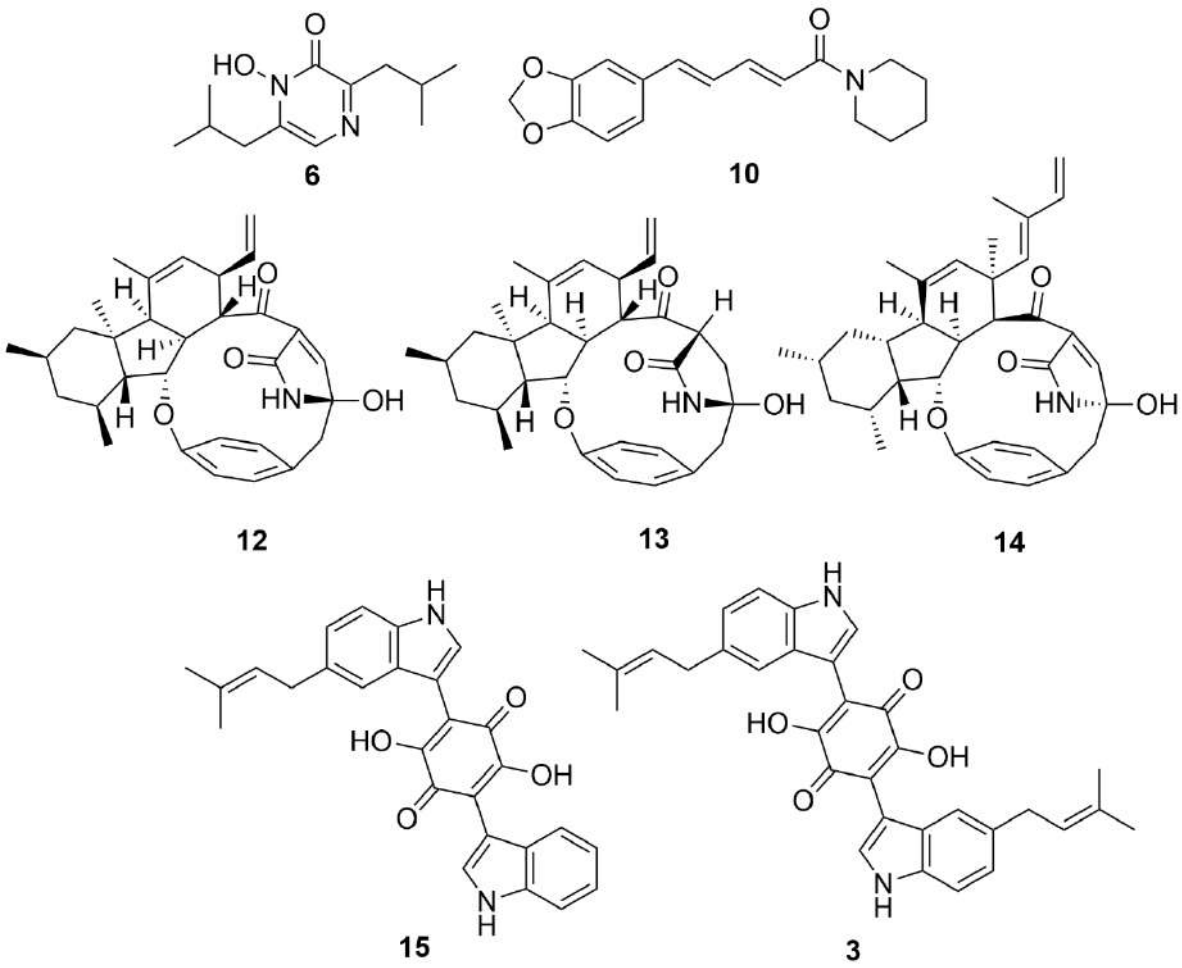

Figure 2. Chemical structures of neoaspergillic acid (6), piperine (10), pyrrocidine A (12), pyrrocidine B (13), semicochliodinol A (15) and cochliodinol (3).

- Peptides

Dipeptides

The 2,5-diketopiperazine derivative, tardioxopiperazine A (**92**), was isolated from culture extract of *Eurotium cristatum* EN-220, an endophytic fungus isolated from the marine alga *Sargassum thunbergii* (Du et al. 2012). This compound exerted antibacterial activity in a well-diffusion method against a strain of *Staphylococcus aureus*, with a MIC value of 8 μg/mL. In addition, tardioxopiperazine A showed no cytotoxic activity against P388, HL-60, BEL-7402 and A-549 cell lines *in vitro* (IC_{50} > 50 μM) (Wang et al. 2007).

Polypeptides

Two cyclopeptides PF1022F (**91**) and halobacillin (**90**) have been isolated from the endophytic fungus *Trichoderma asperellum*, residing in the traditional chinese medicinal plant *Panax notoginseng*. Both compounds showed antibacterial activity *in vitro* in a serial dilution model against *Enterococcus faecium* CGMCC 1.2025 strain with MICs values of 7.3 and 5.4 μg/mL, respectively (Ding et al. 2012). Halobacillin, previously isolated from cultures of *Bacillus* sp. (CND-914) obtained from a deep-sea sediment core, showed also strong cytotoxic

activity, inhibiting the growth of human colon tumor cells (HCT-116) with an IC_{50} of 0.98 µg/mL (Trischman et al. 1994).

In 2013, the cyclic depsipeptide enniatin A1 (**87**), a cyclic hexadepsipeptide of alternating D-α-hydroxyisovaleric acids and N-methyl-L-amino acids, was isolated from the fungal endophyte *Fusarium tricinctum* with antibacterial activity showing MIC value of 2 µg/mL against *Staphylococcus pneumoniae* ATCC 49619. Remarkably, the co-culturing of *F. tricinctum* with the bacterium *Bacillus subtilis* 168 trpC2 resulted in an up to 78-fold increase in the production of enniatin A1 (Ola et al., 2013). Enniatin A1 also possesses anticarcinogenic properties by induction of apoptosis of HepG2 liver cancer cell line and disruption of extracellular signal-regulated kinases signalling pathway. In addition, this compound has been probed as an enzyme inhibitor of acyl-CoA:cholesterol acyltransferase with an IC_{50} of 49 µM in rat liver microsomes (García et al. 2015; Tomoda et al. 1992).

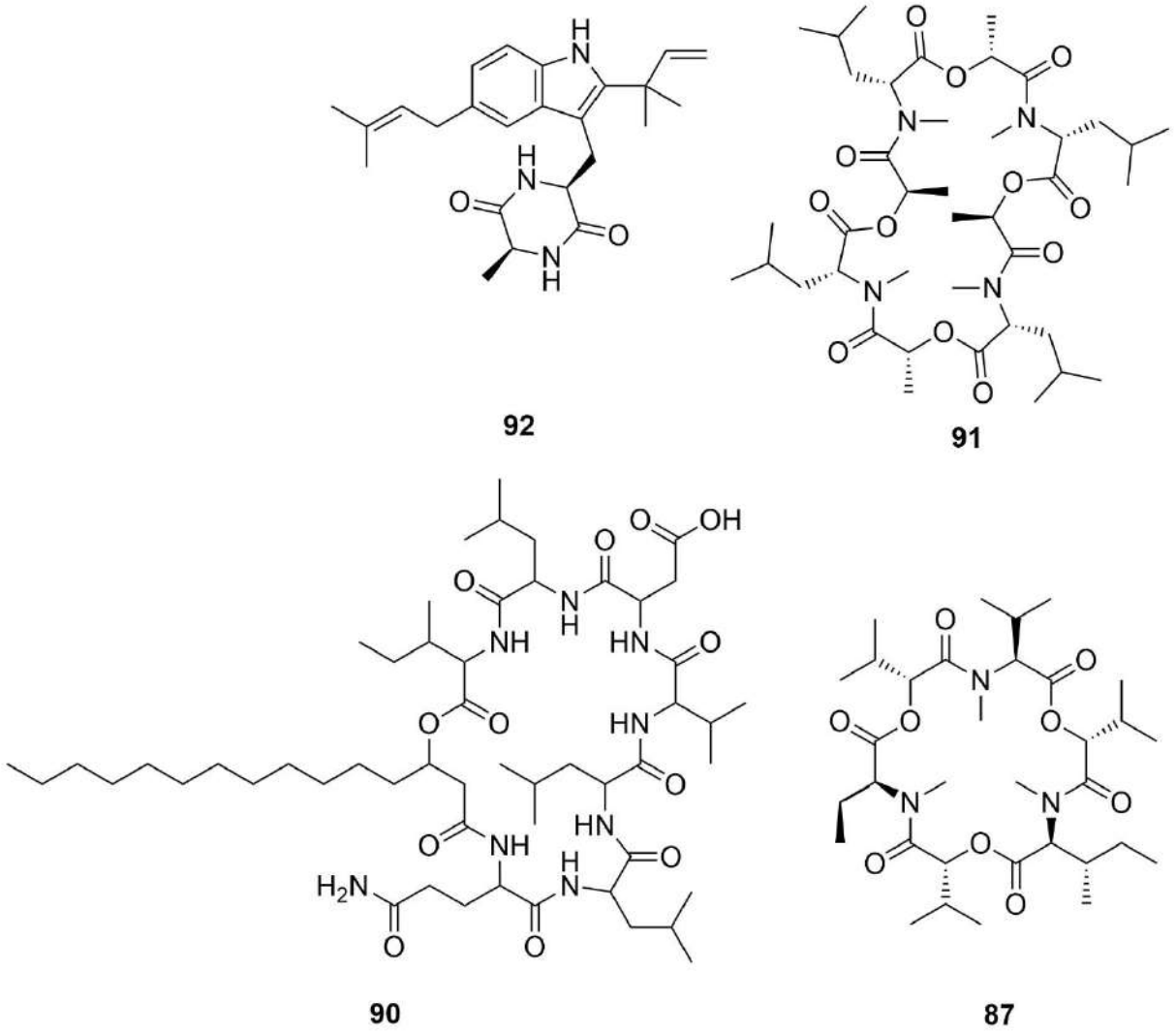

Figure 3. Chemical structures of tardioxopiperazine A (92), PF1022F (91), halobacillin (90) and enniatin A1 (87).

- Polyketides

Chromones

The chromone derivative altechromone A (**37**), firstly isolated from a strain of *Alternaria* sp. in 1992, which was obtained from an ear of oat, was reported as a plant growth promoter. Also isolated from several fungi including *Hypoxylon truncatum*, Ascomycota spp. and from *Alternaria brassicicola*, altechromone A has showed antibacterial activity with a MIC value of 3.9, 3.9, 1.8 and 7.8 µg/mL against *Bacillus subtilis* CGMCC1.1162, *Escherichia coli* CGMCC1.1571, *Pseudomonas fluorescens* CGMCC1.1828 and *Staphylococcus aureus* CGMCC1.1361 strains, respectively (Gu, 2009; Kimura et al., 1992).

Alternariol (**39**), a chromone derivative isolated from the crude extract of *Alternaria alternata* ZHJG5 (an endophytic fungus isolated from healthy leaves of *Cercis chinensis*), showed antibacterial activity against the phytopathogen *Xanthomonas oryzae* pv. oryzae KACC10331 with a MIC value of 4 µg/mL. This activity was further evaluated in a protective rice-infected model, showing protection efficacy of 52.8 and 66.2 % at 100 and 200 µg/ML, respectively, against the same pathogen. Alternariol was found to inhibit the β-ketoacyl-acyl carrier protein synthase III, an essential protein for bacterial fatty acid biosynthesis (Zhao et al. 2020).

Quinones

A new quinone derivative, the 2,3-didehydro-19a-hydroxy-14-epicochlioquinone B (**29**) was isolated from the endophytic fungus *Nigrospora* sp. MA75 obtained from the marine semi-mangrove plant *Pongamia pinnata* (Fabaceae), and showed antibacterial activity in a serial dilution assay with MICs values of 8.0, 4.0, 4.0, 0.5 and 0.5 µg/mL against a methicillin-resistant *Staphylococcus aureus*, *Escherichia coli*, *Pseudomonas aeruginosa*; *P. fluorescens* and *S. epidermidis*, respectively. In addition, this compound showed cytotoxic effect *in vitro* against several tumor cell lines with IC_{50} values of 4, 5 and 7 µg/mL for MCF-7, SW1990 and SMMC7721 strains respectively (Shang et al., 2012).

Xanthones

From the same endophytic fungus of *Nigrospora* sp. MA75 described previously, a xanthone derivative, norlichexanthone (**62**) was isolated and showed antibacterial activity against *Staphylococcus epidermidis* with a MIC value of 0.5 µg/mL. This compound showed cytotoxic effects against HepG2 cell line with a IC_{50} oh 15 µg/mL (Shang et al. 2012). In addition, norlichexanthone has been identified as a selective ligand of estrogen receptor-alpha (ERα) by activating the Gal4/DBD-ERα/LDB fusion protein in a dose-dependently with an EC_{50} of 38.8 nM. The potential efficacy to prevent osteoporosis of norlichexanthone was evaluated in an ovariectomized mouse model, preventing bone loss at the dosage of 1 mg/kg (Wang et al. 2021).

Two novel xanthone dimers derivatives, phomoxanthone A (**69**) and B (**70**), were isolated from culture of the endophytic fungi *Phomopsis* sp. BSS 1323, an endophytic fungus isolated from *Tectona grandis* (Lamiaceae) and showed antitubercular activity against the strain *Mycobacterium tuberculosis* H37Ra with a MIC values of 0.5 and 6.25 µg/mL, respectively (Isaka et al., 2001). In addition, these two xanthone dimers have been shown to inhibit the proliferation of cancer cell lines (IC_{50} of 0.9 and 4.1 µg/mL against KB cells, 0.51 and 0.70 µg/mL against

BC-1 cells and 1.4 and 1.8 µg/mL against vero cells, respectively) and inhibit the tyrosine phosphatase SHP1 in MCF7 cells leading to the upregulation of inflammatory factors (Yang et al. 2020).

Quinones

From the endophyte fungus *Nigrospora* sp. MA75, described previously, two anthraquinones derivatives, tetrahydrobostrycin (**76**) and 4-deoxytetrahydrobostrycin (**30**), were isolated with antibacterial activity with MICs values of 0.5 and 4.0 µg/mL against a strain of *Escherichia coli*, respectively. Tetrahydrobostrycin was active also against a methicillin-resistant *Staphylococcus aureus* with a MIC value of 2.0 µg/mL (Shang et al. 2012). In the same study, only deoxytetrahydrobostrycin showed moderate cytotoxic activity against HeLa cell line with a IC_{50} of 22.0 µg/mL.

Javanicin (**56**), a highly functionalized naphthoquinone, was isolated from an endophytic fungus, *Chloridum* sp. (J. F. H. Beyma), which was obtained from the roots of *Azadirachta indica* (Meliaceae). This compound showed antibacterial activity in a standard plate bioassay test method against *Pseudomonas* spp., *P. aeruginosa* and *P. fluorescens* with a MIC value of 2.0 µg/mL against both species. In addition, javanicin has shown antifungal activity against the fungal plant pathogen species *Cercospora arachidicola*, with a MIC value of 5.0 µg/mL (Kharwar et al. 2009).

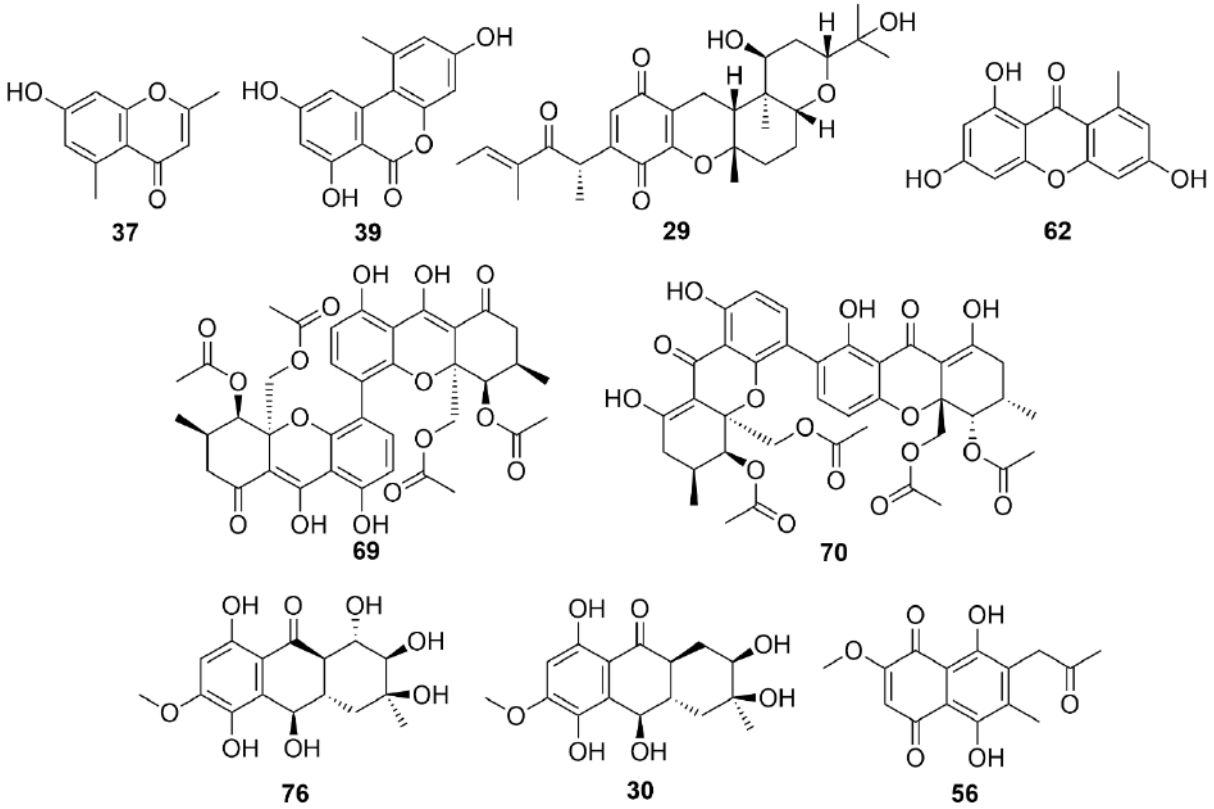

Figure 4. Chemical structures of altechromone A (37), alternariol (39), 2,3-didehydro-19a-hydroxy-14-epicochlioquinone B (29), norlichexanthone (62), phomoxanthone A (69), phomoxanthone B (70), tetrahydrobostrycin (76), 4-deoxytetrahydrobostrycin (30) and javanicin (56).

Benzofurans

Usnic acid (**78**) and two of its derivatives, cercosporamide (**42**) and phomodione (**65**), were isolated from the endophytic fungus *Phoma* sp. NG-25, which was isolated from *Saurauia scaberrima* (Actinidiaceae) and they showed antibacterial activity with MIC values of 2.0 µg per disc with an halo of inhibition of 0.5 mm against the strain *Staphylococcus aureus* ATCC 25923 (Hoffman et al., 2008). Previously, isolated from a lichen, usnic acid showed antibacterial activity against *Clostridium perfringens* ATCC 13124, *Propionibacterium acnes*, and 29 clinical isolated of *Enterococcus faecalis* and 8 clinically isolated strains of methicillin-resistant *S. aureus* with MICs values of 4.0, 2.0, 8.0 and 8.0 µg/mL, respectively (Lauterwein et al., 1995). Usnic acid showed also antibiofilm activity, inhibiting the formation of biofilm by loaded *S. aureus* cells and altering the biofilm morphology formed by *Pseudomonas aeruginosa* cells, indicating the possibility of interference in signaling pathways (Francolini et al; 2004). Recently, the strong inhibition of RNA and DNA synthesis in *Bacillus subtilis* and *S. aureus*, by usnic acid has been demonstrated as a possible antibacterial mechanism of action. Interestingly, DNA synthesis was halted rapidly, suggesting interference of usnic acid with the elongation of DNA replication. It was also observed a slight inhibition of RNA synthesis in a Gram-negative bacterium, *Vibrio harveyi* (Maciag-Dorszynska et al. 2014).

Octaketides

Two new octaketides, cytosporone D (**44**) and E (**45**), were isolated from extracts obtained from the endophytic fungus *Cytospora* sp. CR200, isolated from the tissue of the mangrove shrub *Conocarpus erecta* (Combretaceae). These compounds showed antibacterial activity against representative strains of *Staphylococcus aureus* and *Enterococcus faecalis* with MICs values of 8 µg/mL. In addition, cytosporone D also showed antifungal activity with a MIC value of 4 µg/mL against the fungus *Candida albicans*.

Benzophenones

From the endophyte fungus *Nigrospora* sp. MA75, described previously, a benzophenone identified as griseophenone C (**49**) was also isolated. This compound showed MIC value of 0.5 µg/mL against *Pseudomonas aeruginosa*, *P. fluorescens* and a methicillin-resistant *Staphylococcus aureus* strain.

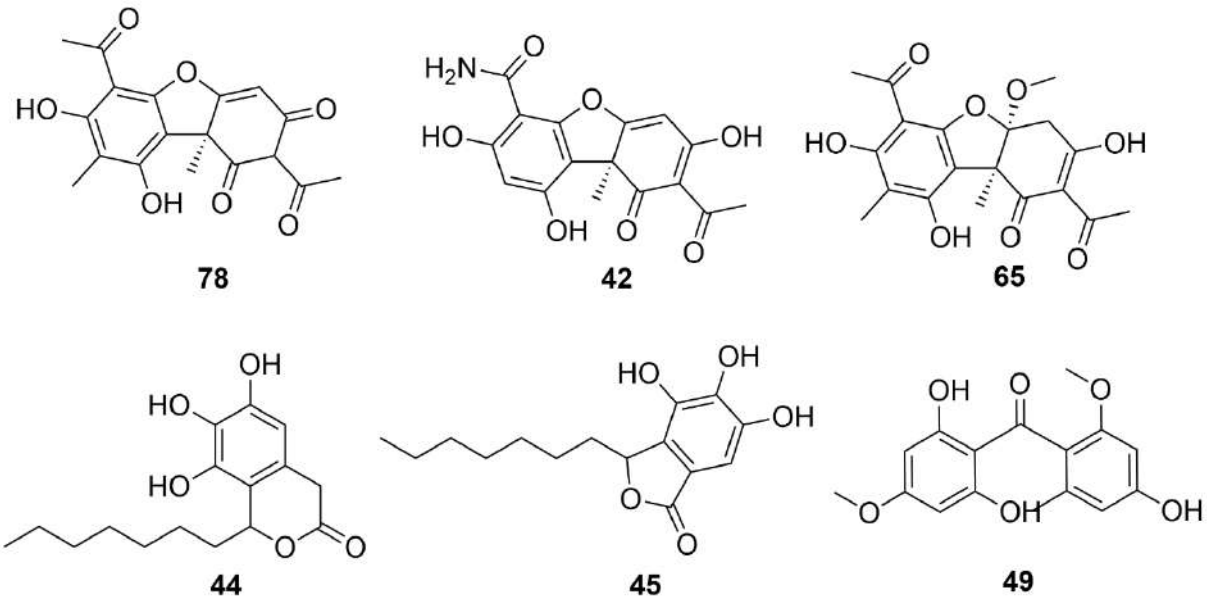

Figure 5. Chemical structures of usnic acid (78), cercosporamide (42), phomodione (65), cytosporone D (44), cytosporone E (45) and griseophenone C (49).

- Terpenoids

A meroterpene with a cyclohexane acid moiety, named fusariumin C (**98**), was isolated from a crude extract of an endophytic fungus *Fusarium oxysporum* ZZP-R1, obtained from the roots of coastal plant *Rumex madaio* (Polygonaceae). This terpenoid possesses significant antibacterial activity against *Staphylococcus aureus* ATCC 25923 strain with a MIC value of 6.25 μg/mL (Chen et al. 2019).

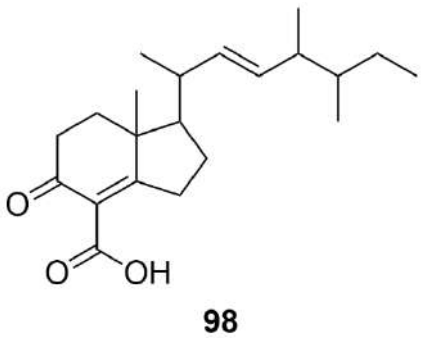

Figure 6. Chemical structure of fusariumin C (98).

Antivirulence compounds

In the last years, and in order to find new strategies to fight some persistent and multidrug pathogens, the expression, production, secretion or activity of different virulence factors have been targeted. Some of these factors are essential in the invasion, colonization and pathogenicity of bacterial infections, such as the production of gelatinase, which is inhibited by ambuic acid (**41**) isolated from different strains of *Pestalotiopsis* sp. and *Monochaetia* sp. (Li et al., 2001 ; Nakayama et al, 2009). In the exploration of new bioactive compounds, scientifics have been screening isolated compounds from endophytic fungi.

During a screening of 100 extracts from 50 *Penicillium* species, 33 were found to produce QS inhibitory (QSI) compounds. From the extracts of the endophytic fungus of *Penicillium radicicola* (IBT 10696) and *Penicillium coprobium* (IBT 6895) bioguided isolation leaded to the identification of penicillic acid (**64**) and patulin (**63**) respectively, as potent quorum system inhibitors of a *Pseudomonas aeruginosa* PA01 strain. These compounds were found to target the transcription of different genes encoding the expression of RhlR and LasR proteins at 80-40 µM (Rasmussen et al. 2005).

From the endophytic fungi *Penicillium restrictum* G85ITS, obtained from healthy parts of *Silybum marianum* (Asteraceae), a series of anti quorum sensing polyhydroxyanthraquinones were isolated. The most active compounds were identified as ω-hydroxyemodin (**82**) and isorhodoptilometrin (**55**) with IC_{50} values of 8.1 and 8.4 respectively against the expression of a functional accessory gene regulator (agr), which is required for the infection of clinical strains of methicillin-resistant *Staphylococcus aureus* (Figueroa et al. 2014).

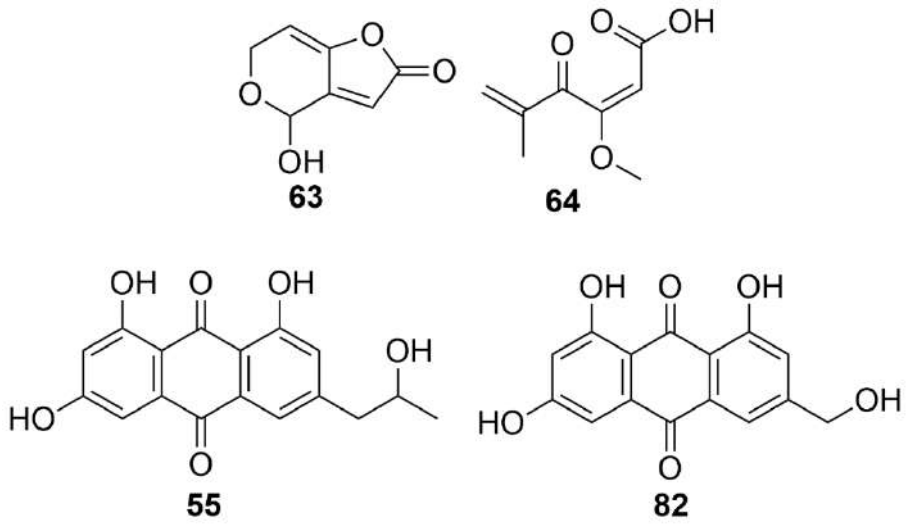

Figure 7. Chemical structures of patulin (63), penicillic acid (64), ω-hydroxyemodin (82) and isorhodoptilometrin (55).

2.2. Antiparasitic compounds

Among all the works carried out on the search for bioactive compounds from endophytic fungi, many studies have focused on their activity against parasitic infections (Ibrahim et al., 2018; Toghueo et al., 2019; Hzounda Fokou et al., 2021). The reported antiparasitic activities in the literature can vary up to IC_{50} >290 µM against *P. falciparum* such as the lactones isolated from *Xylaria* sp. isolated from the leaves of *Siparuna* sp. (Siparunaceae) (Jimenez Romero et al., 2008) or up to IC_{50} > 169 µM against *L. donovani* such as the polyketides isolated from *Mycoleptodiscus indicus* isolated from the plant *Borreria verticillata* (Rubiaceae) (Andrioli et al., 2014). Here, we focused on the compounds with IC_{50} values lower than 10 µM active against *Plasmodium* spp., *Leishmania* spp. and *Trypanosoma* spp. and we describe the culture methods and their potential cytotoxicity against different cancer cell lines. Interestingly, these compounds belong to several chemical classes, such as polyketides, terpenoids, alkaloids and polypeptides.

2.2.1. Antileishmanial

Among the most active compounds isolated from endophytic fungi active against *Leishmania donovani* with an IC_{50} below 1 µM, we can mention preussomerin EG1 (IC_{50} 0.12 µM) followed by FD-838 (IC_{50} 0.2 µM), fumiquinone B and pseurotin D (IC_{50} 0.5 µM), palmarumycin CP18 (IC_{50} 0.62 µM) and purpureone (IC_{50} 0.87 µM). The compounds exhibiting a moderate activity against *L. donovani* with an IC_{50} between 1 and 5 µM are palmarumycin CP17 (IC_{50} 1.34 µM) followed by integracide J (IC_{50} 3.29 µM), palmarumycin CP2 (IC_{50} 3.93 µM), 14-norpseurotin A (IC_{50} 4.4 µM) and integracide H (IC_{50} 4.75 µM). Similarly, cochlioquinone A and isocochlioquinone A exhibited moderate activities with EC_{50} values of 1.7 and 4.1 µM, respectively and were tested against *Leishmania amazonensis* promastigotes (Campos et al., 2008). Finally, the compounds presenting a weaker activity against *L. donovani* with an IC_{50} between 5 and less than 10 µM are pseurotin A (IC_{50} 5.8 µM) and CJ-12,371 (IC_{50} 8.4 µM). Additionally, amphotericin B is one of the reference drugs to be used in biological assays against *Leishmania donovani* exhibiting an IC_{50} value of 0.07 µM, besides being part of one of the most important antileishmanial current treatments.

- **Polyketides**

Isocochlioquinone A, cochlioquinone A

Phytotoxic compounds, isocochlioquinone A (**126**) and cochlioquinone A (**123**), were isolated for the first time from the fungal pathogen *Bipolaris bicolor* (*Cochliobolus* sp.) from a lesioned leaf of *Eleusine coracana* (Poaceae) (Miyagawa et al., 1994). Isocochlioquinone A and cochlioquinone A were later isolated from a different strain of *Cochliobolus* sp. from the plant *Piptadenia adiantoides* (Fabaceae). These compounds were tested against *L. amazonensis* amastigotes, exhibiting an EC_{50} value (effective concentration to kill 50% of the parasites) of 4.1 µM and 1.7 µM, respectively. Additionally, they are considered to possess some degree of selectivity since no cytocidal activity was detected against 3 human cancer cell lines [UACC-62 (melanoma), MCF-7 (breast) and TK-10(renal)] (Campos et al., 2008). Amphotericin B was used at 0.2 µg/mL as a control drug. In another study, the same compounds were isolated but not separated and therefore their activity was tested as a mixture against *L. amazonensis* promastigotes, exhibiting an IC_{50} value of 10.16 µM (do Nascimento et al., 2015).

CJ-12,371

This compound with DNA-gyrase activity was previously isolated from a non-identified fungus (N983-46) (Sakemi et al., 1995) and recently isolated from *Edenia sp.* (Martinez-Luis et al., 2008). In this last study, CJ-12,371 (**122**) exhibited a weak activity with an IC_{50} value of 8.40 µM against the amastigotes of *Leishmania donovani*. Amphotericin B was used as the positive control with an IC_{50} value between 0.07 – 0.12 µM.

Palmarumycin CP17, palmarumycin CP18 (news), preussomerin EG1, palmarumycin CP2

Two new members of the palmarumycin family with potent antileishmanial activity were isolated from an endophytic strain of *Edenia sp.* from a mature leaf of *Petrea volubilis* (Verbenaceae). This fungus was cultivated in malt extract media for 15 days before the mycelium extraction. Palmarumycin CP17 (**133**) and CP18 (**134**) exhibited an IC_{50} of 1.34 µM and 0.62 µM, respectively, against the amastigotes of *Leishmania donovani* (Martinez-Luis et al., 2008). In addition, two already known compounds isolated from *Edenia sp.* exhibited potent antileishmanial activity, being preussomerin EG1 (**139**) the most active (IC_{50}=0.12 µM), followed by palmarumycin CP2 (**135**, IC_{50}=3.93 µM). Amphotericin B was used as the positive control with an IC_{50} value between 0.07 – 0.12 µM. Preussomerin EG1 was first described in *Edenia gomezpompae*, an endophytic fungus isolated from *Callicarpa acuminate* (Verbenaceae) (Macias-Rubacalva et al., 2008) while palmarumycin CP2 was first obtained from *Coniothyrium sp* isolated from the forest soil in West Borneo (Indonesia), being also the first described member of the palmarumycin family (Krohn et al., 1994).

Purpureone

The new ergochrome compound was isolated for the first time from the endophytic fungus *Purpureocillium lilacinum* from the roots of the medicinal plant *Rauvolfia macrophylla* (Apocynaceae). This endophyte was cultivated in a solid rice medium for 3 weeks at room temperature. Purpureone (**140**) possesses a potent activity against the amastigotes of *Leishmania donovani* with an IC_{50} value of 0.87 µM, showing also a good selectivity index (SI=49.5) while control drug miltefosine showed and IC_{50} value of 0.35 µM. Additionally, it exhibited good antimicrobial activity, signalling the promising future investigations for drug development (Lenta et al., 2016).

Fumiquinone B

This compound was first isolated from the culture of a soil-strain of *Aspergillus fumigatus*, and showed a nematicidal activity against *Bursaphelenchus xylophilus* (pine wood nematode) (Hayashi et al., 2007). Later, fumiquinone B (**125**) was also isolated from *Aspergillus* sp. F1544, a fungal endophyte isolated from a mature leaf of *Guapira standleyana* (Nyctaginaceae) in Panama. *Aspergillus* sp. F1544 was cultured in Potato dextrose agar and in Czapek-Dox medium at 30°C during 15 days at 150 rpm for whole culture extraction. Fumiquinone B exhibited a strong activity against the amastigotes of *Leishmania donovani* with an IC_{50} value of 0.5 µM and a moderate activity against *Plasmodium falciparum* with an IC_{50} value of 5.4 µM. Amphotericin B was used as the positive control with an IC_{50} value between 0.07 – 0.12 µM. Additionally, it presented a moderate cytotoxicity against the human breast cancer cell MCF-7 with an IC_{50} value of 23.9 µM (Martinez-Luis et al., 2012).

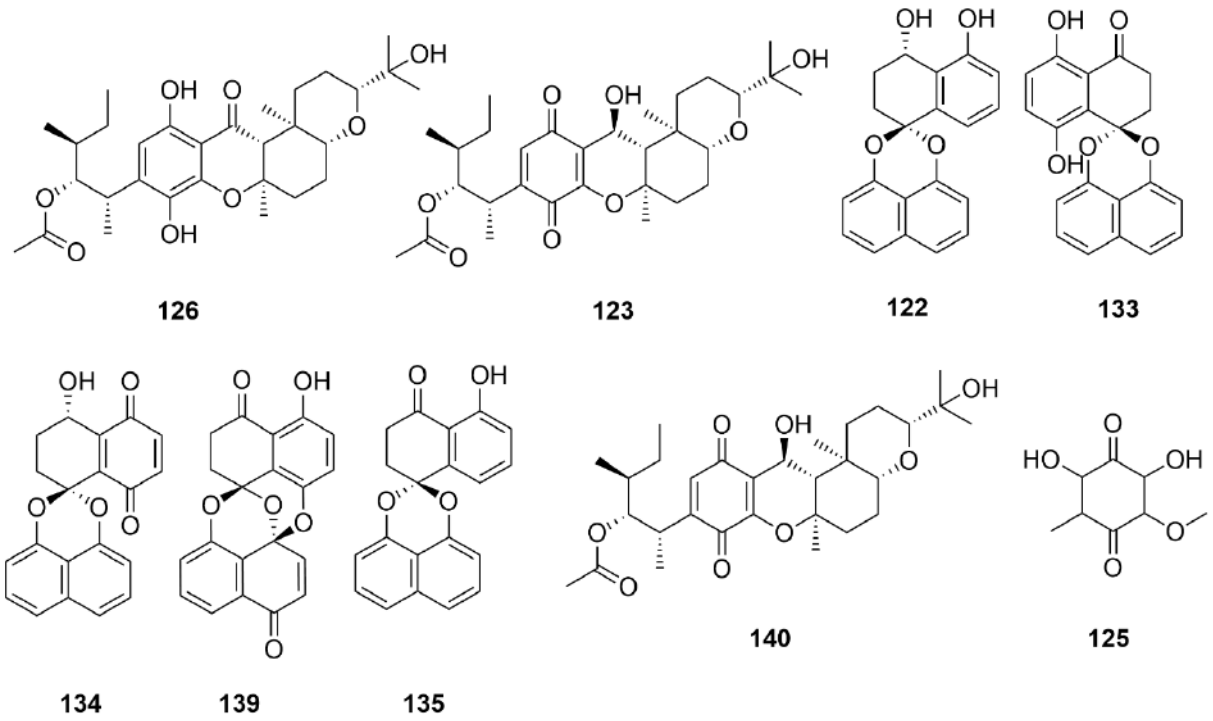

Figure 8. Chemical structures of isocochlioquinone A (126), cochlioquinone A (123), CJ-12,371 (122), palmarumycin CP17 (133), palmarumycin CP18 (134), preussomerin EG1 (139), palmarumycin CP2 (135), purpureone (140) and fumiquinone B (125).

- **Polyketide – Alkaloids**

14-Norpseurotin A, FD-838, pseurotin A, pseurotin D

Along with the isolation of fumiquinone B from endophytic fungus *Aspergillus* sp. F1544, 4 other known compounds were also isolated, 14-norpseurotin A (**142**), FD-838 (**144**), pseurotin A (**145**) and pseurotin D (**146**) (Martinez-Luis et al., 2012). 14-Norpseurotin was first isolated from a marine-derived strain of *Aspergillus sydowii* as a new oxaspirol [4,4]lactam exhibiting a significant antimicrobial activity (Zhang et al., 2008). Pseurotin A was first isolated from *Pseudeurotium ovalis* as a minor metabolite from the culture of this fungus (Bloch & Tamm, 1976) while pseurotin D was isolated 5 years later from the same strain along with other compounds from the same family (pseurotin B, C, D and E) which possess a rare substituted skeleton found in natural product chemistry (Breitenstein et al., 1981). When 14-norpseurotin A, pseurotin A and pseurotin D were tested against the amastigotes of *Leishmania donovani*, they exhibited an IC_{50} value of 4.4, 5.8 and 0.5 μM, respectively. However, compound FD-838 (patent application EP0216607) exhibited the highest antileishmanial activity with an IC_{50} value of 0.2 μM (Martinez-Luis et al., 2012). Amphotericin B was the positive control of the assay exhibiting IC_{50} values between 0.07 – 0.12 μM.

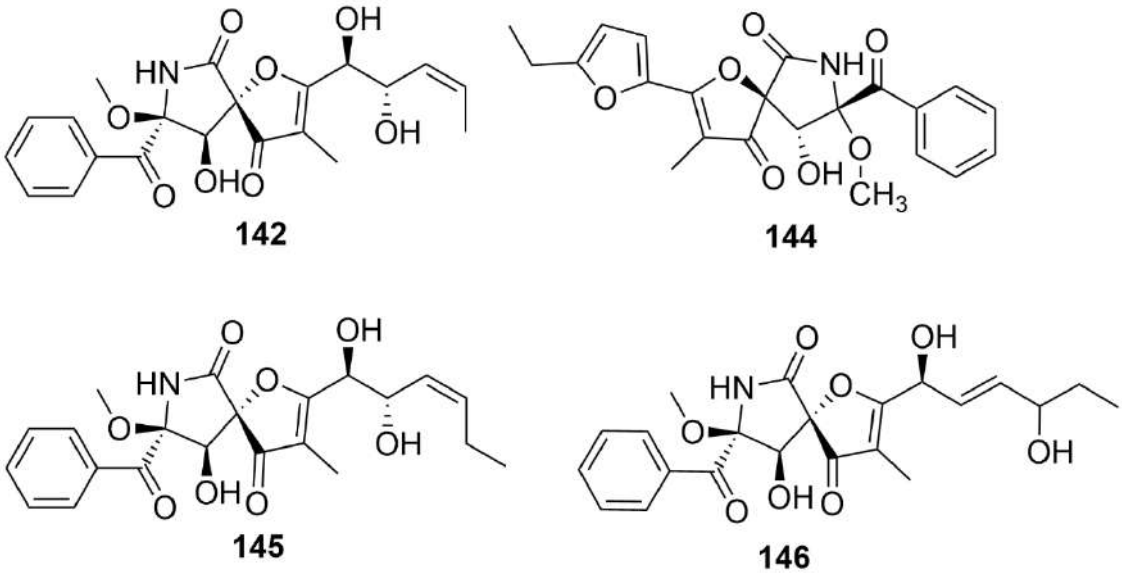

Figure 9. Chemical structures of 14-norpseurotin A (142), FD-838 (144), pseurotin A (145) and pseurotin D (146).

- **Terpenoids**

Integracide H, integracide J

Two new tetracyclic triterpenoids with antileishmanial activity were isolated from *Fusarium* sp. isolated from the roots of *Mentha longifolia* (Lamiaceae). The fungal endophyte was cultivated in a rice solid medium for 30 days at 27°C before extraction. Integracides H (**156**) and J (**157**) exhibited moderate activity against the amastigotes of *Leishmania donovani* with an IC_{50} value of 4.75 and 3.29 µM, respectively (Ibrahim et al., 2016). Pentamidine was used as the positive control with an IC_{50} value of 6.35 µM. Moreover, integracide H presented a high cytotoxicity against the human cancer cell lines BT-549, SKOV and KB with IC_{50} values of 1.82, 1.32 and 0.18 µM, respectively; while Integracide H exhibited IC_{50} values of 2.46, 3.01 and 2.54 µM, respectively (Ibrahim et al., 2016).

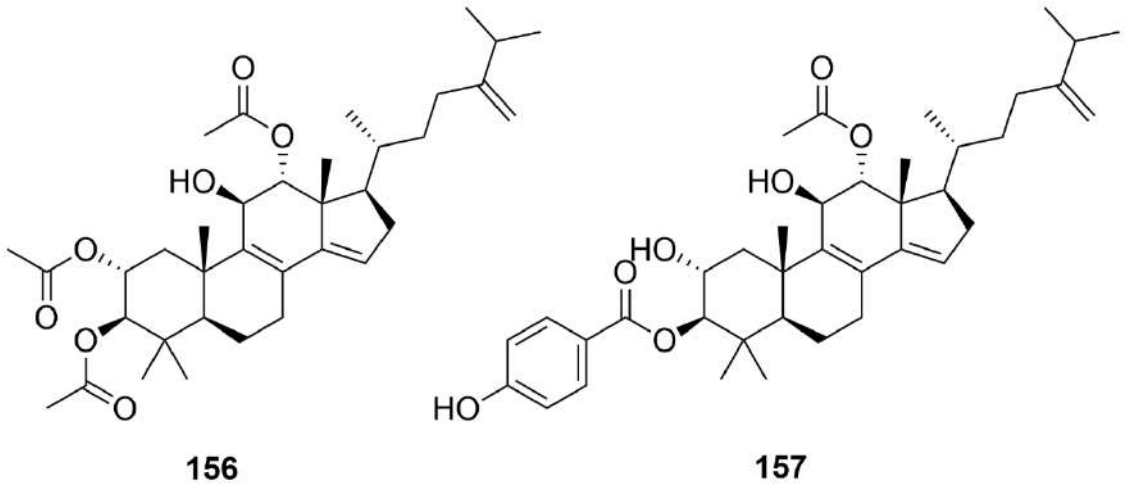

Figure 10. Chemical structures of integracide H (156) and integracide J (157).

2.2.2. Antiplasmodial

The following compounds isolated from endophytic fungi have been tested against different strains of *Plasmodium falciparum*: 3D7 (drug sensitive), D6 (chloroquine sensitive), W2 (chloroquine resistant), NF54 (chloroquine resistant) and K1 (multidrug resistant).

Among the most active compounds against *P. falciparum* 3D7 are cytochalasins H, J and O, 12,13-deoxyroridin E and roridin E with IC_{50} values <0.02 μM, followed by cytochalasin D (IC_{50} 0.0258 μM), 2,5-dihydroxy-1-(hydroxymethyl)pyridin-4-one (IC_{50} 0.127 μM), 7-hydroxy-3,4,5-trimethyl-6-on2,3,4,6- tetrahydroisoquinoline-8-carboxylic acid (IC_{50} 0.129 μM), 19,20-epoxycytochalasin D (IC_{50} 0.136 μM) and dicerandrol D (IC_{50} 0.6 μM). Compounds with potent activity against *P. falciparum* D6 and W2 are 19,20-epoxycytochalasin D with an IC_{50} value of 0.04 μM followed by 19,20-epoxycytochalasin C (IC_{50} 0.05-0.07 μM), epoxycytochalasin H (IC_{50} 0.07-0.1 μM) and 18-deoxy-19,20-epoxycytochalasin C (IC_{50} 0.19-0.56 μM) while fusaripeptide A was tested only against *P. falciparum* D6 and it exhibited an IC_{50} value of 0.34 μM. Three other compounds presented potent activity against *P. falciparum* K1 being phomoxanthone A with an IC_{50} value of 0.15 μM followed by phomoxanthone B (IC_{50} 0.44 μM) and monocerin (IC_{50} 0.68 μM). Additionally, apicidins B and C were tested against *P. falciparum* (strain not specified) exhibiting IC_{50} values of 0.189 and 0.069 μM, respectively.

Compounds presenting a moderate activity in terms of IC_{50}were tested against *P. falciparum* K1, a multidrug resistant strain. Chaetoxanthone B was the most active, with an IC_{50} value of 1.41 μM followed by 2-chloro-5-methoxy-3-methylcyclohexa-2,5- diene-1,4-dione (IC_{50} 1.84 μM), phomoarcherin B (IC_{50} 2.05 μM), 12,12a-dihydro antibiotic PI 016 (IC_{50} 2.95 μM), mollicellin K (IC_{50} 1.84 μM), pullularin B (IC_{50} 4.18 μM) and pullularin A (IC_{50} 4.64 μM). Codinaeopsin was tested against *P. falciparum* 3D7 and exhibited a moderate activity with an IC_{50} value of 4.7 μM.

Finally, those exhibiting a weaker activity in terms of IC_{50}, were also mainly tested against *P. falciparum* K1. Xylariaquinone A presented an IC_{50} value of 6.68 μM followed by mollicellin M (IC_{50} 6.95 μM), mollicellin E (IC_{50} 7.16 μM), 11-hydroxymonocerin (IC_{50} 7.7 μM), 7α,10α-dihydroxy-1βmethoxyeremophil-11(13)-en-12,8β olide (IC_{50} 8.1 μM), 7-butyl-6,8-dihydroxy-3(R)-pentylisochroman-1-one (IC_{50} 8.48 μM), mollicellin L (IC_{50} 8.6 μM) and KS-501a (IC_{50} 9.9 μM). Asterric acid, preussiafuran A and cissetin were tested against *P. falciparum* NF54 exhibiting weak activities with IC_{50} values of 8.67, 8.76 and 10.3 μM, respectively.

- **Alkaloids**

<u>18-Deoxy-19,20-epoxycytochalasin C; 19,20-epoxycytochalasin C; 19,20-epoxycytochalasin D</u>

Three known cytochalasins were obtained from the endophytic fungus *Nemania* sp. isolated from the diseased leaves of *Torreya taxifolia* Arnott (Taxaceae) (Kumarihamy et al., 2019). Compounds 19,20-epoxycytochalasin C (**103**) and D (**104**) were first isolated from the fungus *Xylaria hypoxylon* and by this time, there were many biological activities, such as antibiotic and antitumor activities, that were already reported for this family of compounds (Espada et al., 1997). Moreover, 18-deoxy-19,20-epoxycytochalasin C was first isolated from a non-

identified fungus (KL-1.1) isolated from the leaves of the medicinal plant *Psidium guajava* (Myrtaceae) (Okoye et al., 2015).

For the isolation of secondary metabolites, *Nemania* sp. was cultivated in Potato dextrose broth at 27 °C during 30 days at 100 rpm. These three known cytochalasins exhibited potent *in vitro* activity against two strains of *Plasmodium falciparum* (D6 and W2). Compound 19,20-epoxycytochalasin C (**103**) was isolated as the major compound and it exhibited IC_{50} values of 0.07 and 0.05 µM against the D6 and W2 strains, respectively. Compound 18-deoxy-19,20-epoxycytochalasin C (**102**) exhibited IC_{50} values of 0.56 and 0.19 µM against the D6 and W2 strains, respectively while compound 19,20-epoxycytochalasin D (**104**) exhibited an IC_{50} value of 0.04 µM for both *P. falciparum* strains (Kumarihamy et al., 2019). Positive standard controls used were chloroquine (IC_{50} 0.03 µM) and artemisinin (IC_{50} 0.02 µM). Similarly, when the compound 19,20-epoxycytochalasin D was isolated from endophytic fungus *Diaporthe* sp., it exhibited an IC_{50} value of 0.136 µM against *P. falciparum* 3D7 (Calcul et al., 2013).

Additionally, all three compounds presented moderate toxicity against different tumor cell lines, 19,20-epoxycytochalasin C exhibited an IC_{50} value of 8.02 µM against SK-MEL (malignant melanoma); 19,20-epoxycytochalasin D exhibited IC_{50} values of 7.84 and 8.4 µM against BT-549 (breast ductal carcinoma) and LLC-PK_{11} (kidney epithelial cells), respectively. While 18-Deoxy-19,20-epoxycytochalasin C exhibited an IC_{50} value of 6.89 µM against BT-549. None of these compounds were toxic against Vero Cells (kidney fibroblast), therefore showing their selectivity to *Plasmodium falciparum* strains (Kumarihamy et al., 2019).

Cissetin

Cissetin (**107**) was first isolated from a non-identified fungus (OSI 50185) isolated from a decomposed plant in Peru, showing antibacterial activity against penicillin-resistant *Streptococcus pneumoniae* (MIC 2 µg/mL) (Boros et al., 2003). This compound was later isolated from endophytic fungus *Preussia* sp. isolated from the leaves and barks of the plant *Enantia chlorantha* (Annonaceae) (Talontsi et al., 2014). For the isolation of compounds, *Preussia* sp. was cultivated in a rice medium at 25°C for 30 days under static conditions. Cissetin exhibited a weak activity against *Plasmodium falciparum* (NF54) with an IC_{50} value of 10.3 µM and a weak cytotoxicity against L6 cells (rat skeletal myoblast) with an IC_{50} value of 42.1 µM.

2,5-Dihydroxy-1-(hydroxymethyl)pyridin-4-one; 7-hydroxy-3,4,5-trimethyl-6-on 2,3,4,6-tetrahydroisoquinoline -8-carboxylic acid

Two new alkaloids were isolated from a non-identified endophytic fungus (strain BB4) isolated from the stem and leaves of *Tinospora crispa* (Menispermaceae), a plant traditionally used for malaria treatment. This endophytic fungal strain was cultivated in Potato dextrose broth for 3 weeks for further extraction. Compounds 2,5-dihydroxy-1-(hydroxymethyl)pyridin-4-one (**105**) and 7-hydroxy-3,4,5-trimethyl-6-on-2,3,4,6-tetrahydroisoquinoline-8-carboxylic acid (**106**) exhibited potent activity against *Plasmodium falciparum* (3D7) with IC_{50} values of 0.127 and 0.129 µM, respectively (Elfita et al., 2011). Positive standard chloroquine presented an IC_{50} value of 0.02 µM.

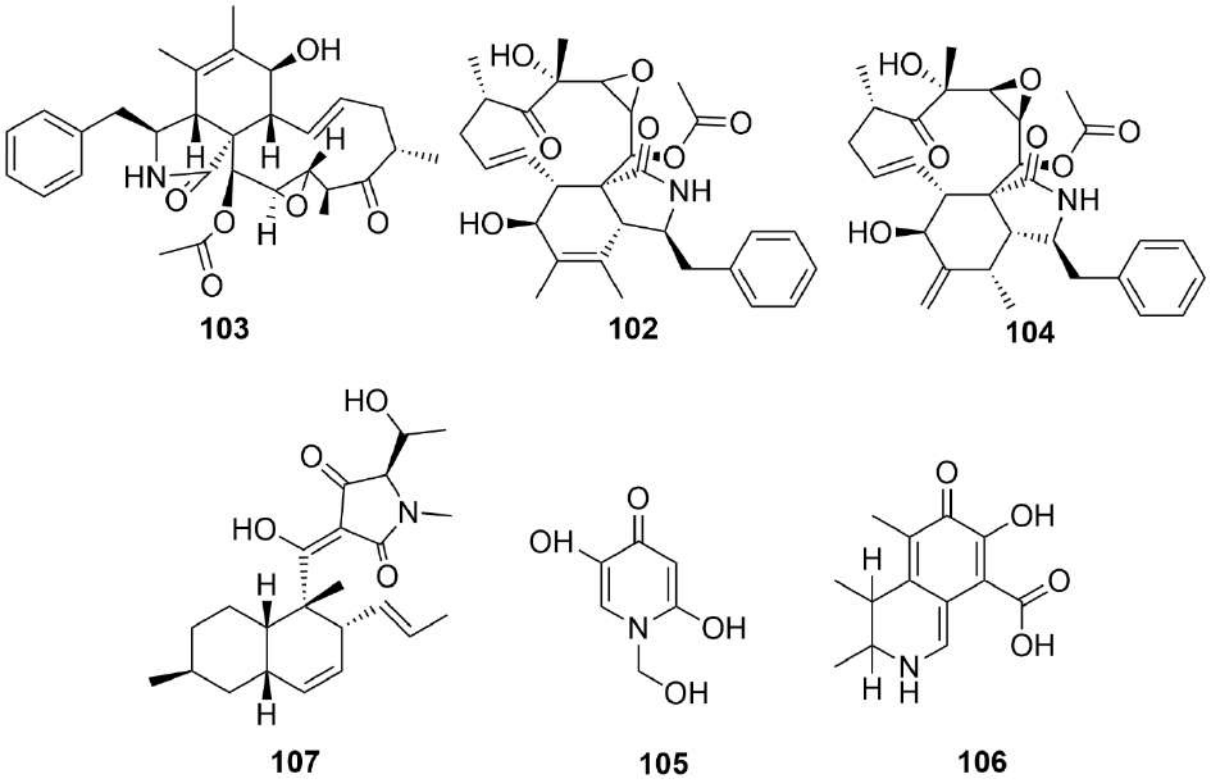

Figure 11. Chemical structures of 18-deoxy-19,20-epoxycytochalasin C (102), 19,20-epoxycytochalasin C (103), 19,20-epoxycytochalasin D (104), cissetin (107), 2,5-dihydroxy-1-(hydroxymethyl)pyridin-4-one (105) and 7-hydroxy-3,4,5-trimethyl-6-on-2,3,4,6-tetrahydroisoquinoline-8-carboxylic acid (106)

Cytochalasin D, cytochalasin H, cytochalasin J, cytochalasin O

Cytochalasin D (**108**) was first isolated from endophytic fungus, *Xylaria* sp. from the plant *Palicourea marcgravii* (Rubiaceae), showing antifungal activity (Cafeu et al., 2005). This compound was able to reduce the attachment of the promastigotes of leishmania by the destabilization of the actin cytoskeleton of macrophages, accompanied by a reduction of the intracellular amastigote load (Roy et al., 2014). Cytochalasin H (**109**) and J (**110**) were previously isolated from *Phomopsis* sp. (Wells et al., 1976; Izawa et al., 1989) while cytochalasin O (**111**) was isolated from the fungus *Hypoxylon terricola* (Edwards et al., 1989). As part of a bigger study, endophytic fungi *Diaporthe* sp., *Xylaria* sp. and *Verticillium* sp. were isolated from the barks and leaves of 3 different plants; *Kandelia obovata* (Rhizophoraceae), *Avicennia marina* (Acanthaceae) and *Lumnitzera racemosa* (Combretaceae). These fungi were cultivated in a liquid medium containing 1% w/v glucose, 0.1% w/v yeast extract and 0.2% w/v peptone during 3 weeks for isolation of secondary metabolites. Cytochalasin D exhibited potent activity against *Plasmodium falciparum* (3D7) with an IC_{50} value of 0.0258 µM while cytochalasins H, J and O presented IC_{50} values of <0.02 µM (Calcul et al., 2013). In this study, the positive standard used was chloroquine presenting an IC_{50} value of 0.0045 µM and dihydroartemisinin with an IC_{50} value of 0.0003 µM.

Epoxycytochalasin H

This compound (**112**) was first isolated from *Phomopsis sojae* isolated from soybean seeds (Cole et al., 1982) and later it was also obtained from the endophytic fungus *Diaporthe miriciae* isolated from the plant *Vellozia gigantea* (Velloziaceae) showing potent antiplasmodial activity. Endophytic fungus *Diaporthe miriciae* was cultured in Potato dextrose agar at 25°C during 15 days for compound extraction. Epoxycytochalasin H exhibited an IC_{50} value of 0.1 and 0.07 μM against D6 and W2 strains of *Plasmodium falciparum*, respectively while no toxicity was detected against Vero cells (mammalian kidney) (Ferreira et al., 2017). Chloroquine and artemisinin were used as positive standards for both plasmodial strains.

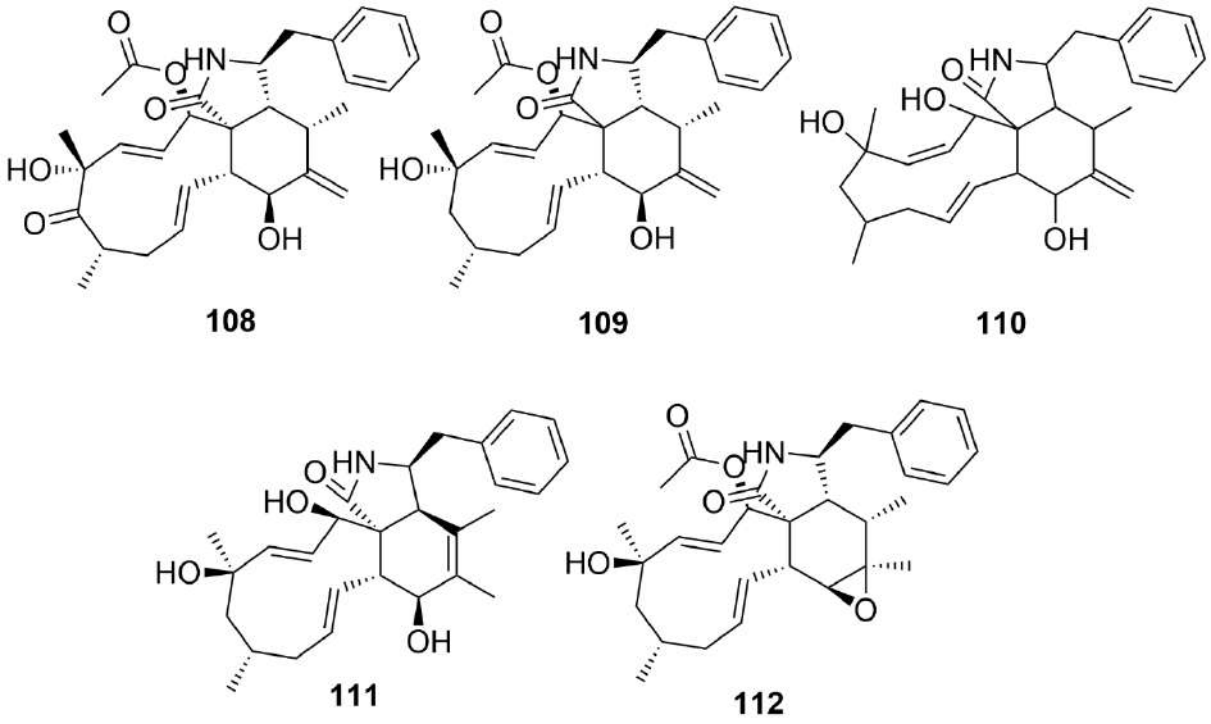

Figure 12. Chemical structures of cytochalasin D (108), cytochalasin H (109), cytochalasin J (110), cytochalasin O (111) and epoxycytochalasin H (112).

- **Polyketides**

11-Hydroxymonocerin, monocerin

Monocerin (**132**) and a new analogue of monocerin (**113**) were isolated from endophytic fungus *Exserohilum rostratum* isolated from the leaves and roots of *Stemona* sp. (Stemonaceae) (Sappapan et al., 2008). Monocerin was first isolated from *Helminthosporium monoceras* along with other related benzopyrans (Alridge et al., 1970). Fungus *Exserohilum rostratum* was cultivated in yeast sucrose extract at 31°C during 21 days under static conditions for supernatant extraction. Compound 11-hydroxymonocerin was weakly active against *Plasmodium falciparum* K1 with an IC_{50} value of 7.7 μM while monocerin exhibited a potent antiplasmodial activity with an

IC_{50} value of 0.68 µM. According to the authors, the presence of the additional –OH group in 11-hydroxymonocerin caused the lower activity compared to monocerin. Dihydroartemisinin was used as the positive standard with an IC_{50} value of 0.004 µM. Additionally, the compounds showed no cytotoxicity against 5 human tumor cell lines BT474 (breast carcinoma), CHAGO (lung carcinoma), Hep-G2 (hepatocarcinoma), KATO-3 (gastric carcinoma), and SW-620 (colon carcinoma) (Sappapan et al., 2008).

2-Chloro-5-methoxy-3-methylcyclohexa-2,5-diene-1,4-dione, xylariaquinone A

Two novel benzoquinones with antiplasmodial activity were isolated from fungal endophyte *Xylaria* sp. isolated from the leaves of *Sandoricum koetjape* (Meliaceae) (Tansuwan et al., 2007). Fungus was cultivated in malt extract broth at 30°C during 5 weeks under static conditions for supernatant extraction. Xylariaquinone A (**141**) was weakly active against *Plasmodium falciparum* K1 with an IC_{50} value of 6.68 µM while 2-chloro-5-methoxy-3-methylcyclohexa-2,5-diene-1,4-dione (**114**) exhibited a moderate antiplasmodial activity with an IC_{50} value of 1.84 µM and cytotoxic activity against Vero cells with an IC_{50} value of 1.35 µM. (Tansuwan et al., 2007). Positive standard dihydroartemisinin exhibited an IC_{50} value of 0.0033 µM.

7 Butyl-6,8-dihydroxy-3(R)-pentylisochroman-1-one

A novel dihydroisocoumarin (**115**) was isolated from fungal endophyte *Geotrichum* sp. isolated from the healthy stems of *Crassocephalum crepidioides* (Asteraceae). The fungus was cultivated in Czapek broth at 25°C during 21 days for supernatant extraction. The 7 Butyl-6,8-dihydroxy-3(R)-pentylisochroman-1-one was weakly active against *Plasmodium falciparum* K1 with an IC_{50} value of 8.48 µM (Kongsaeree et al., 2003). The standard compound Chloroquine presented an IC_{50} value of 0.31 µM.

Asterric acid, preussiafuran A

Asterric acid (**117**) and a novel dibenzofuran (**138**) were isolated from fungal endophyte *Preussia* sp. isolated from the healthy leaves and barks of *Enantia chlorantha* (Annonaceae) (Talontsi et al., 2014). Asterric acid was first isolated from *Aspergillus terreus* (Curtis et al., 1960). The endophytic strain of *Preussia* sp. was cultivated in a rice medium at 25°C during 30 days under static conditions. Asterric acid and preussiafuran A were weakly active against *Plasmodium falciparum* NF54 and they exhibited IC_{50} values of 8.67 and 8.76 µM, respectively. Chloroquine was used as the positive standard. Moreover, asterric acid and preussiafuran A presented moderate cytotoxicity against L6 cell lines (rat skeletal myoblasts) with IC_{50} values of 14.8 and 36.7 µM, respectively.

Chaetoxanthone B

A new compound (**120**) was isolated from the marine-derived fungus *Chaetomium* sp. isolated from an algal species (taxonomy not determined) (Pontius et al., 2008). This fungus was cultivated in malt extract yeast agar at room temperature for 15 days for compound extraction. Chaetoxanthone B exhibited moderate activity against *Plasmodium falciparum* K1 with an IC_{50} value of 1.41 µM while it showed no cytotoxicity against L6 cells (rat skeletal myoblasts). Chloroquine was used as the positive standard.

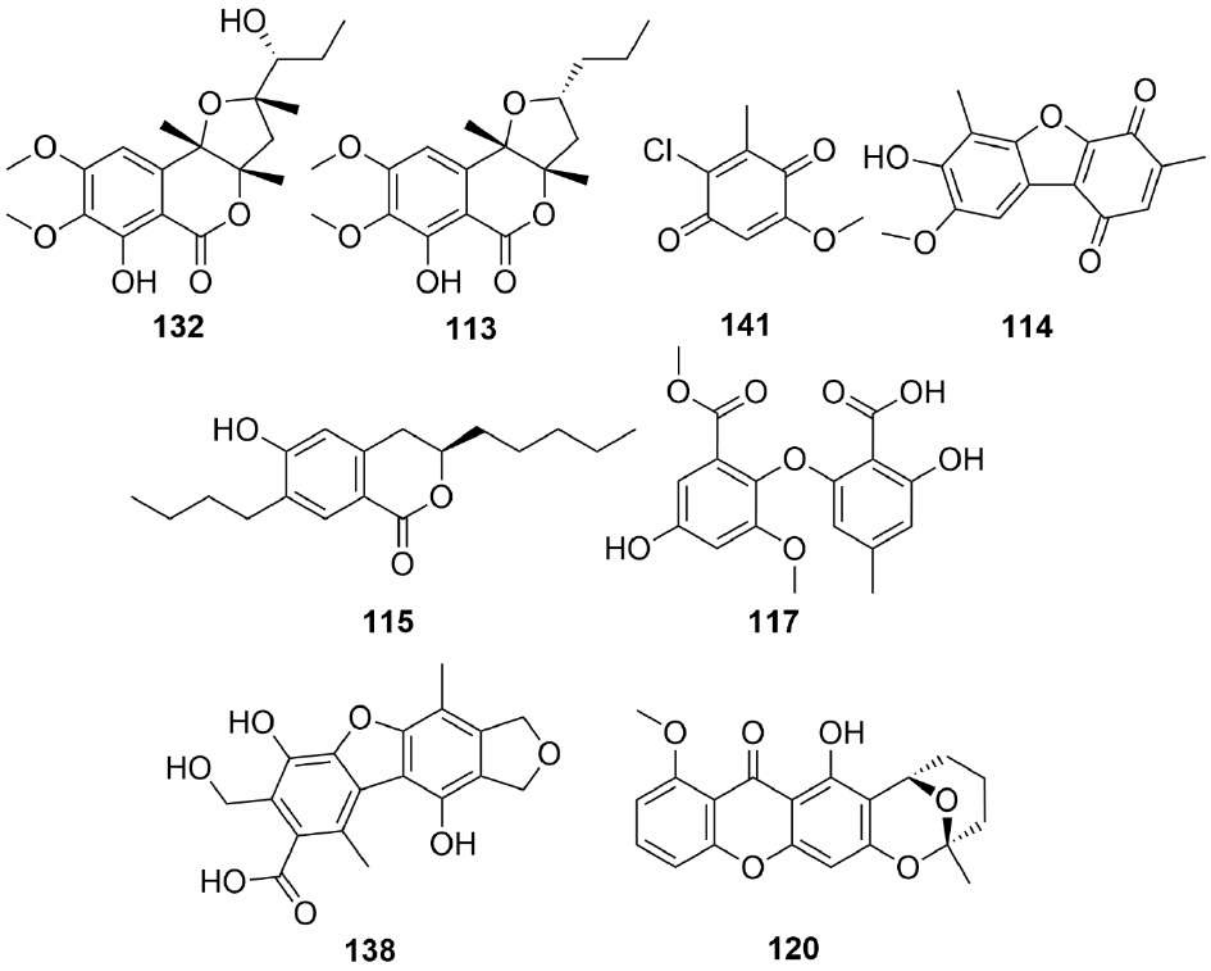

Figure 13. Chemical structures of 11-hydroxymonocerin (113), monocerin (132), 2-chloro-5-methoxy-3-methylcyclohexa-2,5-diene-1,4-dione (114), xylariaquinone A (141), dihydroisocoumarin (115), asterric acid (117), preussiafuran A (138) chaetoxanthone B (120).

Phomoxanthone A, phomoxanthone B

Two novel xanthone dimers were isolated from the fungal endophyte *Phomopsis sp.* isolated from the leaves of *Tectona crispa* (Lamiaceae). This fungus was cultivated in bacto-malt extract broth at 22°C during 20 days for mycelium extraction. Phomoxanthone A (**136**) and B (**137**) exhibited potent activity against *Plasmodium falciparum* K1 with IC_{50} values of 0.15 and 0.44 µM, respectively. However, they presented elevated cytotoxicity against 3 cancer cell lines, KB cells, BC-1 cells and Vero cells (Isaka et al., 2001). Chloroquine diphosphate and artemisinin were used as positive standards.

Dicerandrol D

A new dimeric tetrahydroxanthone was isolated from the fungal endophyte *Diaporthe* sp. along with other known cytochalasins previously mentioned (Calcul et al., 2013). Dicerandrol D (**124**) exhibited a potent activity against

Plasmodium falciparum 3D7 with an IC_{50} value of 0.6 µM and a low cytotoxicity against A549 cells (adenocarcinomic human alveolar epithelial cells) with an IC_{50} value of 7.8 µM.

KS-501a

KS-501a (**127**) was first isolated as a potent inhibitor of Ca^{2+} from *Sporothrix* sp. from a fallen leaf in Japan (Nakanishi et al., 1989). Later, it was also obtained from the culture of *Acremonium* sp. isolated from a palm leaf in Thailand. Here, *Acremonium* sp. was cultivated in Bacto-malt extract broth at 25°C during 32 days at 200 rpm for the isolation of compounds from the supernatant. This compound exhibited a weak activity against *Plasmodium falciparum* K1 with an IC_{50} value of 9.9 µM while its cytotoxic activity possessed an IC_{50} value of 8.8 µM against BC (human breast cancer) cell lines (Bunyapaiboonsri et al., 2008). Dihydroartemisinin was used as the positive standard with an IC_{50} value of 0.004 µM.

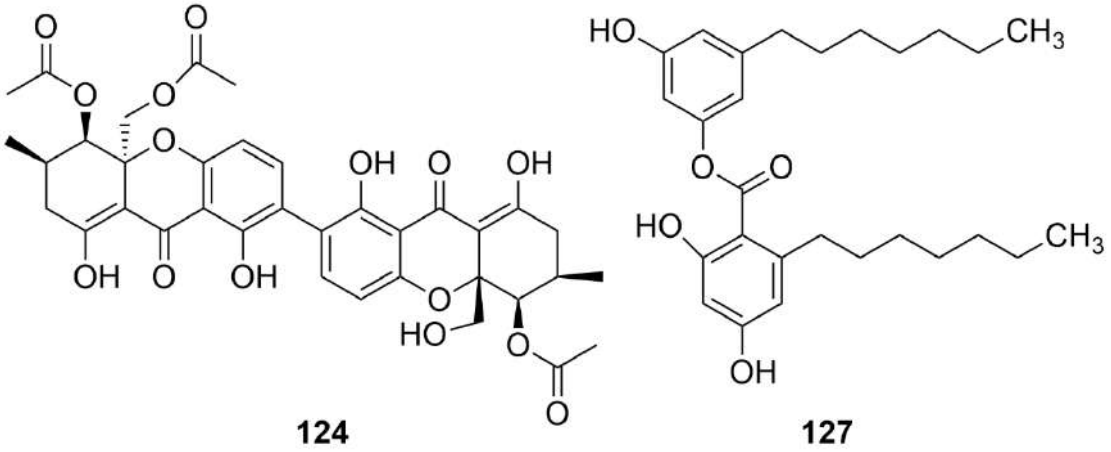

Figure 14. Chemical structures of dicerandrol D (124) and KS-501a (127).

Mollicellin E, mollicellin K, mollicellin L, mollicellin M

Three novel depsidones (mollicellin K, L and M, **129**, **130**, **131**) and one known (mollicellin E, **128**) were isolated from endophytic fungus *Chaetomium brasiliense*, isolated from a leaf collected in the Hala-Bala evergreen forest (Thailand) (Khumkomkhet et al., 2009). Mollicellin E was first isolated from *Chaetonium mollicellum* and its mutagenic and bactericidal activity against *Salmonella typhimurium* was reported (Stark et al., 1978). The strain of *C. brasiliense* was cultured in potato dextrose broth between 25-28 °C during 4 weeks under static conditions for mycelium extraction. Mollicellin E, L and M presented a weak activity against *Plasmodium falciparum* K1, exhibiting IC_{50} values of 7.16, 8.6 and 6.95 µM, respectively. Mollicellin K presented a moderate antiplasmodial activity with an IC_{50} value of 3.13 µM and cytotoxicity against KB cells (human epidermoid carcinoma of the mouth) and NCI-H187 (human small cell lung cancer) with IC_{50} values of 1.9 and 0.35 µM, respectively (Khumkomkhet et al., 2009). The standard compound used was artemisinin. Additionally, the 4 compounds exhibited significant cytotoxicity against 5 cholangiocarcinoma cell lines (KKU-100, KKU-M139, KKU-M156, KKU-M213, and KKUM214).

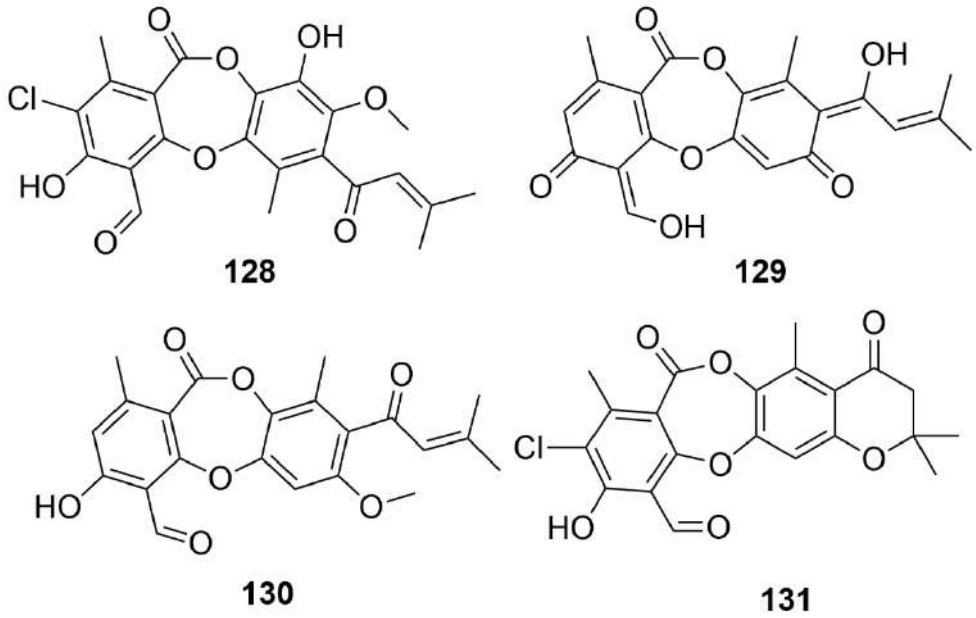

Figure 15. Chemical structures of mollicellin E (128), mollicellin K (129), mollicellin L (130) and mollicellin M (131).

- **Polyketide-Alkaloid**

Codinaeopsin

A novel tryptophan-polyketide hybrid (**143**) was isolated from fungal endophyte *Codinaeopsis gonytrichoidesi* isolated from the tree *Vochysia guatemalensis* (Vochysiaceae). This fungus was cultivated in a rich seed medium at 25°C during 21 days for compound extraction. Codinaeopsin exhibited moderate activity against *Plasmodium falciparum* 3D7 with an IC_{50} value of 4.7 μM (Kontnik et al., 2008).

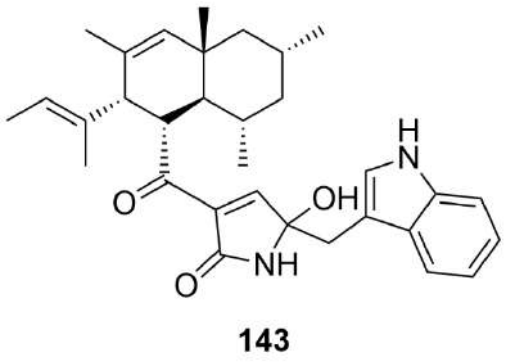

Figure 16. Chemical structure of codinaeopsin (143).

- **Polypeptides**

12,12a-Dihydroantibiotic PI 016

A novel compound (**147**) with antimalarial activity was isolated from fungal endophyte *Menisporopsis theobromae* isolated from the seeds of a plant (not specified) in Thailand. This fungus was grown in potato dextrose broth at 25°C during 24 days at 200 rpm for whole culture extraction. The compound 12,12a-dihydroantibiotic PI 016 exhibited a moderate activity against *Plasmodium falciparum* K1 with an IC_{50} value of 2.95 µM (Chinworrungsee et al., 2006). Moreover, this compound presented cytotoxicity against NCI-H187 cell lines (small cell lung cancer) with an IC_{50} value of 20.3 µM. Dihydroartemisinin was used as the positive standard with an IC_{50} value between 0.004 – 0.014 µM.

Apicidin B, apicidin C

Two novel cyclic tetrapeptides with antiplasmodial activity were isolated from fungal endophyte *Fusarium pallidoroseum* isolated from the branches of *Acacia* sp. (Fabaceae). Apicidin B (**148**) and C (**149**) exhibited significant activity against *Plasmodium falciparum* with MIC values of 0.189 and 0.069 µM, respectively (Singh et al., 2001).

Fusaripeptide A

A novel cyclodepsipeptide was isolated from endophytic fungus *Fusarium* sp. isolated from the roots of *Mentha longifolia* (Lamiaceae). Fungus was cultivated in rice solid medium at room temperature for 30 days. Fusaripeptide A (**151**) exhibited a potent activity against *Plasmodium falciparum* (D6) with an IC_{50} value of 0.34 µM (Ibrahim et al., 2018). Additionally, this compound presented significant cytotoxicity against L5178Y (mouse lymphoma) and PC12 (rat brain cancer) cell lines with IC_{50} values of 5.71 and 9.55 µM, respectively. Fusaripeptide A also presented high antifungal activity against 3 different species of *Candida* and one strain of *Aspergillus fumigatus*. Positive control artemisinin presented an IC_{50} value of 0.57 µM.

Pullularin A, pullularin B

Two new cyclohexadepsipeptides with antiplasmodial activity were isolated from endophytic fungus *Pullularia* sp. (yeast-like) isolated from the leaves of *Calophyllum* sp. (Clusiaceae). This endophyte was cultivated in potato dextrose broth at 25°C during 19 days at static conditions for supernatant extraction. Pullularins A (**152**) and B (**153**) exhibited moderate activity against *Plasmodium falciparum* K1 with IC_{50} values of 4.64 and 4.18 µM, respectively (Isaka et al., 2007). Pullularin A presented cytotoxic activity against Vero cells with an IC_{50} value of 36 µM. Dihydroartemisinin was used as the positive standard.

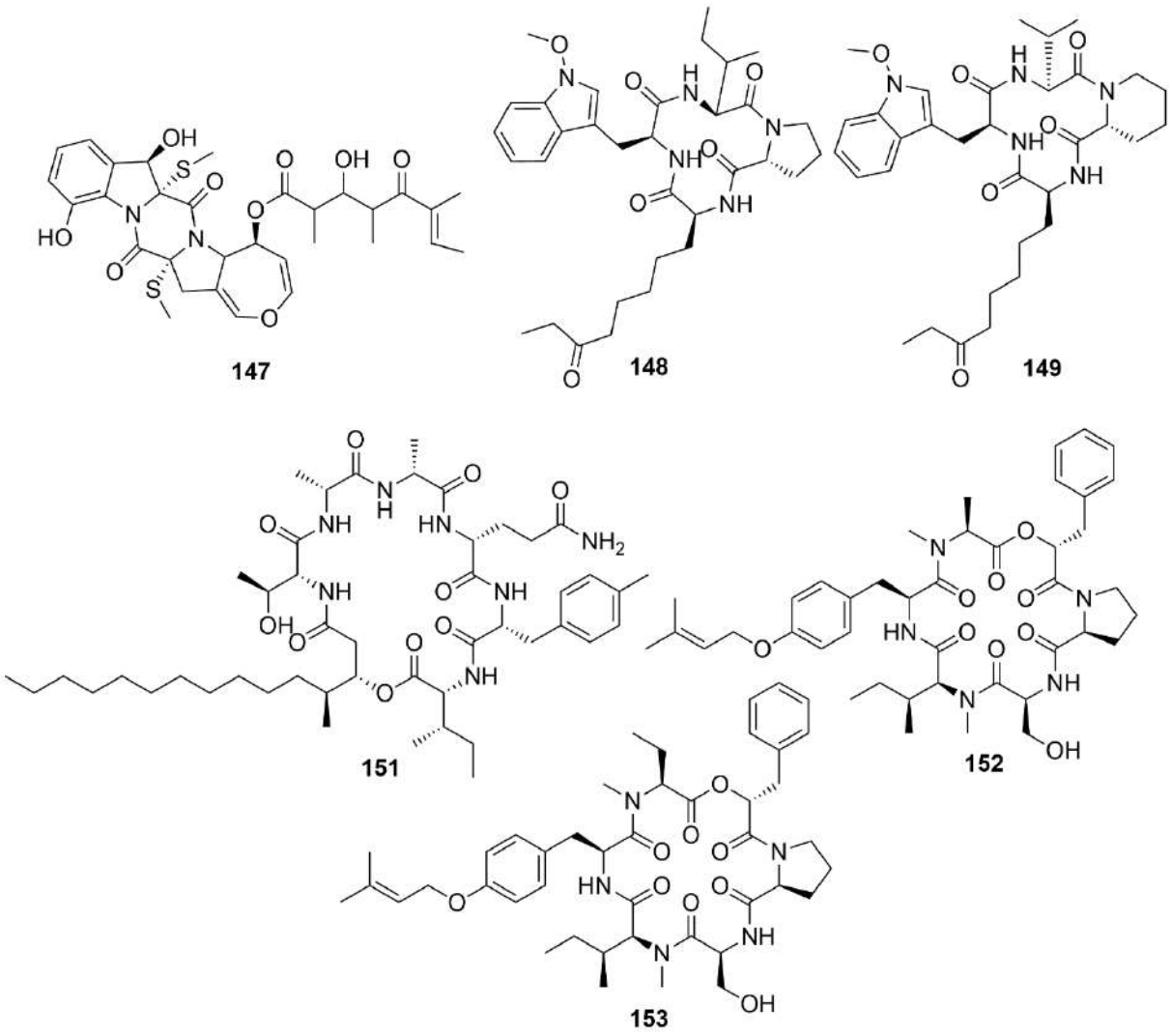

Figure 17. Chemical structures of 12,12a-dihydroantibiotic PI 016 (147), apicidin B (148), apicidin C (149), fusaripeptide A (151), pullularin A (152) and pullularin B (153).

- **Terpenoids**

7α,10α-Dihydroxy-1βmethoxyeremophil-11(13)-en-12,8β olide

A novel eremophilanolide sesquiterpenoid was isolated from *Xylaria* sp. isolated from the palm *Licuala spinosa* (Arecaceae). This fungus was cultivated in potato dextrose broth at 25°C during 30 days at 200 rpm. The compound (**155**) exhibited weak activity against *Plasmodium falciparum* K1 with an IC_{50} value of 8.1 µM (Isaka et al., 2010). Moreover, it presented cytotoxic activity against KB (oral human epidermoid carcinoma), MCF-7 (human breast cancer), NCI-H187 (human small cell lung cancer) and Vero cells (African green monkey kidney fibroblasts) with IC_{50} values of 21, 15, 7.2 and 8.5 µM, respectively. Dihydroartemisinin was used as the positive standard with an IC_{50} value of 0.004 µM.

Phomoarcherin B

A new sesquiterpene was isolated from fungal endophyte *Phomopsis archeri* isolated from the cortex stem of *Vanilla albidia* (Orchidaceae). The fungus was cultivated in potato dextrose broth at 25-28°C during 4 weeks for mycelium extraction. Phomoarcherin B (**158**) exhibited moderate activity against *Plasmodium falciparum* K1 with an IC_{50} value of 2.05 µM (Hemtasin et al., 2011). Additionally, it presented low cytotoxicity against the KB cell line with an IC_{50} value of 9.4 µM. However, it possessed significant toxicity against KKU-M139 and KKU-M156 (cholangiocarcinoma cell lines) with IC_{50} values of 0.1 and 2 µM, respectively. Dihydroartemisinin was used as the positive standard with an IC_{50} value of 0.015 µM.

12,13-Deoxyroridin E, roridin E

Along with the Cytochalasins D, H, J and O and dicerandrol D previously mentioned, two already known terpenoids with potent antiplasmodial activity were isolated from a non-identified strain (CY-3923) isolated from the barks and leaves of 3 different plants; *Kandelia obovata* (Rhizophoraceae), *Avicennia marina* (Acanthaceae) and *Lumnitzera racemosa* (Combretaceae) (Calcul et al., 2013). The compounds 12,13-deoxyroridin E (**154**) and roridin E (**159**) exhibited activity against *Plasmodium falciparum* 3D7, both with an IC_{50} value <0.02 µM. Moreover, they showed no cytotoxicity against A549 cell lines (adenocarcinomic human alveolar epithelial cells).

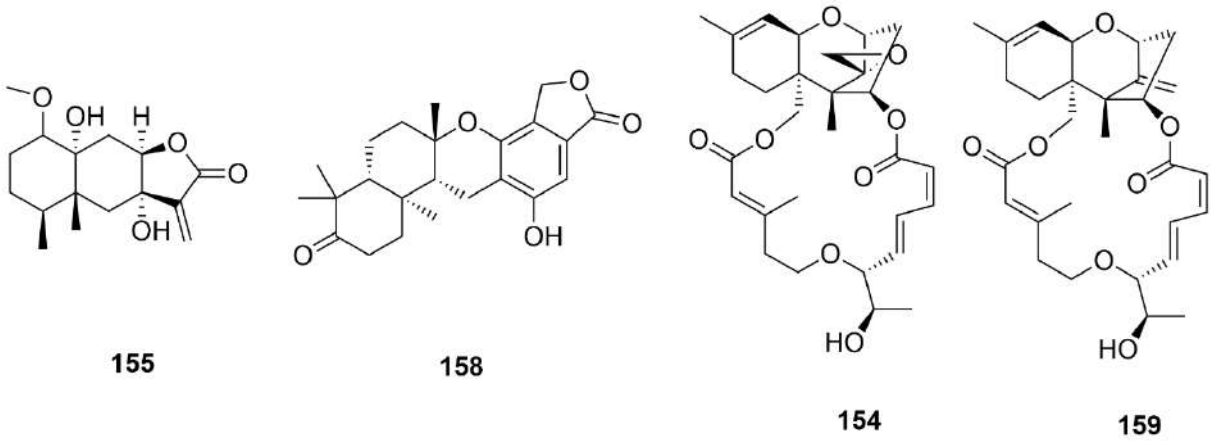

Figure 18. Chemical structures of 7α,10α-dihydroxy-1βmethoxyeremophil-11(13)-en-12,8β olide (155), phomoarcherin B (158), 12,13-deoxyroridin E (154) and roridin E (159).

2.2.3. Antitrypanosomal / Antiplasmodial / Antileishmanial

The most active compounds against *Trypanosoma cruzi* are cercosporin, exhibiting an IC_{50} value of 1.08 µM while its semisynthetic tetra-acetylated derivative presented an IC_{50} value of 0.78 µM. Cercosporin and its tetra-acetylated derivative also exhibited activity against *Leishmania donovani* with IC_{50} values of 0.46 and 0.64 µM, respectively and activity against *Plasmodium falciparum* with IC_{50} values of 1.03 and 2.99 µM, respectively. Moreover, compound Beauvericin exhibited a moderate activity against *T. cruzi* with an IC_{50} value of 2.43µM followed by chaetoxanthone C with an IC_{50} value of 3.83 µM. Altenusin was tested in an assay with the

recombinant enzyme trypanothione reductase, considered as a drug target (Cota et al., 2008) and it exhibited IC_{50} value of 4.3 µM.

- **Polyketides**

Altenusin

Altenusin (**116**) was first isolated from *Alternaria tenuis* (Thomas, 1961). It was also obtained from endophytic fungus *Alternaria* sp. isolated from the leaves of *Trixis vauthieri* DC (Asteraceae). *Alternaria* sp. was cultivated in malt extract agar at 28°C during 9 days at 150 rpm. Altenusin exhibited a moderate activity against the recombinant enzyme trypanothione reductase (TR) from *Trypnanosma cruzi* with an IC_{50} value of 4.3 µM but this activity was not observed for the amastigotes of *Leishmania amazonensis* (Cota et al., 2008). It is suggested that altenusin might not be able to reach the intracellular compartments in *Leishmania* parasites in sufficient quantities to inhibit parasite survival. In this assay, clomipramine was used as a standard TR inhibitor at a concentration of 6 µg/mL.

Chaetoxanthone C

Chaetoxanthone C (**121**) was isolated from endophytic fungus *Chaetomium* sp. along with chaetoxanthone B, which exhibited a moderate antiplasmodial activity as it was previously mentioned (Pontius et al., 2008). Chaetoxanthone C also exhibited a moderate activity against *Trypanosoma cruzi* Tulahuen C4 with an IC_{50} value of 3.83 µM and a low cytotoxicity against L6 cells (rat skeletal myoblasts) with an IC_{50} value of 46.7 µM. Benznidazole was used as a standard compound showing an IC_{50} value of 1.15 µM.

Cercosporin, cercosporin derivative tetra-acetylated

Cercosporin (**118**) was first isolated as a pigment from the cultured mycelia of *Cercospora kikuchii* (Kuyama & Tamura, 1957). Later, it was also obtained from the endophytic fungus *Mycosphaerella* sp. isolated from *Psychotria horizontalis* (Rubiaceae). The fungus was cultivated in potato dextrose at 28°C during 15 days at 200 rpm for mycelium extraction. In this study, cercosporin was acetylated to obtain a tetra-acetylated derivative (**119**), both with potent anti-parasitic activities. Cercosporin and its tetra-acetylated derivative exhibited activity against *Leishmania donovani* with IC_{50} values of 0.46 and 0.64 µM, respectively, against *Plasmodium falciparum* with IC_{50} values of 1.03 and 2.99 µM, respectively and activity against *Trypanosoma cruzi* with IC_{50} values of 1.08 and 0.78 µM, respectively (Moreno et al., 2011). The drugs used as positive controls were amphotericin (IC_{50} 0.08 – 0.13 µM) for *L. donovani*, chloroquine (IC_{50} 0.08 – 0.1 µM) for *P. falciparum* and nifurtimox (IC_{50} 10 - 16 µM) for *T. cruzi*. Additionally, cercosporin and its tetra-acetylated derivative presented cytotoxic activities against MCF-7 (human breast cancer) with IC_{50} values of 4.68 and 3.56 µM, respectively and against Vero cells (African green monkey kidney fibroblasts) with IC_{50} values of 1.54 and 1.24 µM, respectively.

- **Polypeptides**

Beauvericin

The depsipeptide beauvericin (**150**) was first isolated from the fungus *Beauveria bassiana*, known to be a potent insect pathogen (Hamill et al., 1969). This compound was also isolated from the endophytic fungus *Fusarium* sp. isolated from the stems and barks of the endangered species *Caesalpinia echinata* Lam (Fabaceae) (Campos et al., 2015). This fungus was cultivated in potato dextrose agar at 28°C during 14 days for compound extraction. Beauvericin exhibited a moderate activity against *Trypanosoma cruzi* with an IC_{50} value of 2.43 µM. Benznidazole was used as a standard compound showing an IC_{50} value of 3.8 µM. Beauvericin showed cytotoxic activity against L929 (mouse fibroblasts) with an IC_{50} value of 6.38 µM.

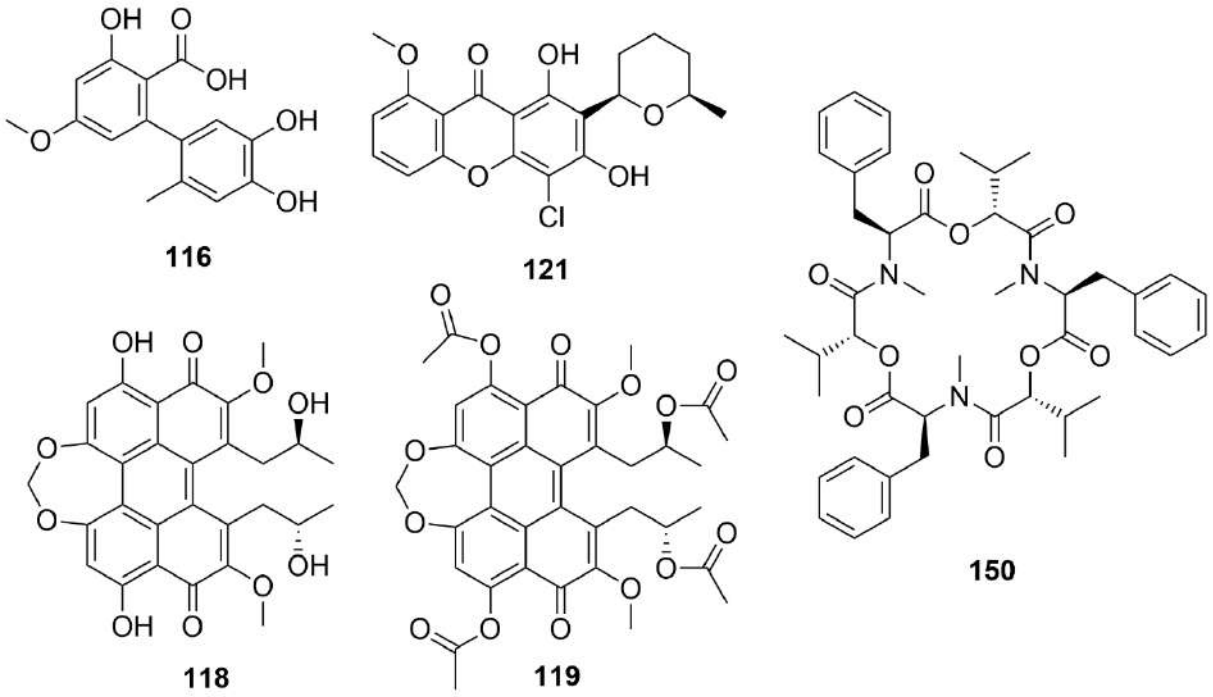

Figure 19. Chemical structures of altenusin (116), chaetoxanthione C (121), cercosporin (118), tetra-acetyl cercosporin derivative (119) and beauvericin (150).

3. Discussions and Conclusions

This work listed 101 antibacterial and 58 antiparasitic compounds isolated from endophytic fungi over the last two decades (2000-2019). These endophytic fungi were obtained from host plants of different botanical families and as shown in Figure 20, Fabaceae, Lamiaceae and Asteraceae are among the most represented families. These families are known to contain a large number of species producing bioactive compounds, as medicinal or toxic plants (Moraes Neto et al., 2019 ; Sharma et al., 2017 ; Bessada et al., 2015 ; Setzer and Setzer, 2006) and they may represent a great target for the researchers bioprospecting for endophytes. More generally, without focusing on antibacterial and antiparasitic properties, most of the bioactive endophytes studied between 2006 and 2016 were mainly isolated from plants corresponding to the families Fabaceae, Lamiaceae, Asteraceae and Araceae

(Martinez-Klimova et al., 2016) while in a recent study, between 2016 and 2019, 254 plants families were studied for their endophytes, with Poaceae, Fabaceae, Pinaceae and Asteraceae as the most studied plant families (Harrison et al., 2020).

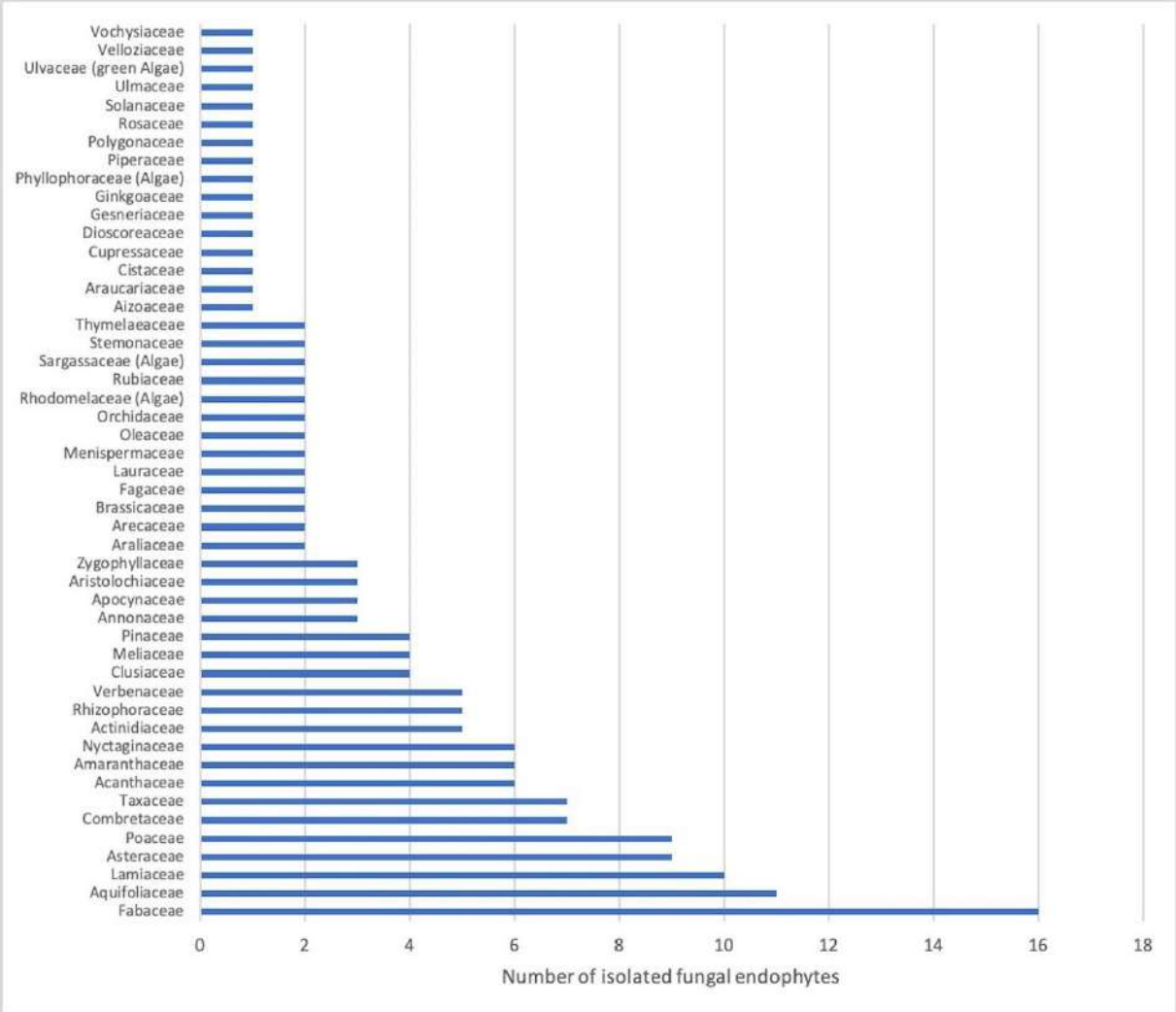

Figure 20. Botanical families of host-plants reported in this work

In this review, endophytes were mostly isolated from leaves tissues, which represent one of the largest microbial habitats on the planet (Oono et al., 2017). Most of the endophytic fungal strains belong to the Pezizomycotina sub-division of Ascomycetes: 53% of the compounds were isolated from Sordariomycetes (85 compounds from 48 fungal strains), 28% from Dothideomycetes (45 compounds from 27 fungal strains) and 12% from Eurotiomycetes (19 compounds from 12 fungal strains). According to Arnold et al. (Arnold, 2007), Dothideomycetes, Sordariomycetes and Eurotiomycetes are the three most common classes of foliar endophytes found from Canadian arctic to the lowland tropical forest of central Panama. Only one Basidiomycete, a strain belonging to the genus Rhizoctonia, has been listed here, as a producer of an antibacterial compound, monomethylsulochrin, a polyketide active against *Helicobacter pylori* (MIC = 10 ug/mL).

Almost 60% of the compounds described herein are polyketides (94 over the 159), 16% are alkaloids (26/159), 9% are polypeptides (15/159) and 8% belong to the terpenoids (13/159). Polyketides is a large class of secondary metabolites with diverse bioactivities, including immunosuppressive, anticancer, and antibacterial properties (Yin and Dickschat, 2021).

More than half of the 58 antiparasitic compounds (30 over the 58) and almost 40% (40 over the 101) of the antibacterial compounds listed here were described for the first time, highlighting the potential of novelty of endophytic fungal metabolites. Almost all the listed compounds were isolated after traditional axenic cultures. Two hypotheses could be made: due to their specific environment these endophytic fungal strains present specific metabolism leading to novel compounds; indeed, interactions between endophytes and their host-plant could enhance the biosynthesis of bioactive specialized metabolites. The second hypothesis is that fungal endophytes listed here may belong to species chemically understudied. Only 4 antibacterial compounds, neoaspergillic acid, lateropyrone, enniatin A1 and enniatin B1, were isolated from extracts of co-cultures with other fungi or bacteria. Surprisingly, all of them were already known, and no new antibacterial or antiparasitic compounds seemed to be *de novo* induced by co-cultures. Nevertheless, interestingly their production rate could be increased by these co-culture conditions, such as enniatin A1. Nowadays, the development of new methods is commonly used in order to reveal some biosynthetic pathway and to induce the production of original specialized metabolites.

Despite the great number of gene clusters found in fungi thanks to molecular techniques, the conditions for gene expression are not fully understood and the presence of silent or cryptic genes and lowly-expressed genes represent one of the main challenges for the isolation of novel secondary metabolites (Brakhage et al., 2011). For the activation of cryptic genes, many approaches are proposed, broadly classified in culture-independent and culture-dependent techniques. Regarding the culture-based techniques, the modification of cultivation conditions focuses on providing a better environment to trigger the expression of cryptic gene clusters.

The set of variations of culture conditions is known as the OSMAC approach (One strain – Many compounds) which is based on the potential of a single strain to expand its chemical diversity under small changes (Bode et al., 2002). These small changes involve different carbon or nitrogen sources, solid or liquid media, temperature variations, aeration or shaking conditions, salinity or pH levels, light conditions and time of development in culture (Romano et al., 2018). Under this approach, many endophytic fungi have already shown to expand their chemical diversity, being able to produce novel secondary metabolites. For example, the endophytic fungus *Trichocladium* sp. was cultured under the OSMAC approach, considering variations of culture media, rice medium and peas medium, allowing the isolation of a new amidepsine derivative and a new reduced spiro azaphilone derivative (Tran-Cong et al., 2019).

In addition to this, chemical elicitation during fungal culture such as treatment with epigenetic modifiers have also shown to elicit secondary metabolism. Biosynthetic gene clusters in fungi are transcriptionally regulated by epigenetic regulators, mainly by DNA methyltransferases (DNMT) and histone deacetylases (HDAC), which change the condensation state of the chromosomes (Brakhage et al., 2013). The use of inhibitors of these enzymes induces the transcription and expression of silenced genes. For instance, the treatment of the endophytic fungus

Dimorphoporicola tragani with 5-azacytidine (DNMT inhibitor) and valproic acid (HDAC inhibitor) elicited the production of 3 different mycotoxins dendrodolides (González-Menéndez et al., 2019).

Similarly, the addition of biosynthetic precursors such as the use of amino acids has been used for the induction of cryptic biosynthetic pathways in fungi. The culture of the marine-derived fungus *Dichotomomyces cejpii* was supplemented with the amino acids L-tryptophan and L-phenylalanine allowing the production of 2 new polyketides, dichocetides B and C and 2 new alkaloids, dichotomocejs E and F and the induction of other known compounds (Wu et al., 2018).

Moreover, considering the natural conditions under which endophytic fungi are found, constant interactions with other microorganisms are occurring, situations that induce the production of different secondary metabolites useful for competition, communication or defense. For this reason, the co-culture of endophytic fungi with another bacterium or fungus might mimic microbial interactions, triggering different signaling pathways and responses. The co-culture of the endophytic fungus *Bionectria* sp. with *Bacillus subtilis* or *Streptomyces lividans* triggered the production of the new molecules, bionectriamines A and B and two other known compounds (Kamdem et al., 2018). To conclude, this review shows the great potential of fungal endophytes as renewable sources of antiparasitic and antibacterial compounds. With the advent of original cultures techniques, fungal endophytes are far from having revealed all their secrets.

ANNEXES

ID	Compound names	Chemical Formula	Endophytic fungal strain	Host plant	Botanical family	Activity	References
	Alkaloids						
1	(+)-flavipucine	$C_{12}H_{15}NO_4$	*Phoma* sp. 7204*	*Salsola oppositifolia* Desf.	Amaranthaceae	6, 17, and 11 mm zone inhibition against *B. subtilis, S. aureus* and *E. coli*	Loesgen et al., 2011
2	Brevianamide M	$C_{18}H_{15}N_3O_3$	*Aspergillus versicolor*	*Sargassum thunbergii* (Mertens ex Roth) Kuntze	Sargassaceae (Algae)	11-10 mm inhibition against *E. coli* and *S. aureus* at 30 µg/disk	Miao et al., 2012
3	Cochliodinol	$C_{32}H_{30}N_2O_4$	*Chaetomium globosum* SNB-GTC2114	*Paspalum virgatum* L.	Poaceae	4 µg/mL MIC against *S. aureus*	Casella et al., 2013
4	Fumigaclavine C	$C_{23}H_{30}N_2O_2$	*Aspergillus* sp. EJC08	*Bauhinia guianensis* Aubl.	Fabaceae	7.81 µg/mL MIC against *B. subtilis*	Pinheiro et al., 2012
5	Fusapyridon A	$C_{29}H_{43}NO_5$	*Fusarium* sp. YG-45	*Maackia chinensis* Takeda	Fabaceae	6.25 µg/mL MIC against *P. aeruginosa*	Tsuchinari et al., 2007
6	Neoaspergillic acid	$C_{12}H_{20}N_2O_2$	*Aspergillus* sp. FSY-01/*Aspergillus* sp. FSW-02 (co-culture)*	*Avicennia marina* (Forssk.) Vierh.	Acanthaceae	0.98-7.80 µg/mL MIC against *S. aureus, S. epidermis, B. subtilis, B. dysenteriae, B. proteus*	Zhu et al., 2011
7	Phomapyrrolidone B	$C_{34}H_{41}NO_4$	*Phoma* sp. NRRL 46751*	*Saurauia scaberrima* Lauterb.	Actinidiaceae	5.9 µM IC50 against *M. tuberculosis* H37Pv	Wijeratne et al., 2013
8	Phomapyrrolidone C	$C_{34}H_{41}NO_5$	*Phoma* sp. NRRL 46751*	*Saurauia scaberrima* Lauterb.	Actinidiaceae	5.2 µM IC50 against *M. tuberculosis* H37Pv	Wijeratne et al., 2013
9	Phomoenamide A	$C_{14}H_{24}N_2O_4$	*Phomopsis* PSU-D15*	*Garcinia dulcis* (Roxb.) Kurz	Clusiaceae	6.25 µg/ml MIC against *M. tuberculosis* H37Ra	Rukachaisirikul et al., 2008
10	Piperine	$C_{17}H_{19}NO_3$	*Periconia* sp	*Piper longum* L.	Piperaceae	2.62 and 1.74 MIC against *M. tuberculosis* and *M. smegmetis*	Verma et al., 2011
11	Pseurotin A	$C_{22}H_{25}NO_8$	*Aspergillus* sp. EJC08	*Bauhinia guianensis* Aubl.	Fabaceae	15.62 µg/mL MIC against *B. subtilis*	Pinheiro et al., 2012
12	Pyrrocidine A	$C_{31}H_{37}NO_4$	*Acremonium zeae* NRRL 13540	*Zea mays* L.	Poaceae	0.25-2 µg/mL MIC against *S. aureus, S. haemolyticus, E. faecalis, E. faecium*	Wicklow et al., 2008
13	Pyrrocidine B	$C_{31}H_{39}NO_4$	*Acremonium zeae* NRRL 13540	*Zea mays* L.	Poaceae	4 µg/mL MIC against *S. aureus, S. haemolyticus, E. faecalis, E. faecium*	Wicklow et al., 2008
14	Pyrrocidine C	$C_{34}H_{41}NO_4$	*Lewia infectoria* SNB-GTC2402*	*Besleria insolita* C.V. Morton	Gesneriaceae	2 µg/mL MIC against *S. aureus*	Casella et al., 2013
15	Semicochliodinol A	$C_{27}H_{22}N_2O_4$	*Chaetomium globosum* SNB-GTC2114	*Paspalum virgatum* L.	Poaceae	2 µg/mL MIC against *S. aureus*	Casella et al., 2013
	Fatty acids						
16	Cerebroside 1	$C_{41}H_{77}NO_9$	*Fusarium* sp. IFB-121*	*Quercus variabilis* Blume	Fagaceae	7.8-3.9 MIC against *B. subtilis, E. coli, P. fluorescens*	Shu et al., 2004
17	Cerebroside 2	$C_{41}H_{75}NO_9$	*Fusarium* sp. IFB-122	*Quercus variabilis* Blume	Fagaceae	1.9-3.9 MIC against *B. subtilis, E. coli, P. fluorescens*	Shu et al., 2004
	Polyketides						
18	(12S)-12-hydroxymonocerin	$C_{16}H_{22}O_7$	*Microdochium bolleyi**	*Fagonia cretica* L.	Zygophyllaceae	10 mm zone inhibition against *E. coli* at 50 µg/disk	Zhang et al., 2008
19	(3R)-5-methylmellein	$C_{11}H_{12}O_3$	*Cytospora* sp.	*Ilex canariensis* Poir.	Aquifoliaceae	20 mm zone inhibition against *B. megaterium* at 50 µg/disk	Lu et al., 2011
20	(4R,5R,6S)-6-acetoxy-4,5-dihydroxy-2-(hydroxymethyl)cyclohex-2-en-1-one	$C_9H_{12}O_6$	*Phoma* sp. 8889	*Salsola oppositifolia* Desf.	Amaranthaceae	10 mm zone inhibition 0.05 mg against *B. megaterium*	Qin et al., 2010
21	(R)-5-((S)-acetate(phenyl)-methyl)dihydrofuran-2(3H)-one	$C_{13}H_{14}O_4$	*Cytospora* sp.*	*Ilex canariensis* Poir.	Aquifoliaceae	20 mm zone inhibition against *B. megaterium* at 50 µg/disk	Lu et al., 2011

ANNEXES

22	(R)-5-((S)-hydroxy(phenyl)-methyl)dihydrofuran-2(3H)-one	$C_{11}H_{12}O_3$	*Cytospora* sp.*	*Ilex canariensis* Poir.	Aquifoliaceae	20 mm zone inhibition against *B. megaterium* at 50 µg/disk	Lu et al., 2011
23	(S)-5-((S)-hydroxy(phenyl)-methyl)dihydrofuran-2(3H)-one	$C_{11}H_{12}O_3$	*Cytospora* sp.	*Ilex canariensis* Poir.	Aquifoliaceae	18 mm zone inhibition against *B. megaterium* at 50 µg/disk	Lu et al., 2011
24	(S)-5-benzyl-dihydrofuran-2(3H)-one	$C_{11}H_{12}O_2$	*Cytospora* sp.*	*Ilex canariensis* Poir.	Aquifoliaceae	20 mm zone inhibition against *B. megaterium* at 50 µg/disk	Lu et al., 2011
25	(S)-5-hydroxy-4-oxo-1,2,3,4-tetrahydronaphthalen-1-yl acetate	$C_{12}H_{12}O_4$	*Cytospora* sp.*	*Ilex canariensis* Poir.	Aquifoliaceae	15 mm zone inhibition against *B. megaterium* at 50 µg/disk	Lu et al., 2011
26	2-hydroxy-3-(hydroxymethyl)anthraquinone	$C_{15}H_{10}O_4$	*Coniothyrium* sp. Zw86*	*Salsola oppositifolia* Desf.	Amaranthaceae	16 and 15 mm zone inhibition against *E. coli* and *B. megaterium* at 50 µg per disk	Sun et al., 2012
27	2,3-didehydro-19a-hydroxy-14-epicochlioquinone B	$C_{28}H_{38}O_7$	*Nigrospora* sp. MA75*	*Pongamia pinnata* (L.) Pierre	Fabaceae	8-0.5 µg/mL MIC against MRSA, *E. coli, P. aeruginosa, P. fluorescens*	Shang et al., 2012
28	3-(2,5-dihydro-4-hydroxy-5-oxo-3-phenyl-2-furyl)propionic acid	$C_{13}H_{12}O_5$	*Cytospora* sp.	*Ilex canariensis* Poir.	Aquifoliaceae	15 mm zone inhibition against *B. megaterium* at 50 µg/disk	Lu et al., 2011
29	3-O-methylalaternin	$C_{16}H_{12}O_6$	*Ampelomyces* sp. EU143250	*Urospermum picroides* (L.) Scop. Ex F.W. Schmidt	Asteraceae	12.5 µg/mL MIC *S. epidermis, E. faecalis, S. aureus*	Aly et al., 2008
30	4-deoxytetrahydrobostrycin	$C_{16}H_{20}O_7$	*Nigrospora* sp. MA75	*Pongamia pinnata* (L.) Pierre	Fabaceae	4 µg/mL MIC against *E. coli*	Shang et al., 2012
31	5-phenyl-4-oxopentanoic acid	$C_{11}H_{12}O_3$	*Cytospora* sp.*	*Ilex canariensis* Poir.	Aquifoliaceae	15 mm zone inhibition against *B. megaterium* at 50 µg/disk	Lu et al., 2011
32	6-hydroxy-2-methyl-4-chromanone	$C_{10}H_{10}O_3$	*Periconia siamensis* CMUGE015	*Thysanolaena latifolia* (Roxb. Ex Hornem.) Honda	Poaceae	12.5-6.25 µg/mL MIC against *B. subtilis, L. monocytogenes, P. aeruginosa*	Bhilabutra et al., 2007
33	6-hydroxyterrefuranone	$C_{14}H_{20}O_4$	*Microdiplodia* sp. KS 75-1*	*Pinus sp*	Pinaceae	16 mm zone inhibition against *S. aureus* at 40 µg/disk	Shiono et al., 2012
34	6(7)-dehydro-8-hydroxyterrefuranone	$C_{14}H_{18}O_3$	*Microdiplodia* sp. KS 75-1*	*Pinus sp*	Pinaceae	15 mm zone inhibition against *S. aureus* at 40 µg/disk	Shiono et al., 2012
35	7-amino-4-methylcoumarin	$C_{10}H_9NO_2$	*Xylaria* sp.YX-28*	*Ginkgo biloba* L.	Ginkgoaceae	20 - 4 µg/mL MIC against *S. aureus, E. coli, Salmonella typhia, Sa. Typhimurium, Sa. Enteritidis, A. hydrophyla, Shigella sp. V. parahaemolyticus*	Liu et al., 2008
36	7,8-dihydonivefuranone A	$C_{15}H_{20}O_4$	*Microdiplodia* sp. KS 75-1*	*Pinus sp*	Pinaceae	15 mm zone inhibition against *S. aureus* at 40 µg/disk	Shiono et al., 2012
37	Altechromone A	$C_{11}H_{10}O_3$	*Alternaria brassicicola* ML-P08	*Malus halliana* Koehne	Rosaceae	3.9, 3.9, 1.8, and 3.9 µg/ml MICs against *Bacillus subtilis, Escherichia coli, Pseudomonas fluorescens and Candida albicans*	Gy et al., 2009
38	Alterlactone	$C_{15}H_{12}O_6$	*Alternaria alternata* ZHJG5	*Cercis chinensis* Bunge	Fabaceae	16 µg/mL MIC value against *Xanthomonas oryzae pv. oryzae*	Zhao et al., 20et al., 20
39	Alternariol	$C_{14}H_{10}O_5$	*Alternaria alternata* ZHJG5	*Cercis chinensis* Bunge	Fabaceae	4 µg/mL MIC value against *Xanthomonas oryzae pv. oryzae*	Zhao et al., 20et al., 20
40	Altersolanol A	$C_{16}H_{16}O_8$	*Ampelomyces* sp. EU143251	*Urospermum picroides* (L.) Scop. Ex F.W. Schmidt	Asteraceae	12.5 µg/mL MIC *S. epidermis, E. faecalis*	Aly et al., 2008
41	Ambuic acid	$C_{19}H_{26}O_6$	4 strains of *Pestalotiopsis microspora, P. guepinii* MSU 214, *Monochaetia* sp. MSU-NC 202	*Taxus baccata* L. ,*Torreya taxifolia* Arn., *Taxodium distichum* (L.) Rich., *Dendrobium speciosum* Sm., *Wollemia nobilis* W.G. Jones, K.D.Hill & J.M. Allen, *Taxus wallichiana* Zucc.	Taxaceae, Taxaceae, Cupressaceae, Orchidaceae, Araucariaceae, Taxaceae	10 µM IC50 inhibited the production of gelatinase by *E. faecalis* OG1RF (anti-QS)	Nakayama et al., 2009, Li et al., 2001
42	Cercosporamide	$C_{16}H_{13}NO_7$	*Phoma* sp. NG-25	*Saurauia scaberrima* Lauterb.	Actinidiaceae	2.0 µg/ml MIC against *S. aureus*	Hoffman et al., 2008
43	Citreorosein	$C_{15}H_{10}O_6$	*Microsphaeropsis* sp. (strain 8875)	*Lycium intricatum* Boiss.	Solanaceae	9 mm zone inhibition against *E. coli*, 10 mm agaisnt *Bacillus megaterium* at 50 µg/disk	Krohn et al., 2009

ANNEXES

44	Cytosporone D	$C_{16}H_{22}O_5$	*Cytospora* sp. CR200 and *Diaporthe* sp. CR146*	*Conocarpus erectus* L. and *Forsteronia spicata* (Jacq.) G. Mey.	Combretaceae and Apocynaceae	8 µg/mL MIC against *S. aureus* and *E. faecalis*	Brady et al., 2000
45	Cytosporone E	$C_{15}H_{20}O_5$	*Cytospora* sp. CR200 and *Diaporthe* sp. CR146*	*Conocarpus erectus* L. and *Forsteronia spicata* (Jacq.) G. Mey.	Combretaceae and Apocynaceae	8 µg/mL MIC against *S. aureus* and *E. faecalis*	Brady et al., 2000
46	Dicerandrol A	$C_{34}H_{34}O_{14}$	*Phomopsis longicolla* MMW29*	*Dicerandra frutescens* Shinners	Lamiaceae	11-10 mm inhibition against *B. subtilis* and *S. aureus*	Wagenaar et al., 2001
47	Dicerandrol B	$C_{36}H_{36}O_{15}$	*Phomopsis longicolla* MMW29*	*Dicerandra frutescens* Shinners	Lamiaceae	9.5-8.5 mm inhibition against *B. subtilis* and *S. aureus*	Wagenaar et al., 2001
48	Dicerandrol C	$C_{38}H_{38}O_{16}$	*Phomopsis longicolla* MMW29*	*Dicerandra frutescens* Shinners	Lamiaceae	8-7 mm inhibition against *B. subtilis* and *S. aureus*	Wagenaar et al., 2001
49	Griseophenone C	$C_{16}H_{16}O_6$	*Nigrospora* sp. MA75	*Pongamia pinnata* (L.) Pierre	Fabaceae	2-0.5 µg/mL MIC against MRSA, *E. coli, P. aeruginosa, P. fluorescens, S. epidermis*	Shang et al., 2012
50	Guanacastepene A	$C_{22}H_{30}O_5$	strain CR115*	*Daphnopsis americana* (Mill.) J.R. Johnst.	Thymelaeaceae	6-8 mm inhibition zone at 6.25 µg per spot against *S. aereus, E. faecium* and *E. coli*	Singh et al., 2000
51	Integracins A	$C_{37}H_{56}O_8$	*Cytospora* sp.	*Ilex canariensis* Poir.	Aquifoliaceae	20 mm zone inhibition against *B. megaterium* at 50 µg/disk	Lu et al., 2011
52	Integracins B	$C_{35}H_{54}O_7$	*Cytospora* sp.	*Ilex canariensis* Poir.	Aquifoliaceae	20 mm zone inhibition against *B. megaterium* at 50 µg/disk	Lu et al., 2011
53	Isofusidienol A	$C_{16}H_{12}O_6$	*Chalara* sp. (strain 6661)*	*Artemisia vulgaris* L.	Asteraceae	23 mm zone inhibition 0.015 mg against *B. subtilis*	Lösgen et al., 2008
54	Isofusidienol B	$C_{16}H_{12}O_7$	*Chalara* sp. (strain 6661)*	*Artemisia vulgaris* L.	Asteraceae	22 mm zone inhibition 0.015 mg against *B. subtilis*	Lösgen et al., 2008
55	Isorhodoptilometrin	$C_{17}H_{14}O_6$	*Penicillium restrictum* G85ITS	*Silybum marianum* (L.) Gaertn.	Asteraceae	8.9 agr P3lux IC50 *S. aereus* MRSA (anti-QS)	Figueroa et al., 2014
56	Javanicin	$C_{15}H_{14}O_6$	*Chloridium* sp	*Azadirachta indica* A. Juss.	Meliaceae	10-2 µg/mL MIC against *Pseudomonas fluorescens, P. aeruginosa*	Kharwar et al., 2009
57	Lateropyrone	$C_{15}H_{10}O_8$	*Fusarium tricinctum*/*Bacillus subtilis* 168 trpC2 (co-culture)	*Aristolochia paucinervis* Pomel	Aristolochiaceae	8-2 µg/mL MIC against *B. subtilis, S. aureus, S. pneumoniae* and *E. faecalis*, MRSA	Ola et al., 2013
58	Modiolide A	$C_{10}H_{14}O_4$	*Periconia siamensis* CMUGE015	*Thysanolaena latifolia* (Roxb. Ex Hornem.) Honda	Poaceae	12.5-3.12 µg/mL MIC against *B. subtilis, L. monocytogenes, P. aeruginosa*	Bhilabutra et al., 2007
59	Monocerin	$C_{16}H_{20}O_6$	*Microdochium bolleyi*	*Fagonia cretica* L.	Zygophyllaceae	10 mm zone inhibition against *E. coli* at 50 µg/disk	Zhang et al., 2008
60	Monomethylsulochrin	$C_{18}H_{18}O_7$	*Rhizoctonia* sp. Cy064	*Cynodon dactylon* (L.) Pers.	Poaceae	10 µg/mL MIC against *H. pylori* ATCC 43504	Ma et al., 2004
61	Nivefuranone A	$C_{15}H_{18}O_4$	*Microdiplodia* sp. KS 75-1	*Pinus sp*	Pinaceae	15 mm zone inhibition against *S. aureus* at 40 µg/disk	Shiono et al., 2012
62	Norlichexanthone	$C_{14}H_{10}O_5$	*Nigrospora* sp. MA75	*Pongamia pinnata* (L.) Pierre	Fabaceae	0.5 µg/mL MIC against *S. epidermis*	Shang et al., 2012
63	Patulin	$C_7H_6O_4$	*Penicillium radicicola* (IBT 10696) and *Penicillium coprobium* (IBT 6895)	*Armoracia rusticana* P. Gaertn., B. Mey. & Scherb./ -	Brassicaceae / -	Abolish of QS-controlled lasB induction at 80 µM (anti-QS)	Rasmussen et al., 2005
64	Penicillic acid	$C_8H_{10}O_4$	*Penicillium radicicola* (IBT 10696) and *Penicillium coprobium* (IBT 6895)	*Armoracia rusticana* P. Gaertn., B. Mey. & Scherb./ -	Brassicaceae / -	Abolish of QS-controlled lasB induction at 40 µM (anti-QS)	Rasmussen et al., 2005
65	Phomodione	$C_{20}H_{22}O_8$	*Phoma* sp. NG-25*	*Saurauia scaberrima* Lauterb.	Actinidiaceae	MIC 1.6 µg/ml *S. aureus*	Hoffman et al., 2008
66	Phomol	$C_{22}H_{36}O_7$	*Phomopsis* sp. strain E02018 *	*Erythrina crista-galli* L.	Fabaceae	10 µg/mL MIC against *Corynebacterium insidiosum*	Weber et al., 2004

ANNEXES

67	Phomosine A	$C_{18}H_{18}O_7$	*Phomopsis* sp 5686	*Ligustrum vulgare* L.	Oleaceae	11 mm zone inhibition against *B. megaterium* at 50 µg/disk	Krhon et al., 2011
68	Phomosine B	$C_{19}H_{22}O_7$	*Phomopsis* sp 5686	*Ligustrum vulgare* L.	Oleaceae	11 mm zone inhibition against *B. megaterium* at 50 µg/disk	Krhon et al., 2011
69	Phomoxanthone A	$C_{38}H_{38}O_{16}$	*Phomopsis* sp. BCC 1323*	*Tectona grandis* L.f.	Lamiaceae	0.5 µg/mL against *M. tuberculosis* H37Ra	Isaka et al., 2001
70	Phomoxanthone B	$C_{38}H_{38}O_{16}$	*Phomopsis* sp. BCC 1323*	*Tectona grandis* L.f.	Lamiaceae	0.5 µg/mL against *M. tuberculosis* H37Ra	Isaka et al., 2001
71	Phyllostine	$C_7H_6O_4$	*Phomopsis* sp	*Notobasis syriaca* (L.) Cass.	Asteraceae	10 mm zone inhibition against *E. coli* at 50 µg/disk	Hussain et al., 2011
72	Primin	$C_{12}H_{16}O_3$	*Botryosphaeria mamane* PSU-M76	*Garcinia* x *mangostana* L.	Clusiaceae	8 µg/mL MIC against *S. aureus* and MRSA	Pongcharoen et al., 2007
73	Pyrenocine L	$C_{14}H_{20}O_6$	*Phomopsis* sp*	*Cistus salviifolius* L.	Cistaceae	10 mm zone inhibition against *E. coli* at 50 µg/disk	Hussain et al., 2012
74	Secalonic acid B	$C_{32}H_{30}O_{14}$	*Blennoria* sp. 7064	*Carpobrotus edulis* (L.) N.E.Br.	Aizoaceae	15 mm zone inhibition against *B. megaterium* at 50 µg/disk	Zhang et al., 2008
75	Spiropreussione A	$C_{19}H_{12}O_5$	*Preussia* sp. CGMCC 2022	*Aquilaria sinensis* (Lour.) Spreng.	Thymelaeaceae	16.4 mm wone inhibition against *S. aureus* at 5 µg/disk	Chen et al., 2009
76	Tetrahydrobostrycin	$C_{16}H_{20}O_8$	*Nigrospora* sp. MA75	*Pongamia pinnata* (L.) Pierre	Fabaceae	2-0.5 µg/mL MIC against MRSA, *E. coli*	Shang et al., 2012
77	Trypethelone	$C_{16}H_{16}O_4$	*Coniothyrium cereale*	*Enteromorpha sp*	Ulvaceae (green Algae)	18, 14, and 12 mm, against *Mycobacterium phlei, S. aureus* and *E.coli* at 20 µg/disk	Elsebai et al., 2011
78	Usnic acid	$C_{18}H_{16}O_7$	*Phoma* sp. NG-25	*Saurauia scaberrima* Lauterb.	Actinidiaceae	MIC 2.0 µg/ml against *S. aureus*	Hoffman et al., 2008
79	xanthone 8-hydroxy-6-methyl-9-oxo-9H-xanthene-1-carboxylic acid methyl ester	$C_{16}H_{12}O_5$	*Microsphaeropsis* sp. (7177)	*Zygophyllum fontanesii* Webb & Berthel.	Zygophyllaceae	13 mm zone inhibition against *B. megaterium* at 50 µg/disk	Krhon et al., 2009
80	Yicathin C	$C_{16}H_{12}O_6$	*Aspergillus wentii* pt-1*	*Gymnogongrus flabelliformis* Harvey	Phyllophoraceae (Algae)	12 mm inhibition against *E. coli* at 10 µg/disk	Sun et al., 2012
81	γ-oxo-benzenepentanoic acid methyl ester	$C_{12}H_{14}O_3$	*Cytospora* sp.*	*Ilex canariensis* Poir.	Aquifoliaceae	25 mm zone inhibition against *B. megaterium* at 50 µg/disk	Lu et al., 2011
82	ω-hydroxyemodin	$C_{15}H_{10}O_6$	*Penicillium restrictum* G85ITS	*Silybum marianum* (L.) Gaertn.	Asteraceae	8.1 agr P3lux IC50 *S. aereus* MRSA (anti-QS)	Figueroa et al., 2014
	Polyketides-Fatty acids						
83	Biscogniazaphilone A	$C_{24}H_{34}O_4$	*Biscogniauxia formosana* BCRC 33718*	*Cinnamomum* sp.	Lauraceae	< 5.12 µg/mL against *M. tuberculosis* H37RV	Cheng et al., 2012
84	Biscogniazaphilone B	$C_{25}H_{32}O_5$	*Biscogniauxia formosana* BCRC 33718*	*Cinnamomum* sp.	Lauraceae	< 2.52 µg/mL against *M. tuberculosis* H37RV	Cheng et al., 2012
	Polypeptides						
85	3,1′-didehydro-3[2″(3‴,3‴-dimethyl-prop-2-enyl)-3″-indolylmethylene]-6-methyl pipera-zine-2,5-dione	$C_{14}H_{13}N_3O_2$	*Penicillium chrysogenum* MTCC 5108*	*Porteresia coarctata* (Roxb.) Tateoka	Poaceae	14-16 mm zone inhibition against *Vibrio cholerae* at 10 µg/disk	Devi et al., 2012
86	Beauvericin	$C_{45}H_{57}N_3O_9$	*Fusarium redolens* Dzf2	*Dioscorea zingiberensis* C.H. Wright	Dioscoreaceae	26.6-18.4 µg/mL MIC against *A. tumefaciens, X. vesicatoria, B. subtilis, S. haemolyticus*	Xu et al., 2010
87	Enniatin A1	$C_{35}H_{61}N_3O_9$	*Fusarium tricinctum/Bacillus subtilis* 168 trpC2 (co-culture)	*Aristolochia paucinervis* Pomel	Aristolochiaceae	8-2 µg/mL MIC against *B. subtilis, S. aureus, S. pneumoniae* and *E. faecalis*, MRSA	Ola et al., 2013
88	Enniatin B	$C_{33}H_{57}N_3O_9$	*Fusarium tricinctum* Salicorn 19	*Salicornia bigelovii* Torr.	Amaranthaceae	13-6 µM MIC against *B. subtilis, E. aerogenes, M. tetragenus*	Zhang et al., 2014

ANNEXES

89	Enniatin B1	$C_{34}H_{59}N_3O_9$	*Fusarium tricinctum/Bacillus subtilis* 168 trpC2 (co-culture)	*Aristolochia paucinervis* Pomel	Aristolochiaceae	16-4 µg/mL MIC against *B. subtilis, S. aureus, S. pneumoniae* and *E. faecalis*, MRSA	Ola et al., 2013
90	Halobacillin	$C_{53}H_{94}N_8O_{12}$	*Trichoderma asperellum*	*Panax notoginseng* (Burkill) F.H. Chen	Araliaceae	5.4 and 14.00 µg/mL IC50 against *E. faecium* and *S. aureus*	Ding et al., 2012
91	PF1022F	$C_{40}H_{68}N_4O_{12}$	*Trichoderma asperellum*	*Panax notoginseng* (Burkill) F.H. Chen	Araliaceae	7.30 and 19.02 µg/mL IC50 against *E. faecium* and *S. aureus*	Ding et al., 2012
92	Tardioxopiperazine A	$C_{24}H_{31}N_3O_2$	*Eurotium cristatum* EN-220	*Sargassum thunbergii* (Mertens ex Roth) Kuntze	Sargassaceae (Algae)	8 µg/mL MIC against *S. aureus* and *E. coli*	Du et al., 2012
	Steroids						
93	Helvolic acid	$C_{33}H_{44}O_8$	Aspergillus sp. CY725	*Cynodon dactylon* (L.) Pers.	Poaceae	5.0 µg/mL MIC against *H. pylori* ATCC 43504	Song et al., 2005
	Terpenoids						
94	1β-Hydroxy-α-cyperone	$C_{15}H_{22}O_2$	*Microsphaeropsis arundinis*	*Ulmus macrocarpa* Hance	Ulmaceae	11.4 µg/mL MIC against *S. aureus*	Luo et al., 2013
95	Conidiogenol	$C_{20}H_{34}O_2$	*Penicillium chrysogenum* QEN-24S	*Laurencia* sp.	Rhodomelaceae (Algae)	16 µg/mL MIC against *P. fluorescens, S. epidermis*	Gao et al., 2011
96	Conidiogenone B	$C_{20}H_{30}O$	*Penicillium chrysogenum* QEN-24S	*Laurencia* sp.	Rhodomelaceae (Algae)	8 µg/mL MIC against MRSA, *P. aeruginosa, P. fluorescens, S. epidermis*	Gao et al., 2011
97	Fusarielin B	$C_{25}H_{40}O_5$	*Fusarium tricinctum* Salicorn 19	*Salicornia bigelovii* Torr.	Amaranthaceae	19-10 µM MIC against *M. smegmatis, B. subtilis, M. phlei, E. coli*	Zhang et al., 2014
98	Fusariumin C	$C_{21}H_{32}O_3$	*Fusarium oxysporum* ZZP-R1*	*Rumex madaio* Makino	Polygonaceae	6.25 µg/mL MIC value against *S. aureus* ATCC 25923	Chen et al., 2019
99	Fusartricin	$C_{21}H_{40}O_8$	*Fusarium tricinctum* Salicorn 19*	*Salicornia bigelovii* Torr.	Amaranthaceae	19 µM MIC against *E. aerogenes, M. tetragenus*	Zhang et al., 2014
100	Periconicin A	$C_{20}H_{28}O_3$	*Periconia* sp OBW-15*	*Taxus cuspidata* Siebold & Zucc.	Taxaceae	12.5-3.12 µg/mL MIC against *S. aureus, S. epidermis, B. subtilis, K. pneumoniae, S. typhimurium*	Kim et al., 2004
	Other						
101	3-nitropropionic acid	$C_3H_5NO_4$	*Phomopsis longicolla*	*Trichilia elegans* A. Juss.	Meliaceae	2.3-1.1 mm zone inhibition against *Xanthomonas axonopodis, Micrococcus luteus, Salmonella typhi*	Flores et al., 2013

ANNEXES

ID	Compound names	Chemical Formula	Endophytic fungal strain	Host plant	Botanical family	Parasite strain	Activity	References
	Alkaloids							
102	18-Deoxy-19,20-epoxycytochalasin C	$C_{30}H_{37}NO_6$	*Nemania* sp. UM10M	*Torreya taxifolia* Arn.	Taxaceae	*P. falciparum* (D6 and W2)	IC50 0.56 µM (280 ng/mL) in D6; 0.19 µM (100 ng/mL) in W2	Kumarihamy et al., 2019
103	19,20-Epoxycytochalasin C	$C_{30}H_{37}NO_7$	*Nemania* sp. UM10M	*Torreya taxifolia* Arn.	Taxaceae	*P. falciparum* (D6 and W2)	IC50 0.07 µM (37 ng/mL) in D6; 0.05 µM (28 ng/mL) in W2	Kumarihamy et al., 2019
104	19,20-Epoxycytochalasin D	$C_{30}H_{37}NO_7$	*Nemania* sp. UM10M	*Torreya taxifolia* Arn.	Taxaceae	*P. falciparum* (D6 and W2)	IC50 0.04 µM (22 ng/mL) in D6; 0.04 µM (20 ng/mL) in W2	Kumarihamy et al., 2019
			Diaporthe sp.	*Guapira standleyana* Woodson	Nyctaginaceae	*P. falciparum* 3D7	IC50 136 nM (0.136 µM)	Calcul et al, 2013
105	2,5-Dihydroxy-1-(hydroxymethyl)pyridin-4-one		Strain BB4*	*Tinospora crispa* (L.) Hook. f. & Thomson	Menispermaceae	*P. falciparum* 3D7	IC50 0.02 µg/mL (0.127 µM)	Elfita et al., 2011
106	7-Hydroxy-3,4,5-trimethyl-6-on 2,3,4,6-tetrahydroisoquinoline-8-carboxylic acid	$C_{13}H_{15}O_3N$	Strain BB4*	*Tinospora crispa* (L.) Hook. f. & Thomson	Menispermaceae	*P. falciparum* 3D7	IC50 0.03 µg/mL (0.129 µM)	Elfita et al., 2011
107	Cissetin	$C_{22}H_{31}NO_5$	*Preussia* sp.	*Enantia chlorantha* Oliv.	Annonaceae	P. falciparum NF54	IC50 10.3 µM	Talontsi et al., 2014
108	Cytochalasin D	$C_{30}H_{37}NO_6$	*Diaporthe* sp., *Xylaria* sp.	*Kandelia obovata* Sheue, H.Y. Liu & J. Yong, *Avicennia marina* (Forssk.) Vierh., *Lumnitzera racemosa* Willd.	Rhizophoraceae, Acanthaceae, Combretaceae	*P. falciparum* 3D7	IC50 25.8 nM (0.0258 µM)	Calcul et al, 2013
109	Cytochalasin H	$C_{30}H_{39}NO_5$	*Diaporthe* sp.	*Kandelia obovata* Sheue, H.Y. Liu & J. Yong, *Avicennia marina* (Forssk.) Vierh., *Lumnitzera racemosa* Willd.	Rhizophoraceae, Acanthaceae, Combretaceae	*P. falciparum* 3D7	IC50<20 nM (<0.02 µM)	Calcul et al, 2013
110	Cytochalasin J	$C_{28}H_{37}NO_4$	*Diaporthe* sp.	*Kandelia obovata* Sheue, H.Y. Liu & J. Yong, *Avicennia marina* (Forssk.) Vierh., *Lumnitzera racemosa* Willd.	Rhizophoraceae, Acanthaceae, Combretaceae	*P. falciparum* 3D7	IC50 <20 nM (<0.02 µM)	Calcul et al, 2013
111	Cytochalasin O	$C_{28}H_{37}NO_4$	*Verticillium* sp.	*Kandelia obovata* Sheue, H.Y. Liu & J. Yong, *Avicennia marina* (Forssk.) Vierh., *Lumnitzera racemosa* Willd.	Rhizophoraceae, Acanthaceae, Combretaceae	*P. falciparum* 3D7	IC50 <20 nM (<0.02 µM)	Calcul et al, 2013
112	Epoxycytochalasin H	$C_{30}H_{39}NO_5$	*Diaporthe miriciae* UFMGCB 9720	*Vellozia gigantea* N. L. Menezes & Mello-Silva	Velloziaceae	*P. falciparum* (D6 and W2)	IC50 51.70 ng/mL in D6 (0.1 µM) and 39.40 ng/mL in W2 (0.07µM)	Ferreira et al., 2017
	Polyketides							
113	11-hydroxymonocerin	$C_{16}H_{20}O_7$	*Exserohilum rostratum**	*Stemona sp*	Stemonaceae	*P. falciparum* K1	IC50 7.70 µM	Sappapan et al., 2008
114	2-chloro-5-methoxy-3-methylcyclohexa-2,5-diene-1,4-dione	$C_8H_7ClO_3$	*Xylaria* sp. PB-30*	*Sandoricum koetjape* (Burm.f.) Merr.	Meliaceae	*P. falciparum* K1	IC50 1.84 µM	Tansuwan et al., 2007
115	7-butyl-6,8-dihydroxy-3(R)-pentylisochroman-1-one	$C_{18}H_{26}O_4$	*Geotrichum* sp.*	*Crassocephalum crepidioides* (Benth.) S. Moore	Asteraceae	*P. falciparum* K1	IC50 2.6 µg/mL (8.48µM)	Kongsaeree et al., 2003
116	Altenusin	$C_{15}H_{14}O_6$	*Alternaria* sp. UFMGCB55	*Trixis vauthieri* DC.	Asteraceae	Inhibits trypanothione reductase	IC50 4.3 - 0.3 µM	Cota et al., 2008
117	Asterric acid	$C_{17}H_{16}O_8$	*Preussia* sp.	*Enantia chlorantha* Oliv.	Annonaceae	*P. falciparum* NF54	IC50 8.67 µM	Talontsi et al., 2014
118	Cercosporin	$C_{29}H_{26}O_{10}$	*Mycosphaerella* sp. nov. strain F2140	*Psychotria horizontalis* Spreng. ex DC.	Rubiaceae	*L. donovani, P. falciparum, T. cruzi*	IC50 0.46 µM, 1.03µM, 1.08 µM	Moreno et al., 2011
119	Cercosporin derivative tetraacetylated *	$C_{37}H_{34}O_{14}$	*Mycosphaerella* sp. nov. strain F2140*	*Psychotria horizontalis* Spreng. ex DC.	Rubiaceae	*L. donovani, P. falciparum, T. cruzi*	IC50 0.64 µM, 2.99 µM, 0.78 µM	Moreno et al., 2011

ANNEXES

120	Chaetoxanthone B	$C_{20}H_{18}O_6$	*Chaetonium* sp*	*Algal species*	-	*P. falciparum* K1	IC50 0.5 µg/mL (1.41 µM)	Pontius et al., 2008
121	Chaetoxanthone C	$C_{20}H_{19}ClO_6$	*Chaetonium* sp*	*Algal species*	-	*T. cruzi* C4	IC50 1.5 µg/mL (3.83 µM)	Pontius et al., 2008
122	CJ-12,371	$C_{20}H_{16}O_4$	*Edenia* sp	*Petrea volubilis* L.	Verbenaceae	*L. donovani* amastigotes	IC50 8.40 µM	Martinez-Luis et al., 2008
123	Cochlioquinone A	$C_{30}H_{44}O_8$	*Cochliobolus* sp	*Piptadenia adiantoides* (Spreng.) J.F. Macbr.	Fabaceae	*L. amazonensis* promastigotes	EC50 1.7 µM	Campos et al., 2008
124	Dicerandrol D	$C_{36}H_{37}O_{15}$	*Diaporthe* sp.*	*Kandelia obovata* Sheue, H.Y. Liu & J. Yong, *Avicennia marina* (Forssk.) Vierh., *Lumnitzera racemosa* Willd.	Rhizophoraceae, Acanthaceae, Combretaceae	*P. falciparum* 3D7	IC50 600 nM (0.6 µM)	Calcul et al, 2013
125	Fumiquinone B	$C_8H_8O_5$	*Aspergillus* sp. F1544	*Guapira standleyana* Woodson	Nyctaginaceae	*L. donovani; P. falciparum*	IC50 0.5 µM, 5.4 µM	Martinez-Luis et al., 2012
126	Isocochlioquinone A	$C_{30}H_{44}O_8$	*Cochliobolus* sp	*Piptadenia adiantoides* (Spreng.) J.F. Macbr.	Fabaceae	*L. amazonensis* promastigotes	EC50 4.1 µM	Campos et al., 2008
127	KS-501a	$C_{33}H_{48}O_{10}$	*Acremonium* sp. BCC 14080	Palm tree	Arecaceae	*P. falciparum* K1	IC50 9.9 µM	Bunyapaiboonsri et al., 2008
128	Mollicellin E	$C_{22}H_{19}ClO_8$	*Chaetonium brasiliense*	Hala-Bala evergreen forest	-	*P. falciparum* K1	IC50 3.2 µg/mL (7.16 µM)	Khumkomkhet et al., 2009
129	Mollicellin K	$C_{21}H_{18}O_7$	*Chaetonium brasiliense**	Hala-Bala evergreen forest	-	*P. falciparum* K1	IC50 1.2 µg/mL (3.13 µM)	Khumkomkhet et al., 2009
130	Mollicellin L	$C_{22}H_{20}O_7$	*Chaetonium brasiliense**	Hala-Bala evergreen forest	-	*P. falciparum* K1	IC50 3.4 µg/mL (8.6 µM)	Khumkomkhet et al., 2009
131	Mollicellin M	$C_{21}H_{17}ClO_7$	*Chaetonium brasiliense**	Hala-Bala evergreen forest	-	*P. falciparum* K1	IC50 2.9 µg/mL (6.95 µM)	Khumkomkhet et al., 2009
132	Monocerin	$C_{16}H_{20}O_6$	*Exserohilum rostratum*	*Stemona* sp	Stemonaceae	*P. falciparum* K1	IC50 0.68 µM	Sappapan et al., 2008
133	Palmarumycin CP17	$C_{20}H_{14}O_5$	*Edenia* sp*	*Petrea volubilis* L.	Verbenaceae	*L. donovani* amastigotes	IC50 1.34 µM	Martinez-Luis et al., 2008
134	Palmarumycin CP18	$C_{20}H_{14}O_5$	*Edenia* sp*	*Petrea volubilis* L.	Verbenaceae	*L. donovani* amastigotes	IC50 0.62 µM	Martinez-Luis et al., 2008
135	Palmarumycin CP2	$C_{20}H_{14}O_4$	*Edenia* sp	*Petrea volubilis* L.	Verbenaceae	*L. donovani* amastigotes	IC50 3.93 µM	Martinez-Luis et al., 2008
136	Phomoxanthone A	$C_{38}H_{38}O_{16}$	*Phomopsis* sp. BCC 1323 *	*Tectona grandis* L.f.	Lamiaceae	*P. falciparum* K1	IC50 0.11 µg/mL (0.15 µM)	Isaka et al., 2001
137	Phomoxanthone B	$C_{38}H_{38}O_{16}$	*Phomopsis* sp. BCC 1323 *	*Tectona grandis* L.f.	Lamiaceae	*P. falciparum* K1	IC50 0.33 µg/mL (0.44 µM)	Isaka et al., 2001
138	Preussiafuran A	$C_{18}H_{16}O_7$	*Preussia* sp.*	*Enantia chlorantha* Oliv.	Annonaceae	P. falciparum NF54	IC50 8.76 µM	Talontsi et al., 2014
139	Preussomerin EG1	$C_{20}H_{12}O_6$	*Edenia* sp	*Petrea volubilis* L.	Verbenaceae	*L. donovani* amastigotes	IC50 0.12 µM	Martinez-Luis et al., 2008
140	Purpureone	$C_{32}H_{30}O_{14}$	*Purpureocillium lilacinum**	*Rauvolfia macrophylla* Ruiz & Pav.	Apocynaceae	*L. donovani* amastigotes	MIC 0.63 µg/mL (0.87 µM)	Lenta et al., 2016
141	Xylariaquinone A	$C_{15}H_{12}O_5$	*Xylaria* sp. PB-30*	*Sandoricum koetjape* (Burm.f.) Merr.	Meliaceae	*P. falciparum* K1	IC50 6.68 µM	Tansuwan et al., 2007
	Polyketides-alkaloids							
142	14-Norpseurotin A	$C_{21}H_{23}NO_8$	*Aspergillus* sp. F1544	*Guapira standleyana* Woodson	Nyctaginaceae	*L. donovani*	IC50 4.4 µM	Martinez-Luis et al., 2012
143	Codinaeopsin	$C_{32}H_{40}N_2O_3$	*Codinaeopsis gonytrichoides* CR127A*	*Vochysia guatemalensis* Donn. Sm.	Vochysiaceae	*P. falciparum* 3D7	IC50 2.3 µg/mL (4.7 µM)	Kontnik et al., 2008
144	FD-838	$C_{22}H_{21}NO_7$	*Aspergillus* sp. F1544	*Guapira standleyana* Woodson	Nyctaginaceae	*L. donovani*	IC50 0.2 µM	Martinez-Luis et al., 2012

145	Pseurotin A	$C_{22}H_{25}NO_8$	*Aspergillus* sp. F1544	*Guapira standleyana* Woodson	Nyctaginaceae	*L. donovani*	IC50 5.8 µM	Martinez-Luis et al., 2012
146	Pseurotin D	$C_{22}H_{25}NO_8$	*Aspergillus* sp. F1544	*Guapira standleyana* Woodson	Nyctaginaceae	*L. donovani*	IC50 0.5 µM	Martinez-Luis et al., 2012
	Polypeptides							
147	12,12a-dihydroantibiotic PI 016	$C_{31}H_{36}N_2O_9S_2$	*Menisporopsis theobromae* BCC 3975*	Seed plant	-	*P. falciparum* K1	IC50 2.95 µM	Chinworrungsee et al. 2006
148	Apicidin B	$C_{33}H_{47}N_5O_6$	*Fusarium pallidoroseum**	*Acacia* sp.	Fabaceae	*P. falciparum*	MIC 189 nM (0.189 µM)	Singh et al., 2001
149	Apicidin C	$C_{33}H_{47}N_5O_6$	*Fusarium pallidoroseum**	*Acacia* sp.	Fabaceae	*P. falciparum*	MIC 69 nM (0.069 µM)	Singh et al., 2001
150	Beauvericin	$C_{45}H_{57}N_3O_9$	*Fusarium* sp. [KF611679]	*Caesalpinia echinata* Lam.	Fabaceae	*T. cruzi*	IC50 2.43 µM	Campos et al., 2015
151	Fusaripeptide A	$C_{46}H_{75}N_7O_{11}$	*Fusarium* sp.*	*Mentha longifolia* (L.) L.	Lamiaceae	*P. falciparum* (DC6)	IC50 0.34 µM	Ibrahim et al., 2017
152	Pullularin A	$C_{42}H_{57}N_5O_9$	*Pullularia* sp. BCC 8613*	*Calophyllum* sp.	Clusiaceae	*P. falciparum* K1	IC50 3.6 µg/mL (4.64 µM)	Isaka et al., 2007
153	Pullularin B	$C_{43}H_{59}N_5O_9$	*Pullularia* sp. BCC 8613*	*Calophyllum* sp.	Clusiaceae	*P. falciparum* K1	IC50 3.3 µg/mL (4.18µM)	Isaka et al., 2007
	Terpenoids							
154	12,13-Deoxyroridin E	$C_{29}H_{38}O_7$	CY-3923 (not identified)	*Kandelia obovata* Sheue, H.Y. Liu & J. Yong, *Avicennia marina* (Forssk.) Vierh., *Lumnitzera racemosa* Willd.	Rhizophoraceae, Acanthaceae, Combretaceae	*P. falciparum* 3D7	IC50 <20 nM (<0.02 µM)	Calcul et al, 2013
155	7α,10α-Dihydroxy-1βmethoxyeremophil-11(13)-en-12,8β olide	$C_{16}H_{24}O_5$	*Xylaria* sp. BCC 21097*	*Licuala spinosa* Wurmb	Arecaceae	*P. falciparum* K1	IC50 8.1 µM	Isaka et al., 2010
156	Integracide H	$C_{36}H_{54}O_7$	*Fusarium* sp*	*Mentha longifolia* (L.) L.	Lamiaceae	*L. donovani* amastigotes	IC50 4.75 µM	Ibrahim et al., 2016
157	Integracide J	$C_{39}H_{54}O_7$	*Fusarium* sp*	*Mentha longifolia* (L.) L.	Lamiaceae	*L. donovani* amastigotes	IC50 3.29 µM	Ibrahim et al., 2016
158	Phomoarcherin B	$C_{23}H_{28}O_5$	*Phomopsis archeri*	*Vanilla albidia* Blume	Ochidaceae	*P. falciparum* K1	IC50 0.79 µg/mL (2.05 µM)	Hemastin et al., 2011
159	Roridin E	$C_{29}H_{38}O_8$	CY-3923 (not identified)	*Kandelia obovata* Sheue, H.Y. Liu & J. Yong, *Avicennia marina* (Forssk.) Vierh., *Lumnitzera racemosa* Willd.	Rhizophoraceae, Acanthaceae, Combretaceae	*P. falciparum* 3D7	IC50 <20 nM (<0.02 µM)	Calcul et al, 2013

* First time isolation of the compound from the fungal strain

ANNEXES

References

Adeleke, B., & Babalola, O. (2021). Pharmacological Potential of Fungal Endophytes Associated with Medicinal Plants: A Review. *Journal of Fungi*, *7*(2), 147. https://doi.org/10.3390/jof7020147

Aldridge, D. C., & Turner, W. B. (1970). Metabolites of Helminthosporium monoceras: structures of monocerin and related benzopyrans. *Journal of the Chemical Society C: Organic*, (18), 2598. https://doi.org/10.1039/j39700002598

Aly, A. H., Debbab, A., & Proksch, P. (2011). Fungal endophytes: unique plant inhabitants with great promises. *Applied Microbiology and Biotechnology*, *90*(6), 1829–1845. https://doi.org/10.1007/s00253-011-3270-y

Aly, A. H., Edrada-Ebel, R. A., Wray, V., Müller, W. E. G., Kozytska, S., Hentschel, U., Proksch, P., & Ebel, R. (2008). Bioactive metabolites from the endophytic fungus Ampelomyces sp. isolated from the medicinal plant Urospermum picroides. *Phytochemistry*, 69(8), 1716–1725. doi: 10.1016/j.phytochem.2008.02.013

Aminov, R. I. (2010). A brief history of the antibiotic era: Lessons learned and challenges for the future. *Frontiers in Microbiology*, *1*(DEC), 1–7. https://doi.org/10.3389/fmicb.2010.00134

Andrioli, W. J., Conti, R., Araújo, M. J., Zanasi, R., Cavalcanti, B. C., Manfrim, V., … Bastos, J. K. (2014). Mycoleptones A-C and polyketides from the endophyte *Mycoleptodiscus indicus*. *Journal of Natural Products*, *77*(1), 70–78. https://doi.org/10.1021/np4006822

Andrzej, C. 2002. Coexistence and coevolution: various levels of interactions I. Internal fungi (endophytes) and their biological significance in coevolution. Wiad. Bot. 46: 35–44.

Arnold, A. E. (2007). Understanding the diversity of foliar endophytic fungi: progress, challenges, and frontiers. *Fungal Biology Reviews*, *21*(2–3), 51–66. https://doi.org/10.1016/j.fbr.2007.05.003

Arnold, A.E. and Lutzoni, F. (2007). Diversity and host range of foliar fungal endophytes: are the tropical leaves biodiversity hotspots? *Ecology*, 88(3), 541-549.

Bérdy, J. (2012). Thoughts and facts about antibiotics: Where we are now and where we are heading. *Journal of Antibiotics*, *65*(8), 385–395. https://doi.org/10.1038/ja.2012.27

Bessada, S.M.F., Barreira, J.C.M. & Oliveira M.B.P.P (2015). Asteraceae species with most prominent bioactivity and their potential applications: a review. *Industrial Crops and Products*, 76, 604-615.

Bhilabutra, W., Techowisan, T., Peberdy, J. F., & Lumyong, S. (2007). Antimicrobial activity of bioactive compounds from *Periconia siamensis* CMUGE015. *Research Journal of Microbiology*, 2(10), 749–755. doi: 10.3923/jm.2007.749.755

Bloch, P., Tamm, C., Bollinger, P., Petcher, T. J., & Weber, H. P. (1976). Pseurotin, a new Metabolite of *Pseudeurotium ovalis* STOLK having an unusual hetero-spirocyclic System. (Preliminary Communication). *Helvetica Chimica Acta*, *59*(1), 133–137. https://doi.org/10.1002/hlca.19760590114

Bode, H. B., Bethe, B., Höfs, R., & Zeeck, A. (2002). Big effects from small changes: possible ways to explore nature's Chemical Diversity. *ChemBioChem*, *3*(7), 619. https://doi.org/10.1002/1439-7633(20020703)3:7<619::AID-CBIC619>3.0.CO;2-9

Boros, C., Dix, A., Katz, B., Vasina, Y., & Pearce, C. (2003). Isolation and identification of cissetin-A setin-like antibiotic with a novel cis-octalin ring fusion. *The Journal of Antibiotics*, *56*(10), 862–865. https://doi.org/10.7164/antibiotics.56.862

Brady, S. F., Wagenaar, M. M., Singh, M. P., Janso, J. E., & Clardy, J. (2000). The cytosporones, new octaketide antibiotics isolated from an endophytic fungus. *Organic Letters*, 2(25), 4043–4046. doi: 10.1021/ol006680s

Brakhage, A. A. (2013). Regulation of fungal secondary metabolism. *Nature Reviews Microbiology*, *11*(1), 21–32. https://doi.org/10.1038/nrmicro2916

Brakhage, A. A., & Schroeckh, V. (2011). Fungal secondary metabolites – Strategies to activate silent gene clusters. *Fungal Genetics and Biology*, *48*(1), 15–22. https://doi.org/10.1016/j.fgb.2010.04.004

ANNEXES

Breitenstein, W., Chexal, K. K., Mohr, P., & Tamm, C. (1981). Pseurotin B, C, D, and E. further new metabolites of *Pseudeurotium ovalis* STOLK. *Helvetica Chimica Acta*, *64*(2), 379–388. https://doi.org/10.1002/hlca.19810640203

Bunyapaiboonsri, T., Yoiprommarat, S., Khonsanit, A., & Komwijit, S. (2008). Phenolic glycosides from the filamentous fungus *Acremonium* sp. BCC 14080. *Journal of Natural Products*, *71*(5), 891–894. https://doi.org/10.1021/np070689m

Cafêu, M. C., Silva, G. H., Teles, H. L., Bolzani, V. da S., Araújo, Â. R., Young, M. C. M., & Pfenning, L. H. (2005). Substâncias antifúngicas de *Xylaria* sp., um fungo endofítico isolado de Palicourea marcgravii (Rubiaceae). *Química Nova*, *28*(6), 991–995. https://doi.org/10.1590/S0100-40422005000600011

Calcul, L., Waterman, C., Ma, W., Lebar, M., Harter, C., Mutka, T., Baker, B. (2013). Screening mangrove endophytic fungi for antimalarial natural products. *Marine Drugs*, *11*(12), 5036–5050. https://doi.org/10.3390/md11125036

Campos, F. F., Rosa, L. H., Cota, B. B., Caligiorne, R. B., Teles Rabello, A. L., Alves, T. M. A., Zani, C. L. (2008). Leishmanicidal metabolites from *Cochliobolus* sp., an endophytic fungus isolated from *Piptadenia adiantoides* (Fabaceae). *PLoS Neglected Tropical Diseases*, *2*(12), 1–11. https://doi.org/10.1371/journal.pntd.0000348

Campos, F. F., Sales Junior, P. A., Romanha, A. J., Araújo, M. S. S., Siqueira, E. P., Resende, J. M., … Cota, B. B. (2015). Bioactive endophytic fungi isolated from *Caesalpinia echinata* Lam. (Brazilwood) and identification of beauvericin as a trypanocidal metabolite from *Fusarium* sp. *Memorias Do Instituto Oswaldo Cruz*, *110*(1), 1–10. https://doi.org/10.1590/0074-02760140243

Casella, T. M., Eparvier, V., Mandavid, H., Bendelac, A., Odonne, G., Dayan, L., Duplais, C., Espindola, L. S., & Stien, D. (2013). Antimicrobial and cytotoxic secondary metabolites from tropical leaf endophytes: Isolation of antibacterial agent pyrrocidine C from *Lewia infectoria* SNB-GTC2402. *Phytochemistry*, 96, 370–377. doi: 10.1016/j.phytochem.2013.10.004

Challinor, V. L., & Bode, H. B. (2015). Bioactive natural products from novel microbial sources. *Annals of the New York Academy of Sciences*, *1354*(1), 82–97. https://doi.org/10.1111/nyas.12954

Chen, J., Bai, X., Hua, Y., Zhang, H., & Wang, H. (2019). Fusariumins C and D, two novel antimicrobial agents from *Fusarium oxysporum* ZZP-R1 symbiotic on Rumex madaio Makino. Fitoterapia, 134, 1–4. doi: 10.1016/j.fitote.2019.01.016

Chen, X., Shi, Q., Lin, G., Guo, S., & Yang, J. (2009). Spirobisnaphthalene analogues from the endophytic fungus *Preussia* sp. *Journal of Natural Products*, 72(9), 1712–1715. doi: 10.1021/np900302w

Cheng, M. J., Wu, M. Der, Yanai, H., Su, Y. S., Chen, I. S., Yuan, G. F., Hsieh, S. Y., & Chen, J. J. (2012). Secondary metabolites from the endophytic fungus *Biscogniauxia formosana* and their antimycobacterial activity. *Phytochemistry Letters*, 5(3), 467–472. doi: 10.1016/j.phytol.2012.04.007

Chinworrungsee, M., Kittakoop, P., Saenboonrueng, J., Kongsaeree, P., & Thebtaranonth, Y. (2006). Bioactive compounds from the seed fungus Menisporopsis theobromae BCC 3975. *Journal of Natural Products*, *69*(10), 1404–1410. https://doi.org/10.1021/np0601197

Cole, R. J., Wilson, D. M., Harper, J. L., Cox, R. H., Cochran, T. W., Cutler, H. G., & Bell, D. K. (1982). Isolation and identification of two new [11]cytochalasins from *Phomopsis sojae*. *Journal of Agricultural and Food Chemistry*, *30*(2), 301–304. https://doi.org/10.1021/jf00110a021

Cota, B. B., Rosa, L. H., Caligiorne, R. B., Rabello, A. L. T., Almeida Alves, T. M., Rosa, C. A., & Zani, C. L. (2008). Altenusin, a biphenyl isolated from the endophytic fungus *Alternaria* sp., inhibits trypanothione reductase from *Trypanosoma cruzi*. *FEMS Microbiology Letters*, *285*(2), 177–182. https://doi.org/10.1111/j.1574-6968.2008.01221.x

Curtis, R. F., Hassall, C. H., Jones, D. W., & Williams, T. W. (1960). The biosynthesis of phenols. Part II. Asterric acid, a metabolic product of *Aspergillus terreus* Thom. *Journal of the Chemical Society (Resumed)*, (4838), 4838. https://doi.org/10.1039/jr9600004838

do Nascimento, A. M., Soares, M. G., da Silva Torchelsen, F. K. V., de Araujo, J. A. V., Lage, P. S., Duarte, M. C., do Nascimento, A. M. (2015). Antileishmanial activity of compounds produced by endophytic fungi derived from medicinal plant *Vernonia polyanthes* and their potential as a source of bioactive substances. *World Journal of Microbiology and Biotechnology*, *31*(11), 1793–1800. https://doi.org/10.1007/s11274-015-1932-0

ANNEXES

Devi, P., Rodrigues, C., Naik, C. G., & D'Souza, L. (2012). Isolation and characterization of antibacterial compound from a mangrove-endophytic fungus, *Penicillium chrysogenum* MTCC 5108. *Indian Journal of Microbiology*, 52(4), 617–623. doi: 10.1007/s12088-012-0277-8

Ding, G., Chen, A. J., Lan, J., Zhang, H., Chen, X., Liu, X., & Zou, Z. (2012). Sesquiterpenes and cyclopeptides from the endophytic fungus *Trichoderma asperellum* Samuels, Lieckf. & Nirenberg. *Chemistry & Biodiversity*, 9(6), 1205–1212. doi: 10.1002/cbdv.201100185

Du, F. Y., Li, X. M., Li, C. S., Shang, Z., & Wang, B. G. (2012). Cristatumins A-D, new indole alkaloids from the marine-derived endophytic fungus *Eurotium cristatum* EN-220. *Bioorganic and Medicinal Chemistry Letters*, 22(14), 4650–4653. doi: 10.1016/j.bmcl.2012.05.088

Edwards, R. L., Maitland, D. J., & Whalley, A. J. S. (1989). Metabolites of the higher fungi. Part 24. Cytochalasin N, O, P, Q, and R. New cytochalasins from the fungus *Hypoxylon terricola* Mill. *Journal of the Chemical Society, Perkin Transactions 1*, (1), 57. https://doi.org/10.1039/p19890000057

Elfita, E., Muharni, M., Munawar, M., Legasari, L., & Darwati, D. (2011). Antimalarial compounds from endophytic fungi of brotowali (*Tinaspora crispa* L). *Indonesian Journal of Chemistry*, *11*(1), 53–58. https://doi.org/10.22146/ijc.21420

Elsebai, M. F., Natesan, L., Kehraus, S., Mohamed, I. E., Schnakenburg, G., Sasse, F., Shaaban, S., Gütschow, M., & König, G. M. (2011). HLE-inhibitory alkaloids with a polyketide skeleton from the marine-derived fungus *Coniothyrium cereale*. *Journal of Natural Products*, 74(10), 2282–2285. doi: 10.1021/np2004227

Engels, D., & Zhou, X. N. (2020). Neglected tropical diseases: An effective global response to local poverty-related disease priorities. *Infectious Diseases of Poverty*, *9*(1), 1–9. https://doi.org/10.1186/s40249-020-0630-9

Espada, A., Rivera-Sagredo, A., de la Fuente, J. M., Hueso-Rodríguez, J. A., & Elson, S. W. (1997). New cytochalasins from the fungus *Xylaria hypoxylon*. *Tetrahedron*, *53*(18), 6485–6492. https://doi.org/10.1016/S0040-4020(97)00305-0

Ferreira, M. C., Cantrell, C. L., Wedge, D. E., Gonçalves, V. N., Jacob, M. R., Khan, S., … Rosa, L. H. (2017). Antimycobacterial and antimalarial activities of endophytic fungi associated with the ancient and narrowly endemic neotropical plant *Vellozia gigantea* from Brazil. *Memorias Do Instituto Oswaldo Cruz*, *112*(10), 692–697. https://doi.org/10.1590/0074-02760170144

Figueroa, M., Jarmusch, A. K., Raja, H. A., El-Elimat, T., Kavanaugh, J. S., Horswill, A. R., Cooks, R. G., Cech, N. B., & Oberlies, N. H. (2014). Polyhydroxyanthraquinones as quorum sensing inhibitors from the guttates of *Penicillium restrictum* and their analysis by desorption electrospray ionization mass spectrometry. *Journal of Natural Products*, 77(6), 1351–1358. doi: 10.1021/np5000704

Francolini, I., Norris, P., Piozzi, A., Donelli, G., Stoodley, P., 2004. Usnic acid, a natural antimicrobial agent able to inhibit bacterial biofilm formation on polymer surfaces. Antimicrob. Agents Chemother. 48, 4360–4365. https://doi.org/10.1128/AAC.48.11.4360-4365.2004

Fredenhagen, A., Petersen, F., Tintelnot-Blomley, M., Rösel, J., Mett, H., Hug, P., 1997. Semicochliodinol A and B: Inhibitors of HIV-1 Protease and EGF-R Protein Tyrosine Kinase Related to Asterriquinones Produced by the Fungus Chrysosporium merdarium. J. Antibiot. (Tokyo). 50, 395–401. https://doi.org/10.7164/antibiotics.50.395

Ganley RJ, Brunsfeld SJ, Newcombe G. 2004. A community of unknown, endophytic fungi in western white pine. *Proceedings of the National, Academy of Sciences* 101, 10107–10112.

Gao, S.-S., Li, X.-M., Zhang, Y., Li, C.-S., & Wang, B.-G. (2011). Conidiogenones H and I, two new diterpenes of cyclopiane class from a marine-derived endophytic fungus *Penicillium chrysogenum* QEN-24S. *Chemistry & Biodiversity*, 8(9), 1748–1753. doi: 10.1002/cbdv.201000378.

Juan-García, A., Ruiz, M.J., Font, G., Manyes, L., 2015. Enniatin A1, enniatin B1 and beauvericin on HepG2: Evaluation of toxic effects. Food Chem. Toxicol. 84, 188–196. https://doi.org/10.1016/j.fct.2015.08.030

Gennaro M, Gonthier P, Nicolotti G, Cellerino GP. (2001). First Report of Tubakia dryina in Buds and Shoots of Quercus cerris and Quercus robur. *Plant Disease* 85(12), 1289. doi: 10.1094/PDIS.2001.85.12.1289B.

ANNEXES

Germida, J.J., S.D. Siciliano, J.R. de Freitas, and A.M. Seib. (1998). Diversity of rootassociated bacteria associated with field grown canola (*Brassica napus* L.) and wheat (*Triticum aestivum* L.). *FEMS Microbiology Ecology* 26, 43-50.

Gómez, O. C., & Luiz, J. H. H. (2018). Endophytic fungi isolated from medicinal plants: future prospects of bioactive natural products from Tabebuia/Handroanthus endophytes. *Applied Microbiology and Biotechnology*, *102*(21), 9105–9119. https://doi.org/10.1007/s00253-018-9344-3

González-Menéndez, V., Crespo, G., Toro, C., Martín, J., de Pedro, N., Tormo, J. R., & Genilloud, O. (2019). Extending the metabolite diversity of the endophyte *Dimorphosporicola tragani*. *Metabolites*, *9*(10), 197. https://doi.org/10.3390/metabo9100197

Gouda, S., Das, G., Sen, S. K., Shin, H. S., & Patra, J. K. (2016). Endophytes: A treasure house of bioactive compounds of medicinal importance. *Frontiers in Microbiology*, *7*(SEP), 1–8. https://doi.org/10.3389/fmicb.2016.01538

Gu, W. (2009). Bioactive metabolites from *Alternaria brassicicola* ML-P08, an endophytic fungus residing in *Malus halliana*. World Journal of Microbiology and Biotechnology, 25(9), 1677–1683. doi: 10.1007/s11274-009-0062-y

Gupta, S., Chaturvedi, P., Kulkarni, M. G., & Van Staden, J. (2020). A critical review on exploiting the pharmaceutical potential of plant endophytic fungi. *Biotechnology Advances*, *39* (September 2019), 107462. https://doi.org/10.1016/j.biotechadv.2019.107462

Gutierrez-Zamora, M. and E. Martinez-Romero. (2001). Natural endophytic association between Rhizobium etli and maize (Zea mays). *Journal of Biotechnology* 91, 117-126.

Hamill, R. L., Higgens, C. E., Boaz, H. E., & Gorman, M. (1969). The structure of beauvericin, a new depsipeptide antibiotic toxic to *Artemia salina*. *Tetrahedron Letters*, *10*(49), 4255–4258. https://doi.org/10.1016/S0040-4039(01)88668-8

Harrison, J. G., & Griffin, E. A. (2020). The diversity and distribution of endophytes across biomes, plant phylogeny and host tissues: how far have we come and where do we go from here? *Environmental Microbiology*, *22*(6), 2107–2123. https://doi.org/10.1111/1462-2920.14968

Hayashi, A., Fujioka, S., Nukina, M., Kawano, T., Shimada, A., & Kimura, Y. (2007). Fumiquinones A and B, nematicidal quinones produced by Aspergillus fumigatus. *Bioscience, Biotechnology and Biochemistry*, *71*(7), 1697–1702. https://doi.org/10.1271/bbb.70110

He, H., Yang, H.Y., Bigelis, R., Solum, E.H., Greenstein, M., Carter, G.T., 2002. Pyrrocidines A and B, new antibiotics produced by a filamentous fungus. Tetrahedron Lett. 43, 1633–1636. https://doi.org/10.1016/S0040-4039(02)00099-0

Hemtasin, C., Kanokmedhakul, S., Kanokmedhakul, K., Hahnvajanawong, C., Soytong, K., Prabpai, S., & Kongsaeree, P. (2011). Cytotoxic pentacyclic and tetracyclic aromatic sesquiterpenes from *Phomopsis archeri*. *Journal of Natural Products*, *74*(4), 609–613. https://doi.org/10.1021/np100632g

Hoff, J.A., N.B. Klopfenstein, G.I. McDonald, J.R. Tonn, M.S. Kim, P.J. Zambino, P.F. Hessburg, J.D. Rogers, T.L. Peever, and L.M. Carris. 2004. Fungal endophytes in woody roots of Douglas-fir (Pseudotsuga menziesii) and ponderosa pine (Pinus ponderosa). *Forest Pathology.* 34, 255-271

Hoffman, A. M., Mayer, S. G., Strobel, G. A., Hess, W. M., Sovocool, G. W., Grange, A. H., Harper, J. K., Arif, A. M., Grant, D. M., & Kelley-Swift, E. G. (2008). Purification, identification and activity of phomodione, a furandione from an endophytic *Phoma* species. *Phytochemistry*, 69(4), 1049–1056. doi: 10.1016/j.phytochem.2007.10.031

Hussain, H., Ahmed, I., Schulz, B., Draeger, S., & Krohn, K. (2012). Pyrenocines J-M: Four new pyrenocines from the endophytic fungus, *Phomopsis* sp. *Fitoterapia*, 83(3), 523–526. doi: 10.1016/j.fitote.2011.12.017

Hussain, H., Tchimene, M. K., Ahmed, I., Meier, K., Steinert, M., Draeger, S., Schulz, B., & Krohn, K. (2011). Antimicrobial chemical constituents from the endophytic fungus Phomopsis sp. from *Notobasis syriaca*. *Natural Product Communications*, 6(12), 1934578X1100601. doi: 10.1177/1934578X1100601228

Hutchings, M. I., Truman, A. W., & Wilkinson, B. (2019). Antibiotics: past, present and future. *Current Opinion in Microbiology*, *51*, 72–80. https://doi.org/10.1016/j.mib.2019.10.008

ANNEXES

Hzounda Fokou, J. B., Dize, D., Etame Loe, G. M., Nko'o, M. H. J., Ngene, J. P., Ngoule, C. C., & Boyom, F. F. (2021). Anti-leishmanial and anti-trypanosomal natural products from endophytes. *Parasitology Research*, *120*(3), 785–796. https://doi.org/10.1007/s00436-020-07035-1

Ibrahim, S. R. M., Abdallah, H. M., Elkhayat, E. S., Al Musayeib, N. M., Asfour, H. Z., Zayed, M. F., & Mohamed, G. A. (2018). Fusaripeptide A: new antifungal and anti-malarial cyclodepsipeptide from the endophytic fungus *Fusarium* sp. *Journal of Asian Natural Products Research*, *20*(1), 75–85. https://doi.org/10.1080/10286020.2017.1320989

Ibrahim, S. R. M., Abdallah, H. M., Mohamed, G. A., & Ross, S. A. (2016). Integracides H-J: New tetracyclic triterpenoids from the endophytic fungus *Fusarium* sp. *Fitoterapia*, *112*, 161–167. https://doi.org/10.1016/j.fitote.2016.06.002

Ibrahim, S. R. M., Mohamed, G. A., Al Haidari, R. A., El-Kholy, A. A., & Zayed, M. F. (2018). Potential anti-malarial agents from endophytic fungi: A review. *Mini-Reviews in Medicinal Chemistry*, *18*(13), 1110–1132. https://doi.org/10.2174/1389557518666180305163151

Isaka, M., Berkaew, P., Intereya, K., Komwijit, S., & Sathitkunanon, T. (2007). Antiplasmodial and antiviral cyclohexadepsipeptides from the endophytic fungus *Pullularia* sp. BCC 8613. *Tetrahedron*, *63*(29), 6855–6860. https://doi.org/10.1016/j.tet.2007.04.062

Isaka, M., Chinthanom, P., Boonruangprapa, T., Rungjindamai, N., & Pinruan, U. (2010). Eremophilane-type sesquiterpenes from the fungus *Xylaria* sp. BCC 21097. *Journal of Natural Products*, *73*(4), 683–687. https://doi.org/10.1021/np100030x

Isaka, M., Jaturapat, A., Rukseree, K., Danwisetkanjana, K., Tanticharoen, M., & Thebtaranonth, Y. (2001). Phomoxanthones A and B, novel xanthone dimers from the endophytic fungus *Phomopsis* species. *Journal of Natural Products*, 64(8), 1015–1018. doi: 10.1021/np010006h

Izawa, Y., Hirose, T., Shimizu (née Tomioka), T., Koyama, K., & Natori, S. (1989). Six new 10-pheynl-[11]cytochalasans, cytochalasins N - S from *Phomopsis* SP. *Tetrahedron*, *45*(8), 2323–2335. https://doi.org/10.1016/S0040-4020(01)83434-7

Jia, M., Chen, L., Xin, H.-L., Zheng, C.-J., Rahman, K., Han, T., & Qin, L.-P. (2016). A Friendly Relationship between Endophytic Fungi and Medicinal Plants: A Systematic Review. *Frontiers in Microbiology*, *7*(JUN), 1–14. https://doi.org/10.3389/fmicb.2016.00906

Jiménez-Romero, C., Ortega-Barría, E., Arnold, A. E., & Cubilla-Rios, L. (2008). Activity against *Plasmodium falciparum* of lactones isolated from the endophytic fungus *Xylaria* sp. *Pharmaceutical Biology*, *46*(10–11), 700–703. https://doi.org/10.1080/13880200802215859

Kamdem, R. S. T., Wang, H., Wafo, P., Ebrahim, W., Özkaya, F. C., Makhloufi, G., Proksch, P. (2018). Induction of new metabolites from the endophytic fungus *Bionectria* sp. through bacterial co-culture. *Fitoterapia*, *124*, 132–136. https://doi.org/10.1016/j.fitote.2017.10.021

Keller, N. P. (2019). Fungal secondary metabolism: regulation, function and drug discovery. *Nature Reviews Microbiology*, *17*(3), 167–180. https://doi.org/10.1038/s41579-018-0121-1

Khare, E., Mishra, J., & Arora, N. K. (2018). Multifaceted Interactions Between Endophytes and Plant: Developments and Prospects. *Frontiers in Microbiology*, *9*. https://doi.org/10.3389/fmicb.2018.02732

Kharwar, R. N., Verma, V. C., Kumar, A., Gond, S. K., Harper, J. K., Hess, W. M., Lobkovosky, E., Ma, C., Ren, Y., & Strobel, G. A. (2009). Javanicin, an antibacterial naphthoquinone from an endophytic fungus of neem, *Chloridium* sp. *Current Microbiology*, 58(3), 233–238. doi: 10.1007/s00284-008-9313-7

Khumkomkhet, P., Kanokmedhakul, S., Kanokmedhakul, K., Hahnvajanawong, C., & Soytong, K. (2009). Antimalarial and cytotoxic depsidones from the fungus *Chaetomium brasiliense*. *Journal of Natural Products*, *72*(8), 1487–1491. https://doi.org/10.1021/np9003189

Kim, S., Shin, D. S., Lee, T., & Oh, K. B. (2004a). Periconicins, two new fusicoccane diterpenes produced by an endophytic fungus *Periconia* sp. with antibacterial activity. *Journal of Natural Products*, 67(3), 448–450. doi: 10.1021/np030384h

Kimura, Y., Mizuno, T., Nakajima, H., Hamasaki, T., 1992. Altechromones A and B, New Plant Growth Regulators Produced by the Fungus, Alternaria sp. Biosci. Biotechnol. Biochem. 56, 1664–1665. https://doi.org/10.1271/bbb.56.1664

ANNEXES

Knight, V., Sanglier, J. J., DiTullio, D., Braccili, S., Bonner, P., Waters, J., Zhang, L. (2003). Diversifying microbial natural products for drug discovery. *Applied Microbiology and Biotechnology*, *62*(5–6), 446–458. https://doi.org/10.1007/s00253-003-1381-9

Kongsaeree, P., Prabpai, S., Sriubolmas, N., Vongvein, C., & Wiyakrutta, S. (2003). Antimalarial dihydroisocoumarins produced by *Geotrichum* sp., an endophytic fungus of *Crassocephalum crepidioides*. *Journal of Natural Products*, *66*(5), 709–711. https://doi.org/10.1021/np0205598

Kontnik, R., & Clardy, J. (2008). Codinaeopsin, an antimalarial fungal polyketide. *Organic Letters*, *10*(18), 4149–4151. https://doi.org/10.1021/ol801726k

Krohn, K., Farooq, U., Hussain, H., Ahmed, I., Rheinheimer, J., Draeger, S., Schulz, B., & van Ree, T. (2011). Phomosines H–J, novel highly substituted biaryl ethers, isolated from the endophytic fungus *Phomopsis* sp. from *Ligustrum vulgare*. *Natural Product Communications*, 6(12), 1934578X1100601. doi: 10.1177/1934578X1100601229

Krohn, K., Kouam, S. F., Kuigoua, G. M., Hussain, H., Cludius-Brandt, S., Flörke, U., Kurtán, T., Pescitelli, G., Di Bari, L., Draeger, S., & Schulz, B. (2009). Xanthones and oxepino[2, 3- b]chromones from three endophytic fungi. *Chemistry - A European Journal*, 15(44), 12121–12132. doi: 10.1002/chem.200900749

Krohn, K., Michel, A., Flörke, U., Aust, H.-J., Draeger, S., & Schulz, B. (1994). Palmarumycins C1–C16 from *Coniothyrium* sp.: isolation, structure elucidation, and biological activity. *Liebigs Annalen Der Chemie*, *1994*(11), 1099–1108. https://doi.org/10.1002/jlac.199419941108

Kumarihamy, M., Ferreira, D., Croom, E. M., Sahu, R., Tekwani, B. L., Duke, S. O., Dhammika Nanayakkara, N. P. (2019). Antiplasmodial and cytotoxic cytochalasins from an endophytic fungus, *Nemania* sp. UM10M, Isolated from a diseased *Torreya taxifolia* leaf. *Molecules*, *24*(4). https://doi.org/10.3390/molecules24040777

Kuyama, S., & Tamura, T. (1957). Cercosporin. A pigment of *Cercosporina Kikuchii* Matsumoto et Tomoyasu. I. Cultivation of fungus, isolation and purification of pigment. *Journal of the American Chemical Society*, *79*(21), 5725–5726. https://doi.org/10.1021/ja01578a038

Lauterwein, M., Oethinger, M., Belsner, K., Peters, T., Marre, R., 1995. In vitro activities of the lichen secondary metabolites vulpinic acid, (+)-usnic acid, and (-)-usnic acid against aerobic and anaerobic microorganisms. Antimicrob. Agents Chemother. 39, 2541–2543. https://doi.org/10.1128/AAC.39.11.2541

Lenta, B. N., Ngatchou, J., Frese, M., Ladoh-Yemeda, F., Voundi, S., Nardella, F., Sewald, N. (2016). Purpureone, an antileishmanial ergochrome from the endophytic fungus *Purpureocillium lilacinum*. *Zeitschrift Für Naturforschung B*, *71*(11), 1159–1167. https://doi.org/10.1515/znb-2016-0128

Li, J.Y., Harper, J.K., Grant, D.M., Tombe, B.O., Bashyal, B., Hess, W.M., Strobel, G.A., 2001. Ambuic acid, a highly functionalized cyclohexenone with antifungal activity from Pestalotiopsis spp. and Monochaetia sp. Phytochemistry 56, 463–468. https://doi.org/10.1016/S0031-9422(00)00408-8

Li, Y., Song, Y. C., Liu, J. Y., Ma, Y. M., & Tan, R. X. (2005). Anti-helicobacter pylori substances from endophytic fungal cultures. *World Journal of Microbiology and Biotechnology*, 21(4), 553–558. doi: 10.1007/s11274-004-3273-2

Liu, X., Dong, M., Chen, X., Jiang, M., Lv, X., & Zhou, J. (2008). Antimicrobial activity of an endophytic *Xylaria* sp.YX-28 and identification of its antimicrobial compound 7-amino-4-methylcoumarin. *Applied Microbiology and Biotechnology*, 78(2), 241–247. doi: 10.1007/s00253-007-1305-1

Loesgen, S., Bruhn, T., Meindl, K., Dix, I., Schulz, B., Zeeck, A., & Bringmann, G. (2011). (+)-Flavipucine, the missing member of the pyridione epoxide family of fungal antibiotics. *European Journal of Organic Chemistry*, 2011(26), 5156–5162. doi: 10.1002/ejoc.201100284

Lösgen, S., Magull, J., Schulz, B., Draeger, S., & Zeeck, A. (2008). Isofusidienols: novel chromone-3-oxepines produced by the endophytic fungus *Chalara* sp. *European Journal of Organic Chemistry*, 2008(4), 698–703. doi: 10.1002/ejoc.200700839

Lu, S., Draeger, S., Schulz, B., Krohn, K., Ahmed, I., Hussain, H., Yi, Y., Li, N., & Zhang, W. (2011). Bioactive Aromatic derivatives from endophytic fungus, *Cytospora* sp. *Natural Product Communications*, 6(5), 661–666. doi: 10.1177/1934578x1100600518

Luo, J., Liu, X., Li, E., Guo, L., & Che, Y. (2013). Arundinols A-C and arundinones A and B from the plant endophytic fungus *Microsphaeropsis arundinis*. *Journal of Natural Products*, 76(1), 107–112. doi: 10.1021/np300806a

Ma, Y. M., Li, Y., Liu, J. Y., Song, Y. C., & Tan, R. X. (2004). Anti-Helicobacter pylori metabolites from *Rhizoctonia* sp. Cy064, an endophytic fungus in *Cynodon dactylon*. *Fitoterapia*, 75(5), 451–456. doi: 10.1016/j.fitote.2004.03.007

Maciag-Dorszyńska, M., Wegrzyn, G., Guzow-Krzemińska, B., 2014. Antibacterial activity of lichen secondary metabolite usnic acid is primarily caused by inhibition of RNA and DNA synthesis. FEMS Microbiol. Lett. https://doi.org/10.1111/1574-6968.12409

Macías-Rubalcava, M. L., Hernández-Bautista, B. E., Jiménez-Estrada, M., González, M. C., Glenn, A. E., Hanlin, R. T., Anaya, A. L. (2008). Naphthoquinone spiroketal with allelochemical activity from the newly discovered endophytic fungus *Edenia gomezpompae*. *Phytochemistry*, *69*(5), 1185–1196. https://doi.org/10.1016/j.phytochem.2007.12.006

Manganyi, M. C., & Ateba, C. N. (2020). Untapped potentials of endophytic fungi: A review of novel bioactive compounds with biological applications. *Microorganisms*, *8*(12), 1–25. https://doi.org/10.3390/microorganisms8121934

Martinez-Klimova, E., Rodríguez-Peña, K., & Sánchez, S. (2017). Endophytes as sources of antibiotics. *Biochemical Pharmacology*, *134*, 1–17. https://doi.org/10.1016/j.bcp.2016.10.010

Martińez-Luis, S., Cherigo, L., Arnold, E., Spadafora, C., Gerwick, W. H., & Cubilla-Rios, L. (2012). Antiparasitic and anticancer constituents of the endophytic fungus *Aspergillus* sp. strain F1544. *Natural Product Communications*, *7*(2), 165–168. https://doi.org/10.1177/1934578x1200700207

Martínez-Luis, S., Della-Togna, G., Coley, P. D., Kursar, T. A., Gerwick, W. H., & Cubilla-Rios, L. (2008). Antileishmanial constituents of the panamanian endophytic fungus *Edenia* sp. *Journal of Natural Products*, *71*(12), 2011–2014. https://doi.org/10.1021/np800472q

Meng, L. H., Li, X. M., Zhang, F. Z., Wang, Y. N., & Wang, B. G. (2020). Talascortenes A-G, highly oxygenated diterpenoid acids from the sea-anemone-derived endozoic fungus *Talaromyces scorteus* AS-242. *Journal of Natural Products*, 83(8), 2528–2536. doi: 10.1021/acs.jnatprod.0c00628

Miao, F.-P., Li, X.-D., Liu, X.-H., Cichewicz, R. H., & Ji, N.-Y. (2012). Secondary Metabolites from an algicolous *Aspergillus versicolor* strain. Marine Drugs, 10(12), 131–139. doi: 10.3390/md10010131

Miller, L. H., Ackerman, H. C., Su, X., & Wellems, T. E. (2013). Malaria biology and disease pathogenesis: insights for new treatments.: KRISALIS DISCOVERY. *Nature Medicine*, 19, 156. Retrieved from http://eds.a.ebscohost.com/eds/pdfviewer/pdfviewer?sid=8938f6da-b205-4cf9-b07f-e99d8e435f65%40sessionmgr4002&vid=0&hid=4111

Miyagawa, H., Nagai, S., Tsurushima, T., Sato, M., Ueno, T., & Fukami, H. (1994). Phytotoxins produced by the plant pathogenic fungus *Bipolar is bicolor* El-1. *Bioscience, Biotechnology, and Biochemistry*, 58(6), 1143–1145. https://doi.org/10.1271/bbb.58.1143

Moraes Neto, R.N., Barros Setubal, R.F., Maciel Higino, T.M., Accioly Brelaz-de-Castro, M.C., Nascimento da Silva, L.C. & dos Santos Alianca, A.S. (2019). Asteraceae plants as sources of compounds against leishmaniasis and Chagas disease, *Frontiers in Pharmacology*, 10, 477. doi: 10.3389/fphar.2019.00477.

Moreno, E., Varughese, T., Spadafora, C., Arnold, A. E., Coley, P. D., Kursar, T. A., Cubilla-Rios, L. (2011). Chemical constituents of the new endophytic fungus *Mycosphaerella* sp. nov. and their anti-parasitic activity. *Natural Product Communications*, 6(6), 1934578X1100600. https://doi.org/10.1177/1934578X1100600620

Nakanishi, S., Ando, K., Kawamoto, I., & Kase, H. (1989). KS-501 and KS-502, new inhibitors of Ca^{2+} and calmodulin-dependent cyclic-nucleotide phosphodiesterase from *Sporothrix* sp. *The Journal of Antibiotics*, 42(7), 1049–1055. https://doi.org/10.7164/antibiotics.42.1049

Nakayama, J., Uemura, Y., Nishiguchi, K., Yoshimura, N., Igarashi, Y., & Sonomoto, K. (2009). Ambuic acid inhibits the biosynthesis of cyclic peptide quormones in gram-positive bacteria. *Antimicrobial Agents and Chemotherapy*, 53(2), 580–586. doi: 10.1128/AAC.00995-08

Ola, A. R. B., Thomy, D., Lai, D., Brötz-Oesterhelt, H., & Proksch, P. (2013). Inducing secondary metabolite production by the endophytic fungus *Fusarium tricinctum* through coculture with *Bacillus subtilis*. *Journal of Natural Products*, 76(11), 2094–2099. doi: 10.1021/np400589h

Newman, D. J., & Cragg, G. M. (2020). Natural products as sources of new drugs over the nearly four decades from 01/1981 to 09/2019. *Journal of Natural Products*, *83*(3), 770–803. https://doi.org/10.1021/acs.jnatprod.9b01285

Okoye, F. B. C., Nworu, C. S., Debbab, A., Esimone, C. O., & Proksch, P. (2015). Two new cytochalasins from an endophytic fungus, KL-1.1 isolated from *Psidium guajava* leaves. *Phytochemistry Letters*, *14*, 51–55. https://doi.org/10.1016/j.phytol.2015.09.004

Oono, R., Rasmussen, A., & Lefèvre, E. (2017). Distance decay relationships in foliar fungal endophytes are driven by rare taxa. Environmental microbiology, 19(7), 2794-2805 doi:10.1111/1462-2920.13799.

Pinheiro, E. A. A., Carvalho, J. M., Dos Santos, D. C. P., De Oliveira Feitosa, A., Marinho, P. S. B., Guilhon, G. M. S. P., De Souza, A. D. L., Da Silva, F. M. A., & Andrey, A. M. (2013). Antibacterial activity of alkaloids produced by endophytic fungus *Aspergillus* sp. EJC08 isolated from medicinal plant *Bauhinia guianensis*. *Natural Product Research*, 27(18), 1633–1638. doi: 10.1080/14786419.2012.750316

Pongcharoen, W., Rukachaisirikul, V., Phongpaichit, S., & Sakayaroj, J. (2007). A New Dihydrobenzofuran Derivative from the Endophytic Fungus *Botryosphaeria mamane* PSU-M76. *Chemical &Pharmaceutical Bulletin*, 55(9), 1404–1405. doi: 10.1248/cpb.55.1404

Pontius, A., Krick, A., Kehraus, S., Brun, R., & König, G. M. (2008). Antiprotozoal activities of heterocyclic-substituted xanthones from the marine-derived fungus *Chaetomium* sp. *Journal of Natural Products*, *71*(9), 1579–1584. https://doi.org/10.1021/np800294q

Qin, S., Hussain, H., Schulz, B., Draeger, S., & Krohn, K. (2010). Two new metabolites, epoxydine A and B, from *Phoma* sp. *Helvetica Chimica Acta*, 93(1), 169–174. doi: 10.1002/hlca.200900199

Ragazzi, A., S. Moricca, P. Capretti, and I. Dellavalle. 1999. Endophytic presence of Discula quercina on declining Quercus cerris. *Journal of Phytopathology* 147, 437-440.

Rasmussen, T. B., Skindersoe, M. E., Bjarnsholt, T., Phipps, R. K., Christensen, K. B., Jensen, P. O., Andersen, J. B., Koch, B., Larsen, T. O., Hentzer, M., Eberl, L., Hoiby, N., & Givskov, M. (2005). Identity and effects of quorum-sensing inhibitors produced by *Penicillium* species. Microbiology, 151(5), 1325–1340. doi: 10.1099/mic.0.27715-0

Raviraja, N.S. (2005). Fungal endophytes in five medicinal plant species from Kudremukh Range, Western Ghats of India. *Journal of Basic Microbiology* 45, 230-235.

Rodriguez, K.F. and G.J. Samuels. 1999. Fungal endophytes of Spondias mombin in Brazil: A preliminary study. *Journal of Basic Microbiology* 39:131-135.

Romano, S., Jackson, S. A., Patry, S., & Dobson, A. D. W. (2018). Extending the "one strain many compounds" (OSMAC) principle to marine microorganisms. *Marine Drugs*, *16*(7), 1–29. https://doi.org/10.3390/md16070244

Roy, S., Kumar, G. A., Jafurulla, M., Mandal, C., & Chattopadhyay, A. (2014). Integrity of the actin cytoskeleton of host macrophages is essential for *Leishmania donovani* infection. *Biochimica et Biophysica Acta - Biomembranes*, *1838*(8), 2011–2018. https://doi.org/10.1016/j.bbamem.2014.04.017

Rukachaisirikul, V., Sommart, U., Phongpaichit, S., Sakayaroj, J., & Kirtikara, K. (2008). Metabolites from the endophytic fungus *Phomopsis* sp. PSU-D15. Phytochemistry, 69(3), 783–787. doi: 10.1016/j.phytochem.2007.09.006

Sakemi, S., Inagaki, T., Kaneda, K., Hirai, H., Iwata, E., Sakakibara, T., Kojima, N. (1995). CJ-12,371 and CJ-12,372, two novel dna gyrase inhibitors. Fermentation, isolation, structural elucidation and biological activities. *The Journal of Antibiotics*, *48*(2), 134–142. https://doi.org/10.7164/antibiotics.48.134

Sappapan, R., Sommit, D., Ngamrojanavanich, N., Pengpreecha, S., Wiyakrutta, S., Sriubolmas, N., & Pudhom, K. (2008). 11-Hydroxymonocerin from the plant endophytic fungus *Exserohilum rostratum*. *Journal of Natural Products*, *71*(12), 2080. https://doi.org/10.1021/np8006167

Schueffler, A., & Anke, T. (2014). Fungal natural products in research and development. *Nat. Prod. Rep.*, *31*(10), 1425–1448. https://doi.org/10.1039/C4NP00060A

Schena, L., F. Nigro, I. Pentimone, A. Ligorio, and A. Ippolito. 2003. Control of postharvest rots of sweet cherries and table grapes with endophytic isolates of Aureobasidium pullulans. *Postharvest Biology and Technology* 30, 209-220.

Setzer, W.N. & Setzer, M.C. (2006). Antitrypanosomal agents from higher plants. In Biologically active natural products for the 21st century, Ed. L.A.D. Williams, 47-95

Shang, Z., Li, X.-M., Li, C.-S., & Wang, B.-G. (2012). Diverse secondary metabolites produced by marine-derived fungus *Nigrospora* sp. MA75 on various culture media. *Chemistry & Biodiversity*, 9(7), 1338–1348. doi: 10.1002/cbdv.201100216

Sharma, A., del Carmen Flores-Vallejo, R., Cardoso-Taketa, A., Villarreal, M.L. (2017). Journal of Ethnopharmacology, 208, 264-329. http://dx.doi.org/10.1016/j.jep.2016.04.045

Sharma, S., Kumar, M., Sharma, S., Nargotra, A., Koul, S., Khan, I.A. (2010). Piperine as an inhibitor of Rv1258c, a putative multidrug efflux pump of *Mycobacterium tuberculosis. Journal of Antimicrobial Chemotherapy,* 65(8), 1694-1701. DOI: 10.1093/jac/dkq186

Shiono, Y., Hatakeyama, T., Murayama, T., & Koseki, T. (2012). Polyketide metabolites from the endophytic fungus *Microdiplodia* sp. KS 75-1. *Natural Product Communications*, 7(8), 1934578X1200700. doi: 10.1177/1934578X1200700825

Shu, R. G., Wang, F. W., Yang, Y. M., Liu, Y. X., & Tan, R. X. (2004). Antibacterial and xanthine oxidase inhibitory cerebrosides from *Fusarium* sp. IFB-121, an endophytic fungus in *Quercus variabilis*. *Lipids*, 39(7), 667–673. doi: 10.1007/s11745-004-1280-9

Siegel, M.R., G.C.M. Latch, and M.C. Johnson. 1987. Fungal endophyte of grasses, *The Annual Review of Phytopathology* 25:293-315

Singh, M. P., Janso, J. E., Luckman, S. W., Brady, S. F., Clardy, J., Greenstein, M., & Maiese, W. M. (2000). Biological activity of guanacastepene, a novel diterpenoid antibiotic produced by an unidentified fungus CR115. *Journal of Antibiotics*, 53(3), 256–261. doi: 10.7164/antibiotics.53.256

Singh, S. B., Zink, D. L., Liesch, J. M., Dombrowski, A. W., Darkin-Rattray, S. J., Schmatz, D. M., & Goetz, M. A. (2001). Structure, histone deacetylase, and antiprotozoal activities of apicidins B and C, congeners of apicidin with proline and valine substitutions. *Organic Letters*, *3*(18), 2815–2818. https://doi.org/10.1021/ol016240g

Smith, H., M.J. Wingfield, and O. Petrini. (1996). Botryosphaeria dothidea endophytic in Eucalyptus grandis and Eucalyptus nitens in South Africa. *Forest Ecology and Management* 89:189-195.

Stark, A. A., Kobbe, B., Matsuo, K., Büchi, G., Wogan, G. N., & Demain, A. L. (1978). Mollicellins: Mutagenic and antibacterial mycotoxins. *Applied and Environmental Microbiology*, *36*(3), 412–420. https://doi.org/10.1128/aem.36.3.412-420.1978

Strobel, G., & Daisy, B. (2003). Bioprospecting for microbial endophytes and their natural products. *Microbiology and molecular biology reviews : MMBR*, 67(4), 491–502. https://doi.org/10.1128/MMBR.67.4.491-502.2003

Strobel, G.A. (2003). Endophytes as sources of bioactive products. *Microbes Infect.* 5(6), 535-544. https://doi.org/10.1016/s1286-4579(03)00073-x.

Sturz, A.V., B.R. Christie, and B.G. Matheson. 1998. Associations of bacterial endophyte populations from red clover and potato crops with potential for beneficial allelopathy. *Canadian Journal of Microbiology* 44, 162-167.

Sun, P., Huo, J., Kurtán, T., Mándi, A., Antus, S., Tang, H., Draeger, S., Schulz, B., Hussain, H., Krohn, K., Pan, W., Yi, Y., & Zhang, W. (2013). Structural and stereochemical studies of hydroxyanthraquinone derivatives from the endophytic fungus *Coniothyrium* sp. *Chirality*, 25(2), 141–148. doi: 10.1002/chir.22128

ANNEXES

Talontsi, F. M., Lamshöft, M., Douanla-Meli, C., Kouam, S. F., & Spiteller, M. (2014). Antiplasmodial and cytotoxic dibenzofurans from *Preussia* sp. harboured in *Enantia chlorantha* Oliv. *Fitoterapia*, *93*, 233–238. https://doi.org/10.1016/j.fitote.2014.01.003

Tansuwan, S., Pornpakakul, S., Roengsumran, S., Petsom, A., Muangsin, N., Sihanonta, P., & Chaichit, N. (2007). Antimalarial benzoquinones from an endophytic fungus, Xylaria sp. *Journal of Natural Products*, *70*(10), 1620–1623. https://doi.org/10.1021/np0701069

Thomas, R. (1961). Studies in the biosynthesis of fungal metabolites. 4. Alternariol monomethyl ether and its relation to other phenolic metabolites of *Alternaria tenuis*. *Biochemical Journal*, *80*(2), 234–240. https://doi.org/10.1042/bj0800234

Toghueo, R. M. K. (2019). Anti-leishmanial and anti-inflammatory agents from endophytes: A review. *Natural Products and Bioprospecting*, *9*(5), 311–328. https://doi.org/10.1007/s13659-019-00220-5

Tomoda, H., Nlshida, H., Huang, X.H., Masuma, R., Kim, Y.K., Ōmura, S., 1992. New cyclodepsipeptides, enniatins d, e and f produced by fusarium sp. fo-1305. J. Antibiot. (Tokyo). 45, 1207–1215. https://doi.org/10.7164/antibiotics.45.1207

Torres-Mendoza, D., Ortega, H. E., & Cubilla-Rios, L. (2020). Patents on endophytic fungi for agriculture and bio- and phytoremediation applications. *Microorganisms*, *8*(8), 1237. https://doi.org/10.3390/microorganisms8081237

Tran-Cong, N. M., Mándi, A., Kurtán, T., Müller, W. E. G., Kalscheuer, R., Lin, W., Proksch, P. (2019). Induction of cryptic metabolites of the endophytic fungus: *Trichocladium* sp. through OSMAC and co-cultivation. *RSC Advances*, *9*(47), 27279–27288. https://doi.org/10.1039/c9ra05469c

Trischman, J.A., Jensen, P.R., Fenical, W., 1994. Halobacillin: A cytotoxic cyclic acylpeptide of the iturin class produced by a marine Bacillus. Tetrahedron Lett. 35, 5571–5574. https://doi.org/10.1016/S0040-4039(00)77249-2

Tsuchinari, M., Shimanuki, K., Hiramatsu, F., Murayama, T., Koseki, T., & Shiono, Y. (2007). Fusapyridons A and B, novel pyridone alkaloids from an endophytic fungus, *Fusarium* sp. YG-45. *Zeitschrift Fur Naturforschung - Section B Journal of Chemical Sciences*, 62(9), 1203–1207. doi: 10.1515/znb-2007-0916

Verma, V. C., Lobkovsky, E., Gange, A. C., Singh, S. K., & Prakash, S. (2011). Piperine production by endophytic fungus *Periconia* sp. isolated from *Piper longum* L. *Journal of Antibiotics*, 64(6), 427–431. doi: 10.1038/ja.2011.27

Wagenaar, M. M., & Clardy, J. (2001). Dicerandrols, new antibiotic and cytotoxic dimers produced by the fungus *Phomopsis longicolla* isolated from an endangered mint. *Journal of Natural Products*, 64(8), 1006–1009. doi: 10.1021/np010020u

Wang, W.L., Lu, Z.Y., Tao, H.W., Zhu, T.J., Fang, Y.C., Gu, Q.Q., Zhu, W.M., 2007. Isoechinulin-type alkaloids, variecolorins A-L, from halotolerant Aspergillus variecolor. J. Nat. Prod. 70, 1558–1564. https://doi.org/10.1021/np070208z

Wang, K., Chen, Y., Gao, S., Wang, M., Ge, M., Yang, Q., Liao, M., Xu, L., Chen, J., Zeng, Z., Chen, H., Zhang, X. kun, Lin, T., Zhou, H., 2021. Norlichexanthone purified from plant endophyte prevents postmenopausal osteoporosis by targeting ERα to inhibit RANKL signaling. Acta Pharm. Sin. B 11, 442–455. https://doi.org/10.1016/j.apsb.2020.09.012

Weber, D., Sterner, O., Anke, T., Gorzalczancy, S., Martino, V., & Acevedo, C. (2004). Phomol, a new antiinflammatory metabolite from an endophyte of the medicinal plant *Erythrina crista-galli*. *Journal of Antibiotics*, 57(9), 559–563. doi: 10.7164/antibiotics.57.559

Wells, J. M., Cutler, H. G., & Cole, R. J. (1976). Toxicity and plant growth regulator effects of cytochalasin H isolated from *Phomopsis* sp. *Canadian Journal of Microbiology*, *22*(8), 1137–1143. https://doi.org/10.1139/m76-165

Wicklow, D. T., & Poling, S. M. (2009). Antimicrobial activity of pyrrocidines from *Acremonium zeae* against endophytes and pathogens of maize. *Phytopathology*, 99(1), 109–115. doi: 10.1094/PHYTO-99-1-0109

ANNEXES

Wijeratne, E. M. K., He, H., Franzblau, S. G., Hoffman, A. M., & Gunatilaka, A. A. L. (2013). Phomapyrrolidones A-C, antitubercular alkaloids from the endophytic fungus *Phoma* sp. NRRL 46751. *Journal of Natural Products*, 76(10), 1860–1865. doi: 10.1021/np400391p

Wu, D. L., Li, H. J., Smith, D. R., Jaratsittisin, J., Xia-Ke-Er, X. F. K. T., Ma, W. Z., Lan, W. J. (2018). Polyketides and alkaloids from the marine-derived fungus *Dichotomomyces cejpii* F31-1 and the antiviral activity of scequinadoline A against dengue virus. *Marine Drugs*, *16*(7), 1–10. https://doi.org/10.3390/md16070229

Xu, L., Wang, J., Zhao, J., Li, P., Shan, T., Wang, J., Li, X., & Zhou, L. (2010). Beauvericin from the endophytic fungus, *Fusarium redolens*, isolated from *Dioscorea zingiberensis* and its antibacterial activity. *Natural Product Communications*, 5(5), 1934578X1000500. doi: 10.1177/1934578X1000500527

Yang, R., Dong, Q., Xu, H., Gao, X.H., Zhao, Z., Qin, J., Chen, C., Luo, D., 2020. Identification of Phomoxanthone A and B as Protein Tyrosine Phosphatase Inhibitors. ACS Omega 5, 25927–25935. https://doi.org/10.1021/acsomega.0c03315

Yin, Z., Dickschat J.S. (2021). Cis double bond formation on polyketide biosynthesis. *Natural Product Reports*, doi: 10.1039/d0np00091d

Zhang, H. W., Song, Y. C., & Tan, R. X. (2006). Biology and chemistry of endophytes. *Natural Product Reports*, *23*(5), 753–771. https://doi.org/10.1039/b609472b

Zhang, J., Liu, D., Wang, H., Liu, T., & Xin, Z. (2015). Fusartricin, a sesquiterpenoid ether produced by an endophytic fungus Fusarium tricinctum Salicorn 19. European Food Research and Technology, 240(4), 805–814. doi: 10.1007/s00217-014-2386-6

Zhang, M., Wang, W.-L., Fang, Y.-C., Zhu, T.-J., Gu, Q.-Q., & Zhu, W.-M. (2008). Cytotoxic Alkaloids and Antibiotic Nordammarane Triterpenoids from the Marine-Derived Fungus Aspergillus sydowii. *Journal of Natural Products*, *71*(6), 985–989. https://doi.org/10.1021/np700737g

Zhang, W., Krohn, K., Draeger, S., & Schulz, B. (2008). Bioactive isocoumarins isolated from the endophytic fungus *Microdochium bolleyi*. *Journal of Natural Products*, 71(6), 1078–1081. doi: 10.1021/np800095g

Zhao, S., Xiao, C., Wang, J., Tian, K., Ji, W., Yang, T., Khan, B., Qian, G., Yan, W., & Ye, Y. (2020). Discovery of natural FabH inhibitors using an immobilized enzyme column and their antibacterial activity against *Xanthomonas oryzae* pv. oryzae. *Journal of Agricultural and Food Chemistry*, 68(48), 14204–14211. doi: 10.1021/acs.jafc.0c06363

Zheng, R., Li, S., Zhang, X., & Zhao, C. (2021). Biological activities of some new secondary metabolites isolated from endophytic fungi: A review study. *International Journal of Molecular Sciences*, 22(2), 1–75. https://doi.org/10.3390/ijms22020959

Zhu, F., Wu, J., Chen, G., Lu, W., Pan, J., 2011. Biosynthesis, characterization and biological evalutation of Fe(III) and Cu(II) complexes of neoaspergillic acid, a hydroxamate siderophore produced by co-cultures of two marine-derived mangrove epiphytic fungi. Nat. Prod. Commun. 6, 1137–1140. https://doi.org/10.1177/1934578x1100600824